Authors In This Issue

P. A. Beck (p. 468A): Born in Budapest, Hungary. Went to Budapest High School and attended Royal Hungarian University of the Technical Sciences and Michigan College of Mining and Technology with degrees of M.S. in Met., and Mechanical Engineering. Is a member of AIME and now lives at University of Notre Dame. He has worked for American Smelting & Refining Co. as research metallurgist, for the Beryllium Corp., as chief metallurgist, and Cleveland Graphite Bronze Co. as superintendent of Metallurgical Lab. His major activities besides writing technical papers are golf and swimming. . . .

J. F. B. Jackson

R. G. Knickerbocker

J. F. B. Jackson (p. 468B): born in Lancashire, England, and graduated from University of Manchester with B.Sc. in Met. degree. Became associated with David Brown & Sons, (Huddersfield) Ltd. as Research Metallurgist, then in succession Foundry Foreman, Technical Superintendent and Technical Controller (Foundries) with that organization. Is currently Director of Research, British Steel Founders' Association. Mr. Jackson is a member of AIME and lives in Sheffield, England. He is a stamp collector, and for relaxation he turns to fishing and golf. . . . **J. G. Mravec** (p. 468B); born in Czechoslovakia, attended high school in Rocky River, Ohio and graduated from Ohio State University with B.Ch.E. degree, Started with Timken Roller Bearing Co, Steel & Tube Div, as Research Assistant and later became Research Engineer, Blooming Mill Metallurgist, Tool Steel Metallurgist, Research Metallurgist and is at present Melt Shop Metallurgist. His home is in Canton, Ohio. Mr. Mravec has previously presented AIME papers on Effects of Refractories on Steel Cleanliness; Determination of Hydrogen in Molten Steel by the Gas-Tube Method. He enjoys traveling and is interested in photography as well as playing bridge. . . .**Guy B. Hunner** (p. 471); born in Eau Clair, Wis. Worked for a time as Superintendent of Menominee Range, Michigan; Superintendent of Clifton Mines, DeGrasse, N. Y.; District Supt. of Cuyuna Range, Minn. Mr. Hunner is a member of AIME and has previously presented a paper before the AIME on Adirondack Magnetite. He enjoys sailing, fishing, hunting and trap shooting. . . . **H. A. Byrns** (p. 474); born in Cleveland, Ohio, attended high school in Lakewood, Ohio, received degree of B.S. in Mech. Eng. from Case Institute of Technology. Worked for a time for American Steel & Wire Co., National Tube Co., Lorain, Ohio as Assistant. Blast Furnace Superintendent, becoming Asst. General Superintnedent Steel Works of the Duluth Works, and General Superintendent Furnaces & Coke Plant at Cleveland of American Steel & Wire Co., and currently General Superintendent of Woodward Iron Co., Alabama. Mr. Byrns lives in Birmingham, Ala., and has previously presented a paper before the AIME on Briquetting of Fine Ores. . . . **A. J. Macdonald** (p. 476); born in Superior, Wisc., attended Central high school there and University of Minnesota. His home is in Buffalo. Mr. Macdonald worked for Youngstown Sheet & Tube Co., Republic Steel Corp. and is at present with Hanna Furnace Corp. His chief recreation is golf. . . . **R. G. Knickerbocker** (p. 481); born in Napoleon, Ohio, attended Logansport, Ind. high school and graduated from the Missouri School of Mines and Metallurgy with B.Sc. and Metallurgical Engineering degree. Now lives in Rolla, Mo. Mr. Knickerbocker is a member of AIME and has presented many previous papers before AIME. . . . **L. M. Fulton** (p. 476E); born in Stewiacke, Nova Scotia, attended Syndey Academy and went to Dalhousie Col-

L. M. Fulton

C. W. Craighead

Journal of METALS

Published to provide a continuing, authoritative, and up-to-date record of technologic, engineering, and economic progress in all branches of the metals industry by the

Metals Branch

American Institute of Mining and Metallurgical Engineers, Inc.
29 West 39th Street, New York 18

* * *

T. W. LIPPERT
Manager of Publications
Editor, Journal of Metals

* * *

JAMES A. STANGARONE
Advertising Manager

* * *

WINIFRED D. GIFFORD, HAROLD N. UNDERHILL, ***Assistant Editors;*** **GRACE PUGSLEY,** ***Production Manager;*** **WALTER J. SEWING,** ***Assistant.***

* * *

OFFICERS, *AIME*

D. H. McLaughlin	*President*
A. B. Kinzel	*Vice President*
Philip Kraft	*Vice President*
R. W. Thomas	*Vice President*
C. H. Benedict	*Vice President*
D. H. McLaughlin	*Vice President*
Andrew Fletcher	*VP & Treasurer*

* * *

AIME STAFF

E. H. Robie	*Secretary*
H. A. Maloney	*Asst. Treasurer*
E. J. Kennedy, Jr.	*Asst. Secretary*
Ernest Kirkendall	*Asst. Secretary*
H. Newell Appleton	*Asst. to Secretary*

* * *

Technical Publications Comittee

E. C. Meagher	*Chairman*
E. J. Kennedy, Jr.	*Secretary*

* * *

Auxiliary Publications Committee

O. B. J. Fraser	*Chairman, IMD*
Michael Tenenbaum	*Chairman, ISD*
Philip T. Stroup	*Chairman, EMD*

* * *

Publications Advisory Committee
J. B. Austin, F. N. Rhines, C. D. King, John D. Sullivan, Fred P. Peters, A. W. Schlechten, Frank T. Sisco, M. Tenenbaum, Felix Wormser

* * *

The AIME Also Publishes
Mining Engineering
and
Journal of Petroleum Technology

IN THIS ISSUE

VOL. 188, NO. 3 MARCH, 1950

COVER

Sendzimir single-stand planetary hot mill, an exclusive first picture. This 7-in. mill is shown here continuously breaking down 3 pct. silicon steel from ⅞-in. thick bars to 0.095-in. hot-coiled strip in one pass at a delivery speed of 65 fpm. Five Selas furnaces heat the steel to rolling temperature. Very low investment and operating costs and small space and manpower requirements are factors certain to interest many mills in this radically different hot mill. A much wider unit, well over 20 in., is already on order for delivery to England.

FEATURES

Authors in This Issue 446
Engineering Employment Service 451
Journal of Metals REPORTER 452C
It's Everyone's Business 452D
Drift of Things 464

NEWS

AIME Annual Meeting Report 454
President D. H. McLaughlin 457
AIME Section Activities 459
Personals, Obituaries 460
New Members 462
Openhearth Meeting Program 466

TECHNICAL ARTICLES

Grain Boundary Migration in High-Purity A1 *Paul A. Beck, P. R. Sperry* 468A
Immersion Thermocouple *J. F. B. Jackson, D. G. Harris, S. G. Mravec* 468B
Operation, Portsmouth Sinter Plant *Guy B. Hunner* 471
Pig Machine Practice at Woodward *H. A. Bryns* 474
Pig Machine Practice at Hanna *A. J. Macdonald* 476
Ferroalloys in 1949 *R. G. Knickerbocker* 476B
Lessons, Hanging Blast Furnace *L. M. Fulton* 476E
Graphite Electrodes *H. G. MacPherson* 481

TRANSACTIONS

Titanium Binary Alloys 485
C. M. Craighead, O. W. Simmons, L. W. Eastwood
Ternary Alloys of Titanium 514
C. M. Craighead, O. W. Simmons, L. W. Eastwood
Quaternary Alloys of Titanium 539
C. M. Craighead, O. W. Simmons, L. W. Eastwood
Diffusion Coefficients, Carbon in Austenite 553
Cyril Wells, Walter Batz, R. F. Mehl
Carbides in Long-Tempered Vanadium Steels 561
Walter Crafts, John L. Lamont
Internal Friction, Cold-Worked Metals at Various Temperatures 575
T'ing-Sui Ke
Recrystallization and Grain Growth by Measurements of Internal Friction 581
T'ing-Sui Ke
Kinetics of the Reactions, Columbium and Tantalum with O_2, N_2 and H_2 586
E. A. Gulbransen, K. F. Andrew
Graphical Representation of Metallurgical Equilibria 600
C. J. Osborn
Conditioning Dwight Lloyd Gases to Increase Bag Life 608
R. E. Shinkoskey
An Improved Automatic Smoke Sampler 610
J. J. Donoso

Published the first day of each month by the American Institute of Mining and Metallurgical Engineers, Inc., 29 West 39th Street, New York 18, N. Y. Telephone: PEnnsylvania 6-9220. Subscription $8 per year for non-AIME members in United States and North, South and Central America; $9, foreign; $6 for AIME members, or $4 in combination with a subscription to *Mining Engineerng* or the *Journal of Petroleum Technology*. Single copies, 75 cents; special issues, $1.50 . . . The AIME is not responsible for any statement made or opinion expressed in its publications. . . . Copyright 1949 by the American Institute of Mining and Metallurgical Engineers, Inc. . . . Registered cable address, AIME New York . . . Indexed in Engineering Index, Industrial Arts Index and Chemical Abstracts . . . Reentered as second-class matter Sept. 21, 1949, at the post office at New York, N. Y., under the Act of March 3, 1879.

Authors In This Issue

P. A. Beck (p. 468A): Born in Budapest, Hungary. Went to Budapest High School and attended Royal Hungarian University of the Technical Sciences and Michigan College of Mining and Technology with degrees of M.S. in Met., and Mechanical Engineering. Is a member of AIME and now lives at University of Notre Dame. He has worked for American Smelting & Refining Co. as research metallurgist, for the Beryllium Corp., as chief metallurgist, and Cleveland Graphite Bronze Co. as superintendent of Metallurgical Lab. His major activities besides writing technical papers are golf and swimming. . . .

J. F. B. Jackson

R. G. Knickerbocker

J. F. B. Jackson (p. 468B): born in Lancashire, England, and graduated from University of Manchester with B.Sc. in Met. degree. Became associated with David Brown & Sons, (Huddersfield) Ltd. as Research Metallurgist, then in succession Foundry Foreman, Technical Superintendent and Technical Controller (Foundries) with that organization. Is currently Director of Research, British Steel Founders' Association. Mr. Jackson is a member of AIME and lives in Sheffield, England. He is a stamp collector, and for relaxation he turns to fishing and golf. . . . **J. G. Mravec** (p. 468B); born in Czechoslovakia, attended high school in Rocky River, Ohio and graduated from Ohio State University with B.Ch.E. degree, Started with Timken Roller Bearing Co, Steel & Tube Div, as Research Assistant and later became Research Engineer, Blooming Mill Metallurgist, Tool Steel Metallurgist, Research Metallurgist and is at present Melt Shop Metallurgist. His home is in Canton, Ohio. Mr. Mravec has previously presented AIME papers on Effects of Refractories on Steel Cleanliness; Determination of Hydrogen in Molten Steel by the Gas-Tube Method. He enjoys traveling and is interested in photography as well as playing bridge. . . .**Guy B. Hunner** (p. 471); born in Eau Clair, Wis. Worked for a time as Superintendent of Menominee Range, Michigan; Superintendent of Clifton Mines, DeGrasse, N. Y.; District Supt. of Cuyuna Range, Minn. Mr. Hunner is a member of AIME and has previously presented a paper before the AIME on Adirondack Magnetite. He enjoys sailing, fishing, hunting and trap shooting. . . . **H. A. Byrns** (p. 474); born in Cleveland, Ohio, attended high school in Lakewood, Ohio, received degree of B.S. in Mech. Eng. from Case Institute of Technology. Worked for a time for American Steel & Wire Co., National Tube Co., Lorain, Ohio as Assistant. Blast Furnace Superintendent, becoming Asst. General Superintnedent Steel Works of the Duluth Works, and General Superintendent Furnaces & Coke Plant at Cleveland of American Steel & Wire Co., and currently General Superintendent of Woodward Iron Co., Alabama. Mr. Byrns lives in Birmingham, Ala., and has previously presented a paper before the AIME on Briquetting of Fine Ores. . . . **A. J. Macdonald** (p. 476); born in Superior, Wisc., attended Central high school there and University of Minnesota. His home is in Buffalo. Mr. Macdonald worked for Youngstown Sheet & Tube Co., Republic Steel Corp. and is at present with Hanna Furnace Corp. His chief recreation is golf. . . . **R. G. Knickerbocker** (p. 481); born in Napoleon, Ohio, attended Logansport, Ind. high school and graduated from the Missouri School of Mines and Metallurgy with B.Sc. and Metallurgical Engineering degree. Now lives in Rolla, Mo. Mr. Knickerbocker is a member of AIME and has presented many previous papers before AIME. . . . **L. M. Fulton** (p. 476E); born in Stewiacke, Nova Scotia, attended Syndey Academy and went to Dalhousie Col-

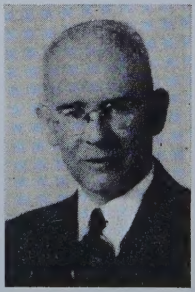
L. M. Fulton

C. W. Craighead

lege. Is a member of AIME, and lives in Sydney, N. S. Has worked for Dominion Steel & Coal Corp., formerly as Chemist, then Assistant Superintendent of Blast Furnace, and at present is Assistant General Superintendent. Mr. Fulton has no particular hobby but admits to membership in Office League of Bowling Champions. . . . **C. M. Craighead** (p. 485); born in Carlisle, Pa., went to Central high school, Harrisburg, Pa. and graduated from Penn State College with B.S. and M.S. degrees. Was Research Metallurgist at Aluminum Research Lab., later with Braeburn Alloy Steel in the same capacity; became Metallurgist for Reynolds Metals Co. and is at present with Battelle Memorial Institute. Mr. Simmons has previously presented AIME papers as co-author on Equilibrium Relations in Aluminum-Magnesium, Silicide Alloys Containing Excess Magnesium. Photography and photography are his chief pleasures. . . . **O. W. Simmons** (p. 485); born in Ilion, N. Y. he attended high school there and took degrees of B.S.-Chem.Eng. and M.S.-Met. Eng. from University of Michigan. His home is in Columbus, Ohio. He worked for Packard Motor Car. Co. as Heattreating Inspector, was Instructor in Metallurgical Eng., Rose Polytechnic Inst., Terre Haute, Ind., and at present is Research Engineer, Battelle Memorial Inst. During the war Mr. Simmons served as Lt.-Comdr. U. S. Navy as O-in-C of Ground Controlled Approach Radar Unit. His hobby is electronic gadgeteering and for relaxation turns to the open spaces for camping and hiking. . . . **L. W. Eastwood** (p. 485). See October 1949. . . . **Walter Crafts** (p. 561). See December 1949. . . . **John L. Lamont** (p. 561). See December 1949. . . . **E. A. Gulbransen** (p. 586). See October 1949. . . . **K. F. Andrew** (p. 586). See October 1949. . . . **C. J. Osborn** (p. 600); born in Melbourne, Australia and attended Wesley College there. He took degrees of B.-Met.E., and Ph.D. respectively from Melbourne University and Lehigh University. Was associated with the Steel Co. of Australia, Australian Council for Scientific &

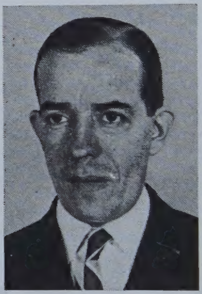

O. W. Simmons

Industrial Research, Lehigh Univ., Norwegian Inst. of Technology. Mr. Osborn is a member of AIME and makes his home in Melbourne. Hiking and skiing rate as his chief pleasures and photography is his hobby.

* A great quantity of long-awaited data on binary, ternary and quaternary alloys of titanium are presented by Craighead, Simmons and Eastwood, of Battelle, on pp. 485-552. Hundreds of alloys have been examined in detail as regards their physical properties. This work adds an entirely new chapter to the rapidly expanding metallurgical concept of titanium metal.

* Electron microscope studies of carbides in vanadium-chromium-molybdenum steels after tempering show that conditions encouraging formation of fine vanadium carbides improve high temperature strength. (p. 561).

* Hanging in blast furnaces is caused by the semi-rigid diaphragm of the fusion zone coming to rest on the top of the bosh either because of lack of preheating time or from amount of lime in the charge. (p. 476E) Hanging is minimized by lowering the bosh and designing for more preheating space.

* Whether Europe is faced with a steel surplus is still a matter of much debate. The secretariat of the ECE steel committee at Geneva several months ago issued a report totaling present and planned steel capacity at 70 million tons and estimating possible demand at 58 million tons. Some opinion is that possible consumption is somewhat higher.

None the less a buyers' market has already appeared even though Europe's steel needs are as yet far from satisfied. The main causes of this impasse are currency payment difficulties and import quotas. ECE is attempting to get import quotas relaxed but is meeting stiff resistance from high cost producers and from the British who want stability more than anything else.

Europe's traditional steel producers are also making extreme efforts to discourage upstart producers such as the Dutch, Greeks and Turks into abandoning their nationalistic plans for building additional steel capacity.

* Three to four billion dollars in the immediate years ahead will be required to maintain the steel industry's producing facilities, according to R. E. Zimmerman, vice-president of the U. S. Steel Corp. In addition to rebuilding the usual worn-out equipment, the money will be needed for developing new iron ore mines, treating taconite ores, beneficiating coking coal, handling industrial wastes to avoid stream and air pollution, and providing pensions and social benefits.

* Delivery of 78,000 tons of steel rails rolled in the German Ruhr to Communist Shanghai, has been stopped by the Allied High Commission. The British subsidiary of the American Trading Co., Commerce International Inc., originally placed the order for the Nationalist government and the contract subsequently was picked up by the communists. This same trading company has recently been shipping tanks and other war materiel to the Nationalists in Formosa.

* Government research is being conducted at Stevens Institute and elsewhere with the object of producing high density powder products for ultimate application to the jet propulsion and high temperature gas turbine projects for Army, Navy and Air Force."

* Carbon molds for pig-casting machines have shown great promise at Hanna Furnace Corp., Buffalo. However, they are difficult to adapt to machines already built for iron molds.

It's Everyone's Business

FEB. 17—The past month found the average citizen backed off just a little more into his blind corner staring glassily at hydrogen bombs, unbalanced budgets, John L. Lewis, more inflation, a rising wave of strikes, the country's only active battleship on a mudbank, a famous scientist in gaol as a traitor, a favorite actress on a Roman holiday, and rising mountains of potatoes, butter and eggs begging for destruction.

About the only bright spot has been industrial activity and employment, but even these are menaced by the coal shortage. Most industries have orders on hand or in prospect to warrant high operations for some time to come. The trend of the Reserve Board's production index is upward except as strikes may interfere. There has been heavy buying at the seasonal merchandise shows, particularly in furniture and household goods. The demand for goods of this kind illustrates greater confidence in the Spring outlook than was generally felt a year ago. Further, the demand also reflects improved market positions due to curtailment of output and reduction of inventories in 1949 and sustained consumer buying power. It demonstrates the strong support that is given directly to many businesses, and indirectly to all, by the phenomenal construction activity that is now under way. The Commerce Department places the number of new dwelling units started in 1949 at the new all-time high of 1,019,000.

Automobile output has been cut some 30,000 to 35,000 cars a week by the strike against Chrysler. An offer has been made to provide employees $100 a month total pension and old-age insurance benefits upon retirement, which conforms to the pattern set in the steel and other cases. However, the union is striving to break old patterns and set new ones and the strike's duration is unpredictable.

Steel producers are hard pressed to satisfy current demands. Among the base metals copper has held steadily at 18½¢ a lb; lead is unchanged at 12¢; zinc is steady at 9¾¢, and tin has slid off gradually to 74½¢ a lb. (See graph.) For the most part buyers of base metals are holding purchases to minimum requirements and this situation is likely to hold until the current strike wave moderates.

President Truman's budget for the fiscal year ending on June 30, 1951, much to the surprise of no one, showed the government again failing to balance its accounts even though peacetime prosperity has achieved heights which were hardly imagined until recently. A year ago the President estimated that the current year's deficit would be less than $900 million on what then seemed to be a rather shaky basis. But that deficit is now put at $5.5 billion. For the 1950-51 period the deficit estimate is only slightly lower—$5.1 billion—and if past experiences are any criteria the final figure will certainly be much larger. Even so, Mr. Truman obviously believes that the national economy is nicely balanced and that it should be possible to maintain stability and steady growth.

The 1951 budget (see graph) provides for an expenditure of $4.7 billion on foreign activities, $1.3 billion, or more than 20 pct less than is estimated for 1950. All segments of the European recovery program, including that portion of aid to western Germany which has previously been provided separately, will be more than $1 billion below the amounts provided for the same purposes in 1950. Only $35 million will be appropriated as the essential first step in the Fourth Point program for the development of backward areas.

With the cut in foreign items substantially greater than the decline in expenditure as a whole, the domestic items are allowed more in 1951 than in 1950. The difference is almost exactly accounted for by national defense expenditures which, including stockpiling and other ancillary items, are up, by $400 million, to $13.5 billion. Estimates for economic development have gone up, as has provision for welfare and social security while benefits to ex-servicemen are $825 million lower on the year.

In the prolonged coal dispute the underlying problem is always the over-expansion of the mines both in capital equipment and number of employees. Approximately two-thirds of the present industry, operated on a full-time basis, could supply all visible peacetime markets. With Mr. Lewis constantly dragging his feet as regards production, the supply problem would have boiled to a crisis much earlier except for the phenomenally mild winter, the steel strike, which eliminated one of the major sources of demand for coal and affected the requirements of related industries and, finally, the failure of the pension plan in its initial phase to reduce the number of miners as much as was expected.

BUDGET, 1951 FISCAL YEAR
IN BILLIONS OF DOLLARS

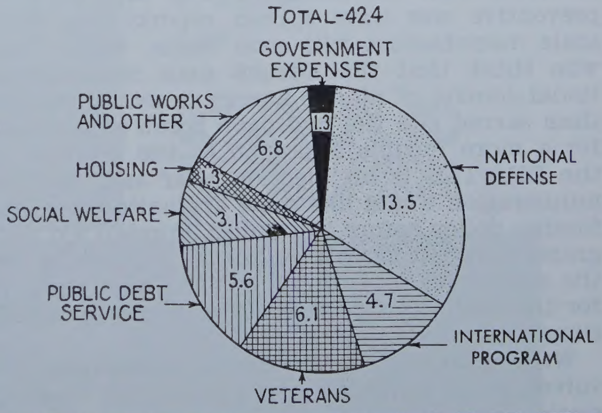

The first sign of movement out of the coal impasse came with the filing by Mr. Denham, general counsel of the NLR, of a request for a court injunction against UMW for refusing to bargain in good faith and attempting to coerce the operators through the three-day week into renewing an illegal contract. The request for this injunction—which is not to be confused with the general injunction prohibiting for 80 days a strike that creates a "national emergency"—went to court, but six days earlier Mr. Lewis outmaneuvered Mr. Denham by promptly accepting an offer of renewed negotiations from the operators, setting the very hour that Mr. Denham was scheduled to appear in court. The operators, however, postponed the meeting until after the court hearing.

The meetings sank beneath the quicksands of Mr. Lewis' usual histrionic mystery as regards specific demands and the operators' insistence on an unbreakable two-year contract and no increase in wages or pension levies. Mr. Truman then entered the arena with the proposal that all miners should return to a full working week for 70 days, while a fact-finding board investigated and drew up recommendations for an equitable settlement. Mr. Lewis' vitriolic reply to this proposal left Mr. Truman with no other recourse but to invoke the "Taft blackjack."

At this writing the miners still aren't digging coal and the next few days may see an injunction leveled at them. Even so, miners are a tough breed and the enforcement of the injunction will be an interesting operation to watch.

The hydrogen bomb, and all the attendant wide-eyed comment, came somewhat as a surprise to most scientists. It was the logical next step in the atomic arsenal. Its principle has been common knowledge for almost two decades awaiting only the atom bomb as a means of supplying the high temperature and pressure necessary to trigger the reaction. But while the next step forward did not surprise scientists, the action certainly was accompanied by a common feeling of revulsion. Atomic fission has at least the possibility of many beneficial peacetime byproducts. But the hydrogen version, atomic fusion, is purely a titanic instrument of destruction with no beneficial byproducts.

On the political front the hydrogen bomb has become primarily a device for scaring people into either a new arms race or a new attempt to come to terms with the Russians. The supporters of preventive war have spread reports that full-scale manufacture will soon begin, while those who think that the Baruch plan for international control of atomic energy is something less than sacred cite the hydrogen bomb as a reason for a more flexible approach to the problem in the UN. This is an election year and the Administration would like some dramatic success in foreign policy before November. Foreign aid programs have not the attraction they once had and the near defeat of the bill to aid Korea bodes ill for the forthcoming requests for money to further support European recovery.

With both the United States and Russia involved in a hydrogen bomb race, the state of world tension which has been normal for the past three years has been screwed up to almost an unbearable pitch. A new attempt to secure international control of atomic energy is certainly in the making. Mr. Churchill has spoken for another meeting with Mr. Stalin and President Truman, despite his denials, certainly is exploring a new attempt for agreement.

However, it is by no means certain that an agreement with the Soviet Union confined simply to the question of the atom bomb would either strengthen western defense or make the need for it less—the only two ways in which the risk of war could be reduced. In return for an American destruction of stockpiles and an undertaking not to continue with the hydrogen bomb, the Russians might agree to put into operation the system of international inspection and control of nationally produced atomc energy which is the maximum they have so far been prepared to concede. But would the risk of war be less even if the Russians made further advances and agreed to transfer some atomic activities to international ownership for an experimental period? On the contrary, the risk might be greater. Even a limited agreement with Russia might be taken as the signal for a slackening of vigilance and a weakening of the defensive effort all along the line. It is better that the cold war should continue until both sides are genuinely ready for a complete settlement than that any new scientific horror should lead to the disarming of one side and the consequent tempting of the other to commit aggression.

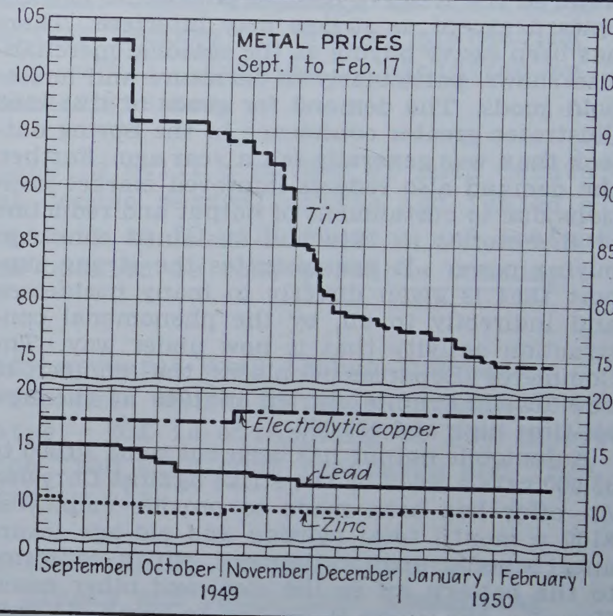

According to the London Economist, even if no friendlier emotion ever stirs the Soviet leaders, surely the possibilities of the hydrogen bomb are horrifying enough to create a comradeship of commun funk. It would certainly be a grave error to allow this or any other opportunity of approaching Russia to slip. The hydrogen bomb does appear to offer a new opening. It should be seized, not simply to discuss the bomb, but to examine once again whether there is any possibility of a general *detente* between the east and west. Such a settlement could not be confined to atomic agreement; it would be dangerous if it were. It should cover all the major issues of policy—spheres of influence, the peace treaties, general disarmament, the elimination of hostile and inflammatory propaganda—which exacerbate tension and distrust in the world today. Only in such a setting of general pacification can specific agreements and concessions make a real contribution to peace. An atomic convention embedded in a larger framework of cordiality and restored confidence would give the world new hope. Without the wider accord there is a risk that it would only weaken the western powers, confuse their defense, divide their will and thus actually increase the likelihood of future war.

AIME's 170TH GENERAL MEETING

Hotel Statler – New York – Feb. 12-16

Sunday morning, Feb. 12, long before many people were astir over three hundred Metals Branch men gathered in the Ball Room of the Statler Hotel, New York City, to get the annual meeting off to an excellent start with J. H. Hollomon's paper on the nature of structural changes during solidification of liquid metal. Practically all of the 300 men stayed through until after 10 p.m. to hear papers by R. F. Mehl and B. R. Queneau. On Monday, Tuesday, Wednesday, and Thursday, sessions started at 9 a.m. in an attempt to fit in all the papers scheduled. Everyone who could took out time Monday to hear General Eisenhower speak at the Welcoming Luncheon. Extractive metallurgists, Institute of Metals and Iron and Steel division men all met in the foyer to the Keystone Room at 6 p.m. Tuesday for cocktails and at 7 p.m. had dinner and heard Evan Just, of E&MJ, tell of his experiences with the ECA. Two more high spots in the busy week were the Institute of Metals Division lecture Wednesday and the Howe Memorial lecture Thursday. E. E. Schumacher based his IMD lecture on Metallurgy Behind the Decimal Point, pointing out the infinitesimal quantities of impurities that would affect the properties of an almost pure metal. Francis B. Foley discussed the factors affecting the deformation and rupture of metals at elevated temperatures. The Metals Branch was well represented among the 1400-odd who enjoyed sirloin, Bombe Statler, and the presentation of awards and medals at the banquet Wednesday. The Metals Branch can be proud of what it took to and got from the 1950 annual meeting.

The Council of Section Delegates met Saturday morning, Feb. 11, to discuss AIME activities and objectives, and to make recommendations. Here is (L to R) Cadwallader Evans, Jr., Pennsylvania Anthracite Section, President-elect D. H. McLaughlin and G. C. Weaver.

Over 300 IMD men were on hand to hear R. F. Mehl, of Carnegie Tech, explain crystal growth.

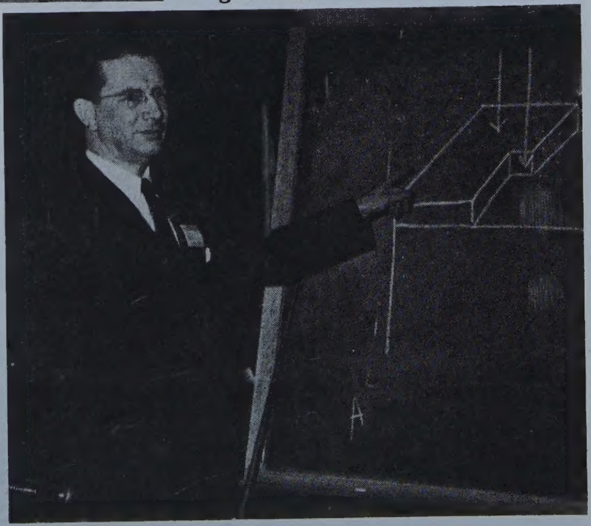

After the Board of Directors meeting on Sunday: (L to R) W. M. Peirce, Gail Moulton and Andrew Fletcher (V.P. and Treas.)

Registering for the Council of Section Delegates: (L to R) Roland D. Park, Section Delegate, with pen in hand; T. B. Counselman, Chairman of the New York Local Section; and James L. Head, AIME Director.

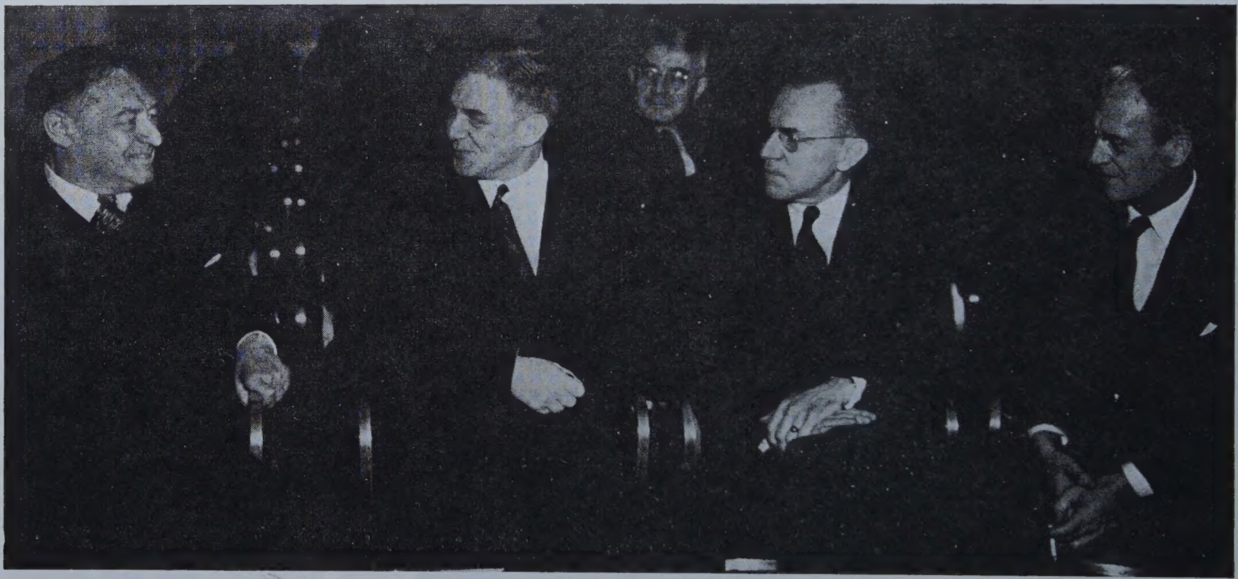

Five directors waiting for the all-day Sunday meeting to start; (L to R) Philip Kraft, A. B. Kinzel, W. M. Peirce, E. E. Schumacher and George P. Swift.

IMD's Symposium on Tube Production Practice; (L to R) T. F. McCormick, of Alcoa, speaking on Al-alloy tube production; W. M. Baldwin, Jr., and J. J. Rutherford, Associate Chairmen.

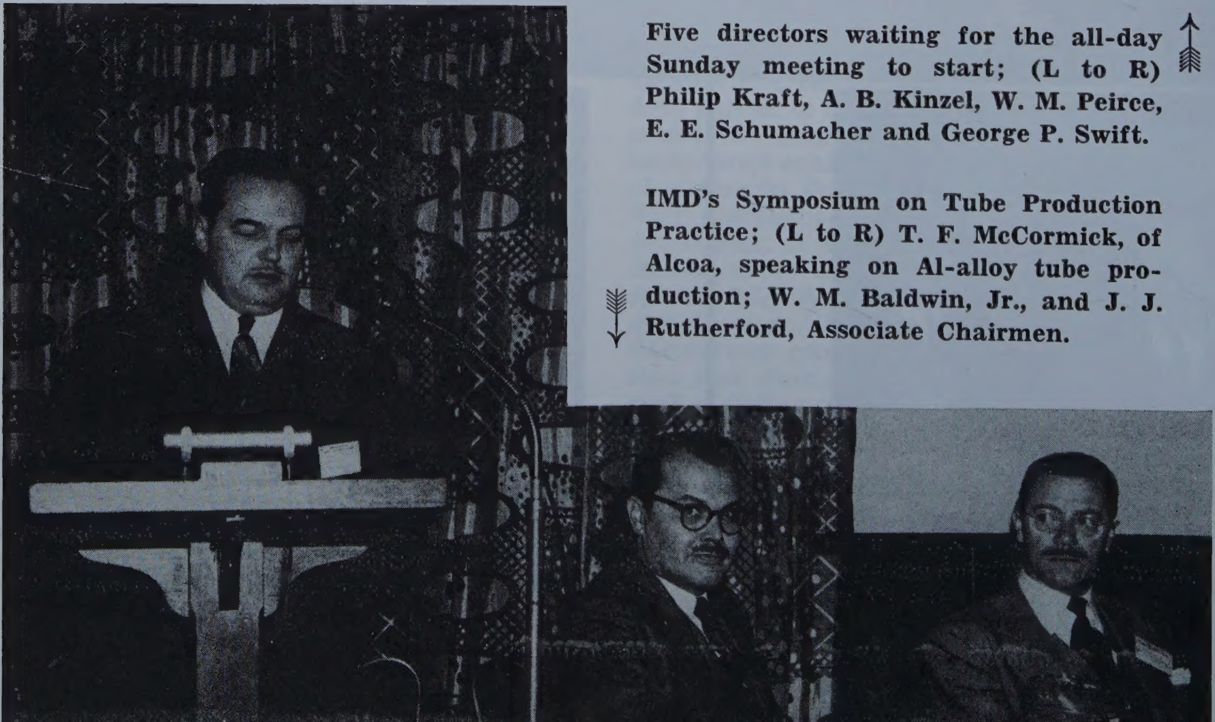

←

The Institute of Metals Division, Executive Committee, started their meeting with a luncheon on Tuesday and were still at it late in the evening. The most difficult problem to resolve was the publishing burden of an unprecedented number of first-rate technical papers.

There were no men busier than these three; (L to R) President-elect D. H. McLaughlin, President L. E. Young and Past-President W. E. Wrather.

**e 27th Howe Memorial Lec-
er; Francis B. Foley, of In-
national Nickel Co., pre-
ted his paper on Factors
ecting Deformation and
pture of Metals at Elevated
mperature.**

**e 29th Institute of Metals
ision lecturer was Earle E.
humacher, Chief Metal-
gist of Bell Telephone
boratories, Inc. His very
pular paper dealt with Met-
urgy Behind the Decimal
nt.**

Donald H. McLaughlin

AIME President

for 1950

To the mining man Homestake and Cerro de Pasco are as well known as Chevrolet and Ford are to the car industry; the mining man connects certain names with the history and development of these two companies as readily as the industry recalls the feats of the various models. One name closely associated with the more recent history of both mining companies is that of Donald Hamilton McLaughlin, who is President of the AIME for 1950.

It's a pretty well known fact that Dr. McLaughlin became head of the Cerro de Pasco Copper Corporation's geological department at an unusually youthful age—he hadn't completed his twenties. It's also common knowledge that Cerro de Pasco's geological department became one of the largest of any mining company, so he had a full time job supervising exploration and development programs of the corporation's extensive copper, silver, and coal deposits in various parts of Peru. As one of the first American engineers to do extensive work in South America, he ranks as a pioneer in a real Pan-American movement.

When he went to Harvard in 1925 as professor of mining engineering and geology, he became one of the youngest professors in the history of the university. (Some dates might help here—Dr. McLaughlin was born in San Francisco on Dec. 15, 1891, graduated from the University of California in 1914, received his doctor's degree in geology from Harvard in 1917, and from 1917 to 1919 was addressed as Lieutenant in the 63rd Infantry, U.S. Army; he went to Peru in 1920.) While at Harvard he became chairman of the Division of Geological Sciences and of the Department of Geology and Geography. In addition to his academic duties he maintained his interest in the field as a consultant, his principal client the Homestake Mining Co. This company was incorporated in California a good many years before Dr. McLaughlin put in his appearance there, but by the time he had acquired a consultant's background he was able to help solve certain geological problems at Homestake, of considerable value both in control of grade as well as in the development of additional reserves of ore. In 1945, after many years as consultant and a director, he became president of the company.

The lure of California called him in 1941 and back he went to become dean of the College of Engineering at his alma mater, the University of California. Big business claimed him two years later when he was made vice-president and director of Cerro de Pasco. Sandwiched in along the way, he has been chairman of the Advisory Committee on Raw Materials of the Atomic Energy Commission; chairman of the National Minerals Advisory Council; and a member of the task force on natural resources of the Hoover Commission. He is a director of the American Trust Co., the Empire Trust Co., the Bunker Hill & Sullivan Mining and Concentrating Co., The Dorr Co., the International Nickel Co. of Canada, San Luis Mining Co., and the Triumph Mining Co.

There has also been time for him to be chairman of the first AIME Committee on Geophysics and to have a hand in getting out the outstanding Geophysical Prospecting volume in 1929; he has served as chairman of the Mining Geology Committee and as a member of the Papers and Publications Committee, and was a member of the Committee on the Lindgren Volume. In 1947 he was a vice-president of the AIME.

Executive and Finance Committees Discuss Budget and Bylaw Changes

Matters discussed by the Executive and Finance Committees of the Institute at their meeting on Jan. 20, 1950 at Institute headquarters were largely of a routine or minor nature, the more important discussion being reserved for the Board meeting on Feb. 12.

A preliminary budget for 1950 was reviewed, indicating a small balance in the black expected for the year, following four years in which expenditures exceeded income by a substantial margin. A balanced budget will be attained chiefly through an expected increase of some $55,000 in dues receipts and some $58,000 in advertising.

The Committees voted to extend to Junior Members who have been on the rolls for ten consecutive years, and who applied for a change of status to Associate Member or Member before Dec. 31, 1949, the privilege of such change of status without the payment of an initiation fee. Previously the limiting date was that of *election* rather than of *application*. Similarly, it was voted that the privilege of election as a Junior Member be extended to those who *apply* for such membership before their thirtieth birthday, instead of to those who are *elected* before they are thirty years old. A change in the bylaw to make this ruling permanent was recommended to the Board, as stated in another column. It was felt that a young man had done his part if his application was made before the time limit expired, and that he should not be responsible for the time consumed in the election procedure.

Another change proposed in the bylaws, which is expected to be acted upon at the Board meeting in April if one is held, has to do with Affiliated Student Societies. It has been found impractical to enforce the distinction between Student Chapters, which are composed entirely of Student Associates, and other student societies composed of many students who are not Student Associates, so it is proposed in future to call all recognized student societies Student Chapters, only the officers of which would be required to be Student Associates. Another item of interest to students was the Committee's vote that all five of the national student prizes for the best papers be for $100. Heretofore one of the two graduate prizes was for $50. The Student prizewinners for 1949 are:

John A. Harrison, ($100) for his paper, "Progress in Mechanization in Underground Coal Mines", entered by the Chicago Section.

L. R. Kalman, ($50) for "Diffusion in Iron and Steel, a Literature Survey", also Chicago Section.

Everett O. Bracken, ($100) for "The Christensen Sillimanite Deposit Southeast of Dillon, Montana", Montana Section.

William H. Humphries, ($100) for "The Effect of Copper and Nickel Upon Rate of Sulphur Transfer", Pittsburgh Section.

Horace K. Thurber, ($100) for "Sodium Sulphate, a Possible New Utah Industry", Utah Section.

The Committee of Award was composed of Clark B. Carpenter, chairman, E. F. Schramm and William A. Staab. Entries were limited to prizewinning papers of the Local Sections that conducted contests.

A prize of $25 was authorized to be paid to Jason E. Everts, of Salt Lake City, for designing the best "key" to be made available to Student Associate members of Student Chapters.

The Committees recommended to the Board that the office of Controller be established, and that George I. Brigden, vice-president and treasurer of the St. Joseph Lead Co., be appointed.

Revised bylaws for the new Mining, Geology and Geophysics Division of the Institute were approved, subject to the approval of that Division.

Institute representatives on Engineers Joint Council for the coming year were named as follows: L. E. Young and Herbert G. Moulton, as "the most available past Presidents", with D. H. McLaughlin and Edward H. Robie, ex officio. It was noted that Dr. Young would be president of EJC for the coming year and Mr. Robie secretary.

Various AIME representatives were named as follows: Harvey S. Mudd reappointed to the Rocky Mountain Income Committee for three years. C. B. Sawyer to succeed C. H. Mathewson on the council of the American Association for the Advancement of Science. Paul Weir at the presentation of the Washington Award for $150 to Wilfred Sykes on Feb. 27. Scott Turner to succeed himself on the Hoover Medal Board of Award for six years.

Proposed Amendments to Bylaws

Notice is hereby given that at its meeting on Jan. 20, 1950, the Executive and Finance Committees voted to bring before the Board at its meeting next following that of Feb. 13 the following changes in the Bylaws:

Substitute for the second and third sentences of Article 1, Section V, the following: "He shall be not more than thirty years of age at the time of his application, and shall not remain a Junior Member beyond his thirty-third birthday."

The effect of the amendment is to make the date of application rather than the date of election the limiting factor in the election of Junior Members, who may thus be permitted to attain their thirtieth birthday between the time of application and the time of election.

An amendment is also proposed to eliminate the distinction between Student Chapters and other Affiliated Student Societies, all of which would hereafter be known as Student Chapters. The proposed amendment is as follows:

In Article XI, Section 4 of the Bylaws, replace the words "Affiliated Student Society" wherever they occur by the words "Student Chapter," the words "Student Society" by "Student Chapter," and the word "Society" by "Chapter." Further, delete the last paragraph of this Section reading "An Affiliated Student Society whose bylaws require all members to be Student Associates of the Institute may use the designation "Student Chapter of AIME."

SECTION ACTIVITIES

Connecticut Section

The Connecticut Section met on Dec. 14 with F. H. Wilson, of the American Brass Co., as the featured speaker. L. E. Thelin, Chairman of the section, opened the meeting by emphasizing the service which present members can give in suggesting eligible candidates for AIME membership. These candidates would then be approached by the section membership committee.

Dr. Wilson's presentation, Intergranular Parting of Brass During Anneals, was in effect a preview of the paper, of which E. W. Palmer is co-author, to be delivered at the annual meeting in February, and published in the December JM.

Cleveland Section

The 65 men who attended the December meeting of the Cleveland Section were treated to a surprise double billing. L. E. Young, President, AIME, came up from Pittsburgh to meet the members. Dr. Young can best be described as an elderly man with a stimulating personality and a youthful and active outlook on life. Knowing that the section consists for the most part of metallurgists, Dr. Young, who is a coal mining engineer and executive, confined his remarks to the more general aspects of his recent visits to other local sections and to England and Turkey. His visit was enthusiastically received; a return engagement is desired.

A. R. Troiano, of Case Institute of Technology, presented the technical lecture. There was no doubt of his enthusiasm and knowledge of his subject, Evaluation of Transformation Characteristics of Ferrous Alloys. The theory, along with all the latest available data, was presented on the quenching behavior of a few typical steels in thin and thick cross sections. Professor Troiano has supervised considerable research on the subject in recent years and included in this lecture many references to his own laboratory work and to his practical shop consulting experience.

Western Section, OHC

Even though it conflicted with the big football game of the year, UCLA vs. USC, the Western Section, OHC, at its Nov. 19 meeting, boasted 86 present at a well planned program designed to interest both the Open Hearth and the Electric Furnace Divisions, as well as members of the steel industry. Technical sessions were followed by a cocktail party and dinner at the Los Angeles Athletic Club. During the evening session, William A. Greene received a cash award from Don N. Watkins, publisher of *Blast Furnace and Steel Plant,* for the best paper presented during 1948. Hal Hibbard, vice-president and chief engineer of the Lockheed Aircraft Corp., was dinner speaker, his subject, Adventures in Space.

Rio de Janeiro Section

At the Dec. 7 meeting of the Rio de Janeiro Section Amaro Lanari, professor of the São Paulo Polytechnic School, gave a talk on the Aliperti Iron and Steel Corp. and its place in the São Paulo steel industry. The Aliperti corporation was founded in 1936 as a mill to manufacture steel strapping material. In 1941 an open hearth was installed and a second one added two years later. Since then the company has been the largest producer of steel in São Paulo, with 1949 production at 27,400 tons.

Economic conditions in the country since the war require a complete and radical reform of the plant and modifications of the methods employed with a larger scale of production. An integrated plant will be constructed in the city of São Paulo, based on the abundant supply of charcoal available there. The expansion program foresees a plant of 120,000 tons annually with two blast furnaces of 120 to 150 tons each, 4 open hearths of 50 tons each and 3 finishing rolls with diameters of 250, 350, and 450 mm. Expansion must be made in stages; the first has been completed, installation of the first blast furnace. Professor Lanari explained that technical improvements in plant practice have enabled management to maintain its past price level in the face of increasing labor costs. It is also realized that only by expansion and increased production can lower costs be obtained.

South Dakota School of Mines and Technology

America's urgent need for trained professional men in mining, metallurgy, and geology was the keynote of the Drill and Crucible Club banquet, South Dakota School of Mines and Technology, on Jan. 14. Celebrating its 30th year as a student chapter, the club is the oldest organization on campus. Arthur I. Johnson, consulting engineer of Keystone, S. Dak., who was one of the officers of the club when it was organized in 1920, spoke of the great need for mining, metallurgical, and geological engineers in this country, whose future welfare depends upon the proper development of mineral resources. Warren E. Wilson, president of the School of Mines, urged the men "to direct energies seriously to prepare for their profession." J. Paul Gries, of the geology department, announced cash prizes in the AIME national contest for papers dealing with aspects of mining development and processing. Dr. Gries, who is chairman of the Black Hills Section, AIME, pointed out that the club precedes its official parent by about 16 years. Guy V. Bennett, president of the club, as master of ceremonies, introduced the speakers.

University of Michigan

The first field trip of the University of Michigan Affiliated Student Society, which, for the convenience of the students and the King Seeley Corp., was divided into two groups, was to the company's Scio, Mich., plant, where students observed zinc die casting, electroplating, and electric timer assembly operations. The second meeting was a tour of the Kaiser-Frazer Corp. metallurgical lab. and included a discussion of operations by host Roger Mather, director. On Dec. 6, C. L. Raynor, chief metallurgist for the Hoskins Mfg. Co., spoke to the students on the electrical alloys produced by his company. Mr. Raynor, in his capacity as the society's industrial councillor, also commented on the advantages of AIME membership.

—Proposed for Membership—

Total AIME membership on Jan. 31, 1950, *was* 16,441; *in addition* 5010 *Student Associates were enrolled.*

ADMISSIONS COMMITTEE

E. C. Meagher, Chairman; Albert J. Phillips, Vice-Chairman; George B. Corless, T. B. Counselman, Ivan A. Given, Robert L. Hallett, Richard D. Mollison, and John Sherman.

Institute members are urged to review this list as soon as the issue is received and immediately to wire the Secretary's office, night message collect, if objection is offered to the admission of any applicant. Details of the objection should follow by air mail. The Institute desires to extend its privileges to every person to whom it can be of service but does not desire to admit persons unless they are qualified.

In the following list C/S means change of status; R, reinstatement; M, Member; J, Junior Member; AM, Associate Member; S, Student Associate.

Alabama

Lewisburg—Sides, Judson B. (M).
Russelville—Britton, Sam Abney, (R,C/S—JA-M).

Arizona

Morenci—Eckhouse, Robert Hermann. (C/S—S-J). Heyde, John Albert. (C/S—S-J). Moolick, Richard Terrence. (C/S—S-J).

Arkansas

Little Rock—Foxhall, Harold B. (M).

California

Bishop—Carpenter, Robert Dickerson. (C/S—J-M).
Burlingame—Shafer, William L. (M).
Long Beach—Wilson, James W. (M).
Los Angeles—Kohn, Arthur Frederic, Jr. (C/S—J-M). Morris, Joel Maurice. (C/S—S-J). Mott, Jack Sheridan. (J). Taves, Max John. (C/S—J-M).
Redondo Beach—Borkovich, George John. (C/S—S-J).
San Francisco—Hatton, Joseph Herbert. (R,C/S—J-M).
San Marino—Irwin, Emmett MacDonald. (M).
Whittier—Smith, Charles Edward. (C/S—J-M).

Colorado

Gilman—Maloit, Frank James. (R—M). Radabaugh, Robert Eugene. (M).
Golden—Aitkenhead, William Charlton. (R—M).
Hamilton—Cutler, William Gifford. (J).

Connecticut

Hartford—Kycia, Michael Anthony. (C/S—S-J).
Waterbury—Blank, Albert Irving. (C/S—J-M).
Westport—Batchelor, Mead Whitlock. (M).

Delaware

Wilmington—Poel, Harlan James. (M).

Florida

Mulberry—Barnett, Grady. (M). Fuller, Robert B. (M). Loehr, Henry Turner. (M). Tillotson, Irving Smith. (M).

Idaho

Boise—Pothier, Oscar Edward. (C/S—J-M).
Kellogg—Haffner, Robert Louis. (J).
Mullan—Hakala, Oiva Waldemar. (C/S—S-J).
North Pocatello—Spencer, Emmett Luther. (C/S—J-M).

Illinois

Centralia—Walker, Bobbie Philbrick. (J).
Chicago—Carney, Dennis Joseph. (C/S—S-J). Niotis, Demetrius John. (M). Robertson, William Donald. (C/S—J-M).
Highland Park—Robbins, F. Peter. (C/S—J-M).
Mt. Vernon—Brehm, Clarence Eckhart. (M).
St. Jacob—Swanbeck, Leonard William. (M).
Wilmette—Davis, Philip David, Jr. (J).

Kansas

Baxter Springs—Childress, Harold Lyle. (M). Landis, Miles Benjamin. (M).
Ellinwood—Lamar, James Riley. (J).
Lyons—Sawvel, Glenn Carl. (C/S—S-J).

Kentucky

Paintsville—Baker, John Augustus. (C/S—S-J).

Louisiana

Houma—Whitman, Harold Anthony, Jr. (C/S—S-J).
Lafayette—Greenley, Richard Edward. (C/S—S-AM).

Massachusetts

Cambridge—deBruyn, Philip Louis. (C/S—J-M). Paranjpe, Vijay Gopal. (C/S—S-J).
Gardner—Moline, Gordon Herbert. (C/S—S-J).
Hamilton—Rice, Charles G. (AM).
Hyde Park—Dunn, William J. (M).
Waltham—Shank, Maurice Edwin. (C/S—S-J).

Michigan

Crystal Falls—Royce, Josiah. (C/S—J-M).
Detroit—Chapman, Richard D. (C/S—J-M). Timmons, George A. (C/S—J-M).
Houghton—Spiroff, Kiril. (R—M).
Ishpeming—Beutner, Edward Louis. (M). Westwater, James Stuart. (C/S—J-M).

Minnesota

Brainerd—Knudsen, Louis. (M).
Duluth—Campbell, Robert Emerson. (J). Hagen, Robert Earl. (C/S—S-J).
Virginia—Manseau, Horace Francis, Jr. (M).

Missouri

Fulton—Reinkensmeyer, Norman William. (J).
Hannibal—Knopp, Charles Roger. (J).
Independence—Steinheider, Wilt Henry. (C/S—J-M).
Rolla—Kershner, Karl K. (M). Rosenbaum, Seymour. (C/S—S-J).
Webb City—Kirk, Whitson John. (M).

Montana

Anaconda—Finnegan, Walter Daniel. (C/S—S-J).
Butte—Mott, William Henry. (AM).

Nevada

Tungsten—McGuire, Philip C. (C/S—J-M).

New Jersey

Arlington—Perch, Michael. (C/S—J-M).
Bound Brook—Brigden, George I. (AM).
Elizabeth—Leslie, William Cairns. (C/S—S-J). Morton, Byron Benson. (M).
Rutherford—Nissley, Roy R. (AM).

New Mexico

Bayard—Eastman, Frank Erastus. (C/S—J-M).
Carlsbad—Barr, Richard Cromer. (J). Blanchard, John Guion. (M). Deviny, William Michael, Jr. (J).
Los Alamos—Wensch, Glen William. (C/S—S-AM).

New York

Bedford Hills—Franceschini, Victor William John. (C/S—J-AM).
Buffalo—Chestnut, Albert Heath. (C/S—J-AM). Jarvis, Herbert O. (M).
Chappaqua—Keith, Stanton Baker. (C/S—J-M).
Crestwood—Jemal, Emile Joseph. (M).
Delmar—Malmgren, Carl Eilertz, (C/S—J-M).
Huntington—Briggs, Fred, Jr. (M).
Kenmore—Kline, James Dickey. (M).
Larchmont—Henault, Emil August. (AM).
New York—Barker, Alexander, Crichlow. (AM). Dohm, Christian F. (M). Gervais, Arthur Joseph. (AM). Hoover, William Harold. (AM). Ingersoll, Vernon LaForge. (AM). Rosenbaum, Joseph. (AM).
Star Lake—Durocher, Roland Edward. (M).

North Dakota

Michigan—Jeffries, Robert L. (C/S—S-J).

Ohio

Cleveland Heights—Cox, Merrill. (M).
Columbus—Frost, Paul Davis. (C/S—J-M).
Elyria—Witte, Otto. (AM).

Oklahoma

Bartlesville—Smith, R. Vincent. (M).
Chickasha—Walker, N. Morgan. (R—M).
Duncan—Olson, Cleo Charles. (M).
Oklahoma City—Gogniat, Stephen. (M). Hegglund, Martin Oliver. (C/S—J-M). Johnson, Charles Teddy. (C/S—S-J). Patty, Duncan Victor. (R,C/S—S-J).
Tulsa—Garlington, Raymond Ellis, Jr. (J). Moore, Wesley Warren. (M). Pearson, Alvin Jerrold. (J). Renberg, Kenneth. (C/S—S-J).

Oregon

Corvallis—Hess, Harold DeWitt. (C/S—S-J). Watkins, Kenneth Oral. (R,C/S—J-M).

Pennsylvania

Evans City—Rape, Sylvester Herman, Jr. (C/S—S-J).
Johnstown—Howell, John P. (C/S—J-M).
Philadelphia—Bounds, Ardrey Middleton. (M).
Pittsburgh—Blood, William Wooster. (M). Giusti, Gino Paul. (J). Snouffer, Richard Dun. (C/S—J-M). Snyder, George M. (C/S—J-M). Wishowki, I. Stanley. (M).
Pottsville—Condit, Merlyn Edwin. (M). Quin, Robert Augustus. (J).
Spangler—Williams, Walter Dewey. (M).
State College—Hill, Robert Grant. (C/S—AM-M).
Temple—Eberly, Warren Samuel. (M).
York—Norris, Bertrand Saunders. (C/S—J-M).

South Carolina

Travelers Rest—Johnson, Henry S., Jr. (C/S—S-J).

Texas

Albany—Smith, Bertram Leon, Jr. (C/S—S-J).
Austin—Barber, Harry Curtis. (J).
Big Lake—Abbott, William Gordon. (J).
Bowie—Koontz, Roderick W. (R,C/S—S-J).
Calvert—McMillan, Frank Ney, Jr. (J)
Corpus Christi—Summers, Paul Howard. (J).
El Paso—Stillinger, Dudley Loomis. (J).
Ft. Worth—Athanas, Gus. (C/S—J-M). Elner, Ray. (C/S—AM-M). Morrison, Paul W. (M).
Houston—Bailey, Charles Woodrow. (M). Clegg, Millard F. (M). Holman, Russell Wesley. (C/S—J-M). O'Rourke, Thomas Floyd. (C/S—J-M). Pickles, William M., Jr. (M). Quinn, Julian William. (M). Shearer, Louis Hollis. (C/S—J-M). Sheets, Martin Meredith. (M). Sloan, J. Paul. (M).
Iraan—Brack, John Raymond. (C/S—S-J).
Levelland—Christner, Jimmie Drue. (J).
Lubbock—Johnston, Paul Shirley. (C/S—S-J). Livermore, George Pogue. (R,C/S—J-M).
Luling—Bilderback. Erwin Glen. (C/S—S-J).
Midland—McCaskill, Neal. (C/S—J-M). Priddy, Charles Horne. (J). Ramage, Bruce Granville. (M).
Odessa—Kendall, Ernest Clayton. (C/S—A-M-M). Lovelady, Isaac William. (M).
Pampa—Bauer, Roy Maurice, Jr. (C/S—S-J).
Silsbee—Williams, Walter Lazenby. (C/S—S-J).
Sundown—Hamann, Lloyd Arthur. (C/S—S-J). Powers, Walter Daniel. (R,C/S—J-M).

Utah

Bingham Canyon—Evans, Hugh Williams. (C/S—S-J). Norden, Joseph Alfred, Jr. (M).
Cedar City—Morgan, Ronald Charles. (C/S—S-J).
Lark—Brownson, Lloyd Daniel. (C/S—S-J).
Provo—Burgin, William Herman. (C/S—J-M).
Salt Lake City—Haley, Fred S. (C/S—J-AM). Kirkland, Archie Glover. (C/S—J-M).

Virginia

Arlington—Reifsnyder, Thomas B. (C/S—S-J).

Washington

Goldendale—Ellett, Richard D. (J).
Holden—Newman, Joseph Melvin. (C/S—J-M).
Metaline Falls—Scott, Marshall Wellington. (C/S—AM-M).

West Virginia

Charleston—Rees, Thomas B. (C/S—J-M).
Glenville—Young, Donald Bell. (C/S—J-M).
Montgomery—Mohtashami, Mansoor. (AM).
Wheeling—Boyd, John Thomas. (M).

Wisconsin

Madison—Tupas, Mateo Hernandez. (C/S—J-AM).

Wyoming

Rock Springs—Simon, Jack Thomas. (C/S—J-M).

Alaska

Nome—Jones, Daniel Amasa. (C/S—S-J).

Alberta

Lethbridge—Livingstone, Robert Donald. (M).

British Columbia

Chapman Camp—Ruffle, James Arthur. (C/S—J-M).

Manitoba

Flin Flon—Carr, John David. (M).

Ontario

Burlington—Warner, Kenneth Melville. (C/S—S-J).
Kirkland Lake—Hopper, Charles Houghton. (M).
Porcupine—Schmitt, Donald E. G. (C/S—J-M).
Toronto—Loree, Robert Jarrell. (C/S—S-J).

Quebec

Montreal—Walker, Walter Samuel. (C/S—J-M).
Noranda—Heino, Kauko Hendrick. (C/S—S-J).
Norrie—Lambert, Donald Platt. (C/S—J-M).

Vera Cruz

Coatzacoalcos—Fackler, William Corliss. (C/S—J-AM).

Guatemala

Coban A.V.—Tufts, John Marshall, Jr. (C/S—J-M).

Bolivia

La Paz—Salter, Russell. (R,C/S—J-M).
Pulacayo—Eck, John. (M).

Chile

Chuquicamata—Becker, Robert Charles. (R,C/S—J-M).
Potrerillos—Brinley, Edward Hermann. (C/S—S-AM).

Ecuador

Quito—Miller, Robert M. (C/S—S-J).

Venezuela

Maracaibo—Dominguez, Jose Rafael. (C/S—J-M).

France

Saint-Servan Ile et Vilaine—Marchal, Jacques Henri. (C/S—S-J).

Germany

Frankfurt a M.—Thieler, Erich Gustav. (R—M).

Italy

Torino—Debenedetti, Arturo. (M).

Norway

Oslo—Poulsen, Arthur Otterbeck. (M).
Trondheim—Smedsland, Tryggve. (C/S—S-J).

Sweden

Stockholm—Kuo, Ke-hsin. (J).

Northern Rhodesia

Luanshya—Smith, James Talbot. (C/S—S-J).

Union of South Africa

Johannesburg—Papenfus, Edward Bossau. (M).
Virginia—Muller, Thomas Frederik. (M).

Saudi Arabia

Abqaiq—Smith, Hugh Ferries. (C/S—J-AM).

Turkey

Karabuk—Ulubay, Ali. (C/S—S-M).

Japan

Tokyo—Nishiwaki, Tikawo. (M).

Australia

Melbourne, Victoria—Wiebenga, William Alexander. (C/S—J-AM).

Philippine Islands

Baguio—Fertig, Claude Edward. (M).

The Drift of Things

as followed by Edward H. Robie

Joe Alford Succeeds Bill Strang

Following the resignation of William H. Strang as executive secretary of the Petroleum Branch of the Institute, the problem immediately arose of securing a successor. Many were suggested for the job, but after the field had been carefully considered one name stood out as the most acceptable candidate—Joe B. Alford, who, since its founding, has been editor of the Journal of Petroleum Technology. His appointment was unanimously approved by both the outgoing and incoming boards of the Petroleum Branch. On general principles we are highly in favor of the promotion of editors to better jobs; specifically, we have every expectation that Joe will meet all his new responsibilities most acceptably. The worst angle to his appointment was that it left JPT without an editor but as this is being written we understand that that position is in a fair way to being filled.

Joe is a native Texan and was graduated from Texas Technological College at Lubbock with a degree in business administration, which training will perhaps stand him in better stead in many aspects of his new work than if he had chosen petroleum engineering. He entered the Army in 1940 and rose from the bottom, being commissioned in 1942 and released with the rank of Major in 1946. He then went to Stanford to get an M.A. in journalism, returning to Dallas in 1947 for a job in that field. His attractive wife, whom he married in 1942, will, incidentally, be no handicap to him in his new work. They have a two-year-old daughter.

Local Section Programs

Study groups, or discussion groups, to exchange opinions on subjects of specific professional interest have been most successful additions to the programs of some Local Sections, particularly in the Petroleum Branch. Those Local Sections that have not tried such meetings might well consider their possibilities.

One such group is being sponsored by the Gulf Coast Section of the Institute. A. G. Gueymard, Secretary-Treasurer, sends us the following brief description of its work: "At the present time we have established one discussion group, which is covering the subject of petroleum reservoir engineering. It is highly possible that other groups will be started in the future to study other phases of petroleum engineering. The present group meets once each month for a period of two to three hours. For each particular meeting a certain phase of reservoir engineering is set up for discussion, and one or more experts on this phase are available to conduct a discussion. Usually the speaker for the evening gives a general talk on the subject and then the floor is open for discussion by all concerned. The length of these meetings depends entirely upon the desires of the members present.

"The discussion group is particularly appealing to younger members of the AIME who are interested in gaining the knowledge and ideas of others on the subjects of their interests. We think the discussions are most beneficial and worthy of the amount of work necessary to keep the group going. The one drawback to this type of study group is that the discussion often becomes too elementary and detailed. Of course this undesirable situation must be prevented if possible by the directors of the group. The discussion group meeting is entirely separate from the regular monthly meeting of the Section; however, all AIME members are invited to attend."

Constant Turmoil

Writing items for this department that have anything to do with the news of the day has become increasingly difficult under the new publishing program, for what we have to say this sixth day of February will not be in the hands of some readers until the latter part of March. It seems fairly safe to say, however, that whenever this is printed a coal strike will either have just been settled, or one will be on, or one will be threatened, so a few remarks on the subject will not completely lack timeliness.

Undoubtedly John L. Lewis has done a lot to secure higher wage rates and shorter hours for the coal miners since he first began to take an interest in them. Also undoubtedly, conditions under which large numbers of them have had to live have been bad, their work hard and dangerous, and their comparatively high wage rates misleading, for most of them do not know what it is to have a steady job five or six days a week throughout the year. And yet, sympathize though we do with them, we do not think the methods used by Mr. Lewis for their betterment are having the results intended. Over the years the increased cost of producing coal has forced prices so high that a good share of the former market has been lost to oil and gas and even to hydroelectric power. Another factor that has influenced some consumers to turn to other fuels is the always present threat of supplies being cut off by a strike, a threat which rarely exists among producers of competitive fuels.

In fact, the market for coal has dwindled to such an extent that Mr. Lewis recently invoked the three-day week in an effort to prevent an undue accumulation of stocks. Now even at the high prevailing wage rates, miners cannot get along on the income from three days of work a week, and many of them have therefore been inclined to stay away from work entirely until a full week's work is available to them. Instead of doing something constructive to provide this work, Mr. Lewis continues to harp on ever-increasing wages, the present demand being for $15 a day instead of $14.05, and an increasing royalty to take care of their old age, which, if they had a good annual income, they should be able to provide for themselves out of earnings. It has been stated that it will take the average miner six to seven years at the 95¢ increase in the daily wage to reimburse him for the time he has lost on strike during the last year.

As the wage rate and royalty payments go up, so will the price of coal, which will result in less of it being used, which will mean less work for the miners, which will mean they will have to have higher wages for the time they *do* work, which is where we came in.

Now there is no particular point in talking about these things unless we have something constructive to suggest, so we hereby offer to the coal miners what we will modestly call the Robie Plan: Determine the average number of hours worked by the coal miners per year for, say, the last two years, and multiply this by the average wage rate, to get the average yearly earnings. Add a fixed amount, say 20%, to this total, and divide the sum by the number of hours that would be worked if the miners had the opportunity of working forty hours a week for fifty weeks in the year. This would give a new average at which the miners would go to work. It would be far below the wage they are getting now—when they get it—but they would have steady work and their annual earnings would be higher by the 20%. The cost of coal mining would drop considerably, and the price as well, so consumption should immediately begin to go up. It might take a little time for the market to absorb all that would be produced through a continuous forty-hour week, but the Government is so used to buying potatoes, and eggs, and fruit, and grain and other things that won't keep, that it shouldn't mind scattering a few stock piles of coal around the country. From cheap coal, gas and synthetic gasoline might be made, competitive with the products of the petroleum industry.

So there's the blue print. Those who know more about the coal industry than we do can work out the details.

Better Than the Atom Bomb

No sooner had the atom bomb, horrible as it was, become accepted in our minds as a possible back-to-the-wall resource in case of war than the hydrogen bomb suddenly appeared on the scene. This is supposed to be a thousand times as destructive as the A-bomb—just like a little chunk of the sun tossed on the earth, so we gather. Rightly, we think, it was decided that we should make it, but it will be quite another question as to whether we should ever use it. Certainly not use it first. And yet, if some one else uses it first, maybe we wouldn't be here to use it second. In any case, whether we have the H-bomb or just a passel of A-bombs, the prospect of war is now too horrible to ponder. Certainly some small percentage at least of what we are spending on military things should be spent on propaganda and methods of assuring peace. Armament races, throughout history, have led to war. It is a fond delusion that by making every effort to keep ahead of our competitors we can achieve "security"—a much overworked and misleading word.

It is heartening to see, therefore, in newspapers like The *New York Times* and the *New York Herald Tribune*, that columns of space are being given to proposals to secure world peace and disarmament. Senator Brien McMahon, the highest Congressional authority on atomic energy, made a thrilling speech on the subject in the Senate on Feb. 3. A month before, the House Foreign Affairs Committee unanimously voted to act on the world federation resolution HCR 64. Nineteen Senators, headed by Charles W. Tobey, are behind a resolution declaring it to be the sense of Congress that the United States should promote the strengthening of the United Nations and "seek its development into a world federation open to all nations with defined and limited powers adequate to preserve peace and prevent aggression through the enactment, interpretation, and enforcement of world law."

At a hearing in Washington on Feb. 3 Senator Wayne Morse described world federation as a "practical step we can take now in our search for lasting peace." Senator Claude Pepper said "the United Nations, through a world federation of nations, must be given powers to prevent war; power to enact, interpret, and enforce law."

Since publication of "The Anatomy of Peace" a few years ago, on which we commented at some length in these columns at the time, several other books have developed the subject further, among the most recent ones being "Peace or Anarchy" by Cord Meyer Jr., and "The World Must Be Governed," by Vernon Nash. The several organizations promoting world peace finally united their activities in the United World Federalists, 7 E. 12th St., New York City 3, which for $1.50 a year publishes a monthly report of progress toward world federation entitled "World Government News." The idea has been spreading fast, and thousands of additional adherents have been stimulated by the prospect of the H-bomb. If a movement may be judged by the character of its enemies, it might be added that Soviet Russia, the Hearst Press, and the *Chicago Tribune* are violently opposed.

World federation and world law may not be the answer, but nothing so far advanced seems as promising. If we can spend fifteen billion dollars a year on armaments, certainly we can afford a billion or so to develop some more civilized and likely plan of securing our future happiness and prosperity than making the H-bomb.

Openhearth, Bessemer Men to Meet

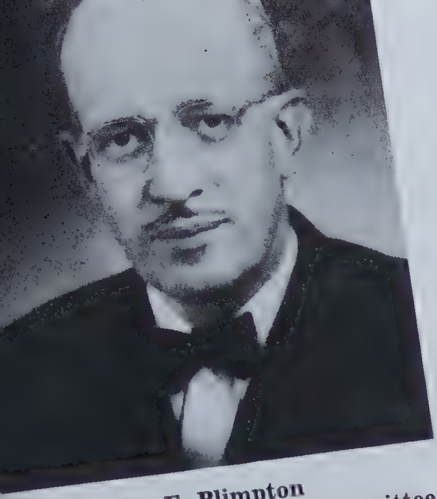
T. F. Plimpton
Chairman, Blast Furnace Committee

A particularly timely program on problems involved in producing more, better and cheaper steel is expected to attract a record gathering of steel operating men, repair and maintenance groups, metallurgists, ceramic and refractory engineers, observers and many others to the AIME Iron and Steel Division's Thirty-Third National Openhearth, Blast Furnace, Coke Oven and Raw Material Conference at the Netherland Plaza Hotel, Cincinnati, for the three days, April 10-12. While this will be the Thirty-Third Conference, it is actually the Silver Anniversary of the Conference, as some of the early meetings were held twice a year.

The local committee has made arrangements to reserve complete tables of ten. Such a table may be reserved by sending a check for eighty-five dollars ($85) to R. S. Bower, 1140 Cleveland Park Hills, Covington, Ky. The only tickets which are assigned to tables will be those that are reserved as complete tables through the local committee.

Plant Trip: Through the courtesy of the Armco Steel Corp., a plant trip has been arranged for Monday, April 10.

OPEN HEARTH GENERAL SESSION

Tuesday, April 11
9:00 a.m.—Hall of Mirrors

(1) Welcoming Remarks
By E. G. Hill, Director of Metallurgy and Development, Wheeling Steel Corp., Wheeling, W. Va., General Chairman, National Open Hearth Committee, AIME

(2) Announcements and Reports

(3) McKune Award Paper

Tuesday, April 11
10:00 a.m.-12:15 p.m.—Hall of Mirrors

BASIC OPENHEARTH OPERATING SESSION I

(Joint Session with Bessemer Committee)

Chairmen: G. B. McMeans, General Superintendent, Kaiser Steel Corp., Fontana, Calif.
D. R. Loughrey, Openhearth and Bessemer Superintendent, Jones & Laughlin Steel Corp., Pittsburgh.

(1) Progress Report on the Use of Oxygen
a For combustion
b For decarburization
c Economics
d Survey of various plants
Paper "Oxygen Production" by E. G. Hickling, Works Manager, Linde Air Products Co., New York.
Paper by Paul Nutting, Openhearth Practice Foreman, Inland Steel Co., E. Chicago.
Paper by A. E. Reinhard, Superintendent Steel Production, Great Lakes Steel Corp., Detroit, on use of oxygen jets in back wall.

(2) Oxygen in the Bessemer Converter

Tuesday, April 11
2:00-5:00 p.m.—Hall of Mirrors

BASIC OPENHEARTH OPERATING SESSION II

Chairmen: C. F. Henzelman, Openhearth Superintendent, Bethlehem Steel Co., Johnstown, Pa.
H. E. Warren, Jr., Division Superintendent, Openhearth Department, Carnegie-Illinois Steel Corp., Munhall, Pa.

(3) Faster Charging Practice
Paper by Vernon W. Jones, Openhearth Superintendent, Armco Steel Corp., Middletown, Ohio.

(4) Stool Stickers
Short Papers by: Jones & Laughlin Steel Corp., Pittsburgh and C. G. McCabe, Openhearth Met. Foreman, Wheeling Steel Corp., Steubenville, Ohio.

(5) New Mold Coatings
Paper by Harold Walker, Republic Steel Corp., Warren, Ohio. (movies to be included)
Paper by J. J. Golden, Superintendent, Steel Production and Central Mills, Carnegie-Illinois Steel Corp., Gary, Ind.

(6) A Method of Nozzle Setting
Paper by A. W. Thornton, Division Superintendent of Blast Furnaces, Openhearth, Bessemer and Rolling Mills, National Tube Co., McKeesport, Pa.

(7) Effect of Changes in Roof Design and Elevation on Furnace Roof Life
Paper by R. P. Carpenter, Openhearth Superintendent, Republic Steel Corp., Cleveland, Ohio.

(8) Use of Refractory Throwing Guns for Maintaining Open Hearth Furnace

Tuesday, April 11
10:00 a.m.-12:15 p.m.—North Hall

ACID OPENHEARTH OPERATIONS

Chairmen: T. D. Collins, Open Hearth Supt., Mackintosh-Hemphill Co., Midland, Pa.
E. E. Callinan, Open Hearth Supt., Standard Steel Works Div., The Baldwin Locomotive Works, Burnham, Pa.

(1) Practical Interpretation of Steel Making
Paper by C. F. Christopher, Metallurgical Engineer, Continental Foundry & Machine Co., East Chicago.

(2) Petrographic Study of Acid Slag
Paper from American Locomotive Co., Latrobe, Pa.

ANNUAL FELLOWSHIP DINNER

Tuesday, April 11
6:00 p.m.—South Hall
Reception and cocktail party for dinner guests
7:00 p.m.—Hall of Mirrors
Annual Fellowship Dinner
Toastmaster: R. L. Bowron, General Superintendent, Tennessee Coal, Iron & R.R. Co., Bessemer, Ala.
Speaker: W. W. Sebald, President, Armco Steel Corp., Middletown, Ohio

Tuesday, April 11
2:00-5:00 p.m.—North Hall

COLD METAL PRACTICE AND BASIC FOUNDRY

Chairmen: H. M. Parker, Openhearth Superintendent, Armco Steel Corp., Butler, Pa.
R. C. Solomon, Openhearth Superintendent, Granite City Steel Co., Granite City, Ill.

(1) Substitutes for Pig Iron
a Natural gas coke

and Blast Furnace
at Cincinnati

Paper by G. S. Baldwin, Assistant to Division vice-president, Standard Steel Works Division, Burnham, Pa.

Paper by Clyde Jenni, Metallurgist, General Steel Castings Corp., Eddystone, Pa.

b Economics and effect on production

Paper from R. C. Solomon, Openhearth Superintendent, Granite City Steel Co., Granite City, Ill.

(2) **Charging Practice and its Effect on Production**

Paper by William Schwinn, Keystone Steel & Wire Co., Peoria, Ill.

(3) **Quality of Raw Materials and their Effect on Production**

Physical and chemical properties of burned lime and spar.

Paper by Gordon McMillan, Metallurgist, General Steel Castings Corp., Eddystone, Pa.

(4) **Cupolas**

Paper by R. L. Baldwin, Chief Chemist, Stanley Works, Bridgeport, Conn.

(5) **Oxygen for Carbon Reduction and Temperature Pick Up**

Paper by E. H. Reyer, Openhearth Superintendent, Keystone Steel & Wire Co., Peoria, Ill.

(6) **Bath Temperature Control and its Effect on Quality of Steel Castings**

Paper by F. Von Gruenigen and W. D. Lawther, American Steel Foundries, Granite City, Ill.

Wednesday, April 12
9:30 a.m.-12:15 p.m.—Hall of Mirrors

BASIC OPENHEARTH QUALITY AND METALLURGY

Chairmen: F. M. Washburn, Assistant General Superintendent, Wisconsin Steel Works, Chicago.
C. R. Taylor, Supervising Metallurgist, Armco Steel Corp., Middletown, Ohio.

(1) **Effect of Analysis**

a Paper, "The Effect of Hydrogen on the Mechanical Properties of Steel", by N. J. Grant, Associate Professor of Process Metallurgy, Massachusetts Institute of Technology, Cambridge, Mass.

b Paper, "The Effect of Aluminum Content on the Internal Quality of a Killed Steel", by Oscar Pearson, Chief Metallurgist and Inspector, Carnegie-Illinois Steel Corp., Gary, Ind.

c Paper, "Use of Vanadium for Non-Aging Rimmed Steels", by Samuel Epstein, Research and Development Department, Bethlehem Steel Co., Bethlehem, Pa.

(2) **Oxidation in Tapping and Ladle Filling**

Paper by T. E. Brower, Associate Physical Chemist, U. S. Steel Corp. of Delaware, Pittsburgh, J. W. Bain and B. M. Larsen, Supervisor of Process Metallurgical Research, U. S. Steel Corp., Kearny, N. J. (High-speed movies of turbulent flow in water and steel streams included)

(3) **Furnace Practice**

a Paper, "Bath Temperature Measurements and Control", by J. A. Creighton, Steel Division Superintendent, Bethlehem Steel Co., Lackawanna, N. Y.

b Paper, "Conservation of Manganese", by Shadburn Marshall, Research Associate, Carnegie-Illinois Steel Corp., Pittsburgh.

Wednesday, April 12
9:30 a.m.—12:15 p.m.—Pavillon Caprice

BASIC OPENHEARTH REFRACTORIES, MASONRY

Chairmen: L. L. Wells, Ceramic Engineer, South Works, Carnegie-Illinois Steel Corp., Chicago
E. R. Westfall, Superintendent Masonry Dept., Armco Steel Corp., Middletown, Ohio

E. G. Hill
Chairman, Openhearth Committee

(1) **Appraisal of European and American Basic Brick Roof Designs**

Paper by R. P. Heuer, V. P., and M. A. Fay, Ceramic Engineer, General Refractories Co., Philadelphia

(2) **Progress Report on All-Basic Furnace**

Paper by M. F. Yarotsky, Division Superintendent of Steel Production, Carnegie-Illinois Steel Corp., Chicago

Paper by A. K. Moore, Openhearth Superintendent, Steel Co. of Canada, Ltd., Hamilton, Ont., Canada

(3) **Comparison of Burned and Unburned Brick in Basic Ends**

Paper by E. R. Westfall, Superintendent Masonry Dept., Armco Steel Corp., Middletown, Ohio

Paper by R. J. Solomon, Openhearth Superintendent, Granite City Steel Co., Granite City, Ill.

(4) **Mixer Linings**

a Progress reports on special refractories

b Methods of estimating mixer lining thickness

Paper by Floyd College, Masonry Superintendent, Carnegie-Illinois Steel Corp., Munhall, Pa.

(5) **Performance of 96 Pct Magnesia Ramming Mixes**

Paper by A. F. Franz, Executive Vice-President, Colorado Fuel & Iron Corp., Pueblo, Colo.

(6) **Performance of Carbonaceous Ladle Refractories**

Paper by E. B. Snyder, Refractories Engineer, Wheeling Steel Corp., Steubenville, Ohio

Paper by Great Lakes Steel Corp.

(7) **Super-Duty Silica Roof Brick**

Wednesday, April 12
2:00-5:00 p.m.—Hall of Mirrors

BASIC OPENHEARTH FUELS AND COMBUSTION

Chairman: J. Morris Brashear, Assistant Superintendent, No. 2 Openhearth, Inland Steel Co., E. Chicago
J. L. Miller, Combustion Engineer, Republic Steel Corp., Cleveland

(1) **Flow and Velocities of Air and Waste Gases**

20-min lead-off paper by H. V. Flagg, Combustion Engineer, Armco Steel Corp., Middletown, Ohio

(2) **The Relation of Heat Size, Infiltration, and Checker Design to Fuel Consumption**

Paper by A. J. Fisher, Assistant Chief Engineer of Construction, Bethlehem Steel Co., Sparrows Point, Md.

(3) **Optimum Firing Rates (At Various Stages and Also Expressed Per Foot of Furnace Length)**

Paper by G. C. Primm, Superintendent of Fuel Utilization, Carnegie-Illinois Steel Corp., South Works, Chicago

(4) **Present Status of Multiple Burners**

Paper by Laurin Woodworth, Carnegie-Illinois Steel Corp., Youngstown, Ohio

(5) **Methods of Training Openhearth Personnel in Use of Fuels**

Paper by Barney Dagan, Openhearth Superintendent, Kaiser Steel Corp., Fontana, Calif.

BLAST FURNACE, COKE OVEN AND RAW MATERIALS CONFERENCE

Tuesday, April 11
9:30 a.m.-12:15 p.m.—Pavillon Caprice

ORE AND AGGLOMERATES SESSION

Chairmen: H. A. Strain, Director of Raw Materials, Fuel and Power, Carnegie-Illinois Steel Corp., Pittsburgh
L. P. Barrett, Vice-President, Jones & Laughlin Ore Co., Interstate Iron Co., Pittsburgh

(1) **An Appraisal of the Iron Ore Resources of the World—An American Estimate**
Preprinted paper by J. W. Gruner, Professor of Geology and Minerology, University of Minnesota, Minneapolis

(2) **Fundamental Factors Influencing the Strength of Green and Burned Pellets Made from Fine Magnetile Ore Concentrates**
Paper by M. Tigerschiold, Director of Research, and P. E. Ilmoni, Research Fellow, Jernkontoret, Stockholm, Sweden

(3) **Pelletizing of Iron-Bearing Fines by Extrusion**
Paper by P. E. Cavanagh, Assistant Director, Department of Engineering and Metallurgy, Ontario Research Foundation, Toronto, Ont., Canada

Tuesday, April 11
2:00-5:00 p.m.—Pavillon Caprice

BLAST FURNACE AUXILIARIES SESSION

Chairmen: C. E. Hoffman, Superintendent of Blast Furnaces, Bethlehem Steel Co., Sparrows Point, Md.
O. E. Clark, General Superintendent, Hamilton Plant, Armco Steel Corp., Hamilton, Ohio

(1) **Fine Gas Cleaners**
Preprinted paper "Application of Superimposed Precipitators", by R. E. Touzalin, Service Engineer, Arthur G. McKee & Co., Cleveland, Ohio
Paper by G. P. Burks, Division Superintendent of Blast Furnaces, Carnegie-Illinois Steel Corp., Gary, Ind.
Preprinted paper, "Gas Washer Developments", by Harry Johnson, General Superintendent of Central Furnaces and Coke Works, American Steel & Wire Co., Cleveland
Paper by Owen Rice, Metallurgical Engineer, Freyn Engineering Co., Chicago

(2) **Pig Machine Practice**
Preprinted paper, "Pig Machine Practice at The Hanna Furnace Corp.", by A. J. Macdonald, Assistant Manager, Hanna Furnace Corp., Buffalo
Paper by R. P. Wheatley, Superintendent of Blast Furnaces, Wisconsin Steel Works, Chicago
Paper, "Pig Casting Machine Practice at the Woodward Iron Co.", by H. A. Byrns, General Superintendent, Woodward Iron Co., Woodward, Ala.
Paper by J. M. Stapleton, Division Superintendent of Blast Furnaces, Carnegie-Illinois Steel Corp., Chicago

Tuesday, April 11
2:00-5:00 p.m.—Rooms A, B, C, & D

COAL AND COKE SESSION

Chairmen: L. P. Kraemer, Operations Engineer, Koppers Co., Inc.
H. V. Lauer, Field Supervisor, Raw Materials, Fuel and Power Division, Carnegie-Illinois Steel Corp., Chicago

(1) **Best Methods of Handling Coal to Reduce Oxidation**
Paper by P. J. Conners, Engineering and Construction Division, Koppers Co., Inc.

(2) **Coke Button Testing and the Agglutinating Value of Coal**
Paper by R. C. Weed, Chief Metallurgist, American Steel & Wire Co., Duluth, Minn.

(3) **Maintenance of Coke Ovens During Shut Downs**
Paper by F. L. McIntire, Superintendent Coke Plant, Jones & Laughlin Steel Corp., Pittsburgh
Paper by H. A. Hager, Assistant Superintendent of Coke Plant, Inland Steel Co., East Chicago
Paper by E. W. Steinweg, Superintendent of Coke Plant, Youngstown Sheet & Tube Co., East Chicago
Paper by G. A. Fort, Superintendent of Coke Plants, Carnegie-Illinois Steel Corp., Gary, Ind.
Paper by James McIntosh, Division Superintendent of Coke Plants, Carnegie-Illinois Steel Corp., Clairton, Pa.
Paper by A. H. Parthum, Assistant superintendent of Campbell Coke Plant, Youngstown Sheet & Tube Co., Campbell, Ohio

Wednesday, April 12
9:30 a.m.-12:15 p.m.—North Hall

GENERAL SESSION

Chairmen: D. P. Cromwell, Assistant Manager of Blast Furnaces and Coke Ovens, Ford Motor Co., Dearborn, Mich.
C. G. Hogberg, U. S. Steel Corp., Pittsburgh

(1) **Present Methods of Grading and Grouping Ores**
Paper by N. H. Thomas, Chief Ore Grader, Pickands-Mather Co., Ironwood, Mich.

(2) **Ore and Coal Bridge Maintenance**
Paper by Stanley Suplick, Chief Inspector, Bridge Operators' Engineering and Inspection Bureau

(3) **Blowing Out Carbon-Hearth Furnaces**
Paper by C. P. Johnson, General Superintendent, Interlake Iron Corp., Chicago
Paper by H. F. Dobscha, Assistant District Manager, Republic Steel Corp., Cleveland
Preprinted paper by G. D. Sells, Blast Furnace Superintendent, Pittsburgh Steel Co., Monessen, Pa.
Paper by H. P. Saxer, Superintendent of Blast Furnaces, Jones & Laughlin Steel Corp., Pittsburgh
Paper by W. F. Zehner, Assistant Superintendent of Blast Furnaces, Bethlehem Steel Co., Bethlehem, Pa.

Wednesday, April 12
9:30 a.m.-12:15 p.m.—South Hall

SINTER SESSION

Chairmen: K. C. McCutcheon, Assistant to Vice-President, Armco Steel Corp., Ashland, Ky.
Samuel Naismith, Evaluation Engineer, Oliver Iron Mining Co., Duluth, Minn.

(1) **Beneficiation of Adirondack Magnetites**
Paper by W. R. Webb, General Superintendent, and R. G. Fleck, Plant Superintendent, Jones & Laughlin Ore Co., Star Lake, N. Y.

(2) **Operating Practices at the Portsmouth Sintering Plant**
Preprinted paper by G. B. Hunner, District Superintendent, Hanna Iron Ore Co., Crosby, Minn.

(3) **Swedish Sintering Practice**
Paper by A. W. Robinson, John Mohr & Sons

Wednesday, April 12
2:00-5:00 p.m.—Pavillon Caprice

OPERATING SESSION

Chairmen: T. L. Joseph, Assistant Dean, School of Mines and Metallurgy, University of Minnesota, Minneapolis
Fordyce Coburn, Vice President, E. & G. Brooke Iron Co., Birdsboro, Pa.

(1) **Use of Adirondack Sinter in Blast Furnaces**
Preprinted paper by E. H. Riddle, Superintendent of Blast Furnace Department, Jones & Laughlin Steel Corp., Aliquippa, Pa.

(2) **Lessons from a Hanging Blast Furnace**
Preprinted paper by L. M. Fulton, Assistant General Superintendent, Dominion Steel & Coal Corp., Ltd., Sydney, N. S., Canada

(3) **Conditions of Outstanding Furnace Operation**
Paper by Kurt Neustaetter, Furnace Engineer, Inland Steel Co., East Chicago

Two Types of Grain Boundary Migration in High-Purity Aluminum

by Paul A. Beck and Philip R. Sperry

A TECHNIQUE has been recently developed[1] for studying grain-boundary migration in aluminum and for ascertaining the **direction** of the migration. Successive positions of the grain boundaries are indicated by etch markings at the specimen surface. The latest set of boundaries are identified by the difference in color between the areas on the two sides of each boundary. Each color area corresponds to a certain lattice orientation. Electrolytic etching is used to form a thin oxide layer on the specimen surface. The crystal orientation of the oxide is related to that of the aluminum grain on which it formed. The optical anisotropy of the aluminum oxide gives rise to the color effects with polarized light.

Paul A. Beck is acting head, Depart. of Metallurgy, University of Notre Dame, and Philip R. Sperry is metallographer at the University of Notre Dame. This work was supported by the office of Naval Research, U. S. Navy, Contract No: N6 ori-165, T.O. 1.

This means of studying grain boundary migration allows clear distinction between the two types of grain boundary migration occurring in high purity aluminum. Fig. 1 shows two sets of grain boundaries resulting from continued annealing at 600°C of material which is essentially strain free, having been previously annealed at that temperature. Observing the direction of migration at the specimen surface, it is noted that almost all boundaries are moving in a direction **toward their centers of curvature.** The driving force of grain boundary migration in essentially strain-free aluminum is the surface energy associated with the grain boundaries. The observed direction of movement is in conformity with that expected with this type of grain boundary migration according to the investigations of Harker and Parker,[2] C. S. Smith,[3] and J. E. Burke.[4]

Fig. 2 shows successive grain boundary positions of migrating boundaries in a specimen of high purity aluminum annealed for four successive periods at 500°C after a rolling reduction of 7.5 pct. In this instance, where the driving force of the boundary movements is the strain energy stored in the deformed grains, the direction of the boundary migration is opposite to that required by surface energy considerations: the boundaries move **away from their centers of curvature.** The surface energy which has to be supplied in order that this type of grain boundary migration may proceed, is provided by the strain-energy gained when the deformed grains are gradually replaced by strain-free grains.

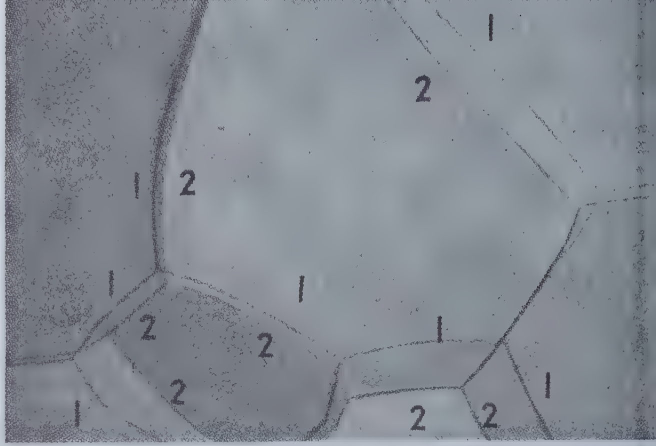

Fig. 1—In grain growth, boundary surfaces migrate toward their centers of curvature. Boundaries in high purity aluminum, after annealing 2 min. at 600°C (1), and after an additional anneal of 30 sec at 600°C (2). Magnification 75X.

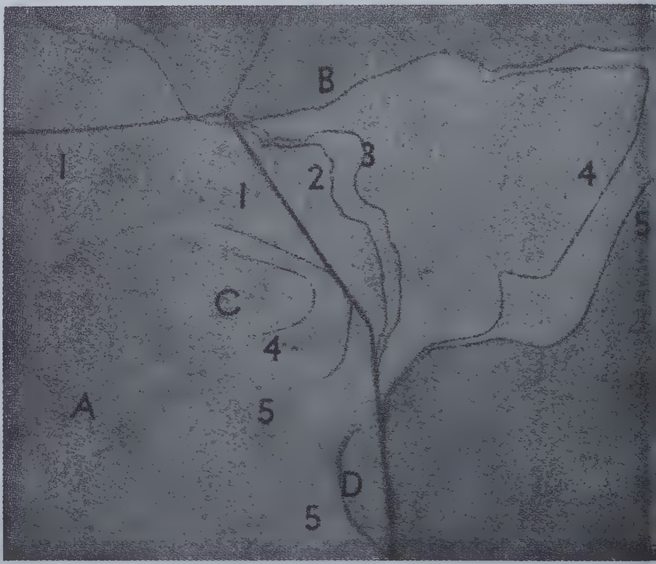

Fig. 2—In recrystallization (grains C, D and E) boundary surfaces migrate away from their centers of curvature. Strain induced growth of grain A at the expense of grain B. High purity aluminum annealed 90 min at 600°C, rolled 7.5 pct [heavily outlined straight boundaries (1)], annealed successively 5 sec (2), 5 sec (3), 15 sec (4) and 7 sec (5) at 500° C. Magnification 75X.

The sharp distinction possible between the two types of grain boundary migration discussed justifies the continuation of the familiar differentiation between surface tension induced boundary migration or grain growth, and strain induced boundary migration or recrystallization. A somewhat more detailed description of the latter process is given in a recent publication.[5]

References

[1] Philip R. Sperry: Method for Studying Grain Boundary Migration in Aluminum. Trans. AIME, (1950) **188**, 103.

[2] D. Harker and E. R. Parker: Grain Shape and Grain Growth, Trans. ASM, (1945) **34**, 156.

[3] C. S. Smith: Grains, Phases, and Interfaces. Trans. AIME (1948) **175**, 15.

[4] J. E. Burke: Some Factors Affecting the Rate of Grain Growth in Metals. Trans. AIME (1949) **180**, 73.

[5] Paul A. Beck and Philip R. Sperry: Strain Induced Grain Boundary Migration in High Purity Aluminum. Jnl. of Applied Physics, (1950) **21**, February issue.

The Immersion Thermocouple

Steel bath temperature control by means of the immersion thermocouple is showing considerable promise in production plants. Here are reports from three users, as presented before the Electric Furnace Steel Committee, Iron and Steel Div., AIME, at Pittsburgh, Dec. 8-10.

APPROXIMATELY 70 pct of British steel castings are produced in foundries employing quick immersion thermocouple technique for liquid steel temperature control, according to J. F. B. Jackson, Technical Controller, David Brown & Sons, Ltd., Huddersfield, England. This fact has been revealed in a survey of steel foundry practice made by the British Steel Founders' Association during August of 1949.

An independent assessment, based upon the overall consumption of silica dipping tubes (protective thermocouple sheaths) shows that in excess of ½ million temperature measurements are made in the United Kingdom each year. On the average this means that one immersion temperature reading is made for every 30 tons of steel melted in Britain today.

In addition to the figures quoted in relation to the steel foundry industry, it is reasonable to assume that in the case of wrought steel products the major portion of alloy steel output and a considerable part of carbon steel production in the U.K. is melted under immersion thermocouple pyrometric control.

While it is known to the author that at least one large American producer of wrought steel products applies the immersion thermocouple technique extensively as a routine control no figures are immediately available relating to steel foundry applications in the U.S.A. upon which a quantitative comparison can be based. Following a recent visit, however, to a number of the leading steel foundries in America it would appear that the use of radiation or optical methods, i.e. the disappearing filament pyrometer in particular, is very much the rule and that immersion pyrometry is the exception.

This difference in practice in temperature measurement and control in the steel foundries of the two countries, while to some extent relatively unimportant insofar as satisfactory measurements are in general obtained by both procedures, inevitably gives rise to the question as to the rational application of the two techniques. That the so-called "quick immersion" method should have established itself so widely in Britain over the last 10 yrs (and recently to some extent also on the Continent) and yet be still a comparatively rare procedure in the U.S.A. is a point which surely demands examination. Has the immersion thermocouple method been oversold in Britain, the country of its origin, or alternatively, has it not yet received the recognition in the U.S.A. which it perhaps deserves.

Since the original publications by Schofield and Grace in 1937[1] and 1939[2] on the subject of immersion thermocouple pyrometry as applied to liquid steel there have been numerous references to the technique both in the British[3] and American[4] scientific press and it is not proposed to include any lengthy description of apparatus on this occasion.

It is perhaps sufficient to say that the original cumbersome immersion apparatus probably required a trolley to convey the thermocouple equipment and usually required two operators, one to immerse the thermocouple and the other to take a potentiometric reading. This has evolved into a very simple one-man outfit which will give a temperature reading upon a large illuminated dial on the furnace stage and at the same time, if desired, a recorded reading upon a chart which may be either upon the furnace stage or in any chosen remote location such as in the melting shop manager's office or the laboratory.

---

[1] *F. H. Schofield, Seventh Report on the Heterogeneity of Steel Ingots (British), Iron & Steel Institute, 1937.*

[2] *F. H. Schofield and A. Grace, Eighth Report on the Heterogeneity of Steel Ingots (British), Iron & Steel Institute, 1939.*

[3] *D. A. Oliver and T. Land, Journal of Iron & Steel Institute (British), 1942 (1).*

[4] *D. Manterfield, The Iron Age, July 25, 1946.*

In principle the operation of the dial indicator and the chart recorder as generally used in British steel foundries and steel plant depends upon an electronic amplifying circuit which produces a dc current directly proportional to the applied thermocouple voltage.

It is present British practice to employ platinum-13 pct rhodium platinum thermocouples using wire of 0.5 mm diam. The hot junction is protected during immersion by a fused silica sheath, usually 125 mm long, 4.5 mm internal diam and 0.75 mm nominal wall thickness.

Compensating leads to offset cold junction temperature variations are used in all known instances.

No difficulty is normally experienced in penetrating basic electric furnace slags when making the thermocouple immersion in the bath, an operation which is assisted by the use of a graphite (old electrode) block at the junction of the silica sheath and the main tubular steel thermocouple housing. The function of the graphite block is of course primarily to protect the steel tubing but in taking openhearth and arc-furnace temperature readings it has the practical advantage of floating the equipment on the slag so that the couple projects into the liquid steel below.

Ladle temperature measurements usually require preliminary clearing of the slag to avoid fracture of the silica sheath.

For high-frequency furnace applications there are of course no problems of slag penetration and the whole thermocouple assembly is of very light construction, with no graphite end block and only 4 ft or so of overall length.

While during the early development stages of immersion pyrometry considerable trouble was taken in the calibration of the thermocouple itself, such measures are not normal practice in Britain at this present date, it being found that the inevitable wastage of thermocouple wire during the immersion process automatically causes the elimination of any contaminated or embrittled platinum or platinum alloy wire which would otherwise introduce inaccuracies in measurement.

It is also found in practice that if for any reason an unsatisfactory temperature indication should be given, the divergence from the true reading is usually so great as to leave no doubt in the mind of the operator that the reading he is getting is false.

While it is by no means the intention of this paper to champion the cause of immersion pyrometry, but rather to stimulate discussion which may lead to a true assessment of its importance in relation to other methods, it can from experience be said that upon the grounds of,

(a) simplicity in actual use,
(b) speed of temperature measurement,
(c) versatility as regards application, i.e. in ladle, in furnace bath, etc., and
(d) accuracy of reading,

the immersion thermocouple technique as it is at present known is either equal or—in the case of (d)—probably superior to radiation methods.

In the matter of cost, however, both as regards capital outlay on equipment and in operational charges, the advantages clearly lie with the optical instrument. In round figures and based upon the BSFA survey of British practice previously mentioned it is reasonable to assume that an immersion thermocouple temperature reading costs probably some 50¢ more that one taken with a disappearing-filament pyrometer.

Does this difference in cost of operation alone account for the comparative lack of application of immersion pyrometry in the steel foundries of America? Or is the disadvantage of cost plus a certain nuisance value entailed in preparing the thermocouple prior to use, responsible for its apparent unpopularity so far? Or is it that the immersion-thermocouple technique in its latest simplified form has not yet been amply demonstrated in the U.S.A.?

Perhaps the rational and balanced answer to these questions may be found in the suggestion that

(1) Insofar as production is concerned with small repetitive furnace melts of carbon and low alloy steels in which the cost of immersion pyrometry is relatively high per ton of steel and where optical pyrometry, applied according to a strict routine will give a comparable and adequate control, British steel foundries would be well advised to adhere to the optical method as generally practiced in America and to discard the immersion thermocouple practice.

while

(2) On the other hand the steel foundries of America might with advantage introduce immersion thermocouple pyrometry in the following instances in substitution for the optical method.
  a—In the production of high-alloy steel castings which have a high inherent value per ton and which also have emissivity characteristics which vary from standard, i.e. carbon and low-alloy steels.
  b—In the production of carbon and low-alloy steel castings which are made from large furnace heats where the cost of immersion pyrometry per ton is relatively low.

THE use of platinum immersion thermocouples for measuring molten steel temperatures in Central Alloy District plants of the Republic Steel Corp. was described by D. G. Harris of Republic's Research Department. The first immersion pyrometer for molten steel temperatures was used at the No. 1 Melt Shop in October of 1945. This complete assembly was given to Republic Steel by the British government. Melt Shop supervision immediately saw the advantages of the platinum couples and had their furnace helpers taking readings around the clock on 52100 types of steel in January of 1946, just three months later. It took only one year to organize a complete setup for the two electric furnace melt shops at Canton with over 85 pct of all heats tapped being followed for temperatures.

The first unit for openhearth temperature measurements was obtained in September 1946 and by April of 1947 all 15 openhearth furnaces in the two melt shops of this district had complete coverage.

The number of readings taken during the development of the present setup has led to 100 pct acceptance by the melt shops. There were 1830 readings in 1946, 32,218 readings in 1947 and over 70,000 readings in 1948. All readings are taken by the furnace men, with the repair and maintenance of the couples and instruments under the control of a thermocouple group under melt shop supervision.

During the development work on the platinum vs platinum—13 pct rhodium couple some unique ideas were developed and a patent application has been filed which has been leased to one of the instrument companies. Also a pilot light was developed and patented which has been a great aid to the melt shop crews in obtaining good readings. This instrument tells them that everything is OK before placing the couple into the furnace and then indicates that the couple is working satisfactorily. Many reductions in cost have occurred, such as a drop in protecting silica tubes from over $1 down to 20¢. Platinum wire is considerably cheaper at the present time. The reduction in cost of materials bought on the outside along with the design of couples has produced an economical couple to maintain in regular mill practice. The accuracy of the platinum couple cannot be approached. Couples off calibration are not found in melt shops. This has been checked many times and even platinum wire has been sent to a laboratory well qualified to test platinum couples and their report on the wire was excellent.

The greatest majority of trouble encountered with the platinum couples is the leadwire wire and couplings, the instruments, and the silica protecting tubes. The melt shops have set up tapping temperature ranges on all types of steel. These temperatures have been changed from time to time and in many instances they have been lowered and raised in a few cases. The setting up of tapping temperatures is a melt shop problem and has to be worked out for the various sizes of furnaces and melt shop conditions. However, there are characteristics, such as freezing ranges for the individual types of steel, that will remain the same regardless of the melt shops. These problems are being investigated and to date definite temperature patterns in the making of a heat of steel have been worked out for certain grades. This work is in progress and probably will continue for some time as there are so many factors that can affect the end product that one has a hard time setting up the definite temperature pattern.

The rewards for using the platinum couples have been large, but to show results in dollars and cents is a problem in itself. Mold life, furnace life, savings on fuel and quality of products such as cold heats and too hot heats are all in the right directions. We would be embarrassed if this instrument were not available.

IN **a final report** on the relative accuracy and cost of using immersion thermocouples for steel bath temperature control, by J. G. Mravec, Melt Shop Metallurgist, Steel and Tube Div., Timkin Roller Bearing Co., it was pointed out that the superiority of the immersion thermocouple over the optical pyrometer for bath temperature control is well established. Since May 1945, when immersion thermocouples were first used to measure electric furnace bath temperatures, a definite conviction has grown that the immersion thermocouple gives more accurate and dependable bath temperature readings than does the optical pyrometer. It is the greater accuracy of temperature measurement that enables the immersion thermocouple to be superior for bath temperature control.

Esteem for the immersion thermocouple is best revealed by the fact that the immersion thermocouple is being used for bath temperature control on all production heats, which consists of six basic electric furnaces and three basic openhearths. The electric furnaces range in size from 25 to 100 tons, while the openhearths are all 120-ton furnaces. When all furnaces are operating, the shop takes approximately 1600 thermocouple readings per month.

Correlation studies in the plant have shown that the application of the immersion thermocouples for bath temperature control has decreased the frequency of skulled and hot heats by approximately 60 pct.

The cost of using the immersion thermocouple, however, is considerably greater than that of the optical pyrometer. A cost study based on 3500 thermocouple readings showed that the material cost of the thermocouple is 75¢ per reading, while the cost of constructing, maintaining and checking of the thermocouples is equivalent to 0.62 man-hr or approximately 90¢ per reading. Total material and maintenance cost per reading is approximately $1.65, exclusive of overhead costs.

A minimum of two thermocouple readings per heat are taken—the average number is about three per heat. During a three-month period in which 85,000 net ingot tons of electric furnace steel were produced from our six electric furnaces, the cost of using immersion thermocouples for temperature control averaged 6.6¢ per net ingot ton.

Some heats for certain applications are poured into molds with carbon plugs in place of clay plugs as an extra precaution against entrapment of fireclay inclusions. Carbon plugs cost 56¢ each as against 12.6¢ per clay plug. Even though half of the carbon plugs may be used a second time, whereas clay plugs are used only once, the cost of using carbon plugs is 12.1¢ per net ingot ton as against 4.1¢ per net ingot ton for clay plugs. Hence, the use of carbon mold plugs in place of clay plugs increases the ingot cost by 8¢ per net ton. This is 1.4¢ per ton higher than the cost of using the immersion thermocouple for closer bath temperature control, which in our opinion is an extremely important factor affecting not only steel quality but also the life of various operating equipment. Unless a heat of steel is tapped and poured within its proper temperature range, its level of quality will be low regardless of what pouring pit practice is employed.

The comparison between the cost of using carbon mold plugs and immersion thermocouples has been presented for the purpose of illustrating that the relative cost of using immersion thermocouples for better temperature control is not so great as one might at first judge on the basis of $1.65 per reading.

Operating Practices

at the

Portsmouth Sinter Plant

by Guy B. Hunner

IN January 1945 the Hanna Ore Co. purchased the sinter plant and Evergreen Mine from the Evergreen Mines Co. Immediately following the purchase this operation was re-named the Portsmouth Mine. This is the only sintering operation located in the Lake Superior Iron Ore District at the present time. This report gives a description of the operating practices at this plant and, in a brief way, will cover some of the principal changes that were put in effect in order to increase the average daily sinter production from 1123 tons in 1945 to 1658 tons in 1949. A short history and description of the plant might first be in order.

It was erected in 1924 by the Minnesota Sintering Co., a subsidiary of the Evergreen Mining Co. The plant was designed to sinter Cuyuna Range iron and manganiferous ores with an objectionable furnace structure because of a large proportion of fines and a high moisture content.

Guy B. Hunner is the District Superintendent, Hanna Iron Ore Co., Crosby, Minn.

This is one of the papers to be presented before the Annual Blast Furnace, Coke Oven and Raw Material Conference, April 10-12, at Cincinnati.

As originally erected it consisted of a Dwight-Lloyd machine, 42 in. by 64 ft. It was equipped with 11-in. side boards and had a theoretical capacity of 500 tons per day. In 1929 a new 72 in. by 76 ft. machine was installed with 18-in. side boards and in 1930 this machine was lengthened to 127 ft. which are the dimensions of the present unit. This last change required the installation of a second fan and the wind-boxes were divided so that the fan on the feed end of the machine pulled through nine wind-boxes and the fan on the discharge end pulled through eleven wind-boxes. The fan on the feed end is a Buffalo Forge design with a capacity of 45,000 cu. ft. per min., or 5000 cu. ft. per min. per wind-box. The fan on the discharge end is of the same design with a capacity of 60,000 cu. ft. per min., or approximately 5000 cu. ft. per min. for the eleven wind-boxes which it originally served. It can readily be seen that this machine is operating on a very low volume of air. According to standard sintering practices on this type of ore each wind-box should have a volume of at least 9000 cu. ft. of air per min. This is somewhat overcome by the additional length of the machine as sintering is merely the function of time, to the volume of air that can be drawn through the sintering charge to burn the carbon.

A rather unusual feature of the plant is the wet dust collectors, one for each fan. These collectors are brick-lined chambers with floors sloping toward the center of the machine. The downcomers from the wind-boxes enter one side of the chamber near the top of the wall where sprays are located to precipitate the dust to the floor. Nozzles along the floor at the upper end of the chamber wash the precipitated dust out of the chamber and into a small de-watering rake where it is returned to the circuit.

The machine when acquired by Hanna was equipped with two ignition furnaces. One being of reverberatory type burning gas obtained by circulating air and 32-deg. gravity oil. This furnace was developed at the Evergreen plant for this particular service. The other furnace was designed for burning pulverized Pocahontas fines and was located ahead of the gas furnace over No. 1 and No. 2 wind-boxes. At least one hour was required to pre-heat this furnace and a like period of time to cool down.

The fine ore for sinter feed was stored in five 70-ton storage bins of wood construction with conical steel bottoms. Sinter fuel was stored in two bins of the same capacity and construction. These bins were located under the screening plant and each fed to a collector belt by means of table feeders driven by a flat belt from a line shaft. The screening plant was also of wood construction and although located adjacent to the discharge end of the sinter plant it was protected by a concrete fire wall.

In 1945, within a few days after the ore season had started, a disastrous fire of unknown origin swept through the screening plant and ore storage building and destroyed this unit for all practical purposes. The remains of the building were hastily dismantled and temporary conveyors were erected so that outside ores which needed no final preparation could be brought in and sintered in the plant which would otherwise have been idle.

Plans were immediately drawn for a new screening and crushing plant and auxiliary buildings necessary for the preparation of Portsmouth ores for either sintering or washing. These consisted of a primary crushing and screening plant in the pit for handling plus 4½-in. material and a 30-in. conveyor from the pit crusher to a direct loading pocket in the plant yards. The ore had previously been hauled from the shovels in the pit to a primary crusher at the plant in 20-ton end dump trucks. The conveyor belt is on 1750 ft. centers and has a total lift of 265 ft. At the direct-loading pocket the ore can either be loaded into railroad cars or by-passed to the secondary crushing and screening plant.

The secondary crushing and screening plant consists first of two 5 x 14-ft. single deck screens. For the separation of sinter-plant feed, screen cloths with a ⅝ x 5-in. opening are used and for the preparation of wash plant feed screens with 1½-in. sq. openings are used. The undersize from these screens is conveyed directly to the sinter plant storage bins or wash-ore storage bins as the case may be. The oversize is shuttled on a reversible belt to either a 36 x 40-in. Dixie hammer mill, or a 42 x 50-in. Jeffrey hammer mill. The Dixie mill is used as a standby unit. Past experience has demonstrated that the soft, high-moisture, Cuyuna Range ores can only be crushed to fine sizes in hammer mills. The 42 x 50-in. Jeffrey mill is of a special design for this service. It is equipped with 30-lb. hammers on a reversible rotor driven by a 400 hp motor. There are two sets of full revolving breaker plates on this unit which are driven independently and which are adjustable on the lower shaft to provide the opening required. Feed for the sinter plant is passed through on one side with ½-in. setting and the rotor is then reversed and feed for the wash plant is passed through the other side with a 2-in. opening. This reversible feature is also helpful in equalizing the wear on both faces of the hammers without having to remove them and reverse them during their life. The discharge from the 2-in. opening on the Jeffrey Mill is conveyed to the wash plant ore storage building together with the undersize from the 1½-in. sq. screens. The discharge from the ½-in. setting is conveyed to a re-screen with ⅝-in. slots from where the undersize is conveyed to the sinter plant storage bins and the oversize is carried to railroad cars and is shipped as a screened manganiferous product.

Located in the ore storage building are two 750-ton capacity steel cylindrical ore storage bins and two 125-ton fuel storage bins of the same design. Ore and fuel are fed to a collector belt by means of 8-ft diam table feeders under the ore bins and 6-ft diam table feeders under the fuel bins. The speed of the feeders is controlled collectively or individually by a variable speed unit with the controls located on the operating floor of the sinter plant. The fuel and ore on the collector belt pass under the hot returns bin where minus ¾-in. hot returns are added to the mixture on its way to the pug mill. Coke breeze is used as fuel.

The sinter plant was operated during the 1945 season without any major mechanical changes. Considerable thought was given to increasing the volume of air on the machine, but due to the unorthodox design no feasible arrangement could be worked out and it was thought that other mechanical changes might be made to partly offset the lack of air. Before the start of operations in 1946 the gas ignition and the coal ignition furnaces were removed and a Morgan-type oil-burning furnace was installed. Ni-Hard grizzly bars were placed under the discharge end of the machine where the sinter is spouted to the railroad cars. Eighty-pound railroad rails had previously been used for grizzly bars and these were constantly warping and breaking, causing frequent delays. The last two wind-boxes on the discharge end of the machine were blanked off. This increased the wind on the remaining nine from 5000 cu. ft. to approximately 6600 cu. ft. per min. These three mechanical changes resulted in decreasing mechanical delays from 2.93 pct of possible operating hours in 1945 to 2.51 pct in 1946 and also effected a saving of 0.10 gal. of fuel oil per ton of sinter produced for that season.

After watching the performance of the Morgan-type furnace in 1946 it was decided that some improvement could be made by a few simple changes. These consisted of placing two additional burners in the back of the furnace, facing down about 5½ deg. from the horizontal, and located 9 in. in from the edge of the pallet side board. These faced the direction of the travel of the bed. The rear of the furnace was elevated 14 in. higher than the front. Of a total of eight burners, four were used, two in the rear and the two in front. This arrangement gave complete ignition on the bed and considerably less arch trouble than had previously been experienced; it also cut ignition fuel consumption 0.14 gal. per ton of sinter over the previous season's experience with this same furnace.

Seal rails had been another source of trouble. As originally designed the machine was equipped with cold-rolled rails having a section 1 x 1½ in. These rails required replacement after two seasons' operation, or a maximum of 600,000 tons of production. Before the start of the 1947 season these rails were replaced with a scarifier steel rail having a section 1 x 1⅝ in. These rails with a greater abrasive resistance and a slightly wider wearing surface have produced over 800,000 tons of sinter to date without any appreciable signs of wear.

There are 153 cast-iron pallets with 18-in. side boards on the Portsmouth machine. Previous practice was to allow a 14-in. open space in the strand for the pallets to drop at the discharge end of the machine. As a consequence of this 14-in. opening or drop it was necessary to replace from 60 to 80 pallets during a season because of breakage or excessive corner wear. This opening has now been closed to 8 in. on the cold machine, or about 4 in. after expansion on the warm machine. Breaker bars were then installed at the discharge end to remove the sinter from the grates instead of removal by impact from the falling pallet. Two pallets were replaced during the 1949 season on account of breakage with practically no corner wear visible on those remaining.

As previously mentioned, the Portsmouth ores have a wet and sticky character. Because of this it was impossible to use a curved swinging spout which would cascade the feed onto the bed. In order to insure an even uninterrupted flow of feed the spout had to be straight and without baffles. Consequently the ore had practically an unbroken drop through the spout and onto the bed. This resulted in a heavy dense bed with very poor porosity under the ignition furnace. To correct this condition a mechanical "fluffer" was built and installed according to the design of "Monk" Morgan. As originally designed this so-called "fluffer" consisted of a 1 x 8-in. mild steel bar 7 ft. long located across the bed under the swinging spout. On the flat side of this bar were clamped two rows of ½ x 10-in. round manganese rods. These rods were spaced 2 in. apart horizontally across the bar and 5 in. apart vertically. The rods in the bottom row were staggered under the openings of the rods in the top row. The bar containing the rods was mounted on edge on springs at either end and vibrated with a syntron vibrator. This device had the effect more or less of a screen and broke the fall of the ore through the 1-in. spacing of the bars and thus fluffed the feed across the bed.

It also had a tendency to separate the larger size returns and cascade them onto the grates to provide a hearth layer. Some trouble was experienced in holding the rods in place on the bar and the operators objected to the constant noise of the vibrator. Experience had proven that the device had considerable merit and it was re-designed. The ½ x 10-in. manganese rods were welded to the 1 x 8-in. bar and extra units were made up and kept on hand for replacement. The bar, instead of being mounted on springs, was mounted on 2 x 4 x 7-in. rubber blocks on each end with another rubber block of the same size on top of the bar at each end to give it a floating action. The vibrator mounted at one end is made up of a housing with bearings at each end and an off-balance crankshaft with the driven sheave mounted on the crankshaft. This is driven by a 3 hp motor using a V-belt drive.

The re-designed "fluffer" was installed prior to the 1948 operating season. During that season 449 tons of sinter were produced per grate-bar change, while in 1947 there were 333 tons of sinter produced per grate-bar change. In 1949 this figure was increased to 729 tons. This is credited chiefly to a better hearth layer of sinter returns and lower sintering temperatures due to a more porous bed. Slotted grates with ¼ x 2¾-in. slots are used on this machine. Each pallet requires six grate bars.

As mentioned previously, coke breeze has been used as a sintering fuel. Prior to the fire in 1945 the Evergreen Mines Co. had been preparing their coke breeze in a rod mill, grinding the fuel to minus ⅛ in. The coke grinding plant was destroyed in the fire and it was necessary to call on suppliers for a prepared size fuel. This was furnished by head-of-the-lakes furnaces but the minimum sizes they could produce were minus 3/16 in. mesh. Comparison has shown that in spite of the larger size fuel the amount of breeze consumed per ton of sinter produced has remained constant and the grate bar cost per ton of sinter has been reduced each year. Portsmouth crude ore for sintering contains 17 pct moisture and this requires 12 pct fuel per ton of sinter produced.

During the 1949 operating season the average daily production of the Portsmouth sinter plant was 1658 tons. The maximum for the season occurred during the month of June when an average of 1810 tons per day were produced. In 1946 mechanical delays accounted for 2.51 pct of possible operating hours. As a result of the operating practices mentioned above this figure has gradually been reduced to 1.14 pct in 1949. It is felt that this reduction in lost time due to mechanical delays has accounted for most of the increased production and has put this plant on a par with most modern twelve-wind box machines today.

Pig-Casting Machine Practice at Woodward

• by H. A. Byrns •

WHEN the Woodward Iron Co. first started operations in the early 1880's, the pigs were cast in the then conventional cast-house sand beds. In 1907 a Ladd and Baker pig breaker was installed, and in 1918 a machine on the order of a large roller that was pulled the length of the cast-shed by the cast-house crane. The indentations made in the sand by this roller formed the runners and molds into which the iron was cast in the shape of pigs. Some time later, to continue the trend of modernization, chill plates were installed. Due to customers' insistence that smaller and cleaner pigs be supplied, a two-strand, 180-ft, Pittsburgh Coal Washer pig machine was installed in 1930.

The machine is located immediately adjacent to a railroad transfer through which there is easy access to seven different railroad lines for serving customers. This location is also close to a good-sized area of ground having topography that is suitable for stocking large tonnages of various grades of pig iron if necessary. At the same time the new machine was built a new 400,000-lb capacity railroad scale was constructed adjacent to the machine over which all pig iron is weighed.

The iron is delivered to the machine in Pollock 75-ton short-pour covered ladles by the hot-metal engine. The only duty of this engine and crew is to get the loaded ladles to the machine and the empty ladles back to the furnaces. The three furnaces are on a 6-hr casting schedule, which means a furnace is casting every 2 hrs. About 1600 gross tons of pig iron per day is the average, and this tonnage is handled with six hot-metal ladles on the run. Because of this transportation setup, and strict adherence to the casting schedule, it is possible to operate this seemingly few iron ladles without trouble or slack wind waiting for the furnaces to be spotted for cast. Due to the ladles being covered and being kept hot because of being constantly in use, a good ladle life and a minimum of scrap are obtained. Ladle linings will last regularly from 2½ to 3 yr, and will handle a minimum of 200,000 gross tons of iron before relining. Seldom are there ladle skulls. The linings consist of 3-4½ courses of brick on the bottom and 2-4½ courses on the side. After the ladle is bricked the sides and bottoms are covered 1½ in. thick with a mixture of 50 pct firebrick ganister and 50 pct stopping clay. This coating is mixed to a consistency that can be easily spread and applied with a trowel.

As is usual in merchant-iron practice, in casting, two ladles are filled at the same time to aid in obtaining uniform analysis. Also, in order to maintain quality, no kind of scrap is placed in

---

H. A. Byrns is General Superintendent, Woodward Iron Co., Woodward, Ala. This is a paper to be presented before the Annual Blast Furnace, Coke Oven and Raw Materials Conference, April 10-12, at Cincinnati.

runners or ladles to be melted by the iron, nor is coke dust thrown on top of the iron in the ladle.

The ladles are delivered to the machine within a very few minutes after finishing cast. They are dumped with a 75-ton Cleveland crane. The operator's cab, which was originally placed directly over the conveyors with the operator facing the ladle, was found to be impractical for Alabama summers, so was moved to the side of the conveyor, where a better view can be had of trough, ladle and molds as well as being away from the intense heat.

In the original construction the pig-machine runners were in the shape of a "Y" with a beveled lip that discharged the molten iron parallel to the mold. This has since been changed to a "T" shape with discharge lip at right-angle to the mold. This type of construction makes easier the equal division of the flow into the molds and considerably less shot-plate scrap is made. The pan collecting the scrap under the molds is dumped every other day. Total pig-machine scrap, including shot-plate scrap, scrap molds and scrap from ladle cleaning was just under 32 lb per gross ton of iron produced for the year 1949.

In the early operation of the machine, difficulties were encountered which caused the conveyors to hang up and break. The slow-speed coupling was redesigned to provide shear pins which were easily replaceable. The couplings were made split so as to allow for replacement without moving the gear reducer.

The discharge guides at the head end of the machine were originally manganese steel. These were changed to forged steel, hard surfaced. The chutes discharging into the car were originally manganese lined. These have since been changed to 100-lb rails with the base trimmed to the same width as the ball of the rail. These two changes have resulted in considerable less maintenance charges on the guides and chutes.

Also, the length of the runner was shortened 4 ft 6 in., or about 20 pct, to reduce scrap production. This was done by moving the tail sprockets as close as possible to the pouring stand.

Ladles are cleaned every other day by tilting them on a tilting stand set low enough that scrap and kish can be raked from floor level into a scrap cinder thimble. When full, the thimble is dumped into a hopper car, taken to the furnace trestle and dumped into scrap bins for recharging into furnace.

The brick in the ladle covers was originally held in place by steel angles. So much trouble was experienced with the steel angle burning and allowing the brick to drop out that a change was made to a cast-iron angle, which resulted in much longer cover life. Covers now will last two to three years. A cast-iron block is also used adjacent to the ladle lips to lock the brick in place. This change resulted in much less trouble with loose brick around the lips.

Pig-machine molds are cast in a foundry pit in a furnace cast house and are made from the grade of iron the furnace is producing at that time. The analysis of the iron on this particular furnace is from 2.00 to 3.25 silicon, sulphur about 0.030, phosphorus 0.72 to 0.83, and manganese 0.24 to 0.75. About 60 molds are changed per month, or approximately 800 tons per mold. Pigs weigh 35 to 40 lb each and the mold weighs about 250 lb, a ratio of approximately six to one. The mold coating is a mixture of 50 pct lime and 50 pct pulverized coal applied by means of an air spray. The specific gravity of the mold coating is closely controlled, depending on grade of iron being pigged. The range will vary from 1.10 for low-silicon iron to 1.02 for high-silicon iron and a "sticker" is rarely encountered.

For replacing worn sections of the conveyor, sections of chain with molds already attached are set up on the pouring platform. These sections are from 15 to 20 molds in length. When necessary to change out a section the worn section is cut loose by removing the wheel axles or pins, and the new section picked up with the crane and set in place. This change can be made in 10 min.

To warn operators in case an axle or pin on the conveyor starts to back out, a lever and electrical contact is set up adjacent to the conveyor track. If a pin backs out it will strike the lever, which in turn will actuate a Klaxon. The operator will immediately stop the machine and make the necessary repair.

The speed of travel of the conveyor is up to 50 fpm and is varied depending on the grade of iron being pigged—the low-silicon iron being poured at the higher rate of travel and the high-silicon iron being poured at the lower rate of speed necessary to produce a perfect surface pig. It has been found that speed of pouring and gravity of the mold wash are the main factors in pig surface appearance. Ordinarily a ladle of iron is poured in 35 to 40 min.

The pouring trough is lined with firebrick and clay, and has a built-in skimming dam. The trough usually lasts about 12 months.

The conveyor is made up of manganese links and wheels with hard-steel pins. As the wheels wear, the hub is drifted out and a hard-steel bushing is pressed in. In this way considerably more life is obtained from the wheels. The operating crew consists of iron pourer, troughman, limeman and laborer. On day turn there is a foreman, crane man and ladle skuller in addition to the regular pouring crew. This crew makes all minor repairs. Shop crews are called for major repairs only.

This machine is depended upon to handle the entire output of the plant. No other equipment is available. Being in such a position requires anticipating the unusual and making plans for any contingency that might arise in order to keep the wind on the furnaces at all times. To handle such contingencies, the big machine has two separate sources of water supply. It has an emergency gasoline-driven air compressor in case of failure of the main plant supply. Because of occasional plant power knockouts due to electrical storms the pig machine has duplicate motor generator sets with separate feeder circuits.

In spite of the fact that the machine is one of the most critical operating centers the pigging cost is less than 20¢ per gross ton of pig produced. Of this 20¢ per gross ton, approximately 11¢ is producing labor, 2½¢ is repair labor, and 2½¢ repair material.

Pig Machine Practice at Hanna

by A. J. Macdonald

HANNA FURNACE CORP., Buffalo, is a producer of merchant iron and thus the pig machine constitutes the finishing end of the plant. Every effort is made to produce a pig iron that customers will like.

There are three pig machines, Nos. 1 and 2 being identical, and each of the three is double-strand, gear-driven, and 140 ft 9 in. center-to-center of sprockets, horizontally. The molds are supported on 18 in. pitch chain links with wheels running on 70-lb rails. There are two molds on each link and 392 molds per strand. The average size of pig is 32 lb. The molds are made in the plant foundry, usually from about 2 pct silicon malleable iron. The pig-machine wheels are of tool steel which has been found to far outlast anything else. The first tool-steel wheels were installed 8 yr ago, and are still good for many more years. Each strand is driven by a 15 hp variable-speed motor. The speed of each strand can be regulated between 22 and 45 fpm. No. 3 machine was built and placed in operation in 1942. It is a double-strand, gear-driven, 155 ft 2 in. center-to-center of sprockets horizontally. On this machine there are 432 molds per strand, each strand driven by a 25 hp variable-speed motor. The speed of each strand may be regulated from 20 to 40 fpm.

Each pig machine has a conventional pouring box, runner and "T" runner to the strands. In the main runner two brick skimmers are placed before the dam. On each machine a ladle skimmer has been installed at the end of a structural steel beam of rugged design. This skimmer is counter-weighted and raised and lowered by a hand-operated winch, and a ladle can be tilted to the point where all the iron will run out and the kish still be held back. In the pig-machine building there are three overhead cranes, an Alliance single-hook crane of 75-tons capacity, with auxiliary 10-ton hoist, a Cleveland 80-ton crane with bale and ladle trunion hooks, also a 25-ton hook on a separate trolley, and a Morgan 30-ton single-hook crane with auxiliary 5-ton hoist and magnet control for handling scrap, clay boxes, etc. A stationary tilting hoist is installed at No. 3 pig machine for pouring iron on this strand.

Pig Knocker on the head end of the pig machine.

The ladles are the open-top, short-pour type, and are of 60 and 75 gross ton capacity. At the head end of each machine there is a pig knocker of very satisfactory and simple design. A shaft is installed over the end of the chain and rails hung from it at a position where they can swing against the mold at the time the pig should drop out. To make the rails swing against the mold, an arm extends toward the molds coming up over the head end of the machine and the side of the mold pushes the arm out, which in turn pushes the rails out and then releases them to fall against the mold as it starts to go under the sprocket. This simple arrangement is very satisfactory and requires no maintenance for long periods of time, and also practically eliminates stickers on an otherwise well kept pig machine.

For cooling the iron sprays are used, made from 27 in. sections of 6-in. pipe welded shut on the ends. A slot is cut lengthwise of the pipe and the water spills downward on the pig at very low pressure. The 6-in. pipe is fed by an 1¼-in. waterline. These sprays are installed as far up towards the head end of the big machine as is possible to put them.

In pouring iron of over 8 pct silicon it is necessary to air-cool the iron, so water sprays were installed on the underside of the molds on the ascending side at the upper end of the machine. These are just perforated pipe with water under pressure and do a very satisfactory job of cooling the molds when no water can be put on the iron. The thermal shock to pig molds as they go around the cycle on the pig machine is not inconsiderable, it being in the range of a 1000°F difference from low to high in 5-min time. This of course does not help mold life, and in the search for longer mold life many different irons have been tried, with additions of molybdenum, vanadium, etc., to the foundry ladle. But, as al-

---

A. J. Macdonald is with Hanna Furnace Corp., Buffalo. This is a paper to be presented before the Annual Blast Furnace, Coke Oven and Raw Materials Conference, April 10-12, at Cincinnati.

ready indicated, malleable iron, with the addition of a little steel scrap in the foundry ladle, has always been the final choice. A mold of uniform wall thickness has been found to be superior. Carbon molds have been tried, with eight molds installed together in one strand. They were used for two weeks and at the end of that time they showed no sign of wear or burning. The carbon molds have a future, but adapting them to a machine already built for iron molds would be very difficult.

Of extreme importance is control of the mold coating. A dead-burned dolomite and powdered coal are used in proportions of 75 pct dolomite and 25 pct coal by volume. The burned dolomite is shipped in container cars and is unloaded into a tank with a capacity of two car loads. Aerators have been installed to prevent the dolomite from sticking in the bin and the results are very satisfactory. At the bottom of the tank there is a screw conveyor leading to a hopper at the bottom of a bucket elevator, and also at the bottom of the elevator is another hopper where powdered coal is measured in. The bucket elevator discharges into a hopper over the slaking tank and between the hopper and slaking tank is a volume-measuring device to deliver the correct amount of material for each batch of mold coat. The coal is crushed and powdered in a ball mill in a separate room adjacent to the limehouse and brought to the elevator in a hand truck. The mold coat is prepared by first heating water in a slaking tank with a steam jet. The coating mixture is then put in the slaking tank, which has a capacity of 550 gal, and agitated with a motor-driven agitator for about 15 min, enough water added to bring the specific gravity to 1.12, and then the solution is pumped to the storage tank which has a capacity of 3000 gal and holds enough to last for 16 hr. In the storage tank is a motor-driven agitator keeping the mold coat stirred up, and from the storage tank the coating is continuously pumped to the three pig machines. The pumps are Aurora centrifugals driven by a 1 hp motor at a speed of 1750 rpm. They have a capacity of 20 to 50 gal per min at 40-ft head. To fill the tanks at the pig machines the operator only has to open a valve and close it when the tank is full. There is a return line from the machines to the storage tank so there can be no settling or precipitation of the lime in the pipes. One man on day turn only takes care of preparing the mold coat for three machines for 24 hr. The mold coat is aspirated into the molds with a steam jet from the tanks beneath the machines.

One other feature of the pig machine is the depressed track and pouring stand for treating high-sulphur iron. As the sulphur limit is 0.050 max, iron that is 0.047 or 0.048 sulphur is often treated so the cold iron will not be over 0.050. An empty ladle is put under the pouring stand on the depressed track and a full ladle poured into it over the stand.

At the head end of the pig machines there are three tracks for pig-iron cars, and a cable-car haul system between tracks. The car man operates the car-haul, with pushbutton control, from a bridge walkway that spans the tracks.

When a cast is finished at the furnace, the blower fills out a card showing ladle numbers and the time cast was finished, and any remarks such as instructions to hold the iron until sulphur is known. The conductor on the ladle engine gives this card to the pig-machine foreman when he delivers the iron. Delivery of hot metal to the pig machine comes first in the transportation department. All the information that has to be exchanged between furnaces, pig machine, and scales, is reduced to writing, as with four furnaces operating on different irons the chance of a mix-up in irons is very possible, and to put a ladle of iron that is outside the analysis on a pile of iron that perhaps has a thousand tons in it is a major calamity.

Because each furnace is usually on a different grade of iron it is necessary to have a separate set of ladles for each furnace. Ladle-lining life is well over 10,000 gross tons, and it is rare to lose more than the inner lining. Ladles are dumped and skulled every 12 hr when they are on the run.

Pouring temperatures on standard iron range from 2400° to 2600°F, mostly between 2500° and 2600°F. There are occasions when better looking iron will result if the temperature is allowed to go down a little, but as a general rule the hotter the iron is when it is poured, the better looking the pigs. Therefore the objective is always to pour hot. On the iron-carbon equilibrium diagram, the temperature at which primary austenite begins to solidify goes up rapidly as the silicon in the iron goes up. So in pouring silvery iron it is especially important to pour it hot.

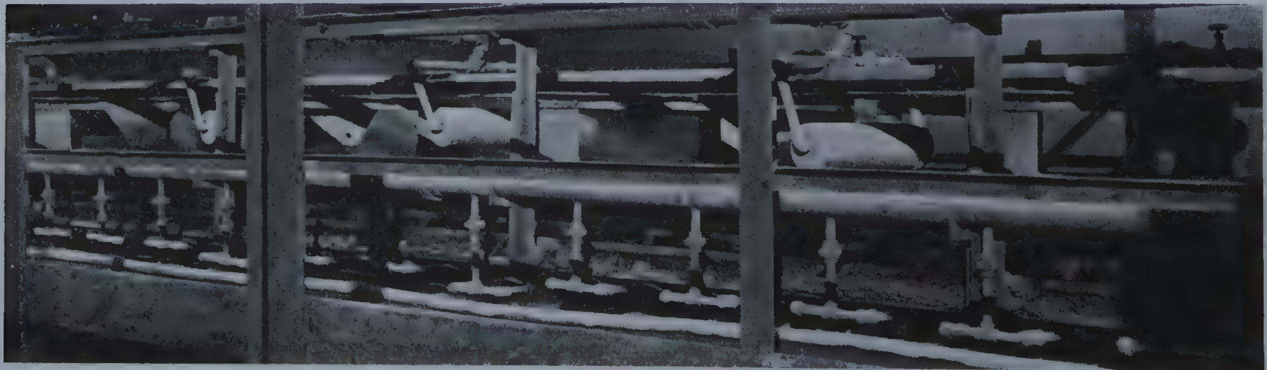

Water box cooling sprays and piping for undercooling.

Ferroalloys in 1949

by R. G. Knickerbocker

A MOST important research and development item on ferroalloys in the calendar year of 1949 was the increase of interest in the recovery of secondary manganese. Owing to the importance of manganese to the nation's welfare, it is most necessary that all possible avenues of research and development on the recovery of this vital metal be investigated.

The principal objective of this new development is to recover manganese from steel furnace slags. Steel furnace slags contain a total of approximately 772,000 tons of metallic manganese which is compared to the 680,000 tons of metallic manganese as ferromanganese that is estimated to be used by the steel industry, annually, at this time.

R. G. Knickerbocker is Metallurgical Engineer at the Bureau of Mines, Rolla, Mo.

To those who are interested in the recovery of primary manganese from low-grade domestic ores containing less than 35 pct manganese, it will be encouraging to know that these slags, containing 5 to 9 pct manganese, are being subjected to considerable research and development work.

The low heat of formation, low viscosity and low specific gravity characteristics of the manganese sulphide-oxide mattes were utilized in Europe during World War II in the treatment of slags and low-grade manganese materials for the recovery of manganese. This is one avenue of investigation of possible value in the program of recovery of domestic primary and secondary manganese.

Results of research work on the influence of temperatures above 1350° C indicate that the affinity of sulphur for copper, manganese and iron is in the order given. Attention is called to the fact that the sulphur in the steel bath is higher when the scrap charge contains copper because of the removal of sulphur from the furnace atmosphere by the copper. That brings up the question of the solubility of copper and manganese sulphides.

The Federal Bureau of Mines initiated new work on the conservation of manganese during the year. Three targets were set up, (1) reduction of sulphur in steel to reduce the necessity for manganese, (2) recovery of manganese from openhearth slags, and (3) development of substitutes for manganese in the making of steel. The steel producers through the American Iron and Steel Institute have furnished the Bureau with $50,000 for these investigations.

A very valuable contribution by the Carnegie Illinois Steel Corp. was made this year covering the details of research work on the removal of sulphur, the effect of the scrap charge, the use of flush-off slags, the importance of distinguishing between the sulphur as introduced by the scrap charge and that introduced in the pig-iron charge in the open-hearth; the effect of time between the pig-iron tap and the openhearth molten bath as regards the sulphur content and the use of manganese ores in the blast furnace. The statement was made that the mechanism for the removal of sulphur was as manganese sulphide in the flush-off slag.

Work on a process for recovering manganese from low-grade domestic ores by leaching with waste pickle liquor, which is produced in large volume in certain steel operations, was reported.

The Standard Mining Co., a subsidiary of Standard Ore and Alloys Corp., started to process manganese ore in the Cushman field near Batesville, Ark., during 1949. The "Potashnick" gravity concentrator which operated during World War II is being utilized for the milling of low-grade manganese ore.

Production of ferromanganese at the Anaconda Copper Mining Co.'s new ferroalloy plant in Anaconda, Mont., was initiated in February 1949.

Electrolytic manganese production and sales were not so good as in 1948 but better than any year prior to 1948. Although no new uses were developed for electrolytic manganese during the past year, the increasing acceptance of the higher purity metal in established fields, particularly for stainless steels, is noteworthy at this time.

The seriousness of the manganese supply problem was recognized by the highest levels in government and in March 1949 the National Security Resources Board, at the request of the President, established the Interdepartmental Manganese Coordination Committee with James Boyd, Director of the Bureau of Mines, as chairman. This committee was assigned the responsibility of coordinating efforts of industry and government to attain a satisfactory balance between total domestic requirements and supplies from all sources.

The imports of manganese to the United States in the first ten months of 1949 from Russia were only 6 pct of the total manganese imported into the country.

In terms of manganese ore plus the ore equivalent of ferromanganese, the African Gold Coast was the largest source in 1949, furnishing approximately 450,000 short tons. India was expected to supply approximately 425,000 short tons and the Union of South Africa is estimated to exceed 300,000 short tons. Inadequate transportation facilities held Brazil's shipments to 144,000 short tons. Total imports of manganese ore during the first ten months were 1,201,240 short tons. Domestic production of manganese ore is estimated as 115,000 short tons—which is slightly less than 1948. Shipments of ferruginous manganese ore and manganiferous iron or containing 5 to 35 pct manganese are estimated at 1,000,000 short tons during 1949.

Ferromanganese consumption decreased 15 pct in 1949 approximating the extent of the lower steel production rate. Imports of 60,000 tons of ferromanganese were received this year.

The price for standard manganese ore rose from approximately 70¢ per long ton unit to abount 82¢ in November; standard ferromanganese rose from $160 per gross ton, in carload lots, to $172 per ton in November.

Ferrochromium

A new chemical method for the treatment of low-grade chrome ore has been developed in Australia which makes use of a sulphuric-chromic acid solvent and electrolytic oxidation. The product contains 95 pct Cr_2O_3 and represents a possible recovery of 75 pct of the chromium in the ore.

A surface-chromizing process has been introduced into this country by the Diffusion Alloys Corp. of New York. This is a British metallurgical development. A pack-carburizing method uses containers with a ferrochromium base material and a suitable catalytic agent. Temperatures range from 1700° to 1850° F, depending upon the carbon content of the steel to be carburized. Chromium penetration in low-carbon steels is about 0.03 to 0.35 in., while in high-carbon steels penetration is 0.003 to 0.005 in.

Important data pertaining to chromium-carbon oxidation and temperature relations have been reported this year by the Union Carbide & Carbon Research Laboratory, Niagara Falls.

The Mead Ferrochrome reduction works of the Chromium Mining & Smelting Co., in the state of Washington, offered to purchase domestic chrome ores during the year. Minimum specifications were 45 pct Cr_2O_3 content, 2.5 to 1 chrome-iron ratio. This does not allow the use of the submarginal Montana chrome ores since the chrome-iron ratio in these concentrates is not high enough. Considerable investigation of the beneficiation of Montana chromite by reducing roast and sulphuric acid leaching of the iron to correct the ratio discrepancy has been conducted.

Some of the African Transvaal chrome ores are reported to require beneficiation of a similar nature and although the detail of the process has not been given, the cost has been stated as approximately 15 shillings per ton.

Imports of chromite during the year were nearly twice the consumption rate and are estimated to have totaled 1,200,000 short net tons. Philippine Republic supplied 30 pct of the total chromite imports and was the largest exporter of chromite to the U. S. Nearly all of the Philippine chromite was of refractory grade. Turkey supplied 24 pct of the total, all of which was metallurgical grade. Domestic production of chromite was estimated to be 300 tons.

The ferrochromium consumption for the first 9 months of 1949 was at a rate of 93,800 tons per year compared with 122,753 tons in 1948.

Cobalt

The Rhokana Corp. in Northern Rhodesia expects to double its present output of 362 tons of cobalt per year. They plan to produce electrolytic cobalt.

The Howe Sound Co. of New York continued exploration and development work on their cobalt property in Idaho and there has been an appreciable increase in the ore reserves there as a result of this work. Preliminary construction was initiated and is planned to be continued through 1950.

The International Nickel Co. of Canada is reported producing at the rate of 15 tons of cobalt monthly. This is cobalt from the nickel ore of the Sudbury Basin.

The Falconbridge Nickel Mines, Ltd. report that they will be producing substantial quantities of cobalt in 1951. This is also from the Sudbury Basin nickel ore.

The Reduction & Refining Co., Kenilworth, N. J., is processing government-owned cobalt ore and subgrade metal.

Union Miniere du Haut Katanga, Belgian Congo, is enlarging their concentrators and the electrolytic plant for copper and cobalt. Hydroelectric power developments are being enlarged to take care of this work.

The Bethlehem Steel Co. was again the only producer of commercial domestic cobalt ore in the United States.

Imports of cobalt into the U. S. for the first nine months of 1949 were 15 pct less than in the corresponding period of 1948.

Effective April 1, 1949 the price of cobalt metal —97 to 99 pct cobalt—was raised to $1.80 per lb.

Exothermic Alloys

Considerable progress has been made in the use of exothermic alloys; they have a definite place in the steel industry and utilize low-grade domestic ores. The use of high-carbon "Chrom-X" now amounts to approximately one-third of the high-carbon ferrochrome used. A "Chrom-Sil-X" is finding considerable use in the cleaning of slags and the making of stainless steel.

Nickel

A report was issued this year on the five years' operation of the Nicaro Nickel Project, a wartime project in Eastern Cuba initiated in February 1942 and concluded in March 1947. Production amounted to 63.5 million lb of nickel chiefly in the oxide form. This oxide was acceptable for use in the iron-steel industry and as such was a substitute for ferronickel.

The International Nickel Co. of Canada reported in June this year a geological exploration revealed nickel was widespread in the Lynn Lake area of Manitoba and two provinces of Venezuela. A new ore body at the Creighton mine, Sudbury district, was largely responsible for increasing ore reserves at the end of 1948 to the all-time record of 246,177,000 short tons.

Imports from Canada, the chief source of supply, were 8 pct less in the first 10 months of 1949 as compared to 1948. This was because of the substantial decline in the output of nickel alloy steels, the steel strike and the production loss in stainless steel.

Molybdenum

Numerous research and development programs have been proposed and are active both on molybdenum metal and as an alloying element to conserve nickel, chromium and manganese in steels. The later programs are based on the plentiful supply of molybdenum which is produced from extensive reserves in Colorado and as a by-product from the copper industry, coupled with the highly satisfactory service the molybdenum alloy steels gave during the recent emergency. Most of the NE or national emergency steels contained 0.15 to 0.25 pct molybdenum.

Advancements made in the melting and fabrication of molybdenum metal has progressed to a commercial stage and the metal is being processed into chemical ware as a replacement for platinum crucibles, etc. Considerable interest continues in the use of molybdenum and high-molybdenum alloys for high-temperature applications since the strength (over 100,000 psi) of the metal does not materially decrease at temperatures as high as 1600°F.

Consumption of molybdenum was 16,201,800 lb in the first nine months—a drop of 8 pct as compared to the same period in 1948.

Tungsten

The Bradley Mining Co. has completed its new tungsten mill to serve the Ima Mine in Idaho. The plant is expected to be in full production during 1949.

Important deposits of tungsten and molybdenum in Guanajuato, Mexico have been discovered.

Brazil has reported possibilities of increasing its production of tungsten, beryllium and tantalite in the northeast section.

There was a 28 pct loss in consumption of tungsten concentrates in the first nine months of 1949 as compared to the same period of 1948. The Tungsten Mining Corp. of North Carolina was the largest domestic producer.

Columbium, Tantalum and Vanadium

The Electro Metallurgical Div. of Union Carbide & Carbon Corp. reports new and increased uses for ferrocolumbium have made it necessary to determine the extent to which tantalum, vanadium and other carbide-formers could be used together with, or in place of, columbium. It has been found that tantalum can be satisfactorily used in the high-temperature alloys where strength at temperature is the major consideration. Vanadium can also be used, but the oxidation resistence of the alloy is affected adversely if the vanadium addition exceeds about half of one percent. The use of tantalum and vanadium for purposes of eliminating susceptibility to intergranular corrosion is possible but these elements are not as effective as columbium. Information on these subjects was available many years ago but had to be reconsidered in the light of new developments and new alloy compositions now being used. Stainless steels very low in carbon (0.03 pct maximum) have proved to be suitable for many uses where the grades containing columbium or titanium were formerly used.

Titanium

The forecast potentialities of titanium and titanium alloys in the not too distant future are of particular interest to the ferroalloy industry. The principal characteristics of the metal are its attractive weight: strength ratio and outstanding corrosion resistance. In the latter respect it compares favorably with platinum as shown in various sea water tests. This new commodity may be expected to gradually replace some of the stainless steels in special applications. Added interest in titanium relations to the steel industry arises from the development of the 36 pct iron ores (containing 32 pct TiO_2) of the Allard Lake area. This reserve of iron ore with titanium byproducts is being processed by the Quebec Iron & Titanium Corp. Its production plant is reported to be able to turn out 175,000 tons of high-grade pig iron and 225,000 tons of titanium slag annually, and tentative plans have already been made to expand capacity.

At least until the titanium commodities have become well established, the metal will remain closely allied with paint pigments, electrode coatings and ferroalloys. In this connection the National Lead Co. acquired certain assets of the Titanium Alloy Mfg. Co. during 1949. Also during the year, Allegheny Ludlum Steel Corp., E. I. du Pont Corp., and Dominion Magnesium, Ltd., announced the production of titanium-metal ingots weighing 25 to 400 lb.

Estimated domestic production of rutile in 1949 was 11,600 tons. Imports of rutile from Australia were 2750 tons for the first 10 months of the year, or slightly more than one-third of receipts for the same period in 1948. Ilmenite prices decreased from $20 per ton to $14-16 during the year. Further exploitation of titanium metal may be expected to materially benefit the economic and production status of these minerals.

Hanging Blast Furnaces

by L. M. Fulton

THE blast furnace concerned used an ore high in silica and phosphorus and a weak coke high in sulphur. After it was provided with high blast temperature and a revolving stock distributor, it developed hanging.

Two types, known as clean and sticky hanging, were encountered. Sticky hanging could be altered to the clean type by temporary use of excess lime or could be reduced greatly in frequency by use of a charge with a high center of gravity on the bell. Clean hanging was practically eliminated by using extra coke when the gas temperature dropped below a critical level but this practice gave undesirably high silicon.

L. M. Fulton is with the Dominion Steel and Coal Corp., Sydney, Nova Scotia. This is one of the papers to be presented before the Annual Blast Furnace, Coke Oven and Raw Materials Conference, April 10, 12, at Cincinnati.

From general thermochemical principles, along with the particular experiences in this operation, a theory of hanging was derived. The theory explained observed correlations of hanging with declining gas temperature and silicon. Furnace design was indicated by the theory as responsible for hanging. Pending opportunity to change furnace design, steam was used in the blast, successfully eliminating hanging while allowing low silicon iron to be made.

Changes in furnace design on this and on a second furnace gave support to the theory. Recently the use of steam on the second furnace confirmed results previously obtained on the first.

Introduction: This paper offers facts concerning the behavior of a blast furnace which frequently encountered hanging. Mainly, the record is chronological but not strictly so. Intermingled with the observed facts are interpretations placed on those facts by the writer. Certain terms are used which, although not obscure in meaning, will be defined, some now, others later.

Hanging: When downward movement of stock either ceases or slows down enough to delay charging beyond the proper time.

Slipping: When stock movement proceeds discontinuously in irregular jumps (slips) of a foot or more at a time. Slipping may be fast enough to allow charging at the proper time.

Blowing-Through: When high pressure gas suddenly blows up through the stock, ejecting material from the bleeders.

Check: An intentional reduction of blast volume of considerable magnitude for any purpose.

Where the adjectives "Uniform" and "constant" are used, they must be interpreted rather liberally to mean approximate rather than strictly defined conditions.

The Furnace: The furnace concerned is No. 1 of the Dominion Steel and Coal Corp.'s integrated steel plant located at Sydney, Nova Scotia, in the middle of the coal areas of Cape Breton Island. At present the furnace has a carbon hearth of 18 ft 3 in. diam. It is just under 79 ft. from the iron notch to the bottom of the closed bell. A dimension which will be referred to later is the height of the bosh, measured from the center line of the tuyeres. This dimension, measured by the cooling line method, is now 13 ft 3 in.

Wabana Ore: Exclusively used is Wabana Ore, mined by the corporation from extensive undersea areas which outcrop on Bell Island, Newfoundland. The ore is mined from two seams which differ in the amount of silica. It is blended in shipping and in stocking at Sydney to give fairly uniform silica, even without further treatment. The size of the ore as received is —4½ in. + 0.

For the past 6 yrs, blending at the crusher, crushing and screening have been carried on at the blast furnace plant, giving three excellently sized fractions, each of very uniform analysis. The sizes are —2 in. + 1 in., —1 in. + ¼ in., and —¼ in.

The iron content of the ore averages 51.00 pct, silica 12.00 pct, and phosphorus 1.00 pct. It has about 4.50 pct alumina and 3.25 pct lime. Sulphur is low, rarely being above 0.06 pct, and the manganese is only 0.12 pct.

Although the ore is an unusual blast furnace material, it is very uniform in analysis and sizing.

Coke from Cape Breton Coal: The coal mines operated by the corporation on Cape Breton Island supply the coal for making coke. These mines are also almost wholly submarine. The coal averages 34.00 pct in volatile matter, 9.00 pct ash, and 2.75 pct sulphur. It is washed before coking.

The coke is about 8.50 pct ash and 2.00 pct sulphur. By the tumbler test it shows a low percentage remaining on the standard 1.06-in. screen, varying from 15 pct to 35 pct. The sizes used in the blast furnaces for the past 15 yrs have been mostly plus 3 in. and —3 in. plus 1½ in., with a small amount of —1½ in. plus ⅞ in., occasionally.

Either the ore or the coke by itself constitutes an abnormal blast furnace material, and their combination in the same operation is probably unique on this Continent.

Iron, Slag, Gas: A typical cast of iron will be of the following analysis: 4.00 pct C, 1.25 Si, 0.025 S, 1.65 P, 0.20 Mn. The slag averages as follows: 30.80 pct silica, 15.20 alumina, 0.40 titania, 48.80 lime, 3.50 magnesia, 0.40 ferrous oxide and 2.50 sulphur. The normal gas contains: 13.0 pct Co_2, 28.0 Co, 1.5 H_2, and 57.5 N_2.

Before Modernization

Until the end of the year 1929 this furnace had operated without the benefit of high blast temperature, or of a revolving top. The furnace gave little or no trouble as far as stock movement was concerned. Hanging was practically unknown and slipping infrequent. The quality of the iron could be controlled easily. However, neither the tonnage nor the coke rate were considered satisfactory, and to improve these new stoves were planned which could supply at least 300°F. higher blast temperature than formerly available.

Lining failures were also a cause for concern. Regularly the brick on one side of the furnace failed badly enough to require a new lining, while the rest of the brick-work was yet in usable condition. To insure better distribution and thus avoid localized lining failure a revolving top was ordered. This distributor was also expected to contribute appreciably to improvement in tonnage and coke rate.

The order of placing materials on the bell was coke first, then the ore and limestone in the following sequence CCOOSCCOOS. The total charge on the bell averaged about 14,000 lb coke, 24,000 lb ore and 8000 lb limestone. The coke was run-of-oven with a maximum size in excess of 4 in. and with the braize screened out at the skip over a 1 in. bar screen. Ore was run-of-pile, about —4½ in. + 0, while the limestone was —7 in. + 0.

The low blast temperature, never over 1100°F., probably was one reason for the absence of hanging. Another was the low resistance to upward bound gas through the coarse materials which the fixed top placed in one sector of the furnace. Into this channel the gas from at least four tuyeres had easy access.

After Modernization

The new equipment went into operation on completion of a relining early in 1930. Blast temperatures in the neighborhood of 1400°F. were used continuously during the early months of operation. Careful examination of the stock, during the later stages of the first filling, showed that the revolving top was giving excellent circumferential distribution.

As an additional protection for the lining, the ore was placed on the bell first so that a layer fell against the wall when the bell was dumped. The order of materials on the bell was OOSCCO-OSCC, with the weight per charge approximately the same as before modernization. This charge when placed on the bell had a lower center of gravity than the former coke first filling, and consequently would spread less towards the center on dumping.

Average tonnages and coke rates were greatly improved and constituted ample justification for the expense of modernization.

In spite of its economy, the operation was very erratic, with sudden and wide swings in iron analysis. Hanging began early in the run and increased in frequency and severity. Periods of normal stock descent seldom lasted more than three days, alternating with spells of hanging, some of which exceeded three days.

The hanging was of two distinct types which came to be known as clean and sticky. The former was the more prevalent. Alteration from one type to the other was sometimes rapidly repeated.

With clean hanging, stock descent virtually ceased, with none but the very slightest movement until the furnace was checked. Sometimes the pressure had to be brought down so low that gas was barely kept from coming back through the tuyeres. Once the stock started to move its descent was sudden with no hesitation whatsoever.

A U-tube water gauge connected with the main dustcatcher gave an indication which was characteristic of clean hanging only. While checking the furnace the gas pressure would drop steadily as the blast volume was reduced. Then suddenly a momentary vacuum of 5 to 10 in. of water would be shown and at the same time stock descent would be indicated by the rodding mechanism. It was as if the stock moved bodily, like a piston in a cylinder.

For a few minutes after the blast was again put on the volume of air entering the tuyeres was considerable although much below normal. Soon this flow became less and less until the coke could be seen lying almost motionless in front of the tuyeres.

The tuyeres remained clean and bright, and slag rarely appeared even when the pressure was brought very low.

The slag from the cinder notch, even when dirty at the start of hanging, soon became clean and hot as the spell progressed. On cast, the slag skimmed cleanly from the iron.

The iron was usually lower in silicon and higher in sulphur than normally when hanging started. As it continued the silicon rose steadily until it had reached an abnormally high level while the sulphur dropped very low. When hanging stopped, which it usually did suddenly, silicon and sulphur rapidly returned to normal.

As the end of a hanging spell approached it was necessary to check at fairly short intervals to avoid heavy slides of material off the wall. With regular checking this wall coating came down gradually with no great interference with the tuyeres. Occasionally, however, a slide occurred which blocked off several tuyeres and required several hours to clear away. The gas temperature and its CO/CO_2 ratio were lower than normal as was also the flue dust produced.

With sticky hanging, stock movement seldom ceased entirely, but it proceeded in slips and was generally too slow to permit charging at the proper time. Usually movement started with less reduction in blast pressure than was the case in clean hanging. However, this was by no means an easier situation because relatively small reductions in pressure allowed slag to appear at the tuyeres, and checking had to be conducted with great care and frequent flushing of slag from the cinder notch to avoid filling the blowpipes.

Stock descent, although it started earlier on a check, often required several minutes to make room for a charge even when no slag appeared at the tuyeres. On a check the U-tube showed a succession of undulations, some starting with a slight drop in pressure, others with a rise. None of them were large and none indicated a vacuum at any moment. When the blast went on again the pressure rise was slower and the volume of air entering the tuyeres was greater than with clean hanging. The reduction in air volume as time passed was not so noticeable.

The tuyeres were rarely bright and descending material could generally be seen.

The slag from the cinder notch was sluggish and below normal temperature at the start gradually becoming foamy and hotter. It did not become clean until the sticky spell had ended. On cast, it was impossible to skim the iron satisfactorily. Silicon and sulphur did not follow the normal inverse variability. For a given silicon, whether high or low, the sulphur was always higher than it should have been and return to a normal relation was slow even after the hanging had disappeared which it did much more leisurely than with clean hanging. Slides of material from the wall, when they occurred, usually filled some of the blowpipes. The gas temperature and its CO/CO_2 ratio were higher than normal. Flue dust was excessively high and besides contained much coke.

The worst feature of sticky hanging, however, was the frequency with which slipping and blowing-through occurred. A slip was generally followed by a moderately rapid increase in gas temperature but when blowing-through took place the gas temperature fairly leaped upwards. The first indication of blowing-through was a sudden drop in blast pressure of two to 5 psi, succeeded instantly by the bleeders opening and stock, including red hot coke, being ejected.

When slipping and blowing-through started, checking had to be regulated to the minute to control it. The slightest delay sometimes allowed a slip or blow-through to occur.

Usually blowing-through resulted in stock movement sufficient to permit a charge and the gas temperature rise could be halted by cold stock. Sometimes there was not enough room for a charge and only the immediate reduction of blast volume prevented the gas temperature reaching levels much too high.

Numerous changes in filling sequence, in tuyere sizes and lengths and in many details of operation were made during the first months. Suggested cures for hanging were tried with a zeal undiminished by uniform failure. Every suggestion that appeared sensible, and some outside this category, received a fair opportunity to work. Although many of them, particularly changes in filling sequence, seemed promising for the first few hours not a single one gave more than temporary relief.

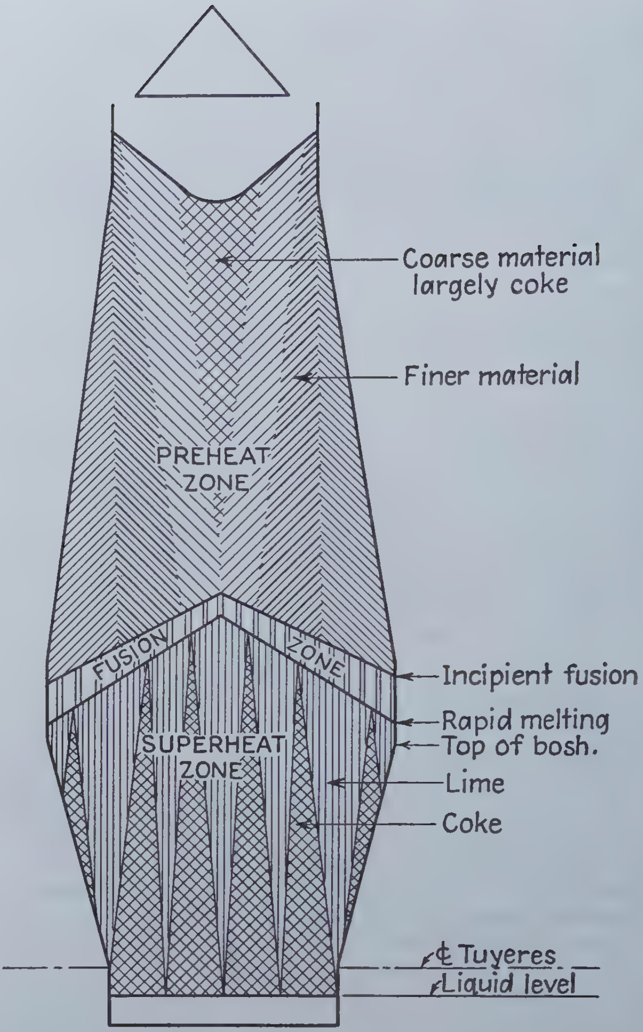

Fig. 1—The three heat zones of a blast furnace fitted with a McKee distributor.

Sticky hanging although less frequent than clean was almost continuous throughout the seventh month of operation. After many changes were made in fruitless efforts to get out of this condition it was decided to revert to the coke first filling. A few days after this the sticky hanging ended although not permanently.

Nevertheless the ore layer against the wall was considered too important to dispense with entirely and for several months a compromise filling of alternate ore and coke first charges was used. Eventually it seemed proven that even this filling caused too much sticky hanging and the ore first charge was omitted.

The coke first filling was continued and so rare did sticky hanging become that the improvement could properly be credited to the change in filling. However, clean hanging came just as often and stayed longer.

A lengthy period late in the first year of operation was devoted to a thorough trial of the effect of low blast temperature on hanging. Reduction of heat to the level used before modernization was made and continued. Contrary to general expectation this drastically lower temperature failed entirely to prevent hanging. In fact, the worst spell of all occurred during this period. It was obvious that high blast temperature was not alone in causing hanging.

Although failing to ward off hanging this low temperature episode provided convincing evidence that the expense of supplying high blast temperature was justified. The tonnage dropped and the coke rate rose until half of the total savings derived from modernization had vanished.

Since the return to the coke first filling, the only new feature of the operation remaining was the revolving top. This equipment was therefore credited with the half economy still left. However, it was obvious also that its functioning contributed in some large measure to hanging.

The fixed top had provided an easy passage through coarse material for the gas from at least four tuyeres all the time. Experiments performed in filling a model furnace showed that the revolving top gave excellent circumferential distribution but that radial distribution was not uniform. As a result the central column of the furnace was mainly coarse material with the finer material in the outer annulus. The larger proportion of the coarse material in the central column was coke.

The chances for gas from one tuyere to get into this central column were no better or worse than those of any other tuyere. Consequently, when the going became difficult for one it became just as difficult for all, and high blast pressure and hanging resulted.

Study of Records Gives Clue

The years following, until early 1934, saw so much idle time that little could be done in the study of hanging. However, a start was made on accumulating and systematizing a mass of data from reports and charts. Study of this soon revealed an encouraging fact. Without exception, every attack of clean hanging had been preceded by a period of declining gas temperature. With almost equal regularity the silicon in the iron had also dropped. However, although a gas temperature decline always preceded an attack of clean hanging, nevertheless clean hanging did not always follow such a decline. These few exceptions to the usual sequence then came in for special investigation.

At last, in one of these exceptions, where hanging did not follow a decline in gas temperature, it was definitely established that under abnormal conditions the coke ovens had produced coke of unusually high density. Coke was charged by volume so that the increase in density gave the furnace more coke than normally. The heavy coke was being charged during this particular period of declining gas temperature.

If the high density coke actually had prevented hanging there were at least two possible interpretations. Either the high density had warded off the promised hanging spell, or merely an additional quantity of coke had done so. Since the conditions which had produced the high density coke could not be continued, there was no opportunity to test this interpretation.

However, it was very easy to test the effect of adding extra coke during a period when the gas temperature was declining. During the next such period a moderate amount of extra coke was charged with very encouraging results. Although hanging did begin, it was over in a few hours. Eventually, by proper timing and adequate doses clean hanging was practically eliminated, and, even when it had started, sufficient extra coke would end it soon after the coke reached the tuyeres.

A certain amount of psychological resistance to this treatment of advanced hanging with extra coke was encountered. To operators accustomed to use extra coke solely for the purpose of increasing the silicon it seemed a strange action to charge extra coke when the silicon was already abnormally high. However, repeated successes in stopping hanging, with consequent rapid reduction in silicon, eventually wore down this understandable reluctance.

Mild cases of sticky hanging sometimes responded to the extra coke treatment, but in general it was not improved. More often the extra coke, particularly if given in blanks (five skip buckets at a time), seemed to aggravate the slipping and blowing-through which were so characteristic of this type of hanging.

As already observed, with sticky hanging there was a disturbance of the normal inverse variability between silicon and sulphur, the latter generally rising with the silicon instead of the reverse. In one prolonged spell, excess lime was used in an attempt to control the sulphur. When surplus lime appeared in the slag there was an abrupt change from sticky to clean hanging. The latter was then quickly stopped by the extra coke treatment.

This became the regular treatment for sticky hanging, first excess lime until an undoubted surplus appeared in the slag, then extra coke to correct the clean hanging which followed. The excess lime was, of course, removed immediately its purpose was attained.

Although hanging was now under control the remedy itself had an undesirable effect. When a furnace is burdened for a certain grade of iron, the charging of extra coke inevitably increases the average silicon. This average silicon was made still higher because of the few occasions when intentional extra coke coincided with an unintentional dose, such as had happened at the time the high density coke led to the discovery of this treatment.

Since properly timed extra coke prevented hanging, the search for a method for retaining this freedom, without the undesirably high silicon, led to speculation on the action of extra coke in the furnace.

Fig. 1 shows schematically the writer's conception of the three distinctive heat zones of a blast furnace equipped with a McKee distributor. The upper, or preheat zone, prepares the stock up to the point where incipient fusion occurs. The fusion zone heats it further until rapid melting takes place, whereupon the molten materials enter the superheat zone for finishing.

Vertical sections of the boundaries of the zone, although represented by straight lines in the diagram, are actually very complex curves determined by the distributions of solid, liquid and gas flow through the furnace.

The arrangement of stock in the upper or preheat zone is based on experiments made in Sydney with a scale model furnace (2 in. to 1 ft). The coke, ore and limestone were also sized in proportion to the sizes actually used in No. 1 Furnace. The model furnace was fitted with skip buckets and a revolving distributor.

The density of the furnace contents was high and fairly uniform for the annular ring bounded on the outside by the wall. Here all three constituents were present in an average proportion of the sizes charged.

When ore was placed on the bell first there was a distinct and fairly heavy layer of ore against the wall which tapered off to a light one in the center. With coke first on the bell there was also a layer of ore against the wall but it was lighter and less distinct than with ore first. However, it was visible across the furnace just as with the ore first charge.

Whether coke or ore was placed on the bell first, there was always a central column containing an excessive proportion of coarse material, largely coke. With ore first on the bell the central column of coke was slightly greater in diameter than with coke first.

The function of the preheat zone is to heat the stock to the point where it is ready for the fusion zone.

Material as it enters the fusion zone begins to soften and get sticky. As it moves downward the softening process continues until eventually rapid melting takes place. The level at which rapid melting occurs is the lower boundary of the fusion zone. Gas channels persist in this softening mass, kept open by the upward force of high-pressure gas.

The fusion zone is therefore a gas permeable floating diaphragm supporting the preheat zone and resting on the superheat zone below. In its upper portion, at least, this diaphragm is semi-rigid because of the cementing effect of its sticky but not fluid condition. The depth of this semi-rigid portion is considerable if the range of temperature between incipient fusion and rapid melting is large, and less if this range is small.

Coke passes through this zone embedded in the matrix of semi-fused material.

Rapid melting can take place before the material is hot enough to absorb all the lime in the charge. This primary slag formed at the lower boundary of the fusion zone, flows down, leaving behind the coke and some of the lime with which it was originally charged.

The molten materials, primary slag and raw metal, trickle downward through the superheat zone, meeting ever increasing temperatures. The coke and residual lime follow but move much more slowly.

The distribution of lime and coke in this zone is not, of course, as it is represented in fig. 1, in wedge formations. The diagram merely illustrates the fact that the molten material leaving the fusion zone meets in its downward flow decreasing lime surfaces and increasing coke surfaces. The amount of residual lime is represented as being greatest under the outer annulus of the preheat zone which contains the heavier proportion of ore and limestone.

Presumptive evidence of increased amounts of residual lime nearer the fusion zone was obtained when with the furnace in good condition the tuyere size was being changed. When one of the tuyeres was removed from the cooler a small amount of coke followed it. In this coke there were a few small fragments of a very limey material. Raking of coke was begun and continued until about twenty cubic feet had been removed from the furnace, all coming from the region just above the tuyere.

The later portion of this coke contained an appreciably greater percentage of these limey fragments, some of them holding embedded small coke. Presumably if raking were further continued the proportion of lime found would increase as the material came from higher regions of the superheat zone.

The primary slag formed at the relatively low temperature of rapid melting flows down through the coke and lime of this zone acquiring heat as it goes. This additional heat allows it to absorb additional lime until, when it reaches the lower boundary of the superheat zone, it has completed its quota.

The raw metal as it trickles through this filter bed of hot coke and lime is heated and refined. Among other changes it picks up silicon.

The Cause of Hanging

With perfectly uniform materials, uniformly distributed, and with gas flow likewise uniform, the level of the fusion zone would remain constant. However, this is not true of blast furnaces. There is enough irregularity in even the smoothest working furnace to cause some variation in the level of the fusion zone.

If the fusion zone lowers sufficiently the semi-rigid portion of the floating diaphragm will come to rest on the top of the bosh. There it must wait until it becomes hot enough to flow into the restricted area below. The pause allows the continuously lowering coke and lime of the superheat zone to create a space beneath the bridge-like diaphragm.

The weight of the preheat zone stock pressing on this immobilized sticky mass tends to close up the gas channels through the diaphragm and so increase the resistance to the upward flow of gas. The blast pressure rises and the initial stage of hanging is entered. With a weakly-knit diaphragm the weight of stock above may break it down at intervals, this process being outwardly manifested by slipping.

If the diaphragm is weak in the central portion the pressure of the gas below may break through to the light central column of coke in the preheat zone. When this happens the gas carries coke with it in a surge upward, opening bleeders or explosion doors, and ejecting coke with some light particles of ore and stone. This is blowing-through.

However, if the diaphragm is uniformly strong neither slipping nor blowing-through take place. The gas channels gradually close until only a small amount of blast enters the tuyeres. To break the bridge it is necessary to bring the blast pressure very low, when the whole weight of the stock above eventually causes the bridge to let go and the mass plunges bodily downward.

The persistence of a dirty slag and of abnormal sulphur for any given silicon with sticky hanging is probably due to material getting through the diaphragm in an unfused condition, particularly following blowing-through. This incompletely prepared material which has not undergone the conditioning of the fusion zone disturbs normal superheat zone functioning.

In uniform operation the rate at which coke enters the superheat zone is the same as the rate at which it is consumed therein. If the rate of consumption exceeds the rate of entry the volume of coke in the superheat zone decreases, and the fusion zone diaphragm, resting on it, drops lower in the furnace.

If, on the other hand, coke enters this zone faster than it is consumed the volume of coke occupying space under and supporting the fusion zone increases. The level of rapid melting gradually moves upward and with it the semi-rigid diaphragm.

Extra coke, therefore, will tend to raise the level of the fusion zone and consequently either ward off hanging or gradually cure clean hanging if it has already started.

Probably the reason for the lack of success in curing sticky hanging with extra coke is that, particularly in blanks, it further weakens the diaphragm just beneath the central coke column. When sticky hanging is allowed to continue it seems that gas flow, and consequently stock flow, are gradually forced more and more towards the central portion of the furnace. This increase in the proportion of gas traveling upward at high velocity through the open column of large coke gives abnormally high gas temperature and flue dust production. At the walls there is little motion and consequently a very great thickness of material builds up and is very difficult to melt off later.

Experience has been that, at the start of sticky hanging, application of a considerable increase in blast temperature may change the hanging to the clean type. If this is not successful, the only other method found useful was to increase the lime temporarily, which it is reasonable to infer increases the strength of the diaphragm in the central area where an abnormally high proportion of the gas has been flowing.

Coke first filling gave less sticky hanging than ore first, probably because it tends to put more ore and limestone in the central column and thus strengthen the diaphragm in this area.

A uniform mixture of slag-forming materials, including lime, will begin to soften at a constant temperature. The amount of lime present cannot alter this temperature of incipient fusion appreciably, any more than the amount of sand in a sand-ice mixture could appreciably alter the temperature at which the ice melts.

The upper boundary of the fusion zone, therefore, is always at the same temperature, whether the fusion zone is high or low, thick or thin.

As the mixture descends to meet higher temperatures the slag is able to incorporate more lime in its composition, but without at first greatly affecting its viscosity which is still too high to allow it to flow freely.

With more heat, even with additional combined lime, the slag could probably flow freely if it were not for the thickening effect of uncombined lime. Thus more heat than is actually required to form a free-running slag is needed to allow rapid melting and escape of the slag from the fusion zone, when a high proportion of lime is contained in the charge.

No one would charge lime enough to cause this delay in forming a fluid slag at the bottom of the fusion zone unless it was thought essential to give the slag certain properties, particularly the ability to take care of sulphur. The temperature of the lower boundary of the fusion zone, therefore, is greater for a high line charge than for a low. However, with a uniform proportion of lime in the charge the temperature of rapid melting at the bottom of the fusion zone is constant.

With uniform materials, therefore, the fusion zone is bounded at the top and at the bottom by constant temperature surfaces. Consequently, whatever the distance between top and bottom, or at whatever level the fusion zone lies, it will always be at approximately the same temperature.

Not only is the fusion zone stock at a constant temperature, but the gas leaving it is also at a constant temperature. The differential in temperature between the heating gas and the heated stock remains approximately constant for any given stock temperature.

As the fusion zone drops lower in the furnace it brings its diaphragm closer to the top of the bosh and thus closer to the start of hanging. The gas, leaving the fusion zone at a constant temperature, must travel further through the material of the preheat zone to reach the stockline. Consequently, as the fusion zone drops and hanging approaches there is a decline in the top gas temperature.

Study of the data on gas declines and hanging disclosed that the gas temperature could be allowed to drop to a certain level before there was much danger of hanging. Thereupon it became standard practice to charge extra coke when the gas temperature dropped below this critical level.

Silicon depends to a considerable extent on the distance the molten materials from the fusion zone have to travel through the hot coke and lime of the superheat zone. As the fusion zone rises or falls, this distance increases or decreases and the silicon in the iron tends to rise or fall. Consequently, silicon usually dropped along with the gas temperature before a hanging spell.

Given a uniform height of fusion zone, one high enough to avoid hanging, the amount of silicon in the iron will be determined largely by two factors. The first is the amount of contact of the molten products of the fusion zone with the hot coke and lime of the superheat zone. The second is the average temperature of the superheat zone.

Specifically acting to increase silicon is the contact of the molten materials with hot coke. Contact with hot lime will not reduce silica to silicon. Therefore, if a greater proportion of lime is maintained in the superheat zone the silicon will be lower in the iron, even though the temperature of the iron is abnormally high.

Presumably also, a thicker average layer of molten material traveling over the hot coke will reduce the amount of contact and consequently the silicon. Faster driving would have this effect. Since it was considered likely that more lime remaining in the superheat zone would increase the lime in a slag already very limey, no attempt was made to test this factor. The blowing engine was already at its maximum capacity so no trial of faster driving by means of increased blast volume was possible.

There remained the possibility of making lower silicon iron by reducing the average temperature of the superheat zone. To do this, either the temperature at the top or the temperature at the bottom, or both, would have to be lowered.

Since the top of the superheat zone is immediately below the level at which rapid melting takes place, the temperature will be determined by that of rapid melting. This, as has been noted, depends on the amount of lime in the charge. Lowering the temperature at the top of the superheat zone, therefore, meant reducing the proportion of lime in the charge.

There was no apparent reason to expect that the slag would handle the sulphur with less lime than was being used. For decades operators had been trying to get along with as little lime as possible. No attempt, therefore, was made at this time to reduce the top superheat zone temperature by reduction in the lime ratio.

To lower the average temperature of the zone, it seemed necessary, therefore, to lower the temperature at the bottom. This temperature is largely determined by the flame temperature at the tuyeres, and the latter could be lowered in more than one way.

The most common method of lowering the flame temperature is by reducing the blast temperature. This had already been tried as a cure for hanging, which previous experience had indicated it might prove to be. However, a reduction of over 300°F had failed to prevent hanging and had been costly in tonnage and coke. This method reduces the heat of the preheat zone but also lowers the total available heat of the furnace.

Injection of cold materials at the tuyeres, materials which ordinarily are charged at the top, would not reduce the total available heat because they have to be heated in any case. However, injection of coke or of lime, the only two suitable materials, presented major mechanical and operational difficulties, and this method was not tried.

Injection of steam into the blast was the easiest method and also the most promising one for lowering the flame temperature without much reduction in the total heat available.

At the tuyeres, steam reacts with coke to form carbon monoxide and hydrogen. The reaction lowers the flame temperature and consumes only as much coke as would be required to form a volume of carbon monoxide from air equal to that formed from the steam. This carbon monoxide is a more effective reducing agent for ore oxides than an equal volume formed from air because it carries with it no diluting nitrogen.

The hydrogen formed is also an excellent reducing agent for most purposes better than carbon monoxide. When a unit of hydrogen combines with ore oxygen to become steam once again, it returns to the furnace all the heat it had abstracted at the tuyeres. If a large proportion of the hydrogen thus recombines with oxygen the overall heat usage may be very small.

Of greater importance, the use of steam would abstract heat from the superheat zone where there was too much heat and return some of it, at least, to the preheat zone, where there was not enough.

Late in 1934 the simple preparations were made for the injection of steam into the cold blast, just as it entered the stove.

The materials required were a few lengths of 2 in. pipe, a valve for each stove, one for the connection to the steam main, and a recording steam meter on the line to the stoves which was checked at intervals by a simple wet and dry bulb device connected to the hot blast main.

First, the furnace was given extra coke and when the silicon began to rise the steam was turned on in small volume. The silicon soon dropped to normal and the process was repeated cautiously. Eventually, not without some errors and adjustments, freedom from hanging was achieved with silicon closely controlled at the desired level.

The total blast moisture required to secure this result was from 1.8 to 2.0 lb per thousand cu ft of dry air, or 12 to 14 grains per cu ft, when using a blast temperature of 1300°F.

The tonnage rose to and remained steadily at a higher level than ever before while no increase in the coke rate was observed.

A considerable decrease in the amount of lime required to handle the sulphur was noted. The cause of this decrease was somewhat obscured by the use of an especially low silica ore which might have been the most important factor.

At the time only one of the four ore mines was being operated due to lack of orders. This mine gave the lowest silica ore which ordinarily was blended with the production from the other mines. Available analyses were limited to those made at Wabana as the cargoes were loaded. In the pile at Sydney these were mixed to some extent with blended ore previously obtained.

As a consequence of this probability that lower silica ore was responsible for the lower lime usage with the steam method, the other probability, that the steam method itself required less lime, was not investigated.

Changes in Furnace Design

Although very satisfactory operation was obtained by using steam in the blast it was recognized that this practice was made necessary by a furnace design not suited to the iron-making materials used. With a properly designed furnace it was hoped that the uniform, although unusual materials available would give free stock movement and uniform iron of the desired quality.

Hanging was caused by the semi-rigid diaphragm of the fusion zone coming to rest on the top of the bosh because, either from lack of preheating time or from the amount of lime in the charge, it was not hot enough to flow freely. Two changes in design would aid in preventing this. The first was a lower bosh, and the second, more preheating space. The lower bosh in itself would achieve both results, unless for some unexpected reason there should be a critical bosh height below which good operation could not be secured.

The present lining of No. 1 Furnace has a cooling line bosh lower than the previous lining and as low as it can be made without major structural alterations. In addition, the present lining is thinner above the mantle and thereby provides more preheating space.

It is impossible to apportion results between these two changes but the improvement has been striking. However, although the changes have been in the right direction they have not been enough to get complete freedom from hanging, and at the next relining the necessary structural changes will be made to get a considerably lower bosh.

In this present lining the bosh as determined by the brickwork was lowered about one foot, as compared with the bosh formed by the noses of the cooling plates. For the first 18 months of operation the performance was the best ever experienced with this furnace. Following this, however, there was a slight falling off in tonnage and a return of the tendency to hang. Presumably the brick had eroded enough in this time to allow the cooling plates to determine the bosh line.

In 1936 a lining constructed in a similar manner, with the brick line bosh about a foot lower than the cooling line bosh, acted in much the same way as the present lining. Several possibilities which existed in the way of explanation for the 1936 lining are not factors with the present lining, so that it may have been really brick erosion that changed the performance of the 1936 lining about two years after blowing in.

Experience With No. 3 Furnace

During the recent war a furnace built many years ago in another location was dismantled and erected at Sydney on the No. 3 site. It was put into commission with all possible speed with practically no change in design. It had a high bosh, about six feet higher than that of No. 1.

This was a very difficult furnace to operate. Within a few days while blast volume was still comparatively low high pressure and hanging were encountered. The hanging was almost completely of the sticky type, and although by excess lime this could be changed to clean, reversion to the sticky type occurred very quickly.

Free stock movement rarely lasted more than an hour or two. The extra coke treatment was ineffective sometimes changing clean hanging back to sticky. The use of steam in the blast failed to effect any improvement in the performance although it gave a little control over silicon.

No. 3 was relined in 1948 and the bosh as determined by the cooling line was lowered 5 ft, as much as could be done without a much longer relining period than was available. It was still about a foot higher than No. 1's bosh.

No. 3, on its second lining, has so far confirmed in every essential detail the results obtained previously with No. 1 furnace. There is comparative freedom from hanging, the extra coke treatment is effective in warding off or curing hanging, and, finally, the use of steam in the blast, formerly of little effect, now operates successfully when required.

Acknowledgments: The writer is grateful to many friends and associates, and particularly grateful to The Dominion Steel and Coal Corp. which displayed such patience and offered so much encouragement during the years when the lessons set forth herein were learned.

• • •

Industry's demand for larger and larger hollow forgings is making it necessary to cast ingots in sizes beyond anything ever before attempted. Recently Bethlehem Steel Co. has completed an ingot mold believed the largest in existence, capable of producing an ingot of 134-in. diam, weighing approximately 720,000 lb. Shown here is the stripping of the first ingot cast in this mold, in No. 3 openhearth at the Bethlehem plant. Ingots of this size will be used in making the hollow forged vessels of large inside diameter required by the chemical industries.

• • •

Graphite Electrodes

Thermal Gradients and Strains During Rapid Cooling. When an electrode column is pulled rapidly out of an electric steel furnace there results a terrific thermal shock. The degree of this shock is calculated, and measurements are described to determine thermal conductivity, thermal expansion, modulus of elasticity and strength.

by H. G. MacPherson

THE electrodes of an electric steel furnace must withstand unusually severe high-temperature operating conditions. An arc electrode must be a good conductor of electricity, highly refractory and sublime directly without melting. Graphite possesses this unique combination of properties. Further, many additional desirable properties of graphite electrodes are required to meet the operating conditions of modern electric steel furnaces. One of these requirements is due to the fact that electric steel furnace operations impose greater thermal shock and strains on the electrodes than are encountered in any other industrial process. Graphite has the greatest resistance to such thermal shock and strains of any material at the high temperatures involved in the making of steel.

This paper was presented before the Seventh Annual Electric Furnace Steel Conference, Iron and Steel Div., AIME, Pittsburgh, Dec. 8-10. H. G. MacPherson is an engineer with National Carbon Corp.

One condition in the operation of an electric furnace will be considered that results in a terrific thermal shock. This occurs when an electrode column is pulled rapidly out of the furnace while hot and the surface of the electrode is rapidly cooled by radiation. Some calculations have been made of typical temperature gradients set up and electrode strains caused by this procedure. The results show the extreme nature of the shock to which the electrode is subjected by the rapid withdrawal of electrodes from the furnace.

The method of calculation of what happens inside the electrode is somewhat complicated by the fact that an analytical solution is not available and it was necessary to use a process of numerical calculation. The method of calculation will be given in some detail because it illustrates the mechanism by which temperature gradients are created and thermal strains are developed.

It is assumed that the electrodes come to equilibrium inside the furnace at the temperature of the bath, or approximately 1650°C, or 300°F, and that the electrodes are pulled out of the furnace rapidly and cooled from the surface by radiation to the surrounding atmosphere. For purposes of calculation the 18-in. diam. electrode was divided into annular zones 5 mm in thickness and each zone was treated as though it were at a uniform temperature. The outside zone was considered to lose its heat by radiation to cold surroundings according to the Stefan-Boltzman law:

$$Q = ekAT^4$$

where A is the area of the surface, T is the absolute temperature, e is the surface emissivity and k is the Stefan-Boltzman constant. Calculation is carried out by small time intervals chosen to be of 1-sec duration. Initially all zones in the electrode are at a uniform temperature of 1650°C. During the first second it is assumed that only the outside zone loses heat, in an amount corresponding to that which would be lost by radiation from the surface. This drops its temperature by the amount

$$T = \frac{Q}{CdV}$$

where Q is the amount of heat lost during a second, C is the specific heat at the temperature of the zone, d is the density of the graphite and V is the volume of the zone. This amounts to a drop in temperature of about 44°C in the first second.

During the next 1-sec period, the outside zone therefore starts at a temperature of 1606°C and radiates heat at a rate corresponding to this new lowered temperature. However, now, in addition to losing heat, it also receives some heat by thermal conduction from the next inner zone because a temperature gradient has been set up over the

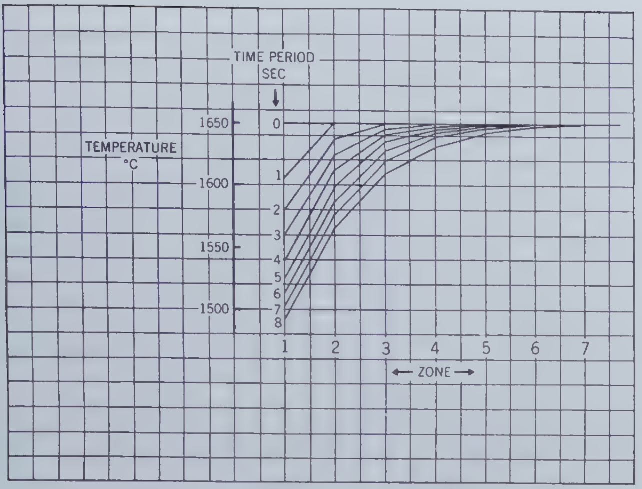

Fig. 1—Calculation of temperature distribution for the first few seconds of cooling.

0.5-cm distance. The net drop in temperature of the outer zone in this second period of time is determined by the difference between the heat lost by radiation and that gained by conduction:

$$\text{Drop in temperature, per sec} = \frac{\text{Heat radiated out per sec minus the heat conducted in per sec.}}{\text{Heat capacity of the zone}}$$

This amounts to 27°. Thus during the first 2 sec the temperature of the outer zone has dropped by 44° plus 27° or a total of 71° and is now at a temperature of 1579°.

During this second period the temperature of the second zone is also decreased by the heat being conducted away to the outer zone. This decrease is given by

$$\text{Drop in temperature of second zone} = \frac{\text{Heat conducted to outer zone}}{\text{Heat capacity of second zone}}$$

This amounts to a 12° temperature drop, and the start of the third period therefore finds the outer zone at 1579°C, the second zone at 1638°C and all others at 1650°C.

During the third-second period heat now radiates from the outer zone at a rate corresponding to a temperature of 1579°C; the heat conducted into it from the second zone is now that corresponding to a temperature gradient of 1638° minus 1579° or 59°C per 0.5 cm, and the further drop in temperature of the outer zone is calculated by the same formula as before. However, the second zone now not only loses heat to the outer zone by conduction but also gains heat by conduction from the third zone since a temperature difference has now been developed between the second and third zones. The new temperature of the second zone is now determined from the relation

$$\text{Drop in temperature of second zone, per sec} = \frac{\text{Heat conducted to outer zone minus heat conducted from third zone}}{\text{Heat capacity of second zone}}$$

It can easily be seen how the calculation proceeds from here. Each succeeding second adds a new zone to the picture of those whose temperature is changing until finally the whole electrode comes into the calculation. The chart in fig. 1 shows the zonewise temperature distribution at the end of the first few time intervals used in the calculation.

Fig. 2—Temperature distribution across a diameter at the end of one and two minutes of cooling.

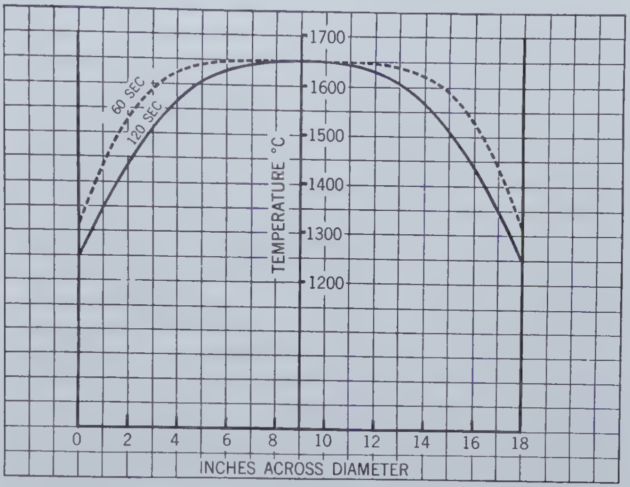

The result of this calculation is a temperature distribution curve giving the temperature at each point in the 18-in. diam. electrode at any time after it starts cooling. Two such curves are given in fig. 2 showing the temperature in various parts of the electrode after 60 sec. and 120 sec. The calculation was not carried any farther than the 2-min period because it is believed that the maximum stresses are obtained within this time.

From the temperature distribution given in fig. 2 the stresses developed in the electrodes may be calculated. A qualitative picture of what happens may be obtained by analogy with the process of putting a steel rim on a wagon wheel. The rim is made of such a size that when it is hot it will just fit over the wheel. When it cools down it shrinks due to its thermal contraction and ends up tightly bonded to the wheel. This tends to compress the wheel and the rim experiences a tensile stress in the tangential direction. Cooling down the outer part of an electrode while leaving the center part hot does the same sort of thing. It shrinks the outer skin, putting it in tension, and tends to split it open. When the temperature distribution within the electrode is known, the tangential stress for any radial distance from the center can be calculated by means of the following formula:

$$S = E\ aT + \frac{1}{R^2}\int_0^R aTxdx + \frac{1}{x^2}\int_0^x aTxdx$$

This formula involves the coefficient of thermal expansion a, the temperature T, the radius of the electrode R and the modulus of elasticity E. Calculations of the tangential stress throughout a typical 18-in. diam. electrode are given in fiig. 3. The dashed curve is the tangential stress developed after 1-min. cooling and the solid curve is that developed after 2-min. of cooling. It is seen that the center part of the electrode is under compression while the outer portion is under tension. The maximum tension is at the outside skin and is calculated to be about 900 psi. At the high temperatures involved here there is a tendency to relieve the maximum stress somewhat by plastic flow. The resulting redistribution of stresses results in a substantially lower tension than the calculated 900 psi. Nevertheless, a very considerable stress will remain that will usually exceed the strength of the electrode, causing it to crack. If the electrodes are withdrawn slowly from the furnace such high thermal gradients and stresses will not develop and this cracking can be avoided. Tests indicate that this rate of withdrawal may be so slow as to be impractical, however.

In making these calculations use is made of certain high-temperature properties of graphite electrodes. For example, in the calculation of the temperature gradients, values for the thermal conductivity, the specific heat, and the emissivity of graphite at temperatures between 1250°C and 1950°C were used. The specific heat has long been known with good accuracy, but new measurements of the thermal conductivity and emissivity were used. The calculations of the stresses developed by this temperature gradient require values for other physical properties, namely, the modulus of elasticity and the thermal expansion. Furthermore, to determine whether the electrode will actually break under the stresses developed it is necessary to know the strength of the graphite. The measurement of these properties will be discussed presently.

It is now possible to see what direction these physical properties should take for a material to be resistant to thermal shock. To keep the temperature gradient at a minimum the thermal conductivity should be as high as possible. To keep the thermal strains low the coefficient of thermal expansion should be as low as possible. So that the resulting stress from these strains will be low the elastic modulus should be low. And, finally, to withstand the thermal stress developed, the strength of the graphite should be as high as possible.

It might be pointed out that graphite with its outstandingly high thermal conductivity, extremely low thermal expansion, and extremely low modulus of elasticity is the only material which has a chance of withstanding severe conditions in the electric arc steel furnace. While its strength at room temperature is not as high as most metals, it maintains this strength to high temperatures and thus can be classed as a strong material at temperatures of the order of 1600°C.

To determine just what thermal conditions an electrode can stand on a quantitative basis it is necessary, as has been indicated in the discussion of the method of calculation, to measure thermal conductivity, thermal expansion, elastic modulus and strength. Of course, these properties are most important at extremely elevated temperatures where measurement is rather difficult and a portion of this research aimed at a better understanding of the operating conditions to which electrodes are subjected has been spent in measuring these high-temperature properties.

The high-temperature thermal expansion measurements were made with a quartz plate interferometer obtained from Gaertner Scientific Corp. A brief description of the method is as follows. The sample consists of three separate pieces of graphite placed between two quartz plates. These pieces rest on the bottom plate and support the top plate. The samples must be of almost exactly the same length so that interference fringes originating between the top surface of the lower plate and the bottom surface of the upper plate can be observed. The assembly of quartz plates with graphite sample between is placed in a furnace consisting of a refractory tube wound with nichrome wire. A rather ingenious optical system permits the projection of filtered light from a mercury lamp to be directed down to the quartz plates and the reflected light to be viewed visually. If the samples are adjusted properly, interference fringes are seen. Any change in length of the sample is observed as a shift in the position of the fringes with reference to the fixed mark on the bottom plate. The position of the fringes can be read to within one-tenth of a fringe, corresponding to a millionth of an inch displacement. Thus for a 0.5-in. sample, for a measurement made over a 100°C temperature range, an expansion of two parts in a hundred million per C° can be determined. This corresponds to an accuracy of 1 pct. The low expansion characteristics of graphite make it necessary to use an extremely sensitive method such as this. Fig. 4 shows the thermal expansion curve of an Acheson graphite electrode.

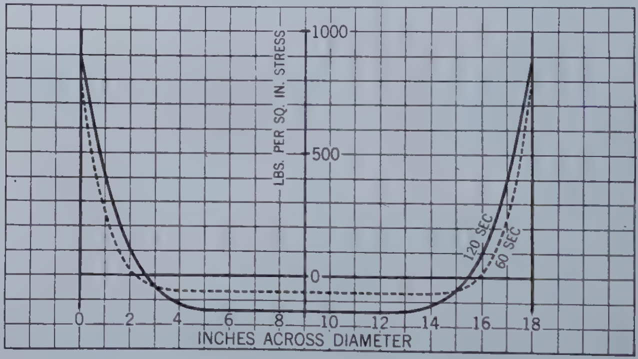

Fig. 3—Tangential stress distribution in 18-in. electrode.

There has recently been developed a method of determining thermal conductivity, based on transient heat flow, that is good up to a temperature of about 1000°C. For this thermal conductivity measurement, a bar of graphite 1 in. in diameter and 6 in. long is strongly heated at one end. Six thermocouples are inserted in the bar at the other end, spaced 0.5 in. apart and starting 0.25 in. from the end. The bar is suspended in acetylene black insulation. The readings of the six thermocouples are recorded with a high-speed six-point potentiometer recorder. In calculating the thermal conductivity the readings of the two thermocouples nearest the heat source are used to determine a thermal gradient, and the rate of rise of temperature as indicated by the last five thermocouples is combined with the specific heat to provide a measure of the heat flow. This method is much more rapid than the usual conventional methods.

There is some correction to be made to allow for heat loss to the insulation, but this correction is minimized by using acetylene black as the insulator. Acetylene black has two virtues; it is a fair insulator, and it has a very low density. The latter factor means that even if an appreciable zone around the graphite is raised in temperature during the rapid heating, no great amount of heat is involved due to the low heat capacity of the insulation. At 1000°C the total correction for loss to insulation is estimated to be only about 15 pct for a highly conducting graphite, and therefore even with a small uncertainty in the correction, fairly accurate thermal conductivity values can be determined.

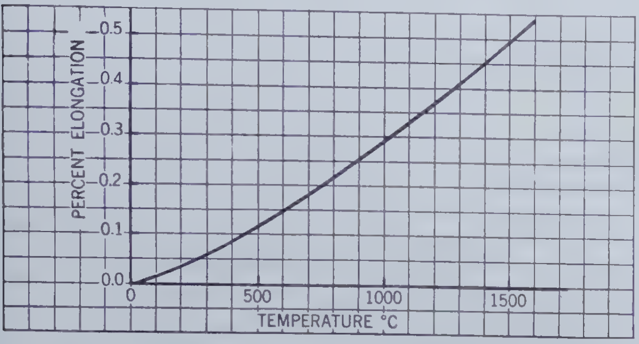

Fig. 4—Thermal expansion — Acheson graphite electrodes—percent elongation.

The rapid heating is accomplished by striking a dc arc of about 80 to 100 amp against the top end of the graphite sample. The sample is made electrically positive and is supported by a 0.5-in. diam graphite rod threaded and tapped into the sample at an angle. This rod also acts as the current contact to the sample.

As a method for determining the thermal conductivity of graphite at still higher temperatures a procedure used by Powell and Schofield in England has been modified. The method consists of heating a graphite rod in vacuum by passing a current through it, and measuring the temperature gradient from the center of the rod to the outside. Heat is generated throughout the mass of the rod by the I^2R loss. The rod is made long enough and is well enough insulated on the ends so that in the center section the heat flow is entirely radial. Two tungsten probes are inserted about 2 in. apart in the central section of the rod and are connected to a Ballantine vacuum tube voltmeter. The rod is heated with alternating current, and a measurement of this current and the voltage across the probes provides a measure of the power input per unit length of the rod. Since there is no longitudinal heat flow and since the rod operates in a vacuum, all of this power input is radiated from the surface of the section.

Temperature measurements of the surface of the rod and of the axis of the rod are made with an optical pyrometer. The axis temperature is taken by sighting to the bottom of a 1/16-in. diameter hole drilled half-way through the rod. Black-body conditions prevail in this case and the axis temperature needs no correction. The surface temperature must be corrected for the emissivity of the graphite and therefore requires a determination of the emissivity.

To determine the emissivity of the graphite surface use is made of the fact that graphite is a true gray-body, and that the spectral emissivity is the same as the total emissivity. From electrical measurements the total energy radiated from the surface is known, and from the Stefan-Boltzman Law this energy is related to the emissivity and the true surface temperature. The emissivity and true surface temperature are also related through Wien's Law to the temperature indicated by the optical pyrometer. This provides two simultaneous equations with two unknowns, the emissivity and the true surface temperature, and they are therefore determined. It is found that the emissivity or radiative power of graphite is constant with temperature and varies between 0.77 and 0.86 for surfaces of different smoothness.

The difference between the axial temperature and the true surface temperature provides the radial temperature gradient, and the electrical energy measurements provide the heat measurement, so that the thermal conductivity can be calculated by a simple formula.

The results of thermal conductivity measurements on two types of apparatus are combined into a single curve (fig. 5) for Acheson graphite. The characteristic feature of this curve is the very high thermal conductivity at low temperatures tapering off to nearly a constant value at high temperatures.

Enough measurements have been made of strength at elevated temperatures to indicate that the strength of graphite does not decrease with increasing temperature within the range of temperatures employed in an electric furnace. It has further been presumed that the elastic modulus is relatively constant with temperature so that there is dependence on rather extensive measurements of strength and elastic modulus made at room temperature.

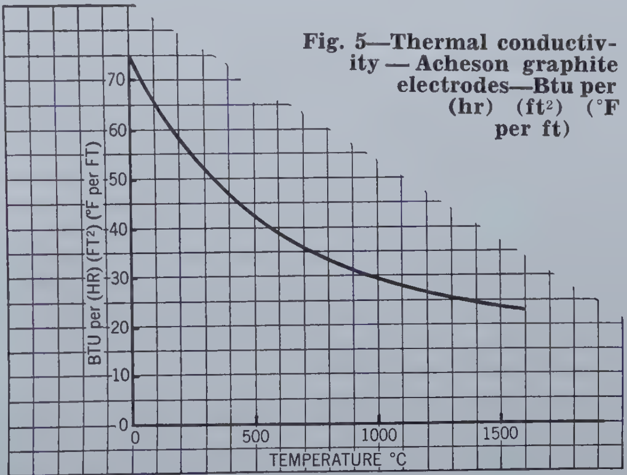

Fig. 5—Thermal conductivity — Acheson graphite electrodes—Btu per (hr) (ft²) (°F per ft)

In conclusion, a typical case of the thermal shock conditions to which graphite electrodes are exposed has been described. It has been shown that the properties of the electrodes which are important for the resistance to thermal shock are a high thermal conductivity, a low thermal expansion, a low modulus of elasticity and a high strength. It has been pointed out that graphite is outstanding in these respects. Finally, measurements made on these properties have been described in order to promote a better understanding of their service.

Titanium Binary Alloys

by C. M. Craighead, O. W. Simmons, and L. W. Eastwood

Binary alloys of titanium with silver, lead, tin, nickel, copper, beryllium, boron, silicon, chromium, molybdenum, manganese, vanadium, iron, and cobalt were studied. One-half-pound ingots of the alloys were prepared in an arc furnace, employing a water-cooled copper crucible, an argon atmosphere, and a water-cooled tungsten electrode. The half-pound ingots were fabricated by forging at 1700°F in air to 1/4-in. slab, followed by hot rolling at 1450°F to 0.060-in. sheet. Tensile properties, minimum bend radii, hardnesses, response to heat treatment and aging treatment, and phase relationships were determined for these alloys.

EARLY in 1947, as one phase of the evaluation of materials for Air Force Project RAND, Battelle successfully arc melted Bureau of Mines titanium and obtained a few basic properties of unalloyed titanium and several titanium-base alloys. The low density, excellent resistance to corrosion, and high tensile properties of these materials stimulated a great deal of interest among metallurgists and designers seeking better materials of construction. As a result of this early work, Battelle, under contract with the Air Materiel Command, Wright-Patterson Air Force Base, has continued extensive studies of titanium alloys. The result of the first year's work is described in three papers. The present one deals with binary alloys, the second with ternary alloys, and the third paper with quaternary alloys.

C. M. CRAIGHEAD, O. W. SIMMONS, and L. W. EASTWOOD are Assistant Supervisor, Research Engineer, and Supervisor, respectively; Battelle Memorial Institute, Columbus, Ohio.

The work described in this paper was sponsored by the Air Materiel Command, Wright-Patterson Air Force Base, Dayton, Ohio.

AIME New York Meeting, Feb. 1950.

TP 2747 E. Discussion (2 copies) may be sent to Transactions *AIME before Apr. 1, 1950, and is scheduled for publication Nov. 1950. Manuscript received Oct. 14, 1949.*

Melting Method

The arc furnace for melting titanium and other refractory metals was developed at Battelle Institute under Air Force Project RAND. During the present work, considerable improvement has been made in the design and operation of this furnace for making small ingots of titanium and titanium alloys. The improved furnace design is illustrated by fig. 1, which shows a cross-sectional view with the dimensions of various parts and their relationship to one another. The essential features of the furnace are the inert argon atmosphere, the water-cooled copper crucible, and the water-cooled tungsten electrode. The melting crucible is formed by spinning 0.064-in. annealed copper sheet. A groove for an O-ring seal is spun into the flange of the crucible. A fiber gasket between the crucible flange and the water-cooled brass cover provides electrical insulation. The brass cover is fitted with a sight glass, an opening for the water-cooled electrode, and a tube through which the material is charged. Direct current is used for melting, with the positive electrical terminal connected to the water jacket and the negative terminal to the electrode.

A typical heat is made in the new furnace as follows: Approximately, 0.20 lb of titanium under 2 mesh per in. and the alloy addition, if any is to be used, are placed in the bottom of the crucible. The cover is clamped on the crucible so that the O-rings make a tight seal. The remainder of the charge is placed in a glass bottle, and this is connected by a rubber hose to the charging tube of the furnace. The crucible and the charge are evacuated with a mechanical pump to a pressure below 50 mm of mercury, or less if desired, and held at this reduced pressure for 5 min. Hot water is circulated through the jacket during the evacuation period to assist in outgassing the crucible. Following the evacuation, tank argon of 99.92+ pct purity is flushed through the crucible for 5 min and then adjusted to give a positive pressure of 1 to 2 psi. During subsequent operation, an argon pressure regulator introduces only enough argon to compensate for the small leakage which occurs through a mercury trap. Re-evacuation and reflushing the melting chamber with argon produced a negligible reduction in contamination.

Two 550-amp generators, connected in parallel, constitute the power source. Normally, about 800 amp are used for melting alloys which are not extremely refractory. The generators are set for 90 v open circuit and 200 amp. The arc is struck and the electrode is withdrawn to produce an arc of 23 to 26 v. This voltage is maintained while the electrode tip is moved slowly around a circle 1 in. smaller than the diameter of the ingot. The current

*This page of Transactions AIME is a continuation from p. 436.
The missing pages appeared in Journal of Metals.*

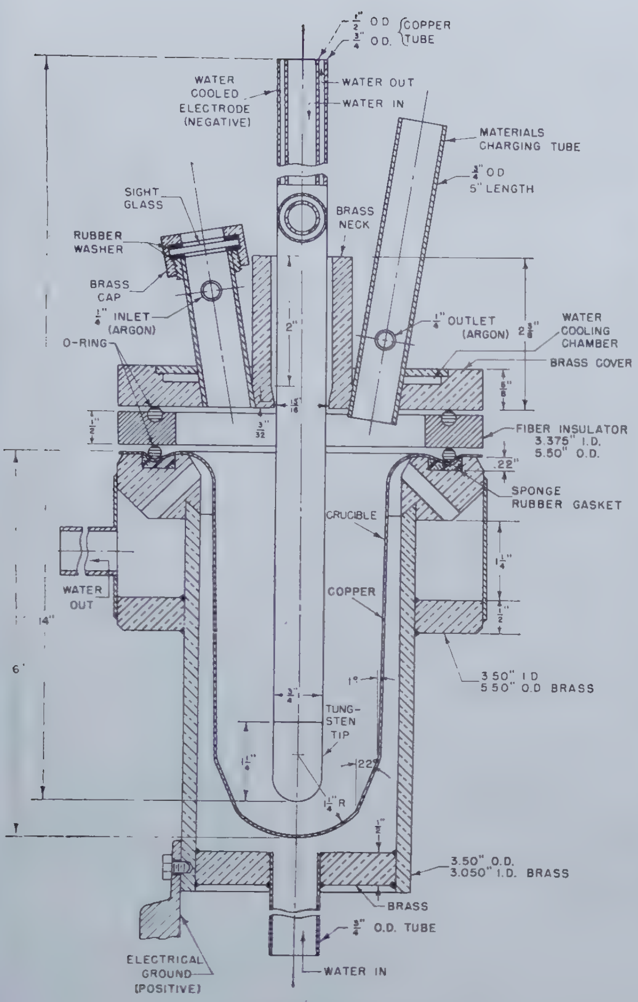

Fig. 1—Sketch of Arc Furnace.

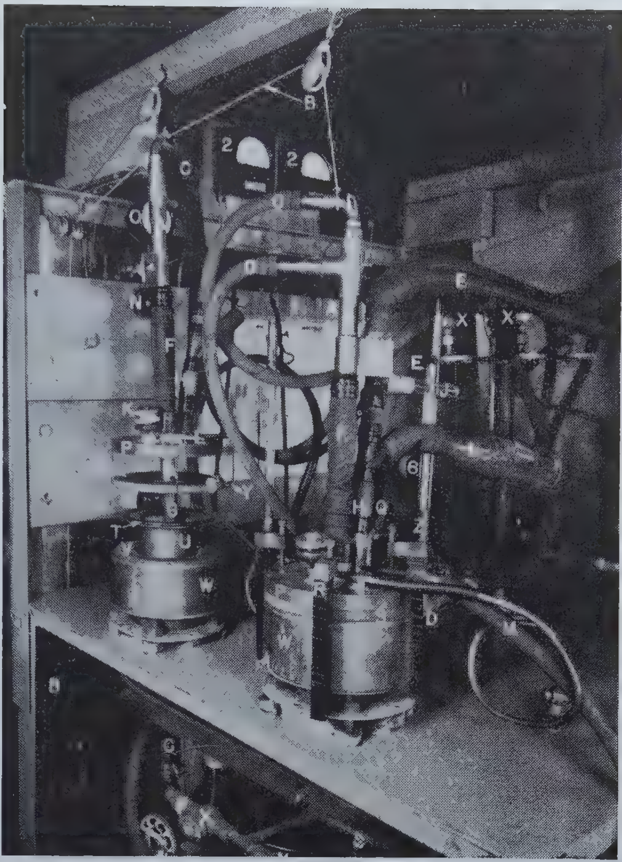

Fig. 2—View showing a small arc furnace assembled for operation and one dismantled to reveal its various parts.

A.	**Electrode (—)**	**Q.**	**Brass cover water leads**
B.	**Electrode counterbalance**	**R.**	**Clamps**
C.	**Electrode water inlet**	**S.**	**Insulating ring (micarta)**
D.	**Electrode water outlet**	**T.**	**O-ring**
E.	**Electrode power lead**	**U.**	**Copper crucible**
F.	**Electrode rubber sleeve**	**V.**	**Sponge rubber gasket**
G.	**Electrode tungsten tip**	**W.**	**Outer water jacket**
H.	**Charging tube**	**X.**	**Water controls**
I.	**Charging bottle (titanium)**	**Y.**	**Water flow manometer**
J.	**Charging bottle (alloy)**	**Z.**	**Exit-water thermometer**
K.	**Sight glass**	**1.**	**Voltmeter**
L.	**Argon inlet**	**2.**	**Ammeter**
M.	**Argon outlet and connection to vacuum pump**	**3.**	**Vacuum manometer**
N.	**Argon regulator**	**4.**	**General switch**
O.	**Argon regulator gauge**	**5.**	**Electric vibrator**
P.	**Brass cover**	**6.**	**Vibrator switch**

is then increased to 700 to 800 amp for a few minutes until the charge is molten.

The electrode is then withdrawn slightly while maintaining the arc, and a small portion of the charge is added through the charging tube in the cover. This portion is then melted in a manner similar to that described previously. The procedure is repeated until the entire charge has been added and melted. The power is gradually reduced as the ingot solidifies. The generator is then shut off, the furnace is allowed to cool for 10 to 15 min, and the ingot withdrawn from the crucible.

Fig. 2 illustrates two of these furnaces which are built and operated together, using a single power source. Using this method, one man can make five to six ½-lb ingots of the easily melted titanium alloys per day.

The contamination which occurs during the melting operation is relatively small. For example, a button ingot of 50 g of Process A titanium was melted and kept molten for 5 min, using the normal operating procedure. The Brinell hardness of the ingot was 130. After remelting, this ingot had a hardness of 143; and after remelting again, the hardness had increased to only 160. These values indicate that only a small amount of contamination takes place during melting.

Acid-leached titanium powder contains too much hydrogen to function satisfactorily in the arc furnace. A rapid evolution of the gas causes excessive spattering. On the other hand, titanium sponge produced by vacuum distillation is too massive, and a careful crushing operation is required to prepare the material for the arc furnace. After some work, the best method of crushing the sponge was found to be as follows: A clean gyratory crusher was employed and the hopper of the crusher was filled with dry titanium sponge which helped to force the stock between the crusher jaws where it was quickly crushed with a minimum of coining and abrasion. The crushed stock was then passed through a 3-mesh screen, and the oversize material was again run through the crusher. All but about 5 pct of the sponge would then pass through a 3-mesh screen. The material finer than 20 mesh is somewhat contaminated and it is not used in the alloy work. Eighty per cent of the crushed titanium sponge lies between 3 and 20 mesh. After screening, this material is washed four successive times in methanol

Table I. The Effects of Thermal and Other Treatments on the Properties of Titanium Alloys[5]

			Tensile Properties				Forming Characteristics	
Heat No.	Treatment	Test Condition	Specimen No.	Tensile Strength psi	Elongation in 1 In., Pct	Hardness (Center) VHN[1]	Minimum Bend Radii,[4] In.	Microstructure of Transverse Specimens
A5007[2]	As hot rolled	Longitudinal specimens	1	118,800	16.0			Structure very fine, grain boundaries not developed on etching. Carbides not observed.
			2	120,000	14.0			
				Avg. 119,400	15.0	254	3/16	
A5007[2]	As hot rolled	Transverse specimens	1	118,800	13.0			
			2	118,800	15.0	237 (Trans.)		
				Avg. 118,800	14.0	266 (Long.)	3/16	
A5007[2]	As hot rolled	Longitudinal specimens — surface ground	1	118,000	15.0			
			2	117,300	15.0			
				Avg. 117,700	15.0			
A5007[2]	Annealed ½ hr in air at 1450°F	Longitudinal specimens	1	100,000	18.5			Grain size less than 0.001 in.
			2	100,000	18.5			
				Avg. 100,000	18.5	224	3/64	
A5007[2]	Annealed ½ hr in air at 1450°F	Longitudinal specimens — surface ground	1	94,000	18.5			
			2	93,300	18.0			
				Avg. 93,700	18.5			
A5007[2]	Annealed 3 hr in air at 1562°F	Longitudinal specimens	1	97,500	15.5			Increase in thickness of surface layer, grain size about 0.001 in.
			2	108,000	15.0			
				Avg. 102,800	15.0	221 (defective specimen)	3/16	
A5007[2]	Annealed 3 hr in air at 1562°F	Transverse specimens	1	96,000	4.0			
			2	95,000	14.0	236 (Trans.)		
				Avg. 95,000	14.0	219 (Long.)	3/32	
A5007[2]	Air cooled from 1750°F	Longitudinal specimens	1	105,000	12.5			Acicular structure, grain size about 0.003 in.
			2	100,000	13.5			
				Avg. 102,500	13.0	226	3/16	
A5007[2]	Quenched in water from 1450°F	Longitudinal specimens	1	93,300	22.0			Grain size about 0.001 in.
			2	93,800	21.0			
				Avg. 93,600	21.5	209	3/64	
A5007[2]	Quenched in water from 1562°F	Longitudinal specimens	1	106,700	18.0			Grain size about 0.001 in.
			2	102,500	17.5			
				Avg. 104,600	18.0	245	1/8	
A5007[2]	Quenched in water from 1750°F	Longitudinal specimens	1	108,800	12.0			Increase in thickness of surface layer, acicular structure, grain size about 0.002 in.
			2	109,400	12.0			
				Avg. 109,100	12.0	241	3/16	
A5007[2]	Annealed 3 hr in air at 1562°F and cold rolled 20 pct	Longitudinal specimens	1	105,300	2.0			Grain boundaries evident in cold-rolled sheet, grain size about 0.001 in., surface skin cracked.
			2	108,000	7.0			
				Avg. 106,700	4.5	255	3/16	
A5007[2]	Annealed 3 hr in air at 1562°F, cold rolled 20 pct, quenched in water from 1450°F	Longitudinal specimens	1	100,000	17.0			
			2	100,000	17.0			
				Avg. 100,000	17.0	221	3/64	
A5008[3]	As hot rolled	Longitudinal specimens	1	121,300	16.5			Grain size about 0.002 in., carbides fine.
			2	121,300	17.0			
				Avg. 121,300	17.0	267	3/16	
A5008[3]	As hot rolled	Transverse specimens	1	126,300	16.0			
			2	127,500	16.5	279 (Trans.)		
				Avg. 126,900	16.5	301 (Long.)	3/16	
A5008[3]	As hot rolled	Longitudinal specimens — surface ground	1	120,000	17.5			
			2	128,600	15.5			
				Avg. 124,300	16.0			
A5008[3]	Annealed ½ hr in air at 1450°F	Longitudinal specimens	1	113,300	18.0			Grain size about 0.001 in., carbides fine.
			2	106,700	18.0			
				Avg. 110,000	18.0	258	1/16	
A5008[3]	Annealed ½ hr in air at 1450°F	Longitudinal specimens — surface ground	1	112,100	17.0			
			2	112,100	17.0			
				Avg. 112,100	17.0			
A5008[3]	Annealed 3 hr in air at 1562°F	Longitudinal specimens	1	112,000	16.5			Increase in thickness of surface layer, grain size about 0.001 in., carbides fine.
			2	112,000	17.0			
				Avg. 112,000	17.0	254	1/8	
A5008[3]	Annealed 3 hr in air at 1562°F	Transverse specimens	1	120,000	13.5			
			2	120,000	7.5	266 (Trans.)		
				Avg. 120,000	10.5	276 (Long.)	1/4	
A5008[3]	Air cooled from 1750°F	Longitudinal specimens	1	108,700	13.5			Carbides relatively large, structure fine, appears to be 2-phase.
			2	110,700	13.5			
				Avg. 109,700	13.5	235	3/16	
A5008[3]	Quenched in water from 1450°F	Longitudinal specimens	1	110,700	20.5			
			2	113,300	18.0			
				Avg. 112,000	19.0	264	1/8	
A5008[3]	Quenched in water from 1562°F	Longitudinal specimens	1	115,300	19.5			Carbides appear fine, grain size about 0.001 in.
			2	113,300	18.5			
				Avg. 114,300	19.0	260	1/8	
A5008[3]	Quenched in water from 1750°F	Longitudinal specimens	1	117,300	11.0			Carbides fine, grain size about 0.001 in.
			2	120,000	16.0			
				Avg. 118,700	13.5	279	3/16	
A5008[3]	Annealed 3 hr in air at 1562°F, cold rolled 20 pct	Longitudinal specimens	1	114,700	9.0			Increase in thickness of surface layer, carbides somewhat larger than above, structure fine, appears to be 2-phase.
			2	116,000	10.0			
				Avg. 115,400	9.5	285	3/16	
A5008[3]	Annealed 3 hr in air at 1562°F, cold rolled 20 pct, quenched in water from 1450°F	Longitudinal specimens	1	116,700	16.0			Grain size about 0.001 in., surface skin cracked from cold work.
			2	116,700	17.0			
				Avg. 116,700	16.5	274	1/8	

---

[1] 10-kg load. Avg of 5 readings—hardness readings taken at the center of the sheet normal to the direction of rolling and the surface unless indicated.

[2] Analysis of Heat A5007—0.14 pct C, 0.048 pct N, 0.91 pct W.

[3] Analysis of Heat A5008—0.38 pct C, 0.069 pct N, 0.48 pct W.

[4] Forming tests made on a specimen sheared 3 in. long by 0.5 in. wide. Specimen formed on an arbor press, using a V-block having a 75° included angle. Radius of forming tool progressively decreased until failure was observed. The radius reported is the smallest showing no evidence of cracking.

[5] 5-lb ingots forged at 1700°F by upsetting to ¾-in. slab, ground, then hot rolled at 1450°F to 0.060-in. sheet. Surface of specimens not ground before testing unless otherwise indicated in Col. 3.

and dried at room temperature and then in a vacuum to 10 microns pressure. The material so produced represents a fairly ideal feed for the arc furnace.

The alloy additions were made as follows:

Element	Form	Remarks
Antimony	8-mesh shot	Relatively little volatilization.
Beryllium	Beryllium chips and titanium powder compacted into pellets, 5/16-in. diam by ½ in. long	
Bismuth	99+ bismuth, 10- to 40-mesh powder	Dissolved readily without appreciable volatilization.
Boron	High-purity boron prepared by decomposition of boron tribromide, granulated, mixed with titanium powder, and pelleted as above	
Carbon	48- to 60-mesh graphite powder	
Chromium	10- to 20-mesh lumps of fused chromium containing 0.45 pct Fe, 0.37 pct Si, $<$0.02 pct Ni, 0.049 pct O, 0.0014 pct H, 0.011 pct N; or electrolytic chromium containing 0.04 pct Fe, 0.01 pct Cu, 0.015 pct S, 0.01 pct C, 0.01 pct N, and 0.31 pct O	Dissolves readily.
Cobalt	Thin, electrolytic flakes containing 0.12 pct Fe, 0.2 pct Ni, 0.02 pct C	
Copper	Clipped wire ¼ to ⅜ in. long	
Iron	4- to 8-mesh particles of electrolytic iron	
Lead	Lead shot	Approximately one-half was lost by volatilization.
Manganese	3- to 30-mesh electrolytic manganese	
Molybdenum	Molybdenum foil 0.03 in. thick by ¼ by ¾ in. bent into S-shaped pieces and mixed with the titanium	
Nickel	48-mesh electrolytic nickel	
Oxygen	10- to 20-mesh granules of a 4 pct oxygen master alloy prepared by melting	
Nitrogen	10- to 20-mesh granules of a 4 pct nitrogen master alloy prepared by melting	
Silicon	8- to 20-mesh granules of 98+ pct silicon, containing 1 pct iron	High-purity amorphous silicon not added successfully.
Silver	8- to 20-mesh 99.5 pct silver shot	
Vanadium	8- to 20-mesh granules of vanadium alloy containing 2 pct Fe, 1 pct Al, 0.9 pct Si. 0.1 pct C, 0.2 pct P, 0.04 pct Mn, and 93 pct V	
Zinc		Not added successfully.
Magnesium		Not added successfully.

Method of Fabrication

The 0.5-lb hemispherical titanium ingots prepared as described in the preceding section were first ground all over to remove defects and cold shuts on the ingot surface which had been in contact with the water-cooled copper crucible. The Brinell hardness of each ingot was then determined. The ingot hardness served as a rough measure of (1) the effect of the alloy addition, (2) any possible inhomogeneity, and (3) in the case of unalloyed titanium, provided a measure of the contamination of the metal either from melting or as a result of the use of an unsatisfactory lot of titanium. When the hardness indicated a substantial degree of inhomogeneity, these ingots were remelted.

The ingots, after grinding out surface defects preparatory to forging, were heated to 1700°F in air in a muffle furnace and forged from 1700°F, usually without reheating, by upsetting the ingots on edge to 0.25-in.-thick slabs. Heating to 1700°F required from 20 to 30 min, depending upon the number of ingots placed in the furnace. This procedure provided a degree of reduction of about 35 to 1.

In general, the titanium alloys forged very satisfactorily at 1700°F, and only a few compositions were discarded because of poor forgeability. Some edge cracking was observed at times, but this was invariably associated with defects which had not been properly ground out of the ingot surface prior to the forging operation.

After forging, scale from the forging operation was removed by sandblasting, and surface defects and edge cracking were removed by grinding. The surface of the slab was ground all over before rolling it to sheet. This conditioning removed the surface contaminated by the atmosphere while the specimen was at 1700°F. The conditioned slabs were then heated in air to 1450°F and hot rolled, using reductions of 0.06 in. per pass until 0.064-in.-thick sheet was obtained. The sheet was reheated after each pass through the rolls. All of the alloy slabs rolled satisfactorily at 1450°F with very little evidence of edge cracking.

In the as-hot-rolled condition, the titanium-alloy sheet had a thin brownish surface scale and a high-nitrogen layer, about 0.0005 in. thick. Measurements showed that the hardness gradient did not extend below the surface to a depth greater than 0.001 to 0.002 in. Specimens heated for 1 hr at 1700°F showed a hardness gradient only 0.005 in. in depth.

The above fabricating procedure carried out on the 0.5-lb ingots resulted in a sheet approximately 20 in. long by 3 to 4 in. wide. The rounded ends, being unsuited for test specimens, were removed and utilized for chemical analyses.

Effects of Various Fabricating Techniques

Early in the work, no information was available on the effects of various fabricating techniques. Likewise, there was no information on the effects of orientation of the specimen in relation to the direction to rolling, or on the effect of surface scale. Consequently, two 5-lb heats of low-alloy titanium were prepared and tested in various ways, as shown by the data in table I. The footnotes to the table contain the chemical compositions of the two alloys.

On the basis of the data in table I, the following conclusions appear to be warranted:

1. The best combination of strength and ductility of both alloys appears to be in the as-hot-rolled condition.
2. The tensile and bend-test results are substantially the same in transverse and longitudinal directions.
3. The high-nitrogen surface layer has had no appreciable effect on the tensile properties in either the as-hot-rolled or annealed conditions. This high-nitrogen layer, even when formed by heating for ½ hr at 1750°F, did not appear to have any significant effect.
4. The properties are not significantly affected by the differences in heating temperature or by the quenching treatments employed.
5. Cold working the annealed alloy did not produce any increase in tensile strength but did produce a marked reduction in elongation. However, annealing after cold working restored the properties, indicating that the metal

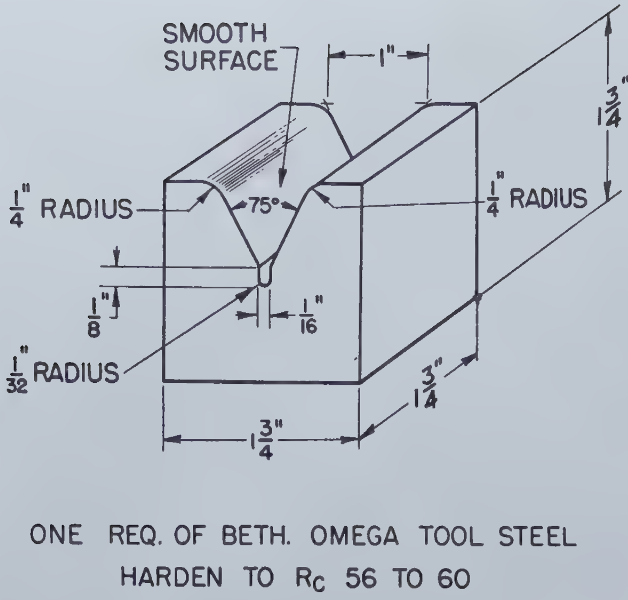

Fig. 3—Forming die for cold-bend test.

had not been damaged by the cold-working operation.

6. Cold working probably would not be a suitable means of increasing the hardness and strength of titanium alloys. It is also probable that the cold-forming characteristics of titanium alloys would be relatively poor.

Testing Methods

Bend Test: The bend test, developed by the Remington Arms Co., involved the use of forming dies shown by fig. 3 and 4. The specimens were bent through 105° by progressively decreasing the radius of the male die until cracking or failure occurred. Limited tests indicated that this procedure yields essentially the same results as those obtained with a single test strip for each male-die radius. The bend radii reported are the smallest values before cracking was observed. A ¼-in. radius was the largest employed. If the bend radii are greater than ¼ in., slight bend ductility is indicated by one asterisk and the absence of any bend ductility is indicated by two asterisks.

Tensile Tests: As a result of the data in table I, all testing was carried out on material with the as-rolled skin intact. Tensile specimens were 3 in. long by 0.375 in. wide with a 0.25-in.-wide reduced section. The load was applied at a rate of 0.04 ipm. Since these specimens were not adapted to the use of a regular strain gauge, yield strengths were not determined. In a limited number of tests, where yield strength was of some interest, the SR-4-type electrical strain gauge was employed. Tensile tests were carried out on duplicate specimens and the average results are reported.

In addition to obtaining tensile data on the as-hot-rolled sheet, data were also obtained on the material after heat treating for ½ hr at 1600°F and quenching in cold water.

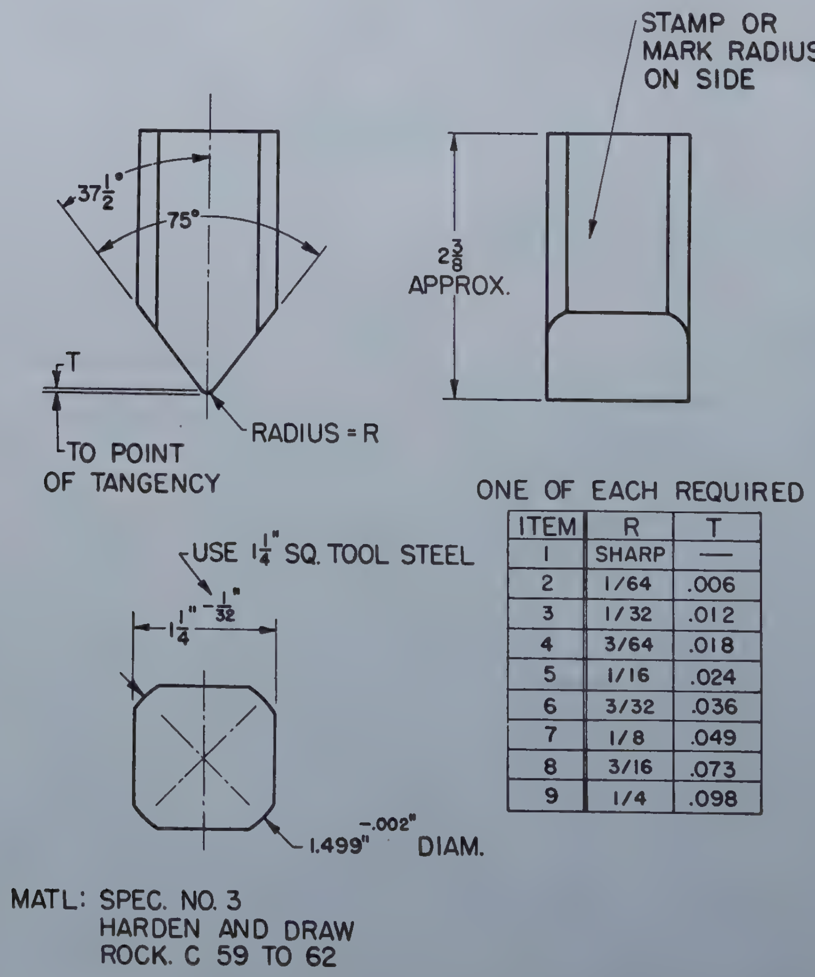

ITEM	R	T
1	SHARP	—
2	1/64	.006
3	1/32	.012
4	3/64	.018
5	1/16	.024
6	3/32	.036
7	1/8	.049
8	3/16	.073
9	1/4	.098

Fig. 4—Bend tools for cold-bend test.

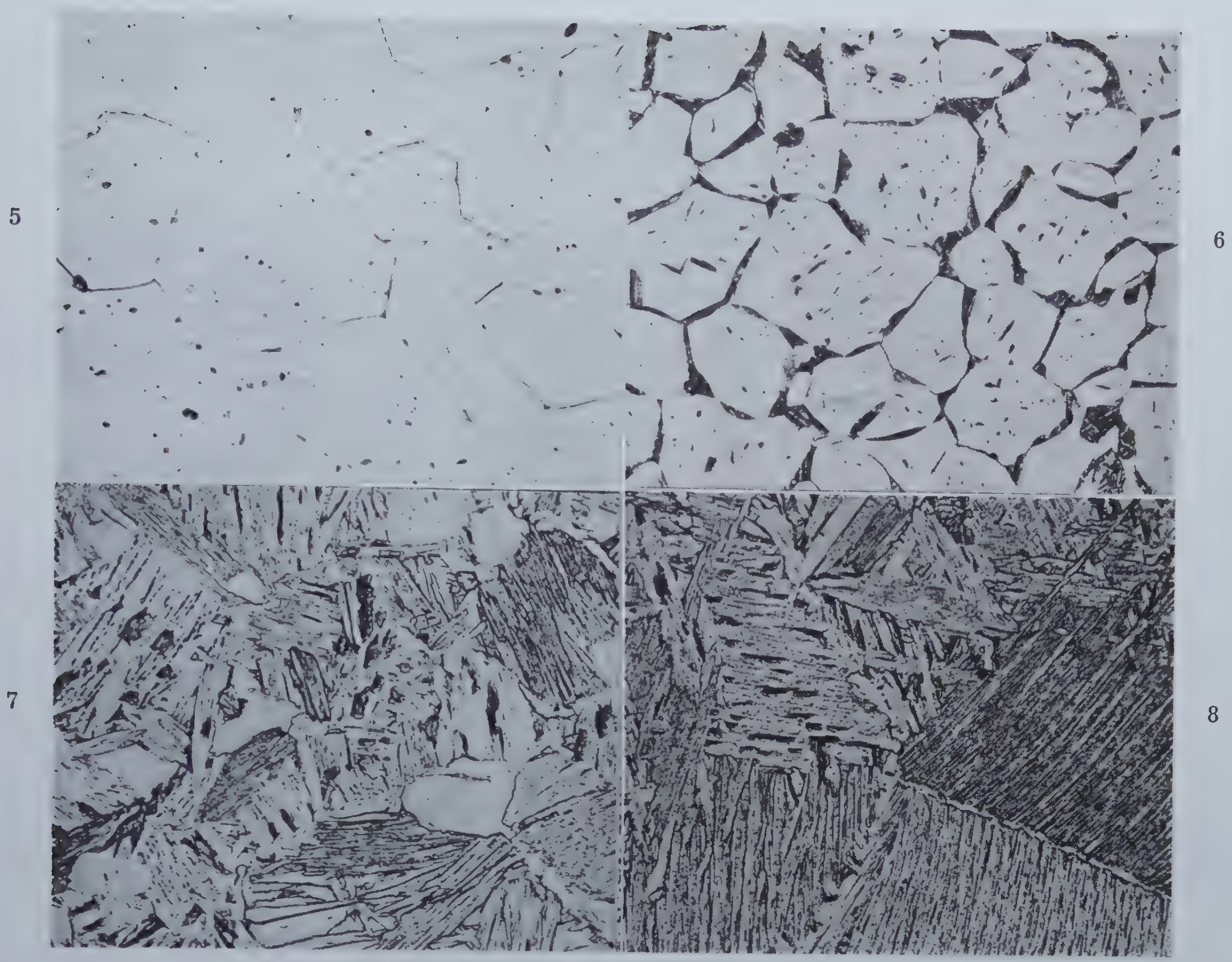

Fig. 5-8—Typical structures observed in unalloyed process A metal.

Fig. 5—Heat WC43 (unalloyed).
0.02 pct C, 0.030 pct N, 0.05 pct W. Quenched from 1450°F in the α field. Equiaxed alpha is shown. 500X.

Fig. 6—Heat WC43 (unalloyed).
0.02 pct C, 0.030 pct N, 0.05 pct W. Quenched from 1600°F in the $\alpha + \beta$ field. Alpha plus transformed beta (acicular alpha) in grain boundaries are shown. 500X.

Fig. 7—Heat WC43 (unalloyed).
0.02 pct C, 0.030 pct N, 0.05 pct W. Quenched from 1650°F in the $\alpha + \beta$ field. Island of alpha (light) in a transformed beta acicular alpha matrix is illustrated. 500X.

Fig. 8—Heat WC43 (unalloyed).
0.02 pct C, 0.030 pct N, 0.05 pct W. Quenched from 1700°F in the β field. Transformed beta (acicular alpha) is shown.

Hardness Tests: The Vickers hardness was determined on the various alloys in the as-hot-rolled condition and after a solution heat treatment consisting of ½ hr in air, generally at temperatures of 1450, 1550, 1600, 1650, 1700, and 1750°F, followed by quenching in cold water. In some of the early work, hardness was determined on specimens annealed ½ hr at 1450°F or 3 hr at 1550°F.

The hardness was determined by using a 10-kg load, and the values reported are the average of at least five readings made on each specimen at the center of the cross section of the sheet taken at 90° to the surface and to the rolling direction. Early in the work, using Process A titanium sheet, hardness anisotropy of as much as 30 points was noted between measurements taken 90° apart in reference to the rolling direction. The hardness at the center of the cross section of the specimen was used in all of the work carried out to evaluate the response of the alloys to solution heat treatment. The center hardnesses were obtained by mounting the solution heat-treated transverse specimens of each alloy in bakelite. The center hardness was then determined 90° to the surface and to the direction of rolling. Subsequently, these mounted specimens were used for metallographic studies.

Because of the large number of hardness readings required for age-hardening studies, hardness measurements for this work were made on the surface after grinding below the high-nitrogen surface layer.

Metallographic Studies: Specimens of each alloy, in the as-hot-rolled temper and after heat treatment in air for ½ hr at 1450, 1550, 1600, 1650, 1700, and 1750°F, were mounted in bakelite for hardness and metallographic studies as described previously. A transverse specimen ⅜ to ½ in. long was cut for this study. After the center hardness was measured, as described previously, the mounted specimens were reground to remove the hardness impressions

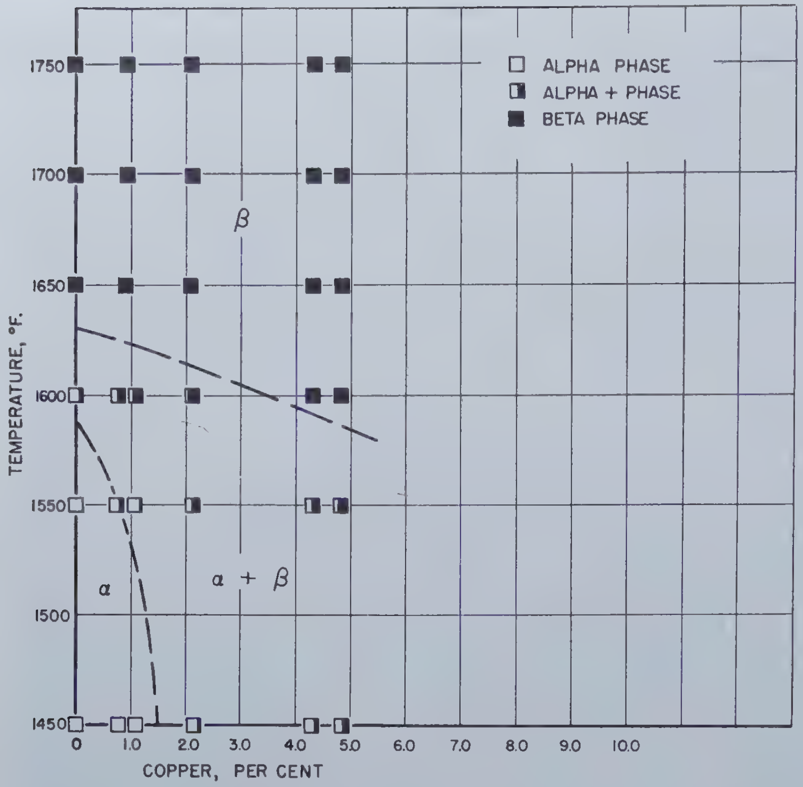

Fig. 9—Tentative diagram showing transformation range of titanium—0 to 5 pct copper alloys made from process A metal.

and then given a metallographic polish. Two etches were used to reveal the structure of the polished specimens as follows: 1. 1.5 pct HF in water. 2. 3.0 pct HNO_3 + 1.5 pct HF in water.

The second etch was particularly useful for developing the alpha-grain boundaries.

The metallographic examination was carried out to provide information on the following: 1. The effect of the various additions on the alpha-to-beta transformation. 2. The establishment of the solubility of the added alloy in both beta and alpha titanium. 3. The identification of second phases, if any, present. 4. The development of a tentative phase diagram.

Structures which could not be resolved by metallographic examination alone were also subjected to X ray diffraction studies to assist in the identification of the phases present.

No difficulties with surface contamination occurred, since this was quite superficial, and the metallographic studies were made near the center of the specimen. Since the specimens were in the rolled condition before heat treatment, it is believed that equilibrium was closely approached by the ½-hr treatment at the temperature. However, the effects of time at temperature were not studied.

Response to Heat Treatment: As indicated in the previous section, the response of titanium alloys to

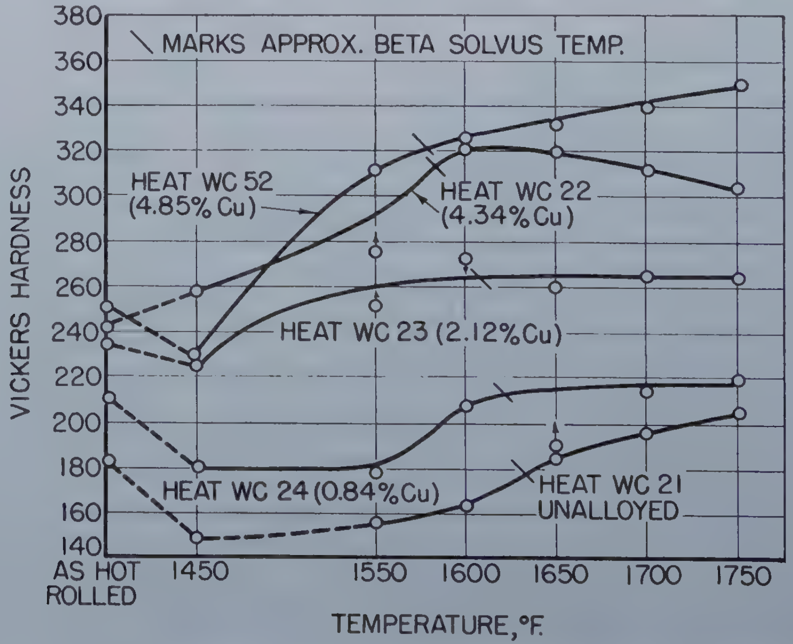

Fig. 10—Effect of solution treatment on the hardness of titanium-copper alloys prepared from process A metal.

Table II. Comparison of Properties of Titanium Alloys in the As-hot-rolled and Heat-treated Conditions[5]

Heat No.	Composition, Pct					As-Hot-Rolled Temper[1]		Heat Treated 1600°F[2], Air		Heat Treated 1600°F[3], Argon	
	Intended	Actual				Tensile Strength,[4] psi	Elongation, Pct in 1 In.	Tensile Strength,[4] psi	Elongation, Pct in 1 In.	Tensile Strength,[4] psi	Elongation, Pct in 1 In.
			C	N	W						
WC21	Unalloyed	0.05 Cu	0.09	0.023	0.10	64,600	21.0	58,300	22.5	64,100	34.0
WC23	2.5 Cu	2.12 Cu	0.06	0.024	0.65	109,900	13.0	110,300	10.0	103,800	10.5
WC29	Unalloyed	0.15 Fe	0.02	0.026	0.28	85,200	21.0	75,000	20.5	71,100	26.0
WC36	2.5 Cu, 0.25 C	2.07 Cu	0.25	0.038	0.08	114,000	14.5	126.600	15.0	101,500	18.0
WC37	2.0 Fe	2.20 Fe	0.05	0.05	0.47	146,500	8.5	146,500	2.5	134,300	8.0
WC33	2.0 Fe, 0.25 C	2.14 Fe	0.19	0.024	0.68	125,000	10.0	125,000	17.0	127,900	8.5
WC44	2.5 Mn	2.08 Mn	0.02	0.029	0.06	128,000	14.0	141,200	7.0	125,100	6.0
WC59	2.5 Mn, 0.25 C	2.24 Mn	0.14	0.019	0.20	132,700	13.0	150,800	7.0	124,700	7.0
WC69	2.5 V	2.38 V	0.03	0.027	0.31	104,000	21.0	118,800	10.0	112,500	12.0
WC73	2.5 V, 0.25 C	2.29 V	0.27	0.044	0.18	113,600	18.0	134,400	5.0	128,700	12.5
WAB2	3.5 Cr	3.27 Cr	0.09	0.088	1.15	169,600	7.5	141,400	2.0	183,400	2.0
WAB1	5.0 Cr	4.78 Cr	0.09	0.118	0.20	182,400	7.0	106,300	1.0	93,300	1.0
WAB4	2.5 Cr, 0.25 C	2.28 Cr	0.28	0.135	0.14	171,200	8.0	165,700	3.0	145,000	4.0
WC15	5.0 Cr, 0.25 C	4.94 Cr	0.25	0.054	0.52	179,900	5.0	125,000	1.0	120,100	2.0

[1] As hot-rolled at 1450°F, tested with surface skin present.
[2] Heat treated in air for ½ hr at 1600°F and quenched in cold water. Tested with surface skin present.
[3] As-fabricated skin ground off, heat treated ½ hr in argon at 1600°F, and quenched in cold water.
[4] Average of 2 longitudinal 14-ga specimens 3 in. long by 0.375 in. wide with a 0.250-in.-wide reduced section.
[5] Forged at 1700°F by upsetting 2¼-in. diam ingot on edge to 0.250-in. slab, then ground and hot rolled at 1450°F to 0.060-in. sheet—total reduction 35:1.

Table III. Properties of Binary Titanium Alloys[6] Prepared from Process A Metal Base (Group I Elements)

Heat No.	Composition, Pct					As-Hot-Rolled Temper[1]				Heat Treated 1600°F[2]			
	Intended	Actual				Tensile Strength,[3] psi	Elongation, Pct in 1 In.	VHN[4]	Minimum Bend Radius,[5] In.	Tensile Strength,[3] psi	Elongation, Pct in 1 In.	VHN[4]	Minimum Bend Radius,[5] In.
			C	N	W								
						Titanium-Copper Alloys							
WC21	Unalloyed	$<$0.05 Cu	0.09	0.023	0.10	64,600	21.0	182	1/32	58,300	22.5	164	1/32
WC29	Unalloyed	0.15 Fe	0.02	0.026	0.28	85,200	21.0	196	3/32	75,000	20.5	169	3/64
WC24	1.0 Cu	0.84 Cu	0.07	0.025	0.52	92,000	19.5	210	3/16	80,700	20.5	208	3/16
WC23	2.5 Cu	2.12 Cu	0.06	0.024	0.65	109,900	13.0	234	3/16	110,300	10.0	273	$>$1/4
WC22	5.0 Cu	4.34 Cu	0.06	0.028	0.05	107,400	9.0	242	3/16	138,300	4.0	322	$>$1/4
WC52	5.0 Cu	4.85 Cu	0.02	0.033	0.01	115,300	13.0	251	3/16	149,500	5.5	326	$>$1/4
WG81	1.0 Cu					88,400	20.5	199	3/32	81.300	14.5	193	$>$1/4*
WG70	Unalloyed					77,800	23.5	180	3/64	66,600	23.5	160	3/64
WC101	Unalloyed					76,700	19.5	189	3/32	76,800	19.0	194	3/32
						Titanium-Silver Alloys							
WC77	Unalloyed		0.04	0.026	0.10	76,700	21.0	184	1/32	74,300	20.0	170	1/32
WC94	1.0 Ag	0.87 Ag	0.03	0.085	0.18	79,000	20.5	197	3/32	76,700	20.0	177	3/32
WC96	2.0 Ag	2.12 Ag	0.02	0.035	0.08	93,200	21.5	207	3/32	83,300	21.0	187	3/32

[1] As hot rolled at 1450°F.
[2] Heated in air ½ hr at 1600°F and quenched in cold water.
[3] Average of 2 longitudinal 14-ga specimens, 3 in. long by 0.375 in. wide with a 0.250-in. wide reduced section. Tested with the surface skin present.
[4] 10-kg load. Hardness at the center of the cross section of the sheet 90° to the surface and to the rolling direction.
[5] Minimum bend radius without cracking on a single longitudinal specimen 3 in. long by 0.5 in. wide. Tested with the surface skin present.
[6] Forged at 1700°F by upsetting the 2¼-in. diam ingot on edge to 0.250-in. slab, then ground and hot rolled at 1450°F to 0.060-in. sheet.
* Some ductility

solution heat treatment in air for ½ hr at temperatures ranging from 1450 to 1750°F was followed by changes in Vickers hardness measured at the center of transverse specimens.

The possibility that some of the alloys might respond to age hardening was studied by following the changes in Vickers hardness. When the aging studies were made by measuring the hardness after progressive intervals of time at the aging temperature, the measurements were made on the surface after grinding off the high-nitrogen layer.

The properties of several alloys were obtained in the as-hot-rolled condition, after heat treatment in air at 1600°F, and after heat treatment in argon at 1600°F; the data are listed in table II. The alloys heat treated in air were tested with the as-fabricated skin present, whereas those heat treated in argon were surface ground prior to heat treatment. Again, it is evident that the best combination of strength and ductility is obtained in the as-hot-rolled condition and that no appreciable benefit is obtained by heat treating in argon or removing the surface skin. Accordingly, all tests on the alloy development have been carried out on specimens with the as-fabricated skin present.

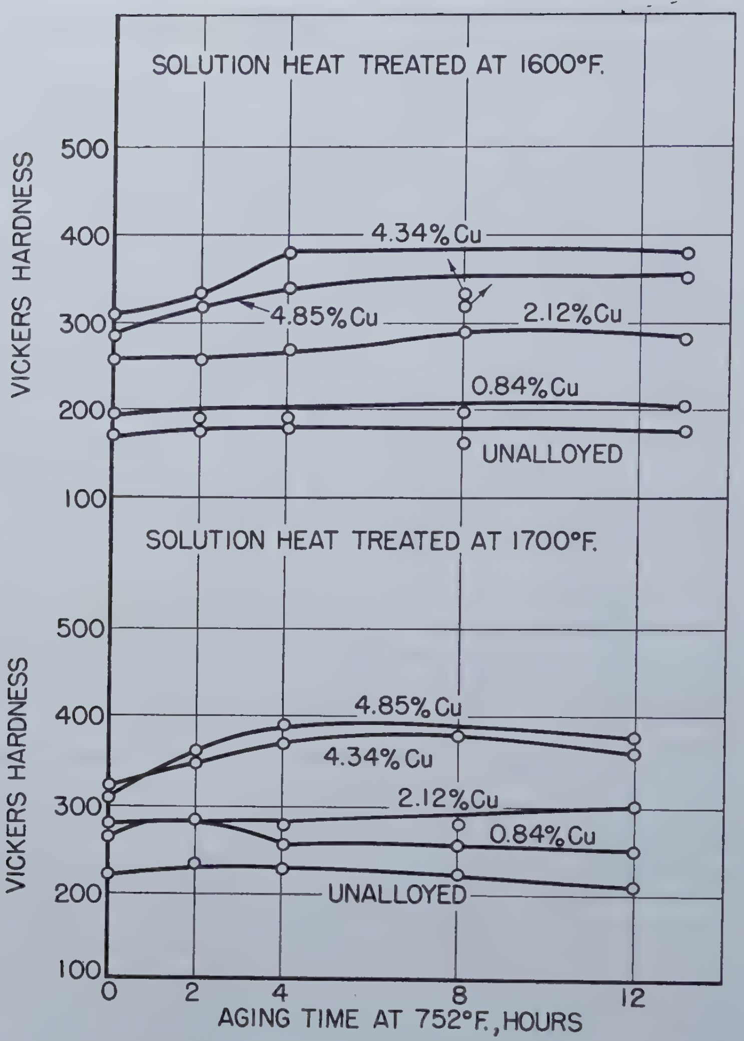

Fig. 11—Effect of aging on the hardness of titanium-copper alloys prepared from process A metal.

Table IV. Properties of Binary Titanium Alloys[7] Prepared from Process A Metal Base (Group II Elements)

Heat No.	Composition, Pct		As-Hot-Rolled Temper[1]				Heat Treated 1600°F[2]			
	Intended	Actual	Tensile Strength,[3] psi	Elong., Pct in 1 In.	VHN[4]	Minimum Bend Radius,[5] In.	Tensile Strength,[3] psi	Elong., Pct in 1 In.	VHN[4]	Minimum Bend Radius,[5] In.
WH107	Unalloyed		87,500	21.5	205	3/32	74,900	21.0	179	3/32
WA22[6]	5.0 Be									
WH103	1.0 Be		101,500	9.0	215	3/16	136,800	5.5	303	>1/4*
WH102	2.0 Be		106,000	2.0	252	>1/4*	111,800	2.0	297	>1/4*

[1] As hot rolled at 1450°F.
[2] Heated in air ½ hr at 1600°F and quenched in cold water.
[3] Average of 2 longitudinal 14-ga specimens, 3 in. long by 0.375 in. wide with a 0.250-in. wide reduced section. Tested with the surface skin present.
[4] 10-kg load. Hardness at the center of the cross section of the sheet 90° to the surface and to the rolling direction.
[5] Minimum bend radius without cracking on a single longitudinal specimen 3 in. long by 0.5 in. wide. Tested with surface skin present.
[6] Too brittle to forge.
[7] Forged at 1700°F by upsetting the 2¼-in.-diam. ingot on edge to 0.250-in. slab, then ground and hot rolled at 1450°F to 0.060-in. sheet—total reduction 35:1.
* Some ductility.

Properties of Unalloyed Titanium Sheet

During the course of this investigation, about forty 0.5-lb ingots of unalloyed Dupont Process A titanium were prepared, fabricated to sheet, and tested with the various series of alloys. The data on these heats served for control and provided data on the uncontrolled variations which might occur in the base material. The minimum, average, and maximum mechanical properties of the unalloyed Process A titanium sheet were as follows:

Property	Minimum	Average	Maximum
Tensile strength, psi	64,600	81,400	91,300
Elongation, pct in 1 in.	18.0	20.8	24.5
Vickers hardness	163	187	205
Minimum bend radius, in.	1/64	1/16	1/8

Analyses have been made on about 12 of the 38

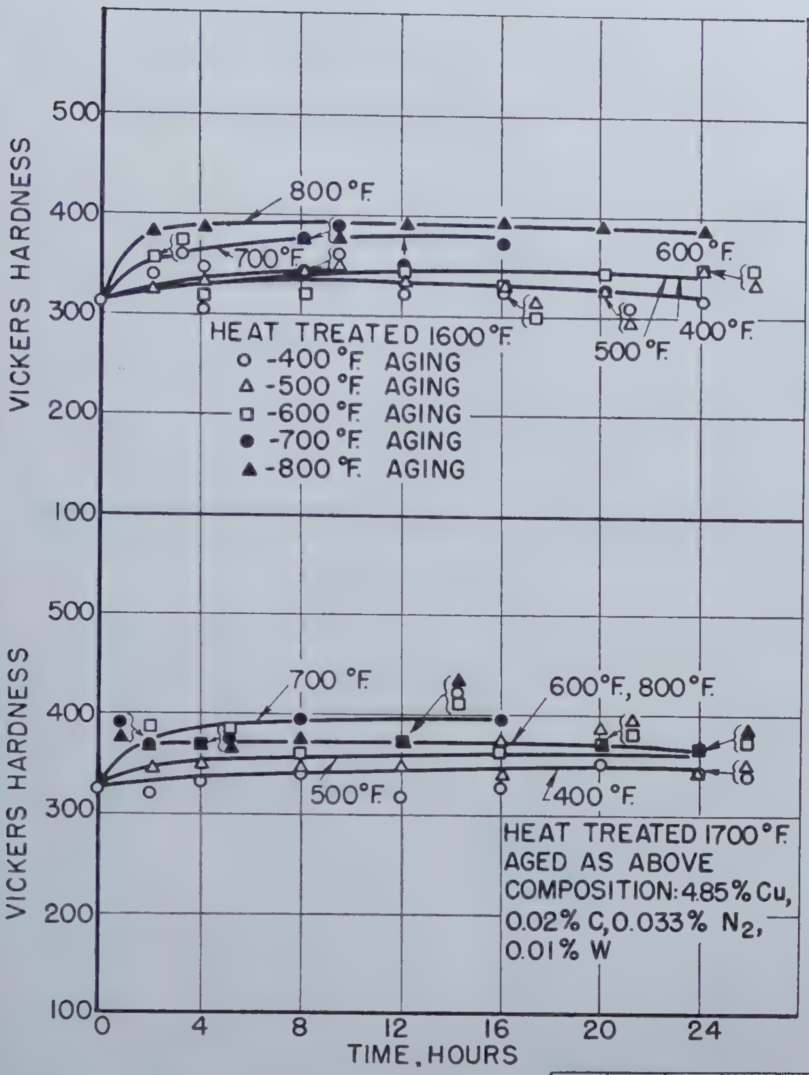

Fig. 12—Aging curves for a titanium-copper alloy (heat WC52) prepared from process A metal.

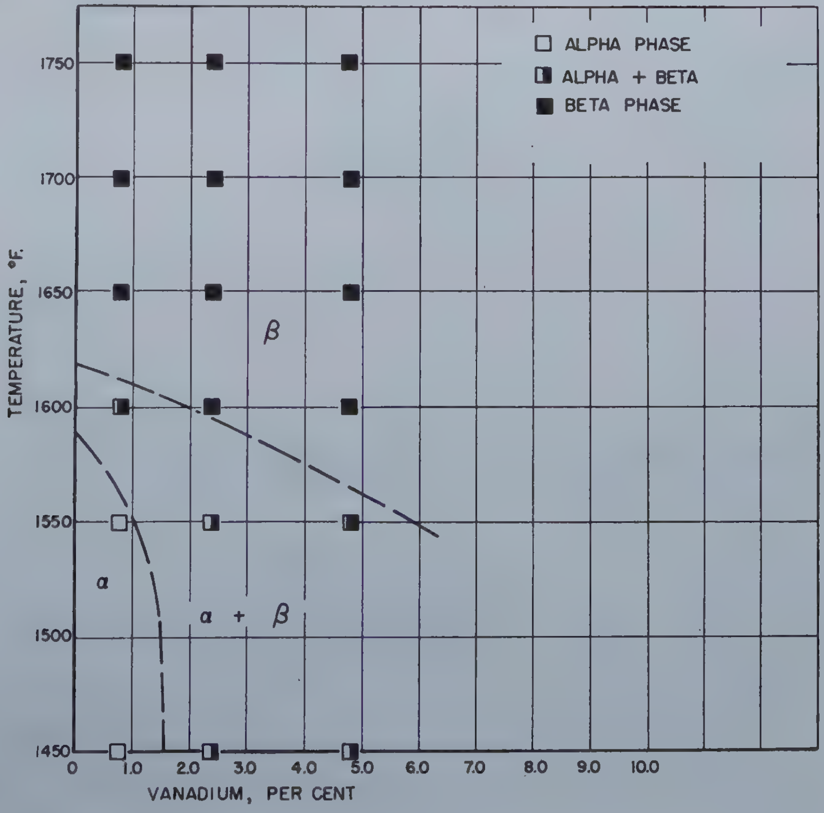

Fig. 13—Tentative diagram showing transformation range of titanium—0 to 5.0 pct vanadium alloys made from process A metal.

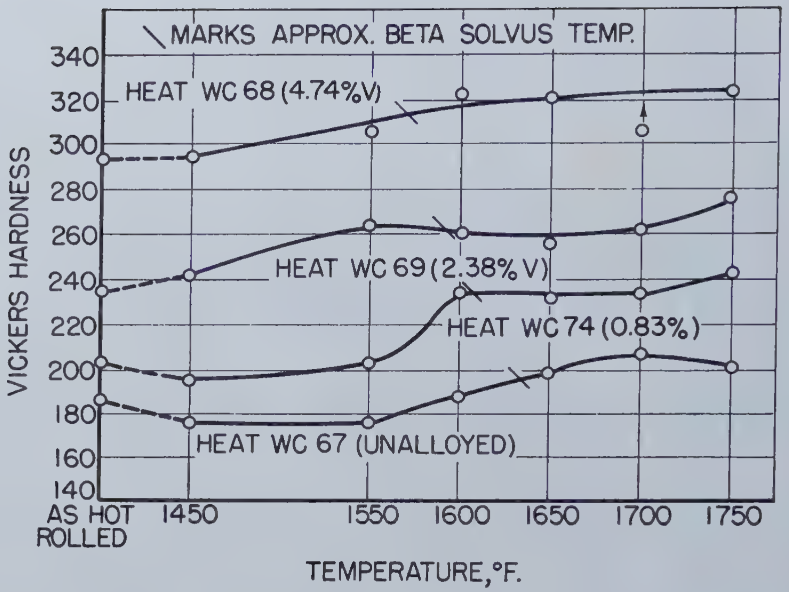

Fig. 14—Effect of solution treatment on the hardness of titanium-vanadium alloys prepared from process A metal.

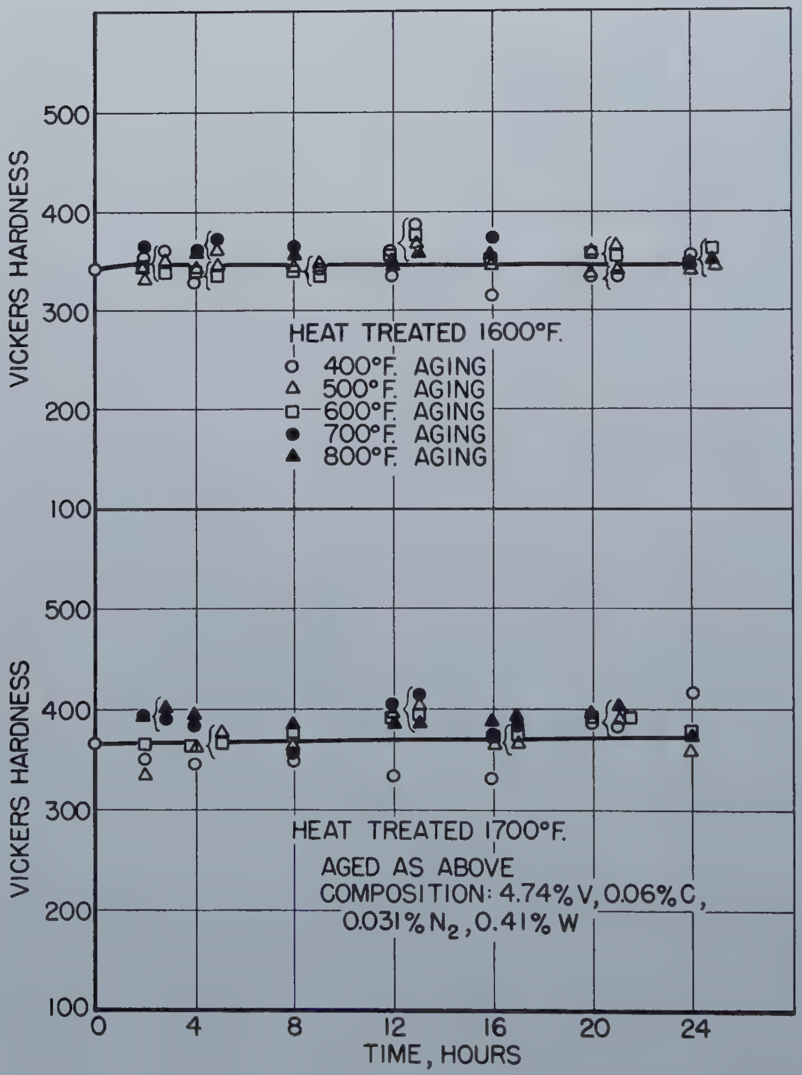

Fig. 15—Aging curves for a titanium-vanadium alloy (heat WC68) prepared from process A metal.

heats. The results of these analyses showed the following:

Carbon — 0.02 to 0.09 pct
Nitrogen — 0.02 to 0.055 pct
Tungsten — 0.04 to 0.46 pct

The average Process A sheet contained 0.04 pct carbon, 0.031 pct nitrogen, and 0.24 pct tungsten. One heat was analyzed and found to contain 0.05 pct copper. Two different heats contained 0.15 and 0.14 pct iron. Undoubtedly, the copper is picked up from the copper crucible and a large portion of the iron is picked up during the crushing operations. Because of the tungsten electrode employed, this element is a normal contaminant of all the arc-melted ingots. At the time this work was done, a method of analyzing for oxygen was not available. Therefore, the degree of this contamination is not known. However, recent analytical results* indicate that Process A titanium sponge contains about 0.13 pct oxygen. The cause of the slight variation in mechanical properties of the unalloyed titanium sheet as noted above could not be established by the analytical work. In all probability, the largest unknown variable is the oxygen content of the metal.

Heat treatment at 1600°F, which is generally in the alpha-plus-beta field, produces properties equivalent to those obtained on the annealed material. The minimum, average, and maximum properties of Process A titanium sheet after solution heat treating the unalloyed material in air for ½ hr at 1600°F were as follows:

Property	Minimum	Average	Maximum
Tensile strength, psi	58,300	74,100	83,100
Elongation, pct in 1 in.	12.0	19.3	26.0
Vickers hardness	147	172	200
Minimum bend radius, in.	1/32	1/16	3/16

In general, a heat having high hardness in the as-hot-rolled condition also had hardness on the high side after heat treatment. This indicates that the high hardness is a function of composition and not of any possible residual cold work in the hot-rolled material. It may be further concluded from these data, as well as from the data on hardness after heat treating at 1450, 1550, 1600, 1650, 1700, and 1750°F and hardness data obtained after quenching from 1600°F and aging at 750°F, that unalloyed titanium does not respond to solution heat treatment or aging treatment. However, a slight increase in hardness does occur when the material is heated into the beta field, presumably because of the formation of acicular alpha instead of the equiaxed alpha which forms when the metal recrystalizes below the transformation temperature.

Twenty-eight of the unalloyed heats, heat treated as described previously, were examined metallographically to establish the transformation range. All of the unalloyed materials in the as-hot-rolled condition consisted of equiaxed alpha. When this material was heated into the alpha-plus-beta field and then into the beta field, larger quantities of transformed beta or acicular alpha were formed when the metal was cooled to room temperature. This is illustrated by the micrographs, fig. 5, 6, 7, and 8.

Of the 28 unalloyed heats examined, 3 began to transform to beta at temperatures slightly under 1450°F. Fourteen began to transform between 1450 and 1550°F, and the remaining 11 began to transform to beta between 1550 and 1600°F. Nineteen of the 28 unalloyed heats were all beta at a temperature between 1600 and 1650°F. The remaining were completely transformed to beta at temperatures between 1650 and 1700°F. All of the heats of unalloyed titanium transformed over a range in temperature rather than at a single temperature. Thus it appears that unalloyed titanium transforms over a range in temperature and a considerable variation occurs in the transformation range of the various heats. These variations in the transformation range are a direct result of the differences in the impurities in the unalloyed material. Small amounts of elements such as oxygen, nitrogen, and tungsten have a very potent effect on the transformation range.

Properties of Titanium Binary Alloys

Binary Titanium-Copper Alloys: Table III contains the data on mechanical properties of the titanium-copper binary alloys in the as-hot-rolled condition and after heat treating at 1600°F. Fig. 45 is a graphical representation of the effects of copper on the tensile properties of the alloys in the as-hot-rolled condition. Fig. 9 shows the effect of copper on the transformation range, while fig. 10 shows the effect of various heat treatments on the hardness of the alloys. These figures show that the 4 or 5 pct copper alloys are hardened appreciably when quenched from the beta field. As shown by the data in table III this treatment increases the tensile strength but markedly lowers the per cent elongation. However, heat treatment of higher copper alloys may be more favorable.

Fig. 11 and 12 show the response of the alloys to the aging treatments. The latter two figures show that the alloys containing 4.5 to 5 pct copper age harden slightly. Data not shown in the paper also indicate that these alloys in the as-hot-rolled condition age harden slightly.

It may be concluded that copper does not produce binary alloys of titanium which have outstanding properties.

Binary Titanium-Silver Alloys: Silver alloys were investigated only up to 2 pct silver. Data on the mechanical properties of these alloys are shown in table III and by fig. 45. Alloys containing up to 2 pct silver do not respond favorably to heat treatment. Data not reproduced in the paper show that 2 pct silver markedly raises the beta solvus line and lowers the alpha solvus line. Alloys containing up to 2 pct silver do not have outstanding properties, though higher silver contents may be somewhat better.

Binary Titanium-Beryllium Alloys: Table IV contains the data on mechanical properties of titanium-beryllium binary alloys in the as-hot-rolled condition and after heat treating at 1600°F. The data on the alloys in the as-hot-rolled condition are also illustrated by fig. 45. The solubility of beryllium in beta titanium at 1750°F is apparently between 1 and 2 pct. The solubility of beryllium in alpha titanium, even at temperatures near the transforma-

---

* Carried out at Naval Research Laboratory, Anacostia, Washington, D. C.

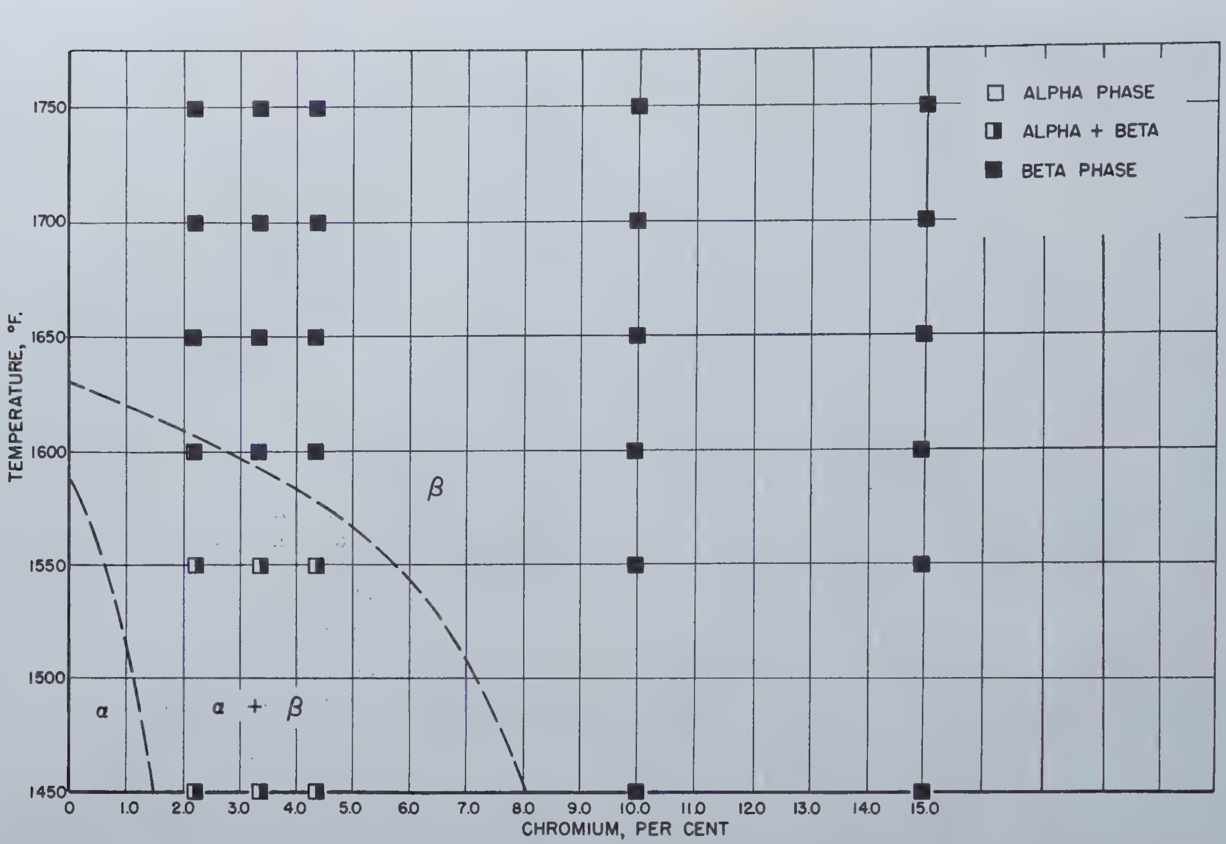

Fig. 16—Tentative diagram showing transformation range of titanium—0 to 15 pct chromium alloys made from process A metal.

tion range, is considerably less than 1 pct. The 1 and 2 pct beryllium alloys were hardened and strengthened by a solution heat treatment at 1600°F, but at considerable sacrifice in ductility. It may be concluded that beryllium is not useful as a major alloying element in titanium, though it may prove to be useful as a minor addition to more complex alloys.

Binary Titanium-Boron Alloys: Table V contains data on the mechanical properties of a few titanium-boron alloys in the as-hot-rolled condition and after heat treating at 1600°F. The limit of solubility of boron in both alpha and beta titanium near the transformation temperature appears to be less than 0.1 pct. None of the alloys was favorably affected by solution heat treatment. Like beryllium, it may be concluded that boron is not useful as a major alloying element in titanium, but it conceivably might be useful as a minor addition in more complex alloys.

Binary Alloys of Titanium With Silicon, Tin, and Lead: The mechanical properties of the binary alloys of titanium with silicon, tin, or lead in the as-hot-rolled condition and after aging at 1600°F are listed in table VI. The data on the silicon alloys in the as-hot-rolled condition are graphically illus-

Table V. Properties of Binary Titanium Alloys Prepared from Process A Metal Base (Group III Elements)

Heat No.	Composition, Pct		As-Hot-Rolled Temper[1]				Heat Treated 1600°F[2]				Annealed 1450°F[6]		
	Intended	Actual	Tensile Strength,[3] psi	Elong., Pct in 1 In.	VHN[4]	Minimum Bend Radius,[5] In.	Tensile Strength,[3] psi	Elong., Pct in 1 In.	VHN[4]	Minimum Bend Radius,[5] In.	Tensile Strength,[7] psi	Elong., Pct in 1 In.	VHN[4]
WAO12[8]	Unalloyed										90,300	16.0	203
WA25[9]	0.1 B										94,700	19.0	245
WH107[8]	Unalloyed		87,500	21.5	205	3/32	79,400	21.0	179	3/32			
WH106[8]	0.1 B		98,300	13.5	214	1/4*	88,800	15.0	205	3/16			
WH105[8]	0.25 B		90,700	16.5	204	3/16	82,800	15.0	192	3/16			
WH104[8]	0.50 B		95,100	13.5	218	3/16	88,000	13.5	201	3/16			

[1] As hot rolled at 1450°F.
[2] Heated in air ½ hr at 1600°F and quenched in cold water.
[3] Average of 2 longitudinal 14-ga specimens, 3 in. long by 0.375 in. wide with a 0.250-in. wide reduced section. Tested with the surface skin present.
[4] 10-kg load. Hardness at the center of the cross section of the sheet 90° to the surface and to the rolling direction.
[5] Minimum bend radius without cracking on a single longitudinal specimen 3 in. long by 0.5 in. wide. Tested with surface skin present.
[6] Annealed ½ hr in air at 1450°F and air cooled.
[7] Longitudinal 8-in. specimens with 0.5-in. reduced section. 14-ga sheet.
[8] Forged at 1700°F by upsetting the 2¼-in. diam ingot on edge to 0.250-in. slab, then ground and hot rolled at 1450°F to 0.060-in. sheet. Total reduction 40:1.
[9] Forged at 1700°F by pancaking the 0.5-in.-thick ingot to 0.250-in. slab. Total reduction 8:1.
* Some ductility.

Table VI. Properties of Binary Titanium Alloys Prepared from Process A Metal Base (Group IV Elements)

Heat No.	Composition, Pct					As-Hot-Rolled Temper[1]				Heat Treated 1600°F[2]				Annealed 1450°F[6]		
	Intended	Actual	C	N	W	Tensile St'gth,[3] psi	Elong., Pct in 1 In.	VHN[4]	Minimum Bend Radius,[5] In.	Tensile St'gth,[3] psi	Elong., Pct in 1 In.	VHN[4]	Minimum Bend Radius,[5] In.	Tensile Strength,[7] psi	Elong., Pct in 1 In.	VHN[4]
						Titanium — Silicon Alloys										
WA012[8]	Unalloyed													90,300	16.0	203
WA7[9]	1.6 Si													133,200	2.0	330
WC86[8]	Unalloyed					91,300	24.5	194	1/16	78,500	24.0	167	1/16			
WC116[8]	0.5 Si	0.44 Si				104,100	17.0	236	3/16	89,700	18.0	216	3/16			
WC117[8]	1.0 Si	0.93 Si				95,000	14.0	239	3/16	93,500	15.0	203	3/16			
WC118[8]	2.0 Si	2.09 Si				122,700	9.0	239	>1/4*	105,300	10.0	228	3/16			
WC119[8]	3.0 Si	2.84 Si				121,900	2.0	258	>1/4*	104,700	5.0	245	>1/4†			
						Titanium — Tin Alloys										
WG70[8]	Unalloyed					77,800	23.5	180	3/64	66,300	23.5	160	3/64			
WG76[8]	0.10 Sn	0.09 Sn				81,000	22.5	189	3/32	69,400	21.5	160	3/64			
WG74[8]	0.25 Sn	0.21 Sn				79,400	21.5	191	3/32	66,900	21.0	165	1/32			
WG75[8]	0.50 Sn	0.31 Sn				80,000	21.0	184	3/64	67,500	19.5	167	3/64			
WG77[8]	1.0 Sn	1.08 Sn				84,400	19.0	192	3/16	69,400	24.0	169	3/64			
WG80[8]	2.0 Sn	1.69 Sn				90,700	20.5	187	3/32	78,800	19.0	171	3/32			
						Titanium — Lead Alloys										
WAO12[8]	Unalloyed													90,300	16.0	203
WC43[8]	Unalloyed		0.02	0.030	0.05	75,000	20.5	190	3/64	71,000	23.5	172	3/64			
WA27[8]	1.0 Pb													121,800	7.0	243
WC51[8]	1.0 Pb	0.53 Pb	0.03	0.041	0.48	91,400	19.5	199	3/64	81,100	23.5	190	1/16			
WC47[8]	2.5 Pb	1.26 Pb	0.02	0.058	1.04	97,500	19.0	211	3/32	97,500	18.0	226	3/64			
WC45[8]	5.0 Pb	2.15 Pb	0.03	0.042	0.28	93,600	20.0	207	3/32	87,900	22.5	217	1/16			

[1] As hot rolled at 1450°F.

[2] Heated in air ½ hr at 1600°F and quenched in cold water.

[3] Average of 2 longitudinal 14-ga specimens, 3 in. long by 0.375 in. wide with a 0.250-in. wide reduced section. Tested with the surface skin present.

[4] 10-kg load. Hardness at the center of the cross section of the sheet 90° to the surface and to the rolling direction.

[5] Minimum bend radius without cracking on a single longitudinal specimen 3 in. long by 0.5 in. wide. Tested with surface skin present.

[6] Annealed ½ hr in air at 1450°F and air cooled.

[7] Average of 2 longitudinal 8-in. specimens with 0.5-in. reduced section. 14-ga sheet.

[8] Forged at 1700°F by upsetting the 2¼-in.-diam. ingot on edge to a 0.250-in. slab, then ground and hot rolled at 1450°F to 0.060-in. sheet. Total reduction 35:1.

[9] Forged at 1700°F by pancaking the 0.5-in.-thick ingot to a 0.250-in. slab, then ground and hot rolled at 1450°F to 0.060-in. sheet. Total reduction 8:1.

* Some ductility.

† Very little ductility.

trated by fig. 45. Metallographic examination indicates that the solubility of silicon in both alpha and beta titanium near the transformation range is somewhat less than 0.4 pct. Like boron and beryllium, silicon is not useful as a major alloying element in titanium, but might be useful as a minor addition to more complex alloys.

Tin, at least up to 1.7 pct, appears to be soluble in both alpha and beta titanium. Up to this concentration, it appears to have relatively little effect on the tensile properties or upon the transformation range. Neither are the alloys benefited by solution or aging heat treatments.

Lead up to 2.1 pct appears to be soluble in both alpha and beta titanium near the transformation range. Lead up to this concentration, according to data not reproduced here, raises the beta solvus temperatures markedly and probably lowers the alpha solvus temperatures slightly. The titanium-lead binary alloys investigated are not favorably affected by solution heat treatments and they did not respond to aging treatments. However, alloys containing higher lead contents are being investigated.

Binary Titanium-Vanadium Alloys: Table VII contains data on mechanical properties of binary titanium-vanadium alloys in the as-hot-rolled condition and after heat treating at 1600°F. Fig. 45 shows some of these data graphically, while fig. 13 shows the effect of vanadium on the transformation range. Fig. 14 shows the effects of various heat treatments on the hardness of the titanium-vanadium binary alloy, while fig. 15 shows the substantial lack of response of the alloys to aging treatments. Vanadium produces moderate increases in strength with some sacrifice in ductility. It limits the alpha field at high temperature and markedly reduces the beta solvus temperature. The alloys do not respond appreciably to solution or aging treatments. However, alloys containing higher vanadium contents merit investigation.

It may be concluded from these data that vanadium is a fairly useful alloy addition to titanium.

Binary Alloys of Titanium With Antimony and Bismuth: Table VII contains some data on the mechanical properties of alloys containing small amounts of antimony or bismuth. The data are insufficient to permit an evaluation of these systems. Further studies are being made.

Binary Titanium-Chromium Alloys: Table VIII contains data on the mechanical properties of titanium-chromium binary alloys in the as-rolled condition and after heat treating at 1600°F. A small amount of data is also available after heat

Table VII. Properties of Binary Titanium Alloys Prepared from Process A Metal Base (Group V Elements)

Heat No.	Composition, Pct					As-Hot-Rolled Temper[1]				Heat Treated 1600°F[2]				Annealed 1450°F[6]		
	Intended	Actual				Tensile Str'gth,[3] psi	Elong., Pct in 1 In.	VHN[4]	Minimum Bend Radius,[5] In.	Tensile Str'gth,[3] psi	Elong., Pct in 1 In.	VHN[4]	Minimum Bend Radius,[5] In.	Tensile Strength,[7] psi	Elong., Pct in 1 In.	VHN[4]
			C	N	W											
Titanium — Vanadium Alloys																
WC67[8]	Unalloyed		0.04	0.024	0.35	80,700	24.0	186	1/16	75,000	22.0	188	1/16			
WAO12[8]	Unalloyed													90,300	16.0	203
WA23[8]	1.0 V													87,900	21.0	216
WC74[8]	1.0 V	0.83 V	0.04	0.032	0.24	91,700	19.0	203	1/16	96,300	14.0	234	3/16			
WC69[8]	2.5 V	2.38 V	0.03	0.027	0.31	104,000	21.0	237	3/16	118,800	10.0	260	>1/4*			
WC68[8]	5.0 V	4.74 V	0.06	0.031	0.41	138,800	10.0	294	3/16	141,300	2.5	322	>1/4*			
Titanium — Antimony Alloys																
WG70[8]	Unalloyed					77,800	23.0	180	3/64	66,300	23.5	160	3/64			144
WAO12[8]	Unalloyed													90,300	16.0	203
WA29[9]	0.1 Sb													87,100	20.0	212
WG58[8]	0.1 Sb	0.06 Sb				81,900	21.5	195	3/16	67,200	26.5	170	3/64			
WG56[8]	0.25 Sb	0.14 Sb				79,400	21.0	186	3/32	66,300	23.0	155	3/64			
WG60[8]	0.50 Sb	0.12 Sb				86,300	21.5	200	3/32	65,700	23.0	168	3/64			
Titanium — Bismuth Alloys																
WG70[8]	Unalloyed					77,800	23.0	180	3/64	66,300	23.5	160	3/64			
WAO12[8]	Unalloyed													90,300	16.0	203
WA30[8]	0.08 Bi													98,100	15.0	243
WG64[8]	0.10 Bi	0.11 Bi				80,400	21.0	201	3/64	67,400	22.0	162	1/32			
WG61[8]	0.25 Bi	0.27 Bi				79,400	22.0	175	3/64	66,600	20.5	154	3/64			
WG65[8]	0.50 Bi	0.29 Bi				68,400	20.5	186	3/64	65,000	21.5	168	3/64			

[1] As hot rolled at 1450°F.

[2] Heated in air ½ hr at 1600°F and quenched in cold water.

[3] Average of 2 longitudinal 14-ga specimens, 3 in. long by 0.375 in. wide with a 0.250-in. wide reduced section. Tested with the surface skin present.

[4] 10-kg load. Hardness at the center of the cross section of the sheet 90° to the surface and to the rolling direction.

[5] Minimum bend radius without cracking on a single longitudinal specimen 3 in. long by 0.5 in. wide. Tested with the surface skin present.

[6] Annealed ½ hr in air at 1450°F and air cooled.

[7] Average of 2 longitudinal 8-in. specimens with 0.5-in. reduced section. 14-ga sheet.

[8] Forged at 1700°F by upsetting the 2¼-in.-diam ingot on edge to a 0.250-in. slab, then ground and hot rolled at 1450°F to 0.060-in. sheet. Total reduction 35:1.

[9] Forged at 1700°F by pancaking the 0.5-in.-thick ingot to 0.250-in. slab, then ground and hot rolled at 1450°F to 0.060-in. sheet. Total reduction 8:1.

treating at 1750°F and annealing at 1450°F. As indicated previously, two different sources of chromium were employed, the fused chromium which is relatively low in oxygen and nitrogen and electrolytic chromium which is relatively high in oxygen and nitrogen. The electrolytic chromium was used to prepare the heats on which a nitrogen analysis was made as listed in table VIII. In general, the low-chromium alloys prepared with electrolytic chromium produce higher tensile properties than the alloys prepared with fused chromium. The effects of chromium on the properties of the alloys in the as-hot-rolled condition are shown by fig. 45.

Fig. 16 shows the effects of chromium on the transformation range and illustrates the very marked limitation of the alpha field produced by the chromium addition and the lowering of the beta solvus temperatures. Fig. 17 to 20, inclusive, illustrate typical structures of titanium-chromium alloys given various treatments.

As with most other titanium alloys, and as shown by fig. 21, increases in hardness are obtained by quenching from higher temperatures, particularly from the beta field. These increases in hardness are quite marked for the 10 pct chromium alloys. As shown by the data in table VIII, quenching from 1600°F did not have an overall beneficial effect on the tensile properties. However, since the 5 to 10 pct alloys do harden by quenching from the beta field, useful heat treatments might be developed.

As shown by fig. 22, the higher chromium alloys age harden quite markedly, even when they are in the hot-rolled condition; presumably, this age hardening is a result of the decomposition of retained beta. Five per cent chromium alloys in the as-hot-rolled condition age harden only slightly.

It may be concluded from this investigation that very good properties can be obtained from titanium-chromium alloys, particularly when some oxygen or nitrogen is present. Thus, alloys in the as-hot-rolled condition and containing 4.8 pct chromium and 0.12 pct nitrogen produced the following properties:

Tensile strength, psi	182,000
Elongation in 1 inch, Pct	7
Vickers hardness	356
Minimum bend radius, in.	3t

Binary Titanium-Molybdenum Alloys: Table VIII contains data on the mechanical properties of titanium-molybdenum binary alloys in the as-hot-rolled condition and after heat treating at 1600°F. The effect of molybdenum on the mechanical properties

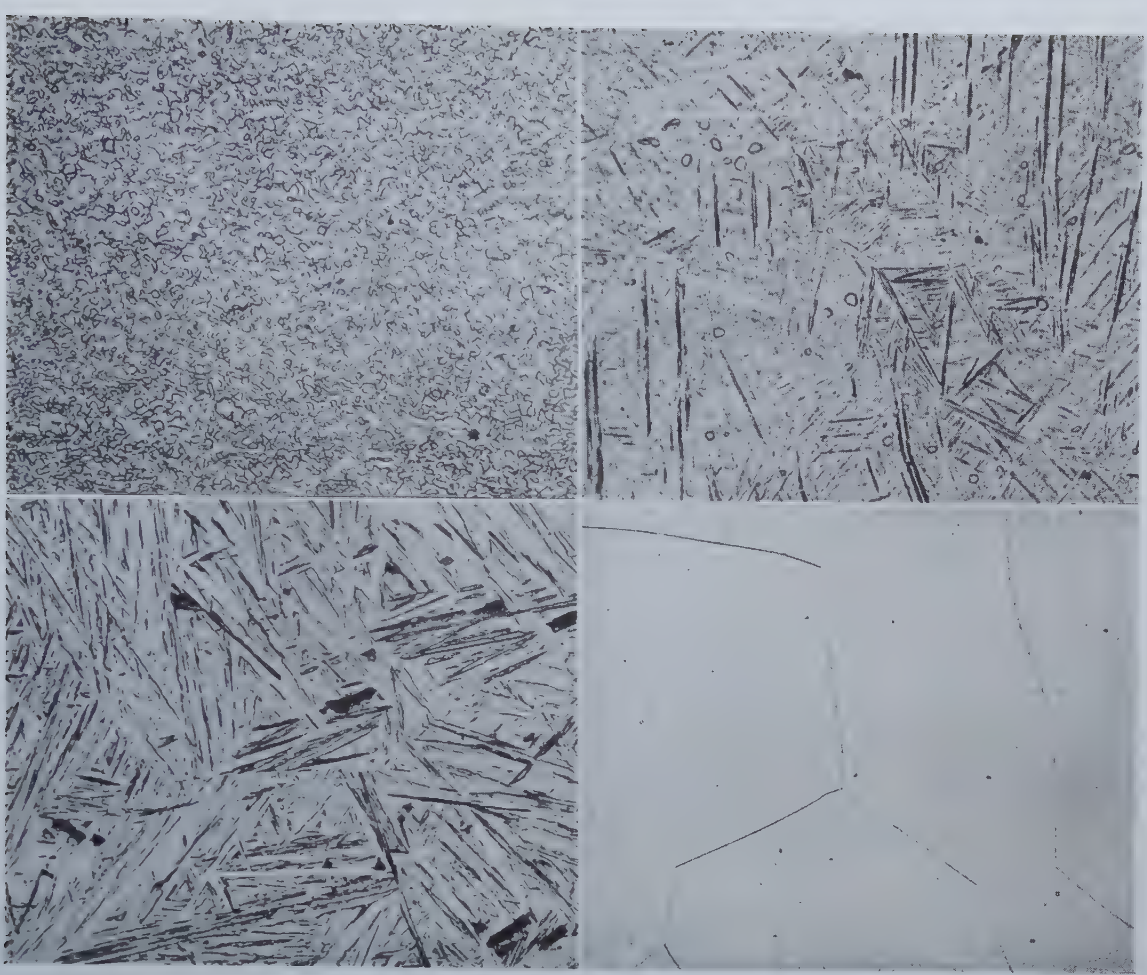

Fig. 17-20—Typical structures observed in binary titanium-chromium alloys made from process A metal.

Fig. 17—Heat WG86, 2.17 pct Cr.

Quenched from 1450°F in the $\alpha + \beta$ field. The alpha phase is distributed in a beta matrix which transformed to alpha during the quench. 500X.

Fig. 18—Heat WG86, 2.17 pct Cr.

Quenched from 1550°F in the $\alpha + \beta$ field. Islands of alpha are distributed in an acicular alpha (transformed beta) matrix. 500X.

Fig. 19—Heat WG86, 2.17 pct Cr.

Quenched from 1600°F in the β field. Acicular alpha formed by transformation of beta during the quench. 500X.

Fig. 20—Heat WC79, 10.0 pct Cr (nominal).

Quenched from 1600°F. This micrograph shows untransformed beta. 500X.

of the as-hot-rolled alloys is represented graphically by fig. 45.

Fig. 23 graphically represents the effect of molybdenum on the transformation range and also illustrates the restriction to the alpha field. Fig. 24, 25, and 26 show typical structures of titanium-molybdenum alloys after various treatments. As shown by the data in table VIII, the tensile properties of the titanium-molybdenum binary alloys are not favorably affected by solution heat treatment from 1600°F. Hardness tests after heat treating at 1450, 1550, 1600, 1650, 1700, and 1750°F showed that little or no increase in hardness occurred as the result of quenching from the beta field. These data are graphically illustrated by fig. 27. This hardness increase is believed to be the result of the formation of acicular alpha instead of the usual equiaxed-type of alpha formed by recrystallization in the alpha field.

Alloys containing up to 5 pct molybdenum do not respond appreciably to solution treatment, though alloys of higher molybdenum content may respond more favorably. Fig. 28 shows the response of the various alloys to aging treatments after quenching from 1450 and 1750°F. These data show that an increase of 70 Vickers numbers occurs in the 5 pct molybdenum alloy after quenching from 1450°F. Slight increases in hardness also occurred when the 5 pct molybdenum alloys in the as-hot-rolled condition were aged at 750°F for 2, 4, and 8 hr.

It may be concluded that molybdenum is a favorable alloy addition to titanium, and that its effects on the properties are similar to those ob-

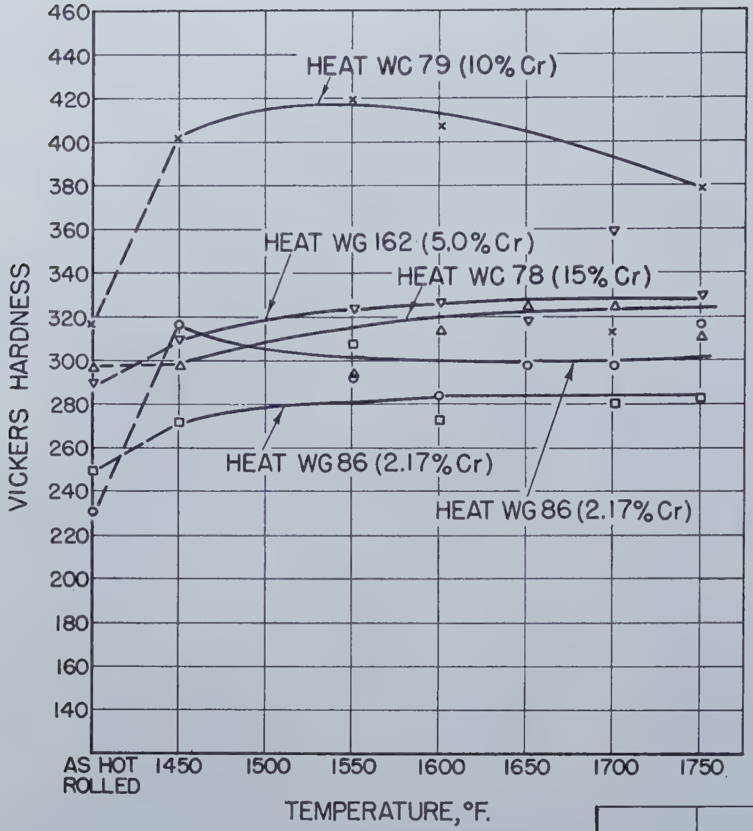

Fig. 21—Effect of solution temperature on the hardness of titanium-chromium alloys prepared from process A metal.

Fig. 22—Effect of aging as-hot-rolled titanium-chromium alloys at 752°F, prepared from process A metal.

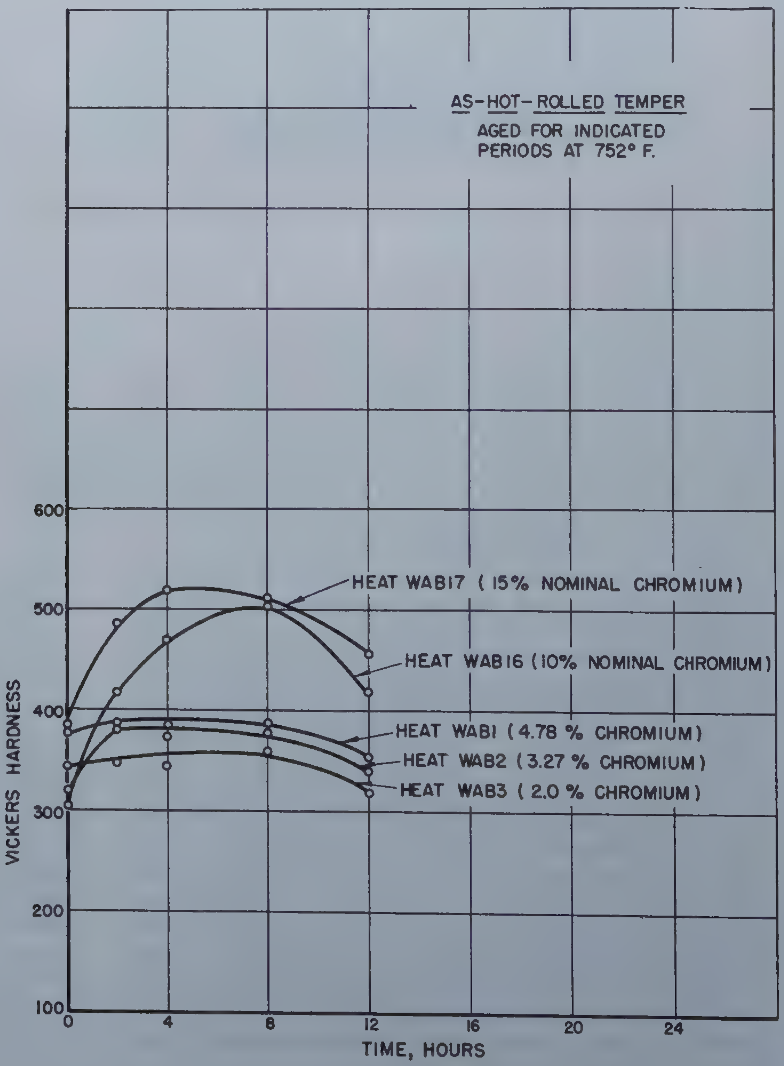

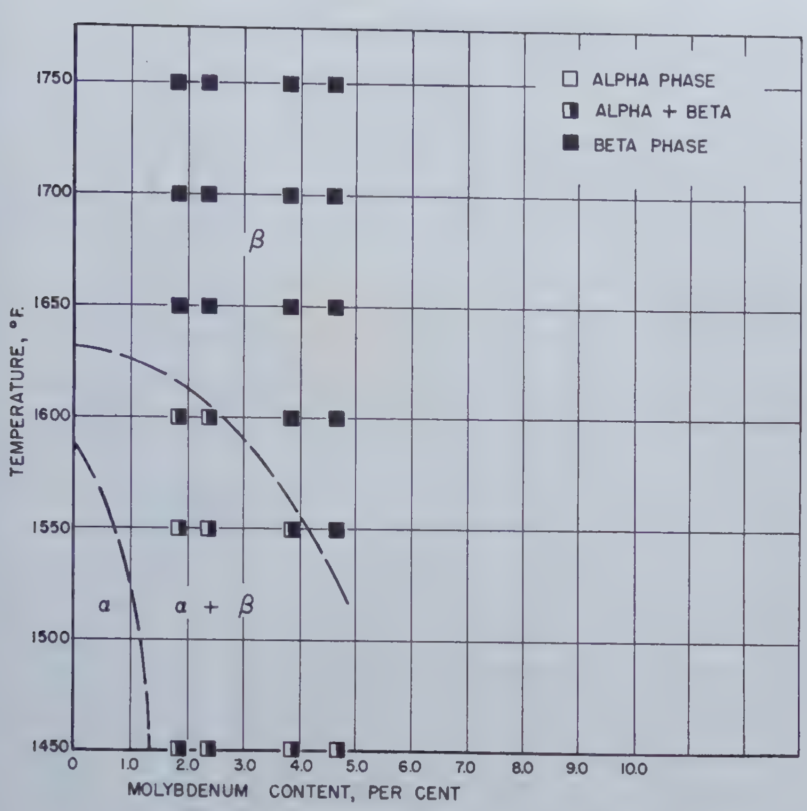

Fig. 23—Tentative diagram showing transformation range of titanium—0 to 5 pct molybdenum alloys made from process A metal.

24

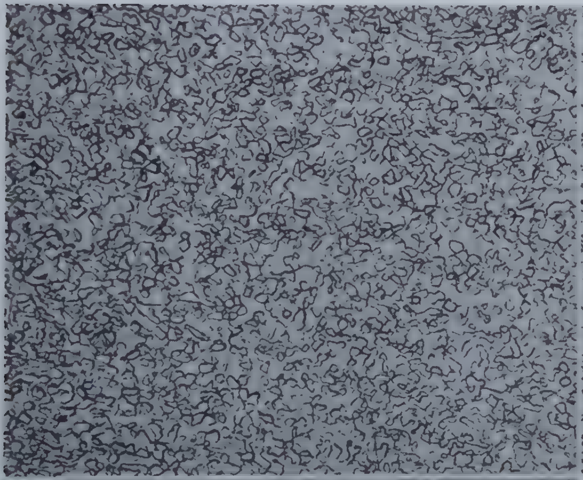

25

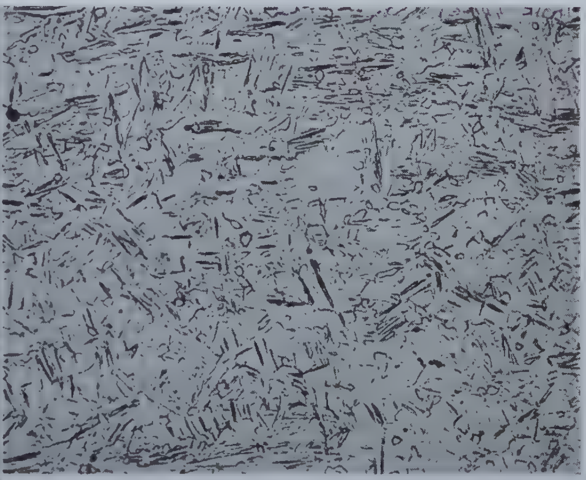

26

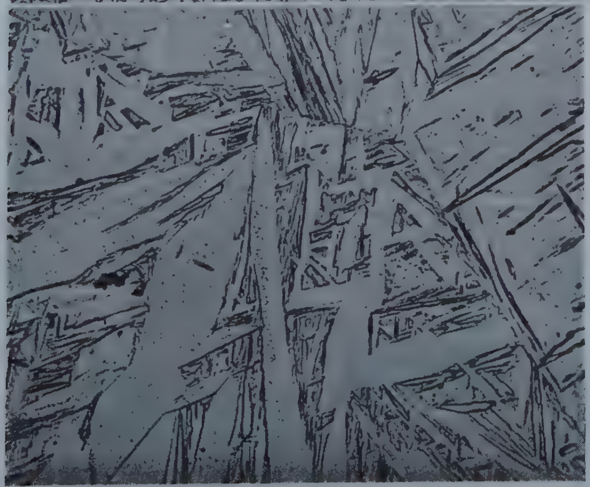

Fig. 24-26—Typical structures observed in binary titanium-molybdenum alloys made from process A metal.

Fig. 24—Heat WC83, 1.86 pct Mo, 0.07 pct C, 0.051 pct N, 0.11 pct W.

Quenched from 1550°F in the $\alpha + \beta$ field. Photograph shows islands of alpha in an alpha matrix, which transformed from beta during the quench. 500X.

Fig. 25—Heat WC83, 1.86 pct Mo, 0.07 pct C, 0.051 pct N, 0.11 pct W.

Quenched from 1600°F in the $\alpha + \beta$ field. Islands of alpha are distributed in an acicular alpha (transformed beta) matrix. 500X.

Fig. 26—Heat WC83, 1.86 pct Mo, 0.07 pct C, 0.051 pct N, 0.11 pct W.

Quenched from 1700°F in the β field. Photograph shows acicular alpha, which transformed from beta during the quench. 500X.

Table VIII. Properties of Titanium Binary Alloys Prepared from Process A Metal Base (Group VI Elements)

Heat No.	Composition, Pct					As-Hot-Rolled Temper[1]				Heat Treated 1600°F[2]				Heat Treated 1750°F[3]				Annealed 1450°F[4]		
	Intended	Actual				Tensile Strength,[5] psi	Elong., Pct in 1 In.	VHN[6]	Minimum Bend Radius,[7] In.	Tensile Strength,[5] psi	Elong., Pct in 1 In.	VHN[6]	Minimum Bend Radius,[7] In.	Tensile Strength,[5] psi	Elong., Pct in 1 In.	VHN[6]	Minimum Bend Radius,[7] In.	Tensile Strength,[8] psi	Elong., Pct in 1 In.	VHN[6]
			C	N	W															
	Titanium-Chromium Alloys																			
WAO[11]	Unalloyed																	91,900	15.0	211
WG69[10]	Unalloyed					75,000	21.5	163	1/64	62,000	26.0	147	3/64							
WG42[10]	Unalloyed					82,100	18.0	163	1/16	74,300	22.0	149	1/16							
WG19[10]	Unalloyed					74,000	22.5	169	1/32	70,000	21.0	157	1/32							
WA4[11]	5 Cr																	193,100	1.0	461
WA5[11]	10 Cr																	188,600	1.5	425
WA6[11]	15 Cr																	152,100	7.0	327
WAB3[10]	2.5 Cr	2.07 Cr	0.07	0.116	0.11	157,900	10.0	306	3/16	150,000	2.0					380	>1/4			
WAB2[10]	3.5 Cr	3.27 Cr	0.09	0.088	1.15	169,600	7.5	330	3/16	141,400	2.0					359	>1/4			
WAB1[10]	5.0 Cr	4.78 Cr	0.09	0.118	0.20	182,400	7.0	356	3/16	106,300	1.0					385	>1/4			
WAB16[9,10]	10.0 Cr		0.19	0.086		158,200	4.5	347	1/4	152,200	3.5			143,700	3.5	349	>1/4			
WAB17[9,10]	15.0 Cr		0.13	0.067		149,700	7.0	306	>1/4	152,200	6.0			139,300	4.5	323	3/64			
WG86[10,12]	2.5 Cr	2.17 Cr				124,400	14.0	248	3/16	146,400	2.5	272	>1/4*			283	>1/4†			
WG67[10,12]	3.5 Cr	3.35 Cr				132,400	9.5	230	3/16	136,000	1.0	283	>1/4†			317	>1/4†			
WG43[10,12]	5.0 Cr	4.38 Cr				186,600	6.0	281	>1/4*	118,700	1.5	316	>1/4†			442	>1/4*			
WC79[10,12]	10.0 Cr					135,900	1.5	316	>1/4*	126,500	11.0	407	1/16			380	>1/4*			
WC78[10,12]	15.0 Cr					153,300	7.0	296	>1/4*	142,200	9.5	314	3/32			311	3/16			
WG162[10,12]	5.0 Cr					150,800	6.5	289	3/16	113,800	1.5	326	>1/4			329	>1/4			
	Titanium-Molybdenum Alloys																			
WC77[10]	Unalloyed		0.04	0.026	0.10	76,700	21.0	184	1/32	74,300	20.0	170	1/32							
WC95[10]	Unalloyed		0.05	0.026	0.43	77,500	22.0	191	1/32	76,700	22.0	169	1/32							
WC80[10]	Unalloyed		0.06	0.020	0.04	71,400	22.5	180	1/16	72,300	24.0	162	1/16							
WAO12[10]	Unalloyed																	90,300	16.0	203
WA1[11]	5.0 Mo																	158,200	6.0	348
WAB10[10]	2.0 Mo		0.12	0.029		128,300	13.0	266	1/4					111,800	2.5	344	>1/4			
WAB11[10]	2.5 Mo		0.32	0.027		135,700	11.0	267	3/16					120,600	2.0	359	>1/4			
WAB9[10]	3.5 Mo		0.16	0.027		121,400	15.5	258	3/16					136,000	2.2	345	>1/4			
WAB8[10]	5.0 Mo		0.14	0.027		152,600	5.5	318	>1/4					109,400	2.5	300	>1/4			
WC83[10]	2.0 Mo	1.86 Mo	0.07	0.051	0.11	109,600	14.0	225	3/32	106,700	7.5	262	3/16							
WC82[10]	2.5 Mo	2.36 Mo	0.07	0.067	0.38	113,300	10.0	233	1/8	114,200	9.5	255	3/16							
WC81[10]	3.5 Mo	3.82 Mo	0.06	0.042	0.26	125,900	11.5	246	3/16	115,500	13.5	248	3/16							
WC84[10]	5.0 Mo	4.65 Mo	0.05	0.049	0.03	144,900	6.5	268	>1/4	110,000	11.5	259	3/16							

* Some ductility.

† Very little ductility.

[1] As hot rolled at 1450°F.

[2] Heated in air ½ hr at 1600°F and quenched in cold water.

[3] Heated in air ½ hr at 1750°F and quenched in cold water.

[4] Annealed ½ hr in air at 1450°F and air cooled.

[5] Average of 2 longitudinal 14-ga specimens 3 in. long by 0.375 in. wide with a 0.250-in.-wide reduced section. Tested with the surface skin present.

[6] 10-kg load. Hardness at the center of the cross section of the sheet 90° to the surface and to the rolling direction.

[7] Minimum bend radius without cracking on a single longitudinal specimen 3 in. long by 0.5 in. wide. Tested with the surface skin present.

[8] Average of 2 longitudinal 8-in. specimens with 0.5-in. reduced section. 14-ga sheet.

[9] Segregation of chromium observed in microscopic examination and no analysis made for chromium, to be replaced by Heats WC79 and WC78, 10 and 15 pct chromium, respectively.

[10] Forged at 1700°F by upsetting the 2¼-in.-diam ingot on edge to 0.250-in. slab, then ground and hot rolled at 1450°F to 0.060-in. sheet. Total reduction 35:1.

[11] Forged at 1700°F by pancaking the 0.5-in.-thick ingot to 0.250-in. slab, then ground and hot rolled at 1450°F to 0.060-in. sheet. Total reduction 8:1.

[12] Chromium added as fused metal low in oxygen and nitrogen.

Table IX. Properties of Titanium Binary Alloys[6] Prepared from Process A Metal Base Group VII Elements

Heat No.	Composition, Pct					As-Hot-Rolled Temper[1]				Heat Treated 1600°F[2]			
	Intended	Actual				Tensile Strength,[3] psi	Elong., Pct in 1 In.	VHN[4]	Minimum Bend Radius,[5] In.	Tensile Strength,[3] psi	Elong., Pct in 1 In.	VHN[4]	Minimum Bend Radius,[5] In.
			C	N	W								
Titanium-Manganese Alloys													
WH48	Unalloyed					87,500	22.5	203	3/64	76,900	16.5	179	3/16
WC43	Unalloyed		0.02	0.030	0.05	75,000	20.5	190	3/64	71,000	23.5	172	3/64
WC63	1.0 Mn	1.0 Mn	0.02	0.034	0.16	101,700	16.0	221	3/32	109,500	15.5	251	3/16
WC44	2.5 Mn	2.08 Mn	0.02	0.029	0.06	128,000	14.0	253	3/32	141,200	7.0	316	1/4
WC41	5.0 Mn	4.37 Mn	0.04	0.042	0.05	157,900	7.5	303	1/16	147,200	2.0	413	>1/4
WH53	1.75 Mn					113,600	14.0	251	3/16	118,500	5.5	266	>1/4*
WH81	2.5 Mn					141,200	10.5	270	3/16	141,700	1.0	343	>1/4*
WH80	3.5 Mn					145,100	11.0	363	3/16	86,400	0.0	348	>1/4†
WH78	5.0 Mn					162,800	6.5	315	3/16	140,700	1.0	397	>1/4†
WH82	7.5 Mn					196,800	2.5	384	>1/4*	100,700	1.0	386	>1/4†
WH57	10.0 Mn					177,400	5.0	394	>1/4†	142,000	3.5	362	>1/4*

* Some ductility.

† Very little ductility.

[1] As hot rolled at 1450°F.

[2] Heated in air ½ hr at 1600°F and quenched in cold water.

[3] Average of 2 longitudinal 14-ga specimens, 3 in. long by 0.375 in. wide with a 0.250-in. wide reduced section. Tested with the surface skin present.

[4] 10-kg load. Hardness at the center of the cross section of the sheet 90° to the surface and to the rolling direction.

[5] Minimum bend radius without cracking on a single longitudinal specimen 3 in. long by 0.5 in. wide. Tested with the surface skin present.

[6] Forged at 1700°F by upsetting the 2¼-in.-diam ingot on edge to 0.250-in. slab, then ground and hot rolled at 1450°F to 0.060-in. sheet. Total reduction 35:1.

Table X. Properties of Titanium Binary Alloys[8] Prepared from Process A Metal Base (Group VIII Elements)

Heat No.	Composition Pct,					As-Hot-Rolled Temper[1]				Heat Treated 1600°F[2]				Annealed 1450°F[3]		
	Intended	Actual				Tensile Strength,[4] psi	Elong., Pct in 1 In.	VHN[5]	Minimum Bend Radius,[6] In.	Tensile Strength,[4] psi	Elong., Pct in 1 In.	VHN[5]	Minimum Bend Radius,[6] In.	Tensile Strength,[7] psi	Elong., Pct in 1 In.	VHN[5]
			C	N	W											
Titanium-Iron Alloys																
WC31	Unalloyed	0.14 Fe	0.04	0.048	0.23	85,900	18.5	199	3/64	74,300	19.5	174	3/64			
WA13	2.0 Fe													136,400	1.5	339
WA14	3.0 Fe													148,300	1.0	440
WC27	0.25 Fe	0.40 Fe	0.04	0.036	0.34	95,300	21.0	211	3/32	80,500	21.0	201	3/32			
WC28	0.50 Fe	0.68 Fe	0.08	0.026	0.51	93,200	17.0	221	3/16	94,600	17.0	232	3/32			
WC25	1.0 Fe	1.15 Fe	0.05	0.037	0.50	110,300	17.0	220	3/16	114,900	10.0	254	>1/4			
WC37	2.0	2.20 Fe	0.05	0.05	0.47	146,500	8.5	305	3/16	146,500	2.5	468	>1/4			
Titanium-Cobalt Alloys																
WC101	Unalloyed		0.03	0.025	0.46	76,700	19.5	189	3/32	70,800	19.0	194	3/32			
WA012	Unalloyed													90,300	16.0	203
WA20	2.0 Co													111,800	14.0	244
WC115	1.0 Co	1.02 Co	0.03	0.047	0.31	108,500	18.5	221	3/16	102,900	10.0	255	>1/4*			
WC103	2.0 Co	1.90 Co	0.04	0.021	0.32	110,700	8.0	242	3/16	115,800	4.0	305	>1/4*			
WC102	3.0 Co	3.05 Co	0.04	0.022	0.23	135,000	10.0	271	3/16	119,400	3.0	354	>1/4†			
Titanium-Nickel Alloys																
WA0	Unalloyed													91,900	15.0	211
WA15	1.0 Ni													94,500	16.0	220
WA16	2.0 Ni													111,600	3.0	271
WA17	5.0 Ni													111,400	2.0	272
WA18	10.0 Ni													100,000	2.0	259
WD1	10.0 Ni	11.4 Ni	0.07	0.029	0.59	100,600	1.0	298	>1/4	78,100	0.0	527	>1/4			

[1] As hot rolled 1450°F.

[2] Heated in air ½ hr at 1600°F and quenched in cold water.

[3] Annealed ½ hr in air at 1450°F and air cooled.

[4] Average of 2 longitudinal 14-ga specimens, 3 in. long by 0.375 in. wide with a 0.250-in.-wide reduced section. Tested with the surface skin present.

[5] 10-kg load. Hardness at the center of the cross section of the sheet 90° to the surface and to the rolling direction.

[6] Minimum bend radius without cracking on a single longitudinal specimen 3 in. long by 0.5 in. wide. Tested with the surface skin present.

[7] Average of 2 longitudinal 8-in. specimens with 0.5-in.-wide reduced section. 14-ga sheet.

[8] Forged at 1700°F by upsetting the 2¼-in.-diam ingot on edge to 0.250-in. slab, then ground and hot rolled at 1450°F to 0.060-in. sheet. Total reduction 35:1.

* Some ductility.

† Very little ductility.

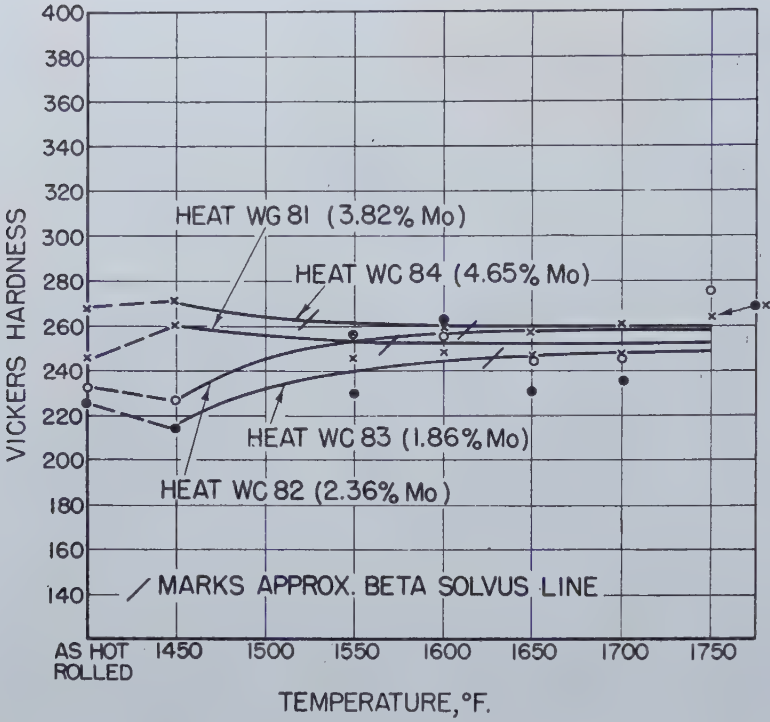

Fig. 27—Effect of solution treatment on the hardness of titanium-molybdenum alloys prepared from process A metal.

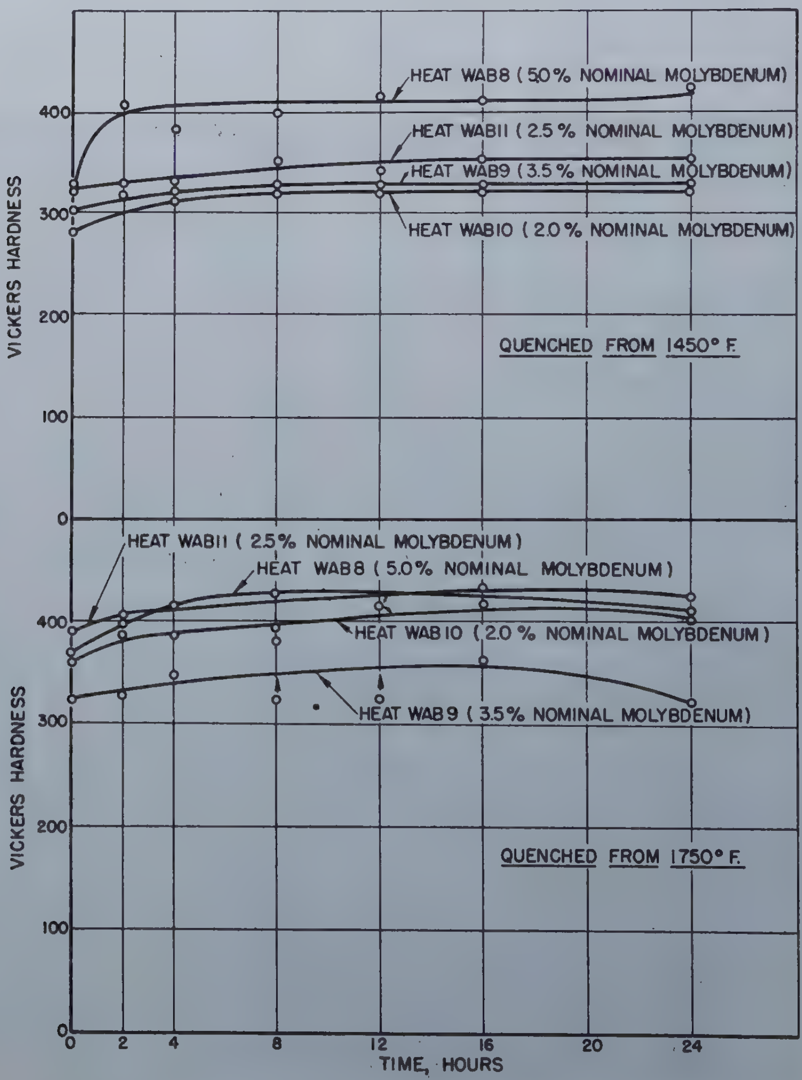

Fig. 28—Effect of aging solution heat-treated titanium-molybdenum alloys at 572°F, process A metal base.

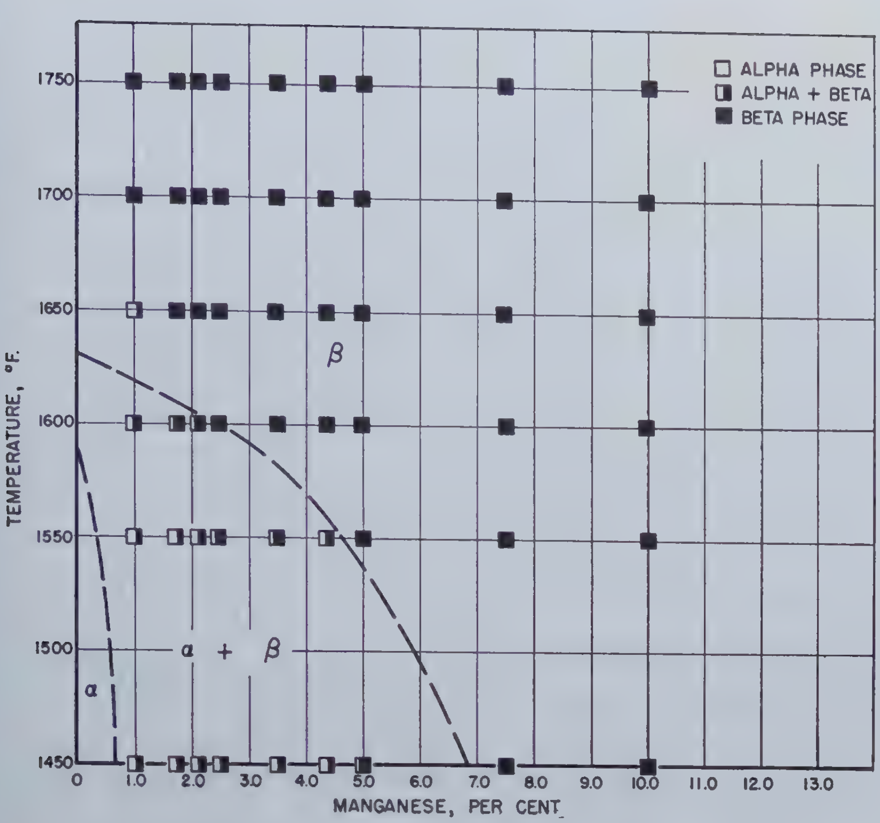

Fig. 29—Tentative diagram showing transformation range of titanium—0 to 10 pct manganese alloys made from process A metal.

Fig. 30-33 (below)—Typical structures observed in binary titanium-manganese alloys made from process A metal.

Fig. 30—Heat WC63, 1.0 pct Mn, 0.02 pct C, 0.034 pct N, 0.16 pct W.

Quenched from 1550° F in the $\alpha + \beta$ field. The predominant phase is alpha with acicular alpha (transformed beta) in the grain boundaries. 500X.

Fig. 31—Heat WC63, 1.0 pct Mn, 0.02 pct C, 0.034 pct N, 0.16 pct W.

Quenched from 1650°F in the $\alpha + \beta$ field. Islands of alpha are shown in an acicular alpha (transformed beta) structure. 500X.

Fig. 32—Heat WC63, 1.0 pct Mn, 0.02 pct C, 0.034 pct N, 0.16 pct W.

Quenched from 1700°F in the β field. The structure shown is acicular alpha which transformed from beta during the quench. 500X.

Fig. 33—Heat WH82, 7.5 pct nominal Mn.

Quenched from 1450°F in the β field. With high manganese present, the beta phase has not transformed in the quenched specimen. 500X.

30

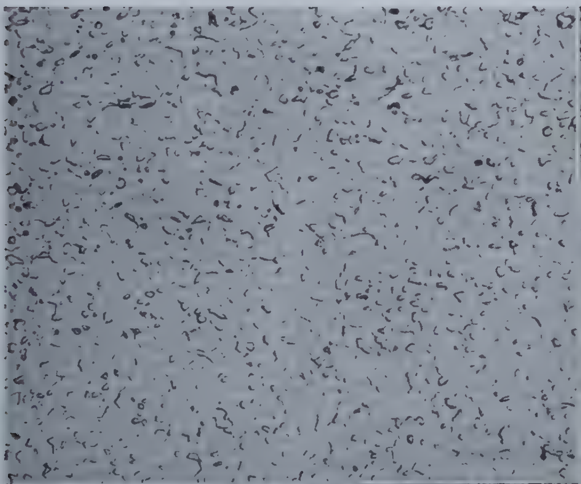

31

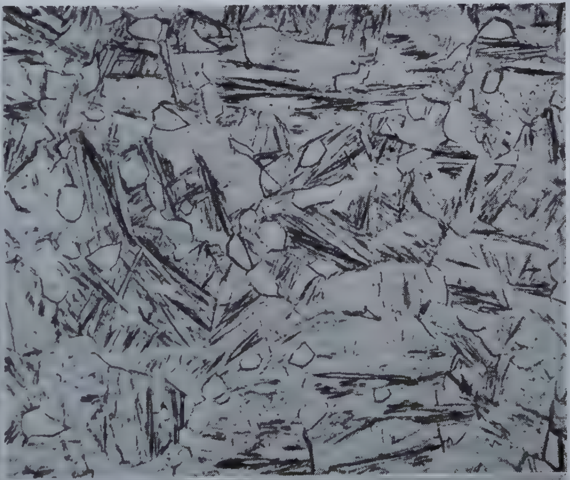

32

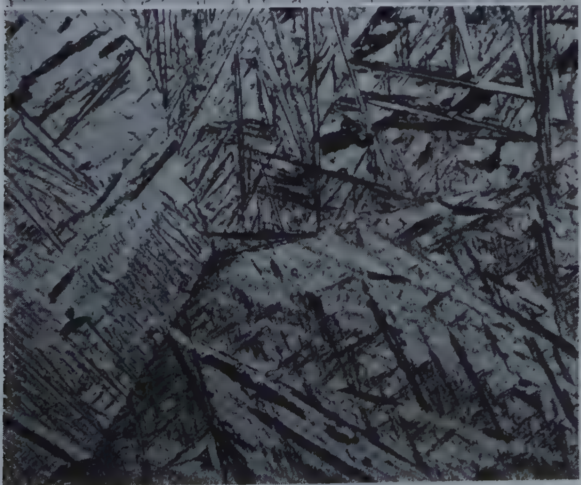

33

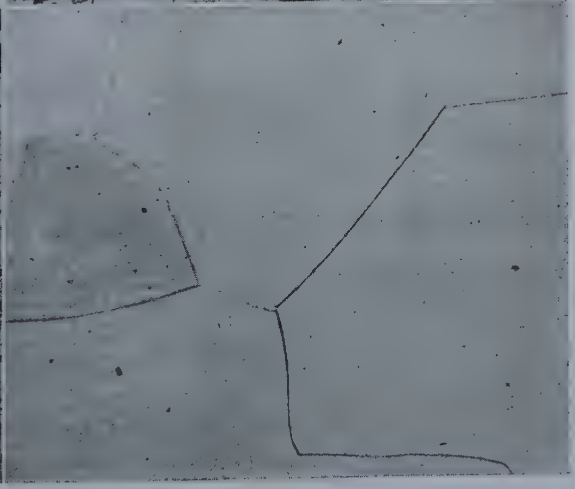

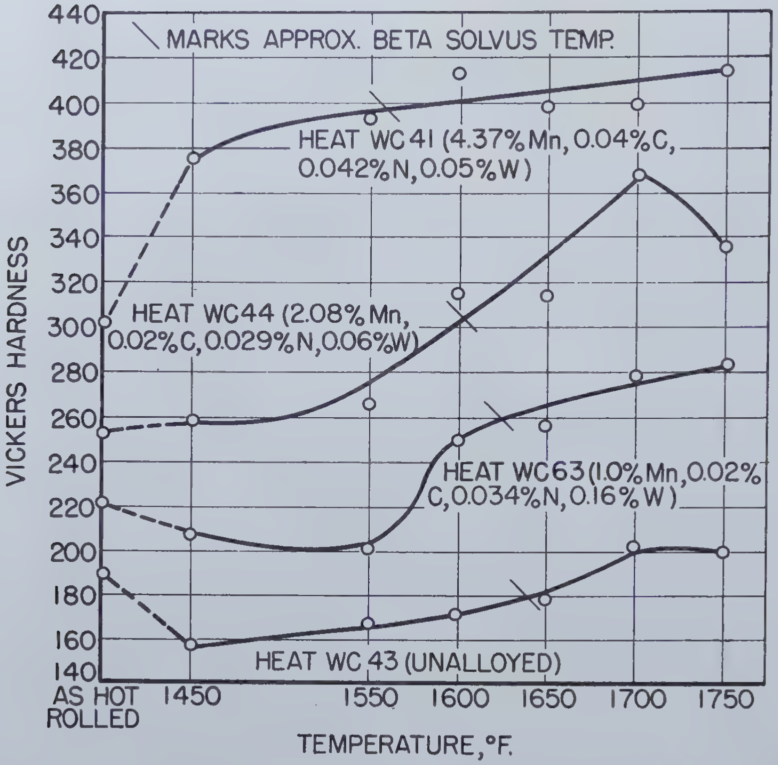

Fig. 34—Effect of solution treatment on the hardness of titanium-manganese alloys prepared from process A metal.

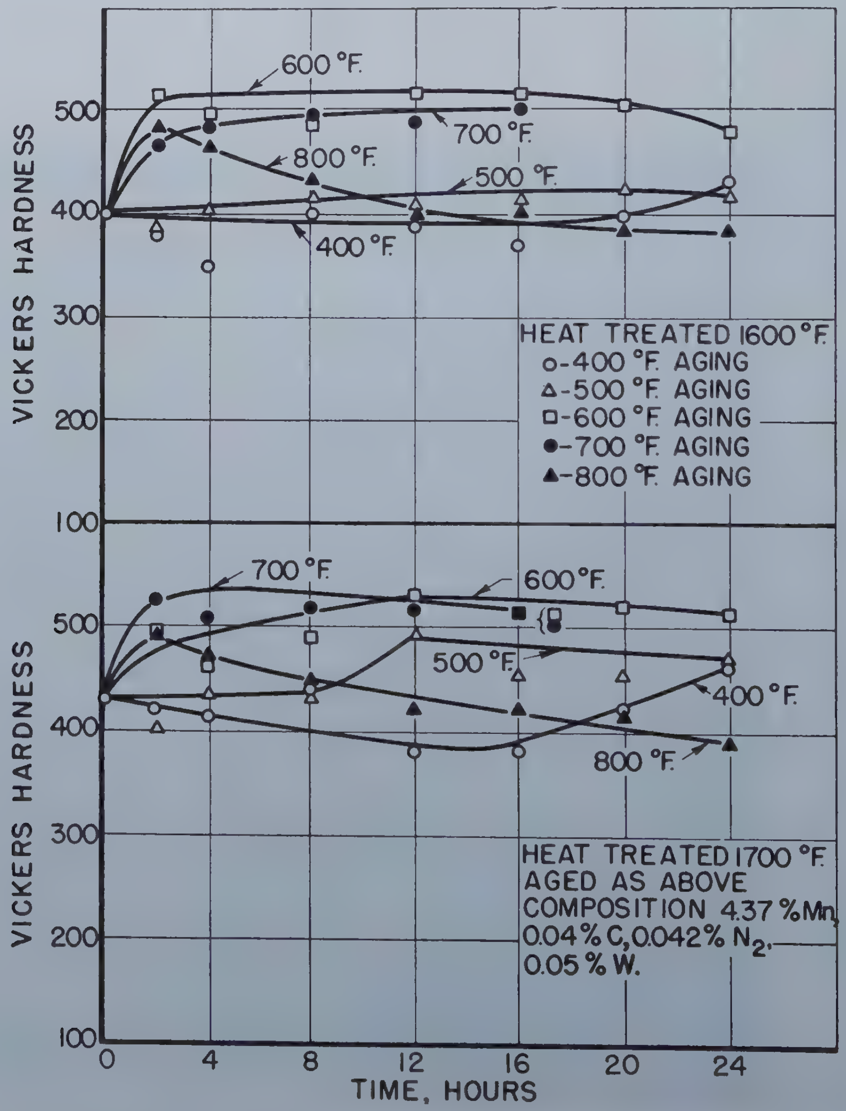

Fig. 35—Aging curves for a titanium-manganese alloy (heat WC41) prepared from process A metal.

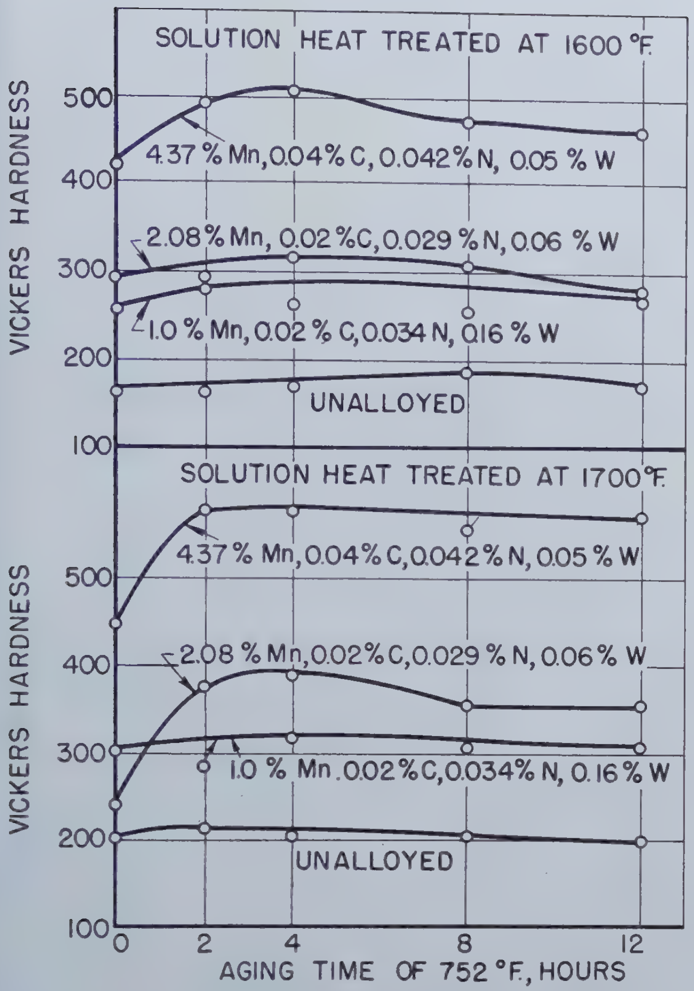

Fig. 36—Effect of aging on the hardness of titanium-manganese alloys prepared from process A metal.

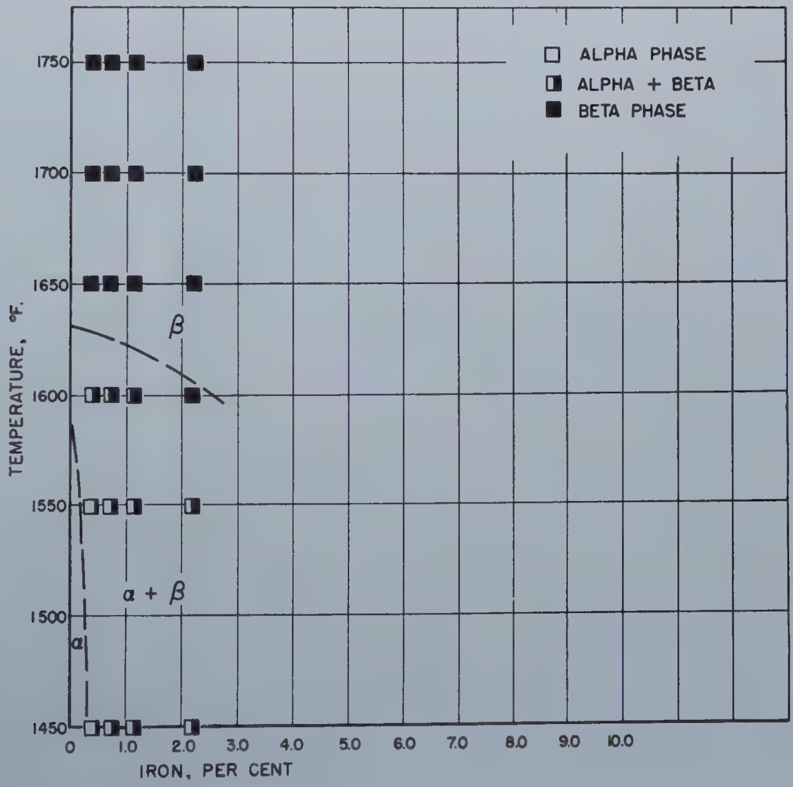

Fig. 37—Tentative diagram showing the transformation range of titanium—0 to 2.0 pct iron alloys made from process A metal.

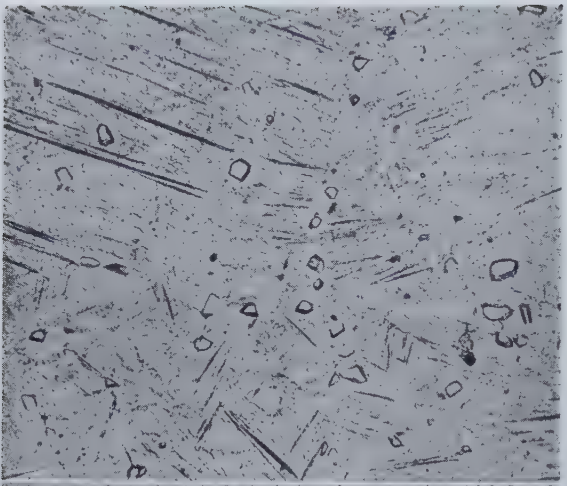

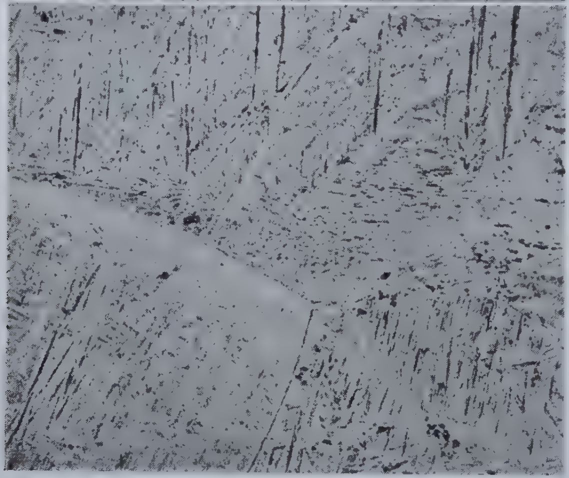

Fig. 38-39—Typical structures observed in binary titanium-iron alloys made from process A metal.

Fig. 38 (above)—Heat WC37, 2.20 pct Fe, 0.05 pct C, 0.05 pct N, 0.47 pct W.
Quenched from 1600°F in the $\alpha + \beta$ field. Islands of alpha in an acicular alpha (transformed beta) matrix are shown 500X.

Fig. 39 (below)—Heat WC37, 2.20 pct Fe, 0.05 pct C, 0.05 pct N, 0.47 pct W.
Quenched from 1650°F in the β field. The structure shown is acicular alpha (transformed beta). 500X.

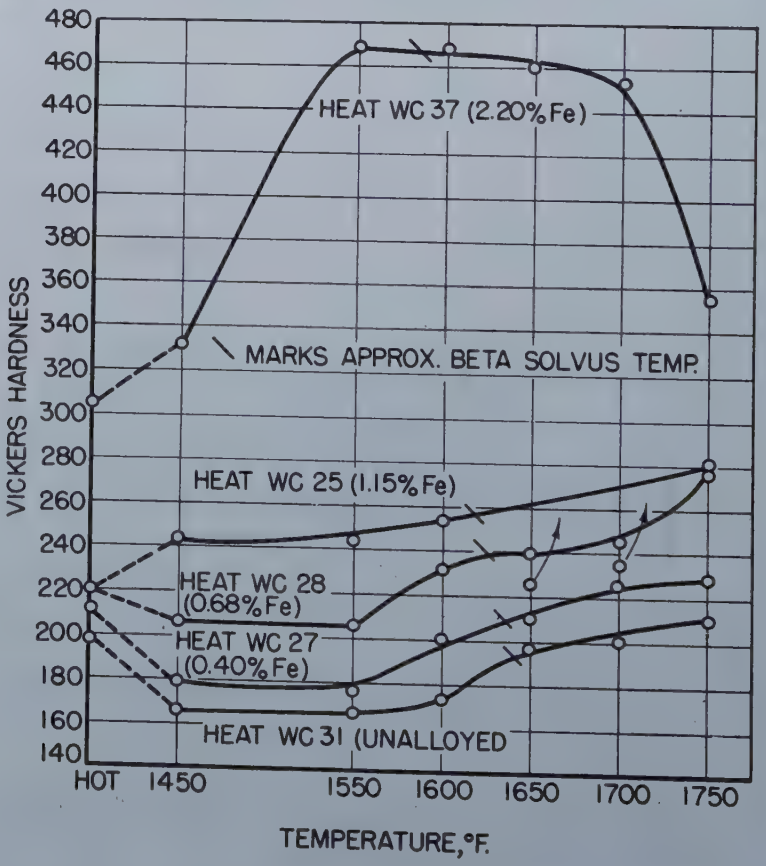

Fig. 40—Effect of solution treatment on the hardness of titanium-iron alloys prepared from process A metal.

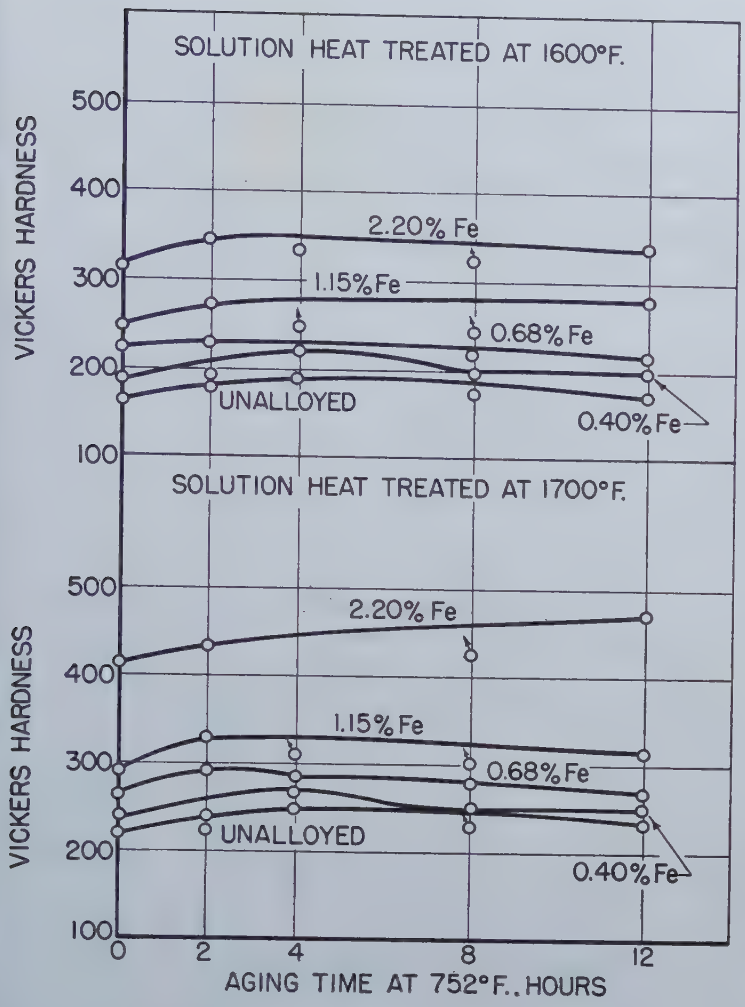

Fig. 41—Effect of aging on the hardness of titanium-iron alloys prepared from process A titanium.

tained by the addition of the fused chromium.

Binary Titanium-Manganese Alloys: The mechanical properties of the titanium-manganese binary alloys in the as-hot-rolled condition and after solution heat treatment at 1600°F are shown by the data in table IX. The effects of manganese on the properties of the alloys in the as-hot-rolled condition are graphically represented by fig. 45.

Fig. 29 shows the effects of manganese on the transformation range and the very marked restriction of the alpha field produced by small additions of manganese. Fig. 30 to 33, inclusive, show representative microstructures of the titanium-manganese binary alloys.

Fig. 34 shows that titanium-manganese binary alloys are hardened by quenching from the higher temperatures, as are some other titanium-base alloys. At 4.37 pct manganese, the hardening is quite marked even at a quenching temperature of 1450°F. The data in table IX show that the tensile properties of these alloys are not favorably affected by quenching from 1600°F. However, since marked hardening occurs, even at low quenching temperatures, favorable heat treatments may be developed. The response of the titanium-manganese alloys to aging is illustrated by fig. 35 and 36. These data show that the quenched alloys containing 2 and 4 pct manganese age substantially at 600 to 750°F. Data not included in the paper show that these alloys containing 3.5 to 10 pct manganese also respond appreciably to aging treatments in the as-hot-rolled condition. At 3.5 pct manganese, the increase in hardness of the as-hot-rolled alloys is only about 30 Vickers. At 10 pct manganese, the increase in hardness is 90 to 100 Vickers points.

It may be concluded from these data that manganese is one of the most interesting alloy additions made to titanium. An addition of 5 or 7.5 pct manganese to titanium produced the following properties:

	5 Pct Mn	7.5 Pct Mn
Tensile strength, psi	162,800	196,800
Elongation in 1 inch, pct	6.5	2.5
Vickers hardness	315	384
Minimum bend radius, in.	3t	>4t

Binary Titanium-Iron Alloys: Table X contains data on the mechanical properties of the titanium-iron alloys in the as-hot-rolled condition and after heat treating at 1600°F. The data on the tensile properties of the alloys in the as-hot-rolled condition are represented graphically by fig. 45. Fig. 37 shows the effects of iron on the transformation range and illustrates the very restricted range of the alpha field. Fig. 38 and 39 illustrate representative

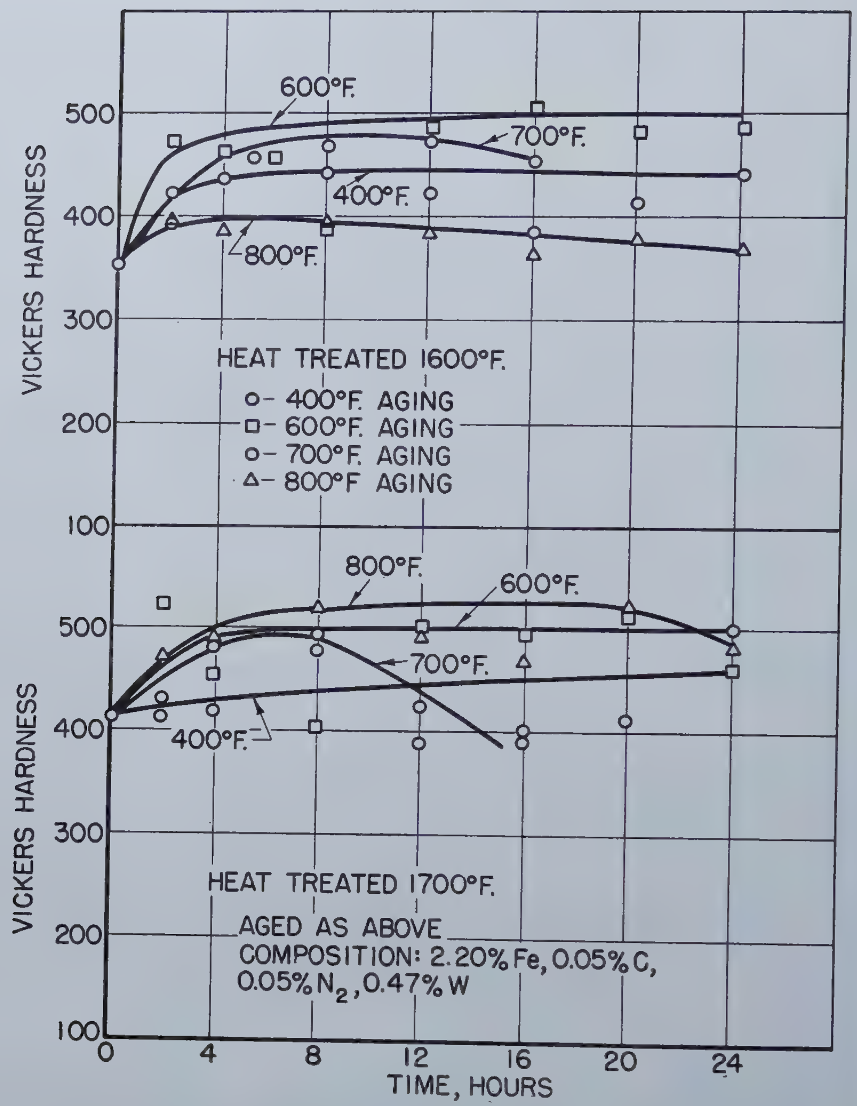

Fig. 42—Aging curves for a titanium-iron alloy (heat WC37), made from process A metal.

microstructures of the titanium-iron binary alloys.

The effects of various heat treatments on the hardness of the titanium-iron binary alloys are illustrated by fig. 40. It is quite evident that the 2.2 pct iron alloy is markedly hardened by quenching from 1550°F. In all probability, such heat treatments will be useful for some applications even though the tensile data, table X, show that a quench from 1600°F was not beneficial.

The response of these binary alloys to aging is illustrated by fig. 41 and 42. It will be noted that the 2 pct iron alloy tends to age slightly after quenching from 1600 or 1700°F. Data not indicated in the table also show that the 2 pct iron alloys age harden about 40 Vickers numbers when the as-hot-rolled material is aged from 2 to 8 hr at 750°F.

Although the increase in strength obtained by additions of iron is accompanied by a considerable sacrifice in ductility, it is quite probable that this element will be a useful alloying addition to titanium.

Binary Titanium-Cobalt Alloys: Data on the mechanical properties of the titanium-cobalt binary alloys in the as-hot-rolled condition and after heat treatment at 1600°F are listed in table X. The tensile properties of the alloys in the as-hot-rolled condition are graphically represented by fig. 45. Fig. 43 shows the effect of cobalt on the transformation range and the restriction to the alpha field.

As with other titanium-base alloys, some increase in hardness occurs when they are quenched from elevated temperatures. The increase is quite marked for the 3 pct cobalt alloy and becomes slightly greater when the temperature is increased to 1750°F. This is shown by fig. 44. However, as indicated by the data in table X, the tensile properties of the alloys are not beneficially affected by the quenching treatment at 1600°F. None of these cobalt alloys age hardens appreciably when the as-hot-rolled material is aged up to 8 hr at 750°F.

Like iron, cobalt produces some increase in strength at a considerable sacrifice in ductility. However, in small amounts, it may have a useful function in complex alloys of titanium.

Binary Titanium-Nickel Alloys: A small amount of data on the mechanical properties of titanium-nickel binary alloys is listed in table X. Relatively few data are available, however, because these alloys were fairly difficult to prepare in the arc furnace. However, alloys have been successfully made recently but data are not yet available.

Summary

Binary alloys of titanium with silver, lead, tin,

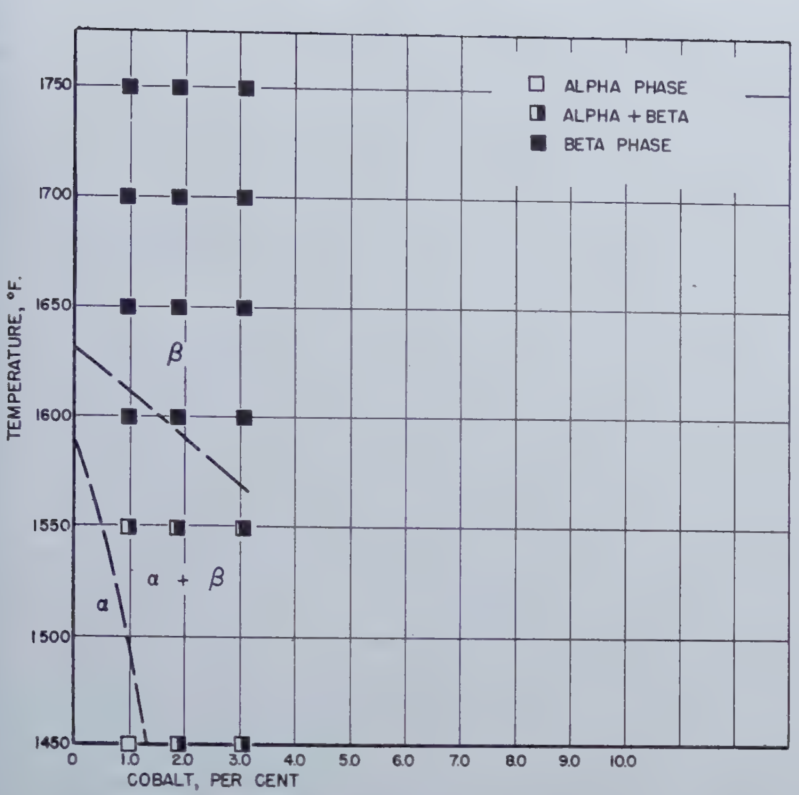

Fig. 43—Tentative diagram showing the transformation range of titanium—0 to 3.0 pct cobalt alloys made from process A metal.

nickel, copper, beryllium, boron, silicon, chromium, molybdenum, manganese, vanadium, iron, and cobalt have been studied. One-half-pound ingots of the alloys were prepared in an arc furnace, employing a water-cooled copper crucible, an argon atmosphere, and a water-cooled tungsten electrode. The ½-lb ingots were then forged at 1700°F in air to a ¼-in. slab and hot rolled at 1450°F to 0.060-in. sheet. Tensile properties, minimum bend radii, hardnesses, response to heat treatment and aging treatment, and phase relationships were determined.

The range of composition of alloys containing silver, lead, tin, or nickel was not adequate. However, the limited data indicate that silver, lead, and tin, though soluble in alpha and beta titanium to the limits investigated, do not produce binary alloys with high tensile properties. Relatively little data are available on titanium-nickel alloys.

Beryllium, boron, and silicon all have very limited solubility in alpha and beta titanium and are not useful as major alloying elements, although they may be useful as minor additions in complex alloys.

Manganese, chromium, molybdenum, vanadium, iron, cobalt, and copper all produced binary alloys with fairly high tensile properties. As illustrated by fig. 45, which shows a comparison of the tensile properties and hardnesses of all the binary systems in the as-hot-rolled condition, the first three are the best and copper is very definitely the poorest. All of these elements were investigated up to their limits of usefulness, and all were soluble in alpha or beta titanium. All produced a lowering in the beta solvus line and all closely limited the extent of the alpha field.

Unalloyed titanium and practically all of the binary alloys are increased in hardness when quenched from elevated temperatures, the increase being greater the higher the temperature, at least up to 1750°F. Alloys, particularly those containing 2 or more pct iron or 5 to 10 pct manganese, are markedly hardened by quenching. Quenching from 1600°F did not produce a beneficial effect on the tensile properties of any of the compositions investigated. However, since marked hardening of some alloys occurs, it is believed that useful heat treatments may be developed.

Several of the binary systems age harden slightly after quenching from a high temperature and even

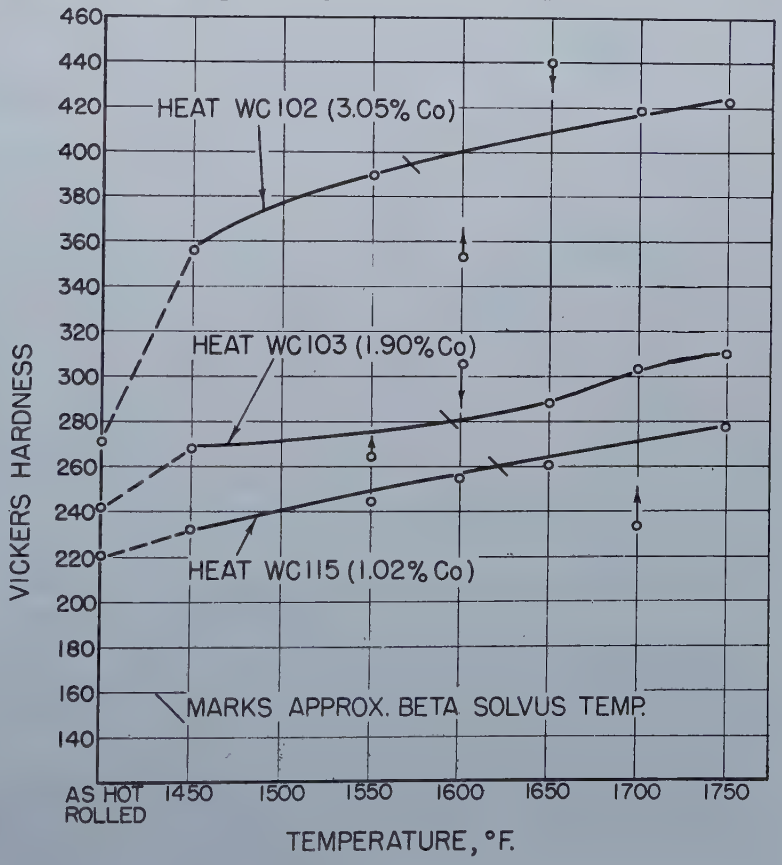

Fig. 44—Effect of solution temperature on the hardness of titanium-cobalt alloys prepared from process A metal.

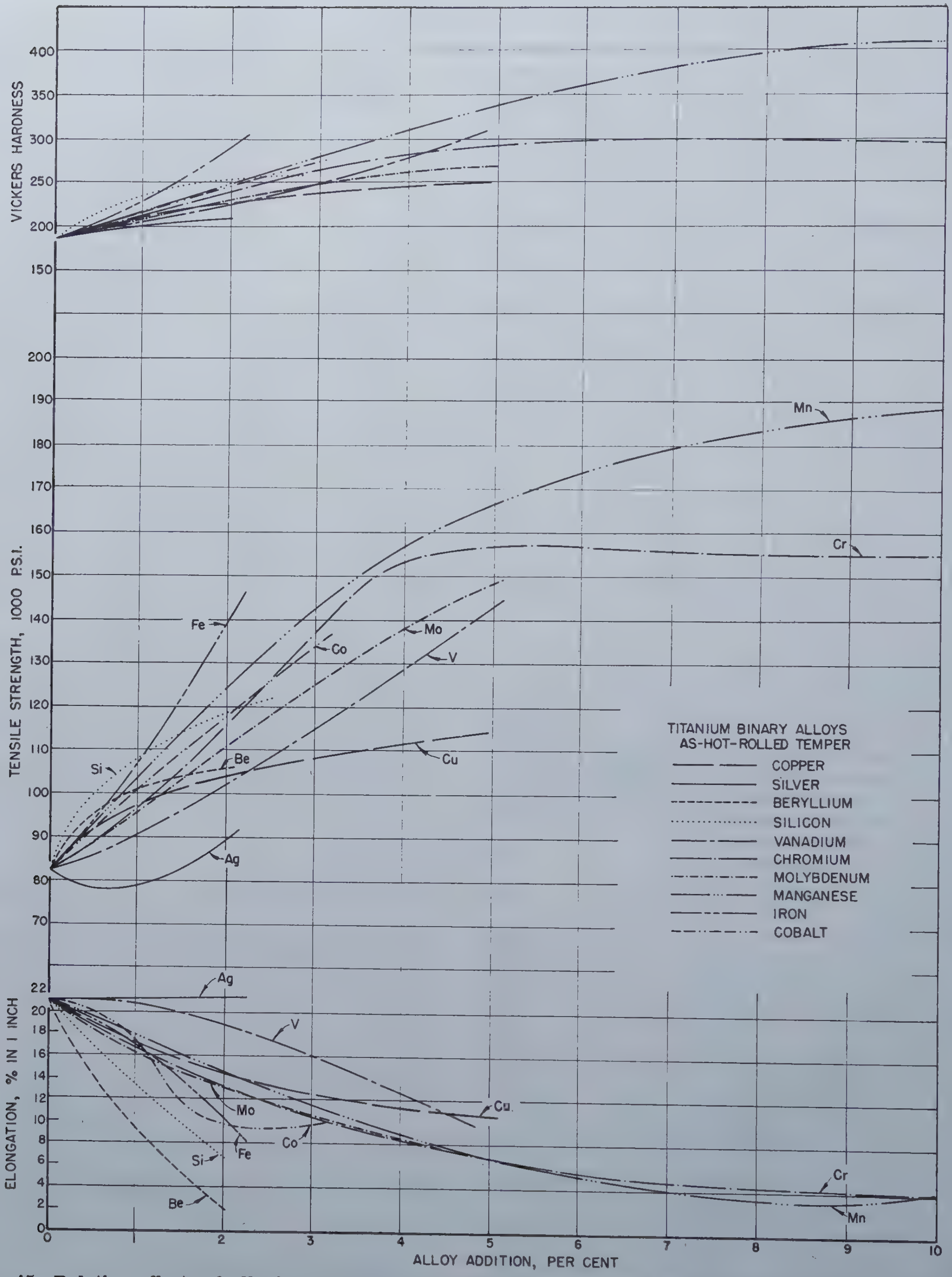

Fig. 45—Relative effects of alloying additions on the tensile properties and hardness of binary titanium alloys prepared from process A metal.

when the alloys are aged in the hot-rolled condition.

The data so far indicate that the best properties of titanium alloys are obtained in the as-hot-rolled condition, though no data are presented on the alloys which have been aged after hot rolling. Annealing produces slightly lower tensile strength with only a slight increase in ductility. Although the data are limited, cold working the annealed alloys does not appear to be beneficial since the loss in ductility is accompanied by only a slight increase in tensile strength.

The studies of titanium-base alloys are being continued under the sponsorship of the Air Materiel Command, Wright-Patterson Air Force Base.

Acknowledgment

The authors wish to express their appreciation to the Air Materiel Command, Wright-Patterson Air Force Base, who sponsored the work and granted permission for its publication.

Ternary Alloys of Titanium

by C. M. Craighead, O. W. Simmons, and L. W. Eastwood

The results of a preliminary study of 113 ternary titanium-base alloys are described. The compositions investigated were as follows:

1. Ternary titanium-carbon alloys containing copper, silicon, vanadium, chromium, manganese, iron, or cobalt.
2. Ternary titanium-nitrogen alloys containing chromium.
3. Ternary titanium-chromium alloys containing additions of vanadium, molybdenum, tungsten, cobalt, or nickel.
4. Ternary titanium-manganese alloys containing additions of silicon, chromium, tungsten, or iron.

Tensile properties, minimum bend radii, hardnesses, response to heat treatment and aging treatment, and phase relationships for these alloys were determined.

THIS is the second in a series of papers describing some of the results of the exploratory work on titanium alloys being conducted at Battelle Memorial Institute for the Wright-Patterson Air Force Base. The work with the binary alloy systems has been described in a previous publication.[1] This paper describes ternary titanium-base alloys as follows:

1. Ternary titanium-carbon alloys containing copper, silicon, vanadium, chromium, manganese, iron, or cobalt.
2. Ternary titanium-nitrogen alloys containing chromium.
3. Ternary titanium-chromium alloys containing additions of vanadium, molybdenum, tungsten, cobalt, or nickel.
4. Ternary titanium-manganese alloys containing additions of silicon, chromium, tungsten, or iron.

As the preparation and fabrication of the 0.5-lb experimental titanium alloy ingots to 14-ga sheet, as well as the methods of testing used in this work, have been described in the first paper of this series, *Titanium Binary Alloys,* no further discussion of these techniques will be given.

Ternary Alloys Containing Carbon

The following alloys of titanium, containing carbon and one other metal, were investigated:

1. 0.25 pct carbon; 1, 2.5, and 5 pct copper.
2. 0.25 pct carbon; 1, 2, and 3 pct silicon.
3. 0.25 pct carbon; 1, 2.5, and 5 pct vanadium.
4. 0.25 pct carbon; 2.5, 3.5, 5, 10, and 15 pct chromium.
5. 0.5 pct carbon; 2.5, 3.5, and 5 pct chromium.
6. 0.25 pct carbon; 1, 1.75, 2.5, 3.5, 5, 7.5, and 10 pct manganese.
7. 0.5 pct carbon; 1.75, 2.5, 3.5, 5, 7.5, and 10 pct manganese.
8. 0.25 pct carbon; 0.25, 0.5, 1, and 2 pct iron.
9. 0.25 pct carbon; 1, 2, and 3 pct cobalt.

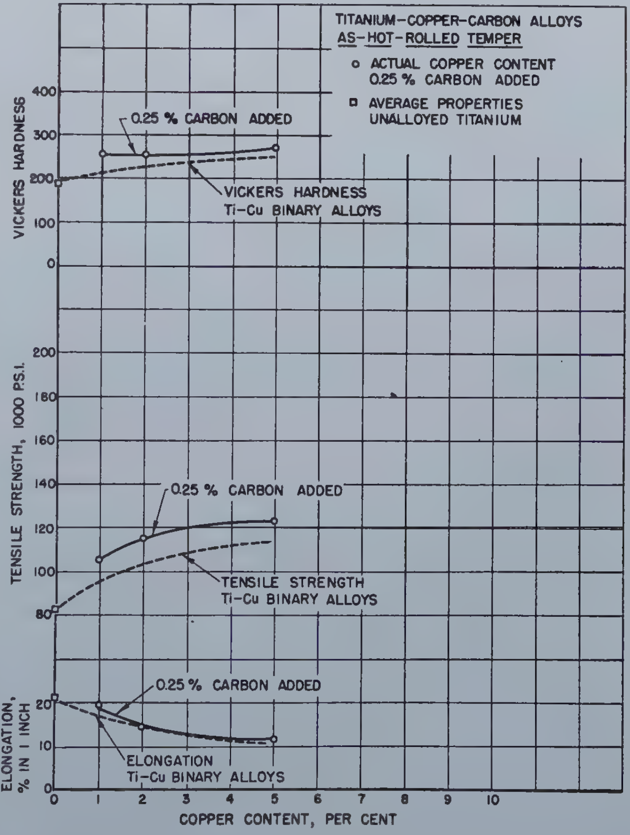

Fig. 1—Effect of carbon on the properties of as-hot-rolled titanium-copper alloys prepared from process A metal.

C. M. CRAIGHEAD, O. W. SIMMONS and L. W. EASTWOOD, Member AIME, are Assistant Supervisor, Research Engineer, and Supervisor, respectively, Battelle Memorial Institute, Columbus, Ohio.

New York Meeting, Feb. 1950.

TP 2748 E. Discussion (2 copies) may be sent to Transactions *AIME before Apr. 1, 1950, and is scheduled for publication Nov. 1950. Manuscript received Oct. 14, 1949.*

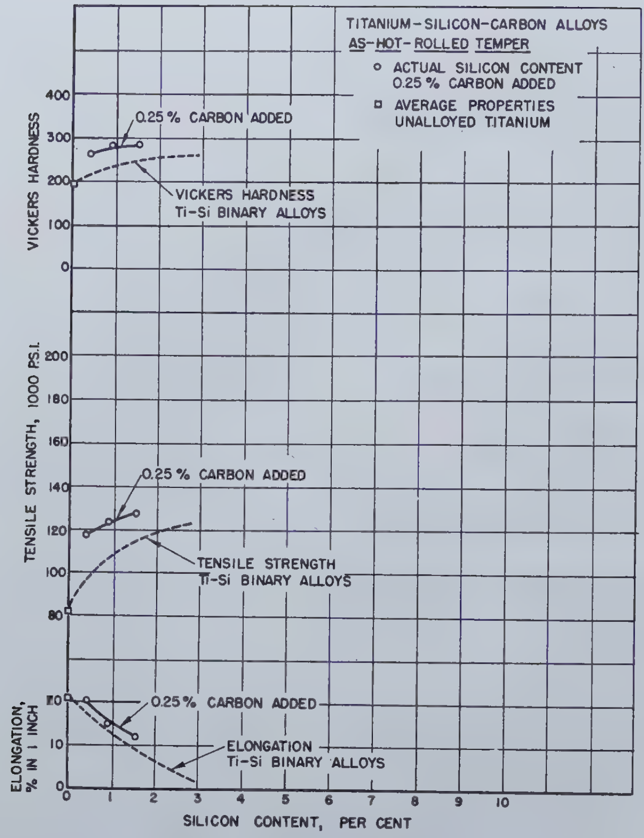

Fig. 2—Effect of carbon on the properties of as-hot-holled titanium-silicon alloys prepared from process A metal.

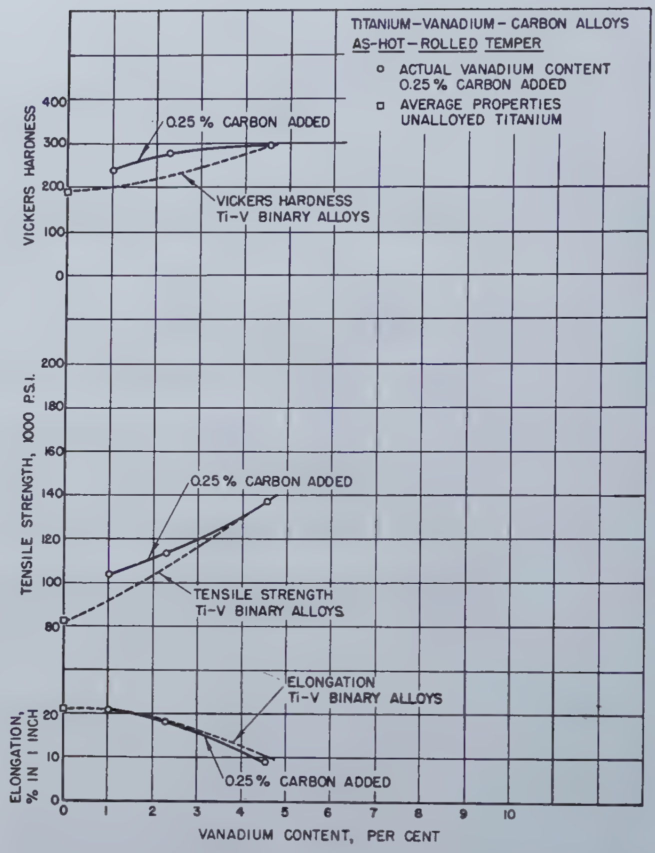

Fig. 3—Effect of carbon on the properties of as-hot-rolled titanium-vanadium alloys prepared from process A metal.

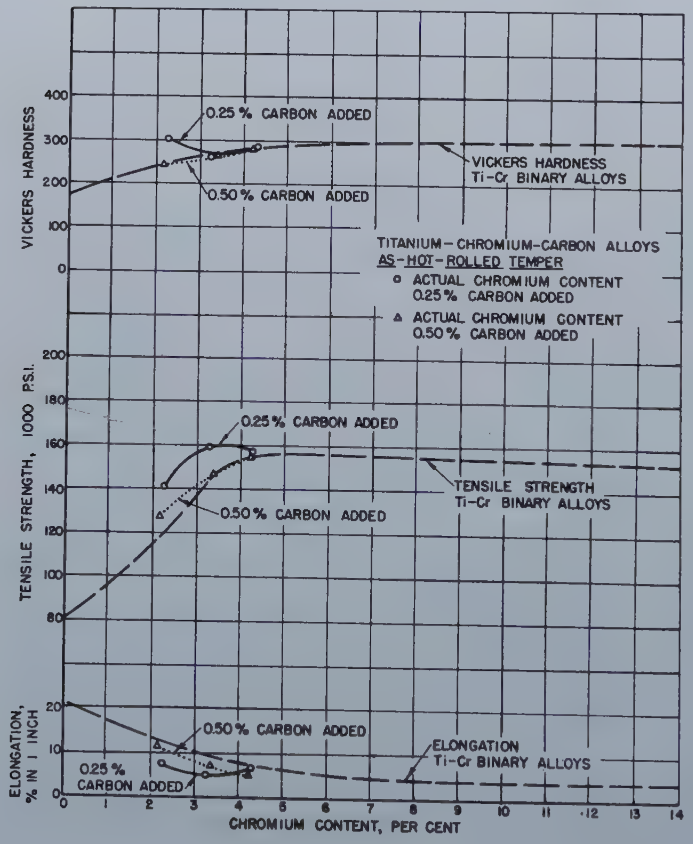

Fig. 4—Effect of carbon on the properties of as-hot-rolled titanium-chromium alloys prepared from process A metal.

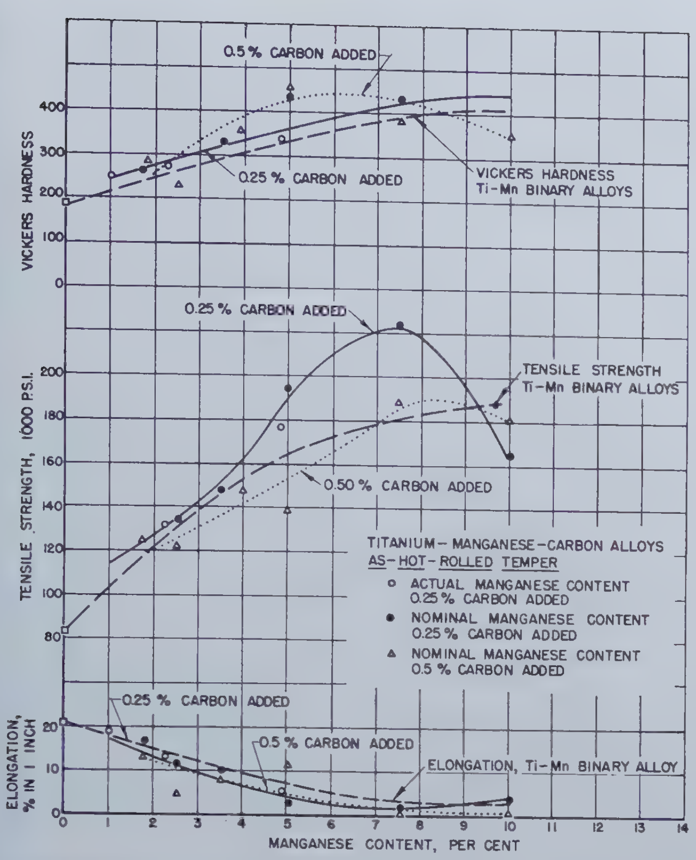

Fig. 5—Effect of carbon on the properties of as-hot-rolled titanium-manganese alloys prepared from process A metal.

Mechanical Properties: The mechanical properties of the above-listed ternary alloys in the as-hot-rolled condition, and after heat treating at 1600°F, are listed in table I. Fig. 1 to 7 show the effect of carbon by a comparison of the properties of the binary and ternary alloys in the as-hot-rolled condition. In these figures, the data for the binary alloys[1] are represented as dashed lines. The curves for the ternary alloys are shown in solid lines.

The addition of 0.25 pct carbon has generally produced an increase in tensile strength and hardness without a serious loss in ductility. However, when 0.5 pct carbon was added to the titanium-chromium and titanium-manganese alloys, the tensile strengths are lower than with 0.25 pct carbon present, as shown by fig. 4 and 5. The amount of the carbide phase present was observed to increase in those alloys containing 0.5 pct carbon and the lower properties are attributed to this condition. Thus, it appears that carbon as an alloying addition should be limited to about 0.25 pct or less.

A comparison of the tensile properties and hardnesses of these ternary alloys in the as-hot-rolled condition is illustrated by fig. 8. The ternary titanium-chromium-carbon and the ternary titanium-manganese-carbon alloys have outstanding tensile strengths. The manganese-carbon alloy containing about 7.5 pct manganese and 0.25 pct carbon had a tensile strength of 221,000 psi, a Vickers hardness of 438, and 2.0 pct elongation in 1 in., but no ductility in the bend test. The structure of this alloy as hot rolled at 1450°F was untransformed beta and titanium carbide. Alloys with lower manganese content produce better ductility with lower strength.

Structure and Transformation Range: Specimens of all the alloys comprising the seven ternary systems containing carbon, were quenched from temperatures of 1450, 1550, 1600, 1650, 1700, and 1750°F. These solution-treated samples were examined microscopically to establish the phase relationship.

No satisfactory etch was found for the titanium-silicon-carbon alloys that would differentiate between the silicon-rich phase, as observed in the binary titanium-silicon alloys,[1] and the carbide phase. The structures of these alloys were fine and the amount of the silicon-rich phase was large so that no estimate of the relative amounts of the alpha and beta phases was possible. Considerably more study will be needed to identify the phases present in the titanium-silicon-carbon system.

Fig. 9 to 13 show typical structures observed in the titanium-chromium-carbon and the titanium-manganese-carbon alloys. As evident from these micrographs, the presence of 0.25 pct or more carbon produced an insoluble carbide phase. This carbide constituent appears to be less soluble at temperatures where beta titanium is the stable phase than at lower temperatures where alpha and beta coexist. The beta phase of alloys containing 10 and 15 pct chromium and those containing 7.5 and 10 pct manganese appeared to be retained at room temperature when the alloys were air cooled after hot working at 1450°F or quenched from temperatures ranging from 1450 to 1750°F. These alloys showed none of the acicular alpha structure characteristic of transformed beta.

The effect of carbon on the transformation range of the titanium-copper, titanium-vanadium, titanium-chromium, titanium-manganese, titanium-iron, and titanium-cobalt systems is shown graphically in fig. 14 to 21. In these figures, the respective binary diagrams[1] have been reproduced as dashed

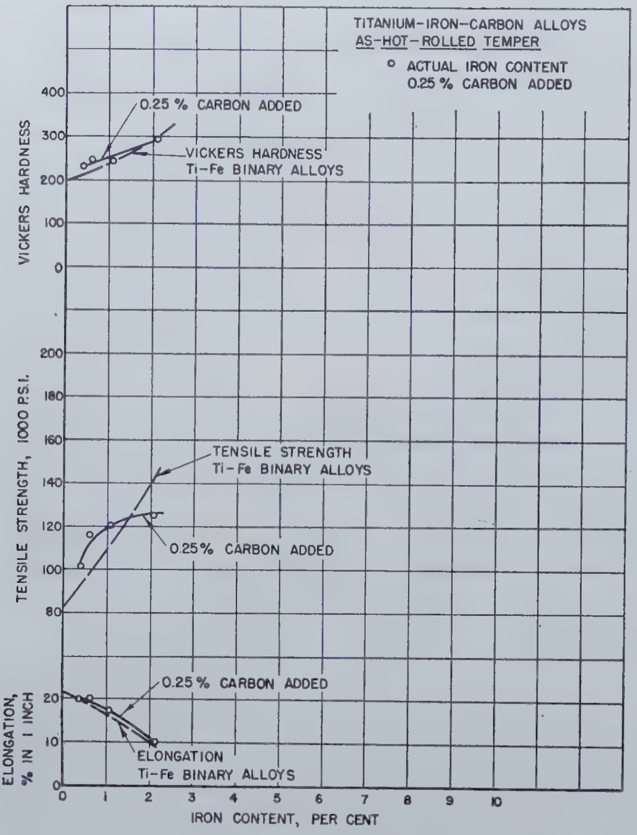

Fig. 6—Effect of carbon on the properties of as-hot-rolled titanium-iron alloys prepared from process A metal.

lines. The phases observed in the ternary alloys at temperatures of 1450 to 1750°F have been superimposed to show the changes resulting from the addition of carbon. Carbon raised the beta solvus line at low-alloy concentrations except in the titanium-chromium and the titanium-cobalt systems.

Response to Heat Treatment and Aging: The response of the ternary alloys containing carbon to solution heat treatment was followed by determining the Vickers hardness of specimens quenched from temperatures of 1450, 1550, 1600, 1650, 1700, and 1750°F. Age-hardening data were obtained in a similar manner on specimens quenched from 1600 and 1700°F and then aged for various periods at 752°F. These hardness data are listed in table II.

As indicated previously, silicon forms an insoluble constituent at very low concentrations. There was very little response of the ternary titanium-silicon-carbon alloys to heat treatment, as shown in table II.

Fig. 22 to 25 show graphically the changes in hardness produced by heat treating the titanium-copper-carbon, the titanium-vanadium-carbon, the titanium-manganese-carbon, and the titanium-iron-carbon alloys. Correlation of the hardness data on the heat-treated ternary alloys with their transformation range as shown by fig. 14 to 20 indicates that the greatest increases in hardness occurred in the more highly alloyed compositions when quenched from the beta-phase field.

The tensile properties of the various alloys after solution heat treatment at 1600°F are listed in table I. Referring to these data and comparing the

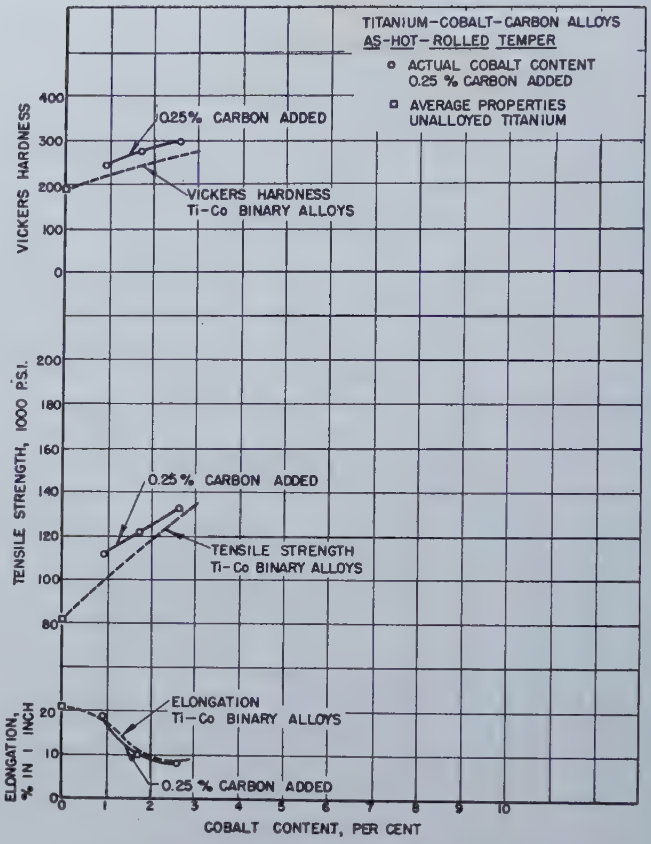

Fig. 7—Effect of carbon on the properties of as-hot-rolled titanium-cobalt alloys prepared from process A metal.

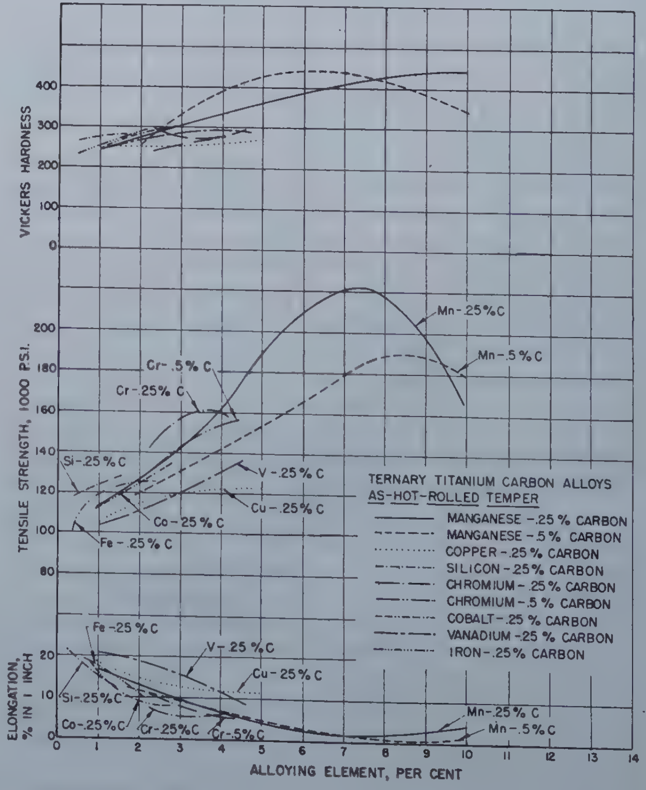

Fig. 8—Relative effects of various elements in titanium-carbon ternary alloys in the as-hot-rolled condition. Process A metal used.

Table I. Properties of Ternary Titanium-Carbon Alloys[8] Prepared from Process *A* Metal Base

Heat No.	Composition, Pct						As-Hot-Rolled Temper[1]				Heat Treated 1600°F[2]			
	Intended		Actual				Tensile Strength,[3] psi	Elong., Pct in 1 In.	VHN[4]	Minimum Bend Radius,[5] In.	Tensile Strength,[3] psi	Elong., Pct in 1 In.	VHN[4]	Minimum Bend Radius,[5] In.
				C	N	W								
							Titanium — Copper — Carbon (0.25 Pct C)							
WC29	Unalloyed		0.15 Fe	0.02	0.026	0.28	85,200	21.0	196	3/32	75,000	20.5	169	3/64
WC30	1.0 Cu	0.25 C	0.98 Cu	0.29	0.033	0.13	105,500	19.5	256	3/16	98,500	23.0	256	3/16
WC36	2.5 Cu	0.25 C	2.07 Cu	0.25	0.038	0.08	114,000	14.5	252	3/16	126,600	15.0	254	>1/4
WC26	5.0 Cu	0.25 C	5.02 Cu	0.25	0.029	0.18	122,700	11.5	271	1/4	137,500	2.5	336	>1/4
							Titanium — Silicon — Carbon (0.25 Pct C)							
WC86	Unalloyed						91,300	24.5	194	1/16	78,500	24.0	167	1/16
WC120	0.5 Si	0.25 C	0.38 Si				116,900	20.5	262	3/16	97,400	24.0	232	3/32
WC122	1.0 Si	0.25 C	0.92 Si				123,300	15.0	281	3/16	122,300	16.5	250	3/16
WC123	2.0 Si	0.25 C	1.52 Si				127,200	12.0	285	>1/4*	102,500	12.0	240	3/16
WC121	3.0 Si	0.25 C							254[6]					
							Titanium — Vanadium — Carbon (0.25 Pct C)							
WC72	Unalloyed			0.05	0.025	0.43	83,300	20.5	192	1/16	82,400	20.0	191	1/16
WC70	1.0 V	0.25 C	1.06 V	0.22	0.026	0.18	103,700	21.0	238	3/16	102,000	21.0	260	3/16
WC73	2.5 V	0.25 C	2.29 V	0.27	0.044	0.18	113,600	18.0	278	3/16	134,400	5.0	287	>1/4*
WC71	5.0 V	0.25 C	4.55 V	0.21	0.026	0.31	137,600	9.0	294	3/16	138,700	6.0	327	>1/4†
							Titanium — Chromium — Carbon (0.25 Pct C)							
WG69	Unalloyed						75,000	21.5	163	1/64	62,000	26.0	147	3/64
WAB4	2.5 Cr	0.25 C	2.28 Cr	0.28	0.135	0.14	171,200	8.0	336	>1/4	165,700	3.0		
WC15[7]	5.0 Cr	0.25 C	4.94 Cr	0.25	0.054	0.52	179,900	5.0	349	1/4	125,000	1.0		
WAB18	10.0 Cr	0.25 C	9.40 Cr	0.28	0.049	0.05	179,400	3.5	383	>1/4	158,800	3.5		
WC13[7]	15.0 Cr	0.25 C	14.4 Cr	0.13	0.045	0.28	171,000	6.0	346	3/16	170,000	5.5		
WG83	2.5 Cr	0.25 C	2.25 Cr				141,400	7.5	305	3/16	147,700	2.5	314	>1/4*
WG66	3.5 Cr	0.25 C	3.23 Cr				160,200	5.0	262	3/16	143,500	2.0	320	>1/4†
WG45	5.0 Cr	0.25 C	4.27 Cr				158,100	6.5	288	3/16	135,000	0.5	303	>1/4†
							Titanium — Chromium — Carbon (0.50 Pct C)							
WG69	Unalloyed						75,000	21.5	163	1/64	62,000	26.0	147	3/64
WG78	2.5 Cr	0.5 C	2.15 Cr				128,200	11.5	245	3/16	150,900	1.0	294	>1/4†
WG68	3.5 Cr	0.5 C	3.35 Cr				146,900	7.0	266	1/4	147,200	1.5	297	>1/4†
WG51	5.0 Cr	0.5 C	4.21 Cr				155,300	5.0	280	3/16	106,500	0.5	301	>1/4†
							Titanium — Manganese — Carbon (0.25 Pct C)							
WH79	Unalloyed						77,000	21.5	194	3/64	79,400	24.0	183	3/64
WC61	Unalloyed			0.02	0.055	0.14	82,400	22.0	186	3/64	75,000	17.0	170	3/64
WC62	1.0 Mn	0.25 C	0.98 Mn	0.18	0.043	0.14	113,000	19.0	252	3/16	114,900	16.0	259	3/16
WC59	2.5 Mn	0.25 C	2.24 Mn	0.14	0.019	0.20	132,700	13.0	272	3/16	150,800	7.0	334	>1/4
WC58	5.0 Mn	0.25 C	4.80 Mn	0.21	0.056	0.22	176,500	5.5	342	>1/4	157,000	1.5	417	>1/4
WH84	1.75 Mn	0.25 C					128,900	17.0	265	3/16	145,800	5.0	314	>1/4†
WH86	2.5 Mn	0.25 C					133,900	11.5	282	3/16	148,000	3.0	387	>1/4†
WH101	3.5 Mn	0.25 C					148,700	10.5	339	3/16	146,700	2.0	403	>1/4†
WH93	5.0 Mn	0.25 C					194,300	2.5	444	3/16	124,300	2.0	443	>1/4†
WH91	7.5 Mn	0.25 C					221,400	2.0	438	>1/4†	164,700	0.5	393	>1/4†
WH89	10.0 Mn	0.25 C					165,000	3.5	361	>1/4*	153,100	2.0	361	>1/4*
							Titanium — Manganese — Carbon (0.50 Pct C)							
WH79	Unalloyed						77,000	21.5	194	3/64	79,400	24.0	183	3/64
WH85	1.75 Mn	0.5 C					126,100	13.0	287	3/16	139,300	4.5	357	>1/4†
WH87	2.5 Mn	0.5 C					123,400	4.5	235	>1/4*	123,200	4.0	269	>1/4†
WH99	3.5 Mn	0.5 C					149,100	8.5	340	3/16	162,500	1.0	429	>1/4†
WH92	5.0 Mn	0.5 C					138,700	11.0	456	>1/4†	131,300	0.0	348	>1/4†
WH100	7.5 Mn	0.5 C					188,000	1.0	387	>1/4†	167,300	0.0	375	>1/4†
WH88	10.0 Mn	0.5 C					181,800	1.0	356	>1/4†	160,000	2.5	345	>1/4†
							Titanium — Iron — Carbon (0.25 Pct C)							
WC39	Unalloyed			0.03	0.043	0.24	83,600	20.5	192	3/32	76,600	22.5	182	3/32
WC40	0.25 Fe	0.25 C	0.40 Fe	0.16	0.035	0.07	100,800	20.0	231	3/16	99,300	20.0	242	3/32
WC38	0.5 Fe	0.25 C	0.63 Fe	0.22	0.034	0.34	117,200	20.0	249	3/16	114,500	14.0	247	3/16
WC42	1.0 Fe	0.25 C	1.10 Fe	0.15	0.03	0.17	120,300	17.5	243	3/16	130,500	10.0	287	>1/4
WC33	2.0 Fe	0.25 C	2.14 Fe	0.19	0.024	0.68	125,000	10.0	289	3/16	125,000	17.0	421	>1/4
							Titanium — Cobalt — Carbon (0.25 Pct C)							
WC101	Unalloyed			0.03	0.025	0.46	76,700	19.5	189	3/32	70,800	19.0	194	3/32
WC114	1.0 Co	0.25 C	0.93 Co	0.22	0.022	0.29	111,800	19.0	243	3/16	107,700	20.0	257	>1/4*
WC112	2.0 Co	0.25 C	1.17 Co	0.23	0.031	0.35	121,750	10.0	274	3/32	117,500	3.5	310	>1/4*
WC113	3.0 Co	0.25 C	2.60 Co	0.23	0.061	0.18	132,400	8.0	296	3/16	125,800	4.0	353	>1/4*

---

[1] As hot rolled 1450°F.

[2] Heated in air ½ hr at 1600°F and quenched in cold water.

[3] Average of 2 longitudinal 14-ga specimens, 3 in. long by 0.375 in. wide with a 0.250-in.-wide reduced section. Tested with the surface skin present.

[4] 10-kg load. Hardness at the center of the cross section of the sheet 90° to the surface and to the rolling direction.

[5] Minimum bend radius without cracking on a single longitudinal specimen 3 in. long by 0.5 in. wide. Tested with the surface skin present.

[6] Broke up on forging.

[7] Analysis — 0.03 pct Mn.

* Some ductility.

† Very little ductility.

[8] Forged at 1700°F by upsetting the 2¼-in. diam ingots on edge to 0.250-in. slab, then ground and hot rolled at 1450°F to 0.060-in. sheet.

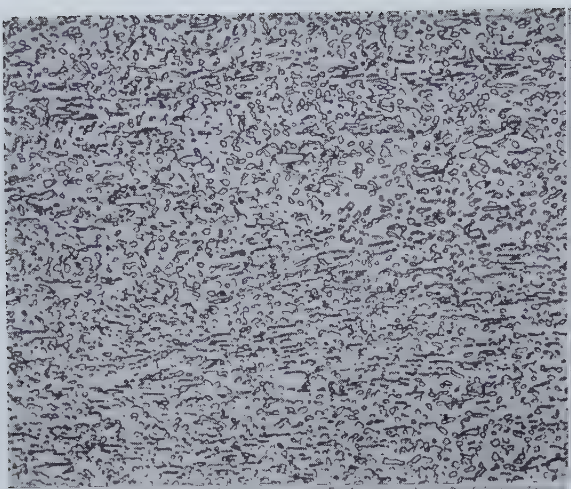

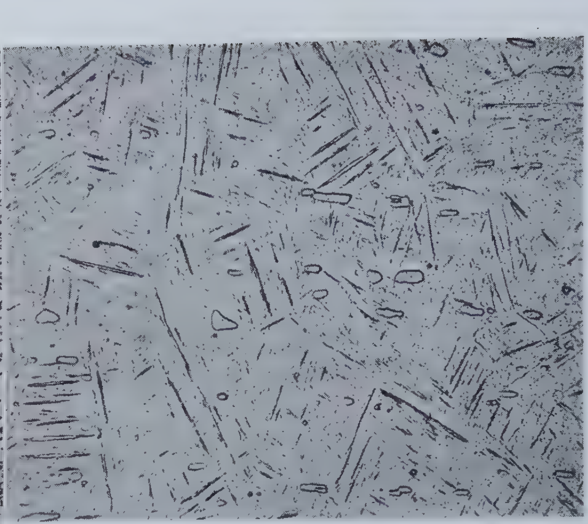

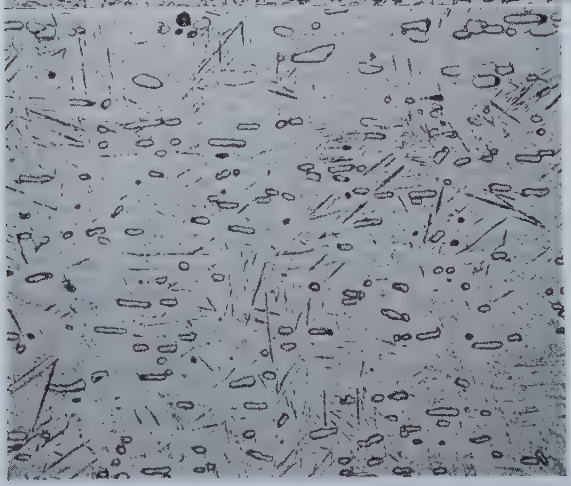

Fig. 9-11 — Typical structures observed in titanium-chromium alloys containing 0.25 and 0.5 pct added carbon, made from process A metal.

Fig. 9 (upper left)—Heat WG45, 4.27 pct Cr, 0.25 pct C (nominal).

Quenched from 1450°F in the $\alpha + \beta +$ TiC field. Background is transformed β with fine particles of alpha and larger gray islands of TiC. 500X.

Fig. 10 (upper right)—Heat WG45, 4.27 pct Cr, 0.25 pct C (nominal).

Quenched from 1550°F in the $\beta +$ TiC field. Acicular alpha (transformed beta) and carbides are shown. 500X.

Fig. 11 (lower left)—Heat WG68, 3.35 pct Cr, 0.5 pct C (nominal).

Quenched from 1550°F in the $\beta +$ TiC field. Acicular alpha (transformed beta) and carbide particles are shown. 500X.

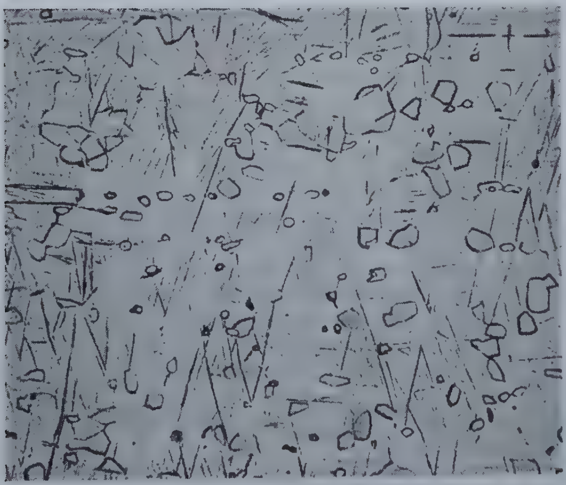

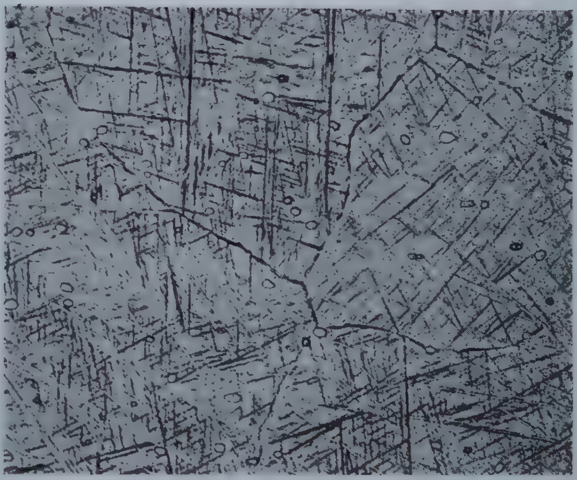

Fig. 12-13 — Typical structures observed in ternary titanium-manganese-carbon alloys made from process A metal.

Fig. 12 (left)—Heat WC59, 2.24 pct Mn, 0.15 pct C, 0.019 pct N, 0.20 pct W.

Quenched from 1650°F in the $\alpha + \beta +$ TiC field. Large islands of alpha and fine carbides in an acicular alpha (transformed beta) matrix are shown. 500X.

Fig. 13 (right)—Heat WC59, 2.24 pct Mn, 0.14 pct C, 0.019 pct N, 0.20 pct W.

Quenched from 1700°F in the $\beta +$ TiC field. Acicular alpha (transformed beta) and the carbide phases are illustrated.

Table II. Aging and Heat-treating Data for Titanium-Carbon Ternary Alloys[13] Prepared from Process *A* Metal Base

Heat No.	Composition, Pct						Heat-Treating Data								Aging Data														
	Intended		Actual				Vickers Hardness[1] After Indicated Treatment								Vickers Hardness[2] After Indicated Treatment														
				C	N	W	As Hot Rolled[3]	Anneal 1450°F[4]	Heat Treated 1450°F[5]	Heat Treated 1550°F[6]	Heat Treated 1600°F[7]	Heat Treated 1650°F[8]	Heat Treated 1700°F[9]	Heat Treated 1750°F[10]	As Hot Rolled[3], Aged 750°F for Indicated Time					Heat Treated 1600°F[7] Aged 752°F for Indicated Period					Heat Treated 1700°F[9] Aged 752°F for Indicated Period				
															0 Hr	2 Hr	4 Hr	8 Hr	12 Hr	0 Hr	2 Hr	4 Hr	8 Hr	12 Hr	0 Hr	2 Hr	4 Hr	8 Hr	12 Hr
Titanium-Copper-Carbon (0.25 Pct C)																													
WC29	Unalloyed		0.15 Fe	0.02	0.026	0.28	196		165	165	169	197	194	199						167	175	175	174	167	204	218	207	221	223
WC30	1.0 Cu	0.25 C	0.98 Cu	0.29	0.033	0.13	256		230	248	256	246	216	225						254	250	262	255	245	205	220	222	221	233
WC36	2.5 Cu	0.25 C	2.07 Cu	0.25	0.038	0.08	252		241	258	254	265	270	258						278	317	309	302	309	261	274	268	292	293
WC26	5.0 Cu	0.25 C	5.02 Cu	0.25	0.029	0.18	271		283	289	336	305	344	350	297	306	322	322		315	349	366	323	334	331	389	396	390	401
Titanium-Silicon Alloys (0.25 Pct C)																													
WC86	Unalloyed						194		161	164	167	187	203	199	194[1]		197[1]												
WC120	0.5 Si	0.25 C	0.38 Si				262		227	229	232	235	236	232	262[1]		257[1]												
WC122	1.0 Si	0.25 C	0.92 Si				281		242	242	250	268	254	273	281[1]		274[1]												
WC123	2.0 Si	0.25 C	1.52 Si				285		232	266	240	227	247	237	285[1]		283[1]												
WC121	3.0 Si	0.25 C					254[12]																						
Titanium-Vanadium Alloys (0.25 Pct C)																													
WC72	Unalloyed			0.05	0.025	0.43	192		183	181	191	210	202	221						193	199	200	199	174	218	222	236	242	204
WC70	1.0 V	0.25 C	1.06 V	0.22	0.026	0.18	238		233	234	260	260	233	254						262	275	274	275	246	218	239	232	260	213
WC73	2.5 V	0.25 C	2.29 V	0.27	0.044	0.18	278		272	279	287	281	270	280						299	298	287	299	272	274	290	304	302	268
WC71	5.0 V	0.25 C	4.55 V	0.21	0.026	0.31	294		304	306	327	327	351	351	300	310	319	325		355	361	384	348	339	388	404	414	405	369
Titanium-Chromium Alloys (0.25 Pct C)																													
WG69	Unalloyed						163		140	145	147	154	161	183	163[1]		186[1]												
WAB4	2.5 Cr	0.25 C	2.28 Cr	0.28	0.135	0.14	336	304	307					377	326	354	363	365	327										
WC15[11]	5.0 Cr	0.25 C	4.94 Cr	0.25	0.054	0.52	349	353	386					392	353	383	387	398	352										
WAB18	10.0 Cr	0.25 C	9.40 Cr	0.28	0.049	0.05	383	443	326					333	376	506	503	482	456										
WC13[11]	15.0 Cr	0.25 C	14.4 Cr	0.13	0.045	0.28	346	337	334					370	317	465	459	488	427										
WG83	2.5 Cr	0.25 C	2.25 Cr				305		301	318	314	327	339	369	305[1]		318[1]												
															262[1]		345[1]												
WG66	3.5 Cr	0.25 C	3.23 Cr				262		312	332	320	321	319	380	287	326	355	351											
															288[1]		357[1]												
WG45	5.0 Cr	0.25 C	4.27 Cr				288		310	376	303	309	312	314	304	338	351	364											
Titanium-Chromium Alloys (0.50 Pct C)																													
WG69	Unalloyed						163		140	145	147	154	161	183	163[1]		186[1]												
WG78	2.5 Cr	0.5 C	2.15 Cr				245		257	291	294	297	306	302	245[1]		301[1]												
WG68	3.5 Cr	0.5 C	3.35 Cr				266		296	295	297	311	313	335	266[1]		321[1]												
WG51	5.0 Cr	0.5 C	4.21 Cr				280		355	305	301	352	446	366	280[1]		355[1]												

Titanium-Manganese Carbon (0.25 Pct C)

WH79	Unalloyed						194		168	176	183	199	200	219	194[1]		194[1]											
WC61	Unalloyed			0.02	0.055	0.14	186		162	167	170	173	184	196					172	169	170	166	165	185	194	221	198	186
WC62	1.0 Mn	0.25 C	0.98 Mn	0.18	0.043	0.14	252		239	228	259	287	280	278					277	303	290	269	278	249	291	266	262	263
WC59	2.5 Mn	0.25 C	2.24 Mn	0.14	0.019	0.20	272		297	300	334	328	337	365					327	319	323	334	319	322	330	324	312	311
WC58	5.0 Mn	0.25 C	4.80 Mn	0.21	0.056	0.22	342		397	410	417	461	475	455					389	536	535	528	493	468	488	483	439	457
WH84	1.75 Mn	0.25 C					265		266	306	314	339	331	351	265[1]		276[1]											
WH86	2.5 Mn	0.25 C					282		304	374	387	387	344	392	282[1]		287[1]											
WH101	3.5 Mn	0.25 C					339		343	387	403	429	409	421	339[1]		314[1]											
WH93	5.0 Mn	0.25 C					444		429	446	443	426	394	406	444[1]		383[1]											
WH91	7.5 Mn	0.25 C					438		356	366	393	367	376	394	438[1]		498[1]											
WH89	10.0 Mn	0.25 C					361		362	351	361	355	350	370	361[1]		501[1]											

Titanium-Manganese Carbon (0.50 Pct C)

WH79	Unalloyed						194		168	176	183	199	200	219	194[1]		194[1]											
WH85	1.75 Mn	0.5 C					287		243	266	357	312	311	380	287[1]		294[1]											
WH87	2.5 Mn	0.5 C					235		242	240	269	294	446	355	235[1]		227[1]											
WH99	3.5 Mn	0.5 C					340		355	405	429	411	425	417	340[1]		362[1]											
															346	341	348	356										
WH92	5.0 Mn	0.5 C					456		303	401	348	379	421	433	456[1]		464[1]											
WH100	7.5 Mn	0.5 C					387		383	373	375	387	380	377	387[1]		525[1]											
WH88	10.0 Mn	0.5 C					356		353	349	345	351	350	360	356[1]		523[1]											

Titanium-Iron Carbon (0.25 Pct C)

WC39	Unalloyed			0.03	0.043	0.24	192		177	173	182	182	203	205					188	190	187	192	195	226	218	220	205	245
WC40	0.25 Fe	0.25 C	0.40 Fe	0.16	0.035	0.07	231		221	216	242	220	218	213					232	236	245	235	244	208	223	212	213	224
WC38	0.5 Fe	0.25 C	0.63 Fe	0.22	0.034	0.34	249		238	279	247	233	238	224					226	212	232	223	232	207	228	225	229	217
WC42	1.0 Fe	0.25 C	1.10 Fe	0.15	0.03	0.17	243		242	272	287	287	274	250					252	265	247	214	267	275	284	283	266	254
WC33	2.0 Fe	0.25 C	2.14 Fe	0.19	0.024	0.68	289		338	336	421	397	473	311					328	306	293	334	379	363	387	309	358	354

Titanium-Cobalt Carbon (0.25 Pct C)

WC101	Unalloyed			0.03	0.025	0.46	189		179	172	194	181	209	248	189[1]		193[1]											
WC114	1.0 Co	0.25 C	0.93 Co	0.22	0.022	0.29	243		253	283	257	268	253	266	243[1]		245[1]											
WC112	2.0 Co	0.25 C	1.71 Co	0.23	0.031	0.35	274		298	366	310	311	319	309	274[1]		281[1]											
WC113	3.0 Co	0.25 C	2.60 Co	0.23	0.061	0.18	296		332	409	353	432	330	348	296[1]		292[1]											

[1] 10-kg load. Hardness at the center of the cross section of the sheet specimen 90° to the surface and to the rolling direction. Average of at least 5 readings.

[2] 10-kg load. Surface hardness after grinding off the high-nitrogen surface layer unless indicated otherwise. Average of at least 5 readings.

[3] As hot rolled 1450°F.

[4] Annealed ½ hr in air at 1450°F and air cooled.

[5] Heated in air ½ hr at 1450°F and quenched in cold water.

[6] Heated in air ½ hr at 1550°F and quenched in cold water.

[7] Heated in air ½ hr at 1600°F and quenched in cold water.

[8] Heated in air ½ hr at 1650°F and quenched in cold water.

[9] Heated in air ½ hr at 1700°F and quenched in cold water.

[10] Heated in air ½ hr at 1750°F and quenched in cold water.

[11] Analysis—0.03 pct manganese.

[12] Broke up on forging.

[13] Forged at 1700°F by upsetting the 2¼-in. slab, then ground and hot rolled at 1450°F to 0.060-in. sheet.

Table III. Properties of Titanium-Chromium-Nitrogen Ternary Alloys[6] Prepared from Process *A* Metal Base

Heat No.	Composition, Pct		As-Hot-Rolled Temper[1]				Heat Treated 1600°F[2]			
	Intended	Actual C N W	Tensile Strength,[3] psi	Elong., Pct in 1 In.	VHN[4]	Minimum Bend Radius,[5] In.	Tensile Strength,[3] psi	Elong., Pct in 1 In.	VHN[4]	Minimum Bend Radius,[5] In.
							Titanium-Chromium-Nitrogen (0.1 Pct N)			
WG168	Unalloyed		77,200	22.5	180	3/64	69,400	15.5	186	3/64
WG176	2.5 Cr 0.1 N		131,200	9.0	313	3/16	152,400	1.0	397	>1/4†
WG174	3.5 Cr 0.1 N		158,500	7.0	311	3/16	140,000	1.0	370	>1/4†
WG172	5.0 Cr 0.1 N		186,800	5.0	295	3/16	84,100	0.0	426	>1/4†
							Titanium-Chromium-Nitrogen (0.2 Pct N)			
WG168	Unalloyed		77,200	22.5	180	3/64	69,400	15.5	186	3/64
WG175	2.5 Cr 0.2 N		154,400	8.0	320	3/16	97,500	0.0	399	>1/4†
WG173	3.5 Cr 0.2 N		163,300	12.0	324	3/16	61,200	0.0	388	>1/4†
WG169	5.0 Cr 0.2 N		185,100	4.0	365	3/16	57,500	0.0	469	>1/4†

[1] As hot rolled 1450°F.
[2] Heated in air ½ hr at 1600°F, and quenched in cold water.
[3] Average of 2 longitudinal 14-ga specimens, 3 in. long by 0.375 in. wide with a 0.250-in.-wide reduced section. Tested with the surface skin present.
[4] 10-kg load. Hardness at the center of the cross section of the sheet 90° to the surface and to the rolling direction. Average of at least 5 readings.
[5] Minimum bend radius without cracking on a single longitudinal specimen 3 in. long by 0.5 in. wide. Tested with the surface skin present.
† Very little ductility.
[6] Forged at 1700°F by upsetting the 2¼-in.-diam ingots on edge to 0.250-in. slab, then ground and hot rolled at 1450°F to 0.060-in sheet.

Table IV. Aging and Heat-treating Data for Titanium-Chromium-Nitrogen Ternary Alloys[10] Prepared from Process *A* Metal Base

Heat No.	Composition, Pct		Heat-Treating Data: Vickers Hardness[1] After Indicated Treatment							Aging Data: Vickers Hardness[2] After Indicated Treatment: As Hot Rolled,[3] Aged 750°F for Indicated Time			
	Intended	Actual C N W	As Hot Rolled[3]	Heat Treated 1450°F[4]	Heat Treated 1550°F[5]	Heat Treated 1600°F[6]	Heat Treated 1650°F[7]	Heat Treated 1700°F[8]	Heat Treated 1750°F[9]	0 Hr	2 Hr	4 Hr	8 Hr
WG168	Unalloyed		180	149	158	186	151	185	201	180[1]		178[1]	
WG176	2.5 Cr 0.1 N		313	260	365	397	384	392	332	313[1]		327[1]	
WG174	3.5 Cr 0.1 N		311	391	355	370	381	373	421	311[1]		321[1]	
WG172	5.0 Cr 0.1 N		295	452	498	426	493	478	489	295[1] 309	327	337[1] 330	335
WG168	Unalloyed		180	149	158	186	151	185	201	180[1]		178[1]	
WG175	2.5 Cr 0.2 N		320	366	358	399	397	408	429	320[1]		355[1]	
WG173	3.5 Cr 0.2 N		324	376	446	388	395	409	433	324[1] 336	342	377[1] 335	350
WG169	5.0 Cr 0.2 N		365	447	405	469	415	505	486	365[1] 364	372	414[1] 397	394

[1] 10-kg load. Hardness at the center of the cross section of the sheet specimen 90° to the surface and to the rolling direction. Average of at least 5 readings.
[2] 10-kg load. Surface hardness after grinding off the high-nitrogen layer unless indicated otherwise. Average of at least 5 readings.
[3] As hot rolled 1450°F.
[4] Heated in air ½ hr at 1450°F and quenched in cold water.
[5] Heated in air ½ hr at 1550°F and quenched in cold water.
[6] Heated in air ½ hr at 1600°F and quenched in cold water.
[7] Heated in air ½ hr at 1650°F and quenched in cold water.
[8] Heated in air ½ hr at 1700°F and quenched in cold water.
[9] Heated in air ½ hr at 1750°F and quenched in cold water.
[10] Forged at 1700°F by upsetting the 2¼-in.-diam ingots on edge to 0.250 in. slab then ground and hot rolled at 1450°F to 0.60-in. sheet.

Table V. Properties of Ternary Titanium-Chromium Alloys[6] Containing Additions of Vanadium, Molybdenum, Tungsten, Cobalt, or Nickel—Process *A* Metal Base

Heat No.	Composition, Pct		As-Hot-Rolled Temper[1]				Heat Treated 1600°F[2]			
	Intended	Actual C N W	Tensile Strength,[3] psi	Elong., Pct in 1 In.	VHN[4]	Minimum Bend Radius,[5] In.	Tensile Strength,[3] psi	Elong., Pct in 1 In.	VHN[4]	Minimum Bend Radius,[5] In.
					Titanium — Chromium — Vanadium (1.0 Pct V)					
WG108	Unalloyed		85,400	20.5	192	3/64	76,900	13.0	183	3/64
WG115	2.5 Cr 1.0 V		128,400	12.0	266	3/16	133,400	2.0	330	>1/4
WG116	3.5 Cr 1.0 V		134,800	10.0	276	3/16	117,100	2.0	350	>1/4
WG163	5.0 Cr 1.0 V		156,600	8.0	318	3/16	93,000	1.5	323	>1/4

Table V (continued). Properties of Ternary Titanium-Chromium Alloys[6] Containing Additions of Vanadium, Molybdenum, Tungsten, Cobalt, or Nickel—Process *A* Metal Base

Heat No.	Composition, Pct				As-Hot-Rolled Temper[1]				Heat Treated 1600°F[2]			
	Intended	Actual			Tensile Strength,[3] psi	Elong., Pct in 1 In.	VHN[4]	Minimum Bend Radius,[5] In.	Tensile Strength,[3] psi	Elong., Pct in 1 In.	VHN[4]	Minimum Bend Radius,[5] In.
		C	N	W								
Titanium — Chromium — Vanadium (2 Pct)												
WG108	Unalloyed				85,400	20.5	192	3/64	76,900	13.0	183	3/64
WG109	2.5 Cr 2.0 V				132,300	7.0	275	3/16	146,700	2.0	350	>1/4
WG100	3.5 Cr 2.0 V				140,700	12.0	407	>1/4*	137,500	2.0	442	>1/4
WG164	5.0 Cr 2.0 V				170,400	5.5	340	3/16	61,300	1.0	350	>1/4
Titanium — Chromium — Molybdenum (1.0 Pct Mo)												
WG103	Unalloyed				82,700	20.0	194	1/8	78,800	12.5	177	1/8
WG101	2.5 Cr 1.0 Mo				132,500	11.0	275	3/32	107,500	0.5	329	>1/4
WG93	3.5 Cr 1.0 Mo				137,200	9.0	284	3/16	114,500	2.0	303	>1/4
WG165	5.0 Cr 1.0 Mo				155,700	6.5	312	3/16	103,300	1.0	343	>1/4
Titanium — Chromium — Molybdenum (2.0 Pct Mo)												
WG103	Unalloyed				82,700	20.0	194	1/8	78,800	12.5	177	1/8
WG95	2.5 Cr 2.0 Mo				146,700	7.0	327	3/16	108,400	1.0	287	>1/4
WG92	3.5 Cr 2.0 Mo				145,700	8.0	322	3/16	94,200	1.0	318	>1/4
WG166	5.0 Cr 2.0 Mo				169,200	4.0	358	3/16	115,700	1.0	402	>1/4
Titanium — Chromium — Tungsten (1.0 Pct W)												
WG177	Unalloyed				89,100	19.5	197	3/32	79,200	16.0	184	3/32
WG186	2.5 Cr 1.0 W				130,400	11.0	267	3/16	117,000	2.0	315	>1/4*
WG183	3.5 Cr 1.0 W				145,900	10.0	303	3/16	120,000	1.0	319	>1/4
WG180	5.0 Cr 1.0 W				146,000	5.5	339	>1/4*	125,000	2.0	319	>1/4
Titanium — Chromium — Tungsten (2.0 Pct W)												
WG177	Unalloyed				89,100	19.5	197	3/32	79,200	16.0	184	3/32
WG185	2.5 Cr 2.0 W				140,000	11.0	272	3/16	123,400	2.0	323	>1/4
WG182	3.5 Cr 2.0 W				148,500	8.0	332	3/16	110,000	1.0	306	>1/4
WG179	5.0 Cr 2.0 W				171,900	4.5	342	3/16	86,500	1.0	314	>1/4
Titanium — Chromium — Tungsten (3.0 Pct W)												
WG177	Unalloyed				89,100	19.5	197	3/32	79,200	16.0	184	3/32
WG184	2.5 Cr 3.0 W				157,900	7.5	282	3/16	133,600	3.0	323	>1/4
WG181	3.5 Cr 3.0 W				154,800	11.0	334	3/16	119,200	1.5	301	>1/4
WG178	5.0 Cr 3.0 W				164,200	6.5	396	3/16	120,300	0.0	399	>1/4*
Titanium — Chromium — Cobalt (1.0 Pct Co)												
WG124	Unalloyed				81,700	21.0	196	1/16	76,800	16.0	177	1/16
WG155	2.5 Cr 1.0 Co				130,000	8.0	263	3/16			427	>1/4
WG158	3.5 Cr 1.0 Co				135,200	11.5	315	3/16	76,700	0.0	440	>1/4
WG156	5.0 Cr 1.0 Co				159,200	6.0	339	3/16	71,300	1.0	452	>1/4
Titanium — Chromium — Cobalt (2.0 Pct Co)												
WG124	Unalloyed				81,700	21.0	196	1/16	76,800	16.0	177	1/16
WG157	2.5 Cr 2.0 Co				125,900	10.0	274	3/16			479	>1/4
WG159	3.5 Cr 2.0 Co				146,100	9.5	320	3/16			530	>1/4
WG154	5.0 Cr 2.0 Co				170,400	3.5	361	3/16	104,700	1.0	473	>1/4
Titanium — Chromium — Nickel (1.0 Pct Ni)												
WG110	Unalloyed				85,700	22.0	186	1/16	77,000	12.0	179	3/32
WG129	2.5 Cr 1.0 Ni				122,500	12.5	249	3/16	101,800	2.0	370	>1/4
WG134	3.5 Cr 1.0 Ni				137,500	9.5	280	3/16	62,500	1.0	388	>1/4
WG167	5.0 Cr 1.0 Ni				150,000	8.0	326	3/16	28,100	0.0	475	>1/4
Titanium — Chromium — Nickel (2.0 Pct Ni)												
WG110	Unalloyed				85,700	22.0	186	1/16*	77,000	12.0	179	3/32
WG135	2.5 Cr 2.0 Ni				137,200	8.0	286	3/16	37,500	1.0	400	>1/4
WG125	3.5 Cr 2.0 Ni				140,800	7.0	292	3/16			486	>1/4
WG170	5.0 Cr 2.0 Ni				161,500	6.0	322	3/32	53,100	1.0	505	>1/4

[1] As hot rolled 1450°F.

[2] Heated in air ½ hr at 1600°F and quenched in cold water.

[3] Average of 2 longitudinal 14-ga specimens, 3 in. long by 0.375 in. wide with a 0.250-in.-wide reduced section. Tested with the surface skin present.

[4] 10-kg load. Hardness at the center of the cross section of the sheet 90° to the surface and to the rolling direction. Average of at least 5 readings.

[5] Minimum bend radius without cracking on a single longitudinal specimen 3 in. long by 0.5 in. wide. Tested with the surface skin present.

* Some ductility.

[6] Forged at 1700°F by upsetting the 2¼-in.-diam ingots on edge to 0.250-in. slab, then ground and hot rolled at 1450°F to 0.060-in. sheet.

Table VI. Aging and Heat-treating Data for Titanium-Chromium Alloys[9] Containing Additions of Vanadium, Molybdenum, Tungsten, Cobalt, or Nickel—Process *A* Metal Base

Heat No.	Composition, Pct			Heat-Treating Data							Aging Data	
				Vickers Hardness[1] After Indicated Treatment							Vickers Hardness[1] After Indicated Treatment	
	Intended	Actual		As Hot Rolled[2]	Heat Treated 1450°F[3]	Heat Treated 1550°F[4]	Heat Treated 1600°F[5]	Heat Treated 1650°F[6]	Heat Treated 1700°F[7]	Heat Treated 1750°F[8]	As Hot Rolled[3], Aged 750°F for Indicated Time	
			C N W								0 Hr	4 Hr
Titanium-Chromium-Vanadium (1.0 Pct V)												
WG108	Unalloyed			192	155	163	183	187	197	219	192	187
WG115	2.5 Cr, 1.0 V			266	277	325	330	334	332	345	266	287
WG116	3.5 Cr, 1.0 V			276	328	357	350	345	362	368	276	282
WG163	5.0 Cr, 1.0 V			318	309	322	323	341	366	389	318	335
Titanium-Chromium-Vanadium (2.0 Pct V)												
WG108	Unalloyed			192	155	163	183	187	197	219	192	187
WG109	2.5 Cr, 2.0 V			275	333	343	350	342	345	354	275	285
WG100	3.5 Cr, 2.0 V			407	437	345	442	357	356	370	407	425
WG164	5.0 Cr, 2.0 V			340	378	433	350	417	426	467	340	365
Titanium-Chromium-Molybdenum (1.0 Pct Mo)												
WG103	Unalloyed			194	157	163	177	172	201	217	194	187
WG101	2.5 Cr, 1.0 Mo			275	259	338	329	319	338	319	275	257
WG93	3.5 Cr, 1.0 Mo			284	289	309	303	310	352	354	284	300
WG165	5.0 Cr, 1.0 Mo			312	371	307	343	370	345	310	312	327
Titanium-Chromium-Molybdenum (2.0 Pct Mo)												
WG103	Unalloyed			194	157	163	177	172	201	217	194	187
WG95	2.5 Cr, 2.0 Mo			327	248	313	287	310	343	315	327	334
WG92	3.5 Cr, 2.0 Mo			322	257	312	318	457	467	465	322	322
WG166	5.0 Cr, 2.0 Mo			358	396	400	402	414	414	478	358	384
Titanium-Chromium-Tungsten (1.0 Pct W)												
WG177	Unalloyed			197	175	183	184	198	200	215	197	196
WG186	2.5 Cr, 1.0 W			267	339	315	315	312	314	319	267	273
WG183	3.5 Cr, 1.0 W			303	294	342	319	337	352	386	303	314
WG180	5.0 Cr, 1.0 W			339	362	399	319	297	325	405	339	349
Titanium-Chromium-Tungsten (2.0 Pct W)												
WG177	Unalloyed			197	175	183	184	198	200	215	197	196
WG185	2.5 Cr, 2.0 W			272	307	329	323	314	322	316	272	281
WG182	3.5 Cr, 2.0 W			332	326	319	306	329	288	349	332	325
WG179	5.0 Cr, 2.0 W			342	322	437	314	431	302	424	342	374
Titanium-Chromium-Tungsten (3.0 Pct W)												
WG177	Unalloyed			197	175	183	184	198	200	215	197	196
WG184	2.5 Cr, 3.0 W			282	339	327	323	329	316	319	282	297
WG181	3.5 Cr, 3.0 W			334	283	318	301	322	326	314	334	378
WG178	5.0 Cr, 3.0 W			396	443	417	399	369	325	437	396	436
Titanium-Chromium-Cobalt (1.0 Pct Co)												
WG124	Unalloyed			196	156	161	177	188	193	196	196	189
WG155	2.5 Cr, 1.0 Co			263	353	397	427	400	467	404	263	267
WG158	3.5 Cr, 1.0 Co			315	527	433	440	493	446	440	315	351
WG156	5.0 Cr, 1.0 Co			339	492	541	452	522	508	435	339	394
Titanium-Chromium-Cobalt (2.0 Pct Co)												
WG124	Unalloyed			196	156	161	177	188	193	196	196	189
WG157	2.5 Cr, 2.0 Co			274	383	421	479	514	534	519	274	292
WG159	3.5 Cr, 2.0 Co			320	536	500	530	505	519	537	320	343
WG154	5.0 Cr, 2.0 Co			361	397	542	473	433	344	442	361	446

Table VI (continued). Aging and Heat-treating Data for Titanium-Chromium Alloys[9] Containing Additions of Vanadium, Molybdenum, Tungsten, Cobalt, or Nickel—Process *A* Metal Base

Heat No.	Composition, Pct			Heat-Treating Data							Aging Data	
				Vickers Hardness[1] After Indicated Treatment							Vickers Hardness[1] After Indicated Treatment	
		Actual									As Hot Rolled[8]. Aged 750°F for Indicated Time	
	Intended		C N W	As Hot Rolled[2]	Heat Treated 1450°F[3]	Heat Treated 1550°F[4]	Heat Treated 1600°F[5]	Heat Treated 1650°F[6]	Heat Treated 1700°F[7]	Heat Treated 1750°F[8]	0 Hr	4 Hr
Titanium-Chromium-Nickel (1.0 Pct Ni)												
WG110	Unalloyed			186	158	157	179	181	204	200	186	184
WG129	2.5 Cr, 1.0 Ni			249	350	372	370	390	401	405	249	264
WG134	3.5 Cr, 1.0 Ni			280	351	368	388	380	377	399	280	300
WG167	5.0 Cr, 1.0 Ni			326	461	464	475	468	490	493	326	337
Titanium-Chromium-Nickel (2.0 Pct Ni)												
WG110	Unalloyed			186	158	157	179	181	204	200	186	184
WG135	2.5 Cr, 2.0 Ni			286	421	406	400	392	487	430	286	285
WG125	3.5 Cr, 2.0 Ni			292	483	498	486	503	508	542	292	301
WG170	5.0 Cr, 2.0 Ni			322	503	508	505	519	488	522	322	343

[1] 10-kg load. Hardness at the center of the cross section of the sheet specimen 90° to the surface and to the rolling direction. Average of at least 5 readings.
[2] As hot rolled 1450°F.
[3] Heated in air ½ hr at 1450°F and quenched in cold water.
[4] Heated in air ½ hr at 1550°F and quenched in cold water.
[5] Heated in air ½ hr at 1600°F and quenched in cold water.
[6] Heated in air ½ hr at 1650°F and quenched in cold water.
[7] Heated in air ½ hr at 1700°F and quenched in cold water.
[8] Heated in air ½ hr at 1750°F and quenched in cold water.
[9] Forged at 1700°F by upsetting the 2¼-in.-diam ingots on edge to 0.250-in. slab, then ground and hot rolled at 1450°F to 0.060-in. sheet.

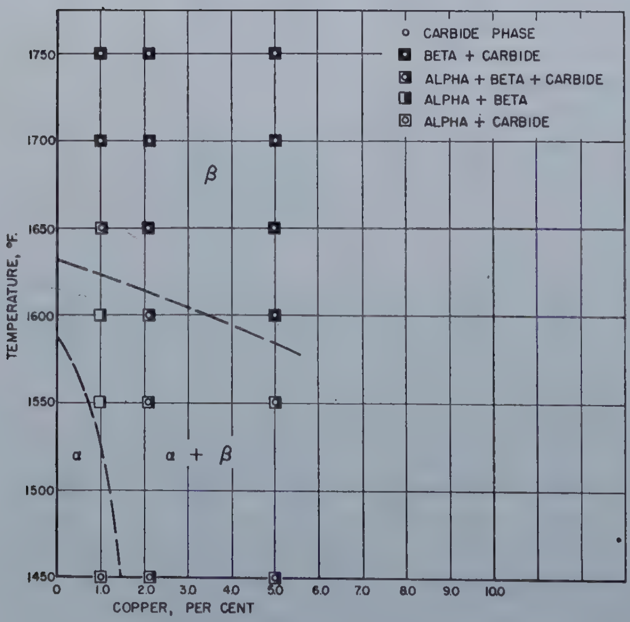

Fig. 14—Effect of 0.25 pct carbon on the transformation range of titanium—0 to 5.0 pct copper alloys made from process A metal.

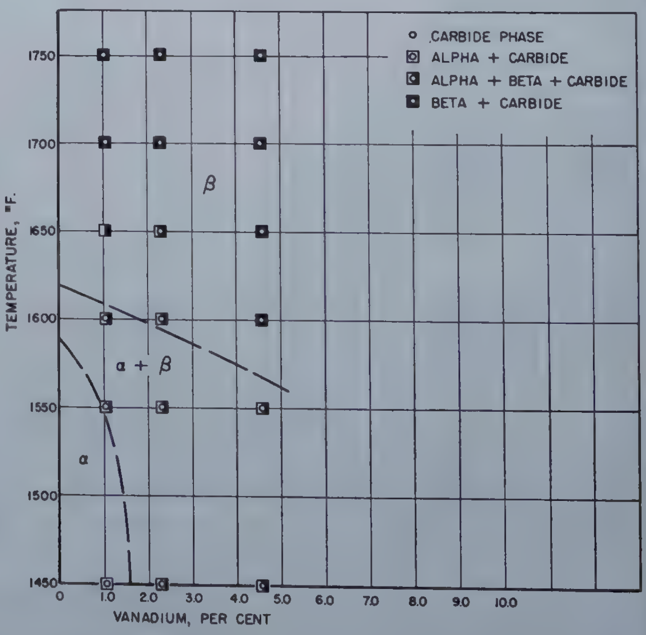

Fig. 15—Effect of 0.25 pct carbon on the transformation range of titanium—0 to 5.0 pct vanadium alloys made from process A metal.

Table VII. Properties of Ternary Titanium-Manganese Alloys[6] with Additions of Silicon, Chromium, Tungsten, or Iron—Process *A* Metal Base

Heat No.	Composition, Pct			As-Hot Rolled Temper[1]				Heat Treated 1600°F[2]			
	Intended	Actual		Tensile Strength,[3] psi	Elong., Pct in 1 In.	VHN[4]	Minimum Bend Radius,[5] In.	Tensile Strength,[3] psi	Elong., Pct in 1 In.	VHN[4]	Minimum Bend Radius,[5] In.
			C N W								
Titanium-Manganese Silicon (1.0 Pct Si)											
WH109	Unalloyed			84,700	18.5	197	3/32	76,900	20.5	177	3/32
WH128	1.75 Mn, 1.0 Si			141,000	6.5	266	3/16	134,000	1.5	376	>1/4*
WH127	2.5 Mn, 1.0 Si			133,300	3.0	287	>1/4*	143,800	1.0	405	>1/4*
WH119	3.5 Mn, 1.0 Si			145,400	6.5	397	>1/4*	136,900	1.0	380	>1/4†
WH114	5.0 Mn, 1.0 Si			152,800	4.5	392	>1/4*	60,600	1.0	419	>1/4†
Titanium-Manganese-Silicon (2.0 Pct Si)											
WH109	Unalloyed			84,700	18.5	197	3/32	76,900	20.5	177	3/32
WH124	1.75 Mn, 2.0 Si			151,300	3.0	305	>1/4†	122,400	1.0	383	>1/4†
WH120	2.5 Mn, 2.0 Si			141,300	7.5	315	>1/4*	118,200	2.0	380	>1/4†
WH113	3.5 Mn, 2.0 Si			152,500	1.5	349	>1/4*	79,400	0.0	438	>1/4†
WH123	5.0 Mn, 2.0 Si			141,000	1.0	356	>1/4*			420	>1/4†
Titanium-Manganese Chromium (1.0 Pct Cr)											
WH59	Unalloyed			87,400	21.5	195	3/64	82,400	16.0	200	3/32
WH63	1.75 Mn, 1.0 Cr			127,500	9.5	260	3/16	129,400	2.0	354	>1/4†
WH64	2.5 Mn, 1.0 Cr			120,000	11.5	258	3/16	120,000	1.5	368	>1/4†
WH67	3.5 Mn, 1.0 Cr			135,300	12.0	290	3/16	160,000	1.0	416	>1/4†
WH68	5.0 Mn, 1.0 Cr			172,400	7.0	383	3/16	91,800	1.5	459	>1/4†
Titanium-Manganese-Chromium (2.0 Pct Cr)											
WH59	Unalloyed			87,400	21.5	195	3/64	82,400	16.0	200	3/32
WH70	1.75 Mn, 2.0 Cr			132,100	13.5	257	3/16	88,200	1.5	364	>1/4†
WH71	2.5 Mn, 2.0 Cr			126,900	10.5	242	3/16	100,800	1.0	396	>1/4†
WH72	3.5 Mn, 2.0 Cr			157,700	5.0	272	3/16	102,100	0.0	414	>1/4†
WH73	5.0 Mn, 2.0 Cr			170,900	5.5	407	>1/4*	97,000	0.0	378	>1/4†
Titanium-Manganese-Tungsten (1.0 Pct W)											
WH130	Unalloyed			85,000	20.5	196	3/32	80,200	17.5	176	3/32
WH141	1.75 Mn, 1.0 W			116,400	12.5	252	3/16	144,300	5.0	340	>1/4*
WH139	2.5 Mn, 1.0 W			154,800	7.5	298	3/16	175,000	1.5	346	>1/4†
WH135	3.5 Mn, 1.0 W			142,000	12.0	365	3/16	126,700	1.5	409	>1/4†
WH131	5.0 Mn, 1.0 W			190,700	4.5	337	3/16	124,300	2.0	415	>1/4†
Titanium-Manganese Tungsten (2.0 Pct W)											
WH130	Unalloyed			85,000	20.5	196	3/32	80,200	17.5	176	3/32
WH140	1.75 Mn, 2.0 W			137,000	11.0	257	3/16	102,900	0.0	297	>1/4*
WH136	2.5 Mn, 2.0 W			135,000	6.5	356	3/16	141,700	1.5	379	>1/4†
WH132	3.5 Mn, 2.0 W			157,900	3.5	322	>1/4*	147,800	1.0	371	>1/4†
WH129	5.0 Mn, 2.0 W			153,400	6.5	373	3/16	134,100	2.0	390	>1/4†
Titanium-Manganese-Iron (1.0 Pct Fe)											
WH107	Unalloyed			87,500	21.5	205	3/32	74,900	21.0	179	3/32
WH108	1.75 Mn, 1.0 Fe			120,800	12.0	271	3/16	164,700	3.0	327	>1/4*
WH112	2.5 Mn, 1.0 Fe			170,000	8.5	260	3/16	101,400	2.0	399	>1/4†
WH143	3.5 Mn, 1.0 Fe			141,200	10.0	295	3/16	141,300	1.0	432	>1/4†
WH118	5.0 Mn, 1.0 Fe			144,300	2.0	315	>1/4*	98,000	1.0	413	>1/4†
Titanium-Manganese Iron (2.0 Pct Fe)											
WH107	Unalloyed			87,500	21.5	205	3/32	74,900	21.0	179	3/32
WH111	1.75 Mn, 2.0 Fe			136,500	8.5	291	3/16			451	>1/4†
WH115	2.5 Mn, 2.0 Fe			152,000	7.5	336	3/16	65,300	1.5	427	>1/4†
WH117	3.5 Mn, 2.0 Fe			175,000	5.5	373	>1/4*			459	>1/4†
WH121	5.0 Mn, 2.0 Fe			180,000	2.0	352	3/16	118,300	0.0	359	>1/4†

* Some ductility.

† Very little ductility.

[1] As hot rolled 1450°F.

[2] Heated in air ½ hr at 1600°F and quenched in cold water.

[3] Average of 2 longitudinal 14-ga specimens 3 in. long by 0.375 in. wide with a 0.250-in.-wide reduced section. Tested with the surface skin present.

[4] 10-kg load. Hardness at the center of the cross section of the sheet 90° to the surface and to the rolling direction. Average of at least 5 readings.

[5] Minimum bend radius without cracking on a single longitudinal specimen 3 in. long by 0.5 in. wide. Tested with the surface skin present.

[6] Forged at 1700°F by upsetting the 2¼-in.-diam ingots on edge to 0.250-in. slab, then ground and hot rolled at 1450°F to 0.060-in. sheet.

Table VIII. Heat-treating and Aging Data for Ternary Titanium Manganese Alloys[9] with Additions of Silicon, Chromium, Tungsten, or Iron—Process *A* Metal Base

Heat No.	Composition, Pct				Heat-Treating Data							Aging Data	
					Vickers Hardness[1] After Indicated Treatment							Vickers Hardness[1] After Indicated Treatment	
	Intended	Actual			As Hot Rolled[2]	Heat Treated 1450°F[3]	Heat Treated 1550°F[4]	Heat Treated 1600°F[5]	Heat Treated 1650°F[6]	Heat Treated 1700°F[7]	Treated Heat 1750°F[8]	As Hot Rolled[2]. Aged 750°F for Indicated Time	
		C	N	W								0 Hr	4 Hr
Titanium-Manganese-Silicon (1.0 Pct Si)													
WH109	Unalloyed				197	167	168	177	186	206	208	197	196
WH128	1.75 Mn, 1.0 Si				266	297	346	376	405	387	362	266	264
WH127	2.5 Mn, 1.0 Si				287	370	364	405	355	441	430	287	298
WH119	3.5 Mn, 1.0 Si				397	319	461	380	417	464	496	397	320
WH114	5.0 Mn, 1.0 Si				392	382	437	419	460	401	444	392	383
Titanium-Manganese-Silicon (2.0 Pct Si)													
WH109	Unalloyed				197	167	168	177	186	206	208	197	196
WH124	1.75 Mn, 2.0 Si				305	274	358	383	401	379	397	305	302
WH120	2.5 Mn, 2.0 Si				315	341	442	380	429	450	395	315	302
WH113	3.5 Mn, 2.0 Si				349	297	437	438	442	425	397	349	382
WH123	5.0 Mn, 2.0 Si				356	389	405	420	450	417	395	356	347
Titanium-Manganese-Chromium (1.0 Pct Cr)													
WH59	Unalloyed				195	175	182	200	174	204	215	195	200
WH63	1.75 Mn, 1.0 Cr				260	281	322	354	319	314	351	260	277
WH64	2.5 Mn, 1.0 Cr				258	273	360	368	363	376	386	258	304
WH67	3.5 Mn, 1.0 Cr				290	357	383	416	413	403	435	290	307
WH68	5.0 Mn, 1.0 Cr				383	384	441	459	433	421	444	383	405
Titanium-Manganese-Chromium (2.0 Pct Cr)													
WH59	Unalloyed				195	175	182	200	174	204	215	195	200
WH70	1.75 Mn, 2.0 Cr				257	346	358	364	366	370	394	257	291
WH71	2.5 Mn, 2.0 Cr				242	292	351	396	381	360	428	242	262
WH72	3.5 Mn, 2.0 Cr				272	405	431	414	416	392	390	272	290
WH73	5.0 Mn, 2.0 Cr				407	387	442	378	406	410	415	407	415
Titanium-Manganese-Tungsten (1.0 Pct W)													
WH130	Unalloyed				196	167	173	176	188	194	216	196	195
WH141	1.75 Mn, 1.0 W				252	270	312	340	309	325	349	252	275
WH139	2.5 Mn, 1.0 W				298	262	370	346	318	409	369	298	317
WH135	3.5 Mn, 1.0 W				365	328	383	409	394	401	429	365	315
WH131	5.0 Mn, 1.0 W				337	361	379	415	413	379	409	337	405
Titanium-Manganese-Tungsten (2.0 Pct W)													
WH130	Unalloyed				196	167	173	176	188	194	216	196	195
WH140	1.75 Mn, 2.0 W				257	274	330	297	339	325	359	257	278
WH136	2.5 Mn, 2.0 W				356	382	336	379	405	400	373	356	401
WH132	3.5 Mn, 2.0 W				322	370	373	371	390	390	384	322	349
WH129	5.0 Mn, 2.0 W				373	376	366	390	383	378	380	373	442
Titanium-Manganese-Iron (1.0 Pct Fe)													
WH107	Unalloyed				205	164	167	179	187	205	202	205	195
WH108	1.75 Mn, 1.0 Fe				271	257	344	327	401	429	437	271	264
WH112	2.5 Mn, 1.0 Fe				260	332	413	399	400	394	438	260	263
WH143	3.5 Mn, 1.0 Fe				295	411	424	432	416	405	429	295	303
WH118	5.0 Mn, 1.0 Fe				315	383	385	413	433	433	446	315	319
Titanium-Manganese-Iron (2.0 Pct Fe)													
WH107	Unalloyed				205	164	167	179	187	205	202	205	195
WH111	1.75 Mn, 2.0 Fe				291	387	502	451	481	473	499	291	265
WH115	2.5 Mn, 2.0 Fe				336	376	468	427	488	472	483	336	338
WH117	3.5 Mn, 2.0 Fe				373	390	426	459	455	437	421	373	364
WH121	5.0 Mn, 2.0 Fe				352	323	427	359	366	373	380	352	373

[1] 10-kg load. Hardness at the center of the cross section of the sheet specimen 90° to the surface and to the rolling direction. Average of at least 5 readings.
[2] As hot rolled 1450°F.
[3] Heated in air ½ hr at 1450°F and quenched in cold water.
[4] Heated in air ½ hr at 1550°F and quenched in cold water.
[5] Heated in air ½ hr at 1600°F and quenched in cold water.
[6] Heated in air ½ hr at 1650°F and quenched in cold water.
[7] Heated in air ½ hr at 1700°F and quenched in cold water.
[8] Heated in air ½ hr at 1750°F and quenched in cold water.
[9] Forged at 1700°F by upsetting the 2¼-in.-diam ingots on edge to 0.250-in. slab, then ground and hot rolled at 1450°F to 0.060-in. sheet.

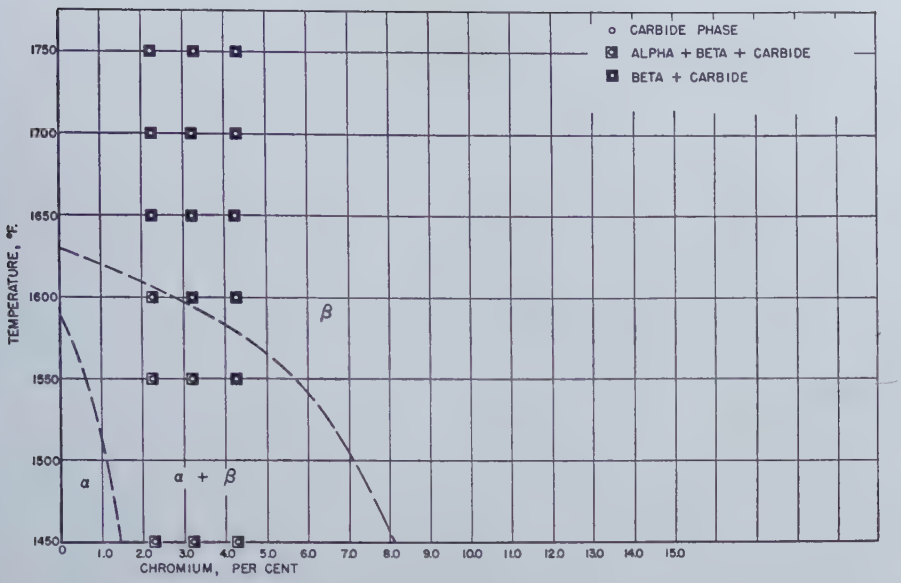

Fig. 16—Effect of 0.25 pct carbon on the transformation range of titanium—0 to 5 pct chromium alloys made from process A metal.

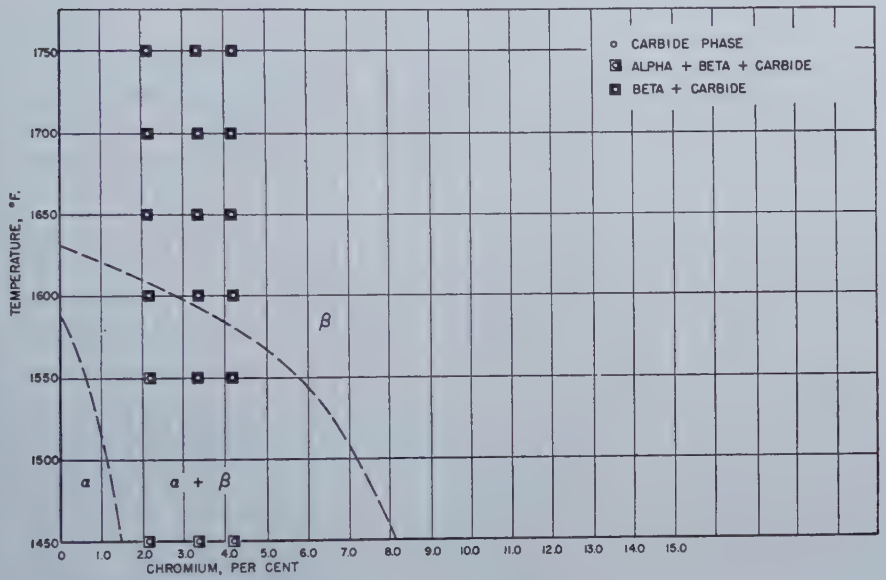

Fig. 17—Effect of 0.50 pct carbon on the transformation range of titanium—0 to 5 pct chromium alloys made from process A metal.

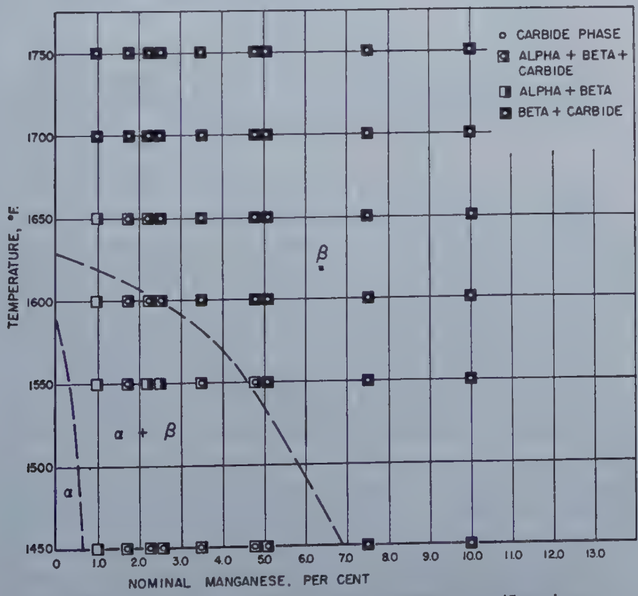

Fig. 18—Effect of 0.25 pct carbon on the transformation range of titanium—0 to 10 pct manganese alloys made from process A metal.

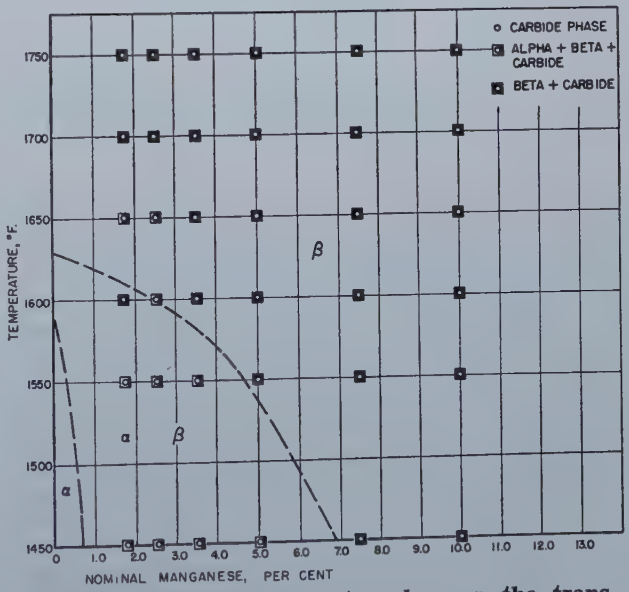

Fig. 19—Effect of 0.5 pct carbon on the transformation range of titanium—0 to 10 pct manganese alloys made from process A metal.

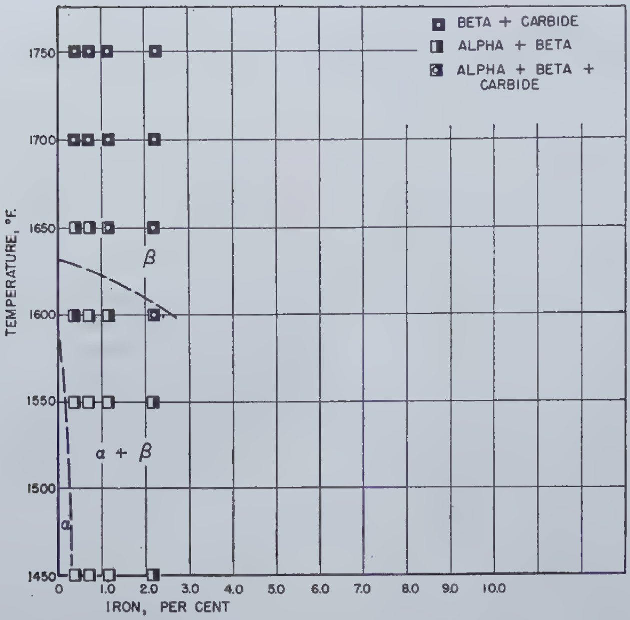

Fig. 20—Effect of 0.25 pct carbon on the transformation range of titanium—0 to 2.0 pct iron alloys made from process A metal.

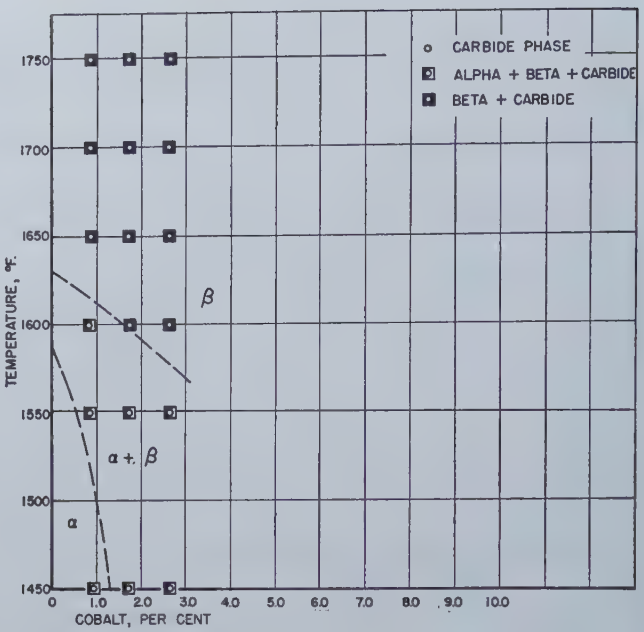

Fig. 21—Effect of 0.25 pct carbon on the transformation range of titanium—0 to 3 pct cobalt alloys made from process A metal.

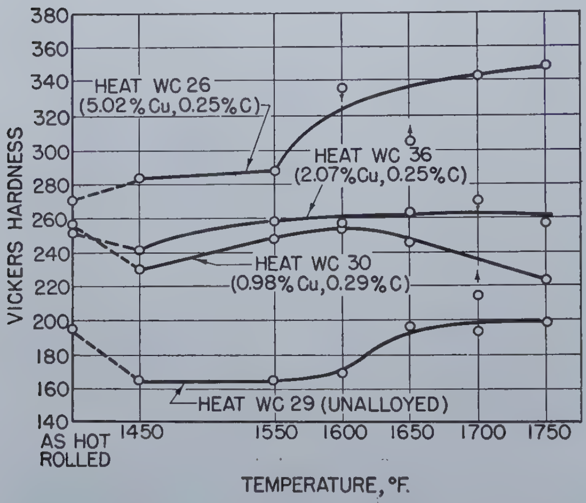

Fig. 22—Effect of solution treatment on the hardness of titanium-copper-carbon alloys prepared from process A metal.

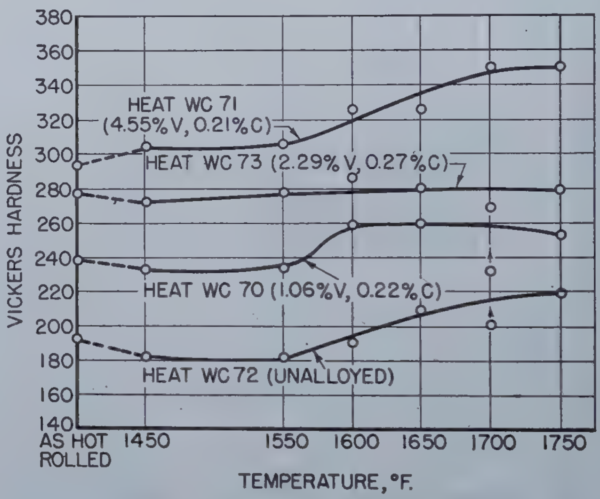

Fig. 23—Effect of solution treatment on the hardness of titanium-vanadium-carbon alloys prepared from process A metal.

properties of the alloys in the as-hot-rolled and heat-treated conditions, it will be observed that there is a marked decrease in elongation when the more highly alloyed compositions are quenched from 1600°F. This loss in ductility following heat treatment is not evident in the properties of either unalloyed titanium or the ternary titanium-silicon-carbon alloys where the silicon addition produces an insoluble phase. Thus, increased hardness and reduced ductility generally characterize the alloys water quenched from or near the beta-phase field.

Of the alloys listed in table I, which show an increase in tensile strength as a result of quenching from 1600°F, all except two compositions, 5.0 pct copper, 0.25 pct carbon, and 3.5 pct manganese, 0.5 pct carbon, consisted of alpha and beta phases at 1600°F.

Age-hardening studies were made on the titanium-copper-carbon, titanium-vanadium-carbon, titanium-manganese-carbon, and titanium-iron-carbon alloys by determining the Vickers hardness of specimens quenched from 1600 and 1700°F and subsequently aging them at 752°F for periods up to 12 hr. These aging data are listed in table II and shown graphically in fig. 26 to 29. The alloys having a high content of copper, manganese, and iron show the greatest increase in hardness when they are aged at 752°F. The titanium-vanadium-carbon alloys showed very little response to aging. Subsequently, selected compositions from these series of alloys which age hardened the most were heat treated at 1600 and 1700°F and aged at temperatures of 400, 500, 600, 700, and 800°F for periods up to 24 hr. Fig. 30 to 33 illustrate these data. Hard-

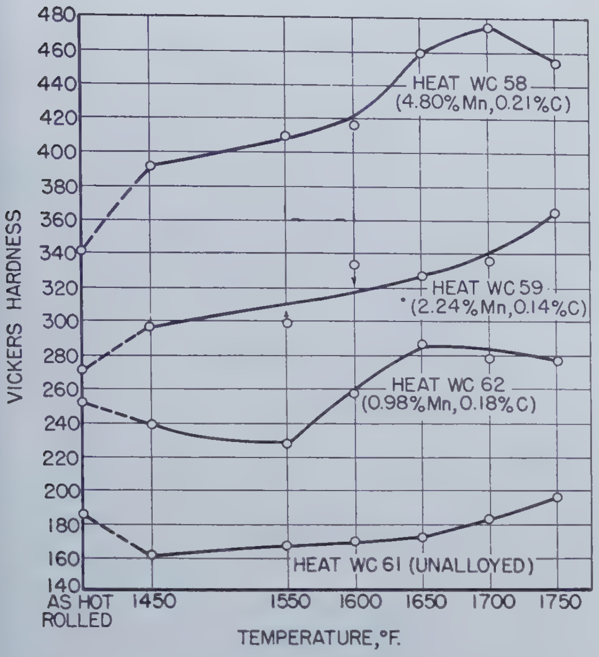

Fig. 24—Effect of solution treatment on the hardness of titanium-manganese-carbon alloys prepared from process A metal.

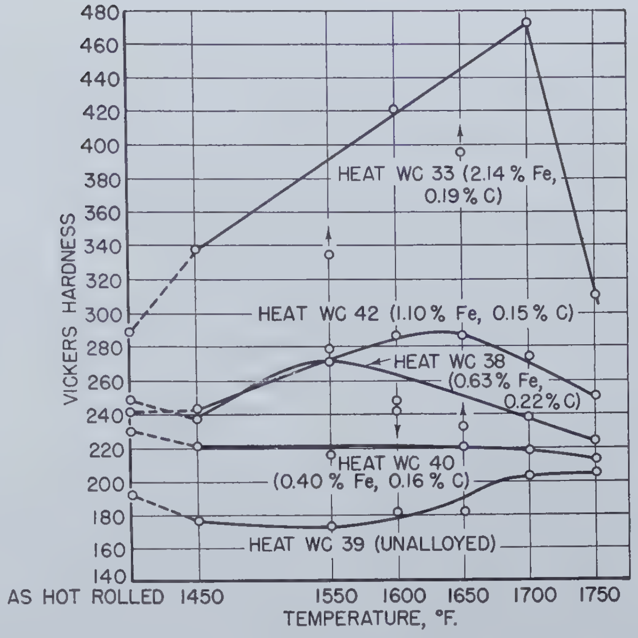

Fig. 25—Effect of solution treatment on the hardness of titanium-iron-carbon alloys prepared from process A metal.

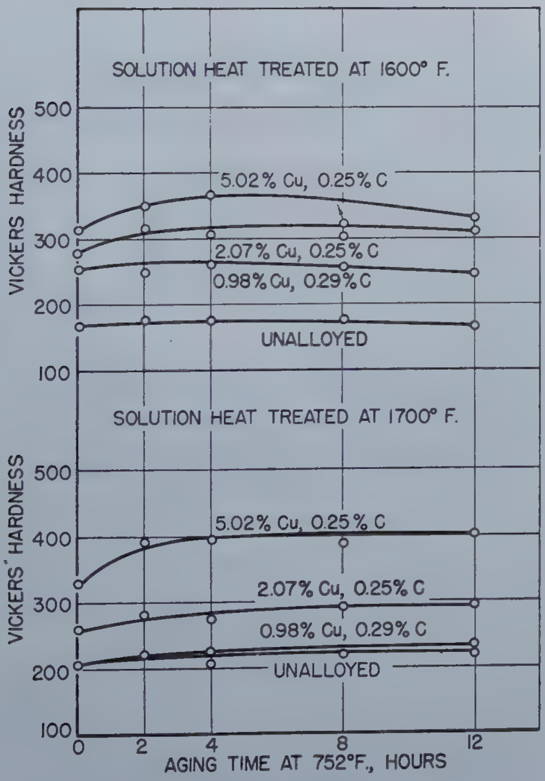

Fig. 26—Effect of aging on the hardness of titanium-copper-carbon alloys prepared from process A metal.

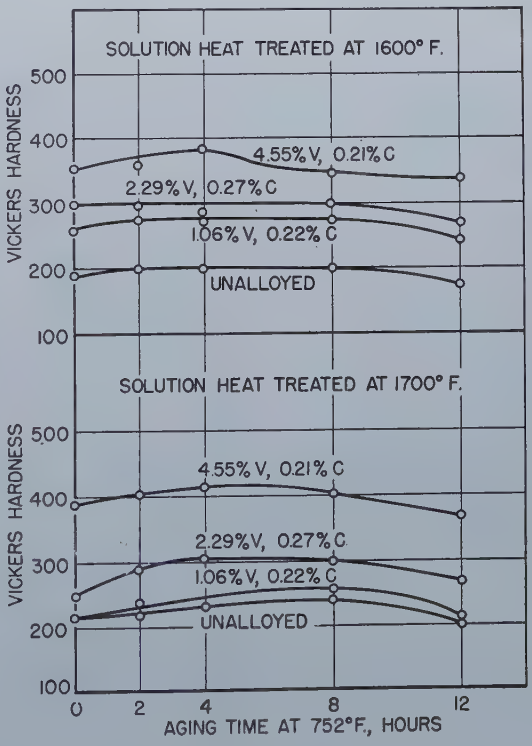

Fig. 27—Effect of aging on the hardness of titanium-vanadium-carbon alloys prepared from process A metal.

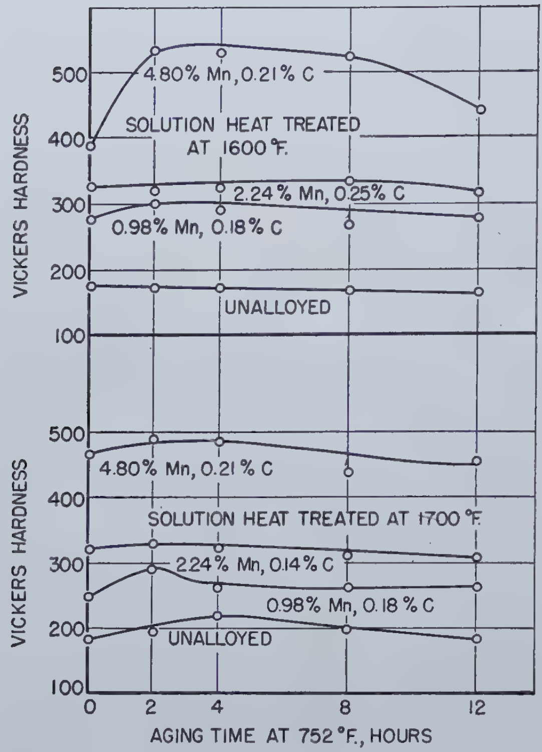

Fig. 28—Effect of aging on the hardness of titanium-manganese-carbon alloys prepared from process A metal.

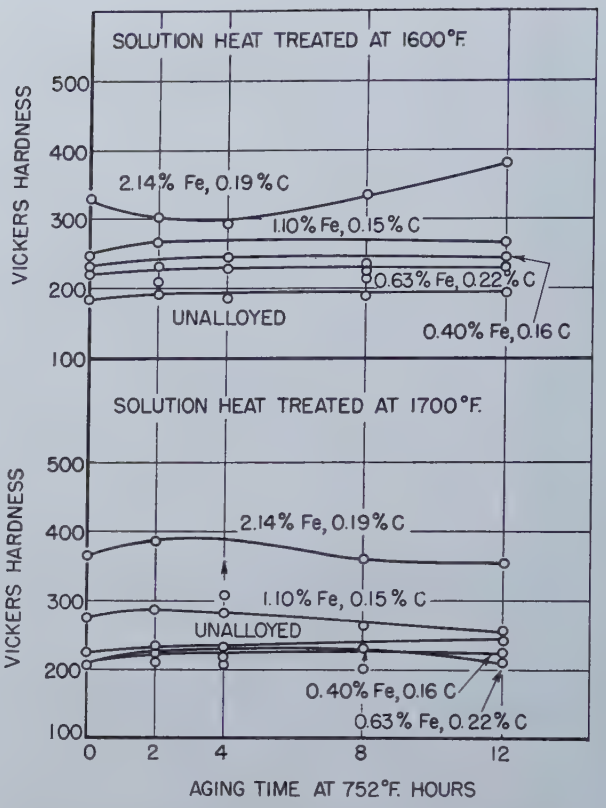

Fig. 29—Effect of aging on the hardness of titanium-iron-carbon alloys prepared from process A metal.

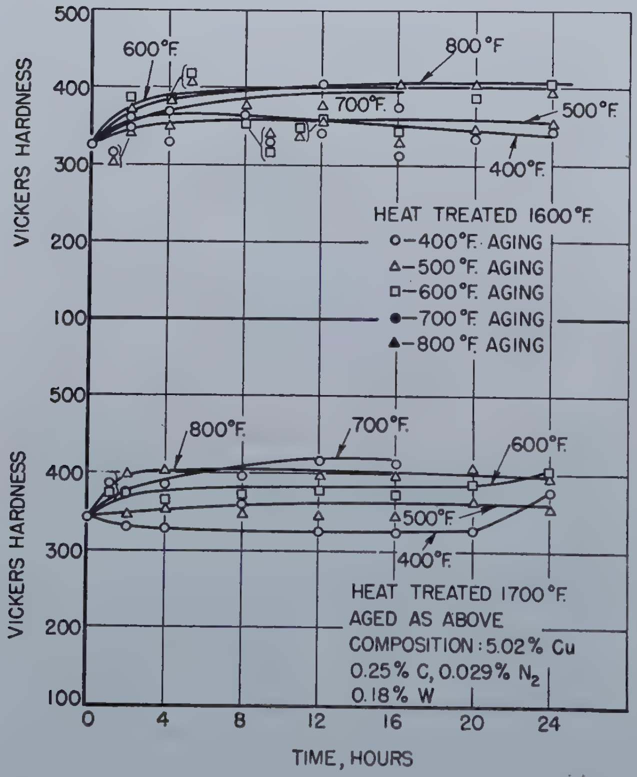

Fig. 30—Aging curves for a titanium-copper-carbon alloy (heat WC26), prepared from process A metal.

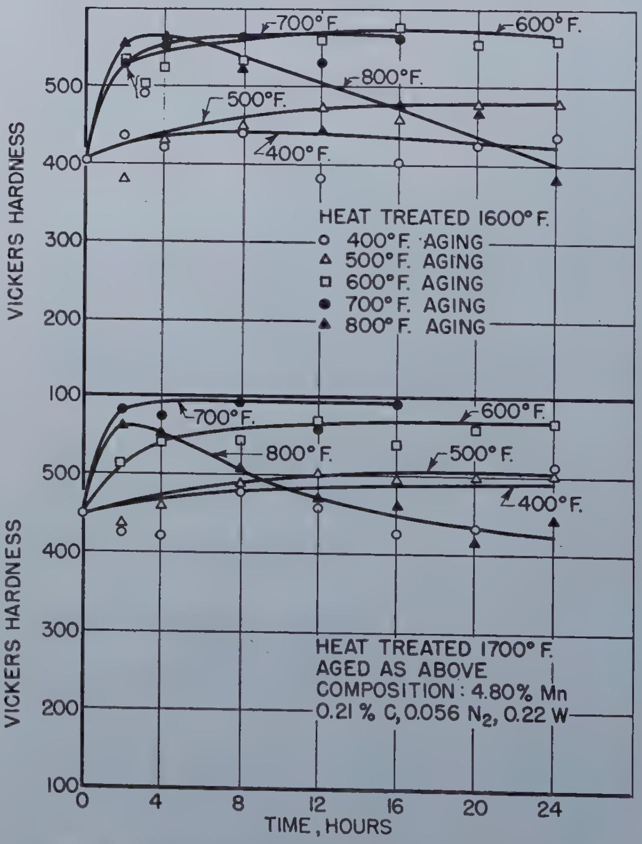

Fig. 31—Aging curves for a titanium-manganese-carbon alloy (heat WC58), prepared from process A metal.

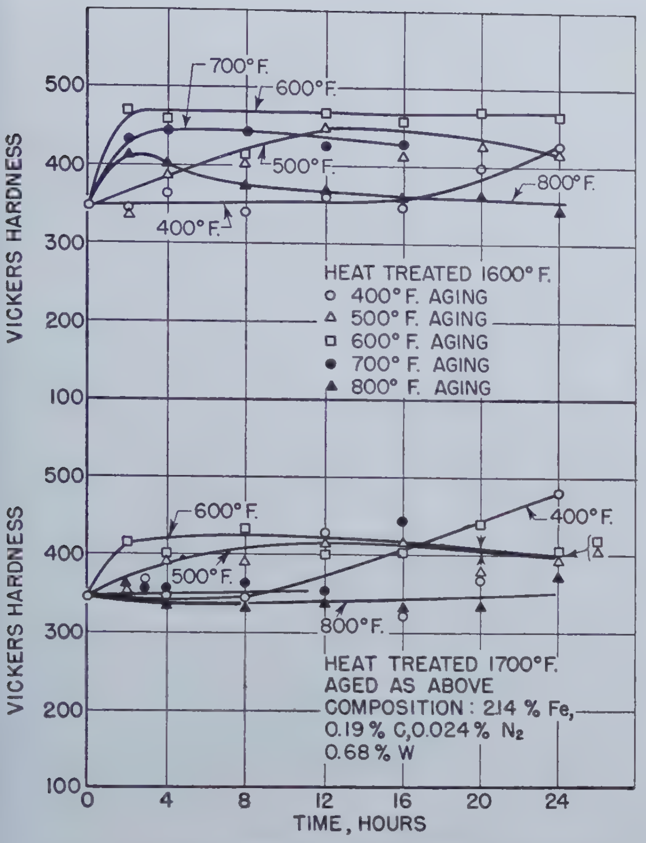

Fig. 32—Aging curves for a titanium-iron-carbon alloy (heat WC33), prepared from process A metal.

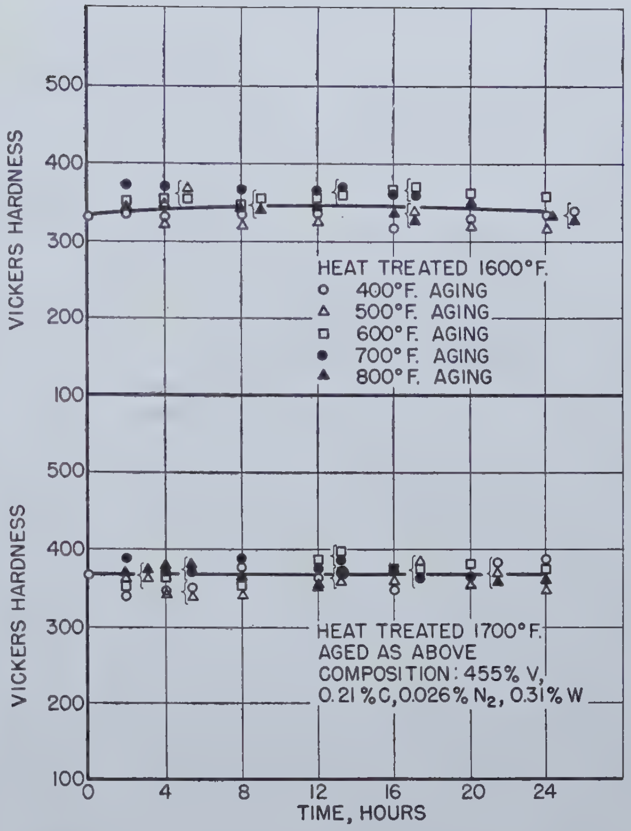

Fig. 33—Aging curves for a titanium-vanadium-carbon alloy (WC71), prepared from process A metal.

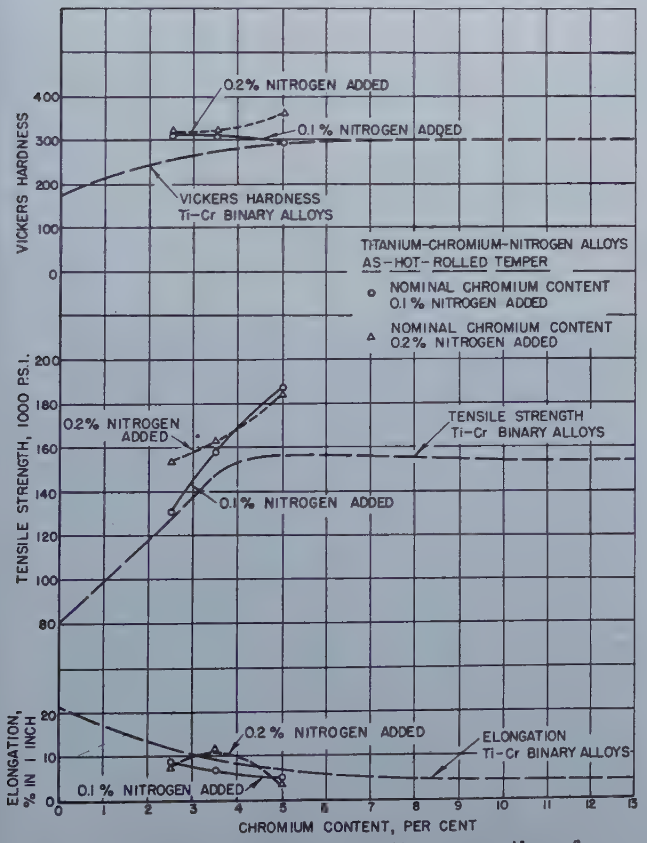

Fig. 34—Effect of nitrogen on the properties of as-hot-rolled titanium-chromium alloys prepared from process A metal.

ness vs. time at the aging temperature are shown for the following alloys:

Fig. 30—5.02 pct copper; 0.25 pct carbon.

Fig. 31—4.80 pct manganese; 0.21 pct carbon.

Fig. 32—2.14 pct iron; 0.19 pct carbon.

Fig. 33—4.55 pct vanadium; 0.21 pct carbon.

The titanium—4.55 pct vanadium—0.21 pct carbon alloy, as shown by fig. 33, did not age harden. The other three alloys age hardened appreciably and the effects of temperature are typical of age-hardening phenomena.

Limited data are available in table II showing the effect on hardness resulting from aging the as-hot-rolled alloys at 750°F. A marked increase in hardness was obtained in the alloys containing the higher concentrations of chromium and manganese. The titanium-silicon-carbon and the titanium-cobalt-carbon alloys show no increase in hardness as a result of aging the alloys in the as-hot-rolled temper.

The mechanism of age-hardening is believed to be the decomposition of the beta phase retained after hot working or quenching. The explanation is supported by the fact that, in the alloys containing the higher concentrations of either manganese or chromium, the beta phase is retained after hot working or quenching and these compositions show the greatest hardness increase during aging.

Ternary Titanium-Chromium-Nitrogen Alloys

The titanium-chromium-nitrogen ternary alloys

Fig. 35—Effect of 0.1 pct nitrogen on the transformation range of titanium—0 to 5 pct chromium alloys made from process A metal.

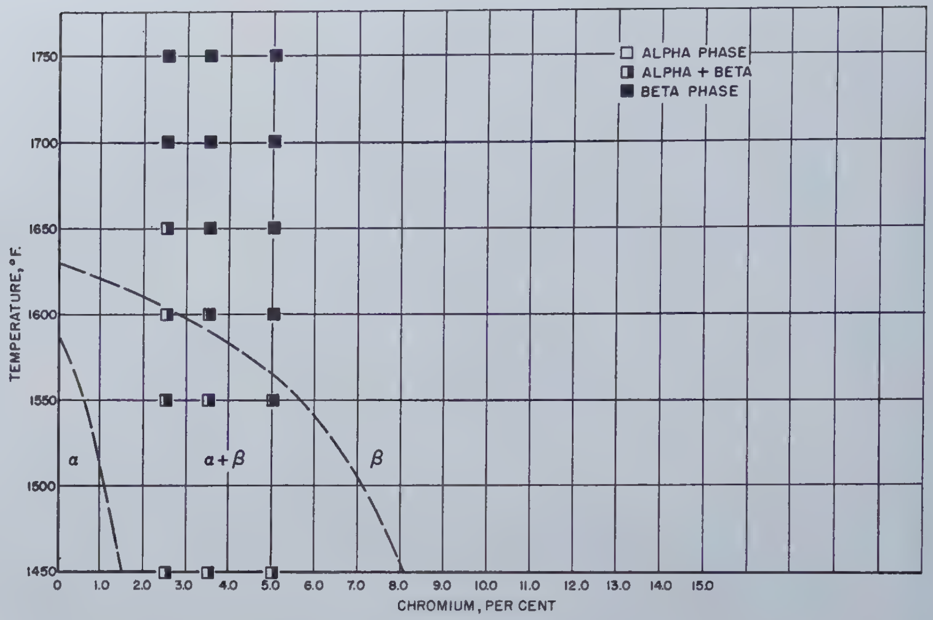

Fig. 36—Effect of 0.2 pct nitrogen on the transformation range of titanium—0 to 5 pct chromium alloys made from process A metal.

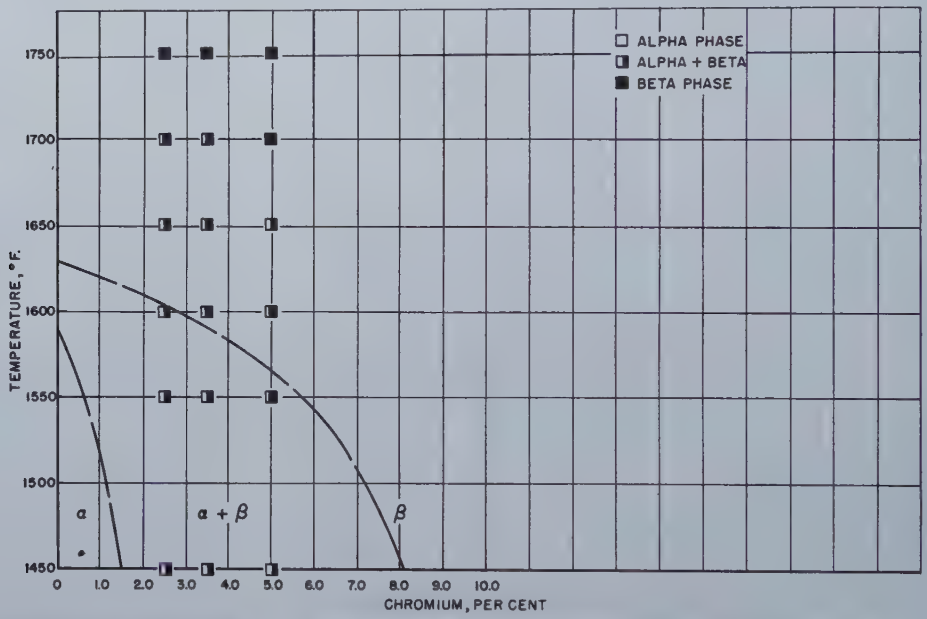

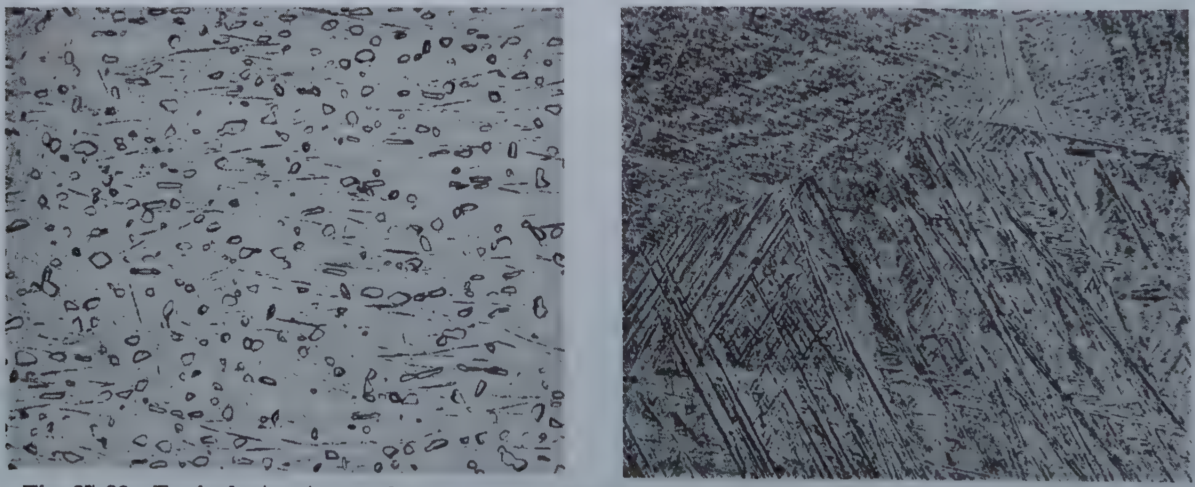

Fig 37-38—Typical structures observed in ternary titanium-chromium-nitrogen alloys made from process A metal. Fig. 37 (left)—Heat WG175, 2.5 pct Cr, 0.20 pct N (nominal). Fig 38 (right)—Heat WG175, 2.5 pct Cr, 0.20 pct N (nominal).

(Fig 37) Quenched from 1700°F in the α + β field. Islands of alpha are in an acicular alpha (transformed beta) matrix. 500X.
(Fig 38) Quenched from 1750°F in the β field. Acicular alpha (transformed beta) is shown. 500X.

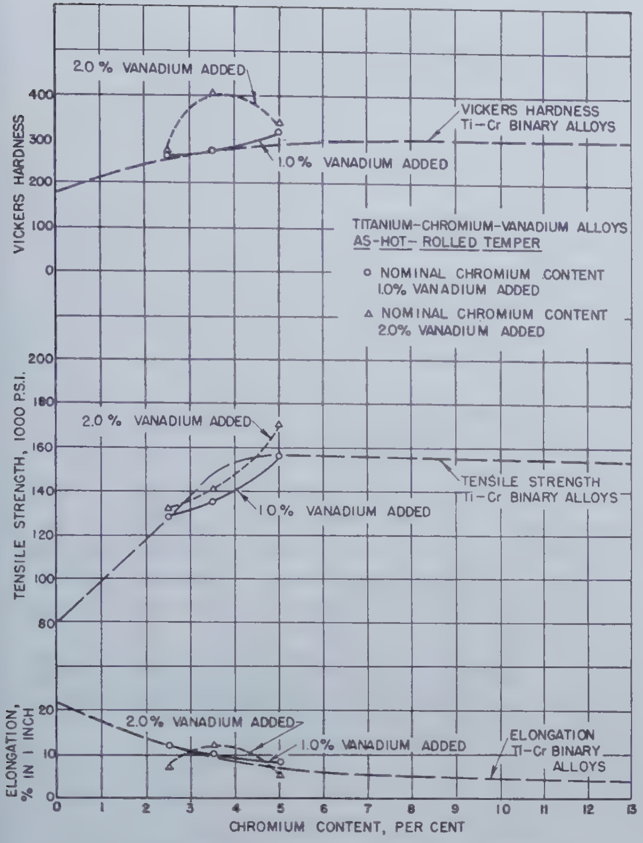

Fig. 39—Effect of vanadium on the properties of as-hot-rolled titanium-chromium alloys prepared from process A metal.

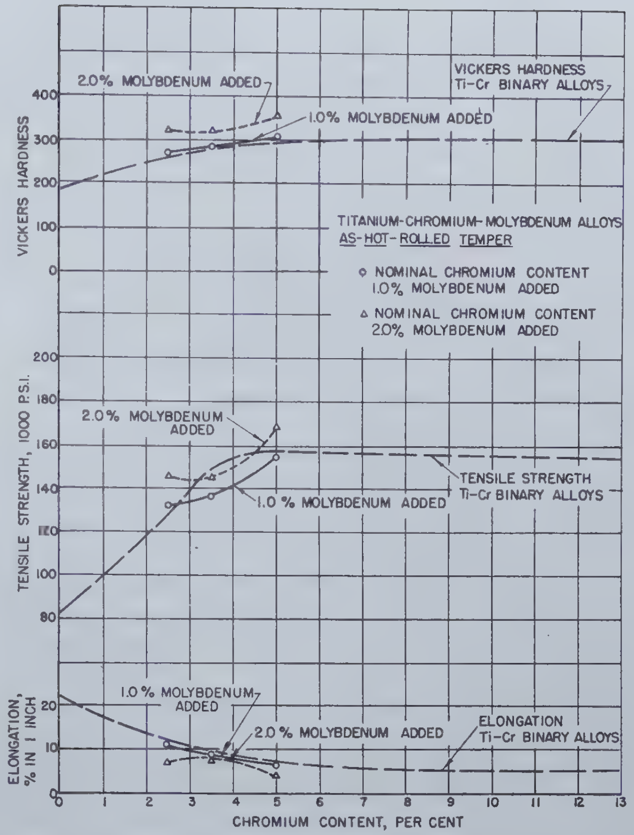

Fig. 40—Effect of molybdenum on the properties of as-hot-rolled titanium-chromium alloys prepared from process A metal.

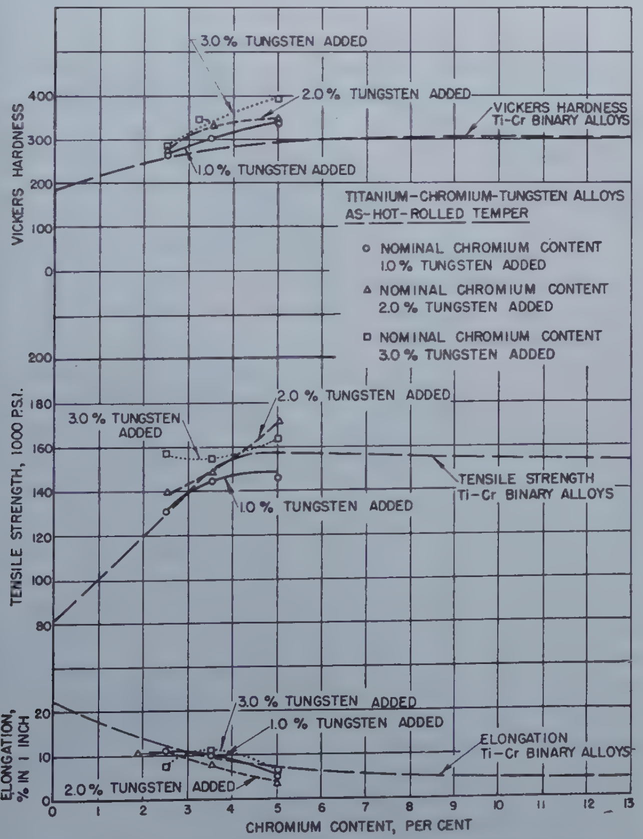

Fig. 41—Effect of tungsten on the properties of as-hot-rolled titanium-chromium alloys prepared from process A metal.

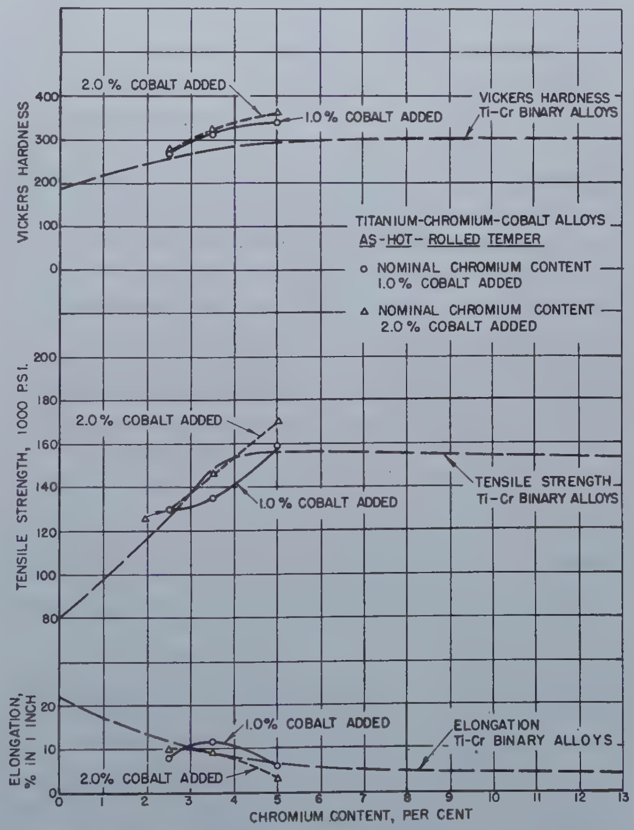

Fig. 42—Effect of cobalt on the properties of as-hot-rolled titanium-chromium alloys prepared from process A metal.

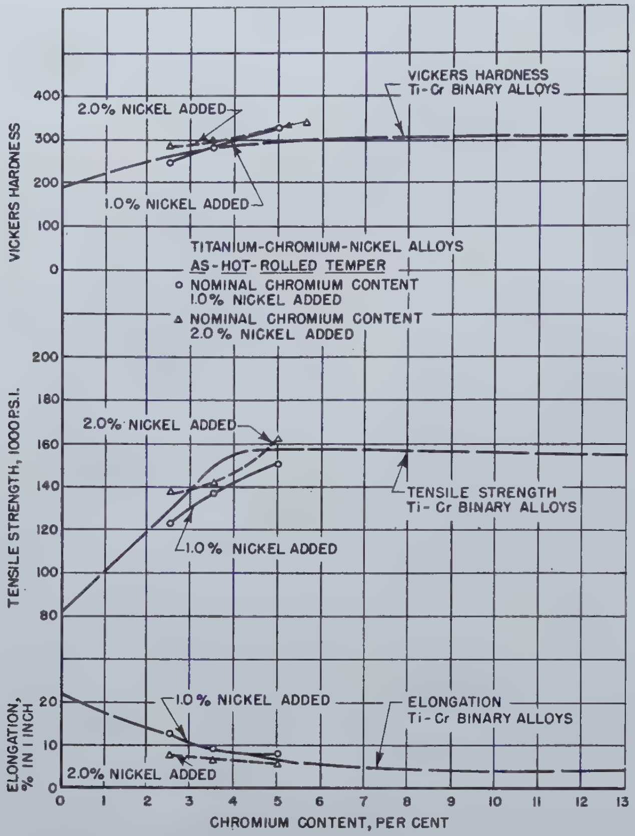

Fig. 43—Effect of nickel on the properties of as-hot-rolled titanium-chromium alloys prepared from process A metal.

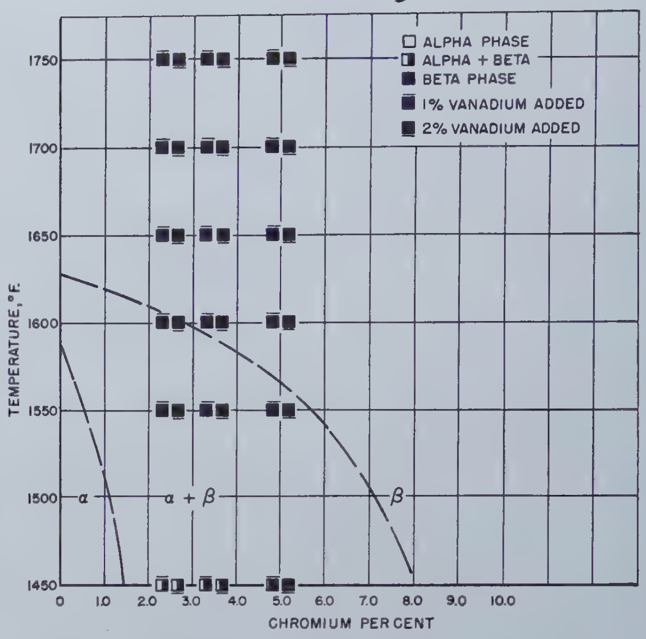

Fig. 44—Effect of 1.0 and 2.0 pct added vanadium on the transformation range of titanium—2.5 to 5.0 pct nominal chromium alloys made from process A metal.

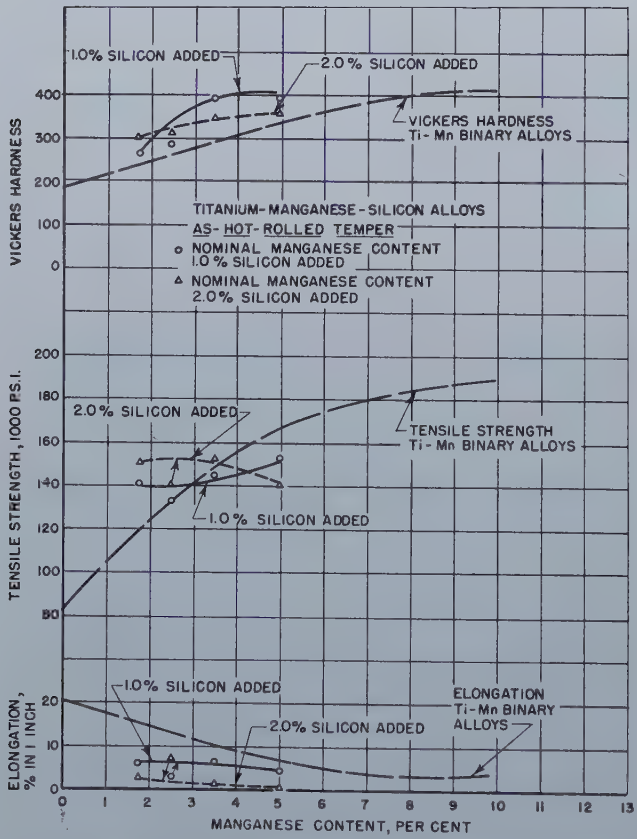

Fig. 45—Effect of silicon on the properties of as-hot-rolled titanium-manganese binary alloys prepared from process A metal.

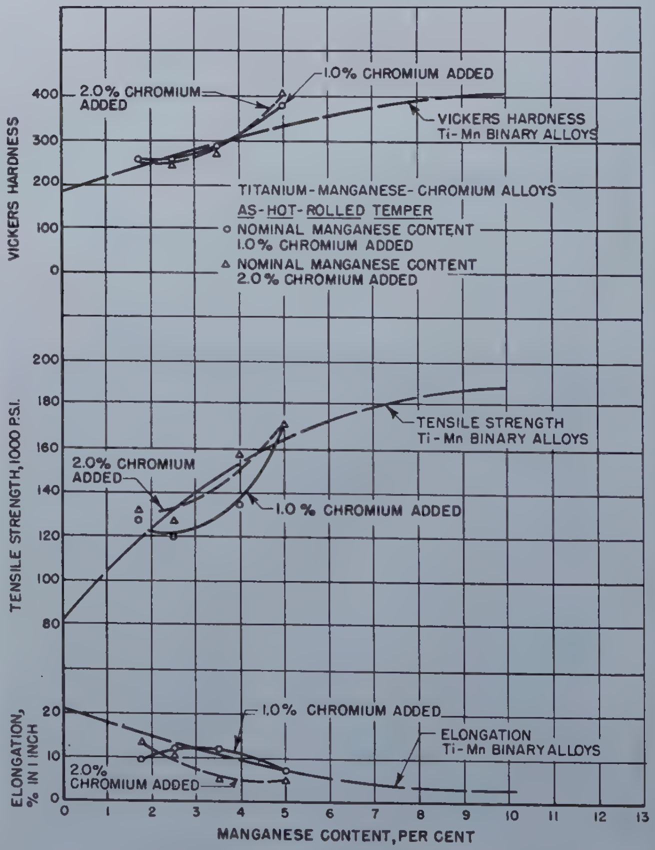

Fig. 46—Effect of chromium on the properties of as-hot-rolled titanium-manganese binary alloys prepared from process A metal.

were investigated at the following levels of composition.

1. Chromium—2.5, 3.5, and 5 pct
2. Nitrogen—0.1 and 0.2 pct

Mechanical Properties: The mechanical properties of the above alloys, in both the as-hot-rolled and heat-treated at 1600°F tempers, are listed in table III. Fig. 34 shows the effect of nitrogen by a comparison of the properties of the binary and ternary alloys in the as-hot-rolled condition. Small additions of nitrogen effectively increase the strength and hardness but slightly reduce the elongation values of titanium-chromium alloys.

With 0.1 pct nitrogen added to a titanium—5 pct chromium alloy, a tensile strength of 187,000 psi with 5.0 pct elongation in 1 in., a Vickers hardness of 295, and a minimum bend radius of 3t was obtained in the as-hot-rolled condition. Corresponding properties for a 5 pct chromium—0.25 pct carbon alloy, prepared from the same chromium metal low in nitrogen and oxygen, were 158,000 psi tensile strength, 6.5 pct elongation in 1 in., a Vickers hardness of 288, and a minimum bend radius of 3t.

Structure and Transformation Range: Specimens from the ternary titanium-chromium-nitrogen alloys were quenched from temperatures of 1450, 1550, 1600, 1650, 1700, and 1750°F. The phase relations observed in these alloys when quenched from the above temperatures are shown in fig. 35 and 36. Nitrogen markedly raises the beta solvus line. The presence of the alpha phase in a specimen containing about 2.5 pct chromium and 0.2 pct nitrogen, when quenched from 1700°F, is shown in fig. 37. When this alloy is heated to 1750°F, the alpha phase is no longer present, as shown by fig. 38. Thus, at 2.5 pct chromium, the beta solvus temperature is between 1700 and 1750°F, when about 0.2 pct nitrogen is present, instead of slightly above 1600°F, when the nitrogen content is low. This is shown by a comparison of the transformation range of the binary titanium-chromium alloys with that of the titanium-chromium-nitrogen ternary alloys.

Response to Heat Treatment and Aging: Hardness data for the ternary titanium-chromium-nitrogen alloys after various solution and aging treatments are listed in table IV.

Correlation of the hardness values after heat treatment with the phase diagrams, fig. 35 and 36, indicates that there was a fairly clear relation between the hardness, the quenching temperature, and the transformation range. High hardness was obtained from specimens quenched from the beta-phase field or where the beta phase predominates.

Referring to the mechanical property data listed in table III, it will be noted that the solution heat treatment has increased the hardness and lowered the ductility. Most of these solution-heat-treated compositions broke in the tension test with a brittle fracture. This condition probably caused the low tensile values reported for the heat-treated alloys.

As shown by the data in table IV, the as-hot-rolled alloy containing 5.0 pct chromium and 0.2 pct nitrogen increased in hardness when it was aged at 750°F.

Ternary Alloys of Titanium and Chromium Containing Additions of Vanadium, Molybdenum, Tungsten, Cobalt, or Nickel: The following ternary compositions were investigated:

1. 2.5, 3.5, 5 pct chromium; 1 and 2 pct vanadium.
2. 2.5, 3.5, 5 pct chromium; 1 and 2 pct molybdenum.
3. 2.5, 3.5, 5 pct chromium; 1, 2, and 3 pct tungsten.
4. 2.5, 3.5, 5 pct chromium; 1 and 2 pct cobalt.
5. 2.5, 3.5, 5 pct chromium; 1 and 2 pct nickel.

Mechanical Properties: The mechanical properties of the above alloys in the as-hot-rolled condition and after heat treating at 1600°F are listed in table V. Fig. 39 to 43 show the effect of the various metal additions by comparing the properties of the binary and ternary alloys in the as-hot-rolled condition.

In the titanium—5 pct chromium base, additions of 2 pct vanadium, 2 pct molybdenum, 2 and 3 pct tungsten, 2 pct cobalt, or 2 pct nickel produced some increase in strength. At levels of 2.5 and 3.5 pct chromium, the various additions generally produced tensile properties quite comparable or inferior to the binary titanium-chromium alloys. As compared to either carbon or nitrogen in the titanium-chromium base, the five elements are relatively ineffective additions.

The combined effect of nitrogen and carbon in a titanium-chromium base is described by the authors in another paper of this series on quaternary alloys.

Structure and Transformation Range: The phase relations observed in these ternary alloys when quenched from temperatures of 1450, 1550, 1600, 1650, 1700, and 1750°F are quite comparable to that shown in fig. 44 for the titanium-chromium-vanadium system. The addition of 1 or 2 pct vanadium, molybdenum, cobalt, or nickel, or 1, 2, or 3 pct tungsten to the titanium-chromium base lowered the beta solvus line. As indicated by the above figure, nearly all of these ternary alloys were in the beta-phase field when they were quenched from 1550°F or from higher temperatures.

Response to Heat Treatment and Aging: Vickers hardness data following solution heat treatment at temperatures of 1450, 1550, 1600, 1650, 1700, and 1750°F are listed in table VI. The hardness of these alloys increased to some extent when quenched from temperatures near or within the beta-phase field.

Referring to the mechanical property data listed in table V, it is evident that the ductility of the alloys quenched from 1600°F has been greatly lowered by the solution treatment and water quench. Most of these solution-heat-treated specimens broke in the tension test with a brittle fracture. For this reason, the tensile strengths are low.

The limited age-hardening data listed in table VI were obtained by aging these hot-rolled alloys for 4 hr at 750°F. Slight increases in hardness were obtained on several of the compositions containing the highest alloy content. This increase was especially marked for the 5 pct chromium and 2 pct cobalt alloy.

Ternary Titanium-Manganese Alloys Containing Additions of Silicon, Chromium, Tungsten, or Iron:

The following alloys of titanium, containing manganese and one other metal, were investigated:

1. 1.75, 2.5, 3.5, 5 pct manganese; 1 or 2 pct silicon.
2. 1.75, 2.5, 3.5, 5 pct manganese; 1 or 2 pct chromium.
3. 1.75, 2.5, 3.5, 5 pct manganese; 1 or 2 pct tungsten.
4. 1.75, 2.5, 3.5, 5 pct manganese; 1 or 2 pct iron.

Mechanical Properties: The mechanical properties of the above alloys, as-hot-rolled and after heat treating at 1600°F, are listed in table VII. Fig. 45 to 48 show, respectively, the effect of silicon, chromium, tungsten, and iron by a comparison of the properties of the binary and ternary alloys. These preliminary data indicate that silicon or chromium were not effective alloy additions in the titanium-manganese base. One per cent tungsten added to a titanium—5 pct manganese alloy and 2 pct iron added to alloys containing 1.75 to 5 pct manganese, produced tensile strengths about 20,000 psi higher than those obtained from the binary titanium-manganese base.

As with the other ternary alloys examined, solution heat treatment at 1600°F followed by quenching in cold water resulted in very low ductility. In the tension test, the heat-treated specimens failed with a brittle fracture. Because of this condition, the tensile strengths are low.

Structure and Transformation Range: The phase relations observed in the ternary titanium-manganese-tungsten, and the titanium-manganese-iron systems were quite comparable to that shown in fig. 49 for the titanium-manganese-chromium system. Chromium, tungsten, and iron, when added to a titanium-manganese base, lower the beta solvus line. Because of the large amount of the silicon-rich phase present in the ternary titanium-manganese-silicon alloys, no estimation of the phases present in these alloys was possible. This insoluble silicon-rich phase undoubtedly accounts for the low ductility shown in table VII for the as-hot-rolled titanium-manganese-silicon alloys.

Response to Heat Treatment and Aging: The hardness data following solution heat treatment or aging these ternary alloys in the as-hot-rolled temper are listed in table VIII. Like the previous ternary systems, the titanium-manganese alloys containing an added metal (silicon, chromium, tungsten, or iron) increased in hardness when they were quenched from or near the beta-phase field. Aging these ternary titanium-manganese base alloys in the as-hot-rolled temper resulted in an appreciable increase in hardness of only a few alloys as shown in table VIII. Compositions containing about 5 pct manganese and 1 pct chromium and 5 pct manganese and 1 or 2 pct tungsten were age hardened appreciably. It appears probable that the tensile properties of these alloys in the as-hot-rolled temper could be further augmented by a simple aging treatment.

Summary

The results of a preliminary study of 113 ternary titanium-base alloys are described. The compositions investigated were as follows:

1. Ternary titanium-carbon alloys containing copper, silicon, vanadium, chromium, manganese, iron, or cobalt.
2. Ternary titanium-nitrogen alloys containing chromium.
3. Ternary titanium-chromium alloys containing additions of vanadium, molybdenum, tungsten, cobalt, or nickel.
4. Ternary titanium-manganese alloys containing additions of silicon, chromium, tungsten, or iron.

All of these elements, excepting carbon and silicon, are soluble in alpha or beta titanium within the composition range studied.

In general, the addition of 0.25 pct carbon in the ternary alloys investigated produced some improvement in the tensile strength of the as-hot-rolled alloys without a serious sacrifice in ductility. At a level of 5 pct manganese and 0.25 pct carbon, a tensile strength of 190,000 psi and 4 pct elongation were obtained in the as-hot-rolled condition. Somewhat less than 0.25 pct carbon resulted in the formation of titanium carbide, indicating limited solubility in these alloys. Carbon raises the beta solvus line at the lower alloy concentrations of all the ternary systems investigated except the titanium-chromium-carbon or the titanium-cobalt-carbon alloys, in which the opposite effect was produced. Some of these compositions in the as-hot-rolled condition respond to aging. It is concluded that carbon up to about 0.25 pct was generally beneficial or permissible in these alloys.

Additions of 0.1 or 0.2 pct nitrogen to titanium-chromium alloys increased the hardness and strength but slightly lowered the ductility of the as-hot-rolled alloys. At 5 pct chromium and 0.1 pct nitrogen, the following properties were obtained:

Ultimate tensile strength,	186,800 psi
Elongation in 1 in.,	5.0 pct
Vickers hardness,	295
Minimum bend radius,	3t

Nitrogen additions raise the beta solvus temperatures, particularly with 0.2 pct nitrogen. The 5 pct chromium-0.2 pct nitrogen alloy in the as-hot-rolled condition increased in hardness when aged at 750°F. It is concluded that 0.1 to 0.2 pct nitrogen may be a useful addition to the titanium-chromium alloys.

Additions of vanadium, molybdenum, tungsten, cobalt, or nickel to titanium-chromium alloys were generally not beneficial. These elements lowered the beta solvus temperature. The titanium chromium-cobalt alloys in the as-hot-rolled condition age hardened appreciably at 750°F.

Of the elements introduced into titanium-manganese alloys, silicon appears to be definitely detrimental. Iron increased the strength considerably but with a sacrifice in ductility. In these tests, the chromium additions were substantially without effect on the tensile properties, while 1 pct tungsten may be useful. An alloy containing 5 pct manganese and 1 pct tungsten produced the following

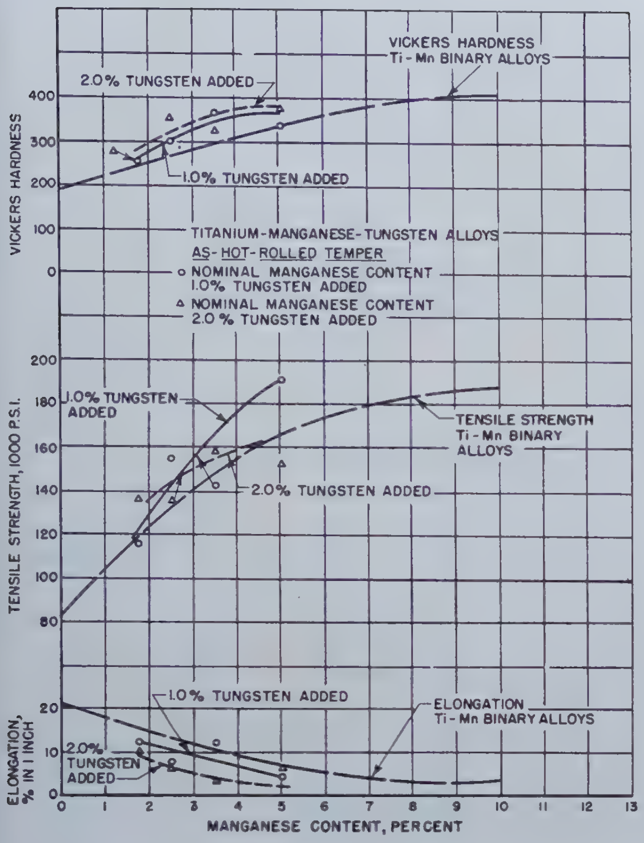

Fig. 47—Effect of tungsten on the properties of as-hot-rolled titanium-manganese binary alloys prepared from process A metal.

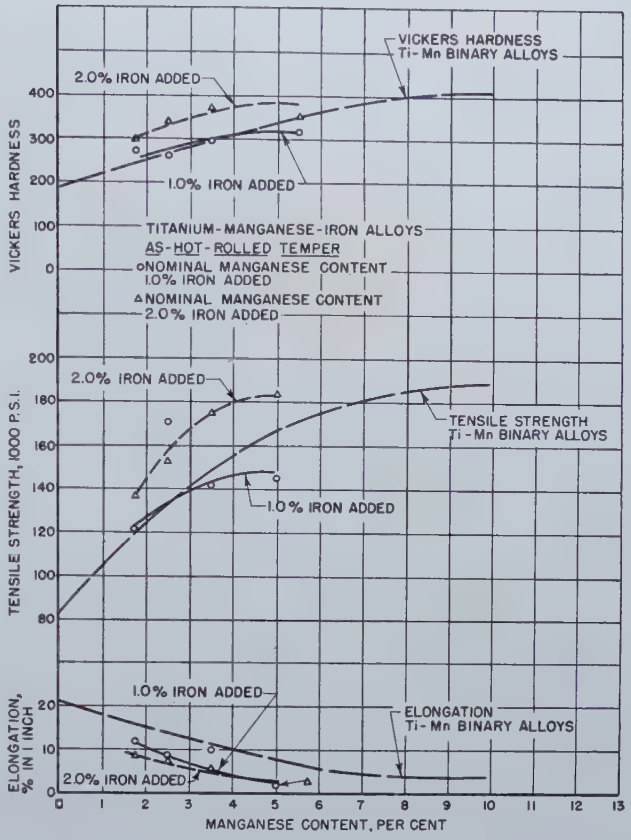

Fig. 48—Effect of iron on the properties of as-hot-rolled titanium-manganese binary alloys prepared from process A metal.

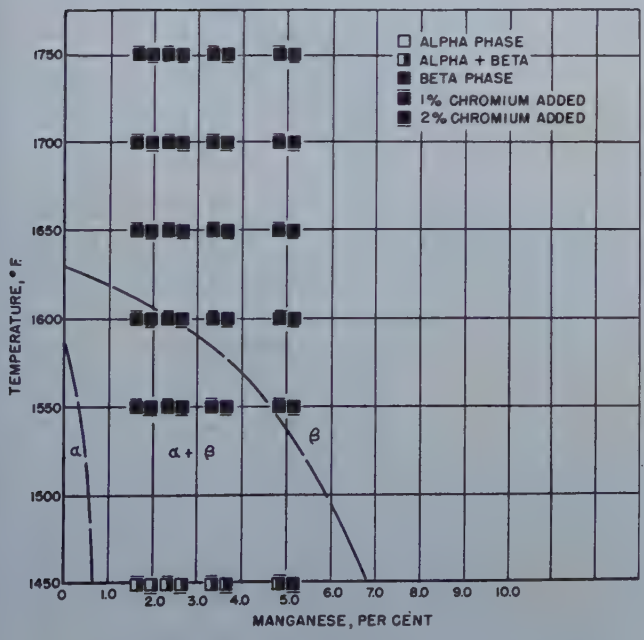

Fig. 49—Effect of 1.0 and 2.0 pct chromium on the transformation range of titanium—1.75 to 5.0 pct manganese alloys made from process A metal.

properties in the as-hot-rolled temper:

Ultimate tensile strength,	190,000 psi
Elongation in 1 in.,	4.5 pct
Vickers hardness number,	337
Minimum bend radius,	3t

Chromium, tungsten, and iron lower the beta solvus temperature. The 5 pct manganese-1 pct tungsten alloy in the as-hot-rolled condition appears to age harden.

In the higher alloy ranges, many of the ternary alloys studied increased in hardness when they were quenched from the beta-phase field. The hardness increase obtained by water quenching from 1600°F was accompanied by a loss in ductility. However, since hardening occurs by quenching from or near the beta field, useful heat treatments may be developed.

Acknowledgments

The authors wish to express their appreciation to the Air Material Command, Wright-Patterson Air Force Base, who sponsored the work described in this paper, and who granted permission for the publication of the results of this investigation.

Reference

[1] C. M. Craighead, O. W. Simmons, and L. W. Eastwood: Binary Alloys of Titanium. *Trans.* AIME (1950) **188**, 485. *Jnl. of Metals*, Mar. 1950. TP 2747.

Quaternary Alloys of Titanium

by C. M. Craighead, O. W. Simmons, and L. W. Eastwood

Eighty-four quaternary titanium-base alloys from the following systems were investigated:

1. Titanium-chromium-carbon-nitrogen.
2. Titanium-chromium-carbon with copper, vanadium, molybdenum, manganese, iron, or nickel.
3. Titanium-chromium-nitrogen with vanadium, molybdenum, or nickel.

The tensile properties, minimum bend radii, hardnesses, response to heat treatment and aging treatment, and phase relationships of these alloys are reported.

THIS paper is the third in a series describing titanium-base alloys. The first paper described titanium binary alloys, and the second contained data on a large number of titanium ternary alloys. Eighty-four heats, comprising three groups of quaternary titanium-base alloys, are described in this paper as follows:

1. Titanium-chromium-carbon-nitrogen alloys.
2. Titanium-chromium-carbon alloys containing copper, vanadium, molybdenum, manganese, iron, or nickel.
3. Titanium-chromium-nitrogen alloys containing vanadium, molybdenum, or nickel.

The methods of preparing, fabricating, and testing the alloys are described in the paper *Binary Titanium Alloys*.

Quaternary Titanium-Chromium-Carbon-Nitrogen Alloys

The properties of titanium-chromium-nitrogen and titanium-chromium-carbon ternary alloys have been described in the paper *Ternary Alloys of Titanium*. Because small amounts of nitrogen and carbon both appear to be somewhat beneficial, these additions have been investigated fairly completely in quaternary alloys containing chromium at the following levels of composition:

2.5, 3.5, and 5.0 pct chromium
0.25 and 0.5 pct carbon
0.1 and 0.2 pct nitrogen

Mechanical Properties: The mechanical properties of these alloys are listed in table I. Fig. 1 and 2 show graphically a comparison of the tensile properties and hardnesses of quaternary alloys with those of the titanium-chromium binary alloys. Fig. 1 shows the comparison at 0.25 pct carbon, whereas fig. 2 shows the comparison at 0.5 pct carbon. It is concluded from these data that 0.25 pct carbon and 0.1 pct nitrogen are desirable additions to the 5 pct chromium-titanium base. It is further concluded that most of this improvement is produced by the nitrogen and that carbon is either harmless or mildly beneficial, at least up to 0.25 pct.

Structure and Transformation Range: The effects of carbon and nitrogen on the transformation range of the titanium-chromium alloys were determined as part of the routine investigation. Additions of 0.25 pct carbon and 0.1 pct nitrogen had no appreciable effect upon the transformation range. However, the addition of 0.25 pct carbon and 0.2 pct nitrogen definitely raised the beta solvus temperature, as shown by fig. 3.

C. M. CRAIGHEAD, O. W. SIMMONS and L. W. EASTWOOD, Member AIME, are Assistant Supervisor, Research Engineer, and Supervisor, respectively, Battelle Memorial Institute, Columbus 1, Ohio.

The work described in this paper was sponsored by the Air Materiel Command, Wright-Patterson Air Force Base, Dayton, Ohio.

AIME New York Meeting, Feb. 1950.

TP 2749 E. Discussion (2 copies) may be sent to Transactions *AIME before Apr. 1, 1950, and is scheduled for publication Nov. 1950. Manuscript received Oct. 14, 1949.*

Table I. Properties of Quaternary Chromium-Titanium Alloys[6] with Additions of Nitrogen and Carbon—Process *A* Metal Base

Heat No.	Composition, Pct					As Hot Rolled[1]				Heat Treated 1600°F[2]			
	Intended	Actual				Tensile Strength,[3] psi	Elong., Pct in 1 In.	VHN[4]	Minimum Bend Radius,[5] In.	Tensile Strength,[3] psi	Elong., Pct in 1 In.	VHN[4]	Minimum Bend Radius,[5] In.
		Cr	C	N	W								
Titanium-Chromium-Carbon (0.25 Pct C) Nitrogen (0.10 and 0.20 Pct N)													
WG69	Unalloyed					75,000	21.5	163	1/64	62,000	26.0	147	3/64
WG82	2.5 Cr, 0.25 C, 0.10 N	2.27				152,600	10.0	311	>1/4*	150,000	1.0	352	>1/4†
WG63	3.5 Cr, 0.25 C, 0.10 N	3.41				163,200	7.0	302	3/16	141,900	1.0	323	>1/4†
WG48	5.0 Cr, 0.25 C, 0.10 N	4.31				183,200	6.0	339	3/16	75,700	1.0	336	>1/4†
WG79	2.5 Cr, 0.25 C, 0.20 N	2.29				167,600	6.0	335	>1/4*	151,000	2.5	376	>1/4†
WG62	3.5 Cr, 0.25 C, 0.20 N	3.37				181,200	5.5	321	>1/4†	110,900	1.0	364	>1/4†
WG49	5.0 Cr, 0.25 C, 0.20 N	4.62				188,600	4.0	319	>1/4*	54,700	0.5	425	>1/4†
Titanium-Chromium-Carbon (0.50 Pct C) Nitrogen (0.10 and 0.20 Pct N)													
WG69	Unalloyed					75,000	21.5	163	1/64	62,000	26.0	147	3/64
WG73	2.5 Cr, 0.50 C, 0.10 N	2.22				155,700	8.0	289	3/16	149,700	2.0	322	>1/4†
WG59	3.5 Cr, 0.50 C, 0.10 N	3.40				159,700	8.5	277	3/16	130,000	1.0	351	>1/4†
WG52	5.0 Cr, 0.50 C, 0.10 N	5.16				174,100	5.5	294	>1/4*	115,100	0.0	450	>1/4†
WG72	2.5 Cr, 0.50 C, 0.20 N	2.22				166,000	7.0	307	>1/4†	146,900	1.0	350	>1/4†
WG57	3.5 Cr, 0.50 C, 0.20 N	3.26				169,900	4.0	302	>1/4†	117,700	1.0	331	>1/4†
WG44	5.0 Cr, 0.50 C, 0.20 N	4.72				190,700	3.0	340	>1/4†	98,700	0.5	417	>1/4†

* Some ductility.

† Very little ductility.

[1] As hot rolled 1450°F.

[2] Heated in air ½ hr at 1600°F and quenched in cold water.

[3] Average of 2 longitudinal 14-ga sheet specimens, 3 in. long by 0.375 in. wide with a 0.250-in.-wide reduced section. Tested with the surface skin present.

[4] 10-kg load. Hardness at the center of the cross section of the sheet 90° to the surface and to the rolling direction. Average of at least 5 readings.

[5] Minimum bend radius without cracking on a single longitudinal specimen 3 in. long by 0.5 in. wide. Tested with the surface skin present.

[6] Forged at 1700°F by upsetting the 2¼-in.-diam ingots on edge to 0.250-in. slab, then ground and hot rolled at 1450°F to 0.060-in. sheet. Total reduction 35:1.

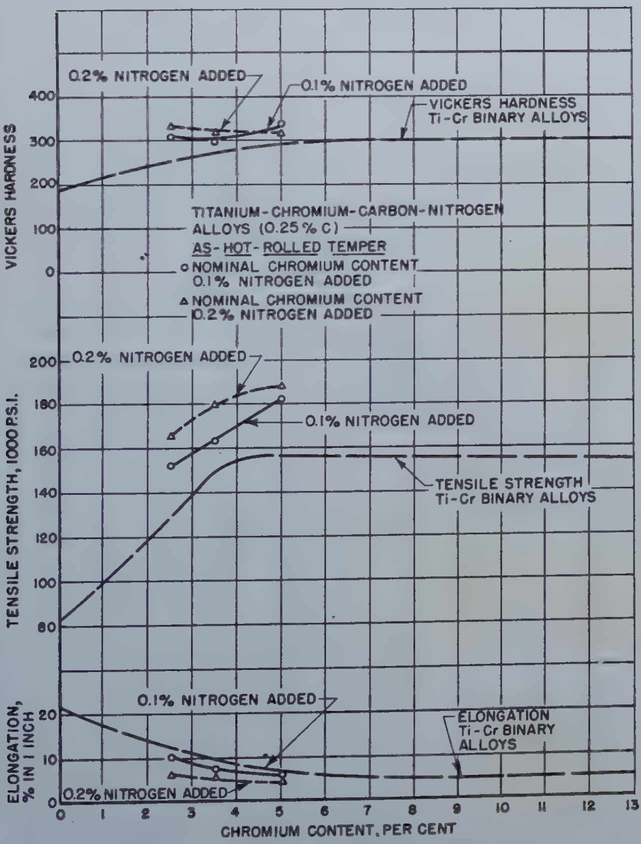

Fig. 1—Effect of carbon and nitrogen on the properties of as-hot-rolled titanium-chromium alloys prepared from process A metal.

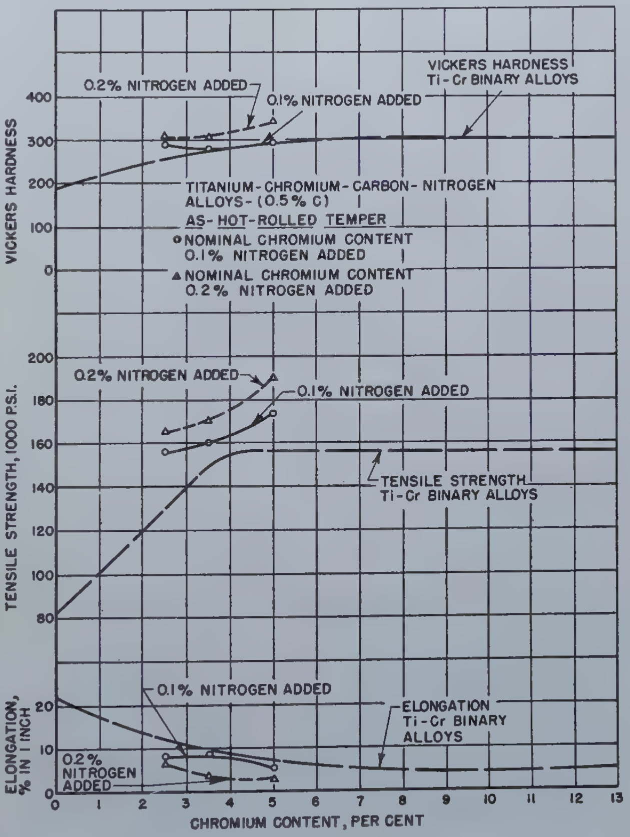

Fig. 2—Effect of carbon and nitrogen on the properties of as-hot-rolled titanium-chromium alloys.

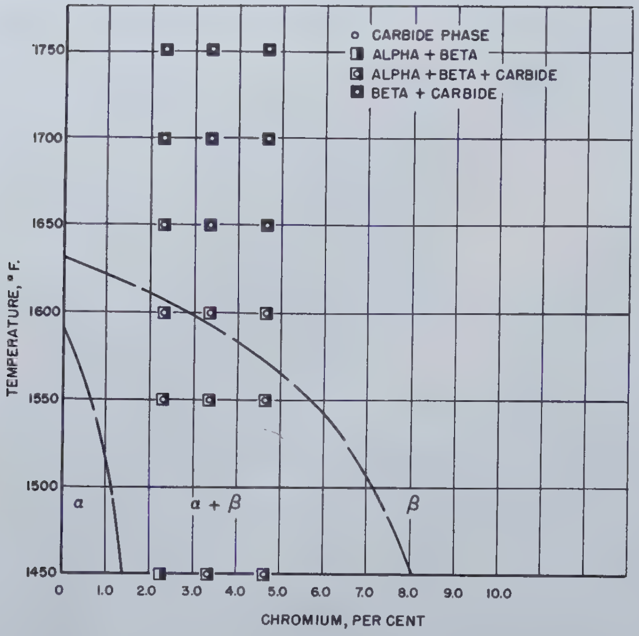

Fig. 3—Effect of 0.25 pct carbon and 0.20 pct nitrogen on the transformation range of titanium-2.5 to 5.0 pct chromium alloys made from process A metal.

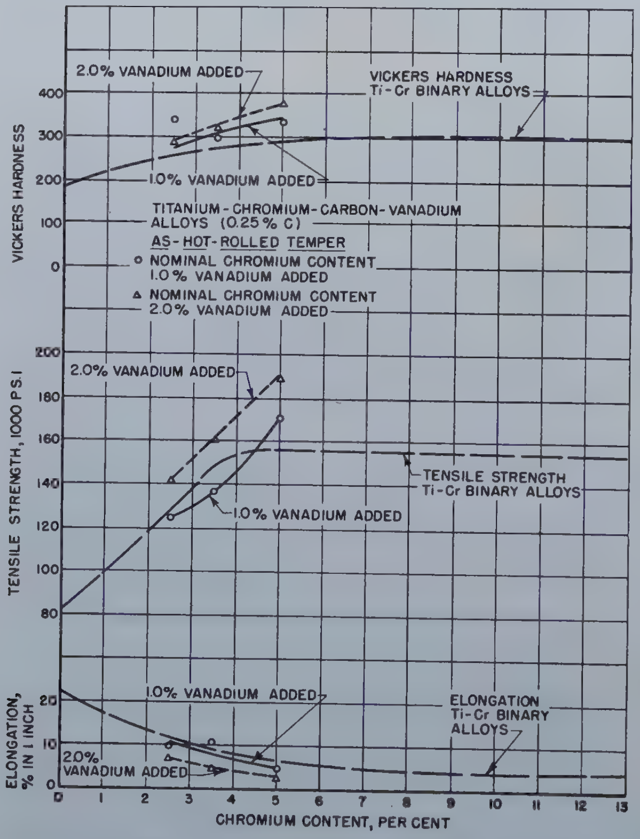

Fig. 5—Effect of vanadium and carbon on the properties of as-hot-rolled titanium-chromium alloys prepared from process A metal.

Fig. 6 (right)—Effect of carbon and iron on the properties of as-hot-rolled titanium-chromium alloys prepared from process A metal.

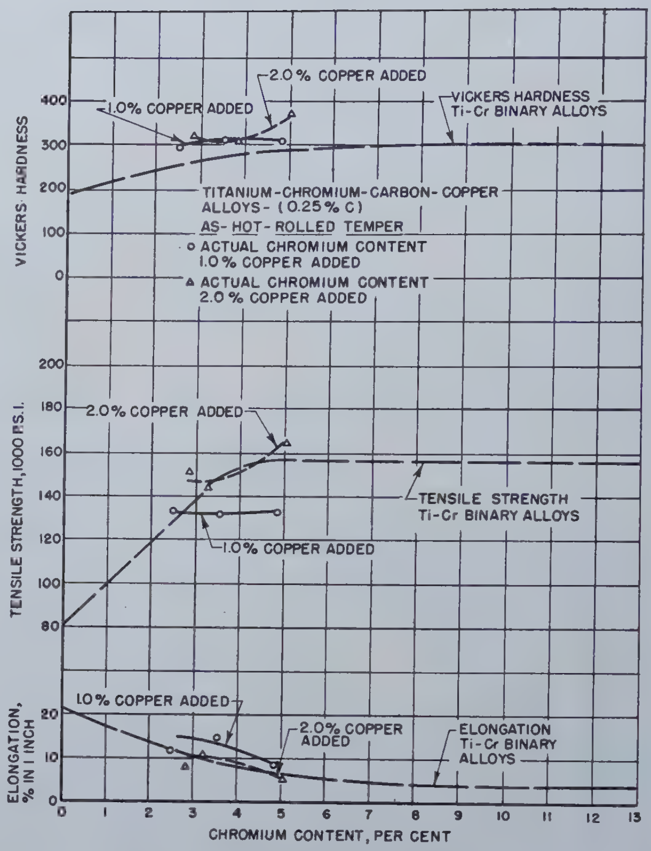

Fig. 4—Effect of copper and carbon on the properties of as-hot-rolled titanium-chromium alloys prepared from process A metal.

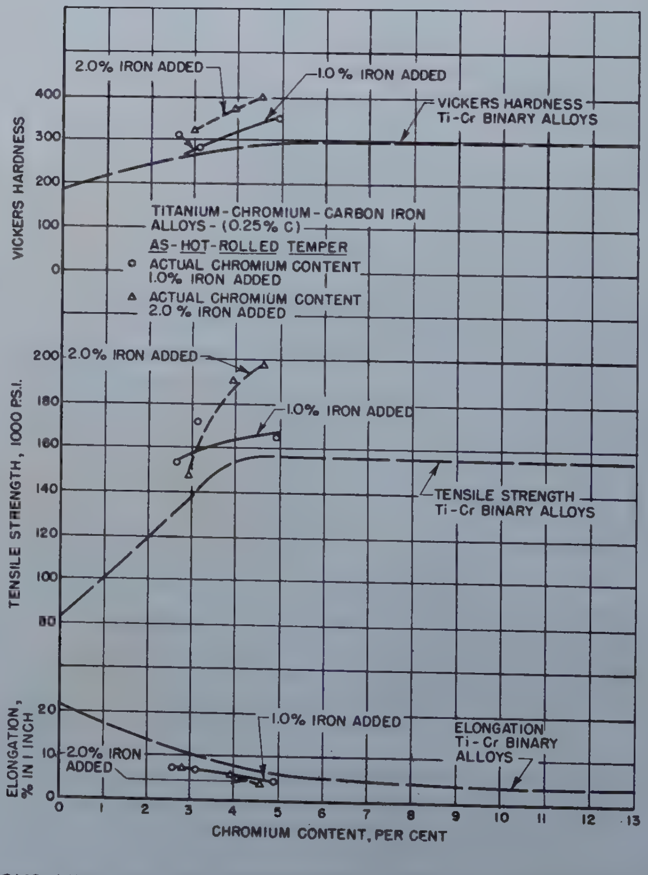

Table II. Aging and Heat-treating Data for Quaternary Chromium-Titanium Alloys with Additions of Carbon and Nitrogen—Process *A* Metal Base

Heat No.	Composition, Pct					Heat-Treating Data							Aging Data	
						Vickers Hardness[1] After Indicated Treatment							Vickers Hardness[1] After Indicated Treatment	
	Intended	Actual											As Hot Rolled,[2] Aged 750°F for Indicated Time	
		Cr	C	N	W	As Hot Rolled[2]	Heat Treated 1450°F[3]	Heat Treated 1550°F[4]	Heat Treated 1600°F[5]	Heat Treated 1650°F[6]	Heat Treated 1700°F[7]	Heat Treated 1750°F[8]	0 Hr	4 Hr
Titanium — Chromium — Carbon (0.25 Pct C) — Nitrogen (0.10 and 0.20 Pct N)														
WG69	Unalloyed					163	140	145	147	154	161	183	163	186
WG82	2.5 Cr, 0.25 C, 0.10 N	2.27				311	324	330	352	364	368	385	311	350
WG63	3.5 Cr, 0.25 C, 0.10 N	3.41				302	314	306	323	317	317	312	302	357
WG48	5.0 Cr, 0.25 C, 0.10 N	4.31				339	337	305	336	312	350	407	339	433
WG79	2.5 Cr, 0.25 C, 0.20 N	2.29				335	357	330	376	381	401	401	335	376
WG62	3.5 Cr, 0.25 C, 0.20 N	3.37				321	352	379	364	366	360	359	321	398
WG49	5.0 Cr, 0.25 C, 0.20 N	4.62				319	395	406	425	405	376	417	319	404
Titanium — Chromium — Carbon (0.50 Pct C) — Nitrogen (0.10 and 0.20 Pct N)														
WG69	Unalloyed					163	140	145	147	154	161	183	163	186
WG73	2.5 Cr, 0.50 C, 0.10 N	2.22				289	280	310	322	314	321	330	289	357
WG59	3.5 Cr, 0.50 C, 0.10 N	3.40				277	340	357	351	361	354	366	277	345
WG52	5.0 Cr, 0.50 C, 0.10 N	5.16				294	373	442	450	328	320	417	294	365
WG72	2.5 Cr, 0.50 C, 0.20 N	2.22				307	322	346	350	358	360	372	307	378
WG57	3.5 Cr, 0.50 C, 0.20 N	3.26				302	340	312	331	332	330	333	302	383
WG44	5.0 Cr, 0.50 C, 0.20 N	4.72				340	403	365	417	359	351	360	340	411

[1] 10-kg load. Hardness at the center of the cross section of the sheet specimen 90° to the surface and to the rolling direction. Average of at least 5 readings.

[2] As hot rolled 1450°F.

[3] Heated in air ½ hr at 1450°F and quenched in cold water.

[4] Heated in air ½ hr at 1550°F and quenched in cold water.

[5] Heated in air ½ hr at 1600°F and quenched in cold water.

[6] Heated in air ½ hr at 1650°F and quenched in cold water.

[7] Heated in air ½ hr at 1700°F and quenched in cold water.

[8] Heated in air ½ hr at 1750°F and quenched in cold water.

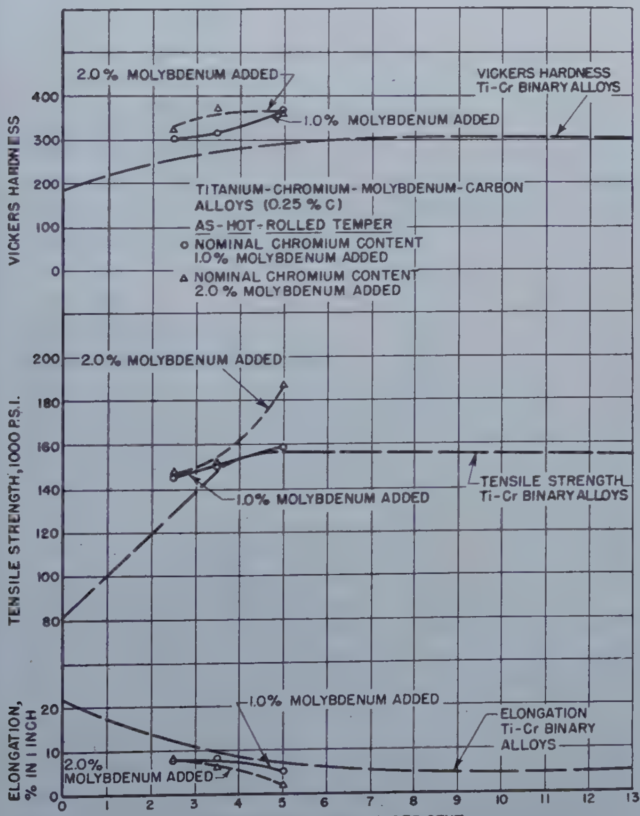

Fig. 7—Effect of molybdenum and carbon on the properties of as-hot-rolled titanium-chromium alloys prepared from process A metal.

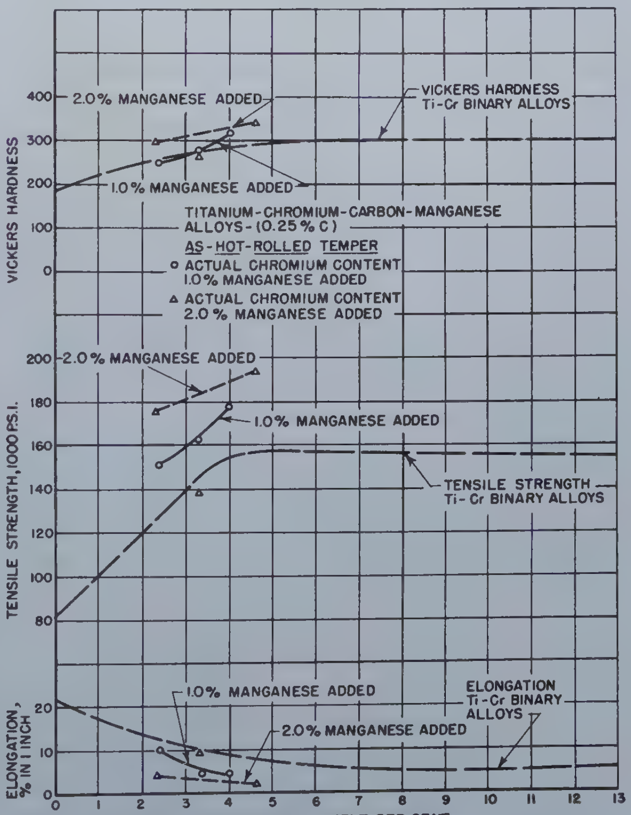

Fig. 8—Effect of carbon and manganese on the properties of as-hot-rolled titanium-chromium alloys prepared from process A metal.

In this figure, the alpha, alpha-plus-beta, and beta fields for the titanium-chromium diagram are shown by the dashed lines. The existence of alpha-plus-beta structures above the dashed line separating the alpha-plus-beta field from the beta field indicates that the addition of 0.25 pct carbon and 0.2 pct nitrogen raises the beta solvus temperatures. This increase in the beta solvus temperature is the direct result of the nitrogen addition since carbon in titanium-chromium alloys tends to lower the beta solvus line. These separate effects of nitrogen and carbon in titanium-chromium alloys are shown in the paper on ternary alloys. One half per cent carbon and 0.1 pct nitrogen tend to lower the beta solvus temperature very slightly, whereas 0.5 pct carbon and 0.2 pct nitrogen tend to raise the beta solvus line. These effects at the mentioned levels of composition are not shown graphically. It is quite obvious, however, that these changes in the beta solvus temperature are a direct result of the two opposite effects of carbon and nitrogen on the beta solvus temperatures of titanium-chromium alloys. Fig. 3 also shows that even 0.25 pct carbon addition introduces the titanium carbide phase in this alloy throughout the temperature range investigated. This indicates that the solubility of carbon is somewhat less than 0.25 pct.

Response to Heat Treatment and Aging: The hardnesses of the various quaternary alloys after solution heat treatment at several temperatures and after an aging treatment are listed in table II. The as-quenched hardnesses of these alloys generally increase with an increase in quenching temperature. At 5 pct chromium, the increase is quite marked, even at the lower quenching temperatures. As shown by the data in table I, quenching from 1600°F has not had a beneficial effect on the tensile properties. It is quite possible, however, that useful heat treatments may be developed for alloys of this type.

Aging of titanium-chromium-carbon-nitrogen alloys in the as-hot-rolled condition for 4 hr at 750°F resulted in an increase of 40 to 90 points in Vickers hardness. Thus, it may be possible to improve further the tensile strength of the quaternary titanium-chromium-carbon-nitrogen alloys by aging them after they have been hot formed. However, the effects of such treatments on the tensile properties have not yet been investigated.

Quaternary Titanium-Chromium-Carbon Alloys Containing One Additional Metal: Quaternary titanium-chromium-carbon alloys containing copper, vanadium, iron, molybdenum, manganese, or nickel were investigated. The base material contained 0.25 pct carbon and 2.5, 3.5, or 5 pct chromium to which a fourth element was added as follows:

	Pct
Copper	— 1 and 2
Vanadium	— 1 and 2
Iron	— 1 and 2
Molybdenum	— 1 and 2
Manganese	— 1 and 2
Nickel	— 1 and 2

Mechanical Properties: The composition, tensile properties, hardnesses, and minimum bend radii of the alloys in the as-hot-rolled condition and after heat treatment at 1600°F are listed in table III. Comparisons of the mechanical properties of the quaternary alloys with the titanium-chromium binary alloys are shown by fig. 4 to 9, inclusive. These figures show the comparison of the properties of the alloys in the as-hot-rolled condition only. As shown in the paper on ternary alloys, 0.25 pct carbon does not produce a marked effect on the properties of the titanium-chromium alloys. It is also useful to compare the properties of the titanium-chromium-0.25 pct carbon ternary alloys with the data represented by fig. 4 to 9, inclusive. It is concluded that 1 and 2 pct iron or manganese produce some improvement in tensile properties in the alloys containing 0.25 pct carbon and 2.5 to 5 pct chromium, and that 1 and 2 pct vanadium is beneficial in the 5 pct chromium-0.25 pct carbon alloys.

Structure and Transformation Range: As part of the routine investigation, the transformation range of the quaternary alloys was determined and compared with the transformation range of the titanium-chromium binary alloys. The chromium addition, of course, greatly lowers the beta solvus temperatures and restricts the alpha field, as shown by the dashed lines in fig. 10. When 0.25 pct carbon and either 1 or 2 pct of copper, vanadium, molybdenum, manganese, iron, or nickel are added to the titanium-chromium base, the beta solvus temperature is still further lowered, as indicated by fig. 10. An examination of this figure shows that the beta-phase field extends to lower temperatures for the quaternary alloys than for the titanium-chromium binary alloys. This figure indicates the phase relations of the quaternary alloys containing titanium, chromium, carbon, and copper. Effects similar to those shown in this figure were obtained with additions of 0.25 pct carbon with 1 and 2 pct vanadium, molybdenum, manganese, iron, or nickel. The portion of the diagram below 1450°F has not yet been developed. Because of the carbon content of the quaternary alloys, this element has caused the formation of titanium carbide throughout the entire temperature range, indicating that the solubility of carbon in these alloys at temperatures from 1450 to 1750°F is less than 0.25 pct.

Response to Heat Treatment and Aging: Table IV contains the hardness data on these quaternary alloys in the as-hot-rolled condition and after they have been quenched from 1450, 1550, 1600, 1650, 1700, and 1750°F. In addition, hardnesses are given for the alloys after they have been aged in the as-hot-rolled condition for 4 hr at 750°F. Table III contains the data on tensile properties of alloys after they were quenched from 1600°F. All of these alloys are hardened to some extent when they are quenched from the beta field. In general, this increase in hardness is greater the higher the quenching temperature and the higher the alloy content of the metal, at least within the limits of composition investigated. Although hardening does take place, as a result of the heat-treating operation, a quench from 1600°F does not produce a beneficial effect on the tensile properties. It is quite possible, however, that useful heat treatments may be developed for these alloys.

An examination of the aging data listed in table IV shows that most of these quaternary alloys in

Table III. Properties of Quaternary Chromium-Titanium Alloys[6] with Additions of Carbon and One Other Metal—Process *A* Metal Base

Heat No.	Composition, Pct				As Hot Rolled[1]				Heat Treated 1600°F[2]			
	Intended	Actual			Tensile Strength,[3] psi	Elong., Pct in 1 In.	VHN[4]	Minimum Bend Radius,[5] In.	Tensile Strength,[3] psi	Elong., Pct in 1 In.	VHN[4]	Minimum Bend Radius,[5] In.
				C N W								
Titanium-Chromium-0.25 Pct Carbon-1.0 and 2.0 Pct Copper												
WG32	Unalloyed				77,400	18.5	163	3/64	71,500	21.5	151	3/64
WG30	2.5 Cr, 1.0 Cu, 0.25 C	2.45 Cr	1.04 Cu		132,900	11.5	287	3/16	144,700	1.5	338	>1/4†
WG22	3.5 Cr, 1.0 Cu, 0.25 C	3.51 Cr	1.05 Cu		131,400	14.5	313	3/16	129,400	0.0	336	>1/4†
WG24	5.0 Cr, 1.0 Cu, 0.25 C	4.78 Cr	0.94 Cu		132,100	8.5	309	3/16	82,900	0.0	407	>1/4†
WG28	2.5 Cr, 2.0 Cu, 0.25 C	2.81 Cr	2.01 Cu		151,300	8.0	322	3/16	163,800	1.0	376	>1/4†
WG26	3.5 Cr, 2.0 Cu, 0.25 C	3.19 Cr	2.01 Cu		144,000	11.0	309	3/16	110,700	1.5	364	>1/4†
WG20	5.0 Cr, 2.0 Cu, 0.25 C	5.03 Cr	2.07 Cu		163,900	5.5	376	>1/4†			456	>1/4†
Titanium-Chromium-0.25 Pct Carbon-1.0 and 2.0 Pct Vanadium												
WG108	Unalloyed				85,400	20.5	192	3/64	76,900	13.0	183	3/64
WG120	2.5 Cr, 1.0 V, 0.25 C				125,000	10.0	347	>1/4	137,500	2.0	322	>1/4
WG102	3.5 Cr, 1.0 V, 0.25 C				137,500	11.0	297	3/16	130,500	2.0	346	>1/4
WH30	5.0 Cr, 1.0 V, 0.25 C				171,900	5.0	336	3/16	63,300	0.5	464	>1/4†
WG99	2.5 Cr, 2.0 V, 0.25 C				142,200	7.5	292	3/16	146,700	0.0	342	>1/4
WG121	3.5 Cr, 2.0 V, 0.25 C				160,500	5.0	327	3/16	121,800	2.0	322	>1/4
WG29	5.0 Cr, 2.0 V, 0.25 C				189,700	3.5	378	3/16	75,000	0.0	464	>1/4†
Titanium-Chromium-0.25 Pct Carbon-1.0 and 2.0 Pct Molybdenum												
WG103	Unalloyed				82,700	20.0	194	1/8	78,800	12.5	177	1/8
WG104	2.5 Cr, 1.0 Mo, 0.25 C				145,400	7.5	301	3/16	142,100	2.0	328	>1/4
WG106	3.5 Cr, 1.0 Mo, 0.25 C				150,800	8.0	315	3/16	125,700	2.0	301	>1/4
WH31	5.0 Cr, 1.0 Mo, 0.25 C				159,200	5.0	370	3/16	84,700	0.0	464	>1/4†
WG105	2.5 Cr, 2.0 Mo, 0.25 C				146,100	8.0	326	>1/4*	130,500	2.5	305	>1/4
WG107	3.5 Cr, 2.0 Mo, 0.25 C				152,400	6.5	372	>1/4*	131,300	1.0	324	>1/4
WH32	5.0 Cr, 2.0 Mo, 0.25 C				186,800	2.0	366	>1/4†	120,500	2.0	334	>1/4†
Titanium-Chromium-0.25 Pct Carbon-1.0 and 2.0 Pct Manganese												
WG32	Unalloyed				77,400	18.5	163	3/64	71,500	21.5	151	3/64
WG33	2.5 Cr, 1.0 Mn, 0.25 C	2.42 Cr	1.68 Mn		151,100	10.0	249	3/16	144,400	1.0	326	>1/4†
WG35	3.5 Cr, 1.0 Mn, 0.25 C	3.33 Cr	1.61 Mn		162,400	4.5	272	3/16	113,800	0.0	334	>1/4†
WG39	5.0 Cr, 1.0 Mn, 0.25 C	4.05 Cr	1.45 Mn		177,200	4.5	317	>1/4†	94,700	1.0	316	>1/4†
WG34	2.5 Cr, 2.0 Mn, 0.25 C	2.30 Cr	2.50 Mn		176,300	4.0	294	>1/4*	140,400	1.0	331	>1/4†
WG36	3.5 Cr, 2.0 Mn, 0.25 C	3.28 Cr	2.18 Mn		137,800	9.5	260	3/16	114,700	1.0	328	>1/4†
WG40	5.0 Cr, 2.0 Mn, 0.25 C	4.63 Cr	2.02 Mn		194,400	2.0	340	3/16	132,400	2.5	425	>1/4†
Titanium-Chromium-0.25 Pct Carbon-1.0 and 2.0 Pct Iron												
WG32	Unalloyed				77,400	18.5	163	3/64	71,500	21.5	151	3/64
WG21	2.5 Cr, 1.0 Fe, 0.25 C	2.64 Cr	1.26 Fe		152,900	7.5	312	3/16	127,400	1.0	390	>1/4*
WG23	3.5 Cr, 1.0 Fe, 0.25 C	3.15 Cr	1.18 Fe		171,700	7.0	288	3/16			473	>1/4*
WG29	5.0 Cr, 1.0 Fe, 0.25 C	4.88 Cr	1.25 Fe		165,000	4.5	355	3/16	131,300	0.0	490	>1/4†
WG25	2.5 Cr, 2.0 Fe, 0.25 C	2.84 Cr	2.15 Fe		147,400	7.5	322	>1/4*			498	>1/4†
WG27	3.5 Cr, 2.0 Fe, 0.25 C	3.93 Cr	1.42 Fe		190,700	6.0	373	3/16			479	>1/4†
WG31	5.0 Cr, 2.0 Fe, 0.25 C	4.66 Cr	2.15 Fe		198,000	4.0	401	>1/4†	160,300	1.0	455	>1/4†
Titanium-Chromium-0.25 Pct Carbon-1.0 and 2.0 Pct Nickel												
WG110	Unalloyed				85,700	22.0	186	1/16	77,000	12.0	179	3/32
WG138	2.5 Cr, 1.0 Ni, 0.25 C				133,300	10.0	280	3/16	98,200	1.0	405	>1/4
WG130	3.5 Cr, 1.0 Ni, 0.25 C				146,500	9.0	294	3/16	76,300	0.5	370	>1/4
WH24	5.0 Cr, 1.0 Ni, 0.25 C				166,800	7.5	429	3/16	86,700	0.0	372	>1/4†
WG139	2.5 Cr, 2.0 Ni, 0.25 C				138,400	9.5	296	3/16	96,700	2.0	412	>1/4
WG126	3.5 Cr, 2.0 Ni, 0.25 C				147,500	8.0	320	3/16			572	>1/4
WH28	5.0 Cr, 2.0 Ni, 0.25 C				173,000	4.0	329	3/16			464	>1/4†

* Some ductility.

† Very little ductility.

[1] As hot rolled 1450°F.

[2] Heated in air ½ hr at 1600°F and quenched in cold water.

[3] Average of 2 longitudinal 14-ga sheet specimens, 3 in. long by 0.375 in. wide with a 0.250-in.-wide reduced section. Tested with the surface skin present.

[4] 10-kg load. Hardness at the center of the cross section of the sheet 90° to the surface and to the rolling direction. Average of at least 5 readings.

[5] Minimum bend radius without cracking on a single longitudinal specimen 3 in. long by 0.5 in. wide. Tested with the surface skin present.

[6] Forged at 1700°F by upsetting the 2¼-in.-diam ingots on edge to 0.250-in. slab, then ground and hot rolled at 1450°F to 0.060-in. sheet. Total reduction 35:1.

Table IV. Aging and Heat-treating Data for Quaternary Chromium-Titanium Alloys with Additions of Carbon and One Metal—Process *A* Metal Base

Heat No.	Composition, Pct				Heat-Treating Data							Aging Data	
					Vickers Hardness[1] After Indicated Treatment							Vickers Hardness[1] After Indicated Treatment	
	Intended	Actual			As Hot Rolled[2]	Heat Treated 1450°F[3]	Heat Treated 1550°F[4]	Heat Treated 1600°F[5]	Heat Treated 1650°F[6]	Heat Treated 1700°F[7]	Heat Treated 1750°F[8]	As Hot Rolled,[2] Aged 750° for Indicated Time	
				C N W								0 Hr	4 Hr
Titanium-Chromium-0.25 Pct Carbon-1.0 and 2.0 Pct Copper													
WG32	Unalloyed				163	138	133	151	175	200	206	163	200
WG30	2.5 Cr, 1.0 Cu, 0.25 C	2.45 Cr	1.04 Cu		287	311	357	338	349	387	413	287	329
WG22	3.5 Cr, 1.0 Cu, 0.25 C	3.51 Cr	1.05 Cu		313	358	373	336	352	417	387	313	358
WG24	5.0 Cr, 1.0 Cu, 0.25 C	4.78 Cr	0.94 Cu		309	437	387	407	346	345	439	309	357
WG28	2.5 Cr, 2.0 Cu, 0.25 C	2.81 Cr	2.01 Cu		322	339	376	376	384	396	398	322	335
WG26	3.5 Cr, 2.0 Cu, 0.25 C	3.19 Cr	2.01 Cu		309	421	394	364	340	370	361	309	352
WG20	5.0 Cr, 2.0 Cu, 0.25 C	5.03 Cr	2.07 Cu		376	461	466	456	487	498	498	376	432
Titanium-Chromium-0.25-Pct Carbon-1.0 and 2.0 Pct Vanadium													
WG108	Unalloyed				192	155	163	183	187	197	219	192	187
WG120	2.5 Cr, 1.0 V, 0.25 C				347	345	325	322	327	281	262	347	268
WG102	3.5 Cr, 1.0 V, 0.25 C				297	301	342	346	358	367	397	297	310
WH30	5.0 Cr, 1.0 V, 0.25 C				336	453	498	464	518	467	493	336	398
WG99	2.5 Cr, 2.0 V, 0.25 C				292	317	323	342	357	352	348	292	290
WG121	3.5 Cr, 2.0 V, 0.25 C				327	310	335	322	314	349	379	327	341
WH29	5.0 Cr, 2.0 V, 0.25 C				378	427	425	464	468	480	483	378	437
Titanium-Chromium-0.25 Pct Carbon-1.0 and 2.0 Pct Molybdenum													
WG103	Unalloyed				194	157	163	177	172	201	217	194	187
WG104	2.5 Cr, 1.0 Mo, 0.25 C				301	294	157	328	177	321	337	301	318
WG106	3.5 Cr, 1.0 Mo, 0.25 C				315	354	302	301	300	306	308	315	332
WH31	5.0 Cr, 1.0 Mo, 0.25 C				370	413	423	464	453	459	441	370	366
WG105	2.5 Cr, 2.0 Mo, 0.25 C				326	381	332	305	315	298	380	326	333
WG107	3.5 Cr, 2.0 Mo, 0.25 C				390	273	313	324	313	351	468	390	461
WH32	5.0 Cr, 2.0 Mo, 0.25 C				366	383	365	334	383	425	355	366	480
Titanium-Chromium-0.25 Pct Carbon-1.0 and 2.0 Pct Manganese													
WG32	Unalloyed				163	138	133	151	175	200	206	163	200
WG33	2.5 Cr, 1.0 Mn, 0.25 C	2.42 Cr	1.68 Mn		249	294	312	326	338	345	341	249	337
WG35	3.5 Cr, 1.0 Mn, 0.25 C	3.33 Cr	1.61 Mn		272	336	314	334	348	368	319	272	349
WG39	5.0 Cr, 1.0 Mn, 0.25 C	4.05 Cr	1.45 Mn		317	351	306	316	366	354	367	317	428
WG34	2.5 Cr, 2.0 Mn, 0.25 C	2.30 Cr	2.50 Mn		294	292	312	331	322	403	319	294	349
WG36	3.5 Cr, 2.0 Mn, 0.25 C	3.28 Cr	2.18 Mn		260	319	328	328	301	342	341	260	398
WG40	5.0 Cr, 2.0 Mn, 0.25 C	4.63 Cr	2.02 Mn		340	431	430	425	366	366	417	340	426
Titanium-Chromium-0.25 Pct Carbon-1.0 and 2.0 Pct Iron													
WG32	Unalloyed				163	138	133	151	175	200	206	163	200
WG21	2.5 Cr, 1.0 Fe, 0.25 C	2.64 Cr	1.26 Fe		312	340	401	390	418	400	423	312	344
WG23	3.5 Cr, 1.0 Fe, 0.25 C	3.15 Cr	1.18 Fe		288	405	372	473	437	461	460	288	334
WG29	5.0 Cr, 1.0 Fe, 0.25 C	4.88 Cr	1.25 Fe		355	431	498	490	494	505	442	355	379
WG25	2.5 Cr, 2.0 Fe, 0.25 C	2.84 Cr	2.15 Fe		322	395	498	498	462	485	494	322	372
WG27	3.5 Cr, 2.0 Fe, 0.25 C	3.93 Cr	1.42 Fe		373	442	432	479	459	495	458	373	381
WG31	5.0 Cr, 2.0 Fe, 0.25 C	4.66 Cr	2.15 Fe		401	441	443	455	514	464	461	401	437
Titanium-Chromium-0.25 Pct Carbon-1.0 and 2.0 Pct Nickel													
WG110	Unalloyed				186	158	157	179	181	204	200	186	184
WG138	2.5 Cr, 1.0 Ni, 0.25 C				280	360	405	405	421	442	459	280	287
WG130	3.5 Cr, 1.0 Ni, 0.25 C				294	384	355	370	405	405	395	294	304
WH24	5.0 Cr, 1.0 Ni, 0.25 C				429	483	442	372	488	485	493	429	405
WG139	2.5 Cr, 2.0 Ni, 0.25 C				296	420	394	412	493	480	494	296	315
WG126	3.5 Cr, 2.0 Ni, 0.25 C				320	506	488	572	542	546	530	320	335
WH28	5.0 Cr, 2.0 Ni, 0.25 C				349	437	466	464	485	479	442	349	373

[1] 10-kg load. Hardness at the center of the cross section of the sheet specimen 90° to the surface and to the rolling direction. Average of at least 5 readings.

[2] As hot rolled 1450°F.

[3] Heated in air ½ hr at 1450°F and quenched in cold water.

[4] Heated in air ½ hr at 1550°F and quenched in cold water.

[5] Heated in air ½ hr at 1600°F and quenched in cold water.

[6] Heated in air ½ hr at 1650°F and quenched in cold water.

[7] Heated in air ½ hr at 1700°F and quenched in cold water.

[8] Heated in air ½ hr at 1750°F and quenched in cold water.

Table V. Properties of Quaternary Chromium-Titanium Alloys[6] with Additions of Nitrogen Plus Metals—Process *A* Metal Base

Heat No.	Composition, Pct				As Hot Rolled[1]				Heat Treated 1600°F[2]			
	Intended	Actual			Tensile Strength,[3] psi	Elong., Pct in 1 In.	VHN[4]	Minimum Bend Radius,[5] In.	Tensile Strength,[3] psi	Elong., Pct in 1 In.	VHN[4]	Minimum Bend Radius,[5] In.
		C	N	W								
Titanium-Chromium-1.0 Pct Vanadium-0.10 and 0.20 Pct Nitrogen												
WG108	Unalloyed				85,400	20.5	192	3/64	76,900	13.0	183	3/64
WG141	2.5 Cr, 1.0 V, 0.10 N				147,700	11.0	303	3/16	146,900	2.0	366	>1/4
WG133	3.0 Cr, 1.0 V, 0.10 N				161,800	8.5	324	3/16	75,600	1.5	384	>1/4
WH56	5.0 Cr, 1.0 V, 0.10 N				170,300	5.0	344	3/16	53,100	1.0	373	>1/4†
WG127	2.5 Cr, 1.0 V, 0.20 N				160,600	9.0	357	>1/4*	90,700	0.5	380	>1/4
WG136	3.5 Cr, 1.0 V, 0.20 N				172,100	9.0	387	3/16	89,900	1.0	387	>1/4
WH55	5.0 Cr, 1.0 V, 0.20 N				207,800	3.5	390	>1/4*	85,700	0.0	536	>1/4†
Titanium-Chromium-2.0 Pct Vanadium-0.10 and 0.20 Pct Nitrogen												
WG108	Unalloyed				85,400	20.5	192	3/64	76,900	13.0	183	3/64
WG128	2.5 Cr, 2.0 V, 0.10 N				154,700	11.0	307	3/16	128,200	0.0	384	>1/4
WG137	3.5 Cr, 2.0 V, 0.10 N				165,700	7.0	337	3/16	72,100	0.0	375	>1/4
WH54	5.0 Cr, 2.0 V, 0.10 N				181,400	4.0	434	>1/4†	62,000	0.5	519	>1/4†
WG132	2.5 Cr, 2.0 V, 0.20 N				166,900	2.0	355	3/16	79,000	0.5	391	>1/4
WG140	3.5 Cr, 2.0 V, 0.20 N				177,200	6.0	383	3/16	63,300	0.5	431	>1/4
WH50	5.0 Cr, 2.0 V, 0.20 N				200,000	3.0	383	>1/4†	41,300	0.0	542	>1/4†
Titanium-Chromium-1.0 Pct Molybdenum-0.10 and 0.20 Pct Nitrogen												
WG103	Unalloyed				82,700	20.0	194	1/8	78,800	12.5	177	1/8
WG111	2.5 Cr, 1.0 Mo, 0.10 N				143,600	8.5	313	3/16	118,800	2.0	371	>1/4
WG123	3.5 Cr, 1.0 Mo, 0.10 N				157,400	7.0	337	3/16	128,700	1.5	400	>1/4
WH49	5.0 Cr, 1.0 Mo, 0.10 N				175,000	4.5	367	3/16	100,000	1.5	413	>1/4†
WG113	2.5 Cr, 1.0 Mo, 0.20 N				188,500	6.0	378	3/16	84,500	0.0	387	>1/4
WG119	3.5 Cr, 1.0 Mo, 0.20 N				190,000	7.0	379	3/16	73,500	1.0	425	>1/4
WH47	5.0 Cr, 1.0 Mo, 0.20 N				191,900	4.5	501	>1/4†	85,300	1.0	473	>1/4†
Titanium-Chromium-2.0 Pct Molybdenum-0.10 and 0.20 Pct Nitrogen												
WG103	Unalloyed				82,700	20.0	194	1/8	78,800	12.5	177	1/8
WG118	2.5 Cr, 2.0 Mo, 0.10 N				166,400	6.5	336	3/16	125,800	2.0	347	>1/4
WG114	3.5 Cr, 2.0 Mo, 0.10 N				176,600	6.0	375	3/16	111,000	2.0	341	>1/4*
WH46	5.0 Cr, 2.0 Mo, 0.10				193,100	2.0	380	>1/4†	96,500	0.0	433	>1/4†
WG122	2.5 Cr, 2.0 Mo, 0.20 N				181,300	6.0	375	3/16	114,100	1.0	386	>1/4
WG112	3.5 Cr, 2.0 Mo, 0.20 N				179,500	6.0	377	>1/4*	104,700	1.5	414	>1/4
WH45	5.0 Cr, 2.0 Mo. 0.20 N				201,200	2.0	411	>1/4†	96,700	0.5	482	>1/4†
Titanium-Chromium-1.0 Pct Nickel-0.10 and 0.20 Pct Nitrogen												
WG110	Unalloyed				85,700	22.0	186	1/16	77,000	12.0	179	3/32
WG150	2.5 Cr, 1.0 Ni, 0.10 N				138,600	11.0	298	3/16	109,400	2.0	409	>1/4
WG152	3.5 Cr, 1.0 Ni, 0.10 N				143,400	8.0	326	3/16			416	>1/4
WH23	5.0 Cr, 1.0 Ni, 0.10 N				182,000	5.0	377	3/16			514	>1/4†
WG146	2.5 Cr, 1.0 Ni, 0.20 N				162,900	10.0	339	3/16	88,300	1.0	434	>1/4
WG149	3.5 Cr, 1.0 Ni, 0.20 N				171,900	7.0	360	3/16	68,000	0.0	429	>1/4
WH43	5.0 Cr, 1.0 Ni, 0.20 N				175,300	4.5	419	3/16	70,600	0.0	430	>1/4†
Titanium-Chromium-2.0-Pct Nickel-0.10 and 0.20 Pct Nitrogen												
WG110	Unalloyed				85,700	22.0	186	1/16	77,000	12.0	179	3/32
WG148	2.5 Cr, 2.0 Ni, 0.10 N				153,100	10.5	326	3/16			413	>1/4
WG144	3.5 Cr, 2.0 Ni, 0.10 N				163,100	8.0	333	3/16			502	>1/4
WH26	5.0 Cr, 2.0 Ni, 0.10 N				171,500	5.0	440	3/16	50,000	0.0	510	>1/4†
WG151	2.5 Cr, 2.0 Ni, 0.20 N				171,100	6.5	356	3/16			484	>1/4
WG145	3.5 Cr, 2.0 Ni, 0.20 N				168,300	3.5	353	3/16			464	>1/4
WH27	5.0 Cr, 2.0 Ni, 0.20 N				194,700	3.0	417	3/16			548	>1/4†

* Some ductility.

† Very little ductility.

[1] As hot rolled 1450°F.

[2] Heated in air ½ hr at 1600°F and quenched in cold water.

[3] Average of 2 longitudinal 14-ga sheet specimens, 3 in. long by 0.375 in. wide with a 0.250-in.-wide reduced section. Tested with the surface skin present.

[4] 10-kg load. Hardness at the center of the cross section of the sheet 90° to the surface and to the rolling direction. Average of at least 5 readings.

[5] Minimum bend radius without cracking on a single longitudinal specimen 3 in. long by 0.5 in. wide. Tested with the surface skin present.

[6] Forged at 1700°F by upsetting the 2¼-in.-diam ingots on edge to 0.250-in. slab, then ground and hot rolled at 1450°F to 0.060-in. sheet. Total reduction 35:1.

Table VI. Aging and Heat-treating Data for Quaternary Chromium-Titanium Alloys with Additions of Nitrogen Plus Metals—Process *A* Metal Base

Heat No.	Composition, Pct		Heat-Treating Data: Vickers Hardness[1] After Indicated Treatment							Aging Data: Vickers Hardness[1] After Indicated Treatment — As Hot Rolled,[2] Aged 750°F for Indicated Time	
	Intended	Actual C N W	As Hot Rolled[2]	Heat Treated 1450°F[3]	Heat Treated 1550°F[4]	Heat Treated 1600°F[5]	Heat Treated 1650°F[6]	Heat Treated 1700°F[7]	Heat Treated 1750°F[8]	0 Hr	4 Hr
Titanium — Chromium (1.0 Pct) — Vanadium (0.10 Pct and 0.20 Pct) — Nitrogen											
WG108	Unalloyed		192	155	163	183	187	197	219	192	187
WG141	2.5 Cr, 1.0 V, 0.10 N		303	362	381	366	386	380	379	303	310
WG133	3.5 Cr, 1.0 V, 0.10 N		324	319	409	384	368	378	372	324	326
WH56	5.0 Cr, 1.0 V, 0.10 N		344	448	350	373	455	390	464	344	376
WG127	2.5 Cr, 1.0 V, 0.20 N		357	383	382	380	405	417	413	357	345
WG136	3.5 Cr, 1.0 V, 0.20 N		387	395	434	387	410	401	387	387	381
WH55	5.0 Cr, 1.0 V, 0.20 N		390	428	508	536	543	488	498	390	464
Titanium — Chromium (2.0 Pct) — Vanadium (0.10 Pct and 0.20 Pct) — Nitrogen											
WG108	Unalloyed		192	155	163	183	187	197	219	192	187
WG128	2.5 Cr, 2.0 V, 0.10 N		307	409	394	384	383	376	401	307	323
WG137	3.5 Cr, 2.0 V, 0.10 N		337	406	388	375	413	369	401	337	358
WH54	5.0 Cr, 2.0 V, 0.10 N		434	446	400	519	454	429	446	434	481
WG132	2.5 Cr, 2.0 V, 0.20 N		355	398	369	391	405	407	394	355	368
WG140	3.5 Cr, 2.0 V, 0.20 N		383	496	437	431	462	464	490	383	405
WH50	5.0 Cr, 2.0 V, 0.20 N		383	466	464	542	553	517	483	383	472
Titanium — Chromium (1.0 Pct) —Molybdenum (0.10 Pct and 0.20 Pct) — Nitrogen											
WG103	Unalloyed		194	157	163	177	172	201	217	194	187
WG111	2.5 Cr, 1.0 Mo, 0.10 N		313	345	357	371	357	369	364	313	334
WG123	3.5 Cr, 1.0 Mo, 0.10 N		337	424	389	400	354	416	383	337	341
WH49	5.0 Cr, 1.0 Mo, 0.10 N		367	373	447	413	491	461	498	367	432
WG113	2.5 Cr, 1.0 Mo, 0.20 N		378	425	364	387	383	413	419	378	373
WG119	3.5 Cr, 1.0 Mo, 0.20 N		379	450	425	425	412	401	448	379	376
WH47	5.0 Cr, 1.0 Mo, 0.20 N		403	474	461	473	500	450	417	403	487
Titanum — Chromium (2.0 Pct) — Molybdenum (0.10 Pct and 0.20 Pct) — Nitrogen											
WG103	Unalloyed		194	157	163	177	172	201	217	194	187
WG118	2.5 Cr, 2.0 Mo, 0.10 N		336	433	401	347	357	371	442	336	357
WG114	3.5 Cr, 2.0 Mo, 0.10 N		375	418	353	341	325	358	354	375	357
WH46	5.0 Cr, 2.0 Mo, 0.10 N		380	415	433	433	456	467	376	380	440
WG122	2.5 Cr, 2.0 Mo, 0.20 N		375	360	357	386	387	397	387	375	384
WG112	3.5 Cr, 2.0 Mo, 0.20 N		377	410	340	414	425	382	379	377	397
WH45	5.0 Cr, 2.0 Mo, 0.20 N		411	394	459	482	467	459	429	411	503
Titanium — Chromium (1.0 Pct) — Nickel (0.10 Pct and 0.20 Pct) — Nitrogen											
WG110	Unalloyed		186	158	157	179	181	204	200	186	184
WG150	2.5 Cr, 1.0 Ni, 0.10 N		298	419	387	409	491	442	413	298	290
WG152	3.5 Cr, 1.0 Ni, 0.10 N		326	452	432	416	443	450	433	326	337
WH23	5.0 Cr, 1.0 Ni, 0.10 N		377	462	498	514	525	536	437	377	397
WG146	2.5 Cr, 1.0 Ni, 0.20 N		339	421	447	434	429	464	483	339	361
WG149	3.5 Cr, 1.0 Ni, 0.20 N		360	532	477	429	473	455	488	360	380
WH43	5.0 Cr, 1.0 Ni, 0.20 N		419	433	452	430	429	438	443	419	500
Titanium — Chromium (2.0 Pct) — Nickel (0.10 Pct and 0.20 Pct) — Nitrogen											
WG110	Unalloyed		186	158	157	179	181	204	200	186	184
WG148	2.5 Cr, 2.0 Ni, 0.10 N		326	455	505	413	562	550	532	326	344
WG144	3.5 Cr, 2.0 Ni, 0.10 N		333	502	530	502	543	530	536	333	367
WH26	5.0 Cr, 2.0 Ni, 0.10 N		440	446	499	510	509	514	519	440	417
WG151	2.5 Cr, 2.0 Ni, 0.20 N		356	456	489	484	547	480	516	356	361
WG145	3.5 Cr, 2.0 Ni, 0.20 N		353	456	497	464	520	498	522	353	442
WH27	5.0 Cr, 2.0 Ni, 0.20 N		417	397	514	548	510	542	525	417	446

[1] 10-kg load. Hardness at the center of the cross section of the sheet specimen 90° to the surface and to the rolling direction. Average of at least 5 readings.

[2] As hot rolled 1450°F.

[3] Heated in air ½ hr at 1450°F and quenched in cold water.

[4] Heated in air ½ hr at 1550°F and quenched in cold water.

[5] Heated in air ½ hr at 1600°F and quenched in cold water.

[6] Heated in air ½ hr at 1650°F and quenched in cold water.

[7] Heated in air ½ hr at 1700°F and quenched in cold water.

[8] Heated in air ½ hr at 1750°F and quenched in cold water.

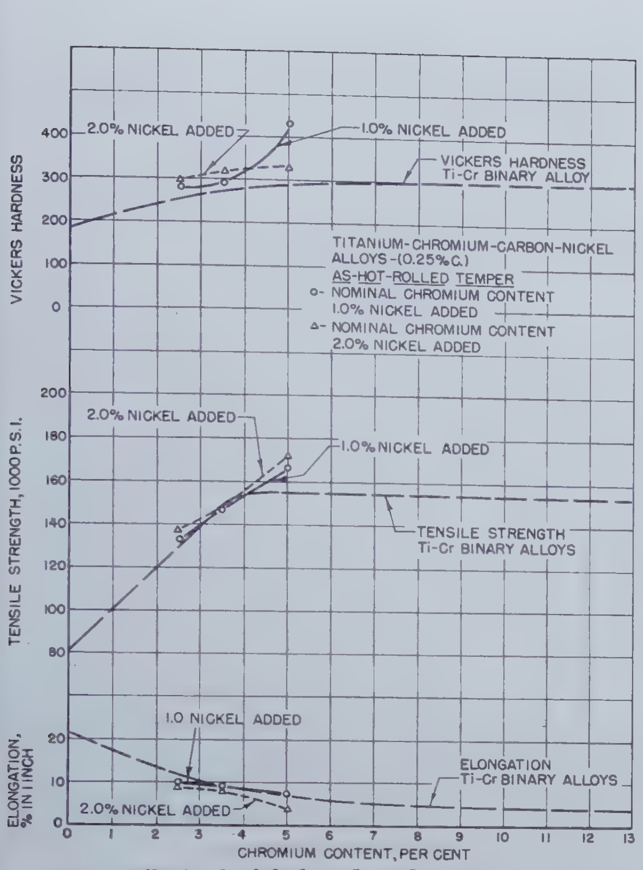

Fig. 9—Effect of nickel and carbon on the properties of as-hot-rolled titanium-chromium alloys prepared from process A metal.

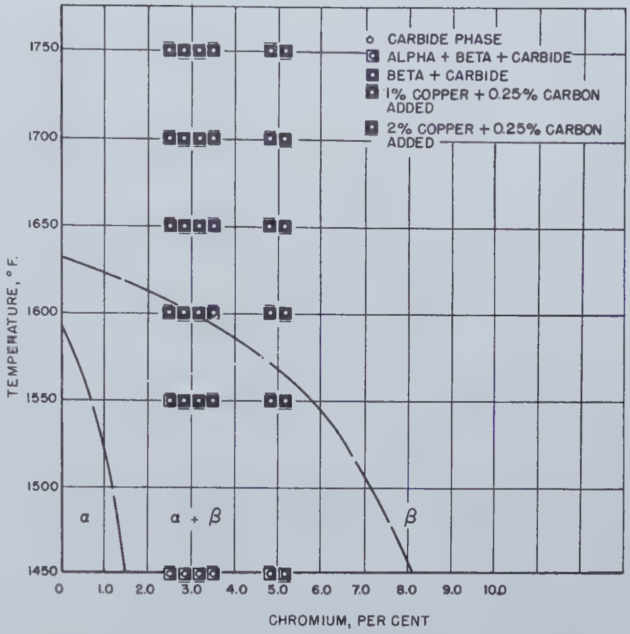

Fig. 10—Effect of 1.0 and 2.0 pct copper and 0.25 pct carbon on the transformation range of titanium-2.5 to 5.0 pct chromium alloys made from process A metal.

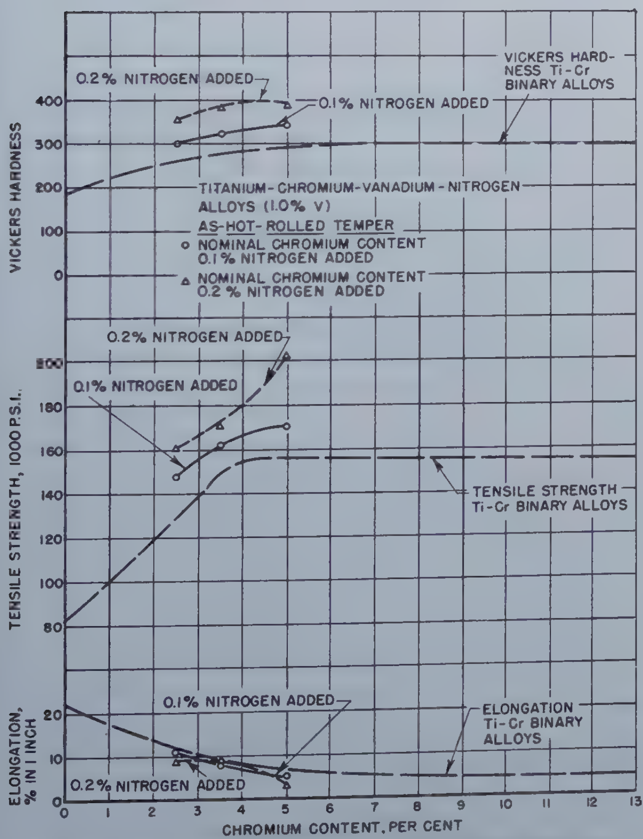

Fig. 11—Effect of vanadium and nitrogen on the properties of as-hot-rolled titanium-chromium alloys prepared from process A metal.

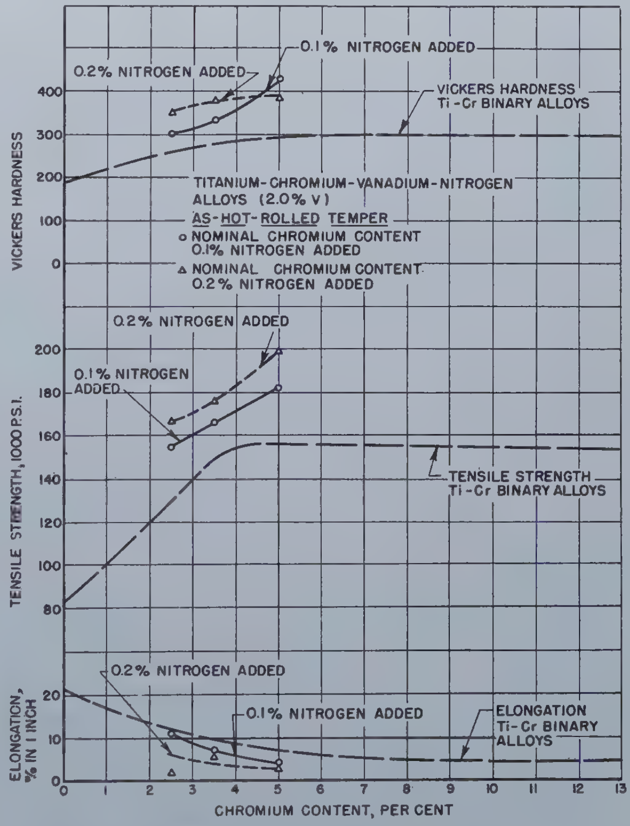

Fig. 12—Effect of vanadium and nitrogen on the properties of as-hot-rolled titanium-chromium alloys prepared from process A metal.

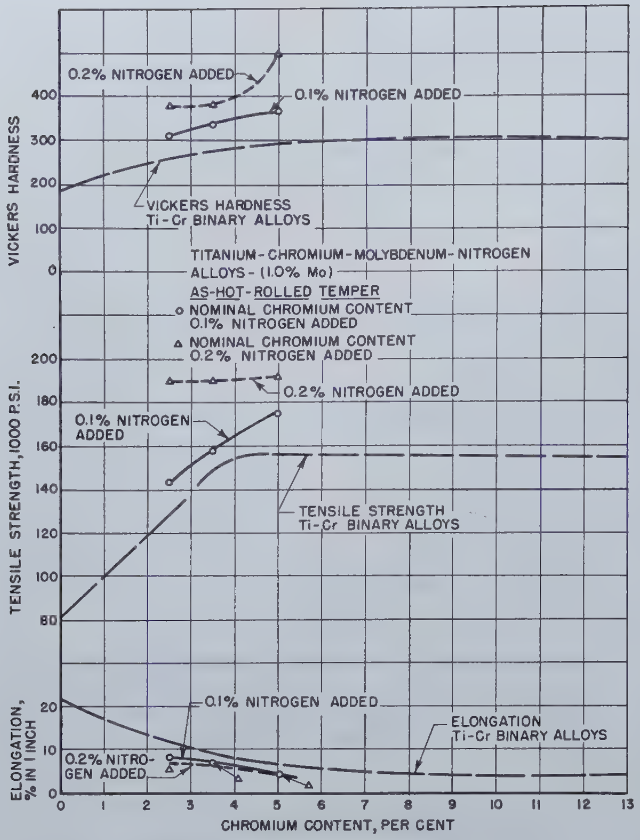

Fig. 13—Effect of molybdenum and nitrogen on the properties of as-hot-rolled titanium-chromium alloys prepared from process A metal.

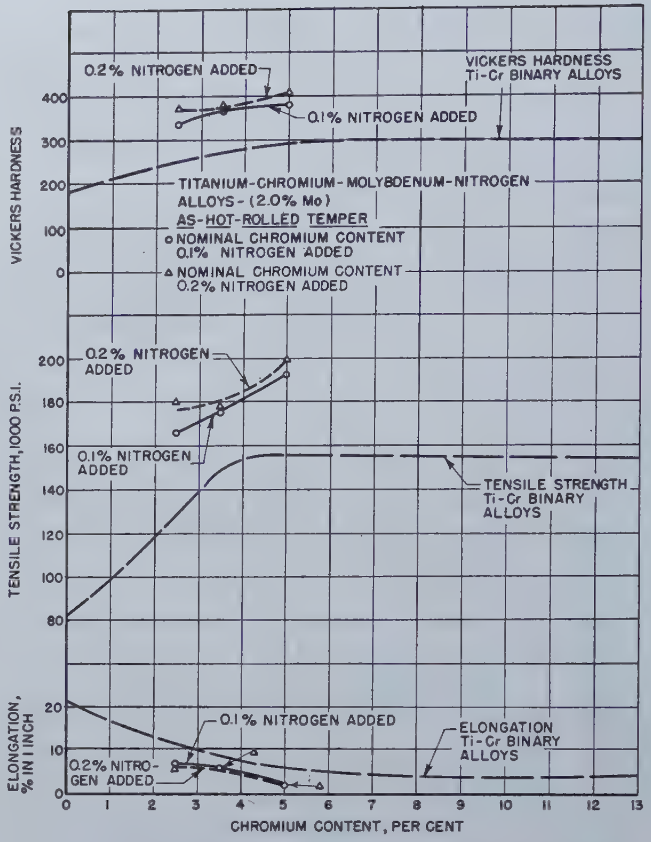

Fig. 14—The effect of molybdenum and nitrogen on the properties of as-hot-rolled titanium-chromium alloys prepared from process A metal.

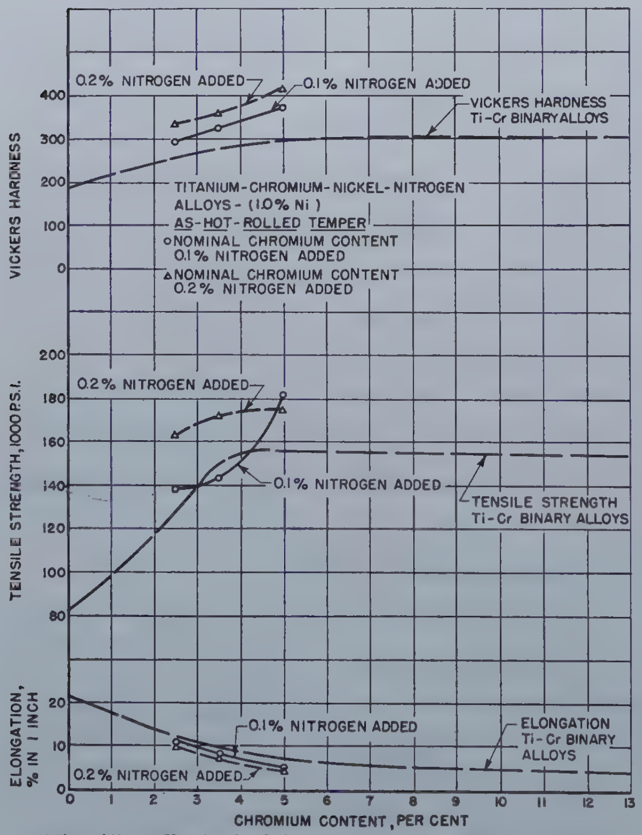

Fig. 15—Effect of nickel and nitrogen on the properties of as-hot-rolled titanium-chromium alloys prepared from process A metal.

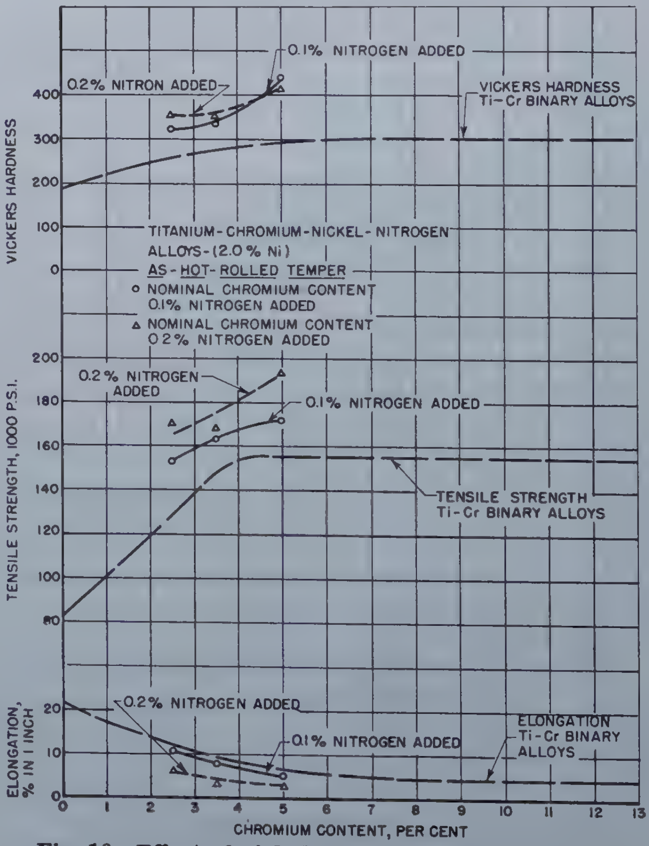

Fig. 16—Effect of nickel and nitrogen on the properties of as-hot-rolled titanium-chromium alloys prepared from process A metal.

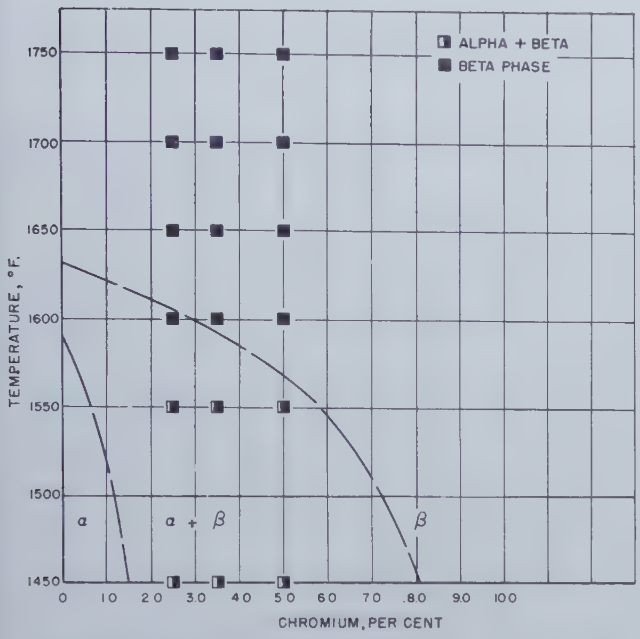

Fig. 17—Effect of 2.0 pct vanadium and 0.10 pct nitrogen on the transformation range of titanium-2.5 to 5.0 pct chromium alloys made from process A metal.

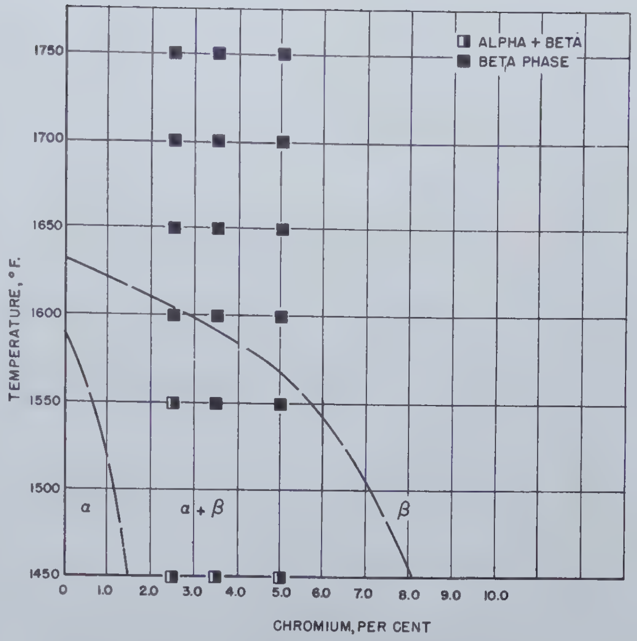

Fig. 18—Effect of 2.0 pct molybdenum and 0.10 pct nitrogen on the transformation range of titanium-2.5 to 5.0 pct chromium alloys made from process A metal.

the as-hot-rolled condition increased in hardness when they are aged for 4 hr at 750°F. Again, this increase in hardness is usually higher for the materials of higher alloy content. The titanium-chromium-carbon alloys containing manganese are particularly susceptible to age hardening, the increase being of the order of 100 Vickers numbers.

Quaternary Titanium-Chromium-Nitrogen Alloys Containing Vanadium, Molybdenum, or Nickel: Quaternary titanium-chromium-nitrogen alloys containing one other metal were studied because nitrogen has been shown to be a useful alloying element in titanium-chromium alloys. The properties of the titanium-chromium-nitrogen ternary alloys are described in another paper of this series. The alloys studied contained 2.5, 3.5, or 5 pct chromium and 0.1 or 0.2 pct nitrogen with 1 and 2 pct vanadium, 1 and 2 pct molybdenum, or 1 and 2 pct nickel.

Mechanical Properties: Table V contains the compositions, tensile properties, hardnesses, and minimum bend radii of the alloys in the as-hot-rolled condition and after heat treatment at 1600°F. The tensile and hardness data on the alloys in the as-hot-rolled condition are graphically represented by fig. 11 to 16, inclusive. These figures not only show the tensile and hardness properties of the as-hot-rolled alloys, but they also permit a comparison of the properties of the quaternary alloys with those of the titanium-chromium binary alloys.

By referring to the paper on ternary alloys, the properties of the titanium-chromium-nitrogen ternary alloys can also be compared with those of the corresponding quaternary alloys containing vanadium, molybdenum, or nickel. This comparison has been made, and it is concluded that 1 and 2 pct vanadium, 1 and 2 pct nickel, and 1 and 2 pct molybdenum appear to be slightly beneficial in these alloys.

Structure and Transformation Range: Nitrogen tends to raise the beta solvus temperatures of titanium and titanium-chromium alloys, whereas vanadium, molybdenum, or nickel tend to lower them. Therefore, the addition of nitrogen and one of these elements will raise or lower the beta solvus temperatures, depending upon the relative amounts of nitrogen and the metal which have been added. For example, as shown by fig. 17, 2 pct vanadium and 0.1 pct nitrogen did not have an appreciable effect on the beta solvus temperatures of the titanium-chromium alloys. On the other hand, 2 pct molybdenum and 0.1 pct nitrogen tends to lower the beta solvus temperatures slightly, as shown by fig. 18, but when the nitrogen content is increased to 0.2 pct, the beta solvus line is markedly raised, as shown by fig. 19. Two per cent nickel and 0.1 pct nitrogen also lowers the beta solvus temperatures, as shown by fig. 20, but when the nitrogen is increased to 0.2 pct, the beta solvus temperatures are quite markedly raised, as shown by fig. 21.

Response to Heat Treatment and Aging: The hardnesses of the quaternary alloys in the as-hot-rolled condition, after quenching from 1450, 1550, 1600, 1650, 1700, and 1750°F and after aging the as-hot-rolled alloys for 4 hr at 750°F, are listed in table VI. Again, the alloys are hardened when they are quenched from the beta field, and this increase is greater the higher the temperature and the higher the alloy content of the materials, at least within the range of composition investigated. Although marked hardening occurred in some of the alloys when they are quenched, this treatment has not been beneficial to the tensile properties when the

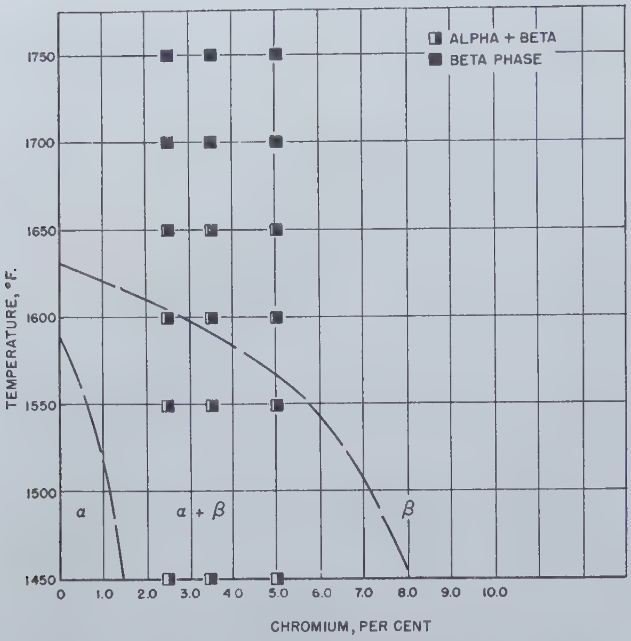

Fig. 19—Effect of 2.0 pct molybdenum and 0.20 pct nitrogen on the transformation range of titanium-2.5 to 5.0 pct chromium alloys made from process A metal.

Table VII. Analysis and Properties of Process *A* Titanium Alloys Whose Tensile Strength Is Higher Than Would Be Expected From the Vickers Hardness Number

Heat No.	Intended Analysis	Tensile Strength, psi	Elong., Pct in 1 In.	Vickers Hardness
WG31	5 Cr - 2 Fe - 0.25 C	190,700	6.0	373
WG40	5 Cr - 2 Mn - 0.25 C	194,400	2.0	340
WG43	4.38 Cr*	186,600	6.0	281
WG44	5 Cr - 0.5 C - 0.2 N	190,700	3.0	340
WG49	5 Cr - 0.25 C - 0.1 N	186,600	4.0	319
WG62	3.5 Cr - 0.25 C - 0.2 N	181,200	5.5	321
WG66	3.23 Cr - 0.25 C	160,200	5.0	262
WG113	2.5 Cr - 1 Mo - 0.2 N	188,500	6.0	378
WG119	3.5 Cr - 1 Mo - 0.2 N	190,000	7.0	379
WG169	5 Cr - 0.2 N	185,100	4.0	365
WG172	5 Cr - 0.1 N	186,800	5.0	295
WH27	5 Cr - 2 Ni - 0.2 N	194,700	3.0	417
WH45	5 Cr - 2 Mo - 0.2 N	201,000	2.0	411
WH50	5 Cr - 2 V - 0.2 N	200,000	3.0	383
WH55	5 Cr - 1 V - 0.2 N	207,800	3.5	390
WH82	7.5 Mn	196,800	2.5	384
WH91	7.5 Mn - 0.25 C	221,400	2.0	438
WH100	7.5 Mn - 0.5 C	188,000	1.0	387

* Actual analysis.

heat-treating temperature was 1600°F. These data are shown in table V. It is quite possible, however, that useful heat treatments may be developed for alloys of this type.

Increases in hardness are obtained by aging the as-hot-rolled alloys for 4 hr at 750°F. This age-hardening effect is quite marked in several of the alloys containing the greatest total alloy content. Tensile properties of the alloys in this condition are not yet available.

Correlation of Hardness with Tensile Properties: Fig. 22 shows the relationship of tensile strength to the hardness of the as-hot-rolled titanium-base alloys prepared from Process A metal. The data are plotted so that the information on binary, ternary, and quaternary alloys is distinguishable.

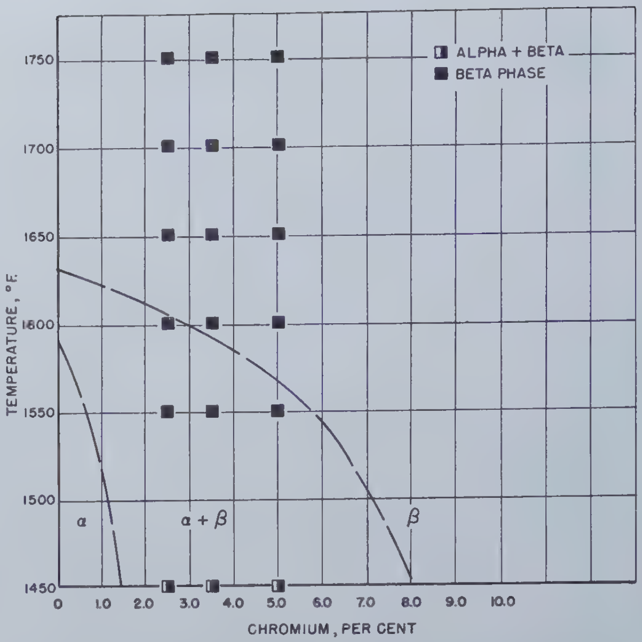

Fig. 20—Effect of 2.0 pct nickel and 0.10 pct nitrogen on the transformation range of titanium-2.5 to 5.0 pct chromium alloys made from process A metal.

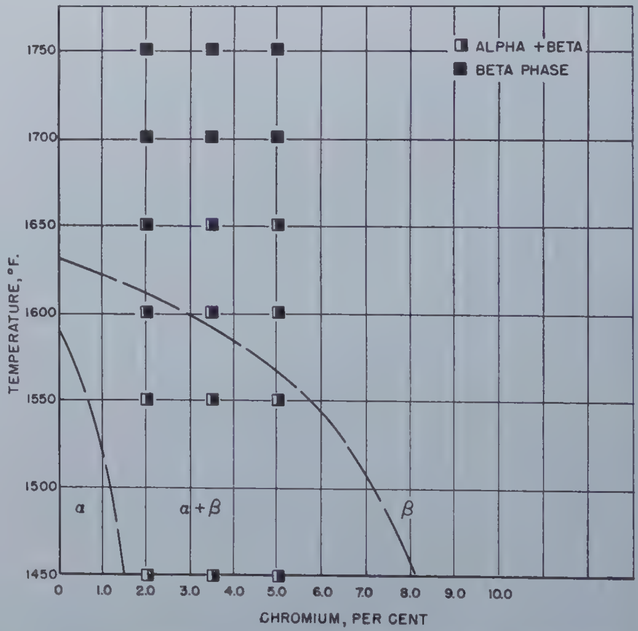

Fig. 21—Effect of 2.0 pct nickel and 0.2 pct nitrogen on the transformation range of titanium-2.5 to 5.0 pct chromium alloys made from process A metal.

In addition, the data on the alloys consisting of alpha, alpha-plus-beta, or beta structures at the hot-working temperature of 1450°F are also noted. A very large proportion of the binary, ternary, and more complex alloys consists of alpha and transformed beta (acicular alpha) at room temperature. The tensile strength of this type of alloy is roughly 475 times the Vickers number. There is, of course, considerable scatter in the results, and the tensile strengths of a number of alloys lie substantially above the average line relating hardness to tensile

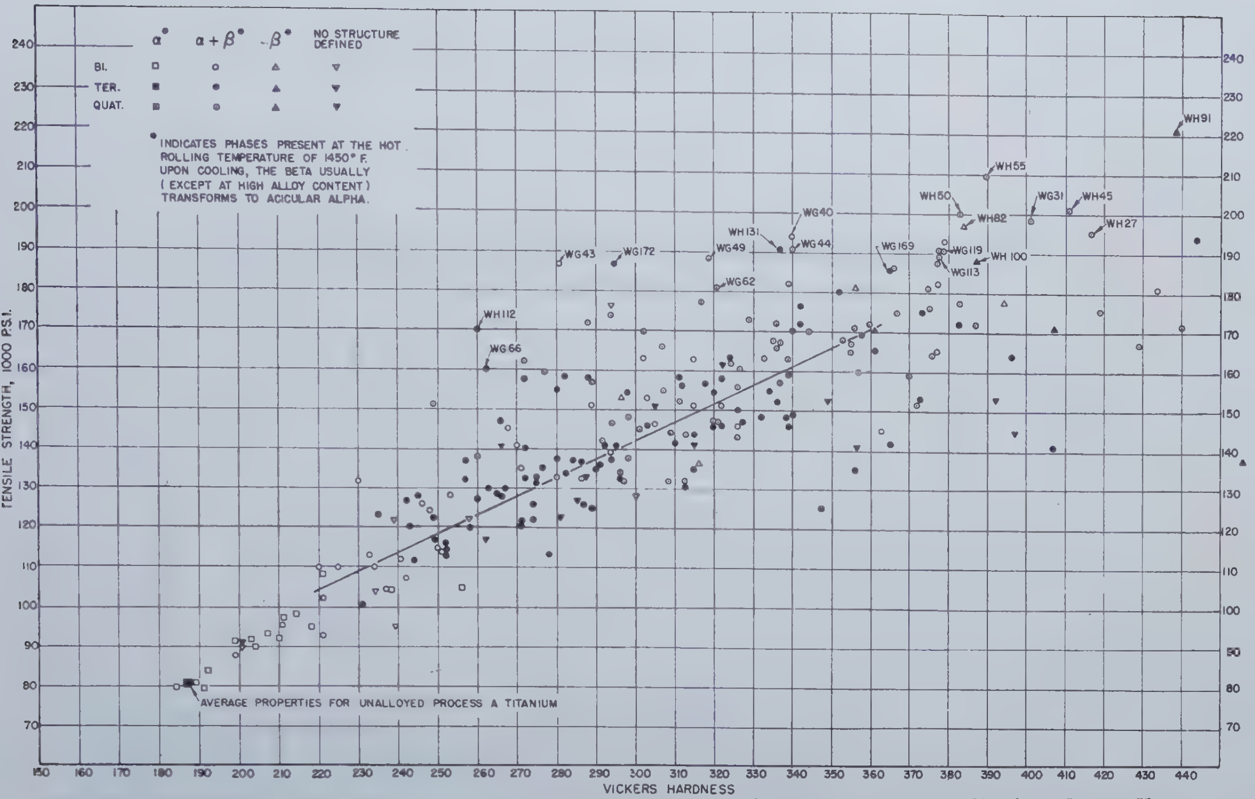

Fig. 22—Correlation of hardness and tensile strength of as-hot-rolled process A titanium base alloys.

Table VIII. Several of Best Quaternary Alloys and Their Properties

Heat No.	Intended Composition, Pct	Ultimate Tensile Strength, psi	Elong., Pct in 1 In.	Vickers Hardness No.	Minimum Bend Radius	Increase in Vickers Hardness by Aging As-Hot-Rolled Alloys
WG63	3.5 Cr, 0.25 C, 0.1 N	163,200	7.0	302	3t	55
WG48	5.0 Cr, 0.25 C, 0.1 N	183,200	6.0	339	3t	92
WH30	5.0 Cr, 1.0 V, 0.25 C	171,900	5.0	336	3t	62
WH29	5.0 Cr, 2.0 V, 0.25 C	189,700	3.5	378	3t	59
WG35	3.5 Cr, 1.0 Mn, 0.25 C	162,400	4.5	272	3t	77
WG39	5.0 Cr, 1.0 Mn, 0.25 C	177,200	4.5	317	4t	111
WG36	3.5 Cr, 2.0 Mn, 0.25 C	137,800	9.5	260	3t	138
WG40	5.0 Cr, 2.0 Mn, 0.25 C	194,400	2.0	340	3t	86
WG27	3.5 Cr, 2.0 Fe, 0.25 C	190,700	6.0	373	3t	50
WG140	3.5 Cr, 2.0 V, 0.2 N	177,200	6.0	383	3t	22
WH49	5.0 Cr, 1.0 Mo, 0.1 N	175,000	4.5	367	3t	65
WG119	3.5 Cr, 1.0 Mo, 0.2 N	190,000	7.0	379	3t	0
WH23	5.0 Cr, 1.0 Ni, 0.1 N	182,000	5.0	377	3t	20
WH27	5.0 Cr, 2.0 Ni, 0.2 N	194,700	3.0	417	3t	29

strength. Hardness data were not obtained on the tensile specimens. Therefore, slight nonuniformity in composition of the sheet also accounts for some of the scatter. As would be expected, this scatter becomes more pronounced as the hardness increases. The composition and properties of the potentially useful alloys, namely, those whose tensile strengths are substantially greater than that predicted from the hardness value, are listed in table VII. It will be noted that most of these alloys contain 3.5 to 5 pct chromium or 7.5 pct manganese. These are the principal additions which produce the most outstanding alloys to date.

Summary

Eighty-four quaternary alloys have been studied from the following systems:

1. Titanium-chromium-carbon-nitrogen.
2. Titanium-chromium-carbon with copper, vanadium, molybdenum, manganese, iron, or nickel.
3. Titanium-chromium-nitrogen alloys containing vanadium, molybdenum, or nickel.

All of these additions, except carbon above about 0.2 pct, are soluble in either alpha or beta titanium and all tend to lower the beta solvus temperatures, excepting nitrogen, which raises it markedly. All of the quaternary alloys have a very narrow alpha field at the hot-working temperature of 1450°F so that all of them, after cooling to room temperature, consisted of equiaxed alpha and acicular alpha which transformed from the beta present at the hot-working temperature. All of the alloys are increased in hardness by quenching from the beta field, but the tensile properties of none were beneficially affected by quenching in water from 1600°F. However, since the hardening by quenching from a temperature in or near the beta field is quite marked, useful heat treatments may be developed after further investigation. Most of these titanium-chromium alloys, particularly those containing 3.5 and 5 pct chromium, age harden appreciably in the as-hot-rolled condition, employing an aging treatment consisting of 4 hr at 750°F. No tensile data are available as yet on these alloys in the aged condition.

Several of the best quaternary alloys and their properties are listed in table VIII.

Acknowledgments

The authors wish to express their appreciation to the Air Materiel Command, Wright-Patterson Air Force Base, who sponsored the work reported in this paper, and who granted permission for its publication.

Diffusion Coefficient of Carbon in Austenite

by Cyril Wells,

Walter Batz,

and Robert F. Mehl

Diffusion coefficient values for carbon in austenite covering a wide range of temperature and composition have been determined employing statistical methods. In addition, the relation between concentration and each of the following, D (diffusion coefficient), Q (activation heat of diffusion), and A (the constant in the diffusion equation), has been obtained.

A study of the rates of diffusion of austenite was published in *Metals Technology* in 1940.[1] The present investigation is an extension of the earlier work, undertaken (1) to obtain values of the coefficient of diffusion, *D*, over a much wider range of carbon concentration, and (2) to provide data in all ranges of concentration and temperature in such abundance that statistical methods could be employed to evaluate the accuracy of the data with unusual precision.

Composition of Materials: Composition of materials used in this research program are listed in table I. These materials, all forged to about 1¼ in. rounds, consist of a high-purity iron, Armco iron, a large number of laboratory-made plain carbon steels containing amounts of impurities normally expected in high-quality commercial steels, and three silicon steels. Since it was known at the time these steels were being made that impurities in the amounts present were unlikely to affect carbon diffusion rates[1] significantly, the effort made to obtain high-purity steels was not as persistent as it otherwise would have been.

Procedure: In general, the procedure followed by Wells and Mehl and described in detail in an earlier publication[1] is the one used by the present authors. However, certain modifications have been made which it is believed allow diffusion data to be interpreted more objectively and correctly. These are described completely under appropriate subheadings which follow.

Experimental Procedure: Experimental procedure includes (1) the preparation of specimens by welding steels of different carbon contents, (2) the heating of these for certain times at selected temperatures in order to diffuse carbon along the specimens across the welded "interface," and (3) the determination of the carbon distribution across the diffusion zone.

Preparation of Specimens: Prior to welding steel of one carbon content to iron or steel of another carbon content, surfaces to be welded are machined perpendicular to the longitudinal axis of cylinders which are about ¾ in. in diam and 1½ in. long. The prepared, flat, parallel surfaces are brought together and butt-welded electrically. Evidence of a good weld is given in fig. 1. Welding temperature

---

CYRIL WELLS, Member AIME, and WALTER BATZ are associated with the Metals Research Laboratory, Carnegie Institute of Technology, Pittsburgh, Pa.; and ROBERT F. MEHL, Member AIME, is Director, Metals Research Laboratory, and Head, Department of Metallurgical Engineering.

AIME New York Meeting, Feb. 1950.

TP 2792 E. Discussion (2 copies) may be sent to Transactions *AIME before Apr. 1, 1950, and will be published Nov. 1950. Manuscript received Oct. 17, 1949; revision received Nov. 30, 1949.*

Table I. Composition of Materials

Material No.	Composition												
	Atomic Per Cent	Weight, Per Cent											
	C	C	Mn	P	S	Si	Cu	Ni	Cr	Mo	B	Co	O
1	0.02	0.005	0.00	0.001	0.003	0.001	0.00	0.004	0.00	0.00		0.001	0.040
2	0.07	0.015	0.04	0.007	0.020	0.006	0.04	0.07	0.03	0.01			
3	0.09	0.020	0.02	0.007	0.016	0.010	0.04	0.07	0.01	0.00			
4	0.33	0.070	0.25	0.015	0.027	2.18	0.10	0.18	0.06	0.04			
5	0.63	0.136	0.38	0.010	0.026	0.23	0.09	0.06	0.25	0.05			
6	1.04	0.224	0.26	0.014	0.025	0.03	0.08	0.14	0.30	0.03	0.009		
7	1.14	0.247	0.51	0.012	0.024	0.30	0.05	0.12	0.13	0.04			
8	2.47	0.54	0.61	0.012	0.027	0.27	0.08	0.14	0.14	0.03			
9	3.14	0.69	0.51	0.013	0.028	0.19	0.05	0.11	0.13	0.03			
10	3.80	0.84	0.25	0.012	0.012	0.26	0.04	0.08	0.06	0.03			
11	4.07	0.90	0.17	0.012	0.017	2.04	0.04	0.09	0.04	0.01			
12	4.20	0.93	0.24	0.005	0.019	0.20	0.05	0.07	0.09	0.02			
13	4.72	1.05	0.28	0.011	0.010	0.28	0.04	0.06	0.08	0.02			
14	4.93	1.10	0.34	0.008	0.017	0.004	0.04	0.04	0.02	0.01			
15	5.24	1.17	0.36	0.016	0.010	0.40	0.04	0.09	0.11	0.04			
16	5.66	1.27	0.16	0.009	0.023	0.008	0.06	0.06	0.02	0.01			
17	5.83	1.31	0.25	0.010	0.012	0.29	0.05	0.09	0.05	0.04			
18	6.13	1.38	0.27	0.005	0.018	0.24	0.04	0.07	0.05	0.01			
19	6.21	1.40	0.60	0.011	0.040	0.22	0.05	0.08	0.14	0.04			
20	6.47	1.46	0.23	0.009	0.024	0.006	0.04	0.06	0.02	0.01			
21	6.64	1.50	0.43	0.007	0.037	0.21	0.08	0.12	0.14	0.03	0.009		
22	6.64	1.50	0.43	0.010	0.038	2.12	0.11	0.21	0.13	0.04			
23	6.68	1.51	0.33	0.004	0.014	0.004	0.04	0.04	0.02	0.01			
24	7.67	1.75	0.72	0.010	0.042	0.33	0.06	0.09	0.12	0.04			

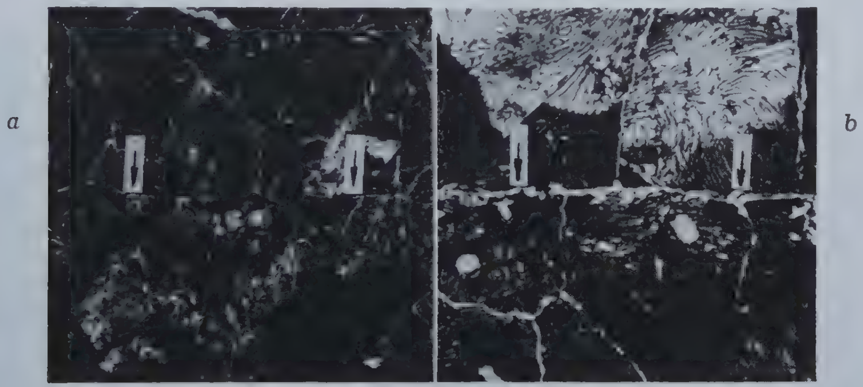

Fig. 1—Evidence of a good weld.

Arrows indicate weld positions. Plain carbon steels welded contain 1.31 and 1.38 wt pct carbon, respectively. Specimen etched with 2 pct nital. Magnification: *a.* X250; *b.* X1500.

is so low and welding time so short that diffusion occurring during this operation is negligible. A more detailed account of preparation of specimens is given in an earlier paper.[1]

Diffusion-anneal: Specimens were heated in argon at temperatures and for times recorded in table II. Temperatures were controlled within 1°C and are probably correct within ±5°C. Errors in reported elapsed times are negligible. Precautions taken have already been adequately reported elsewhere.[1]

Microscopic evidence showed that with few exceptions practically no decarburization of specimens occurred as a result of heating them at diffusion temperatures for long times.

Determination of Carbon Distribution: After the diffusion-anneal, all material which was thought might be decarburized was removed from each specimen and discarded. Subsequently, consecutive layers 0.050 in. thick and perpendicular to the longitudinal axis of the specimen were machined for analysis. The plane of the machined surface was kept as parallel as possible with the plane of the weld. It is believed that a carbon analysis value is rarely in error by more than 0.01 wt pct or a distance measurement in error by more than 0.0005 in.

Typical data obtained in a determination of carbon distribution in one specimen are given in table III, col. 2 and 3. It may be noted that each distance is reported as the number of centimeters from the weld to the center of a layer. The center of Layer 1, for example, is 1.776 cm from the weld. The average carbon content of Layer 1 is 1.762 wt pct and this is accepted as the carbon concentration at the center of the layer.

Plotting of Concentration-penetration Curves: In an effort to draw concentration-penetration curves each one of which best represents the relation between carbon content and distance from the weld in a specimen, a procedure has been used which involves (1) the computation of C/C_o ratios, (2) the plotting on probability paper of a curve relating C/C_o and distance, and (3) the drawing of a concentration-penetration curve. To make it easier to describe this procedure briefly and yet as clearly as possible, certain typical data have been selected. These are for Test 16 and are listed in table III.

The specimen used in Test 16 consisted of Steel 24 containing 7.67 at. pct carbon (1.75 wt pct) welded to Iron 2 containing 0.07 at. pct carbon (0.015 wt pct). In this instance $C_o = C_{max.} — C_{min.} = 7.67 — 0.07 = 7.60$ at. pct and C = at. pct at center of layer — 0.07.

Computed C/C_o ratios are plotted on a probability

Table II. Diffusion-anneal Data

Test No.	Material A Welded to Material B*		Temperature of Diffusion, °C	Time of Diffusion, hr	Test No.	Material A Welded to Material B		Temperature of Diffusion, °C	Time of Diffusion, hr
	No. of A Material	No. of B Material				No. of A Material	No. of B Material		
1	18	15	995	24.00	29	21	6	1127	20.50
2	12	10	995	24.00	30	21	6	1129	20.33
3	15	12	987	24.00	31	7	2	1130	20.25
4	13	10	997	24.00	32	8	7	1128	20.00
5	17	13	1000	24.00	33	22	4	1125	19.25
6	18	15	1000	24.00	34	8	7	1126	19.25
7	18	1	999	24.00	35	7	2	1124	22.67
8	18	1	1010	25.00	36	24	2	1128	20.50
9	17	1	905	72.00	37	16	9	1127	20.00
10	17	1	957	48.00	38	23	16	1122	20.25
11	17	1	950	48.00	39	19	14	1126	20.75
12	15	1	910	71.50	40	19	14	1132	20.25
13	15	10	916	73.00	41	12	8	1121	20.25
14	23	2	1038	21.50	42	12	8	1130	20.67
15	23	2	1042	20.75	43	8	7	1000	47.20
16	24	2	1127	19.50	44	19	14	1002	47.30
17	23	2	1195	11.92	45	19	16	1003	46.00
18	23	2	1195	9.42	46	14	9	1004	44.25
19	19	2	1255	5.33	47	14	9	1002	47.25
20	14	2	909	72.00	48	8	7	1001	53.75
21	16	2	956	73.00	49	19	16	997	45.00
22	13	5	847	163.00	50	14	2	1301	5.83
23	13	5	848	163.00	51	24	19	1130	23.00
24	12	7	802	212.00	52	7	3	1002	44.50
25	12	7	800	212.00	53	24	19	1127	23.17
26	10	8	750	286.50	54	14	3	1305	5.17
27	10	8	754	286.50	55	23	3	1005	47.66
28	22	4	1128	20.75	56	23	3	1000	43.50

* Analyses of materials given in table I.

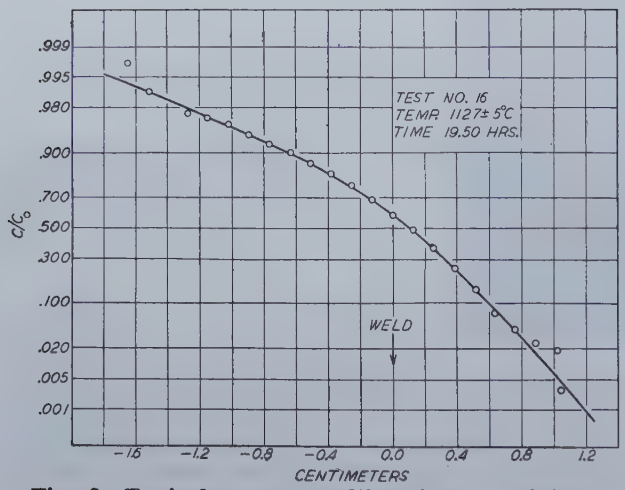

Fig. 2—Typical curve resulting from a plot on probability paper of C/C_0 values versus distances from the weld to centers of layers machined from the couple.

Plots of this kind provide a basis for drawing concentration-penetration curves more accurately and more objectively.

scale, distances from the weld to centers of layers machined from the couple are plotted on a linear scale, and a curve is drawn as indicated in fig. 2. Next, C/C_0 ratios at 0.1 cm intervals between the limits of 1.3 cm on the low and 1.7 cm on the high carbon side of the couple are read from the curve. Concentrations at these distances are obtained by adding $C_{min.}$ to the product of C/C_0 and C_0 and the data obtained are plotted as points (centers of open circles) as shown in fig. 3. The concentration-penetration curve is then drawn through these points. Centers of closed circles in the figure are actual data points.

In some instances all data points representing the relation between C/C_0 and distance fall practically on a straight line when plotted on probability paper. This is the case whenever the difference between maximum and minimum carbon concentration in a couple is sufficiently small so that the variation of D, diffusion coefficient, with concentration is insignificant. In such a situation as this, a regression line is calculated using the method of least squares.

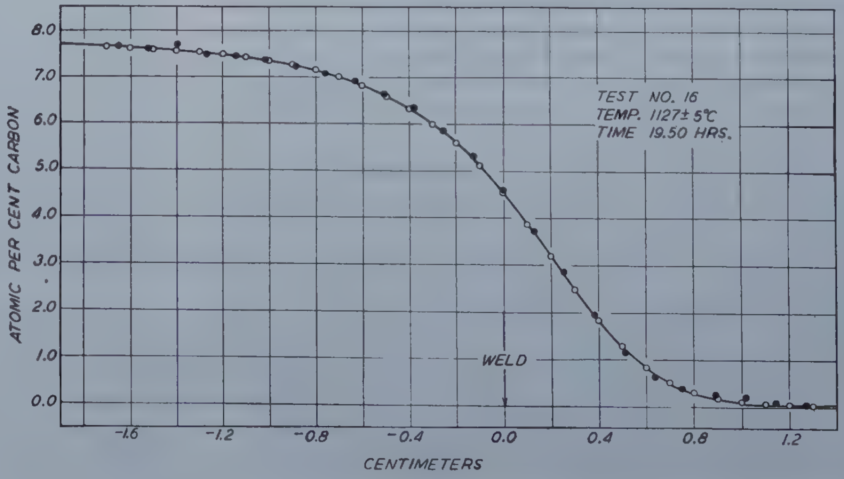

Fig. 3 — Typical concentration-penetration curve.

Centers of closed circles are actual data points. Centers of open circles represent computed concentrations at selected distances from the weld. In computing concentrations C_{min} is added to the product of $C/C_0 \cdot C_{min}$ and C_0 values are known (footnote table III) and values of C/C_0 at selected distances are represented by points on the curve of fig. 2.

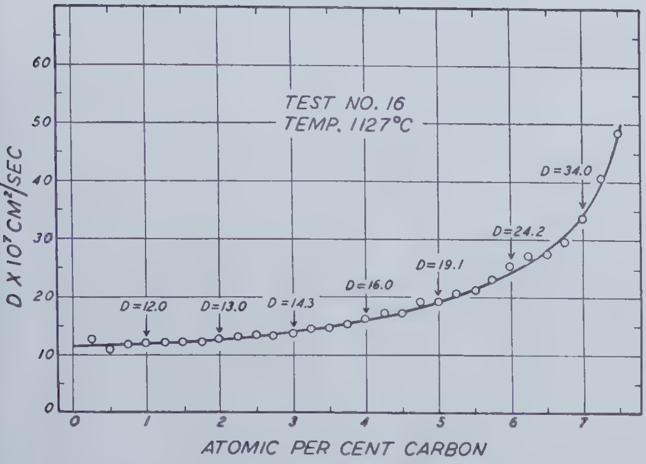

Fig. 4—A typical curve showing diffusion coefficient, D, at a given temperature to vary with concentration.

Values of D at concentrations of 1, 2, 3, 4, 5, 6, and 7 at. pct have been read from such curves and these, after being corrected, are reported in table IV.

Table III. Data from Test 16

Layer No.	Distance from Weld to Center of Layer, cm	Weight Per Cent of Carbon	Atomic Per Cent of Carbon	C	$\frac{C}{C_o}$
1	—1.776	1.762	7.72		
2	—1.649	1.745	7.65	7.58	0.997
3	—1.522	1.729	7.59	7.52	0.990
4	—1.395	1.754	7.69		
5	—1.268	1.702	7.48	7.41	0.975
6	—1.141	1.694	7.44	7.37	0.970
7	—1.014	1.677	7.37	7.30	0.961
8	—0.887	1.642	7.23	7.16	0.942
9	—0.760	1.606	7.08	7.01	0.922
10	—0.633	1.568	6.92	6.85	0.901
11	—0.506	1.500	6.64	6.57	0.864
12	—0.379	1.429	6.34	6.27	0.825
13	—0.253	1.320	5.88	5.81	0.764
14	—0.125	1.189	5.32	5.25	0.691
15	0.003	1.023	4.60	4.53	0.596
16	0.130	0.825	3.74	3.67	0.483
17	0.257	0.626	2.86	2.79	0.367
18	0.384	0.425	1.95	1.88	0.247
19	0.511	0.251	1.16	1.09	0.143
20	0.638	0.136	0.63	0.56	0.074
21	0.765	0.082	0.38	0.31	0.041
22	0.892	0.055	0.26	0.19	0.025
23	1.019	0.045	0.21	0.14	0.018
24	1.146	0.020	0.09	0.02	0.003
25	1.273	0.012	0.06		

In Test 16, Steel 24 (7.67 at. pct carbon) was welded to Iron 2 (0.07 at. pct carbon).

$C_o = C_{max.} - C_{min.}$ Values of $C_{max.}$ and $C_{min.}$ are 7.67 and 0.07 at. pct, respectively.

C = At. pct at center of layer — $C_{min.}$

Values of concentration at given distances from the weld are then computed and a concentration-penetration (error function) curve is plotted.

Calculation of Diffusion Coefficient Values: Diffusion coefficient values are calculated from information provided by concentration-penetration curves. A concentration-penetration curve is not utilized in the determination of D values if the upper flat portion of the curve represents a carbon content which is lower than the determined carbon content of the original steel by more than 0.03 wt pct.*

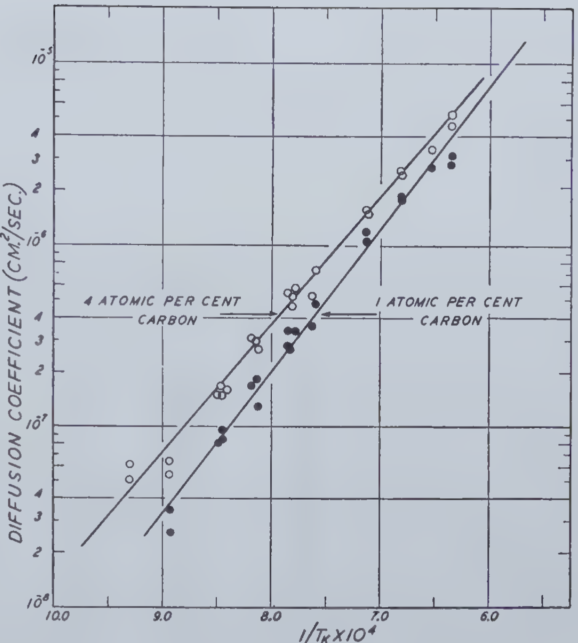

Fig. 5—Plot of diffusion coefficient at each of two concentrations against reciprocal of temperature.

Scale of diffusion values is logarithmic and T_K is given in Kelvin units. Open circles, 4 at. pct (0.88 wt pct) carbon; closed circles, 1 at. pct (0.22 wt pct) carbon.

Matano and Grube methods for computing D values are the ones used by the authors. These have been adequately described and discussed by Rhines and Mehl[2] and are well-known. Matano's solution of Fick's law provides for a variation of diffusion coefficient, D, with concentration. Grube's solution is based on the assumption that D does not vary with concentration. Obviously before D values computed by the Grube method are accepted, one should know that the variation of D with concentration is unlikely to cause the computed values to be in error by an amount greater than that which should be tolerated.

Since the variation of D with concentration in the range of concentration covered by Test 16 is considerable, as indicated by the amount of deviation of the curve in fig. 2 from a straight line, the Matano method was used for computing the D values represented by the centers of open circles in fig. 4.

Values of D at a number of temperatures and for several concentrations have been computed using the Matano method and curves showing the relation between D and concentration at a number of temperatures have been drawn. Values of D at concentrations of 1, 2, 3, 4, 5, 6, and 7 at. pct carbon* have been read from such curves† and these, after being corrected, are reported in table IV.‡

---

* When the carbon content represented by the upper flat portion of a diffusion-penetration curve is lower than the determined carbon content of the original steel by more than 0.03 wt pct carbon, it is suspected that material used for analyses may have been sufficiently decarburized to affect results on which the curve is based. This is the reason for not utilizing such a curve in determinations of D.

* Approximately, atomic per cent carbon is equal to weight per cent multiplied by 4.5.

† To correct data read from these curves, each value was multiplied by K^2 where K represents the expected length of a piece of pure iron at the diffusion-anneal temperature[3,4] when its length at about 25°C (room temperature) is 1 in.

‡ Data in table IV are based on results given in table IVa. Table IVa, which lists the original experimental data from which the concentration-penetration curves were plotted and the diffusion coefficients, such as are given in table IV, were calculated, has been issued through Auxiliary Publication and may be obtained from the American Documentation Institute, 1719 N St., N.W., Washington 6, D. C., by ordering Document No. 2728, remitting $0.50 for copy in microfilm (read enlarged in full size on reading machines now widely available), or $1.40 for copy in paper photoprints legible without mechanical aid.

Table IV. Data Used for Plotting, on Semi-log Paper, Diffusion Coefficient at Constant Concentration Versus Reciprocal of Temperature

Test No.	Temperature °C	Temperature °K	$\frac{10^4}{T_K}$	Wt Pct Carbon 0.22	0.44	0.66	0.88	1.12	1.35	1.59
				At Pct Carbon 1	2	3	4	5	6	7
				D x 10^7 cm² per sec.						
26	750	1023	9.78			(0.18)				
27	754	1027	9.74			(0.20)				
25	800	1073	9.32		0.27	0.35	0.52			
24	802	1075	9.30		0.30	0.41	0.63			
22	847	1120	8.93	0.35	0.39	0.44	0.56			
23	848	1121	8.92	0.27	0.36	0.47	0.67			
9	905	1178	8.49	0.82	1.03	1.33	1.54	1.95		
20	909	1182	8.46	0.98	1.13	1.35	1.71	2.98		
12	910	1183	8.45	0.87	0.98	1.23	1.54	2.26		
13	916	1189	8.41				1.63	3.16		
11	950	1223	8.18	1.74	2.15	2.66	3.27	4.09		
21	956	1229	8.14	1.89	2.20	2.56	3.07	4.09		
10	958	1231	8.12	1.33	1.74	2.15	2.76	3.99		
7	999	1272	7.86	3.48	4.10	4.71	5.43	6.66	12.29	
56	1000	1273	7.85	2.87	3.48	4.40	5.63	7.17	10.03	
55	1005	1278	7.82	2.71	3.09	3.74	4.73	6.25	8.50	
8	1010	1283	7.79	3.48	3.99	4.81	6.04	7.89	10.24	
14	1038	1311	7.63	3.69	4.20	4.72	5.44	6.46	8.00	
15	1042	1315	7.60	4.92	5.54	6.36	7.49	8.92	11.08	
16	1127	1400	7.14	12.35	13.38	14.72	16.47	19.66	24.91	35.03
36	1128	1401	7.14	10.81	12.35	13.89	15.95	19.04	26.45	40.67
17	1195	1468	6.81	19.41	21.16	23.12	25.81	30.97	42.53	
18	1195	1468	6.81	18.79	21.26	23.74	26.63	30.97	41.29	
19	1255	1528	6.54	27.96	30.03	32.10	35.20	40.38	55.91	
50	1301	1574	6.35	29.06	33.21	39.44	55.00			
54	1305	1578	6.34	33.22	36.33	41.00	48.37	57.30		

The Grube method was used to calculate values in parenthesis.
°K signifies temperature is given in Kelvin units.
* See footnote‡ p. 556.

Table V. Data Showing that Within the Limits of Experimental Error Neither Boron up to 0.009 pct Nor Silicon up to 2 pct Significantly Affects the Rate of Diffusion of Carbon in Austenite

Test No.	Temperature °C	Boron Weight Pct	Silicon Weight Pct	Atomic Pct Carbon 2	2½	3	3½	4	4½	5
				D x 10^7 cm² per sec						
16	1127			13.1	14.0	14.3	15.2	16.9	17.8	20.0
36	1128			12.9	13.5	14.1	14.5	15.6	17.5	19.2
		Average		13.0	13.8	14.2	14.9	16.3	17.7	19.6
29	1127	0.009		11.5	12.6	12.8	14.6	15.8	16.5	17.8
30	1129	0.009		10.9	11.9	12.9	13.4	15.0	15.8	15.2
		Average		11.2	12.3	12.9	14.0	15.4	16.2	16.5
28	1128		2.15	11.2	11.7	13.9	14.2	15.4	16.5	16.9
33	1125		2.15	10.5	11.2	11.5	11.6	11.5	12.1	14.5
		Average		10.9	11.5	12.7	12.9	13.5	14.3	15.7

Approximately, Weight Pct Carbon $= \frac{\text{Atomic Pct Carbon}}{4.5}$

Determination of Relation between D and 1/T: The best estimate of the relation between D and $1/T$ at each of six carbon concentrations was computed from data given in table IV utilizing the method of least squares. The six estimates are represented by six straight lines drawn in fig. 5, 6, and 7.

Determination of Relation between D and Concentration: Two methods, A and B, have been used for determining the relation between D and concentration. In both methods distributions of carbon in welded couples subjected to diffusion-anneal treatments were determined.

In Method A carbon concentration limits in each couple, heated for a long time at a diffusion-anneal temperature of "X"°C, were essentially the limits for austenite at "X"°C as indicated by the iron-carbon diagram. Thus the limits of carbon concentration in the couple used in Test 16 and heated at 1127°C for 19½ hr are 0.07 at. pct carbon (0.015 wt pct) and 7.67 at. pct carbon (1.75 wt pct), respectively, and the limits of carbon concentration for austenite at 1127°C are 0.00 and approximately 1.8 wt pct. When Method A was used, a concentration-penetration curve was drawn and D values at

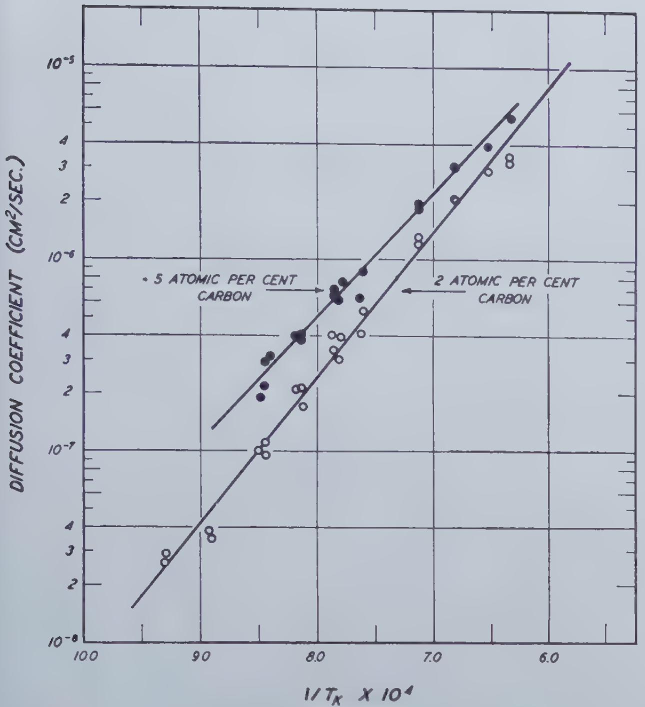

Fig. 6—Plot of diffusion coefficient at each of two concentrations against reciprocal of temperature.

Scale of diffusion values is logarithmic and T_K is given in Kelvin units. Open circles, 2 at. pct (0.44 wt pct) carbon; closed circles, 5 at. pct (1.11 wt pct) carbon.

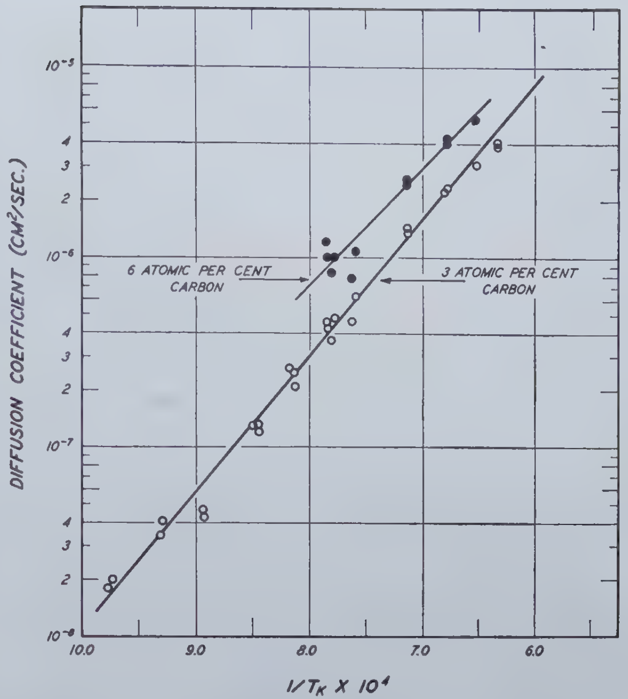

Fig. 7—Plot of diffusion coefficient at each of two concentrations against reciprocal of temperature.

Scale of diffusion values is logarithmic and T_K is given in Kelvin units. Open circles, 3 at. pct (0.66 wt pct) carbon; closed circles, 6 at. pct (1.35 wt pct) carbon.

a given temperature (the diffusion-anneal temperature) were computed for each of several compositions using Matano's procedure.

In Method *B*, the minimum carbon concentration range in a couple was 0.40 at. pct (max. 4.20, min. 3.80 at. pct) and the maximum range was 2.52 at. pct (max. 5.66, min. 3.14 at. pct). C/C_o values at known distances from the weld, computed from carbon distribution data as already described, were plotted on a probability scale. The equation for a straight line of best fit was computed by the method of least squares. The line was then drawn and a *D* value was calculated using Grube's procedure. This *D* value was assumed to be that at the temperature of the diffusion-anneal and for the average carbon concentration of the couple.

Method *B* data (centers of circles) and Method *A* curves (curves *A* + *B*) showing the relation between *D* and concentration are given in fig. 8.

Determination of Relation between Q and Carbon Concentration: To determine the relation between *Q*, the activation heat of diffusion, and carbon concentration, *Q* was first computed for each of the concentrations 1, 2, 3, 4, 5, and 6 at. pct carbon and then the curve showing the relation between *Q* and concentration was drawn (fig. 9). To compute *Q* for a given concentration, the slope of the line showing the relation between *D* (logarithmic scale) and $1/T$ for that concentration was multiplied by 4.58.*

Determination of Relation between A and Carbon Concentration: To determine the relation between *A* and carbon concentration, *A* was computed for each of the concentrations 1, 2, 3, 4, 5, and 6 at. pct carbon and then the curve showing the relation between *A* and concentration was drawn (fig. 10). Each *A* value for a given concentration was computed from the diffusion equation, $D = Ae^{\frac{-Q}{RT}}$, after appropriate substitutions of values of *D*, *Q*, *e*, *R*, and *T* had been made.

Discussion of Results

Results are given in tables 4 and 5 and in fig. 5 to 10 inclusive. They are discussed primarily with respect to their accuracy and to the information they disclose.

Accuracy of D: Standard error of estimate* values have been computed and found to be such that a single determined *D* is "quite likely"† to be within ±50 pct of the true value and that the *D* at a given temperature and for a given carbon concentration, represented by a point on the appropriate line showing the determined relation between *D* (log scale) and $1/T$, is quite likely to be within ±10 pct of the true value. The validity of these conclusions depends on the validity of assumptions that (1) the distribution of *D* values, at a given temperature and composition, for the hypothetical population from which *D* values are drawn is represented by a normal curve where the scale for *D* values is logarithmic and the scale for frequency is linear, and (2) sampling is random. Since data points around each line representing the relation between *D* (log scale) and $1/T$ (fig. 5, 6, and 7) fall within the

---

* 4.58 is the product of the gas constant, *R*, value in appropriate units and the factor of conversion from common to Naperian logarithmic units. As is well-known[2], Q/R is the slope of the straight line obtained by plotting the Naperian logarithm of *D* (for a given concentration) versus the reciprocal of the absolute temperature.

* The meaning of standard error of estimate and examples illustrating its usefulness in estimating limits of accuracy for a set of data are described in many statistical texts and technical papers.[5,6]

† If on the average 19 or more times out of 20 a determined *D* is within 50 pct of the true value, then it is assumed that any determined value is "quite likely" to be within 50 pct of the true value.

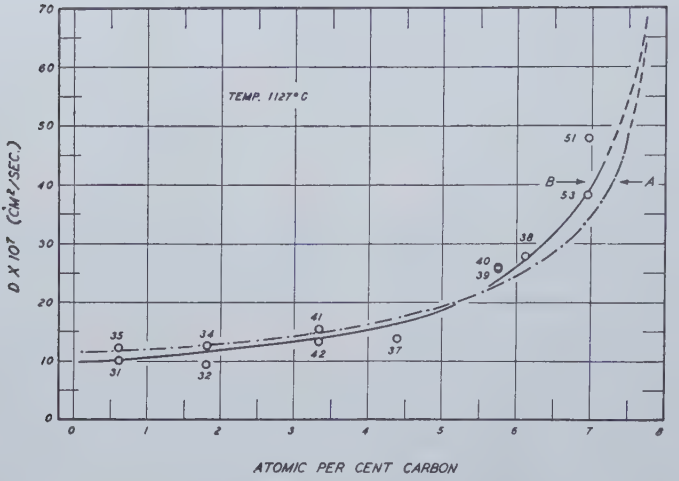

Fig. 8—Shows the relation between diffusion coefficient at 1127°C and carbon concentration.

Curves A and B are based on results from Method A, and data points (centers of circles) are based on results from Method B. Method A involves the Matano and Method B the Grube solution of Fick's law. Numbers close to data points are test numbers.

limits expected (all within 3 times the standard error of estimate), the authors have accepted the assumptions as being justified.

Accuracy of Q: It appears "quite likely" that the difference between computed and true Q values at a given concentration is less than 2,000 g-cal per g atom when the concentrations lie between 2 and 5 at. pct carbon. The difference between computed and true Q values is "quite likely" less than 2,500 cal when the concentration is 1 at. pct, and less than 4,500 cal when it is 6 at. pct. These conclusions are based on a computed value of the standard error of each slope.*

Accuracy of A: As already mentioned, values of A are computed after substituting determined values of D and Q, accepted values of e and R, and an assumed value of T in the diffusion equation. Obviously if the diffusion equation and all the substituted values were correct, then computed and "true" A values would be alike. Actually, determined Q and D values normally differ sufficiently to cause together considerable error in A.

Since it appears quite likely that (1) a D value at a given temperature and for a given concentration represented by a point on the appropriate line showing the determined relation between D (log scale) and $1/T$ is within ±10 pct of the true value and (2) a determined Q value for the same concentration (providing it falls within 2 and 5 at. pct) is within 2,000 cal of the true Q value, the influence of a 10 pct error in D and of a 2,000 cal error in Q on computed A values have been calculated. Actually a 2,000 cal change in Q causes a much greater error in computed A values than does a 10 pct change in D. An increase of 2,000 cal in Q causes the determined A value to be increased by about 125 pct and a decrease of 2,000 cal in Q causes the determined value to be decreased by about 60 pct. A 10 pct error in D causes a 10 pct error in A.

It is estimated that if the relation between D and $1/T$ for a given concentration in the range between 2 and 5 at. pct carbon were determined as in this investigation a sufficiently large number of times and appropriate D (log scale) versus $1/T$ lines were drawn, then on the average (1) D values at a given temperature represented by comparable points on the lines would be so distributed that about 5 pct of the estimated D values would be higher or lower than the true D value by 10 pct or more, (2) slopes of the D (log scale) versus $1/T$ lines would be so distributed that about 5 pct of the determined Q values would be higher or lower than the true Q value by 2,000 cal or more, and (3) about 2.5 pct of the computed A values would be higher than the true A value by 125 pct or more and about 2.5 pct would be lower by about 60 pct or more.

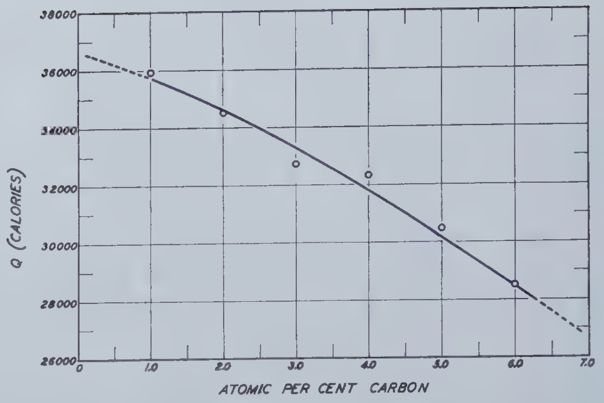

Fig. 9—Curve showing the relation between Q, activation heat of diffusion, and carbon concentration.

Q is given in gram-calories per gram atom.

Relation between D and 1/T: The relation between the diffusion coefficient, D, and the reciprocal of temperature at several carbon concentrations is indicated by straight lines in fig. 5, 6, and 7. The lines together with the data points plotted in these figures are self-explanatory. Straight lines representing the relation are drawn because (1) the diffusion equation indicates that a linear relation exists between log D and $1/T$, (2) the pattern of each set of data points suggest a straight line, and (3) a statistical analysis of each set of data, with one exception, indicates that between 98 and 99 pct of the total variation observed in log D is probably caused by the variation of $1/T$, leaving only 1 or 2 pct to be explained as due to other causes.* It appears reasonable to accept this 1 or 2 pct as resulting from experimental error.

Matano's Solution of Fick's Law: Results indicate that the provision in Matano's equation for taking into account the variation of D with concentration when one computes D is probably correct. Consider, for example, D values at 1127°C and for a composition of 6.17 at. pct computed from data for Test 36 and for Test 38. In Test 36, Steel 24 (7.67 at. pct — 1.75 wt pct carbon) was welded to Iron 2 (0.07 at. pct — 0.015 wt pct carbon). The couple was heated at 1128°C for 20.5 hr. A D value at 1127°C and for a carbon concentration of 6.17 at. pct was computed

---

* Information showing how to calculate the standard error of b, the slope in the equation, $y = a + bx$, and an explanation of the meaning of the standard error of b (designated σ_b) is given in Ezekiel's book,[7] p. 312 to 315.

* This conclusion is based on the fact that determined correlation coefficients for the six sets of data showing the relation between D (log scale) and $1/T$ at six concentrations are —0.993, —0.994, —0.995, —0.994, —0.992, and —0.966, respectively. The interaction of one variable on another, $1/T$ on log D in this instance, may be expressed approximately by r^2 where r represents the correlation coefficient.

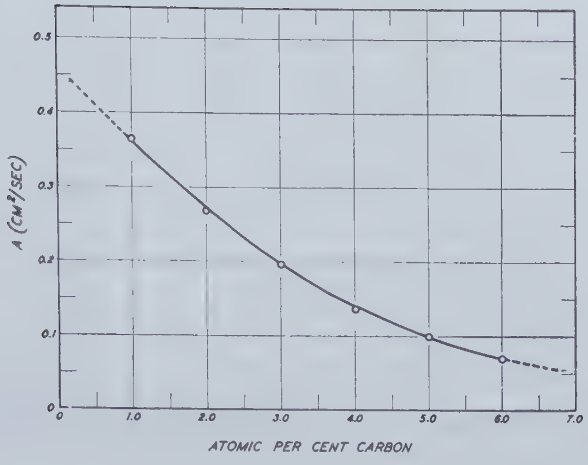

Fig. 10—Curve showing the relation between the constant A in the diffusion equation and carbon concentration.

using the Matano solution and found to be 27.5 x 10^{-7} cm² per sec. In Test 38, Steel 23 (6.68 at. pct — 1.51 wt pct carbon) was welded to Steel 16 (5.66 at. pct — 1.27 wt pct carbon). The couple was heated at 1122°C for 20.25 hr. A D value at 1127°C and for a carbon concentration of 6.17 at. pct was computed using the Grube solution and found to be 27.7 x 10^{-7} cm² per sec. Agreement between the two values of D, 27.5 and 27.7 x 10^{-7} cm² per sec., respectively, supports the conclusion given above. Apparently the difference between the volume change accompanying diffusion in the Test 36 couple and the volume change accompanying diffusion in the Test 38 couple did not affect computed D values.

Effect of Concentration on D, Q, and A: The effect of concentration on D, Q, and A is shown in fig. 4, 8, 9, and 10. D increases while Q and A decrease with increasing concentration.

Effect of Boron and Silicon on D: Results listed in table V show that within the limit of experimental error neither boron up to 0.009 pct nor silicon up to 2 pct significantly affects D. While it is suspected that both boron and silicon lower D slightly, the evidence is not conclusive.

Summary

1. The diffusion coefficient, D, has been determined in a temperature range of 750° to 1300°C and in a composition range of 1 to 7 at. pct carbon. D values represented by points on each line showing the relation between D (log scale) and the reciprocal of temperature are probably correct within ±10 pct.
2. Values of Q, the activation heat of diffusion, have been calculated and found to decrease with increasing concentration. Q values are probably correct within (1) ±2,500 cal at a concentration of 1 at. pct carbon, (2) ±2000 cal at concentrations between 2 and 5 at. pct and (3) ±4500 cal at a concentration of 6 at. pct.
3. The value of the A constant in the diffusion equation at each of several concentrations has been computed. A has been observed to decrease with increasing concentration. If the determined Q should be 2,000 cal higher than true Q, A would be in error by about 125 pct and if Q should be 2,000 cal lower than true Q, A would be in error by about 60 pct.
4. D increases first slowly and then more rapidly with increasing concentration.
5. While it appears that each element, boron up to 0.009 pct and silicon up to 2 pct, lowers D slightly, the evidence is not conclusive.
6. Evidence is given supporting the belief that the provision in Matano's equation for taking into account the variation of D with concentration is essentially correct.

Acknowledgment

This work was done under a contract with the Office of Naval Research. The authors are indebted to many of their friends in the steel industry for making alloys and analyses. The Metallurgical Department of the Central Alloy District of the Republic Steel Corporation made most of the alloys and chemical analyses. Other companies that made analyses include the Bethlehem Steel Co., Allegheny Ludlem Steel Corporation, Edgewater Steel Co., the Midvale Co., and Jones & Laughlin Steel Corporation.

The authors also wish to thank Dr. G. Derge, Dr. C. E. Birchenall, Dr. R. Smoluchowski, Miss A. M. Hanna, Miss M. A. Redmerski, and other members of the Metals Research Laboratory staff for their assistance.

References

[1] C. Wells and R. F. Mehl: *Trans.* AIME (1940) **140**, 279.

[2] F. N. Rhines and R. F. Mehl: *Trans.* AIME (1938) **128**, 185.

[3] F. M. Walters and M. Gensamer: *Trans.* A.S.S.T. (1932) **19**, 614.

[4] H. E. Cleaves and J. G. Thompson: The Metal-Iron, First Ed., McGraw Hill Book Co., New York (1935) 160.

[5] H. Arkin and R. R. Colton: An Outline of Statistical Methods, Fourth Ed., Barnes and Noble, Inc., New York. (1939).

[6] C. Wells and R. F. Mehl: *Trans.* A.S.M. (1949) **41**, 715.

[7] M. Ezekiel: Methods of Correlation Analysis, Second Ed., John Wiley and Sons, Inc., New York (1941).

Carbides in Long-tempered Vanadium Steels

by Walter Crafts and John L. Lamont

Study with the electron microscope of the carbides in vanadium-chromium-molybdenum steels after tempering up to 1000 hr at 600 to 1400°F confirmed that alloy carbides are formed at the secondary hardening temperature by decomposition of the plate-like iron carbides. It was also demonstrated that vanadium carbide persists as much smaller particles than do chromium- or molybdenum-bearing carbides. Conditions conducive to the formation of fine vanadium carbides are indicated to be favorable for high temperature strength.

IN order to determine the effects of long exposure at high temperatures on vanadium-bearing steels, a survey has been made of their hardness and carbide structure. The behavior of carbides in the tempering of martensite was studied by X ray diffraction and electron microscope examination of electrolytically extracted residues in greater detail than in an earlier investigation.[1]

A group of steels with about 0.25 pct carbon and containing chromium up to 5 pct, molybdenum up to 1 pct, and vanadium up to 1 pct was either quenched or annealed and then tempered for periods of up to 1000 hr at 600° to 1400°F. Their hardness after tempering agreed with the Hollomon and Jaffe[2] relation of equivalency of time and temperature, and with the degree of secondary hardening predicted from composition. Further, the appearance of the carbides indicated that the time and temperature equivalency relation was also applicable to the degree of carbide development. The mechanism of the tempering of martensite was demonstrated more clearly than in the earlier study. It was confirmed that carbides develop from martensite as poorly defined plates of the Fe_2C type carbide followed by thickening of the plates with a transition to Fe_3C. Finally the plate structure deteriorates into a lacy mass from which alloy carbides emerge as chunky particles that grow slowly with further increase of tempering temperature.

Vanadium carbide derived from tempered martensite was found in characteristically small particles that tended to grow very slowly. The addition of chromium or molybdenum to a steel with predominant vanadium carbide tended to introduce carbides of a chromium- or molybdenum-bearing type having a somewhat larger particle size. The Cr_7C_3 type carbide particles were larger than those of the V_4C_3 type and somewhat smaller than the carbides in steel containing both Cr_4C and M_6C. Similar observations were made of the carbides in the pearlite of annealed steels. It appeared that high temperature properties would be benefited by the retention of the fine carbide particles that result from a balance of composition and heat-treatment designed to produce a maximum amount of vanadium carbide.

Procedure: The steels used in the investigation were made with a base of Armco iron in a high-frequency furnace at the Union Carbide and Carbon Research Labs., Inc. The steels were deoxidized

---

WALTER CRAFTS, Member AIME, and JOHN L. LAMONT are Chief Metallurgist and Research Metallurgist, respectively, Union Carbide and Carbon Research Labs., Inc., Niagara Falls, N. Y.

AIME New York Meeting, Feb. 1950.

TP 2750 E. Discussion (2 copies) may be sent to Transactions *AIME before Apr. 1, 1950, and is scheduled for publication Nov. 1950. Manuscript received Oct. 14, 1949.*

Table I. Analyses of Steels

Steel No.	Steel Composition, Pct					
	C	Mn	Si	Cr	Mo	V
1	0.26	0.32	0.24	0.93		
2	0.25	0.36	0.32	2.83		
3	0.21	0.30	0.21	4.79		
4	0.16	0.34	0.26	0.90		0.29
5	0.20	0.35	0.31	0.96		0.52
6	0.23	0.36	0.37	0.98		1.04
7	0.28	0.35	0.34	3.01		0.30
8	0.28	0.38	0.36	2.96		1.05
9	0.25	0.32	0.21	4.76		0.29
10	0.26	0.28	0.24	4.69		1.03
11	0.21	0.31	0.19	4.58	0.99	0.29
12	0.25	0.31	0.23	4.66	0.92	1.02

with manganese and silicon only. The analyses of the steels are given in table I.

The 3-in. square ingots of the steels were forged to 1-in. square bars which were cut into 8-in. lengths for heat-treatment. Annealing was carried out in electric muffle furnaces at 1830°F after a holding time of 1 hr at temperature. Quenching treatments were from a salt bath at 2200°F after a 12-min immersion. This high temperature was considered to be necessary to dissolve vanadium carbide in austenite. Prior to the high temperature treatment the specimens were held in a salt bath at 1600°F for ¾ hr and then transferred to the high temperature salt bath. After quenching or annealing, the specimens were immediately immersed in liquid oxygen to minimize residual austenite. The heat-treated bars were cut into ¼-in. slices and tempered at 600°, 800°, 1000°, 1200°, and in some cases at 1400°F for periods of 1, 2, 10, 100, and 1000 hr.

Hardness Tests: The tempered slices were carefully ground to remove scale and decarburization. Hardness was measured as Rockwell C, but for interpretation it was found desirable to convert the hardness data to Vickers Pyramid Hardness by use of the A.S.T.M. Spec. E48-T43 conversion table.

Because of their volume, it is impossible to present the whole mass of hardness data obtained in this investigation. Generally, the annealed samples were low in hardness (—10 to +15 R_C) and changed little in hardness with either tempering temperature or time except at the very highest temperatures. The tempered hardness data from the samples that were oil-quenched from 2200°F prior to tempering are presented graphically in fig. 1. The tempering temperatures for periods of 1, 2, 10, 100, and 1000 hr were calculated by the Hollomon and Jaffe relation[2] to hypothetical temperatures that would give an equivalent degree of tempering in a 2-hr period. In fig. 1, the data are plotted logarithmically as Vickers hardness and calculated absolute temperature. The experimentally determined hardness values were consistent with the hardness calculated from composition[1].

The balance in alloy content, at this carbon level, necessary to maintain the as-quenched hardness after tempering at high temperatures is illustrated in the diagrams of fig. 1. In the plain 1 pct chromium steel the hardness decreased progressively with increase in tempering temperature. As the steel was enriched with vanadium secondary hardening took place and reached a maximum at about 1000°F (for 2 hr). The maximum secondary hardness attainable for this carbon content was not obtained until 1 pct vanadium was present. Increasing the chromium content to 3 pct eliminated the intermediate softening observed in the lower chromium steels, and at 1 pct vanadium maximum hardness was maintained after tempering at temperatures up to 1000°F (for 2 hr). With 5 pct chromium, 0.3 pct vanadium was effective in preventing softening at temperatures below 1000°F (for 2 hr), while the addition of 1 pct vanadium extended this maximum temperature to about 1050°F (for 2 hr). In the 5 pct chromium-1 pct molybdenum steel, 0.3 pct vanadium appeared to be as effective as 1 pct vanadium in retarding softening.

It is apparent that the tendency toward secondary hardening in the range of 1000 to 1050°F (for 2 hr) is principally governed by the amount of alloy in the steel. Even though the method of calculating secondary hardening in tempering[1] is made by arbitrarily assuming that the carbon is associated with the alloying elements as alloy carbides, the hardness basically is proportional to the amount and kind of alloy present. It was found, however, in the work described below that the hardness of steels tempered for long times at temperatures above the secondary hardening temperature was governed more by the type and size of carbide particles than by the total amount of alloy present.

Metallographic Study of Tempering Reactions: After a preliminary microscopic examination, a selection of the more typical specimens was made in order to determine the progress of tempering, and the effects of alloy composition with respect to the constitution and appearance of electrolytically extracted carbide residues. Steel No. 10 (4.69 pct Cr-1.03 pct V) was selected for examination of all of the specimens oil-quenched from 2200°F and tempered over the complete range of time (1 to 1000 hr) and temperature (600 to 1400°F). This panel of specimens was designed to show the progress of tempering in a much more continuous and detailed manner than was possible in the earlier work and to study the equivalence of time and temperature on the carbide structure. This survey was supplemented by a group of annealed specimens of the same steel that had been tempered for 1000 hr at 600° to 1400°F.

After examination of the metal section on the light microscope, carbide residues were extracted from the samples in the same manner as in previous investigations[1,3]. The electron micrographs were taken at an original magnification of 5,000 X or 12,500 X and enlarged to 25,000 X. The compositions designated for the carbides were not determined by analysis but are used for convenience in referring to the type of carbide structure. The *d* values for the carbide types are given in table II.

The constituents identified by the X ray diffraction of the carbide residues of Steel No. 10 are given in table III and the corresponding micrographs are shown in fig. 2 to 7. The X ray diffraction data from the quenched specimens have been divided in table III into three parts to distinguish the three main stages in the tempering process. The first stage, which is characterized by the transition

Table II. Carbide Types Observed in X ray Diffraction Patterns of Electrolytically Extracted Residues

Fe_2C Type		V_4C_3 (VC) Type		Cr_7C_3 Type		Cr_4C_3 ($Cr_{23}C_6$) Type		M_6C type*	
d-Å	Relative Intensity	d-Å	Relative Intensity	d-Å	Relative Intensity	d-Å	Relative Intensity	d-Å	Relative Intensity
2.37	1	2.39	8	2.29	5	2.37	8	2.74	1
2.05	3	2.06	10	2.10	8	2.16	8	2.51	3
1.49	1	1.46	5	2.03	10	2.035	10	2.25	5
		1.25	5	1.88	1	1.87	5	2.12	8
				1.84	5	1.79	5	1.94	5
				1.80	5	1.76	3	1.84	1
				1.75	3	1.59	5	1.54	1
				1.43	1	1.32	1	1.435	1
				1.34	3	1.285	5	1.34	1
				1.200	5	1.245	8	1.295	8
				1.180	5	1.22	5	1.215	1
				1.165	3	1.185	3	1.200	1
						1.164	5	1.195	1
								1.170	1

* The metallic components of M_6C not determined.

Table III. Carbides in Residues Extracted from Steel No. 10 (5 pct Cr-1 pct V) Oil-Quenched from 2200°F

Tempering Time Hr		Tempering Temperature °F				
		600	800	1000	1200	1400
1	Carbide Type Hardness V.P.H. Equiv. 2 Hr Temp*	Fe_2C ^{1} 473 584°F	Fe_3C ^{1} 466 781°F	Fe_3C ^{2} 472 978°F	Cr_7C_3 ^{2} V_4C_3 ^{1} 376 1175°F	Cr_7C_3 ^{3} V_4C_3 ^{3} 236 1372°F
2	Carbide Type Hardness V.P.H.	Fe_2C ^{1} 468 600°F	Fe_3C ^{2} 458 800°F	Blank 466 1000°F	Cr_7C_3 ^{3} V_4C_3 ^{1} 342 1200°F	Cr_7C_3 ^{3} V_4C_3 ^{3} 232 1400°F
10	Carbide Type Hardness V.P.H. Equiv. 2 Hr Temp*	Fe_3C ^{2} 458 637°F	Fe_3C ^{2} 455 845°F	Cr_7C_3 ? 462 1052°F	Cr_7C_3 ^{3} V_4C_3 ^{3} 263 1259°F	Cr_7C_3 ^{3} V_4C_3 ^{4} 189 1456°F
100	Carbide Type Hardness V.P.H. Equiv. 2 Hr Temp*	Fe_3C ^{2} 459 691°F	Fe_3C ^{2} 466 908°F	Cr_7C_3 ^{3} V_4C_3 ^{1} 398 1125°F	Cr_7C_3 ^{4} V_4C_3 ^{4} 231 1343°F	Cr_7C_3 ^{4} V_4C_3 ^{3} 174 1560°F
1000	Carbide Type Hardness V.P.H. Equiv. 2 Hr Temp*	Fe_3C ^{1} 451 744°F	Fe_3C ^{2} 475 972°F	Cr_7C_3 ^{3} V_4C_3 ^{2} 316 1199°F	Cr^7C_3 ^{3} V_4C_3 ^{4} 194 1426°F	Cr_7C_3 ^{4} V_4C_3 ^{4} 129 1654°F
		Annealed from 1830°F†				
1000	Carbide Type Hardness V.P.H.	Cr_7C_3 ^{3} V_4C_3 ^{4} 140	Cr_7C_3 ^{3} V_4C_3 ^{4} 141	Cr_7C_3 ^{3} V_4C_3 ^{4} 138	Cr^7C_3 ^{3} V_4C_3 ^{4} 132	Cr_7C_3 ^{3} V_4C_3 ^{4} 107

* Calculated to 2-hr tempering period by Hollomon and Jaffe relation.
† As-annealed carbide types Cr_7C_3 (²) and V_4C_3 (⁴)—Hardness 155 V.P.H.
[1] Weak Intensity
[2] Fair Intensity
[3] Good Intensity
[4] Strong Intensity

carbide, designated at Fe_2C, was found only after short times at 600°F. The second stage, representing the development of the Fe_3C type carbide, extended from longer tempering periods at 600°F to the short time treatments at 1000°F. The third stage, characterized by the presence of alloy carbide, was encountered after the longer periods at 1000°F and at higher temperatures. The transition from the second to the third stage was accompanied by weakening of the Fe_3C pattern, especially after 2 and 10 hours at 1000°F, and gradual strengthening of the patterns of Cr_7C_3 and V_4C_3 type carbides. As has been observed previously, the transition to alloy carbide coincided with the maximum tendency toward secondary hardening. The temperatures corresponding to 2-hr tempering periods calculated according to the relation of Hollomon and Jaffe[2] are given in table III for comparison of equivalent tempering treatments. It will be noted that the hardness of specimens tempered for 1 hr tended to be relatively high, as if an incorrect allowance had been made of the time required for heating. There is also a slight and inconsistent tendency for the carbide structure of these specimens to show a rela-

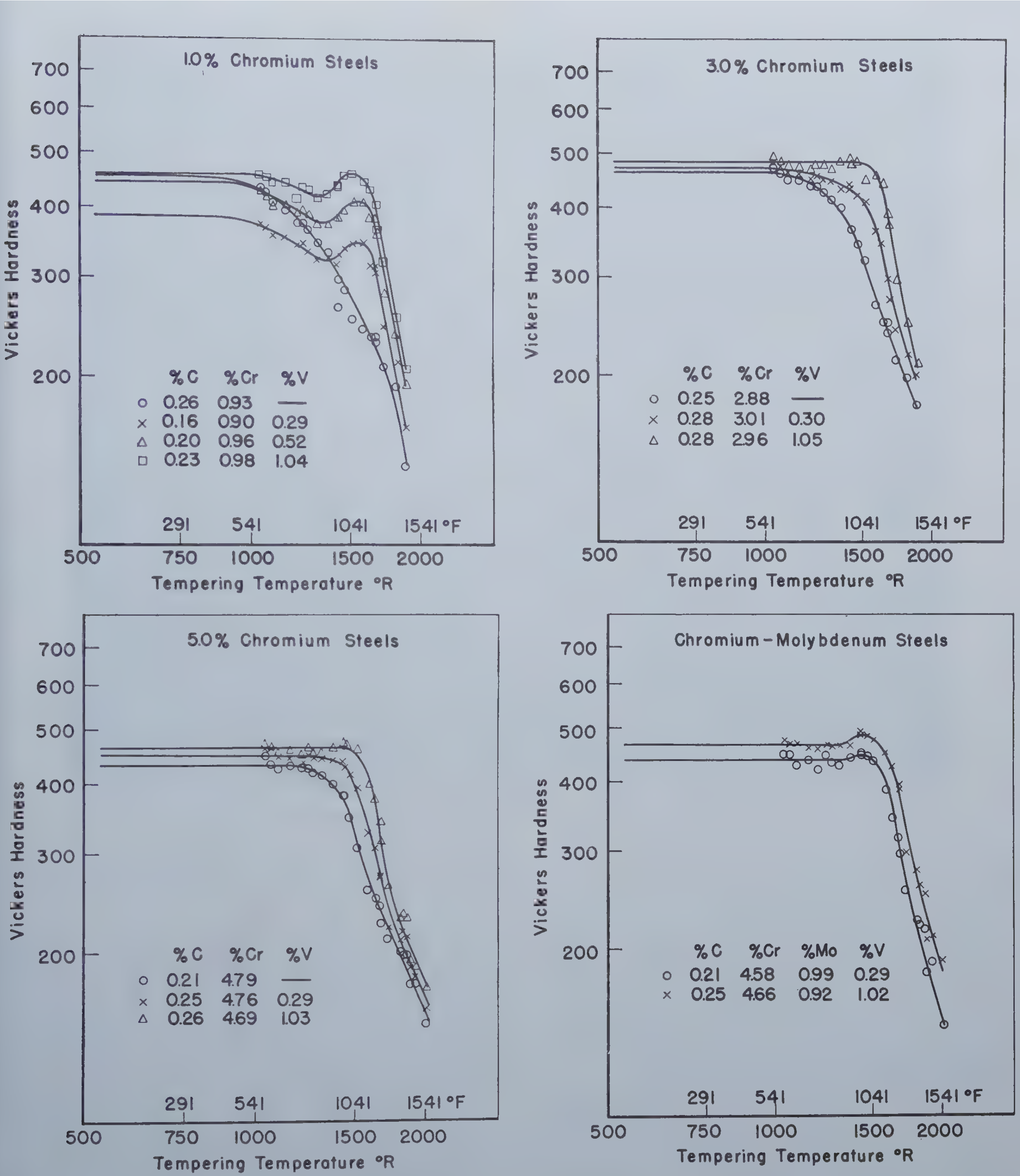

Fig. 1—Hardness of steels oil quenched from 2200°F.

After tempering up to 1000 hr. (Temperatures converted to 2-hr tempering period.)

tively poor development. If the 1-hr specimens are neglected, the others follow a fairly regular gradation at intervals of about 50°F in calculated equivalent degree of tempering, and it may be seen that the intensity of the X ray diffraction patterns and the stage of development of the carbides, fig. 2-6, are fairly consistent with the calculated degree of tempering regardless of the specific time and temperature of treatment.

The residue of the as-quenched specimen of Steel No. 10 (not shown) had the amorphous cloudy structure typical of that of martensite. After tempering 1 hr at 600°F (fig. 2*a*) considerable coagulation to a fuzzy plate-like structure had taken place. From the specimen tempered 1 hr at 600°F, through the longer times at 600°F (fig. 2*b*, *c*), and those tempered up to 100 hr at 800°F (fig. 3*a*, *b*) there was a gradual tendency toward increase of the amount and definition of the plate-like material. The nebulous ground mass finally tended to merge

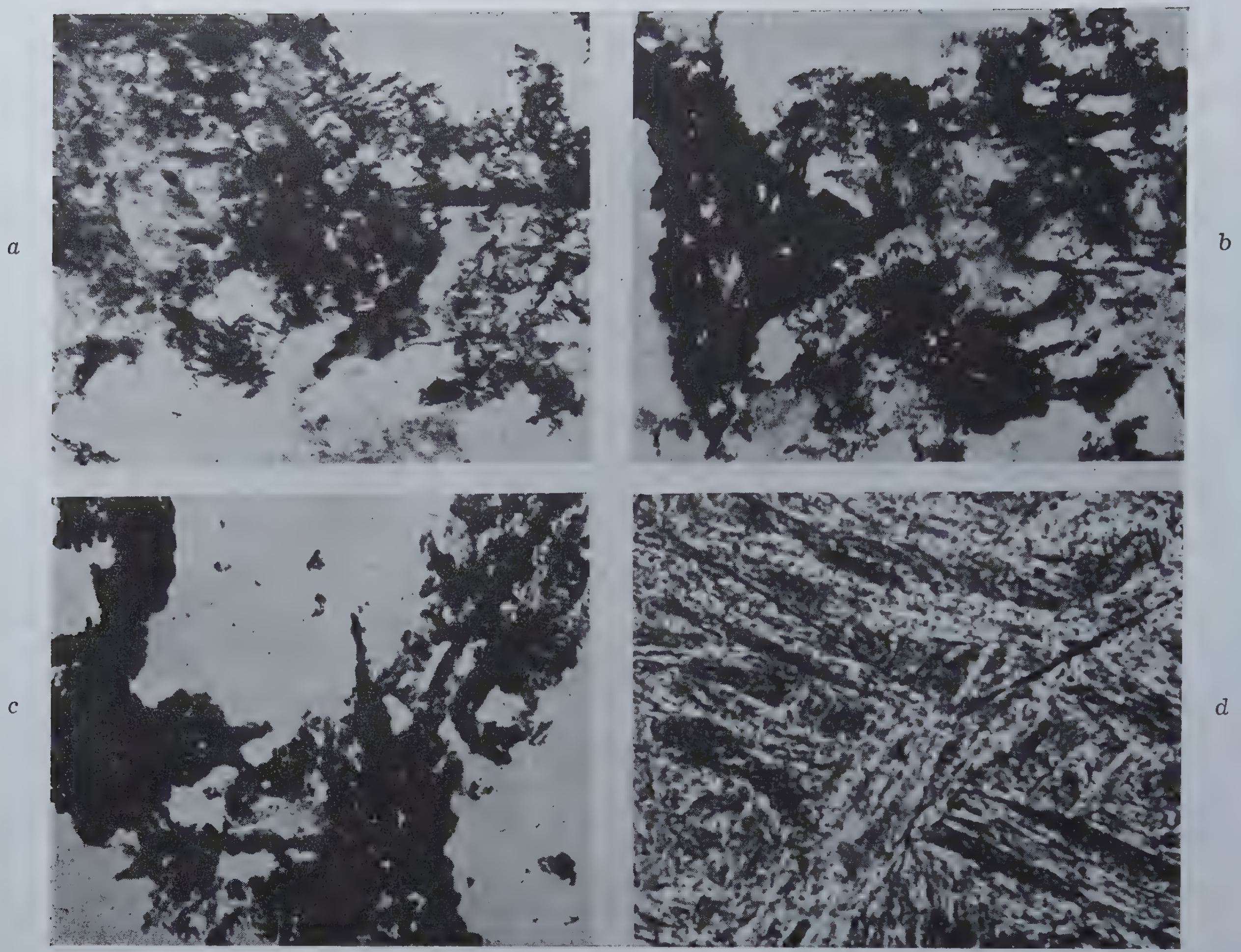

Fig. 2—Steel No. 10—0.26 pct C-4.69 pct Cr-1.03 pct V.

Oil quenched from 2200°F. Cooled in liquid oxygen. Tempered at 600°F. Electron micrographs × 25,000. *a.* 1 hr. *b.* 100 hr. *c.* 1000 hr. *d.* Microstructure after 1000 hr. X2000. Slightly reduced in reproduction.

into the plates. The transition from the Fe_2C to the Fe_3C type of carbide after 2 hr at 600°F was not reflected in a discontinuous change in the structures.

As the degree of tempering was extended beyond 100 hr at 800°F, there was a significant decomposition of the plate structure. After 1000 hr at 800°F (fig. 3*c*) the plates tended to become indistinct and a granular or lacy cloud-like structure appeared. This deterioration of the plates was more evident after 2 hr at 1000°F (fig. 4*b*) and the plate structure had virtually disappeared after 10 hr at 1000°F (fig. 4*c*). These cloud-like structures also gave blank or very weak X ray diffraction patterns as a result of their very fine or confused nature.

On further tempering the cloud-like structure coarsened somewhat with the eventual development of connected fine particles. In addition, there was a rather abrupt appearance of fairly well defined, moderately coarse particles after tempering for 100 hr at 1000°F (fig. 4*d*). Some dark spots in fig. 4*c* might be considered to be the same constituent, but the progression is not as obvious as in the further development of the particles at higher degrees of tempering. The appearance of these particles coincided with the identification of alloy carbides of the Cr_7C_3 and V_4C_3 types. The microstructures of the metal after 1000 hr tempering at 600°, 800°, and 1000°F (fig. 2*d*, 3*d*, and 4*f*) revealed only a gradual progression of the tempering reaction, even though they represent specimens in which the appearance of the carbide residues was significantly different.

Tempering at 1200° and 1400°F resulted in additional growth but little qualitative change in the appearance of the carbides. After 1000 hr at 1200°F the microstructure of the metal (fig. 5*d*) indicated a spheroidized condition. The corresponding electron micrograph of the carbide residue (fig. 5*c*) revealed some fine carbides that were translucent to the electron beam and larger carbide particles tending toward idiomorphic shapes. Further growth took place in tempering at 1400°F and after 1000 hr the carbides were moderately large (fig. 6*c*) and their crystalline shape could even be visualized in the microstructure of the metal (fig. 6*d*). Although the X ray diffraction patterns became stronger with more severe tempering, there was no change in the carbide types and Cr_7C_3 and V_4C_3 persisted at all tempering treatments beyond 100 hr at 1000°F. The carbide particles that remained small and thin after strong tempering are believed to be of the V_4C_3 type, whereas the larger particles are considered to be Cr_7C_3.

The appearance of carbides in the annealed condition and after tempering the annealed specimens for 1000 hr is illustrated in fig. 7. The larger carbide particles were similar to those formed in isothermally transformed pearlitic chromium steels[3]

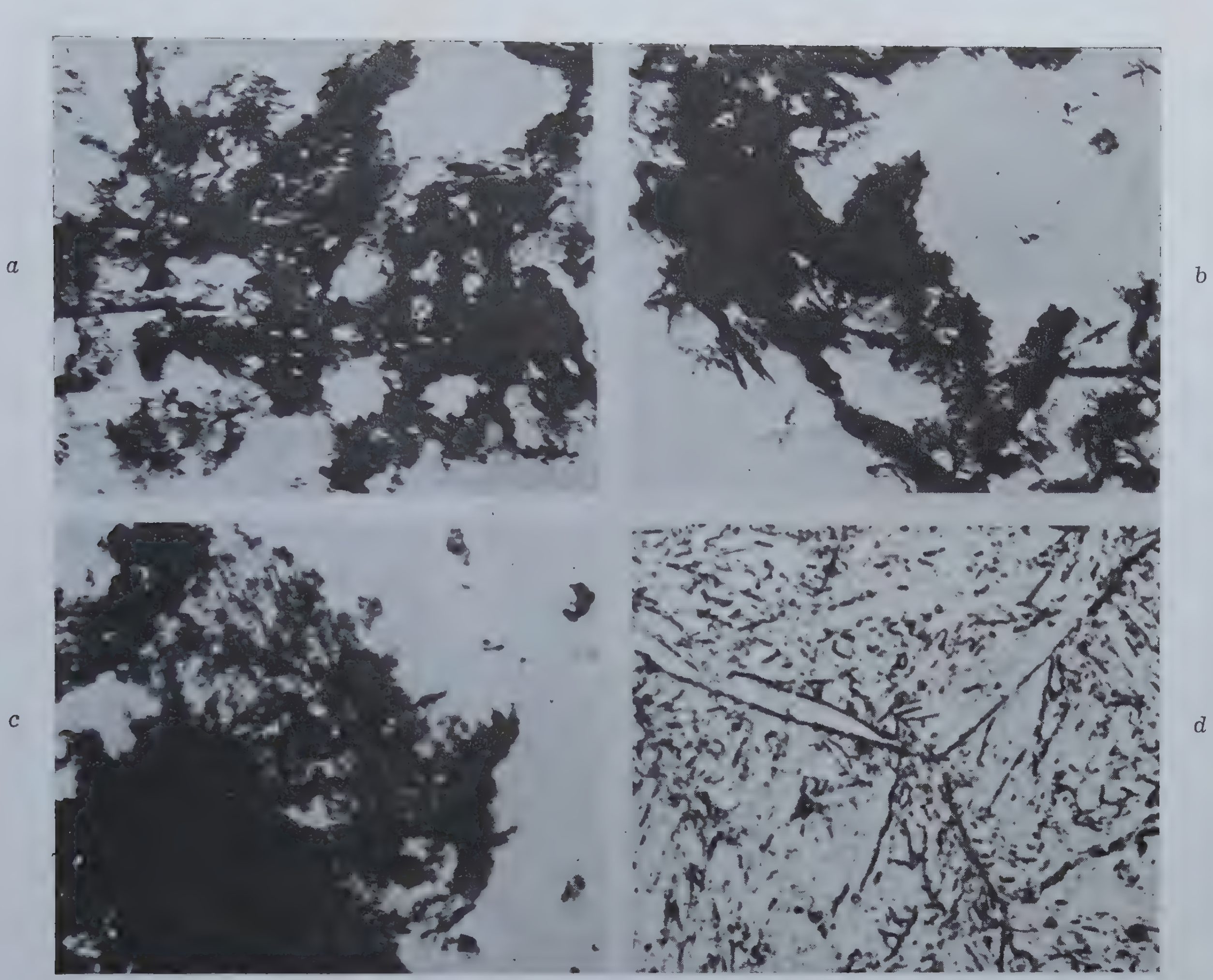

Fig. 3—Steel No. 10—0.26 pct C-4.69 pct Cr-1.03 pct V.

Oil quenched from 2200°F. Cooled in liquid oxygen. Tempered at 800°F. Electron micrographs × 25,000. *a.* 2 hr. *b.* 100 hr. *c.* 1000 hr. *d.* Microstructure after 1000 hr. X2000. Slightly reduced in reproduction.

and were changed little by tempering as high as 1200°F. As shown in fig. 7*a* the as-annealed specimen contained an appreciable amount of very fine particles of many different shapes and the microscopic specimen (fig. 7*b*) tended to stain in etching, probably as a result of the presence of some austenite transformation at low temperatures. There was an initial tendency toward growth of the small particles in tempering at 600°F (fig. 7*c*) that was accompanied by a lessened tendency toward staining in etching of the microscopic specimen (fig. 7*d*), but many of these particles remained small and thin enough to be translucent to the electron beam even after strong tempering. The appearance of the larger carbides (fig. 7*a, c,* and *e*) is considered to indicate no significant change as a result of tempering up to a temperature of 1400°F (fig. 7*g*) at which some growth occurred. This observation was also confirmed by the appearance of the microstructure of the metal specimens in which growth of the carbides was apparent after tempering at 1400°F (fig. 7*h*). The constituents indicated by X ray diffraction were the Cr_7C_3 and V_4C_3 types throughout the whole range of tempering. It is considered probable that the larger carbide type is Cr_7C_3 and that the smaller is V_4C_3.

Effects of Alloys on Tempered Carbides: A study was also made of the carbide structures of some of the steels listed in table I in order to determine the effect of different alloy compositions on carbide type and size. A plain 5 pct chromium steel (No. 3), a low chromium-vanadium steel (No. 6) and two molybdenum-bearing chromium-vanadium steels (Nos. 11 and 12) were selected to secure a variety of carbide types. The examination was made on specimens that were oil-quenched from 2200°F or annealed from 1830°F and tempered for 1000 hr at 1200°F. The structures are illustrated in fig. 8 to 11 and the X ray diffraction and hardness data are shown in tables IV and V.

The structures found in Steel No. 3 (4.79 pct Cr) are shown in fig. 8. The carbides in the quenched and tempered specimen were of the Cr_7C_3 type and of the appearance shown in fig. 8*a*. Both elongated and more massive particles of fairly well defined crystalline shapes were present. The size of the carbides in this plain chromium steel was considerably larger than that of the carbides that were presumed to be of the Cr_7C_3 type in the corresponding specimen of chromium-vanadium Steel No. 10 (fig. 5*c*). The annealed and tempered specimen (fig. 8*c*) had long rod-like carbides that were very

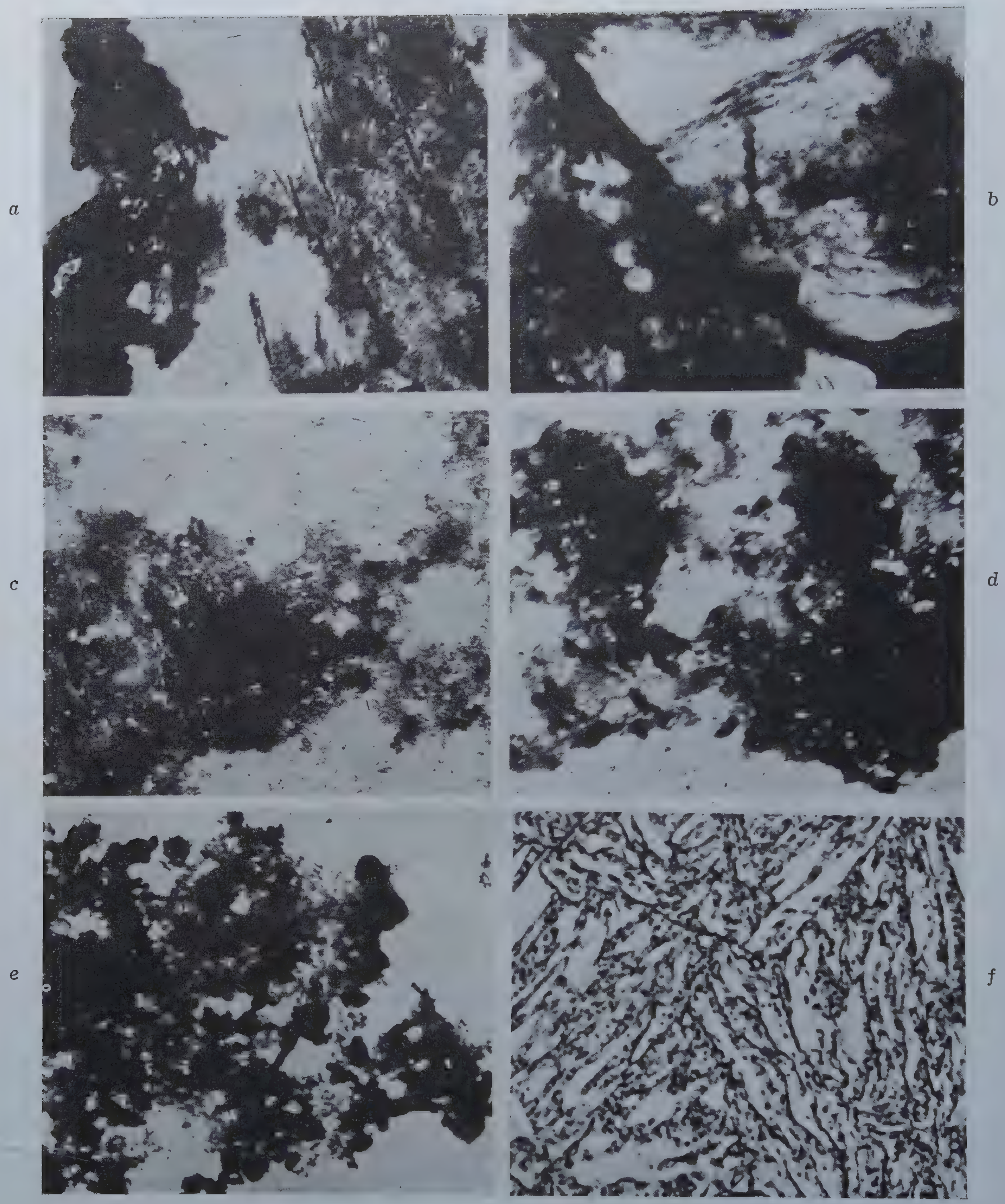

Fig. 4—Steel No. 10—0.26 pct C-4.69 pct Cr-1.03 pct V.

Oil quenched from 2200°F. Cooled in liquid oxygen. Tempered at 1000°F. Electron micrographs × 25,000. *a.* 1 hr. *b.* 2 hr. *c.* 10 hr. *d.* 100 hr. *e.* 1000 hr. *f.* Microstructure after 1000 hr. X2000. Slightly reduced in reproduction.

similar to those found in isothermally transformed plain chromium steel[3], and it is probable that tempering at 1200°F had little effect on their appearance.

In Steel No. 6 (0.98 pct Cr-1.04 pct V) only the V_4C_3 type carbide was identified. As shown in fig. 9*a*, the carbide particles formed by tempering martensite were smaller than in the comparable specimen (fig. 5*c*) of Steel No. 10 which contained 5 pct chromium, 1 pct vanadium, and both Cr_7C_3 and V_4C_3 types of carbides. Similarly, in the annealed and tempered condition (fig. 9*c*), the carbides derived from pearlite were relatively small and chunky as compared with the elongated and larger

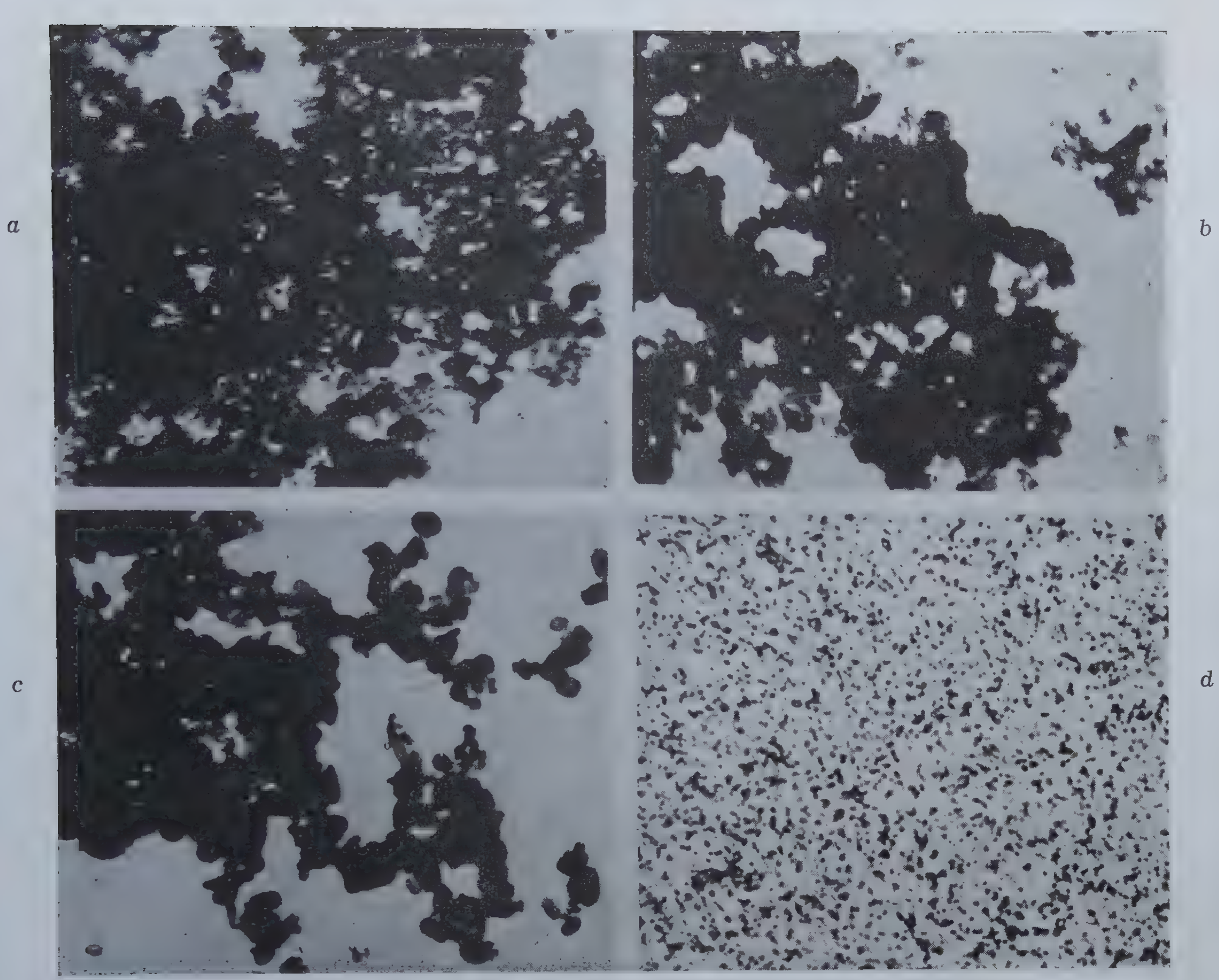

Fig. 5—Steel No. 10—0.26 pct C-4.69 pct Cr-1.03 pct V.

Oil quenched from 2200°F. Cooled in liquid oxygen. Tempered at 1200°F. Electron micrographs × 25,000. *a.* 10 hr. *b.* 100 hr. *c.* 1000 hr. *d.* Microstructure after 1000 hr. X2000. Slightly reduced in reproduction.

Table IV. Carbides in Residues Extracted from Samples Tempered 1000 hr at 1200°F

Steel No.	Pct Cr	Pct Mo	Pct V		Quenched from 2200°F	Annealed from 1800°F
3	4.79			Carbide Type Hardness V.P.H.	Cr_7C_3 [4] 176	Cr_7C_3 [3] 138
6	0.98		1.04	Carbide Type Hardness V.P.H.	V_4C_3 [4] 206	V_4C_3 [4] 133
11	4.58	0.99	0.29	Carbide Type Hardness V.P.H.	Cr_4C [4] M_6C [4] 181	Cr_4C [3] M_6C [3] 217

[3] Good Intensity
[4] Strong Intensity

carbides found in the pearlitic steels in which Cr_7C_3 was the predominant carbide type.

Steel No. 11 (4.58 pct Cr-0.99 pct Mo-0.29 pct V), in the quenched and tempered condition exhibited relatively coarse carbides (fig. 10*a*) as compared with other steels treated in a similar manner. The carbide types were Cr_4C and M_6C. There appeared to be two characteristic sizes of carbide in this specimen but particle size was not identified with carbide type. It would appear that under these conditions of heat-treatment the Cr_4C or M_6C type of carbide tends to grow more rapidly than the V_4C_3 or Cr_7C_3 types. In the annealed specimen (fig. 10*c*), which also contained Cr_4C and M_6C, there appeared to be two forms of carbide particles. One was the elongated type typical of pearlite in chromium steel and the other was a small chunky type.

The more highly alloyed Steel No. 12 (4.66 pct Cr-0.92 pct Mo-1.02 pct V) was examined after quench-

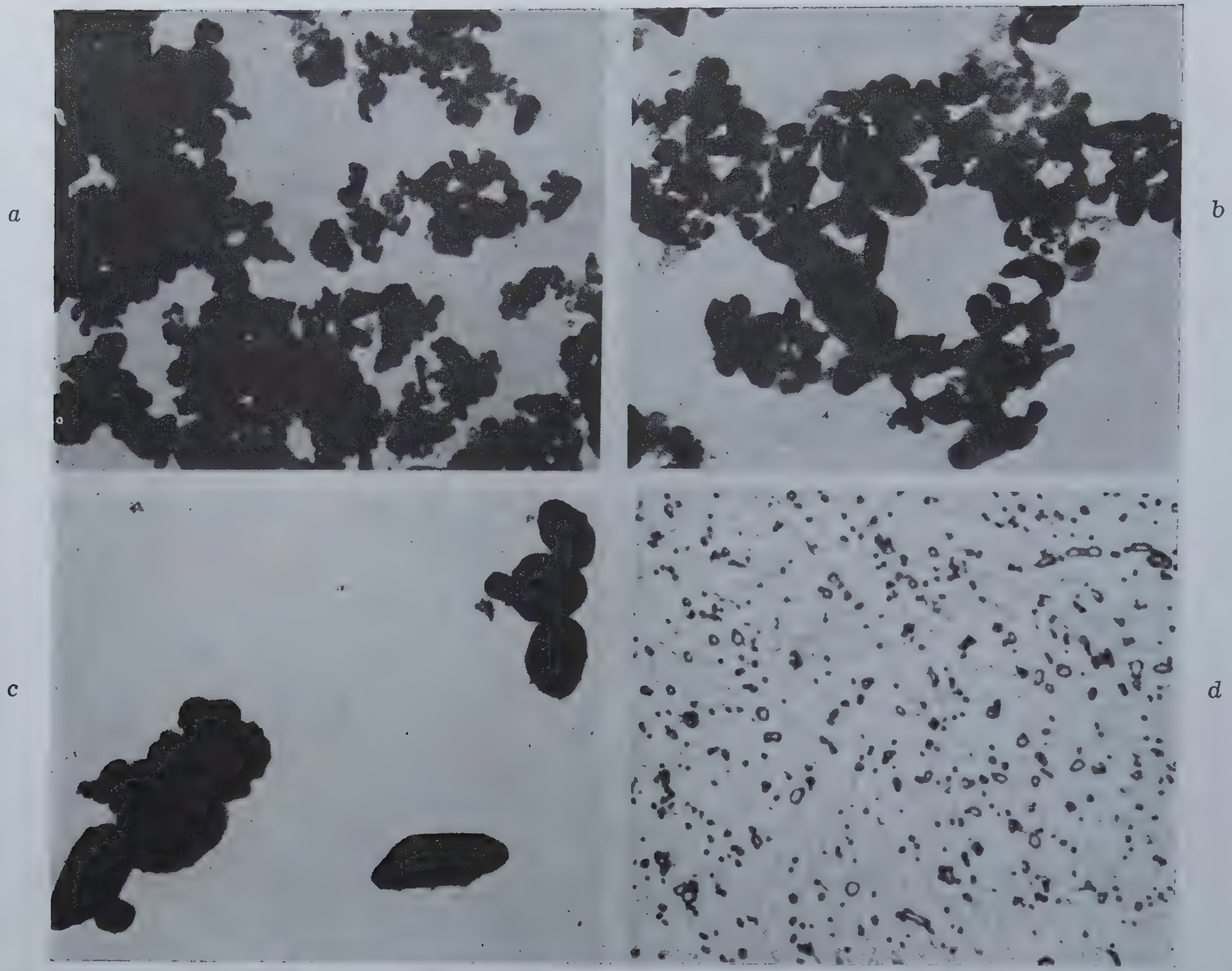

Fig. 6—Steel No. 10—0.26 pct C-4.69 pct Cr-1.03 pct V.

Oil quenched from 2200°F. Cooled in liquid oxygen. Tempered at 1400°F. Electron micrographs × 25,000. *a.* 10 hr. *b.* 100 hr. *c.* 1000 hr. *d.* Microstructure after 1000 hr. X2000. Slightly reduced in reproduction.

Table V. Carbides in Residues Extracted from Steel No. 12 (5 pct Cr-1 pct Mo-1 pct V) Tempered 1000 Hr

Oil-Quenched from 2200°F

	Before Tempering	Tempering Temperature °C			
		600	800	1000	1100
Carbide Type	Blank	Fe_3C [1]	Fe_3C [1]	V_4C_3 [1]	Cr_4C_3 [3] V_4C_3 [3] M_6C [3]
Hardness V.P.H.	457	458	492	395	208
Annealed from 1830°F					
Carbide Type	Cr_4C [2] V_4C_3 [3]	Cr_4C_3 [3] V_4C_3 [3]	Cr_4C_3 [3] V_4C_3 [3]	Cr_4C_3 [3] V_4C_3 [3]	Cr_4C_3 [3] V_4C_3 [3] M_6C [3]
Hardness V.P.H.	181	172	175	174	152

[1] Weak Intensity
[2] Fair Intensity
[3] Good Intensity

ing or annealing and tempering for 1000 hr at 600° to 1200°F. The X ray diffraction results are given in table V. The quenched specimens contained Fe_3C after tempering at 600° and 800°F, but after tempering at 1000°F, only V_4C_3 was found, and after tempering at 1200°F, V_4C_3, Cr_4C, and M_6C were present. As illustrated in fig. 11*a*, the carbide particles were relatively small but quite mixed in size, some being comparable to those in Steel No. 10 (fig. 5c) while many, believed to be V_4C_3, were so thin as to be readily penetrated by the electron beam. A somewhat similar condition was found in the annealed specimen (fig. 11c) which, in addition, contained some very large particles.

In reviewing these structures it is apparent that different types of carbide have specific tendencies to growth, so that they have characteristic particle sizes after a given heat-treatment. Vanadium carbide tended to persist at a much smaller average size than the other carbides. The typical carbides found in the molybdenum-bearing steels, Cr_4C or M_6C or both, were somewhat larger than in the steels containing Cr_7C_3 type carbides. It is, therefore, concluded that the growth tendency in the carbides studied is least for V_4C_3, intermediate for Cr_7C_3, and greatest for Cr_4C or M_6C. As is well known, the formation of specific alloy carbide types depends on the balance of carbon and alloy elements. Thus, the retention of fine carbide particles

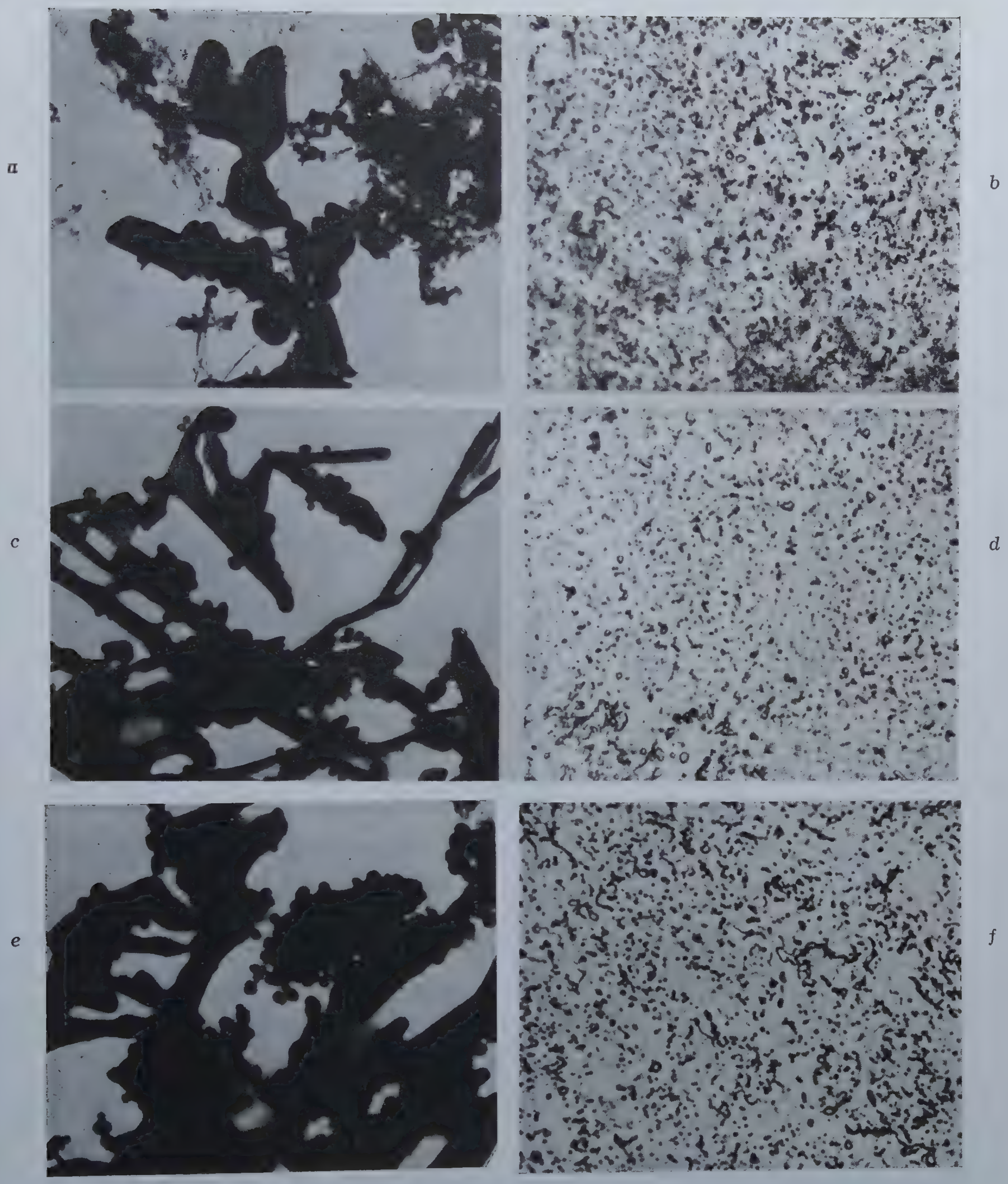

Fig. 7—Steel No. 10—0.26 pct C-4.69 pct Cr-1.03 pct V.

Annealed from 1830°F. Cooled in liquid oxygen. Tempered 1000 hr. *a, b.* As-annealed. *c, d.* 600°F. *e, f.* 1200°F. *g, h.* 1400°F. Extracted residue. X25,000 microstructure. X2000. Slightly reduced in reproduction.

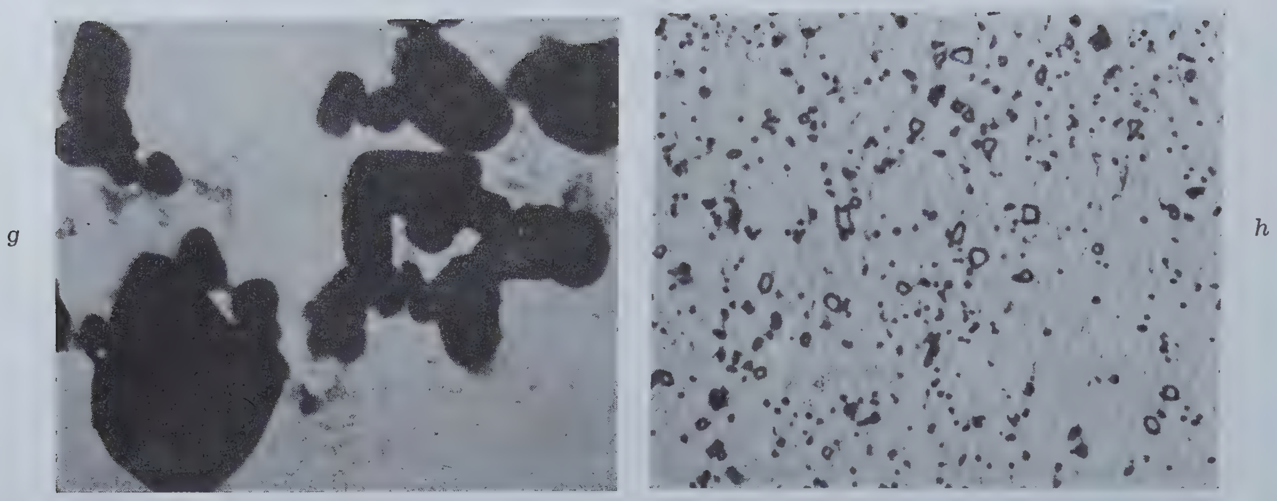

Fig. 7 (continued)—Steel No. 10—0.26 pct C-4.69 pct Cr-1.03 pct V.

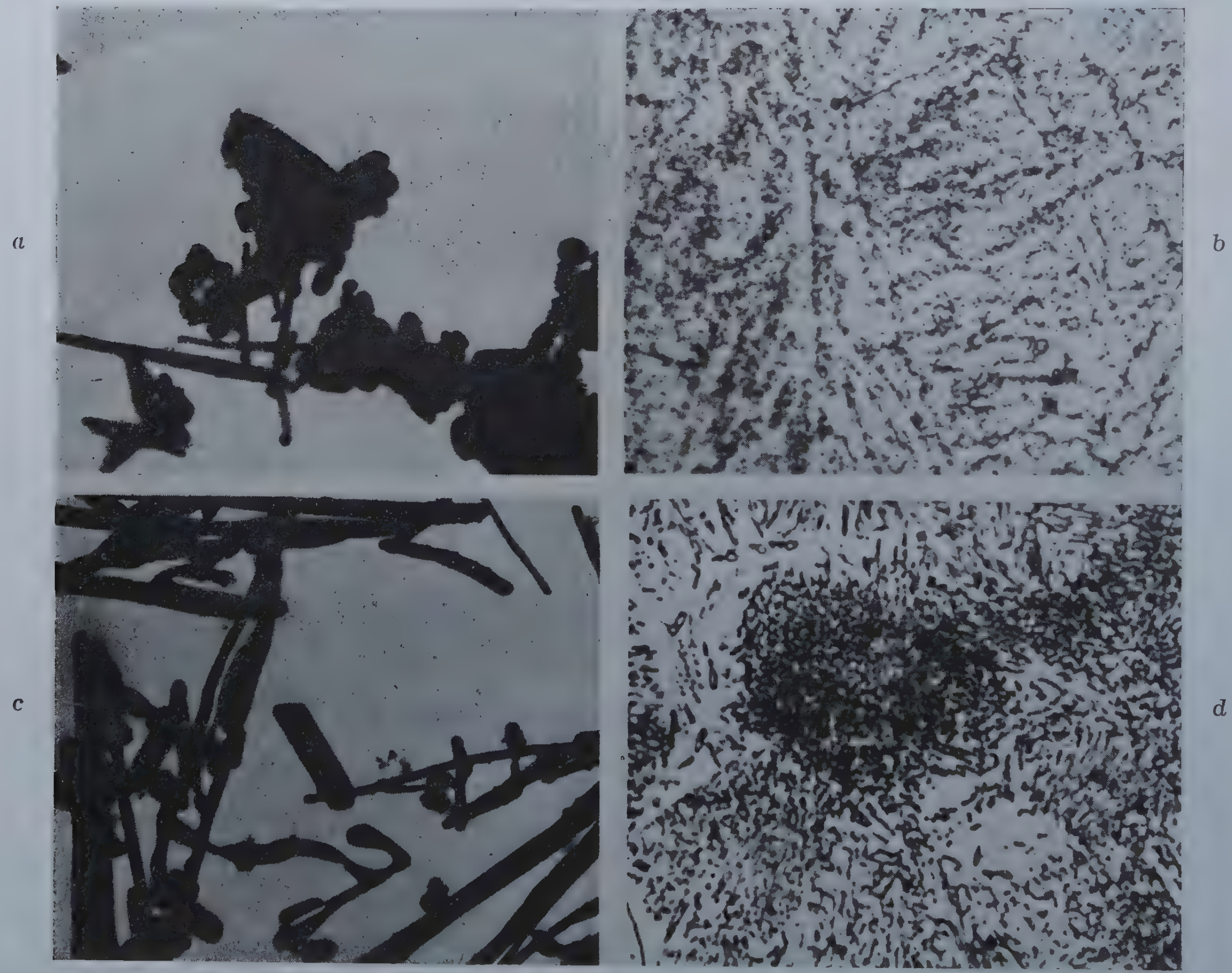

Fig. 8—Steel No. 3—0.21 pct C-4.79 pct Cr. Tempered 1000 hr at 1200°F.

a, b. Oil quenched 2200°F. Cooled in liquid oxygen. *c, d.* Annealed from 1830°F. Cooled in liquid oxygen. Extracted residue. X25,000 microstructure. X2000. Slightly reduced in reproduction.

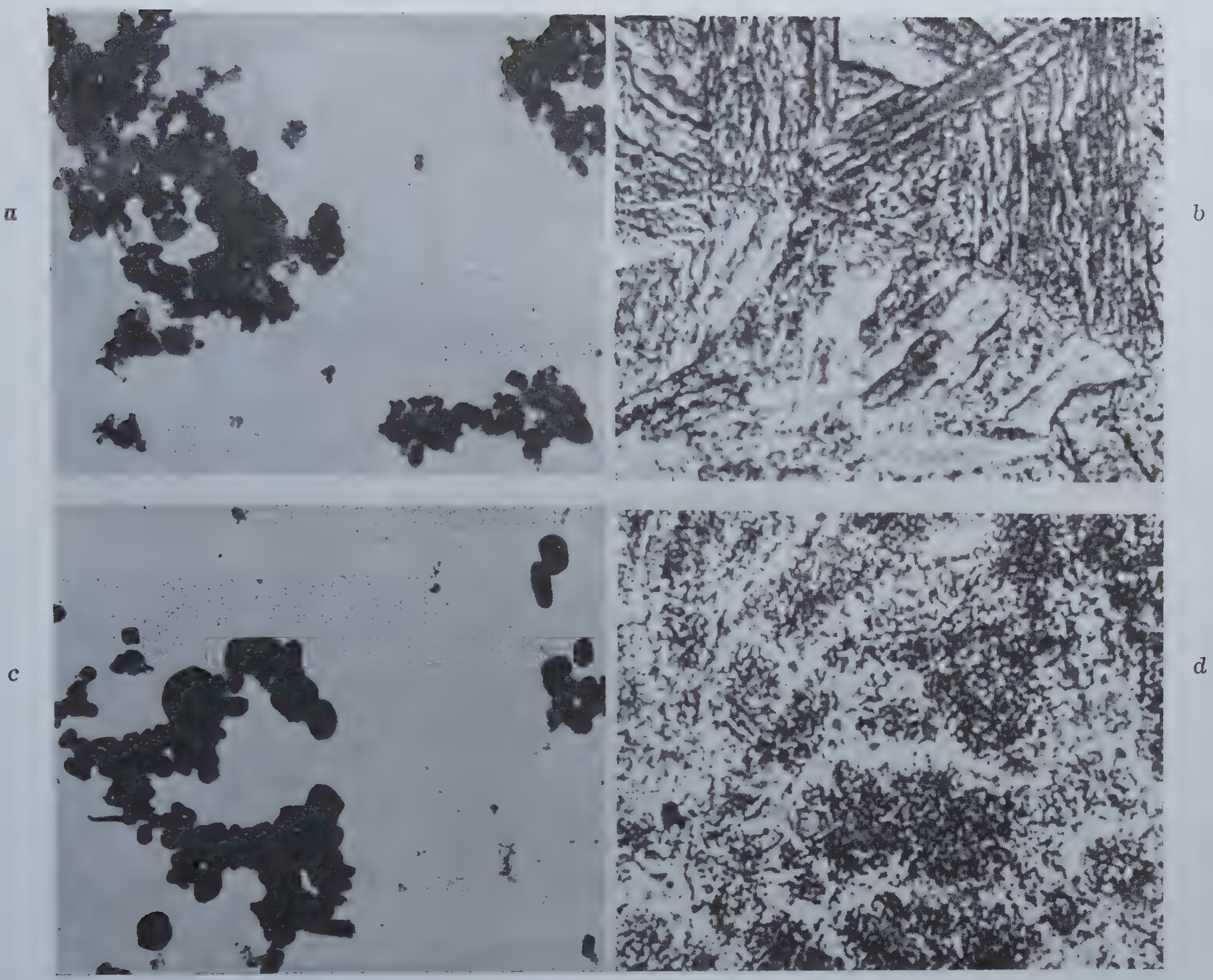

Fig. 9—Steel No. 6—0.23 pct C-0.98 pct Cr-1.08 pct V.

Tempered 1000 hr at 1200°F. *a, b.* Oil quenched 2200°F. Cooled in liquid oxygen. *c, d.* Annealed from 1830°F. Cooled in liquid oxygen. Extracted residue. X25,000 microstructure. X2000. Slightly reduced in reproduction.

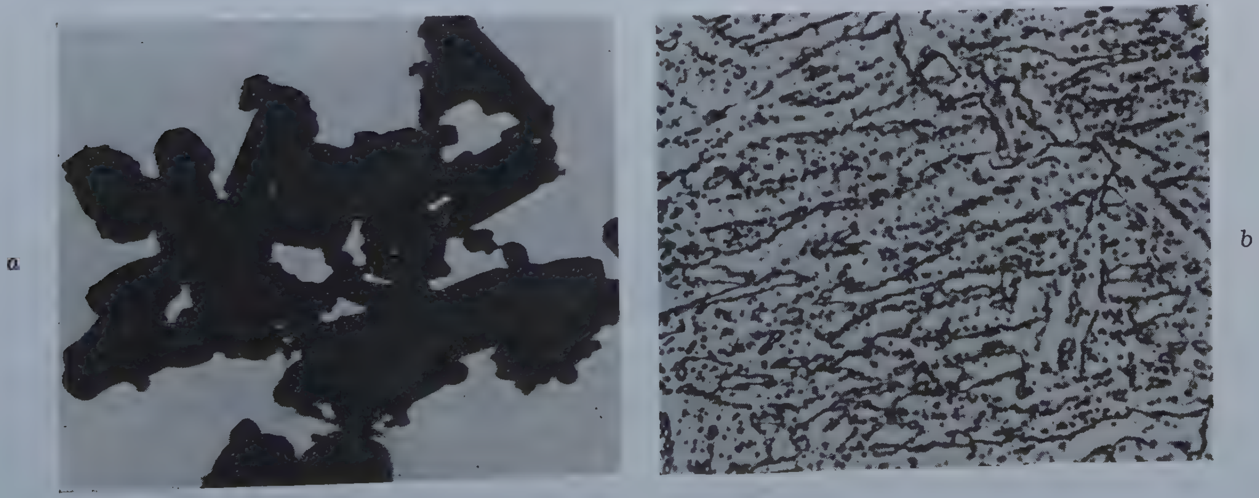

Fig. 10—Steel No. 11—0.21 pct C-4.58 pct Cr-0.99 pct Mo-0.29 pct V.

Tempered 1000 hr at 1200°F. *a, b.* Oil quenched 2200°F. Cooled in liquid oxygen. *c, d.* Annealed from 1830°F. Cooled in liquid oxygen. Extracted residue. X25,000 microstructure. X2000. Slightly reduced in reproduction.

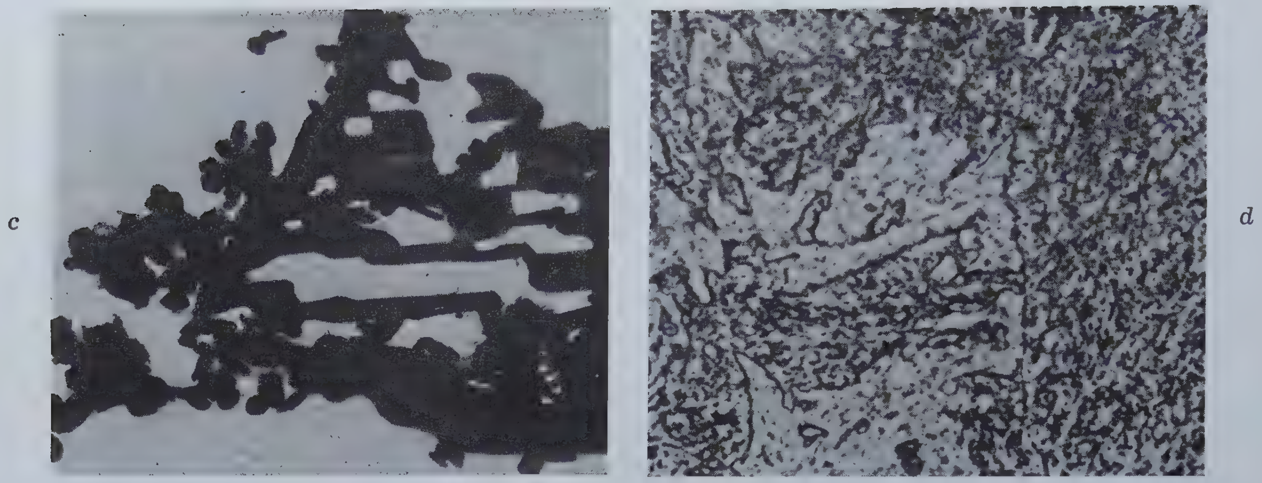

Fig. 10 (continued)—Steel No. 11—0.21 pct C-4.58 pct Cr-0.99 pct Mo-0.29 pct V.

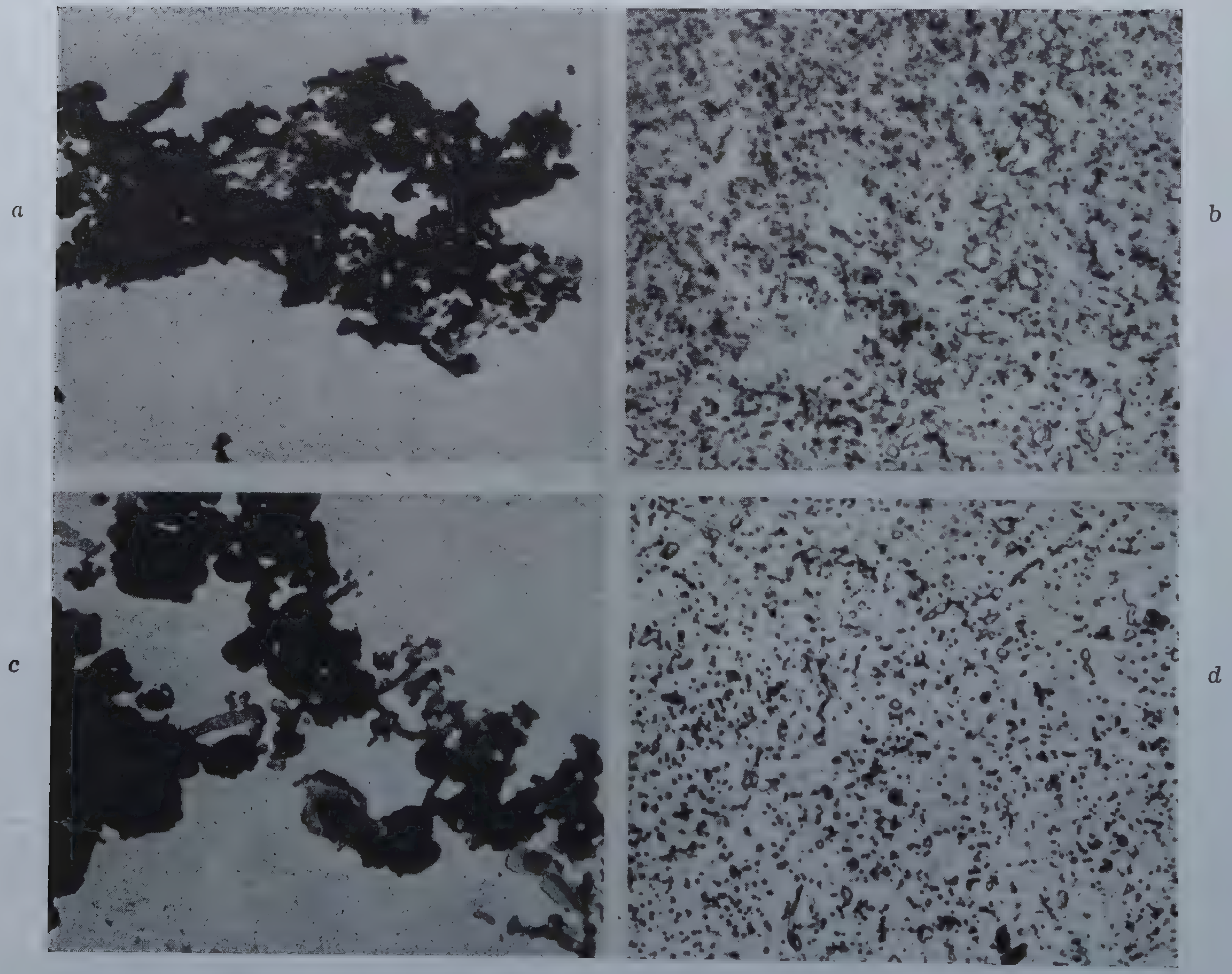

Fig. 11—Steel No. 12—0.25 pct C-4.66 pct Cr-0.92 pct Mo-1.02 pct V.

Tempered 1000 hr at 1200° F. *a*, *b*. Oil quenched 2200°F. Cooled in liquid oxygen. *c*, *d*. Annealed from 1830°F. Cooled in liquid oxygen. Extracted residue. X25,000 microstructure. X2000. Slightly reduced in reproduction.

requires a relatively high proportion of vanadium to carbon and strongly carbide-forming elements. For example, an increase of chromium from 1 pct in Steel No. 6 (fig. 9*a*) to 5 pct in Steel No. 10 (fig. 5*c*) produced a noticeable increase in the average carbide size accompanying the partial change to Cr_7C_3. Similarly, the presence of 1 pct molybdenum and 0.3 pct vanadium in Steel No. 11 (fig. 10*a*) as compared with the plain chromium Steel No. 3 (fig. 8*a*) resulted in a change of carbide type and an increase of particle size. Since the relations between steel composition and carbide types are quite complex, much more information is required in order to control the types of alloy carbides.

In addition to the general order of size characteristic of each type of carbide there were strong indications that the alloy composition of the steel and its previous treatment influenced the characteristic size of a given type of carbide. For example, the size of Cr_7C_3 particles in the quenched and tempered specimen of vanadium-bearing Steel No. 10 (fig. 5*c*) was smaller than in the similar vanadium-free Steel No. 3 (fig. 8*a*). Also in the specimen of Steel No. 11 (fig. 10*a*) that was quenched and tempered at 1200°F, the Cr_4C or M_6C particles were much coarser than in the comparable specimen of the higher vanadium Steel No. 12 (fig. 11*a*). It is also notable that the specimen of Steel No. 12 that was quenched and tempered at 1000°F contained only the V_4C_3 type of carbide, whereas tempering at 1200°F produced V_4C_3, Cr_4C, and M_6C. This suggests that the initial appearance of Cr_4C and M_6C came at a later stage in the tempering as a transition from V_4C_3 and that there might have been insufficient opportunity for the new carbides to develop or that the slow growth tendency of V_4C_3 was inherited. The large particles in the annealed specimen of this steel suggest that the presence of vanadium in the steel did not greatly change the composition of Cr_4C or M_6C carbides and that eventually similar growth might be expected in the further tempering of quenched specimens. These observations indicate that carbide particle size is not only affected by the type of alloy carbide, but also by the manner in which it was formed and the types of parent and associated carbides.

For those applications in which carbide size is critical, and it is presumed that high temperature service would be such a case, it is evident that proper balancing of composition and heat-treatment is very important. In view of the uncertainty in the factors that control creep strength, a categorical assumption of optimum carbide form and size is not possible, although it would appear that the very large carbides remaining after an ineffective austenitizing treatment are less effective than the smaller carbides precipitated from austenite or martensite. A relatively high temperature austenitizing treatment would, therefore, appear to be desirable, especially in high vanadium steels in which the solubility of vanadium carbide is limited. It would not only increase the amount of effective carbide, but also increase the proportion of the more preferable vanadium carbide. The optimum structure resulting from transformation during cooling might depend on the specific type of carbide, but in steels in which vanadium carbide is predominant, and associated with other carbides, it would appear that a quench to martensite would help to produce fine carbide particles and to preserve them longer in subsequent exposure at high temperatures.*

Conclusions

From this investigation of the mechanism of tempering on the carbides in vanadium steels, it may be concluded that:

1. Secondary hardening of tempered martensitic steels was developed to the degree anticipated, and tempering temperature and time were equivalent with respect to both hardness and progress of carbide transition and growth. After severe tempering the hardness was governed by the size of the carbide particles.

2. Carbide residues extracted electrolytically from quenched steel tempered at intervals of equivalent temperature of about 50°F revealed the initial decomposition of martensite into a plate-like structure containing Fe_2C type carbide. The plate structure became better defined with more tempering and the carbide type changed to Fe_3C. After tempering at 800° to 1000°F the plate structure decomposed to a lacy cloud-like condition from which alloy carbides emerged. With further tempering the alloy carbide particles grew larger and tended to assume idiomorphic shapes. The tempering of annealed steel resulted in the early consolidation of incidental fine carbide particles, but little significant change in pearlitic carbides was observed until a more severe tempering than 1000 hr at 1200°F was imposed on the steel.

3. Depending upon the composition and alloy balance of the steel, alloy carbides of the V_4C_3, Cr_7C_3, Cr_4C, and M_6C types were found in steels tempered for 1000 hr at 1200°F. Each type had a characteristic size and tendency to grow larger. The V_4C_3 type was outstanding in its tendency to resist growth. The Cr_7C_3 type was intermediate and either Cr_4C or M_6C or both tended to develop into larger particles. The carbides of pearlite in the annealed specimens were characteristically elongated in the case of chromium and small and chunky in the case of vanadium.

4. In order to retain fine carbides most persistently during exposure at elevated temperatures in complex vanadium steels, the composition should be balanced to make vanadium carbide the predominant carbide phase. The heat-treatment should be designed to increase the effective amount of vanadium carbide and to avoid the early formation of alloy carbides other than vanadium carbide.

Acknowledgments

The authors wish to acknowledge the generous cooperation of the staff of the Union Carbide and Carbon Research Laboratories, Inc. Special acknowledgment is due to W. D. Forgeng for the metallographic and X ray studies and to A. C. Jenkins of the Research Laboratories of The Linde Air Products Co. for preparing the electron micrographs.

References

[1] W. Crafts and J. L. Lamont: Secondary Hardening of Tempered Martensitic Alloy Steels. *Trans.* AIME (1949) **180**. *Metals Tech.*, Sept. 1948. TP 2439.

[2] J. H. Hollomon and L. D. Jaffe: Time-Temperature Relations in Tempering Steel. *Trans.* AIME (1945) **162**, 223-249.

[3] W. Crafts and J. L. Lamont: Carbides in Isothermally Transformed Chromium Steels. *Trans.* AIME (1949) **185**, 957. *Jnl. of Metals* Dec. 1949. TP 2709.

[4] G. Wood and J. R. Rait: Ferritic Steels for Gas Turbines. *The Iron and Coal Trades Rev.*, Feb. 4-11, 1949.

---

* A significant example of the benefit to be derived from careful balancing of composition and heat-treatment was recently reported by Wood and Rait.[4] A steel with 0.25 pct carbon, 3 pct chromium, 0.5 pct molybdenum, 0.5 pct tungsten, and 0.75 pct vanadium was carefully studied with respect to heat-treatment and carbon content. By using high temperature normalizing and oil-quenching treatments to bring carbides into solution and by lowering carbon with the probable suppression of Cr_7C_3 and development of V_4C_3, they were able to produce a profound improvement in the stress-to-rupture time and the creep strength of the steel.

Internal Friction of Cold-worked Metals

At Various Temperatures

by T'ing-Sui Kê

NUMEROUS investigators have observed that internal friction accompanies cold-working of metals and the effect of annealing is to reduce this internal friction.[1, 2] However, most of the experiments were made at high stress amplitudes and the principal purpose was to study the increase of internal friction as a result of the applied cyclic stress during measurement. In order to study the internal friction introduced by cold-working applied prior to the measurement, the stress level applied during the measurement of internal friction must be sufficiently small. The results of measurement are significant and can be used for a base of comparison only when the applied cyclic stress is so small that the internal friction is independent of stress amplitude.

Internal friction of cold-worked metals under small stress level has been studied by a number of workers.[3-6] The internal friction was measured around room temperature with a frequency of vibration of the order of kilocycles per second. The purpose of this paper is to report a study of the change of internal friction when severely cold-worked aluminum was annealed at successively higher temperatures until it was completely recrystallized. The measurements of internal friction were made over a range of temperature extending from room temperature up to the temperature of prior anneal. The frequency of vibrations used was about one cycle per second.

The apparatus used for the internal friction measurements to be reported in this paper was a torsion pendulum with the specimen in wire form as the suspension fiber. The description of this apparatus and the method of measurement have been previously given.[7, 8] The applied stress was sufficiently small so that the magnitude of internal friction is independent of stress level at each temperature range concerned. Corresponding to this stress the maximum shearing strain on the surface of the specimen is of the order of 10^{-5} and lower. The internal friction (Q^{-1}) is reported as $1/\pi$ times the logarithmic decrement.

Internal Friction Versus Temperature of Anneal: Fig. 1 shows the internal friction measurements performed upon 99.991 pct aluminum subjected to 95 pct reduction in area. The final diameter of the wire is 0.033 in. This figure gives a general survey of the effect of temperature of anneal and of temperature of measurement. The internal friction of the cold-worked specimen was first measured at room temperature. It was then annealed at 50°C for one hour and the internal friction measured at 50°C and at room temperature. The same wire was successively annealed at higher temperatures for one hour and measurements were taken at the annealing temperatures and lower temperatures as before. Such a procedure was followed in order to stabilize the internal friction at the temperature of measurement so that during the measurement which generally takes about half a minute, there is no detectable change in internal friction. This series of measurements was made up to 450°C. After each annealing a short test piece of the specimen, which had received the same past thermal and mechanical treatments, was taken out for metallographic examination.

It is seen from fig. 1 that up to the annealing temperature of 250°C we have the following observations: for any given temperature of measurement, the internal friction is lower the higher the temperature of prior anneal. When the annealing temperature is 290°C or higher, the internal friction at the annealing temperature drops abruptly to a value which is much smaller than that for the previous curve. Metallographic examinations showed that the recrystallization of the specimen was completed after the annealing at 290°C.

Fig. 1 shows that, as far as internal friction is concerned, there is no abrupt transition between the processes of recovery and recrystallization. Averbach has also reached the conclusion that recovery may be a process analogous to recrystallization on the basis of X ray extinction measurements in brass.[9]

The effect of annealing temperature upon the internal friction at room temperature is shown by curve I of fig. 2. In this figure the internal friction at room temperature was plotted as a function of annealing temperature. It is seen that the internal friction decreases rapidly at first with an increase

---

T'ING-SUI KÊ, Member AIME, is Research Associate with rank of Assistant Professor, Institute for the Study of Metals, University of Chicago.

This research has been supported in part by ONR (Contract No. N-6ori-20-IV, NR 019 302).

AIME New York Meeting, Feb. 1950.

TP 2788 E. Discussion (2 copies) may be sent to Transactions *AIME before Apr. 1, 1950, and will be published Nov. 1950. Manuscript received Oct. 17, 1949.*

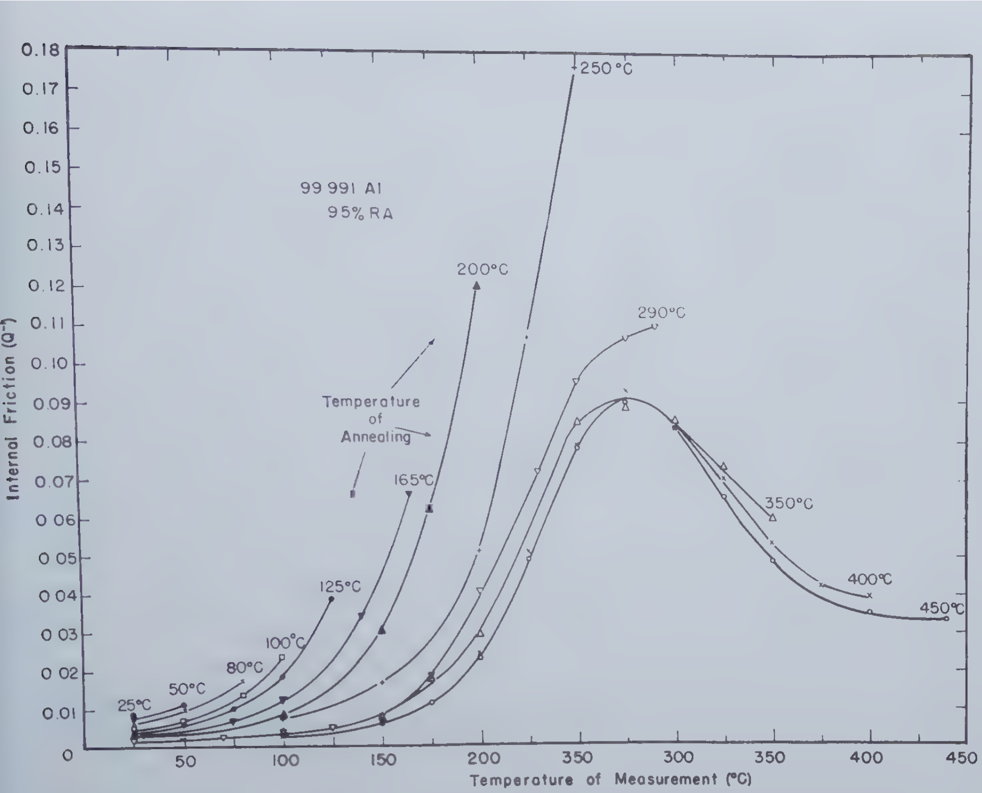

Fig. 1—Effect of temperature of measurement and of prior anneal upon internal friction of cold-worked 99.991 aluminum.

(95 pct reduction area).

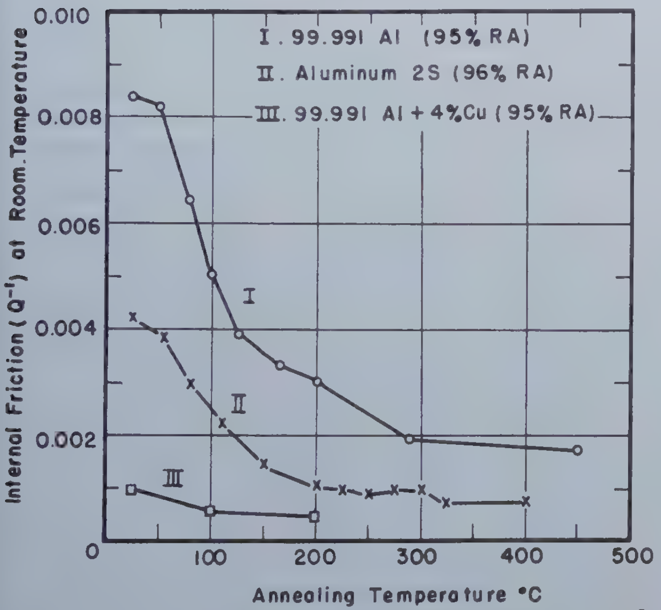

Fig. 2—Effect of annealing temperature upon internal friction at room temperature of cold-worked 99.991 aluminum and other less pure aluminum.

of annealing temperature. However, it becomes somewhat constant after a temperature of abut 300° C at which the specimen has recrystallized. This is in conformity with the high frequency measurements of Zener, Clarke and Smith on cold-worked alpha brass for the range of annealing temperatures up to 225°C.[6] The largest cold-working to which they subjected the specimen was 30 pct elongation. The internal friction they observed was more than one hundred times smaller.

In Wegel and Walther's study of the effect of annealing upon the room temperature internal friction of copper and of commercial brass,[8] and in Norton's study in the case of alpha-brass,[10] they all found that the internal friction at room temperature first decreases and then increases with annealing temperature when the recrystallization temperature is reached. The measurements for aluminum with low frequency of vibration, as shown in fig. 2, are different from these observations.

The effect of annealing temperature upon the internal friction at room temperature of cold-worked aluminum specimens containing various amounts of impurities is shown by curves II and III in fig. 2. The internal friction of each specimen was also lowered by annealing at a higher temperature until a somewhat constant value was reached. The lowest internal friction observed at room temperature was 0.00041 when a specimen containing 4 pct copper was annealed at 200°C. This low value of internal friction assures us that the "constant" parts of internal friction in curves I and II are much higher than the internal friction background due to apparatus loss. We may thus consider that the room temperature internal friction is composed of two parts. One part is readily eliminated by annealing at a higher temperature while the other part is not. Fig. 2 shows that both parts were reduced by the presence of impurities.

It is seen that the "residual" internal friction shown in fig. 2 cannot be eliminated by annealing even at very high temperatures at which the specimen has completely recrystallized. Consequently this internal friction possibly may not be connected with cold-working. Its superposition with the internal friction introduced by cold-working may have caused the inconsistencies and discrepancies observed by previous workers especially in the cases where the cold-work internal friction is comparably small.

Internal Friction Versus Temperature of Measurement: Fig. 1 also shows that for a given temperature of prior anneal the internal friction introduced by cold-work is higher the higher the temperature of measurement. The temperature dependence of internal friction is, however, smaller at lower temperatures of measurement or for higher temperatures of anneal. Similar results have previously been observed in the cases of iron free from carbon and nitrogen[8] and of alpha brass.[11] These results are different from those observed by Zener, Clarke and Smith in slightly cold-worked alpha brass (2.4 pct elongation) with a frequency of vibration of 2,000 cycles per sec. They found that within the temperature range of 20-90°C, the internal friction introduced by cold-work decreases slightly with increasing temperature of measurement.

The internal friction at 250°C after one hour annealing at this temperature is shown to be as high as 0.18. Such a high internal friction has not been reported previously in the literature.

It is seen from fig. 1 that an internal friction peak (versus temperature) was well defined after the 350°C anneal. We have shown previously that this peak is associated with the viscous behavior of grain boundaries in recrystallized specimens.[7, 8] The height of this peak for the several metals observed was around 0.10 and this is much smaller than the high internal friction of 0.18 observed after the 250°C annealing. The drop in internal friction is thus connected in some way to the complete recrystallization of the cold-worked specimen. This question will be analyzed in some detail in a following article.[12]

Fig. 1 shows that the abrupt drop of internal friction occurred after the specimen was annealed at 290°C. Annealing at this temperature had also eliminated that part of internal friction at room temperature which is readily removed by annealing (curve I of fig. 2).

It is seen from fig. 1 that at very high temperatures, the internal friction peak did not drop as rapidly as expected if this peak is entirely due to the viscous behavior of grain boundaries. The factors influencing this additional internal friction at very high temperatures and its possible physical origins will be discussed elsewhere.[13]

Internal Friction Versus Aging Time: We have shown above that the cold-work internal friction is lower the higher the temperature of prior anneal. It has also been observed that this internal friction is also lowered by aging at the same temperature. Fig. 3 shows the effect of annealing at 200°C upon the internal friction of cold-worked (95 pct reduction area) 99.991 aluminum at 200°C. The internal friction decreases rapidly at first and then decreases slowly with the aging time. This behavior is illustrated more markedly in fig. 4 in which the annealing and measurement were made at 245°C. The internal friction in this case is so extremely high that it was found necessary to develop a new type of apparatus for the measurement of internal friction by determining the angle by which strain lags behind the stress in forced cyclic vibration.[14] The frequency of vibration used in this measurement was 0.05 cycles per sec and the internal friction was reported as tan α where α is the angle of phase lag.

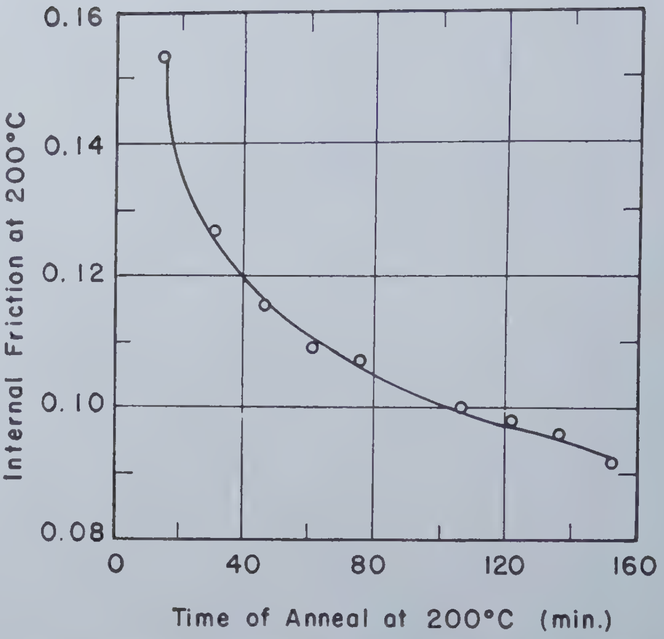

Fig. 3—Effect of annealing time (at 200°C) upon internal friction at 200°C of cold-worked 99.991 aluminum.
(95 pct reduction area).

Fig. 4 shows that the internal friction at 245°C is 0.45 after an anneal of 5 min at 245°C. This internal friction approaches a somewhat stable value of 0.15 after a prolonged aging of over 50 hr at 245°C. This value is still much higher than the maximum value of the internal friction associated with the viscous behavior of the grain boundaries in a recrystallized specimen which is about 0.09, as shown in fig. 1. This suggests that this high internal friction originates from some effect introduced by cold-working which can be completely eliminated only after the "complete" recrystallization of the cold-worked specimen.

Internal Friction Versus Amount of Cold-Work: To compare with fig. 1, a similar series of internal friction curves was determined for 99.991 aluminum subjected to a smaller amount of cold-work: 5 pct, 10 pct and 34 pct reduction area. The series of curves for 34 pct reduction area is shown in fig. 5. The general feature of the curves is similar to that of fig. 1 except that the value of the internal friction at each temperature is smaller than that of the corresponding case of the specimen subjected to a cold-work of 95 pct reduction area. In this case the abrupt drop of internal friction is observed when the temperature of prior anneal is 400°C. Metallographic examination again showed that the specimen has recrystallized after the 400°C annealing.

It was observed by Zener, Clarke and Smith that the room temperature internal friction of cold-worked alpha brass is initially increased by increased amount of cold-work. However, they found that there is an optimum amount of cold-working beyond which the internal friction decreases.[6] The range of cold-working they covered was from 0.02 to about 30 pct of elongation and the frequency of measurement they used was about 2000 cycles per sec. Our observations thus differ again from those

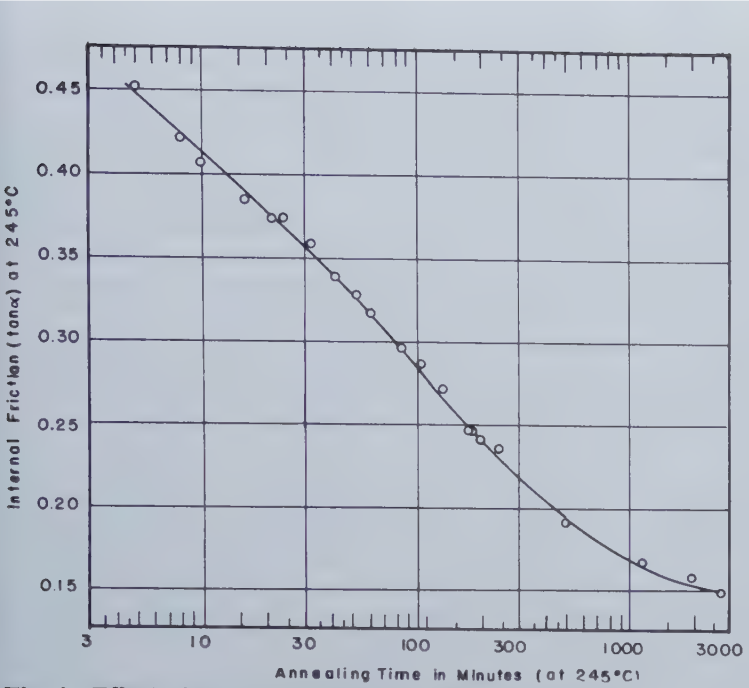

Fig. 4—Effect of annealing time (at 245°C) upon internal friction at 245°C of cold-worked 99.991 aluminum.
(95 pct reduction area).

of the above authors since the internal friction was found to increase monotonously with increasing amount of cold-work ranging from 5 pct to 95 pct reduction area.

Effect of Impurities: Internal Friction in Cold-Worked Aluminum 2S: In order to study the effect of impurities upon the internal friction introduced by cold work, a series of internal friction curves were determined for aluminum 2S under similar conditions as shown in fig. 1 for 99.991 aluminum. This is shown in fig. 6. The impurity content in aluminum 2S is 0.14 pct Cu, 0.48 pct Fe and 0.11 pct Si. The cold-work performed on the specimen was 96 pct reduction area which is close to the 95 pct reduction area performed on the 99.991 specimen. The annealing time at each temperature was also one hour, as before. A general comparison of fig. 6 with fig. 1 shows that at any given temperature and for any given temperature of prior anneal, the internal friction is much smaller in the case of aluminum 2S. This indicates that the internal friction is reduced by the presence of impurities in a cold-worked specimen. The Cu, Fe and Si present as impurities in aluminum are presumably in the form of precipitates in the cold-worked specimen. The effect of the precipitated impurities is thus to block the "relaxation centers" from stress relaxation under conditions in which the stress relaxation is apt to occur in the case of high purity aluminum.

In fig. 1 for 99.991 aluminum the internal friction curve for a higher prior anneal is always lower than that for a lower prior anneal, up to an annealing temperature after which the specimen has completely recrystallized. This is also the case when aluminum 2S was annealed at 250°C and lower temperatures. However, as is shown in fig. 6 and has also been found in another specimen, when aluminum 2S was annealed at 275°C for one hour and the internal friction measured at this and lower temperatures, the internal friction curve began to cross the 250°C anneal curve at a temperature of about 200°C and to cross the 225° and 200°C curves at still lower temperatures. The maximum stress amplitude used in the internal friction measurements was kept the same for all cases. Some change must have occurred in the specimen after the 275° C annealing resulting in an anomalous increase of internal friction.

Such anomalous increase of internal friction disappeared after the specimen was further annealed at 300°C for one hour. Fig. 6 shows that there is an abrupt drop in internal friction after this anneal. Metallographic examination showed that the specimen has completely recrystallized after this annealing in the sense that equiaxed grain rather than irregular grains were observed in the specimen. This may indicate that complete recrystallization

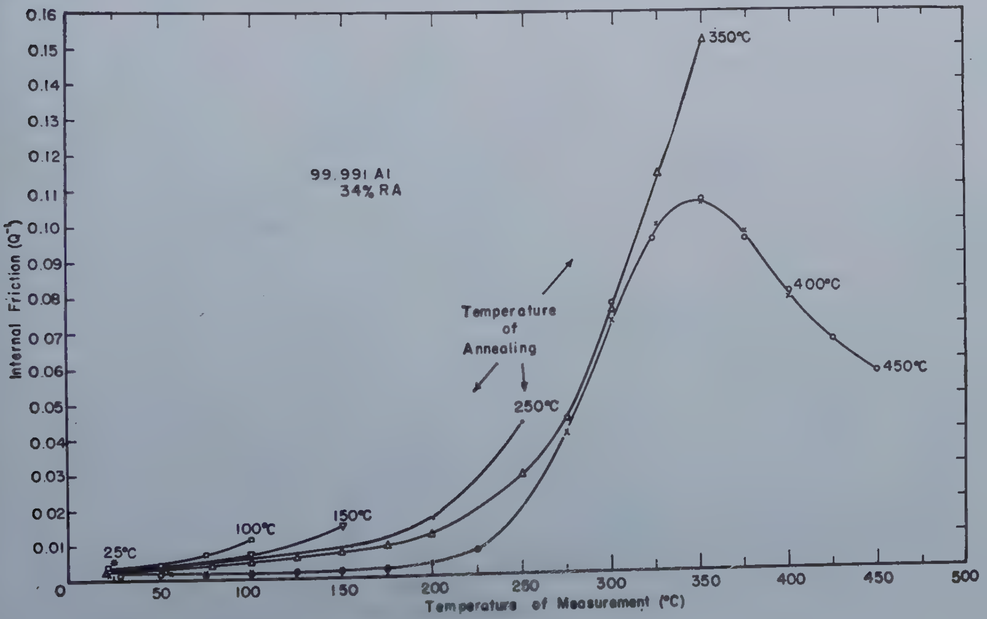

Fig. 5—Effect of temperature of measurement and of prior anneal upon internal friction of cold-worked 99.991 aluminum.

(34 pct reduction area).

eliminates the causes of the anomalous internal friction. It seems thus that the occurrence of this anomalous internal friction requires the presence of impurities and of some effects of cold-work. Internal friction of similar behavior has been observed previously by Snoek[15] and further studied by this writer[8] in the case of cold-worked iron containing nitrogen and carbon as impurities. Such anomalous internal friction has recently been observed by this writer also in the case of cold-worked 99.991 aluminum alloyed with ½ pct copper. A detailed account on this observation will be reported elsewhere.[16]

The effect of impurities upon the internal friction at room temperature after annealing at successively higher temperatures has been already described in fig. 2.

Fig. 6 also shows that the internal friction peak associated with the viscous behavior of grain boundaries in completely recrystallized aluminum 2S specimen is much lower than the case of 99.991 aluminum. The blocking of the viscous slip of grain boundaries by impurities has been discussed elsewhere.[17]

Discussion of Results

The internal friction observed in severely cold-worked 99.991 aluminum in low frequency experiments over a wide range of temperatures shows that the internal friction introduced by severe cold-working is quite complicated and is heterogeneous in nature. The results observed under these conditions may not be compared with those observed by previous investigators in high frequency experiments around room temperature on slightly cold-worked specimens. The internal friction observed in the present experiments is more than one hundred times higher than that observed by previous investigators.

Aside from the "residual" internal friction which cannot be eliminated even after the complete recrystallization of the cold-worked specimen, the internal friction introduced by cold-working has been observed to have the following behavior.

This internal friction predominates at temperatures higher than room temperature. It increases rapidly with the amount of cold-work, is readily lowered by aging or by annealing at a higher temperature. The temperature dependence of this internal friction is remarkable; the internal friction increases very rapidly with a rise of temperature of measurement up to a temperature at which the specimen has completely recrystallized. It is considerably reduced by the presence of impurities.

There are several viewpoints as to the origin of the internal friction introduced by cold-working.[1] One viewpoint is that the internal friction is due to the residual stresses introduced by cold-working. This is a favorable theory in explaining the hysteresis loop or the damping capacity of a plastically deformed specimen under high stress levels. The application of a high external stress raises the local residual stress to a value higher than the yield stress and thus initiates slip. This results in a hysteresis loss when the applied stress is cyclic. It is easily seen that the internal friction resulting from such a mechanism would be strongly sensitive to stress amplitude. The internal friction would vanish when the stress amplitude is sufficiently small. Accordingly this mechanism cannot be applied to the cases of low stress internal friction which stays constant at sufficiently low stress level.

An older view has been advanced that internal friction in cold-worked metals may be explained in terms of a two phase system, a continuous elastic phase and a discontinuous viscous phase. The essential characteristic of a dispersed viscous phase is that it cannot permanently sustain a shearing stress, however small the stress may be. Such a viewpoint has been more recently advocated by Zener.[18, 19] In his study of the anelastic properties of iron, the writer has adopted this viewpoint in explaining the observed behavior of the internal friction of iron introduced by cold-working.[8] It was then assumed that the internal friction is associated with the viscous behavior of the slip band material. The observations on the cold-work internal friction described above are in agreement with the viewpoint that the disorganized material within the slip bands gradually acquires the order of the surrounding

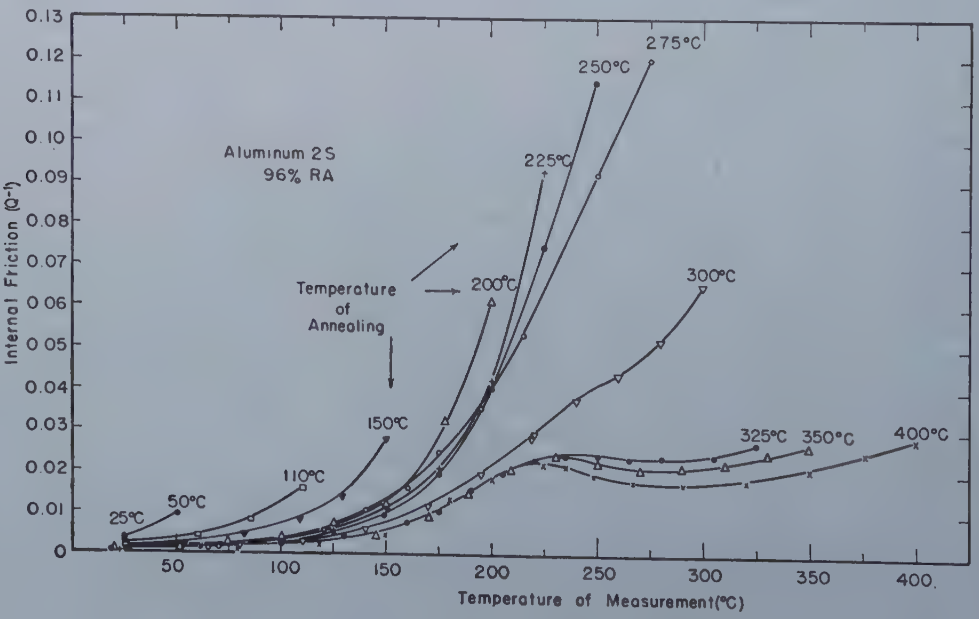

Fig. 6—Effect of temperature of measurement and of prior anneal upon internal friction of cold-worked aluminum 2S.

(96 pct reduction area).

matrix as the specimen is annealed, and with the viewpoint that the rate of shear strain within the disorganized material increases rapidly with an increase of temperature. In the language of dislocation theory, a slip band can be considered as a high concentration of dislocations. A high concentration of dislocations would behave in a viscous manner as a slip band does.

However, the observations that the internal friction remains extremely high after prolonged annealing at a very high temperature short of complete recrystallization of the specimen cannot be understood in terms of the viscous behavior of slip bands as originally recognized by Rosenhain. Slip bands were considered to behave in a viscous manner only when they are freshly formed and that this viscous behavior disappears gradually with aging or annealing at a higher temperature.

In addition to slip bands there may be other dispersed viscous phases in a cold-worked metal. When a metal is severely deformed the grains are broken down into much smaller elements. The boundaries between such "crystallites" may behave in a viscous manner similar to grain boundaries. Such a viscous behavior may also be exhibited by the boundaries of the newly formed grains during recrystallization. As the crystallites and the newly formed grains may have very irregular sizes, the total amount of stress relaxation across such a system could be much larger than the case of essentially equiaxed grains of approximately uniform size in completely recrystallized specimens in which the extent of stress relaxation is blocked by grain corners. The internal friction associated with the viscous behavior of such boundaries can thus be considerably higher than in the case of the boundaries of recrystallized grains.

There are numerous dislocations in the interior of a cold-worked specimen. It is recognized that the stress-induced movement of dislocations can give rise to internal friction although the mechanism involved would be extremely complicated in the case of a severely cold-worked specimen. A detailed analysis in terms of a concrete model of dislocations requires further extensive quantitative experiments.

Summary

Low stress internal friction measurements in torsion were made on severely cold-worked 99.991 aluminum when it was annealed at successively higher temperatures until it had completely recrystallized. The measurements of internal friction were made over a range of temperature extending from room temperature up to the temperature for complete recrystallization.

Factors affecting the internal friction were then examined. These factors include the temperature of prior anneal, the temperature of measurement, the amount of cold-working, the annealing time, and the presence of impurities.

Observations indicate that there is a "residual" internal friction predominating around room temperature. It cannot be eliminated by annealing even after the specimen had completely recrystallized. This internal friction possibly may not be connected with the cold-working performed on the specimen.

The internal friction introduced by cold-working was found to predominate at high temperatures. It increases with the amount of cold-work, is lowered by aging or by annealing at a higher temperature. It increases rapidly with the temperature of measurement and it is extremely high at temperatures just before the specimen has completely recrystallized. This high internal friction is eliminated only after the complete recrystallization of the specimen.

The origin of this internal friction appears to be manifold. It may be associated with the behavior of a discontinuous viscous phase in the cold-worked specimen such as slip bands, crystallite boundaries, the boundaries of the newly formed grains during recrystallization, or with the stress-induced movement of the dislocations inside the strained grains.

Both the residual and the cold-work internal friction were found to be reduced by the presence of impurities. The presence of impurities in cold-worked aluminum also gives rise to an anomalous internal friction similar to that previously observed in the case of cold-worked iron containing nitrogen or carbon as impurities.

References

[1] See C. Zener: Elasticity and Anelasticity of Metals (Univ. of Chicago Press, 1948), pp. 136-138.

[2] See F. Seitz: The Physics of Metals. (McGraw-Hill Book Co., 1943), Chap. X.

[3] R. L. Wegel and H. Walther: Internal Dissipation in Solids for Small Cyclid Strains. *Physics* (1935), **6**, 141.

[4] F. Forster and W. Köster: *Ztsch. Metallkde.* (1937), **29**, 116.

[5] W. Köster and K. Rosenthal: *Ztsch. Metallkde.* (1938), **30**, 345.

[6] C. Zener, H. Clarke and C. S. Smith: Effect of Cold-work and Annealing Upon Internal Friction of Alpha-Brass. *Trans.* AIME (1942), **147**, 90.

[7] T. S. Kê: Experimental Evidence of the Viscous Behavior of Grain Boundaries in Metals. *Phys. Rev.* (1947), **71**, 533.

[8] T. S. Kê: Anelastic Properties of Iron. *Trans.* AIME (1948), **176**, 448. *Metals Tech.* June 1948. TP 2370.

[9] B. L. Averbach: Recovery and Recrystallization in Brass. *Trans.* AIME (1949) **185**, 491. *Jnl. of Metals,* Aug. 1949. TP 2636.

[10] J. T. Norton: Changes in Damping Capacity During Annealing of Alpha Brass. *Trans.* AIME (1940), **137**, 49.

[11] T. S. Kê: unpublished results.

[12] T. S. Kê: A Study of Recrystallization and Grain Growth by Measurements of Internal Friction. *Trans.* AIME (1950) **188**, 581. *Jnl. of Metals,* March 1950. TP 2789.

[13] T. S. Kê: Internal Friction of Metals at Very High Temperatures. Communicated to *Jnl. Appl. Phys.* (1949).

[14] T. S. Kê and Marc Ross: An Apparatus for Measurement of Extremely High Internal Friction. *Rev. Sci. Instr.* (1949), **20**, Nov. issue.

[15] J. L. Snoek: Effect of Small Quantities of Carbon and Nitrogen on the Elastic and Plastic Properties of Iron. *Physica* (1941), **8**, 711.

[16] T. S. Kê: Anomalous Internal Friction Associated with the Precipitation of Cu in Plastically Deformed Al-Cu Alloys (to be published). An abstract of this paper has appeared in *Phys. Rev.* (1949), **76**, 470.

[17] T. S. Kê: A Grain Boundary Model and the Mechanism of Viscous Intercrystalline Slip. *Jnl. Appl. Phys.* (1949), **20**, 274.

[18] C. Zener: Anelasticity of Metals. *Trans.* AIME (1946), **167**, 155. *Met. Tech.* Aug. 1946. TP 1992.

[19] C. Zener: Dynamics of Slip Bands. Chapter in *A Seminar on the Cold-Working of Metals* (A.S.M., 1949), p. 180.

A Study of Recrystallization and Grain Growth by Measurements of Internal Friction

by T'ing-Sui Kê

THE subject of recrystallization and grain growth has been much studied and the literature on this subject is numerous. Such studies have been mostly carried out by metallographic examination of X ray methods.

Since recrystallization and grain growth involve elementary atomic processes, their mechanism can best be elucidated by a study of some properties which can be readily traced back in terms of such atomic processes. Prior to a detailed quantitative study, however, it is necessary to explore first the possibility and practicability of utilizing any particular property for obtaining the desired information.

We have pointed out in a preceding article[1] that the internal friction of cold-worked metals is extremely high during recrystallization and it drops abruptly once the recrystallization is complete. Previous work has also shown that the viscosity of grain boundaries in a recrystallized specimen at a given temperature is raised by grain growth.[2] It seems thus that the measurements of internal friction may furnish a useful tool for the study of the mechanism of recrystallization and grain growth in terms of elementary atomic processes.

The purpose of this paper is to report results of a study along this line. We will demonstrate that the internal friction method does give results in agreement with those furnished by conventional metallographic examinations. Once such a correlation has been established, we will be in a position to take further steps to achieve new information which cannot be achieved by conventional methods.

The measurements of internal friction were made using apparatus and procedures similar to those used in the preceding article. All the measurements were made under such a small stress level that the internal friction is independent of stress level. The frequency of vibration is, unless mentioned otherwise, about one cycle per second in all cases.

Internal Friction and Recrystallization

Complete Recrystallization Temperature: Fig. 1 shows the internal friction curve during annealing of a few metals: aluminum, alpha brass and iron. These curves were determined in the following manner. In the curve for aluminum, internal friction measurements were performed upon 99.991 aluminum subjected to 95 pct reduction area. The internal friction was first measured at room temperature. The specimen was then annealed at 50°C

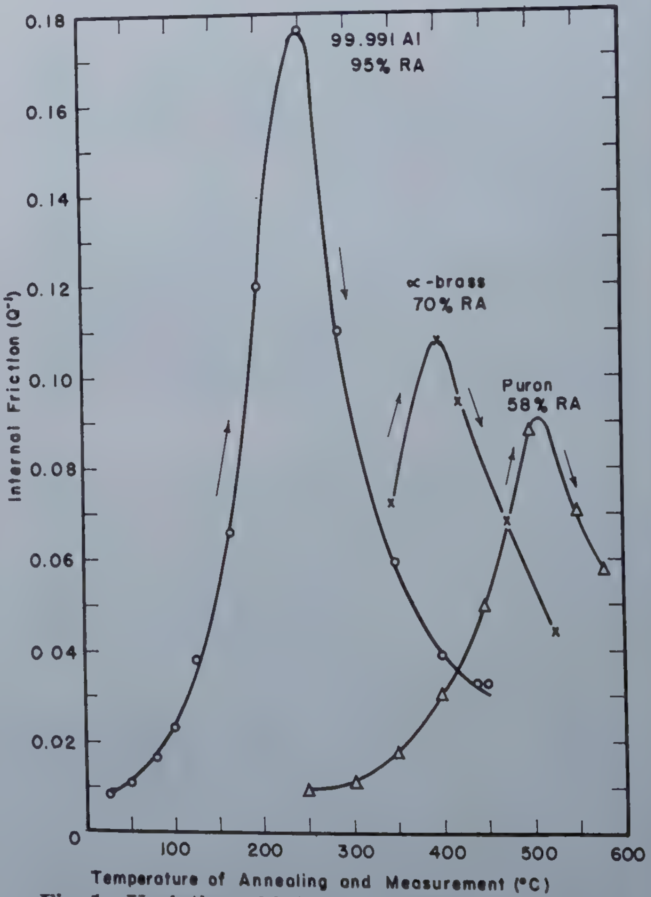

Fig. 1—Variation of internal friction with the temperature of anneal and of measurement of cold-worked aluminum, alpha brass and iron.

The arrows shown with the curves indicate the direction of increase of annealing temperature. The temperature at which the internal friction drops with increasing temperature is defined as the "complete recrystallization temperature".

T'ING-SUI KÊ, Member AIME, is Research Associate with rank of Assistant Professor, Institute for the Study of Metals, University of Chicago.

This research has been supported in part by ONR (Contract No. N-6ori-20-IV, NR 019302).

AIME New York Meeting, Feb. 1950.

TP 2789 E. Discussion (2 copies) may be sent to Transactions *AIME before Apr. 1, 1950, and will be published Nov. 1950. Manuscript received Oct. 17, 1949.*

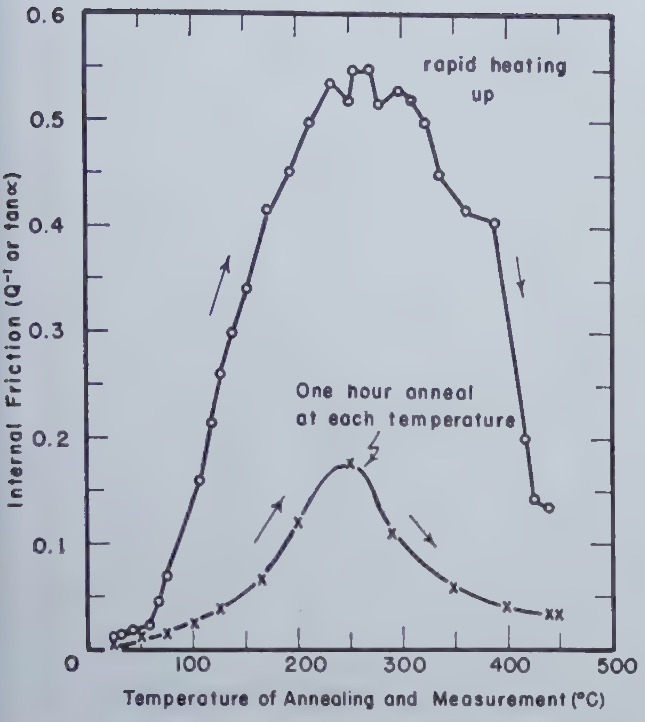

Fig. 2—Effect of rate of heating upon the internal friction and "complete recrystallization temperature" of 99.991 aluminum (95 pct reduction area).

for one hour after which the internal friction was measured at this temperature. The same procedure was repeated for successively higher annealing temperatures. The internal friction measured at each annealing temperature was plotted against that temperature as shown in fig. 1. After each annealing a short test piece of the specimen which has received the same past thermal and mechanical treatments was taken out for metallographic examinations. After the 290°C annealing, the specimen was found to be completely recrystallized and the majority of the newly formed grains are essentially perfect. From the curve it is seen that this temperature for achieving perfect grains (for one hour anneal) is also the temperature at which the internal friction is lowered with a rise of temperature.

The curves for alpha brass and iron (Westinghouse Puron) were determined and plotted in fig. 1 in the same manner as that for aluminum. The annealing time for all cases was one hour. However, the previous cold-working was different in these cases, being 70 pct reduction area for alpha brass and 58 pct for Puron. Metallographic examination on test pieces of these two metals also showed that the annealing temperature for achieving perfect newly formed grains corresponds to the temperature for which the internal friction begins to drop with increasing temperature. The arrows shown with the curves in fig. 1 are to indicate the direction of increase of annealing temperature. These curves are not reproducible when the temperature is lowered from the highest annealing temperature.

For the purpose of qualitative comparison we may call the temperature for maximum internal friction the complete recrystallization temperature for one hour annealing and for the given amount of previous cold-working. Such a temperature is obviously higher than the conventional "recrystallization temperature" which was often defined as the lowest temperature at which recrystallization can occur in a readily measured time under the normal conditions of cold-work employed in commercial fabrication. According to fig. 1 this complete recrystallization temperature for the conditions specified is 250° C for aluminum, 400°C for alpha brass and 515°C for iron.

In the following we will examine the factors that affect this so defined "complete recrystallization temperature."

Effect of Annealing Time: It is recognized that increasing time of annealing displaces recrystallization to a lower temperature. In fig. 1 for 99.991 aluminum (95 pct reduction area) the annealing time at each temperature was one hour. This is reproduced in fig. 2 as the lower curve. In order to find out the effect of annealing time or the rate of heating upon the complete recrystallization temperature, another 99.991 aluminum specimen was heated up fairly rapidly (temperature of specimen reached 250°C in about an hour after it was subjected to a cold-work of 95 pct reduction area. The internal friction was measured while the temperature was going up by an apparatus specially designed for the measurement of extremely high internal friction.[3] The upper curve in fig. 2 shows the value of internal friction at various annealing temperatures. The optimum temperature for the peak of the internal friction is about 260°C, which is only about 10°C higher than the former case.

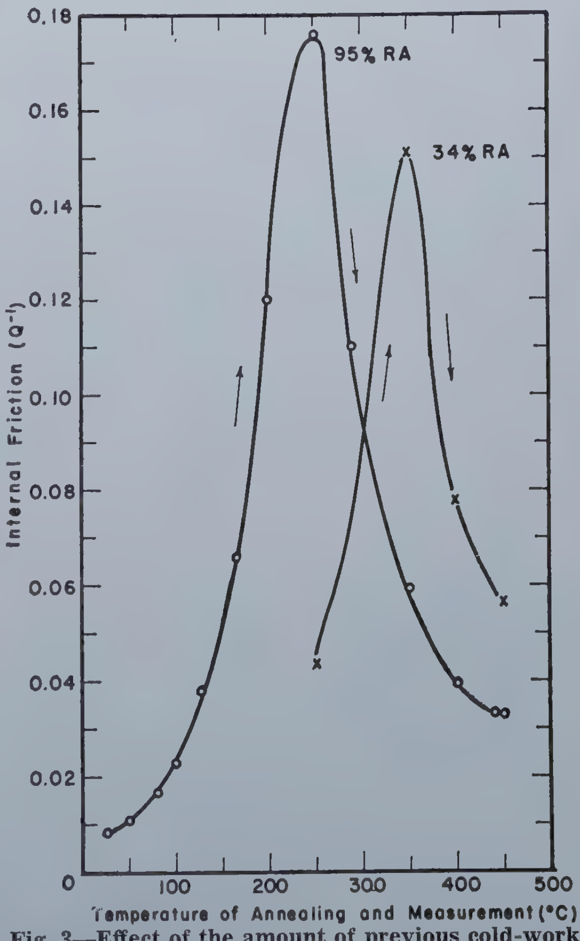

Fig. 3—Effect of the amount of previous cold-work upon the internal friction and "complete recrystallization temperature" of 99.991 aluminum.

In considering that the highest internal friction reached in rapid heating is more than three times higher than that reached in slow heating, a shift of complete recrystallization temperature of only 10°C in these two cases can only be considered as indicating that this temperature is relatively insensitive to annealing time or the rate of heating. This is not readily understandable in terms of our conventional concept of nucleation and growth during recrystallization.

It is seen that the highest internal friction reached in rapid heating is about 0.55, which is by far the highest internal friction ever reported in the literature. It would be fascinating to find out how high an internal friction the specimen would manifest during recrystallization if we could heat up the specimen extremely rapidly. A detailed study of the origin of such a high internal friction and a study of its change during recrystallization will likely throw considerable light toward the understanding of the elementary atomic processes involved in recrystallization. Some internal friction-annealing curves have already been reported in the preceding article (ref. 1, fig. 3 and 4).

Effect of Previous Cold-Work: It is also recognized that recrystallization occurs at a higher temperature, the smaller the degree of previous deformation. This has also been found to be the case of complete recrystallization as is shown in fig. 3. The internal friction curves were determined for 99.991 aluminum with previous deformation of 95 and 34 pct reduction area. The annealing time in both cases was one hour. Fig. 3 shows that complete recrystallization occurs at a temperature 100°C higher in the case of the smaller previous deformation.

The internal friction peak for the case of smaller deformation is seen to be also smaller.

Effect of Impurities: A study of the effect of impurities upon the complete recrystallization temperature of aluminum is shown in fig. 4 for 99.991 aluminum, aluminum 2S and 99.991 aluminum alloyed with ½ pct of copper. The previous deformation was 95 pct reduction area and the annealing was one hour for all specimens. Although the internal friction is lower in a specimen containing a larger amount of impurities, the optimum temperature for

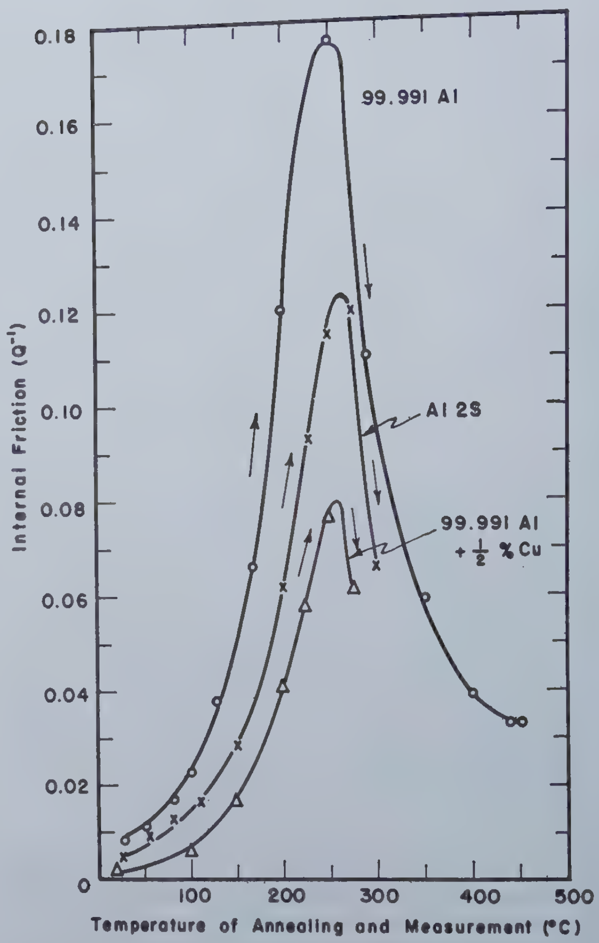

Fig. 4—Effect of impurity content upon the internal friction and "complete recrystallization temperature" of aluminum (95 pct reduction area).

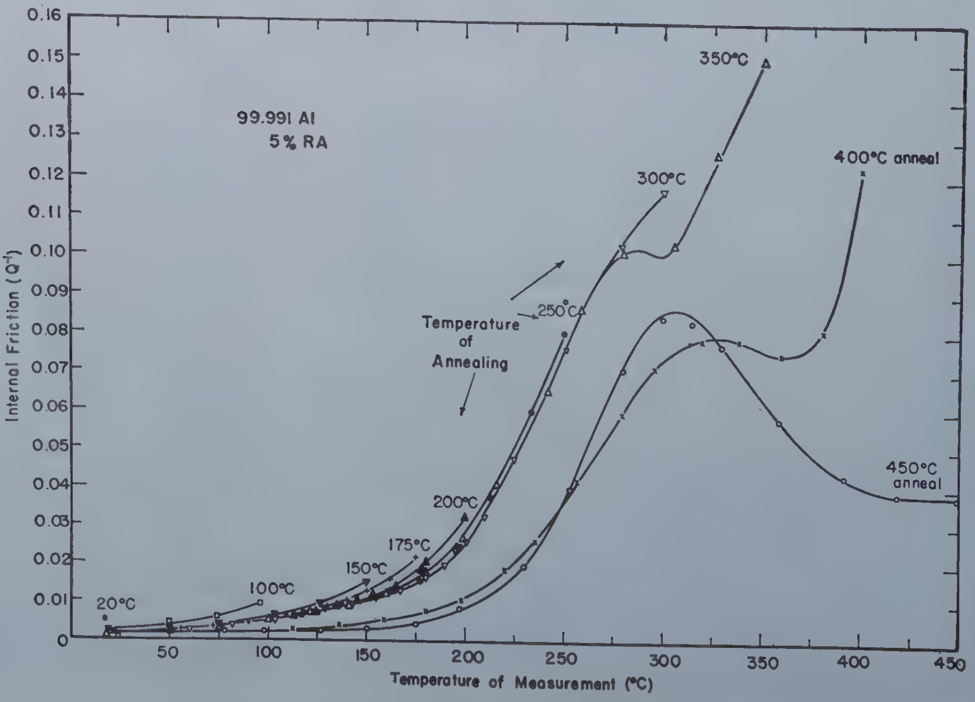

Fig. 5—Effect of temperature of measurement and of prior anneal upon internal friction of slightly cold-worked 99.991 aluminum (5 pct reduction area).

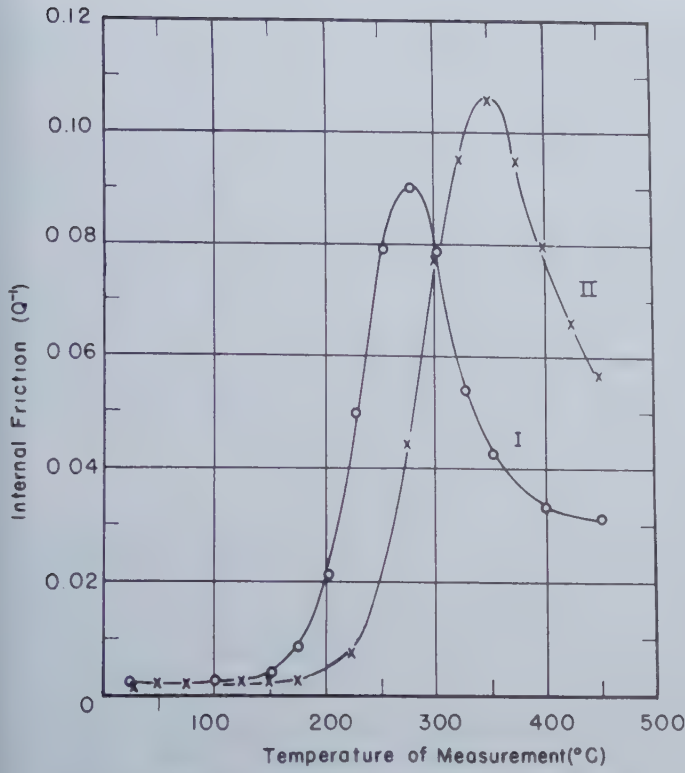

Fig. 6—Effect of previous deformation upon the internal friction peak associated with the viscous behavior of grain boundaries in recrystallized aluminum.

Curve I, 70 pct reduction area; curve II, 34 pct reduction area.

maximum internal friction seems to be insensitive to the impurity content. Under the conditions described, the impurities in the specimens of aluminum 2S and 99.991 aluminum + ½ pct Cu are probably in a precipitated state. Although undissolved impurities have been recognized to have a remarkable effect in lowering the temperature for the occurrence of recrystallization, the observations shown in figure 4 indicate that the precipitated impurity content does not have an appreciable effect upon the temperature for complete recrystallization.

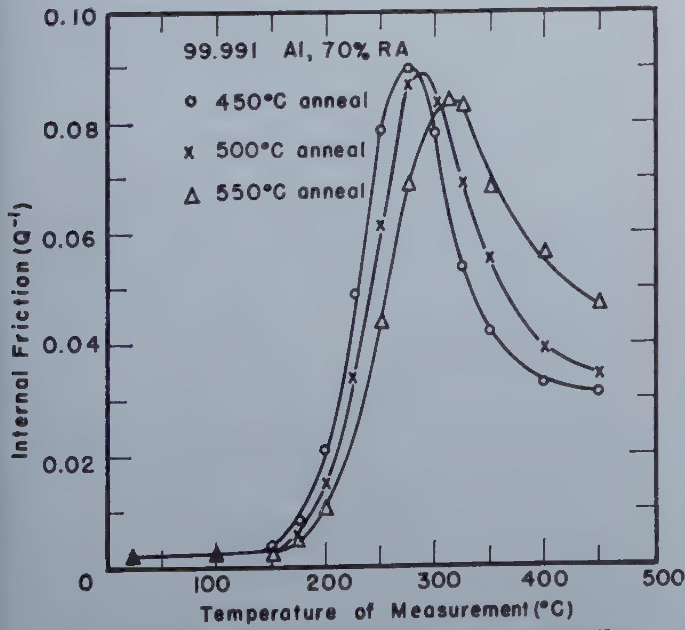

Fig. 7—Effect of annealing temperature upon the grain boundary internal friction peak of recrystallized aluminum which was subjected to a previous cold-working of 70 pct reduction area.

Grain growth was observed.

The Case of Very Small Previous Deformation: Fig. 5 shows a series of internal friction curves for 99.991 aluminum determined in the same manner as was previously reported (fig. 1 and 5 of ref. 1) except that the previous deformation was only 5 pct reduction area and the annealing time at each annealing temperature was 15 min. The highest annealing was made at 450°C for 2 hr. After this annealing we get a well-defined internal friction peak associated with the viscous behavior of the grain boundaries, as shown. It is to be noticed that in the cases of the 350° and 400°C annealings, the internal friction curves are composed of two parts: an apparent peak and a continuous rising branch at high temperatures. Such a behavior has not been observed, at least not so markedly, in the cases of severely deformed specimens. A plausible explanation is that the small amount of cold-working introduces a widespread inhomogeneous straining in the specimen. The high strain regions in the specimen recrystallize at a low temperature to form equiaxed grains. The apparent internal friction peak is associated with the stress relaxation across the boundaries of these recrystallized grains. And the rising portion of the internal friction at high temperatures has its origin in the unrecrystallized strained grains. The abrupt drop of this latter internal friction by annealing at higher temperatures is probably caused by the rapid elimination of the strained grains to form equiaxed grains. It is seen from fig. 5 that after the 450°C annealing, the internal friction peak associated with the boundaries of the recrystallized grains is raised as the rising portion of internal friction is lowered.

Internal Friction and Grain Growth

We have previously reported that the grain boundary viscosity is lower in a specimen subjected to a heavier deformation prior to its recrystallization.[4] Fig. 6 shows the internal friction curves associated with the viscous behavior of grain boundaries in recrystallized 99.991 aluminum subjected to different amounts of previous deformation: curve I for the case of 70 pct reduction area and curve II for the case of 34 pct reduction area. It is seen that the maximum internal friction in curve II occurs at a temperature 65°C higher than that in curve I. A shift of internal friction curve toward higher temperature indicates an increase of relaxation time and thus a rise in coefficient of viscosity at a given temperature. This means that the grain boundary in a specimen subjected to a less previous cold-work has a higher coefficient of viscosity.

The influence of previous deformation on grain boundary viscosity described above has been found to be connected with the phenomenon of grain growth. Metallographic examinations showed that in the 70 pct reduction area specimen, grains grow as the annealing temperature is raised. Such grain growth was also detected by measurements of internal friction, as shown in fig. 7. The internal friction curve is seen to shift to a higher temperature after the specimen was annealed at successively higher

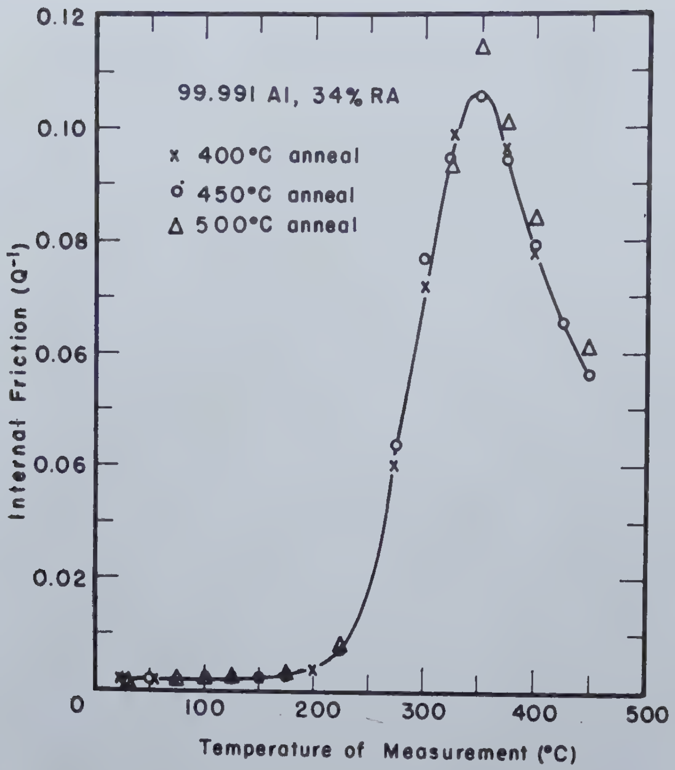

Fig. 8—Effect of annealing temperature upon the grain boundary internal friction peak of recrystallized aluminum which was subjected to a previous cold-working of 34 pct reduction area.

No grain growth was observed.

temperatures. Such a shift to a higher temperature signifies an increase of grain size as has been previously discussed.[2]

However, in the case of the 34 pct reduction area specimen, it was found metallographically that grains did not grow under similar annealing conditions. Thus after the 34 pct reduction area specimen was annealed at 400°C for one hour, the subsequent anneal at 450°C for 2 hr and 500°C anneal for 3 hr did not noticeably change the grain size. The internal friction curves for the 34 pct reduction area specimen after it was annealed at the temperatures mentioned are shown in fig. 8 in which it is seen that these curves coincide within experimental error. This also indicates that no grain growth had taken place under these conditions.

As the grain boundary viscosity of the 34 pct reduction area specimen is higher than that of the 70 pct reduction area specimen at a given temperature, the observations described above indicate that the conditions favoring grain growth or grain boundary migration correspond to conditions for a lower coefficient of viscosity at the grain boundary.

X ray examinations have shown that the dependence of grain boundary viscosity upon previous deformation is not attributable to the difference in the relative orientation of neighboring grains. It appears as if holes or "disordered groups" of atoms were created in the interior of the grains by the cold-working, and that the number of holes created increases with the amount of cold-working.[4] When a cold-worked metal is annealed, these holes migrate because of thermal agitation. Finally, a certain portion of these holes will reach and stay at the grain boundaries during recrystallization, presumably reducing the viscosity of the grain boundaries. The number of holes migrated to and accumulated at the grain boundary will be larger if the specimen is subjected to a larger amount of cold-work prior to recrystallization because, initially, there are more holes in the interior of the grains. This explains the observed effect that the grain boundaries in a specimen subjected to a larger amount of previous cold-working have a lower grain boundary viscosity.

Now, the presence of impurity atoms at the grain boundaries has been recognized to have the effect of inhibiting grain growth.[5] If the accumulation of holes at the grain boundaries facilitates grain growth as we discussed above, then the effect of hole is a reverse of that of impurity atoms.

Summary

1. It is shown that a study of the change of internal friction during recrystallization and grain growth furnishes a new method of approach toward the understanding of recrystallization and grain growth in terms of elementary atomic processes.
2. There is a definite temperature for each metal at which the internal friction of a cold-worked specimen drops abruptly with an increase of temperature of anneal and of meaurement. This temperature which can be defined as the complete recrystallization temperature, is higher than the conventional recrystallization temperature. It is displaced toward a higher temperature for a small amount of prior cold-work. It seems, however, to be relatively insensitive to the variation of the rate of heating and of the impurity content although the magnitude of internal friction is considerably reduced by slow heating or the presence of impurities.
3. Internal friction measurements on a slightly cold-worked specimen indicate that the recrystallization process is heterogeneous under these conditions. The internal friction curve is composed of an apparent peak and a continuous rising branch at high temperatures. The former is associated with the stress relaxation across the boundaries of the recrystallized grains and the latter has its origin in the unrecrystallized strained grains.
4. The conditions favoring grain growth or grain boundary migration are shown to correspond to conditions for a lower coefficient of viscosity at the grain boundary. It is suggested that the grain boundary viscosity is lowered by the accumulation of diffused holes at the grain boundaries. This viewpoint indicates that the effect of holes is a reverse of that of impurity atoms.

References

[1] T. S. Kê: Internal Friction of Cold-Worked Metals at Various Temperatures. *Trans.* AIME (1950) **188**, 575. *Jnl. of Metals*, March 1950. TP 2788.

[2] T. S. Kê: Stress Relaxation Across Grain Boundaries in Metals. *Phys. Rev.* (1947) **72**, 41.

[3] T. S. Kê and M. Ross: An Apparatus for Measurement of Extremely High Internal Friction. *Rev. Sci. Instr.* (1949) **20**, Nov.

[4] T. S. Kê: A Grain Boundary Model and the Mechanism of Viscous Intercrystalline Slip. *Jnl. Appl. Phys.* (1949) **20**, 274.

[5] J. E. Burke: Some Factors Affecting the Rate of Grain Growth in Metals. *Trans.* AIME (1949) **180**. *Met. Tech.* Oct. 1948. TP 2472.

Kinetics of the

Reactions of Columbium and Tantalum

with O_2, N_2 and H_2

by **Earl A. Gulbransen and Kenneth F. Andrew**

THIS paper will present the results of our studies on the kinetics of the gas phase reactions of columbium and tantalum with O_2, N_2 and H_2. Studies on zirconium and titanium have been previously reported.[9, 11]

Due to their high melting points and their many excellent physical and chemical properties, columbium and tantalum have been finding their places as useful metals in science and industry. Chemically the metals are very inert to gas and liquid phase corrosion at room temperature. However, at moderate temperatures of 250°C and higher the metals react readily with oxygen and hydrogen.

It is of interest to study the gas phase reactions of these metals for the following reasons: (1) to compare the rates of the several reactions with those of other metals and to correlate the rate data with theory and structure predictions, (2) to add basic information on the practical difficulties of the reduction, refining and working of columbium and tantalum, (3) to anticipate new uses for the metals and (4) to understand the role that the metals play as components in high temperature alloys.

Literature Survey

A number of papers exist in the literature on the gas phase reactions of columbium and tantalum with O_2, N_2 and H_2; however, only fragmentary data have been reported on the kinetics of these reactions. Although the free energy of formation of the oxide Ta_2O_5[20] at 25°C has been determined and some thermodynamic work has been reported on columbium and its oxides, the data are not sufficient to make equilibria calculations at elevated temperatures.

Oxidation: 1. *Kinetics:* The rate of oxidation of columbium and tantalum has been studied by McAdam and Geil[23] using the interference color method. Tantalum is reported to oxidize more slowly than columbium, zirconium and iron.

The amounts of oxidation of columbium after 20 hr in air for several temperatures are reported by the Fansteel Metallurgical Corporation.[36] Columbium starts to oxidize in air at about 200°C. The oxide is said to be adherent and prevents further oxidation until the temperature is raised. Columbium is reported not to become brittle on heating in air for short periods like tantalum because the oxide film prevents further reaction. The columbium oxides dissolve into the metal when heated in a vacuum at temperatures between red heat and 1200°C. Above 1200°C the oxides are reported to evaporate. Columbium, in the oxide free state, is an active getter in vacuum tubes.

2. *Preparation and Structure:* G. Grube, O. Kubaschewski and K. Zwiauer[15] have studied the decomposition of Cb_2O_5 in argon. They find that CbO_2 is formed slowly at 1150° and rapidly at 1300°C. Cb_2O_5 can be reduced to CbO_2 by moist H_2. The reduction of this dioxide to the lower oxides is rapid. By varying conditions CbO_2, Cb_2O_3, CbO and Cb_2O can be formed. CbO_2, CbO and Cb_2O have independent lattices while Cb_2O_3 is a stoichiometric mixture of CbO and CbO_2. In a later paper O. Kubaschewski[21] has shown that CbO is cubic and that CbO_2 has a rutile type of lattice.

The most exhaustive work on the oxides of columbium is that of G. Brauer.[6] The number and constitution of the solid phases in the binary system Cb-O were investigated by the preparative, analytical and X ray methods. He indicates that only the oxides Cb_2O_5, CbO_2 and CbO exist with limited regions of homogeneity. The solid oxide Cb_2O_5 exists

---

E. A. GULBRANSEN, Member AIME, and K. F. ANDREW are associated with Westinghouse Research Laboratories, East Pittsburgh, Pa.

AIME New York Meeting, Feb. 1950.

TP 2793 E. Discussion (2 copies) may be sent to Transactions *AIME before Apr. 1, 1950, and will be published Nov. 1950. Manuscript received Oct. 14, 1949; revision received Dec. 2, 1949.*

in three forms designated as (*L*) low, middle (*M*) and high (*H*). The X ray pattern of the *L* form is isomorphous with Ta_2O_5. The *L* form is stable to 900°C. At temperatures of 1000° to 1100°C the *M* form results which at still higher temperatures transforms to the *H* form. The crystal structure of the 3 modifications has not been determined.

CbO_2 is obtained from Cb_2O_5 as a black powder by reduction with H_2 or with Cb powder. X ray analyses show that CbO_2 has a structure closely related to rutile with $a = 4.84$, $c = 2.99$ and $c/a = 0.618$. The homogeneity range of CbO_2 is very limited.

The phase CbO has no extensive homogeneity range and the crystal structure is cubic with $a = 4.203$. The CbO lattice is a new type and can be derived from a NaCl lattice by the removal of molecules in such a way that 75 pct of the lattice positions are occupied and the unoccupied ones are distributed in an orderly manner. The solvent power of Cb for O is less than 0.8 pct by weight. A small expansion in the lattice is caused by this small amount of oxygen.

Phelps, Gulbransen and Hickman[29] observed CbO on the surface of columbium after oxidation at 400°C using the reflection electron diffraction method. A study of the same film by the transmission method after stripping from the metal shows a mixture of Cb_2O_5 and CbO.

An X ray diffraction study of the oxide Ta_2O_5 has been made and the results reported in the A.S.T.M. cards.[1] *d/N* values and intensities are tabulated although no structure is given.

Nitrogen Reaction: 1. *Absorption:* The absorption of nitrogen by tantalum has been studied by a number of workers.[2, 24, 40, 43] Andrews[2] has studied the absorption of nitrogen at low pressures and to a temperature of 3400°K. Absorption takes place with the formation of TaN and increases with pressure until 100 volumes are absorbed. At this point the equilibrium pressure drops as the absorption increases. Wright[43] has observed that nitrogen is absorbed at 1 micron pressure and at 700°C for a clean filament. The absorption becomes rapid above 1000°C. In the oxidized condition no absorption is found below 850°C although the absorption becomes rapid above 1200°C. All of the gas cleaned up at 1000°C is liberated at 2100°C.

2. *Preparation and Structure:* Two nitrides of columbium are reported in the literature, CbN and Cb_2N. Becker and Ebert[5] have observed that CbN has a face-centered cubic structure with a lattice parameter of 4.41Å. Horn and Ziegler[18] in a recent study confirm this structure for a sample of CbN of 47.3 at. pct of nitrogen. They find a lattice parameter of 4.375 ±0.004Å.

Aschermann, Friederich, Justi and Kramer[3] in a study of the superconductivity of columbium compounds prepared CbN. They find a face-centered cubic lattice and a lattice parameter of 4.39Å. From the X ray parameters the ideal lattice corresponds to a density of 8.35. This value falls to 7.28 as the lattice deviates from the stoichiometric ratio.

Umanski[37] has observed a hexagonal lattice for a columbium nitride containing 8.8 pct of nitrogen. The lattice parameters for this structure are $a = 3.017Å$ and $c = 5.580Å$. Brauer[6] has prepared Cb_2N by heating CbN with Cb at 1700°C for 15 min. Cb_2N has a Hägg interstitial type of structure possessing a close-packed hexagonal lattice of columbium atoms with the N atoms in the larger gaps.

Aschermann, Friederich, Justi and Kramer[3] observe a tetragonal lattice for the subnitride with $a = 4.35Å$ and $c/a = 0.98$. This subnitride corresponding to Cb_2N contained 7 pct of nitrogen and checks closely the stoichiometrical value of 7.03 pct.

Two nitrides of tantalum are reported, TaN[38] and Ta_2N.[3] TaN has been shown by Van Arkel[38] to have the hexagonal (ZnS) structure with $a = 3.05Å$ and $c/a = 1.62$. In a study of the superconductivity of tantalum compounds Aschermann, Friederich, Justi and Kramer[3] only observed Ta_2N having lattice parameters and structure identical with that for TaN, observed by Van Arkel.[38] There appears to be some question as to the formation of two nitrides.

Hydrogen Reaction: 1. *Solubility and Structure:* The solubility of hydrogen in columbium has been studied by Hagen and Sieverts[16] and by Sieverts and Moritz.[33] In the latter study a purer source of columbium was used. The solubility was measured at 760 mm of Hg gas pressure and over the temperature range of 20° to 900°C. The solubility decreases rapidly with temperature between 400° and 600°C. A value of 65.6 cc per g of columbium is found at 450°C and 4 cc per g at 900°C. At high temperatures (600°C) the solubility is proportional to the square root of the pressure.

Umanski[37] has studied the crystal structures for this system. A sample of columbium containing 0.42 pct of hydrogen gave patterns corresponding to two isometric lattices with spacings of 3.300-3.307Å and 3.416-3.420Å. The first belongs to columbium and the second probably to an undetermined hydride. The hydride spacings disappear after heating in a vacuum at 800°C.

Horn and Ziegler[18] have made a systematic study of the columbium-hydrogen system. From an X ray diffraction study they observe that a homogeneous product is formed from 0 to about 10 at. pct. The body-centered cubic lattice expands slightly with increased hydrogenation. From 23.78 at. pct to 32.76 at. pct of hydrogen the diffraction patterns showed not only the cubic structure but also a second structure which has not been determined.

Tantalum behaves to hydrogen much like palladium. The solubility has been studied by Sieverts and Bergner[31] and by Sieverts and Bruning.[32] If the metal is heated in vacua or argon, a low permeability is found. At high temperatures the metal absorbs readily and retains its permeability on cooling. The solubility is a maximum at low temperatures and decreases as the temperature is raised.

The absorption of tantalum at low pressure is found to be a function of the condition of the surface.[2, 43] Wright[43] found that if the metal is degassed below 1500°C, surface oxide remained, which prevented the cleanup of hydrogen below 400°C. Heating the strip to 1900°C gave a maximum absorption at room temperature which followed Sievert's solubility curve as the temperature is raised. The cleanup followed the square root of pressure law in the pressure range studied. Exposure of the strip at room temperature to oxygen restored the first type

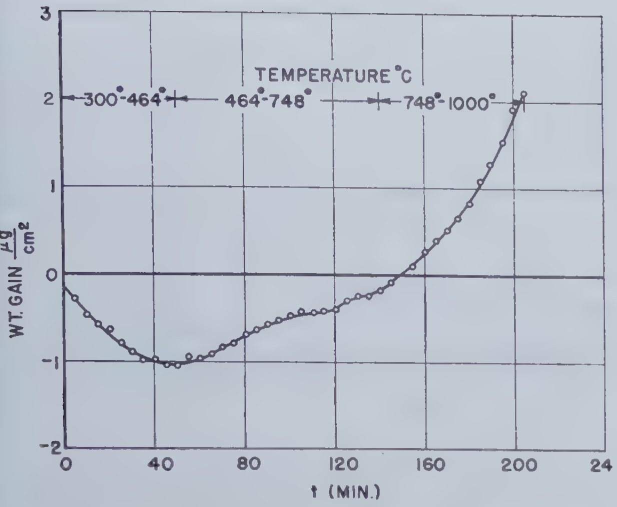

Fig. 1—Reaction of Cb in vacua zircon furnace tube.

of behavior. All of the gas cleaned up at 20°C is liberated at 950°-1000°C and partially liberated at a lower temperature.

Hägg[17] has made an extensive study of tantalum-hydrogen system using the X ray diffraction method. The following phases are proposed to interpret the results: (1) alpha-phase, consists of a solid solution of hydrogen in the body-centered cubic structure, (2) beta-phase, corresponds to Ta_2H and has the hexagonal close packed structure with $a = 3.094$Å and $c = 4.923$Å and (3) gamma-phase, corresponds to TaH and has a face centered rhombic structure with $a = 4.811$Å, $b = 4.781$Å and $c = 3.434$Å. Smith[34] in a recent publication questions the methods used by Hägg[17] and his interpretation of the data.

Metal: The structure of columbium and tantalum are body-centered cubic with lattice parameters of 3.2941 ± 0.0003Å[28] and 3.2959 ± 0.0003Å[27] respectively. The densities are 8.509 and 16.655 respectively.

Apparatus and Method: The vacuum microbalance and associated equipment are used for all of the kinetic measurements.[12, 14] The sensitivity of the balance is 0.86 divisions per microgram and the weight change can be estimated to 0.3 microgram.

The vacuum system, ceramic furnace tube and associated equipment have been described.[8,10,12,14] The double-walled zircon furnace tube is sealed directly to the all glass vacuum system. McLeod gauge pressures of 10^{-6} mm of Hg or lower can be achieved at temperatures of 1175°C and perhaps higher. With this vacuum system we can heat columbium and tantalum to the reaction temperature without appreciable reaction.

The purification of O_2, N_2 and H_2 has been described.[9, 12, 14] Nitrogen gas is the most difficult gas to prepare free from objectionable impurities[9] since the reaction of nitrogen with columbium and tantalum is much slower than the reactions with oxygen and hydrogen. Lamp grade of nitrogen is used as the source in the preparation of the nitrogen. The nitrogen gas used shows an oxygen content of about 0.01 pct.

The methods used in carrying out the experiments have been described.[9, 12, 14]

Samples: The columbium metal is obtained from the Fansteel Metallurgical Corporation in the form of a sheet 3.3 mils thick. According to the manufacturer the columbium specimens contain 0.01 pct of carbon as a maximum and no more than a trace of Fe, Ti, Ta, Sn and Zr, while the tantalum specimens contain 99.9 pct of Ta, 0.03 pct C, maximum and 0.01 pct of Fe, maximum.

The specimens are cut from the sheet and weigh 0.6840 g. They have surface areas of about 20 sq cm for columbium and 10.5 sq cm for tantalum. The specimens are abraded starting with No. 1 grit paper and finishing with 4/0 paper. The last two stages of the abrading are carried out under purified kerosene. The kerosene is removed by washing in petroleum ether and finally washing in absolute alcohol. They are kept in a dessicator prior to use.

Discussion of Results

High Vacuum Reaction: In order to obtain reproducible data of scientific significance it is necessary to minimize the formation of oxide films in preparing the specimens and heating the specimens to the reaction temperature. The reactive metals are excellent getters to the small quantities of gas normally present in the best of high vacua.

By carrying out the last stages in the abrading procedures under purified kerosene, we tend to minimize the formation of films. Such specimens will contain the room temperature oxide film. These specimens are then heated to the reaction temperature as quickly as is feasible in the best of vacua that we can obtain.

Fig. 1 shows the behavior of a sample of columbium on heating between 300° and 1000°C in a vacuum of 10^{-6} mm of Hg or better. The weight change in micrograms per cm^2 is plotted against the time and the temperature is given at the top of the chart. During the initial period of the reaction, 300° to 464°C, gas is evolved and the specimen loses weight. Above 464°C the sample gains weight and the metal behaves as a getter to the gases present in the high vacuum. This behavior is similar to that found for zirconium.[9] Over a part of this temperature range the surface is probably film free and no film barrier exists to limit the reaction. The reaction is only limited by the rate at which the gases present collide with the metal.

Tantalum reacts in a similar manner to columbium when heated in a high vacuum although the extent of the reaction is considerably smaller.

The results show that if contamination of the columbium and tantalum is to be avoided at high temperatures care must be used to obtain the best possible vacuum conditions. The extent of this vacuum reaction is probably negligible below 400°C, the maximum temperature for the hydrogen and oxygen experiments. For the nitrogen reaction, temperatures of 500° to 800°C are used. At these temperatures some reaction is unavoidable. We estimate that this vacuum reaction can be made less than 0.5 micrograms per cm^2 for the maximum temperature if the specimens are brought to temperature in a period of 20 min.

Reaction with Oxygen: The reaction is studied as a function of the time, temperature and pressure and the results given in fig. 2-8. The weight gain in micrograms per cm^2 is plotted against the time in

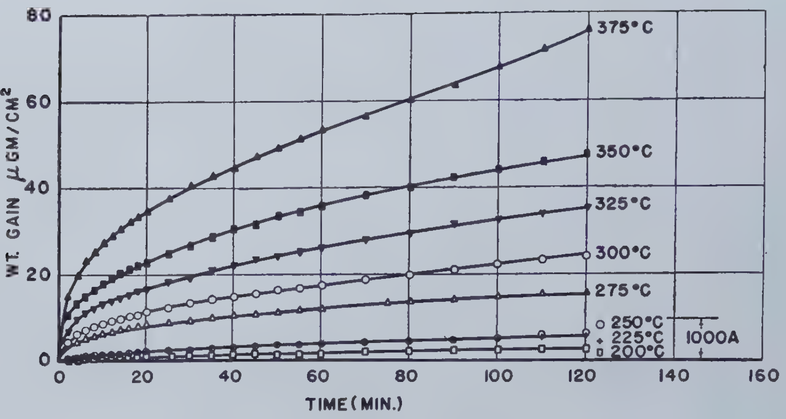

Fig. 2—Reaction of Cb with oxygen. Effect of temperature.

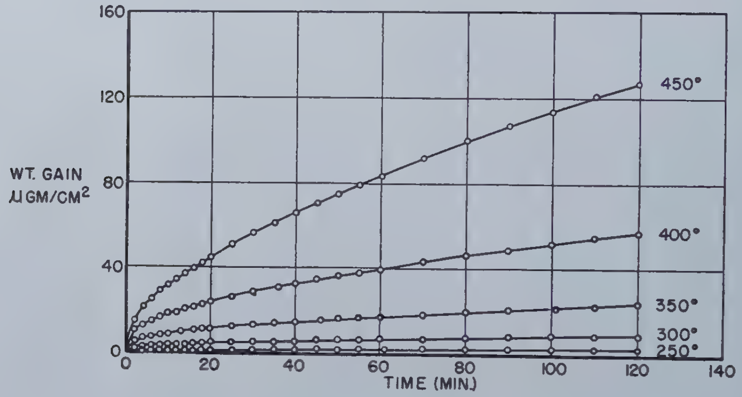

Fig. 3—Reaction of Ta with O_2. Effect of temperature.

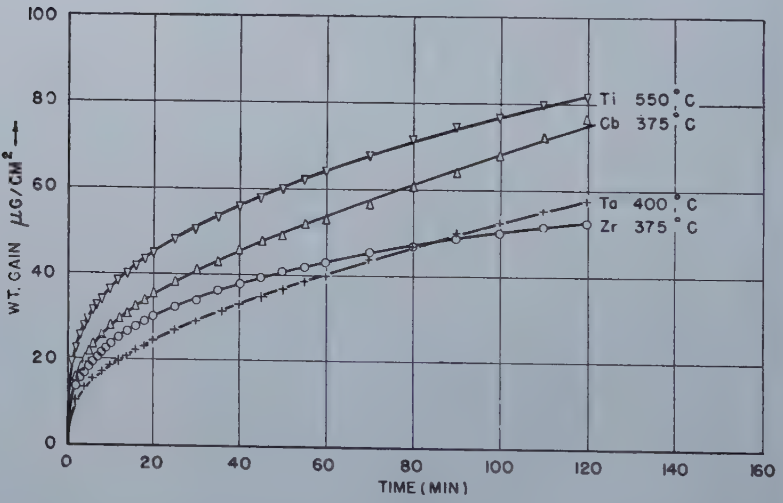

Fig. 4—Comparison oxidation of Ta with Cb, Ti and Zr.

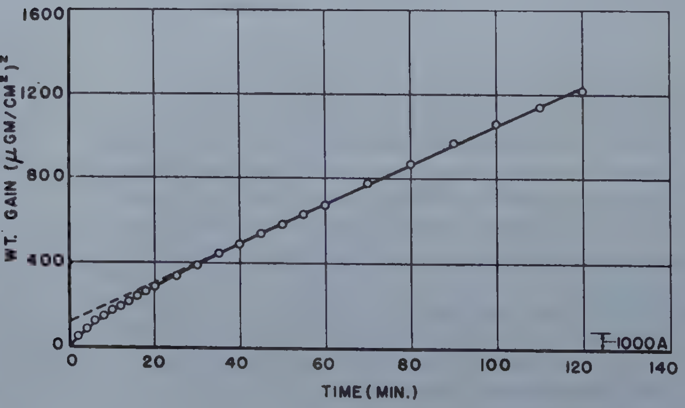

Fig. 5—Reaction of Cb with O_2. Parabolic plot.

minutes. Assuming the ratio of the real to measured area to be unity and the oxide to be CbO[29] for columbium and Ta_2O_5[1] for tantalum the thickness of the film in Angstroms is 108.5 and 69 times respectively the weight gain in micrograms per cm². Since the structure of the surface oxide film on tantalum has not been studied the conversion factor to Angstroms may be changed if the surface oxide turns out to be a structure different from Ta_2O_5.

1. *Time and Temperature:* Fig. 2 shows the time course of the oxidation experiments for the temperature range of 250° to 375°C for columbium and for an oxygen pressure of 7.6 cm of Hg while fig. 3 shows similar results for tantalum in the temperature range of 250° to 450°C. A rapid reaction is found for the initial part of the reaction and the rate of reaction decreases with the film thickness. In this sense the oxide film has protective properties.

Colored oxide films are observed on columbium after 2 hr of reaction for all of the temperatures. At 200°C a very faint straw tint to the film can be noticed. As the temperature is raised to 250°C the straw tint becomes more definite. At 300°C a blue film is found and at 350° and 375°C gray films are observed. It must be concluded that at these temperatures the rate of solution of the oxide is much less than the rate of reaction. At some higher temperature the rate of solution of the oxide becomes more rapid than the rate of formation of the film since no visible oxide films are observed.

The oxide films observed after 2 hr of reaction on tantalum for all of the temperatures show gray films at the oxidation temperatures of 250° to 350°C and blue gray films at 400° and 450°C. It must be concluded that at these temperatures the rate of solution of the oxide is much less than the rate of reaction.

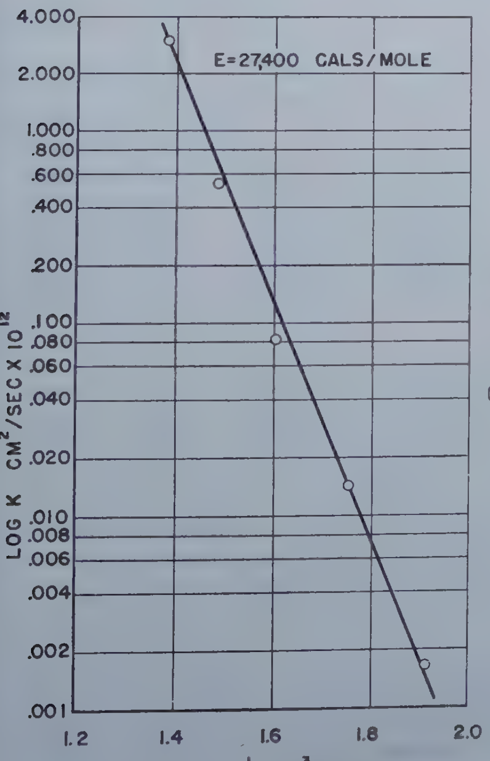

Fig. 6—Reaction of Ta with O_2. Log K vs $\frac{1}{T}$ (250°-450°C).

The effect of temperature on the time courses of the oxidation reaction for columbium is shown also in fig. 2. The temperature effect is very marked and the reaction appears to follow an exponential law. A comparison of the 200°C curve with the 375°C curve shows a film of 290Å to be formed after 2 hr of reaction at 200°C and a film of 8250Å at 375°C.

The effect of temperature on the time courses of the oxidation reaction for tantalum is shown in fig. 3. A comparison of the 250°C curve with the 450°C curve shows that after 2 hr of reaction a weight gain of 3.25 micrograms per cm² is found while a similar reaction time at 450°C gives a total reaction of 127.2 micrograms per cm². The temperature effect is uniform and appears to follow an exponential rate law.

Fig. 4 shows a comparison of the oxidation behavior of columbium and tantalum with titanium and zirconium. Although the reaction temperatures differ it is evident that tantalum oxidizes more rapidly than titanium but slower than columbium and zirconium.

2. *Time and Temperature Equations:* Three equations have been used to explain the time variation of the oxidation rate. These are:

(1) the parabolic law[25, 30, 41] $W^2 = Kt + c$
(2) the linear law $W = K't + c$ and
(3) the logarithmic law[35] $t = \beta\,(e^{W/\alpha} - 1)$

In the above equations W refers to the weight gain, t the time and K', K, c, β and α are constants.

The following equations are used to explain the temperature dependence of the reaction:

(1) Arrhenius equation[7] $K = Ae^{-E/RT}$
(2) Transition State Theory[13]

$$K = \frac{2kT}{h}\,\lambda^2\, e^{\Delta S^*/R}\, e^{-E/RT}$$

ΔS^* and E are the entropy and energy of activation, λ is the interatomic distance between diffusion sites, k is Boltzman's constant, h is Planck's constant, K is the parabolic rate law constant and A is the frequency factor. In the second equation the frequency factor A is identified with universal constants, λ^2 and the temperature independent factor $e^{\Delta S^*/R}$. For our purposes ΔS^* determines what fraction of ions or atoms with a definite energy pass over the energy barrier for reaction.

3. *Time and Temperature Correlation:* A study of fig. 2 and 3 shows that the data are not fitted by a linear rate law while plots of the weight gain vs. the logarithm of the time show smooth curves of increasing slope. The logarithmic law or linear rate laws do not apply for the conditions studied here.

Fig. 5 shows a parabolic rate law plot for the 325°C oxidation of columbium at 7.6 cm of O_2. The square of the weight gain is plotted against the time. Although some deviation is noted from the straight line during the initial stages of the reaction the fit is good. Deviations of this type from the parabolic have been predicted by the recent analyses of Mott.[26] Similar agreement with the parabolic rate law is found for the oxidation of tantalum.

4. *Temperature Dependence and Activation Energy:* The importance of the evaluation of the temperature coefficient of the reaction rate has been previously discussed.[9] Since the oxidation reaction

follows the predictions of the parabolic rate law it is possible to calculate not only the diffusion coefficients but also the energy and entropy of activation of the rate limiting process.

The temperature is involved in the transition state theory as part of the exponential term $e^{-E/RT}$ and also directly as T. However, the effect of the linear term is small compared to the exponential term. In the evaluation of E, logarithms of the parabolic rate constants for tantalum in units of cm² per sec are plotted against $\frac{1}{T}$ in fig. 6. The parabolic rate law constants vary from 1.25×10^{-15} at 200°C to 1.064×10^{-12} at 375°C for columbium and from 0.66×10^{-15} at 250°C to 1.205×10^{-12} at 450°C for tantalum. The density of the oxide CbO is assumed to be 6.27 while the density of the oxide Ta_2O_5 is assumed to be 8.015.[22] The slopes are evaluated for the time range of 60 to 120 min.

The data shown in fig. 6 show a straight line relationship. An energy of activation of 27,400 cal per mol is calculated for the oxidation reaction of tantalum. The temperature independent factors $e^{\Delta S^*/R}$ are evaluated from the transition state theory expression for K.

Similar analyses of the columbium oxidation data give an activation energy of 22,800 cal per mol.

Table I shows the values of the parabolic rate law constants, diffusion constants and the energies, entropies and free energies of the rate controlling process in the oxidation of columbium and tantalum.

It is of interest to compare in table II the parabolic rate law constants, the diffusion constants and the energies, entropies and free energies of activation for columbium, tantalum, titanium and zirconium with iron. The data on the values for K show that the order of increasing resistance to oxidation is columbium, tantalum, zirconium, titanium and iron. This can be shown also by a comparison of the ΔF^* for the reaction. Although tantalum has the highest energy of activation it is not as resistant to oxidation as iron, for example, since the entropy factor is not sufficiently negative to make the overall potential barrier as high. These results differ with those reported by McAdam and Geil[28] in which tantalum is stated to oxidize more slowly than zirconium and iron.

5. *Calculation of Diffusion Constants:* The calculation and interpretation of diffusion constants from the parabolic rate law expression have been discussed by Wagner,[42] Mott[35] and by the authors in a previous paper.[9] The diffusion coefficient D can be calculated from the parabolic rate law constant by the equation $D = \frac{K}{2}$. Typical values of D for columbium in its oxide are 3.68×10^{-15} cm² per sec at 250°C and 0.503×10^{-12} cm² per sec at 375°C while typical values for tantalum in its oxide are 3.3×10^{-16} cm² per sec at 250°C and 6.00×10^{-13} cm² per sec at 450°C. These values represent the coefficients of self diffusion of tantalum in its oxide.

Calculations by Huntington and Seitz[19] have shown that for the diffusion of copper in copper the diffusion of lattice defects is the most probable mechanism. It is possible that a similar conclusion holds for the formation of oxide films. The diffusion coefficients and activation energy thus may be associated with the formation and diffusion of metal lattice defects in the oxide.

6. *Pressure Effect:* The effect of pressure on the reaction at 400°C for tantalum is shown in fig. 7. The pressure is varied by a factor of 50 from 7.6 cm to 0.15 cm of oxygen. No simple relationship of the effect of pressure on the reaction rate can be determined. Similar results are observed in the oxidation of columbium for this pressure range. It is apparent that the reaction rate does not follow a simple linear or square root function of the pressure. Such relationship may be expected if the concentration gradient of the diffusing specie is dependent upon the external pressure.[4] We conclude that the small effects noted are in agreement with the fact that the limiting factor in the reaction is the diffusion of columbium or tantalum ions through the oxide film.

7. *Surface Preparation:* Fig. 8 shows a comparison of the oxidation curves of abraded with unabraded columbium at 300°C and for a pressure of

Table I. Parabolic Rate Constants and Diffusion Constants, Entropies, Energies and Free Energies of Activation for the Oxidation Process

A. Columbium

t°C	K, cm² per sec	Do, cm² per sec	ΔS^* Cal per mol per° C	E Cal per mol	$T \Delta S^*$ Cal per mol	ΔF^* Cal per mol
200	1.25×10^{-15}	2.07×10^{-5}	—12.0	22,800	—5680	28,480
225	5.24×10^{-15}	2.62×10^{-5}	—11.65	22,800	—5800	28,600
250	7.36×10^{-15}	1.195×10^{-5}	—13.3	22,800	—6960	29,760
275	6.51×10^{-14}	3.91×10^{-5}	—11.05	22,800	—6070	28,870
300	8.70×10^{-14}	2.08×10^{-5}	—12.40	22,800	—7110	29,910
325	1.11×10^{-13}	1.15×10^{-5}	—13.65	22,800	—8170	30,970
350	3.30×10^{-13}	1.57×10^{-5}	—13.10	22,800	—8160	30,960
375	1.06×10^{-12}	2.53×10^{-5}	—12.25	22,800	—7950	30,750

B. Tantalum

t°C	K, cm² per sec	Do, cm² per sec	ΔS^* Cal per mol per° C	E Cal per mol	$T \Delta S^*$ Cal per mol	ΔF^* Cal per mol
250	0.66×10^{-15}	8.85×10^{-5}	—9.33	27,400	—4880	32,280
300	0.57×10^{-14}	7.65×10^{-5}	—9.80	27,400	—5610	33,010
350	3.37×10^{-14}	6.70×10^{-5}	—10.20	27,400	—6360	33,760
400	2.165×10^{-13}	8.60×10^{-5}	—9.80	27,400	—6600	34,000
450	1.205×10^{-12}	11.5×10^{-5}	—9.45	27,400	—6845	34,245

Table II. Comparison of the Parabolic Rate Law and Diffusion Constants and the Energies, Entropies and Free Energies of Activation for the Active Metals with Iron at 350°C and 7.6 cm of O_2

Function	Ta	Cb	Ti	Zr	Fe
K cm² per sec	3.37×10^{-14}	3.30×10^{-13}	1.90×10^{-15}	4.28×10^{-14}	1.2×10^{-15}
Do cm² per sec	6.70×10^{-5}	1.57×10^{-5}	1.34×10^{-6}	5.3×10^{-8}	5.48×10^{-8}
E Cal per mol	27,400	22,800	26,000	18,200	22,600
ΔS^* entropy units	—10.20	—13.10	—18.00	—25.1	—24.60
ΔF^* Cal per mol	33,760	30,960	37,200	33,800	37,950

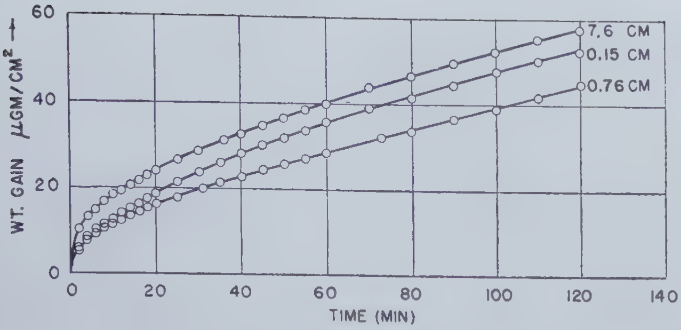

Fig. 7—Reaction of Ta with O_2. Effect of pressure 400°C.

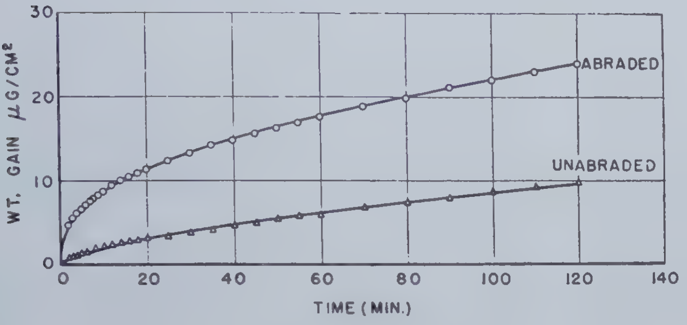

Fig. 8—Reaction of Cb with O_2. Effect of abrasion.

7.6 cm of O_2. The abraded sample reacts more rapidly than the unabraded. Without further knowledge of the history of the specimens before we receive them it is difficult to say whether the difference in reaction rates is due to the presence of a film or to structural differences in the metal.

Reaction with Nitrogen: In this section the reactions of columbium and tantalum with a purified lamp grade of nitrogen are studied as a function of time, temperature and pressure. The stability of the nitrogen reaction product to high vacuum conditions at high temperatures is also observed. The results are given in fig. 9 to 14. The weight of nitrogen absorbed in micrograms per cm² is plotted against the time in minutes. Thickness calculations are not made due to the uncertainty in the nature of the nitrogen reaction product.

Carefully purified lamp grade of nitrogen is used in the following experiments in order to avoid extraneous reactions with the impurities present in many sources of nitrogen.[9] The specimens are heated to the reaction temperature only after the system has been pumped down to pressures of 10^{-6} mm of Hg or lower in order to minimize the vacuum reaction.

1. *Comparison of Nitrogen Reaction on Tantalum with Columbium, Titanium and Zirconium:* Fig. 9 shows the comparison. Tantalum reacts at 700°C with nitrogen at about the same rate as columbium, faster than zirconium and somewhat slower than commercial titanium.

2. *Time and Temperature:* Fig. 10 and 11 show the time course of the reaction of columbium and tantalum with purified lamp grade of nitrogen for several temperatures. The reaction rate decreases as the reaction proceeds. The temperature effect is uniform. For columbium, at 800°C, a total reaction of 74 micrograms per cm² is observed while at 400°C a total reaction of 3.1 micrograms per cm² is found for a reaction time of 2 hr. For tantalum, at 850°C, a total reaction of 154.2 micrograms per cm² is observed while at 400°C a total reaction of 7.4 micrograms per cm² is found for a reaction time of 2 hr. The shapes of these curves are similar to what has been observed in other nitrogen reactions.[9, 11]

Table III. Parabolic Rate Law Constants. Nitrogen Reaction

t°C	T°K	1/T x 10³	K (g per cm²)² sec⁻¹
A. Columbium			
400	673.1	1.48566	1.55×10^{-15}
500	773.1	1.29349	5.55×10^{-15}
600	873.1	1.14534	2.97×10^{-14}
700	973.1	1.02764	1.512×10^{-13}
800	1073.1	0.93188	5.42×10^{-13}
B. Tantalum			
500	773.1	1.29349	9.6×10^{-15}
600	873.1	1.14534	1.78×10^{-14}
700	973.1	1.02764	1.89×10^{-13}
750	1023.1	0.97742	5.28×10^{-13}
800	1073.1	0.93188	1.14×10^{-12}
850	1123.1	0.89039	2.94×10^{-12}

The reactions of zirconium[9] and titanium[11] with nitrogen followed the parabolic rate law as a function of time. Fig. 12 shows a plot of the weight gain squared against the time in minutes, for the reaction of tantalum with pure nitrogen at 700°C and 7.6 cm of N_2. A similar correlation is found for columbium. The data deviate from the straight line during the early stages of the reaction. However, a straight line does fit the reaction over a considerable part of the time course. The parabolic rate law $W^2 = Kt + C$ explains empirically the time variation of the reaction.

In previous papers[9, 11] we have tried to place the nitrogen reaction on a physical basis. The method of van Liempt[30] was suggested to explain the time behavior of the reaction. Van Liempt has applied an approximate method for the solution of the diffusion equation for a flat plate. His equation is:

$$Q/Q_o = \frac{8}{d}\sqrt{\frac{Dt}{\pi}}$$

Here Q is the quantity of gas taken up or evolved at any time t, Q_o is the original quantity of gas in the metal, D is the diffusion coefficient and d is the thickness of the specimen. This expression also holds for the reverse process of absorption of gas in the metal. The expression reduces to the parabolic rate law, $W^2/W_o^2 = Kt + C$. Here W is the weight gain and W_o is the solubility at the temperature T. Since K involves the diffusion coefficient D and W_o is temperature dependent it is impossible to evaluate D unless W_o is known. We can, however, calculate an empirical energy of activation for the reaction.

Table III shows the parabolic rate law constants for the nitrogen reaction on columbium and tantalum while fig. 13 shows a logarithmic plot of the parabolic rate law constants K for the nitrogen reaction on tantalum against $\frac{1}{T}$. The data can be fitted by a straight line although at low temperatures a deviation occurs. An empirical energy of activation of 39,400 cal per mol is calculated. This value can be compared with a value of 25,400 obtained for the corresponding columbium reaction and values of 39,200 and 36,300 obtained for the zirconium and titanium reactions respectively.

It is of interest to note that the specimens after reaction with nitrogen show no visible evidence of colored films. The electron diffraction evidence is difficult to interpret. No patterns can be obtained from the surfaces. However, a slight abrasion of the surface gives a pattern which we have not been able to identify with any known structure although similar lines are found in our studies of the oxidation reaction. Whether these films are formed initially in the vacuum of the apparatus or as a result of abrasion has to be established.

3. *Pressure:* The effect of pressure on the time course of the nitrogen reaction at a temperature of 700°C for tantalum is shown in fig. 14. Similar results are observed for the reaction with columbium. The pressure is varied from 7.6 cm to 0.15 cm or by a factor of 50. Compared to the predictions of a linear or square root of pressure laws[4] the effect of pressure on the reaction rate is small. The largest effect is noted for the initial periods of the reaction.

The influence of pressure on the permeability of metals to gases has been discussed by Barrer[4] and by the authors.[9] Two permeation rate-pressure relationships have been used to explain the data. These are: (1) the linear rate law which is based on the mechanism of activated diffusion of nitrogen without dissociation and (2) the square root law which is based on the mechanism of activated diffusion with dissociation.

Since the pressure dependence does not fit either of the above rate expressions we are led to the conclusion that the factor W_o in the rate expression is not influenced by the gas pressure following Henry's law. Similar conclusions were reached for the nitrogen reaction on zirconium[9] and titanium.[11] In our previous papers we suggested that a film of nitride

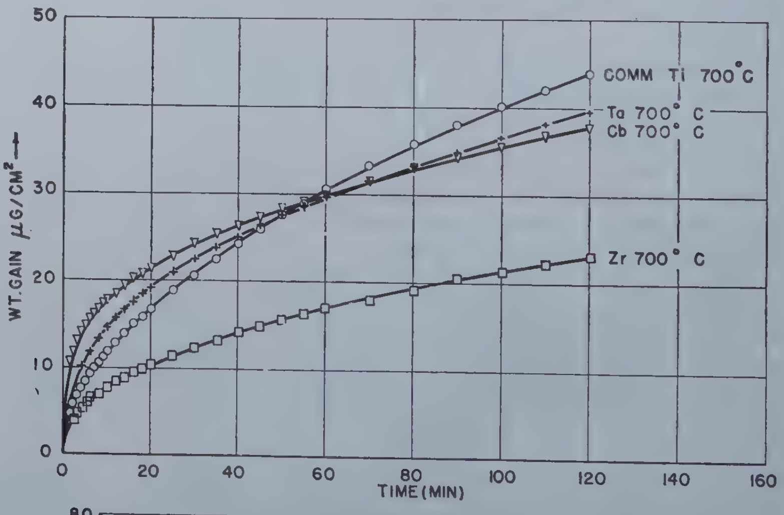

Fig. 9—Comparison N_2 reaction Ta with Cb, Zr and Ti 700°C.

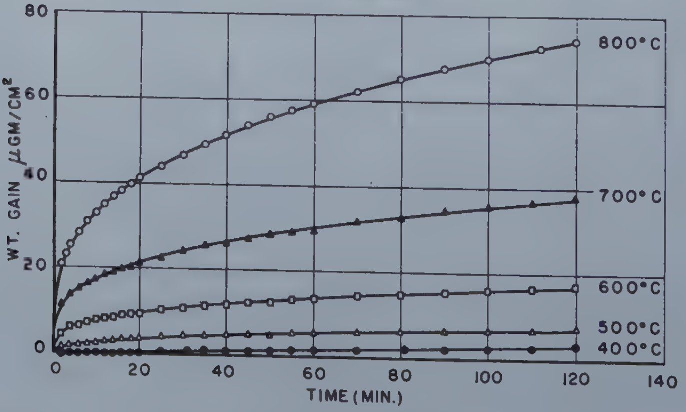

Fig. 10—Reaction of Cb with N_2. Effect of temperature.

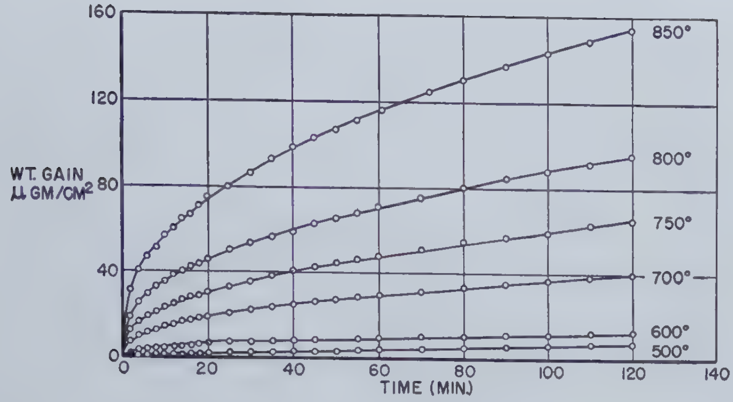

Fig. 11—Reaction of Ta with N_2. Effect of temperature.

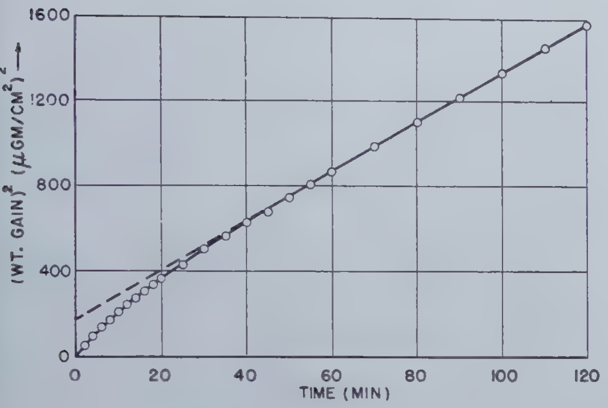

Fig. 12—Reaction of Ta with N_2. 700°C parabolic plot.

is present during the reaction which prevents the operation of Henry's law. This film disappears upon removing the reacting gas since the solution process continues after the gas is removed.

4. *Stability of Nitrogen Reaction Product:* The stability of the nitrogen reaction product on tantalum to high temperatures and high vacuum is tested by heating the 750° specimen containing 61.9 micrograms of nitrogen per cm² to 923°C in a vacuum of 10^{-6} mm of Hg or lower. Observations on the weight and pressure in the system showed that the specimen continued to react slowly with the gases given off in the vacuum. The nitrogen reaction product is stable to at least 923°C. These observations are in agreement with those of Wright[43] and of Andrews.[2]

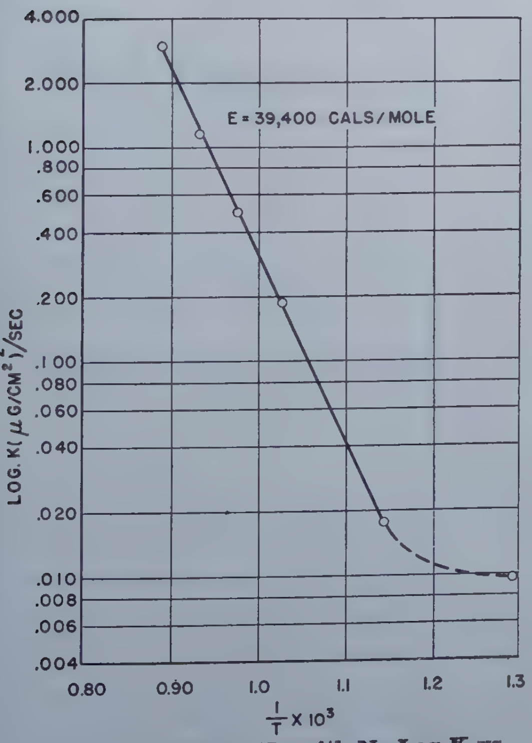

Fig. 13—Reaction of Ta with N_2. Log K vs. $\frac{1}{T}$ 500°-850°C.

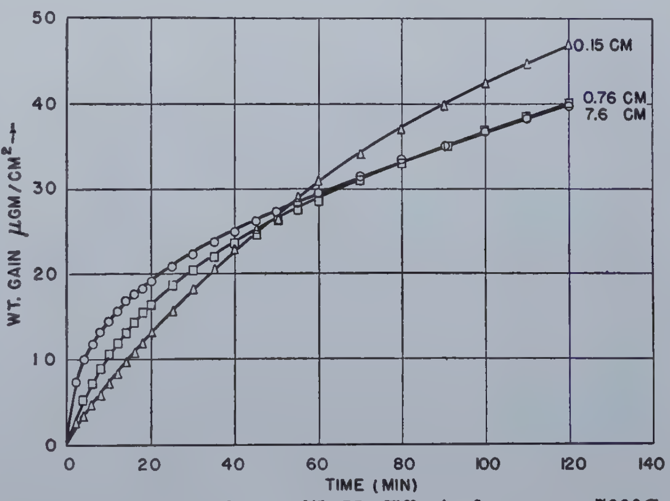

Fig. 14—Reaction of Ta with N_2. Effect of pressure 700°C.

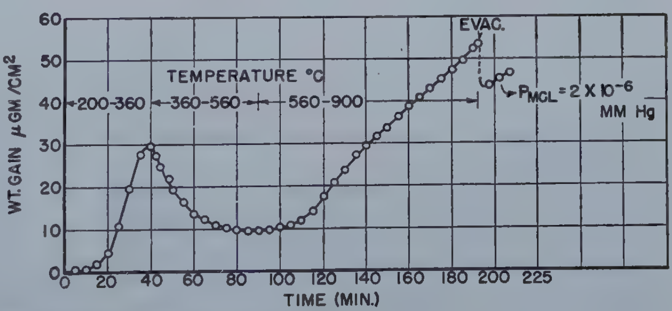

Fig. 15—Reaction of Cb with H_2. 200°-900°C. 2.4 cm H_2.

Fig. 16—Reaction of Ta with H_2. 200°-643°.

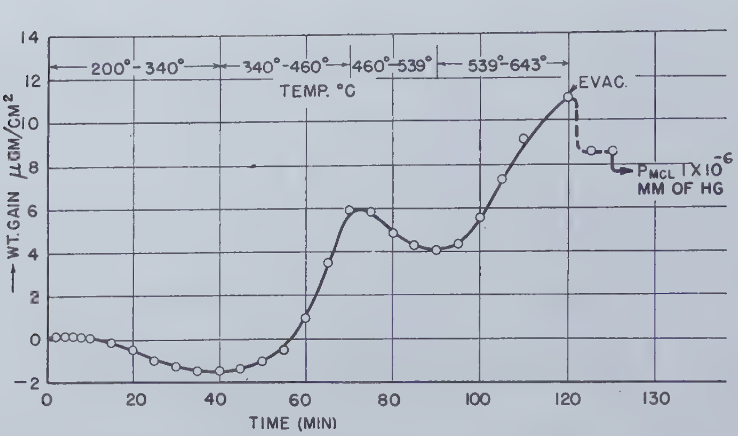

A similar study has been made on the stability of the nitrogen reaction product on columbium. No evidence is noted for decomposition of the nitrogen reaction product at temperatures up to 925°C.

Reaction with Hydrogen: The reaction is studied as a function of time, temperature and pressure and the results compared with the corresponding reactions on titanium and zirconium. The stability of the reaction product to high vacuum is studied as a function of the temperature. Fig. 15 to 27 show the results. The hydrogen used is prepared by diffusing a purified source through a palladium tube.

Preliminary studies of the reaction of columbium and tantalum with hydrogen are shown in fig. 15 and 16. The specimens are heated at approximately a uniform rate in the low pressure hydrogen atmosphere from 200°C to the maximum temperature. The weight gain in micrograms per cm² is plotted against the time in minutes and the temperature indicated at the top of the graph.

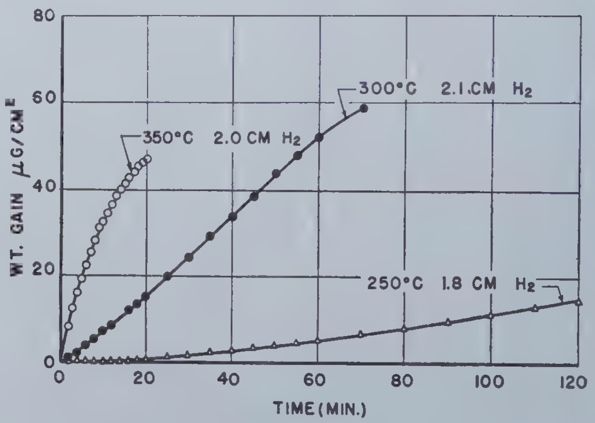

Fig. 17 (above)—Reaction Cb with H_2. 250°-350°C. Effect of temperature.

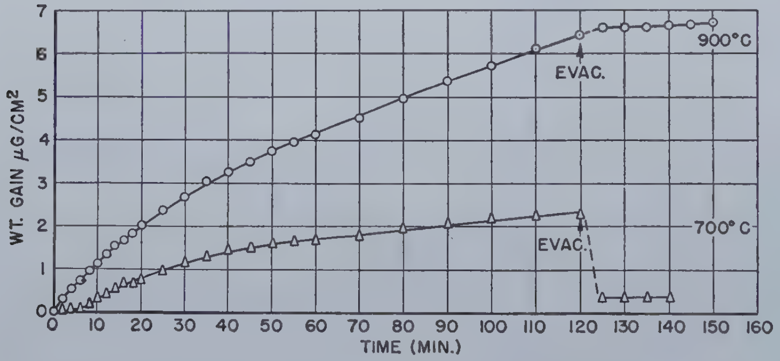

Fig. 18 (left)—Reaction Cb with H_2. 700°-900°C. Effect of temperature.

For columbium the reaction starts at a temperature of 250°C and increases rapidly as the temperature is raised. Above 360°C the sample loses weight and the low temperature hydride decomposes in the hydrogen atmosphere. At a temperature of 560°C columbium again reacts with the hydrogen and the rate increases with the temperature. Evacuation of the hydrogen at 900°C shows that the main part of the added hydrogen remains with the metal. In fact, the metal reacts at 900°C with the small quantities of hydrogen released from the ceramic vessel during the evacuation at a pressure of $2x10^{-6}$ mm of Hg. This reaction curve shows that two

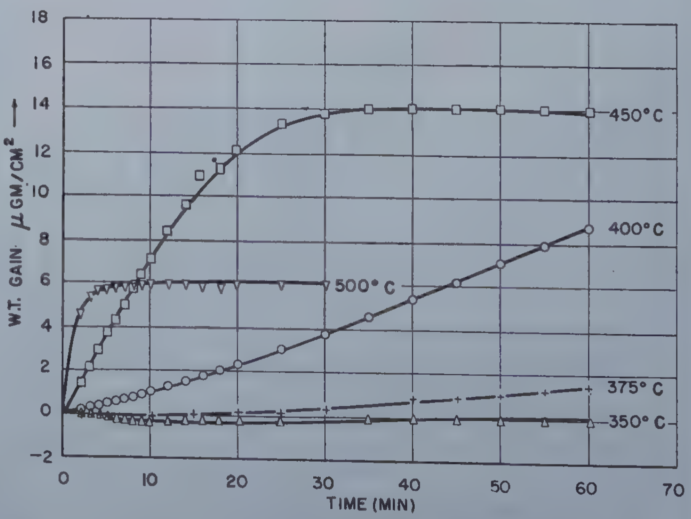

Fig. 19—Reaction of Ta with H_2. Effect of temperature 350°-500°C.

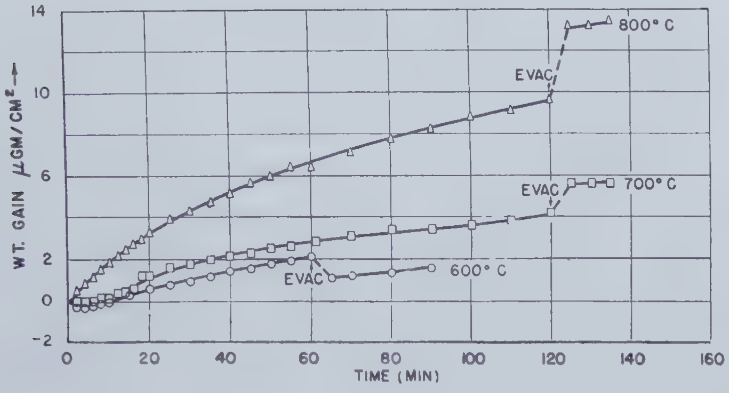

Fig. 20—Reaction of Ta with H_2. Effect of temperature 600°-800°C.

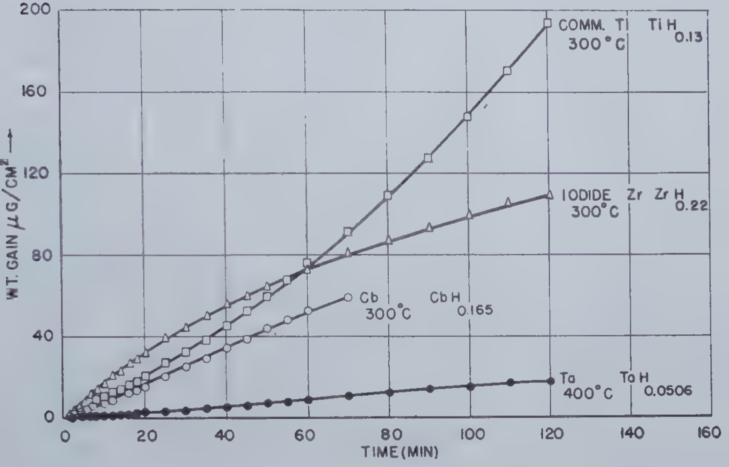

Fig. 21—Comparison of H_2 reaction Cb, Ti, Ta and Zr.

hydrides may form each with its range of stability. We have not attempted to determine the structure of these complexes or compounds.

In the case of tantalum the reaction starts at a temperature of 340° and the rate of reaction increases rapidly to a temperature of 460°C. Above this temperature the reaction stops and the specimen loses weight. We interpret this as indicating that the decomposition pressure of the hydride exceeds 2.8 cm of Hg. After a temperature of 539°C is reached the specimen again gains weight indicating that a new hydride is formed. The rate of the reaction appears to decrease above 643°C. Upon evacuating to a pressure of 10^{-6} mm of Hg or lower a part of the weight gain is removed. However, the major part of the added weight is stable.

1. *Time and Temperature:* Typical time and temperature curves for the hydrogen reaction on columbium are shown in fig. 17 and 18 for the temperature ranges of 250° to 350°C and 700° to 900°C. Each of the low temperature curves obeys a different rate law. The 300°C curve follows a linear rate law while at 350°C the rate decreases as the reaction proceeds. At 250°C the reaction rate increases as the reaction proceeds.

Typical time and temperature curves for the hydrogen reaction on tantalum are shown in fig. 19 and 20 for the temperature ranges of 350° to 500°C and for the range of 600° to 800°C. The shapes of the curves at 450° and 500°C in fig. 19 show a rapid initial reaction with a maximum amount of absorption attained after a certain period of reaction. The maximum absorption and the time to reach this maximum decrease as the temperature is raised. The 350°, 375° and 400°C curves show a linear reaction rate and that the maximum absorption has not been reached. The amount of hydrogen absorbed at 500°C corresponds to the formula $TaH_{0.017}$. It is of interest to note that the reactions above 350°C and up to 500°C all show an unstable reaction product. The absorption curves shown in fig. 20 for the temperature range of 600° to 800°C indicate a stable hydride to be formed and the rate of the reaction follows the predictions of the parabolic rate law.

A tentative physical basis for the several rate

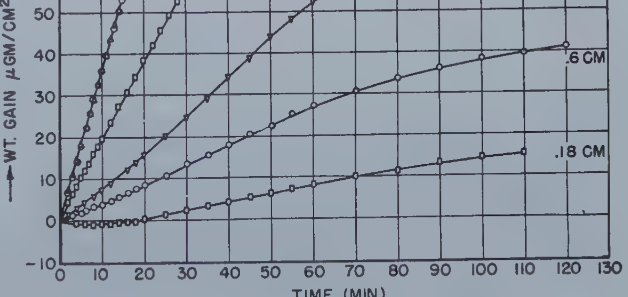

Fig. 22—Reaction Cb with H_2. Effect of pressure 300°C.

Fig. 23—Reaction Cb with H_2. Max. rate vs. $P^{1/2}$.

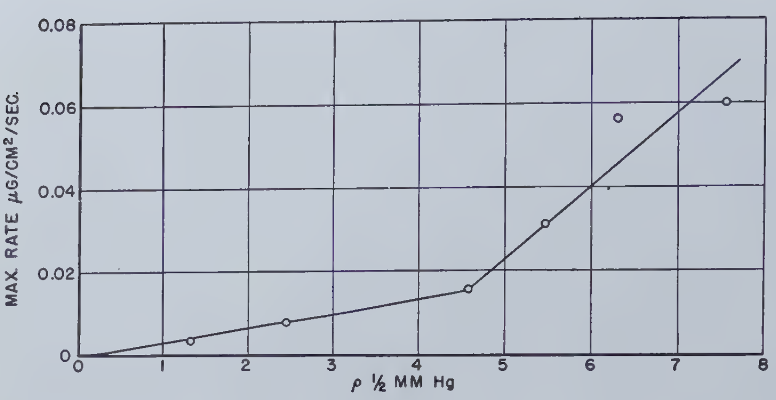

laws has been discussed by Smith[34] for the diffusion of hydrogen in palladium. Two processes are assumed. The first is the primary diffusion of hydrogen through the rifts in the metal and the second is the secondary diffusion of hydrogen from the rifts into the metal lattice.

If we assume the same theory for the hydrogen reaction on columbium and tantalum the governing process for the linear rate law at 300°C is the passage of hydrogen through the entry rifts and into an interior network where the hydrogen concentration remains small. The declining rate law observed at 350°C is explained by Smith[34] as due to the metal recovering from a thermal opening while the increasing rate curve observed at 250°C must be attributed to a process in which new openings are formed as the reaction proceeds.

The absorption data shown in fig. 18 and 20 for 700° and 900°C indicate a declining rate of reaction. A parabolic plot of the rate data indicates a straight line behavior. This special case of the declining rate law may be explained using the expression of van Liempt[39] $W/W_0 = K\sqrt{t}$ for the absorption of gases in metals. This equation has been discussed by Barrer[4] and by the authors under *Reaction with Nitrogen.*

The effect of temperature on the rate of reaction $\frac{dW}{dt}$ for tantalum may be discussed qualitatively. The low temperature hydride appears to have, from an analysis of fig. 19, a very high temperature coefficient while the high temperature form has a smaller temperature coefficient. Due to the extreme sensitivity of the hydride reaction to surface films, impurities and inhomogeneities in the metal it is difficult to evaluate the temperature coefficient and energy of activation.

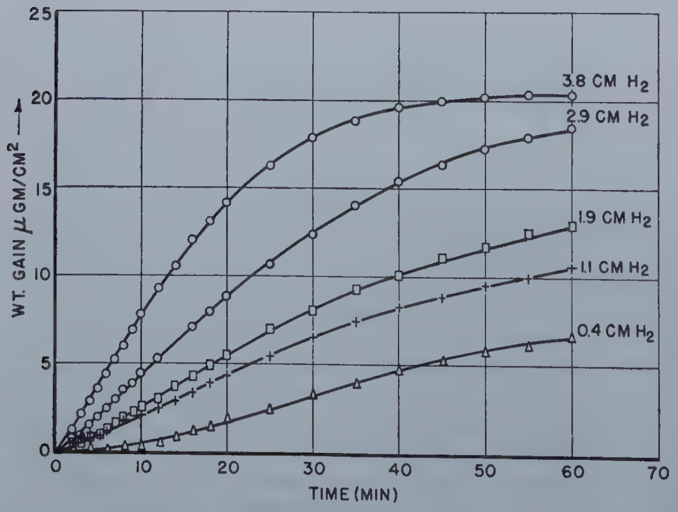

Fig. 24—Reaction of Ta with H_2. Effect of pressure.

2. *Comparison of the Hydrogen Reaction:* A comparison of the hydrogen reaction on the four metals is shown in fig. 21. Tantalum reacts at a much slower rate than the metals columbium, zirconium and titanium.

3. *Pressure:* Columbium: Fig. 22 shows the effect of pressure on the reaction at a temperature of 300°C over the pressure range of 5.7 cm to 0.18 cm of H_2. The effect of pressure is in marked contrast with what is found for the nitrogen reaction. Fig. 23 shows a plot of the initial reaction rates $\frac{dW}{dt}$ as a function of the square root of the pressure. The data can be fitted best by two straight lines. These results may be explained by the following rate law: $\frac{dW}{dt} = k\, p^{1/2}\, e^{-b/T}$ in which k takes on two different values. The agreement of the data with the simple square root law is observed for the hydrogen reactions on zirconium and titanium. The theoretical basis of the square root of pressure law has been discussed by Barrer[4] and by the authors.[9] The present theory indicates that the diffusion of hydrogen into the metal is occurring by atoms of hydrogen.

Tantalum: Fig. 24 shows the effect of pressure on the reaction at 400°C over the pressure range of 3.8 cm to 0.4 cm of Hg. Fig. 25 shows a plot of the initial reaction rates $\frac{dW}{dt}$ as a function of the square root of the pressure for two types of specimens. The upper curve shows the results for specimens abraded immediately before using while the lower curve shows similar results for specimens which had been abraded for several weeks and stored in a dessicator. The results show that the square root law is probably obeyed for pressures below about 2.5 cm of Hg. Above this pressure a break appears in the plot. The freshly abraded specimens give faster reaction rates than the regular abraded

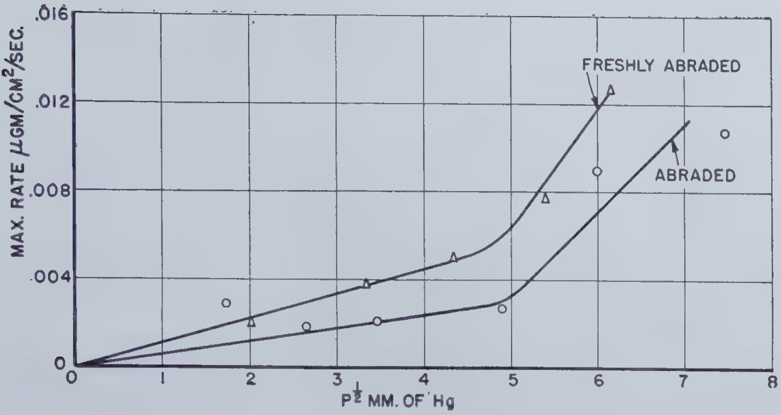

Fig. 25—Reaction of Ta with H_2. 400°C. Max. rate vs. $P^{1/2}$ mm.

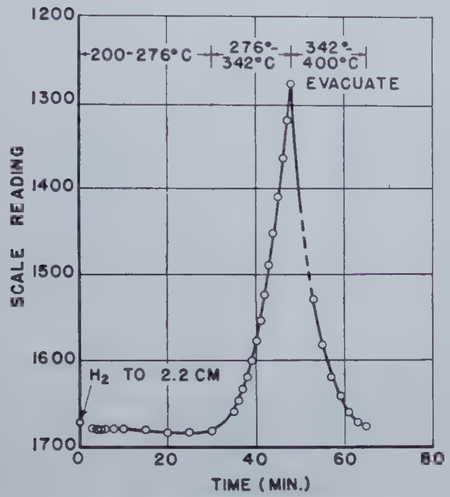

Fig. 26—Reaction Cb with H_2. 200°-400°C stability.

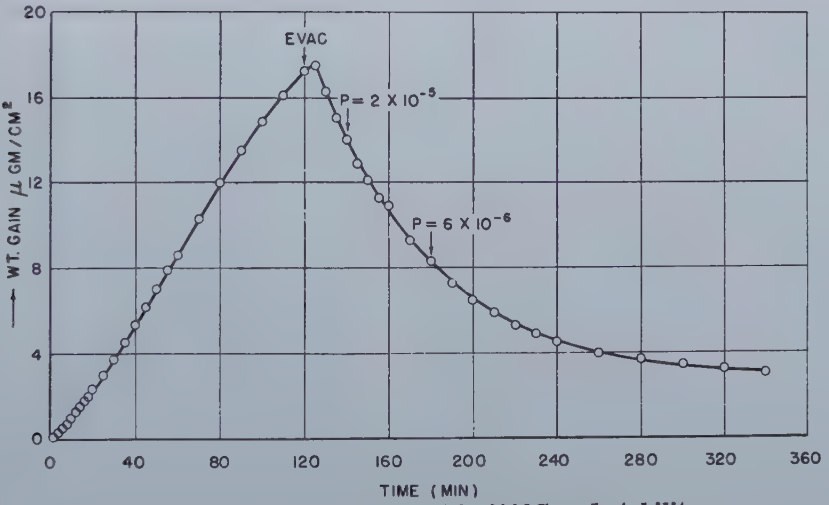

Fig. 27—Reaction of Ta with H_2. 400°C and stability.

samples. The results fit the same rate law as is found for the columbium reaction.

4. *Stability:* Columbium: The stability of the hydrogen reaction product formed at the several temperatures is tested by evacuating to 10^{-6} mm of Hg and observing the weight of the specimen and the pressure in the system. The reaction product is found to be relatively stable at 250°C. However, the reaction products formed at 300° and 350°C are unstable. An example of an unstable reaction product is shown in fig. 26. After evacuating at 342°C the reaction product decomposes. After the hydrogen is evolved the weight of the sample returns to its original value. These experiments indicate that at temperatures of between 250° and 300°C the hydrogen reaction product becomes unstable in high vacua. The hydrogen complex of columbium decomposes at a lower temperature than the corresponding complexes of titanium and zirconium.

The stability of the high temperature hydride formed at 700° and 900°C is shown in fig. 18. After evacuating to 10^{-6} mm of Hg the 900°C experiment shows that the reaction product is stable. However, the 700°C curve shows that a large part of the hydrogen is lost on evacuation.

Tantalum: Fig. 27 shows the reaction with hydrogen at 400°C in 2.4 cm of hydrogen. An absorption of 17.0 micrograms per cm² occurred in 2 hr of reaction. Upon evacuation the hydride decomposes in the vacuum. A similar study at 350°C shows that the hydride is stable to a vacua of 10^{-6} mm of Hg. Long period measurements may show a very small loss of hydrogen. The hydride formed at 500°C decomposed completely in a few minutes.

The hydrides formed at 700° and 800°C are stable as shown by the readings taken in a vacuum of 10^{-6} mm of Hg or lower in fig. 20. The weight change on evacuation is due to a buoyancy correction. The experiment at 600°C shows a stable hydride to be formed. Due to the buoyancy correction it is difficult to say whether there is present, in addition, a hydride which decomposed on evacuation.

Conclusions

The reactions of columbium and tantalum with oxygen, nitrogen and hydrogen and in high vacua are studied using the vacuum microbalance method.

In vacua of 10^{-6} mm or lower columbium loses weight below 464°C and tantalum loses weight below 605°C while at higher temperatures the metals act as getters in a similar manner to zirconium and columbium.

The reaction of columbium with oxygen is studied over the temperature range of 200° to 375°C and tantalum over the temperature range of 250° to 450°C. A modified form of the parabolic rate law is found to fit the data and energies of activation of 22,800 cal per mol and 27,400 cal per mol are calculated from the temperature dependence of the rate law constants for the columbium and tantalum reactions. Using the transition state theory, the entropies and free energies of activation of the rate controlling process are calculated and the values compared to those of other metals. At 350°C the order of increasing rates of reaction is titanium, zirconium, tantalum and columbium. The effect of pressure on the oxidation reaction is small.

The reactions of columbium and tantalum with nitrogen are studied over the temperature range of 500° to 850°C. The parabolic rate law may be fitted to the data. Using the method of van Liempt the parabolic rate law may be deduced from direct diffusion of nitrogen, into the metal. The reactions are not sensitive to pressure. The evidence indicates that the reactions are not taking place directly on the base metal but rather through a film of nitride which limits the pressure from exerting its normal influence on this type of reaction. The nitride film thickness is governed by the rate of formation and the rate of solution. The reaction products are stable to the highest temperature tested, namely 923°C.

A study of the hydrogen reaction shows that the rate of reaction is a function of the square root of the pressure. This evidence indicates that the hydrogen is diffusing into the columbium or tantalum lattice as atoms and the surface is essentially free from a hydride film. The hydrogen reaction product on columbium is stable in vacua of 10^{-6} mm of Hg to a temperature of 250°C. Above this temperature the reaction product decomposes. A high temperature reaction product is also observed. This reaction product is stable at 900°C to a vacua of the order of 10^{-6} mm of Hg. The reaction of tantalum with hydrogen shows that two possible stable hydrides are formed. A low temperature form exists below 350°C in high vacua and a high temperature form at temperatures above 700°C.

References

[1] Am. Soc. Test. Materials. "Original Set of X-ray Diffraction Patterns" (1942).

[2] M. R. Andrews: *Jnl.* Am. Chem. Soc. (1932) **54**, 1845-1854.

[3] G. Aschermann, E. Friederich, E. Justi and J. Kramer: *Physikalische. Ztschr.* (1941) **42**, 349-360.

[4] R. M. Barrer: Diffusion In and Through Solids. Univ. Press, Cambridge, England, 1941.

[5] K. Becker and F. Ebert: *Ztsch. f. Phys.* (1925) **31**, 268-272.

[6] G. Brauer: *Ztsch. anorg. allgem. Chem.* (1941) **248**, 1-31.

[7] J. S. Dunn: *Jnl.* Chem. Soc. (1929) 1149-1150.

[8] E. A. Gulbransen and K. Andrew: *Jnl. Phys. and Colloid Chem.* (1949) **53**, 690-711.

[9] E. A. Gulbransen and K. Andrew: *Trans.* AIME (1949) **185**, 515. *Jnl. of Metals,* Aug. 1949.

[10] E. A. Gulbransen and K. Andrew: *Jnl. Ind. and Eng. Chem.* In Press.

[11] E. A. Gulbransen and K. Andrew: *Trans.* AIME (1949) **185**, 741. *Jnl. of Metals,* Oct. 1949.

[12] E. A. Gulbransen: *Trans.* Electrochem. Soc. (1942) **81**, 187-197.

[13] E. A. Gulbransen: *Trans.* Electrochem. Soc. (1943) **83**, 301-313.

[14] E. A. Gulbransen: *Rev. Sci. Instr.* (1944) **15**, 201-204.

[15] G. Grube, O. Kubaschewski and K. Zwiauer: *Ztsch. Elektrochem* (1939) **45**, 885-888.

[16] H. Hagen and A. Sieverts: *Ztsch. anorg. allgem. Chem.* (1930) **185**, 225-238.

[17] G. Hägg: *Ztsch. phys. Chem.* (1930) **B11**. 433-454.

[18] F. H. Horn and W. T. Ziegler: J.A.C.S. (1947) **69**, 2762-2769.

[19] H. B. Huntington and F. Seitz: *Phys. Rev.* (1942) **61**, 315, 325.

[20] K. K. Kelley: *Jnl.* Am. Chem. Soc. (1940) **62**, 818-819.

[21] O. Kubaschewski: *Ztsch. Elektrochem.* (1940) **46**, 284-287.

[22] Landholt-Bornstein: Eg III a, p. 304.

[23] D. J. McAdam and G. G. Geil: *Jnl. Research* Natl. Bur. Stand. (1942) **28**, 593-635.

[24] H. Moissan: Bull. Soc. Chim (3) (1909) **28**, 434.

[25] N. F. Mott: *Trans.* Faraday Society (1940) **36**, 472.

[26] N. F. Mott: *Jnl.* Inst. of Metals. London (1946) **12**, 367-380.

[27] M. C. Neuberger: *Ztsch. Kristallogr.* (1936) **A 93**, 312-313.

[28] M. C. Neuberger: *Ztsch. Kristallogr.* (1936) **A 93**, 158-159.

[29] R. T. Phelps, E. A. Gulbransen and J. W. Hickman: I. and E. C. Analytical Ed. (1946) **18**, 391-400.

[30] N. B. Pilling and R. E. Bedworth: *Jnl.* Inst. Metals (1923) **29**, 529-582.

[31] A. Sieverts and E. Bergner: *Ber. Deutsch Chem. Ges.* (1911) **44**, 2394-2402. Quoted by D. P. Smith.

[32] A. Sieverts and H. Bruning: *Ztsch. f. phys. Chem.* (1935) **A 174**, 365-369.

[33] A. Sieverts and H. Moritz: *Ztsch. anorg. allgem. Chem.* (1941) **247**, 124-130.

[34] D. P. Smith: "Hydrogen in Metals". Univ. of Chicago Press, Chicago, Ill. (1948).

[35] G. Tammann and W. Köster: *Ztsch. anorg. allgem. Chem.* (1922) **123**, 196.

[36] Tech. Bull., Fansteel Metallurgical Corp. (1945) Chicago, Ill.

[37] Y. S. Umanski: *Jnl. Phys. Chem.* (U.S.S.R.) (1940) **14**, 332-339.

[38] A. E. Van Arkel: *Physica* (1924) **4**, 301.

[39] J. Van Liempt: Quoted by Barrer (ref. 4).

[40] W. Von Bolton: *Ztsch. Elektrochem* (1905) **11**, 47.

[41] C. Wagner and K. Grünewald: *Ztsch. Phys. Chem.* (1938) **40B**, 455.

[42] C. Wagner: *Ztsch. f. Elektrochemie* (1941) **47**, 696-704.

[43] D. A. Wright: *Nature* (1938) **142**, 794.

The Graphical Representation of Metallurgical Equilibria

by C. J. Osborn

The temperature dependence of the free energies of formation of metallurgically important oxides, sulphides, chlorides, carbonates and sulphates is presented graphically, whereby the task of deriving practical metallurgical information is greatly simplified.

The diagrams have been revised according to the latest available thermodynamic data.

WHILE it is true that much careful investigational work remains to be done, there are already available in the literature sufficient thermodynamic data to enable the metallurgist to predict with reasonable confidence the equilibrium conditions to be expected in most important, and potentially important, metallurgical reactions. In this connection, the careful, critical compilations of K. K. Kelley and his collaborators in numerous U. S. Bureau of Mines Bulletins are particularly valuable. However, the translation of reliable thermodynamic data into metallurgical language unfortunately involves lengthy manipulations of the cumbersome formulas which can be set up from heat of formation, entropy, and heat capacity data. Many years ago, Kelley[20] predicted that thermodynamic calculations would be made in the future "with the aid of free energy, heat content, and entropy tables, rather than by means of the algebraic methods employed at present", and where such tables are available they greatly simplify the task of deriving practical metallurgical information. However, in addition to these tables, there are also available one or two reliable graphical presentations, particularly of free energy data, which may be used in the same way as the tables, but which have the added advantages that interpolation is never necessary, and that the behavior of different metals or compounds may be compared at a glance.

Some years ago Professor Robert Lepsöe, Head of the Department of Metallurgy at Norways Institute of Technology (N.T.H.), began a compilation of curves showing the temperature dependence of the heat contents of the elements, and the heat contents and heats and free energies of formation of the common metallurgical compounds. With such a compilation, the thermal and free energy requirements of a reaction may be read from curves in a matter of seconds; and this statement applies not only to the formation of compounds from their elements, and to the reverse dissociation, but to any reaction involving substances whose thermodynamic properties are available. This follows from the fact that heats and free energies of formation are completely additive. For example, the free energy change associated with the chlorination of a metallic oxide at any temperature, T, is given by the free energy of formation of the chloride at temperature T minus that of the oxide also at T; both of these quantities may be read directly from curves of the type suggested above.

Since this early, unpublished work of Lepsöe, both Ellingham[7] and Richardson and Jeffes[46] have

---

C. J. OSBORN was formerly Research Fellow, Metallurgy Department, Norways Institute of Technology (Norges Tekniske Högskole), in Trondheim, Norway. He is now with the Council for Scientific and Industrial Research, Div. of Aeronautics, Melbourne, Australia.

TP 2720 CDE. Discussion (2 copies) may be sent to Transactions *AIME before Apr. 1, 1950, and will be published Nov. 1950. Manuscript received July 22, 1949; revision received Nov. 22, 1949.*

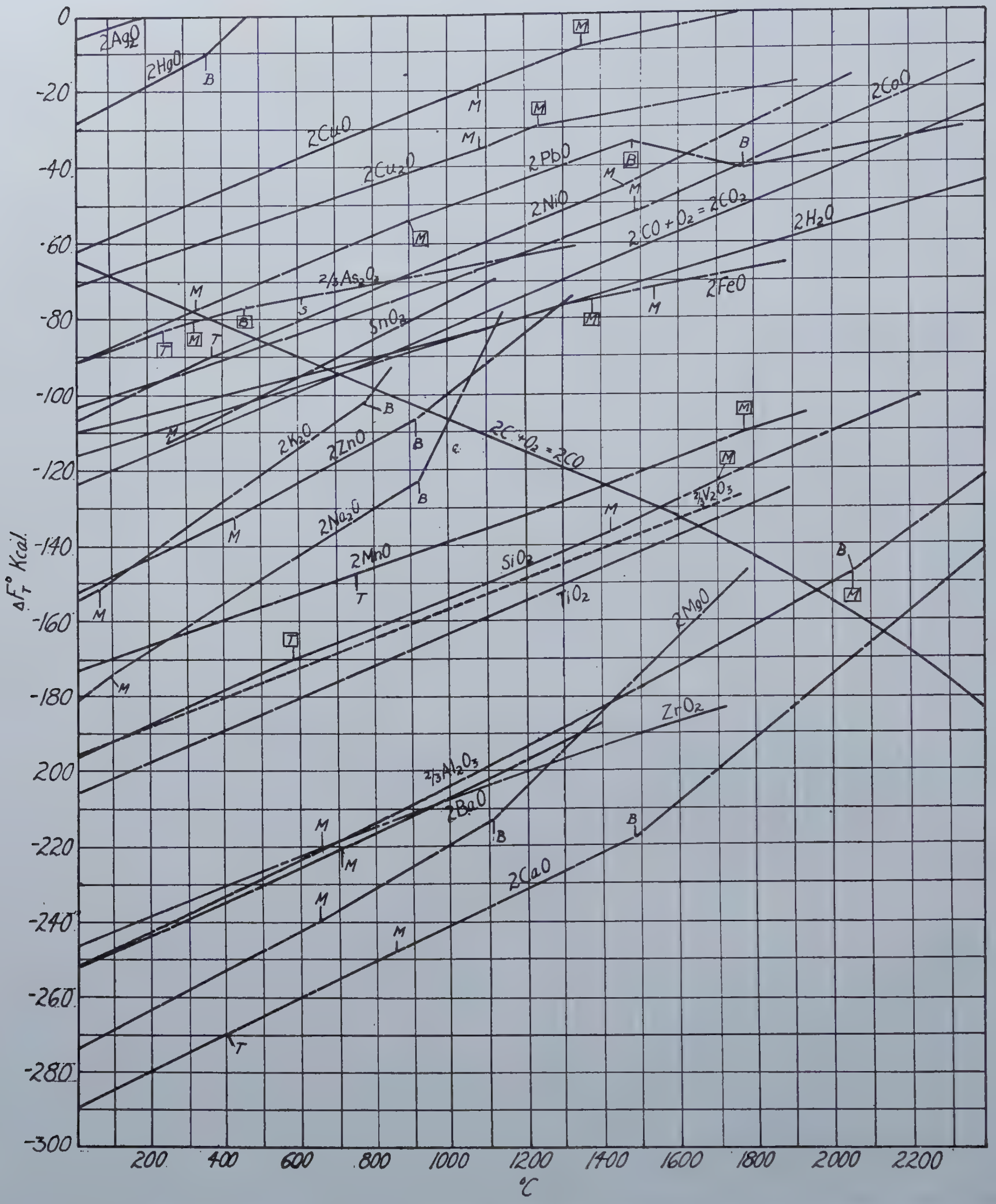

Fig. 1—Standard free energies of formation of metal oxides, for reactions involving 1 gram mol of oxygen.

published free energy curves, but there has been a need for a revised and more complete compilation. It is the aim of the present paper to meet this need, but it must be stated at the outset that some of the available curves of minor importance have been omitted from the diagrams in order to avoid congestion.

Standard Free Energy Changes: In the present paper, attention will be confined to curves illustrating the temperature dependence of the free energy of formation, because it is this type of curve which shows directly the equilibrium conditions to be expected. The significance of the free energy function cannot be discussed in detail in a paper of this nature, but there are two points in particular which may be emphasized before proceeding to a study of the actual curves. First, the decrease in free energy (—ΔF) accompanying any reaction is a measure of the tendency for the reaction to proceed, under the specified conditions. Second, the magnitude of the decrease in free energy accompanying a reaction at any temperature, T, depends on the activities of the participating substances.

Thus, for any chemical reaction:

$$aA + bB \ldots\ldots \rightleftarrows lL + mM + \ldots\ldots \quad [1]$$

the change in free energy at a given temperature and pressure is given by the van't Hoff "reaction isotherm"

$$\Delta F_{T,P} = -RT \ln K + RT \ln \frac{a^l{}_L a^m{}_M \ldots\ldots}{a^a{}_A a^b{}_B \ldots\ldots} \quad [2]$$

$$= -RT \ln K + RT \ln J_a, \quad [3]$$

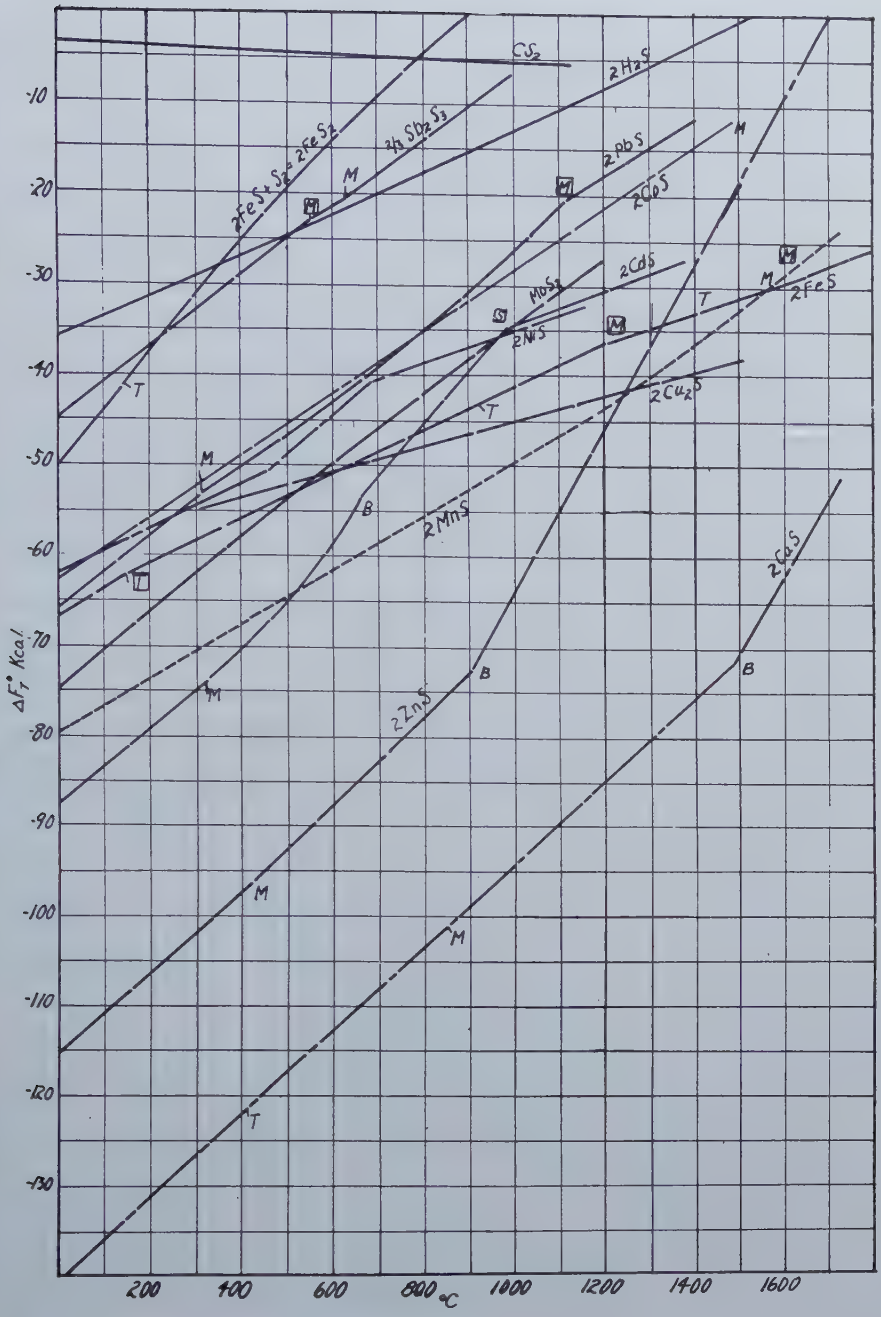

Fig. 2—Standard free energies of formation of metal sulphides, for reactions involving 1 gram mol of S_2 gas.

(With the exception of the curve for CaS, which involves 2 CaS + 100 k cal.)

where K is the equilibrium constant of the reaction at temperature, T, and is equal to the value of the activity function, J_a, at equilibrium. R is the gas constant ($R = 1.987$ cal. per deg.), T is the temperature in degrees Kelvin, and a_L, etc. are the activities of the various products and reactants. Since there is very little information available on the activities in solutions at high temperatures, it is generally necessary to assume that the activities in liquid or solid solutions are equal to the mol fractions, and that activities in gases are equal to the partial pressures. The activity of a pure liquid or solid phase is defined as unity.

If the activities of all reactants and products are unity, $J_a = 1$, the change in free energy is termed the "standard free energy change", ΔF°_T, and we may write

$$\Delta F^\circ_T = -RT \ln K \qquad [4]$$

or, for a reaction involving arbitrary activities,

$$\Delta F_T = \Delta F^\circ_T + RT \ln J_a \qquad [5]$$

Hence, if the standard free energy change, ΔF°_T, can be read from curves, the value of ΔF_T for any arbitrary values of the activities may be obtained simply by adding the activity correction, $RT \ln J_a$. Frequently this correction is not necessary, but a simple graphical method for applying it will be described later. Furthermore, it can be seen from Eq 4 that curves showing the variation of the standard free energy change, can be used to obtain the equilibrium constant, K, at any temperature, and from this it is usually a simple matter to calculate the equilibrium composition of the system at that temperature.

For a full discussion of the free energy concept, reference may be made to any of the standard texts on thermodynamics, such as those of Lewis and Randall[29], and Glasstone[9].

Methods of Calculation and Presentation: The curves to be presented in this paper were plotted from expressions for the standard free energy of formation as a function of temperature, which were derived by the usual methods from heat capacity, heat of formation, entropy and free energy data. Briefly, if the specific heats, C_p, of all substances concerned are known as functions of the absolute temperature, T, the heat of formation at any temperature is given by the relation

$$\Delta H_T = \Delta H_o + \int_0^T C_p \, dT \qquad [6]$$

An expression may then be derived for the standard free energy change by making use of the Gibbs-Helmholtz equation:

$$\left[\frac{\partial(\Delta F^\circ/_T)}{\partial T}\right]_p = -\frac{\Delta H}{T^2} \qquad [7]$$

Where phase changes occur in one of the substances involved, the expression derived by means of Eq 7 may be corrected by adding or subtracting a similar expression for the standard free energy change associated with the phase transformation.

In some cases, the curves have been plotted directly from expressions derived by Kelley[20, 25], Thompson[62], or Richardson and Jeffes[46]; wherever possible more recent data have been used.

The method of plotting free energies is similar to that used by Ellingham[7], in which the standard free energy of formation associated with the utilization of one gram-mol of the combining gas is plotted against the temperature. Five sets of compounds—

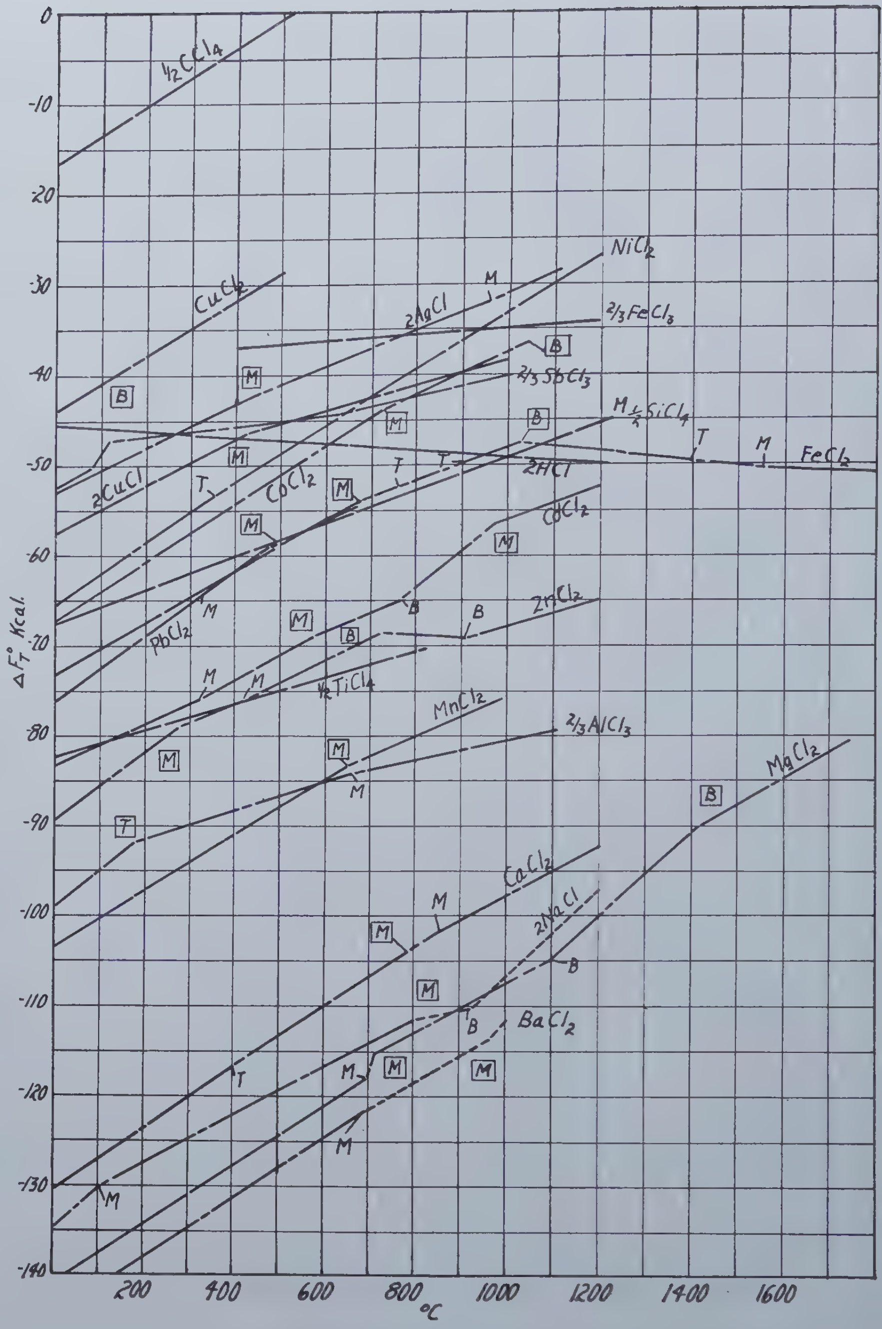

Fig. 3—Standard free energies of formation of metal chlorides, for reactions involving 1 gram mol of Cl_2 gas.

oxides, sulphides, chlorides, sulphates and carbonates—are given in fig. 1-5, and in each case the free energy change is that associated with the reaction of one gram-mol of the gas—O_2, S_2, Cl_2, SO_3, and CO_2 respectively—with the corresponding stoichiometric amounts of the metal or oxide. Actually, the curves for sulphates and carbonates give a free energy of reaction between the oxide and either sulphur trioxide or carbon dioxide, and not the usual free energy of formation from the elements.

This method of plotting has the advantage that, in any one class of compounds, it shows immediately which metals form more stable compounds than others. For example, in fig. 1, if at a particular temperature, *T*, the curve for the oxidation of the element *A* lies below that for the element *B*, the oxide of element *A* is more stable than that of element *B*, and there will be a tendency for element *A*, in the presence of the oxide of element *B*, to displace *B* from the oxide.

An attempt has been made to estimate the accuracy of the various curves, and to classify them according to the scheme suggested by Richardson and Jeffes[46]. Table I shows the method used to represent curves of different accuracy, but it must be emphasized that these accuracy ratings are only roughly correct. On the one hand, great care has been taken to use values which are considered most probably correct, but in some cases where very few experimental results are available, there is no means of assessing the correctness of the values chosen, so that the accuracy rating may become a matter of guess-work. In this connection it should be mentioned that the sulphate curves show a considerable discrepancy from results obtained by vapor pressure measurements for the decomposition of sulphates, Zn SO_4 and Fe SO_4 in particular. Due to the metallurgical importance of roasting reactions, there is an urgent need for further investigation of these equilibria.

A diagram showing the effect of temperature on the free energy of formation of various silicates (fig. 6) is reproduced here from a paper by Richardson[45].

Data Used for Calculations: The sources of data used in constructing fig. 1-5 are summarized in table II, but for the sake of simplicity only the information necessary to set up the basic free energy equation is given. Unless specifically listed in table II, all figures for melting points, heats of fusion, boiling points and heats of vaporization have been taken from either Metals Handbook, 1948[36], (elements only), from the compilations of K. K. Kelley[21, 22], or, when these sources failed, from Hodgman's "Handbook of Chemistry and Physics".[13]

The derivation of most of the oxide curves was described in greater detail in a previous paper[40].

Method of Correcting for Activities: The activity correction term, "$RT \ln J_a$", may be estimated for most practical cases from fig. 7, which shows the function $RT \ln a$ for $a = 2, 5, 10, 100,$ and 1000. For each of the participating substances which is not present in its standard state of unit activity, a correction term may be read from fig. 7 and then multiplied by the numerical coefficient of its molecular formula in the reaction equation (i.e. the factors $a, b, l, m, \ldots$ in Eq 1). This correction term must be added to ΔF°_T if it concerns a reaction

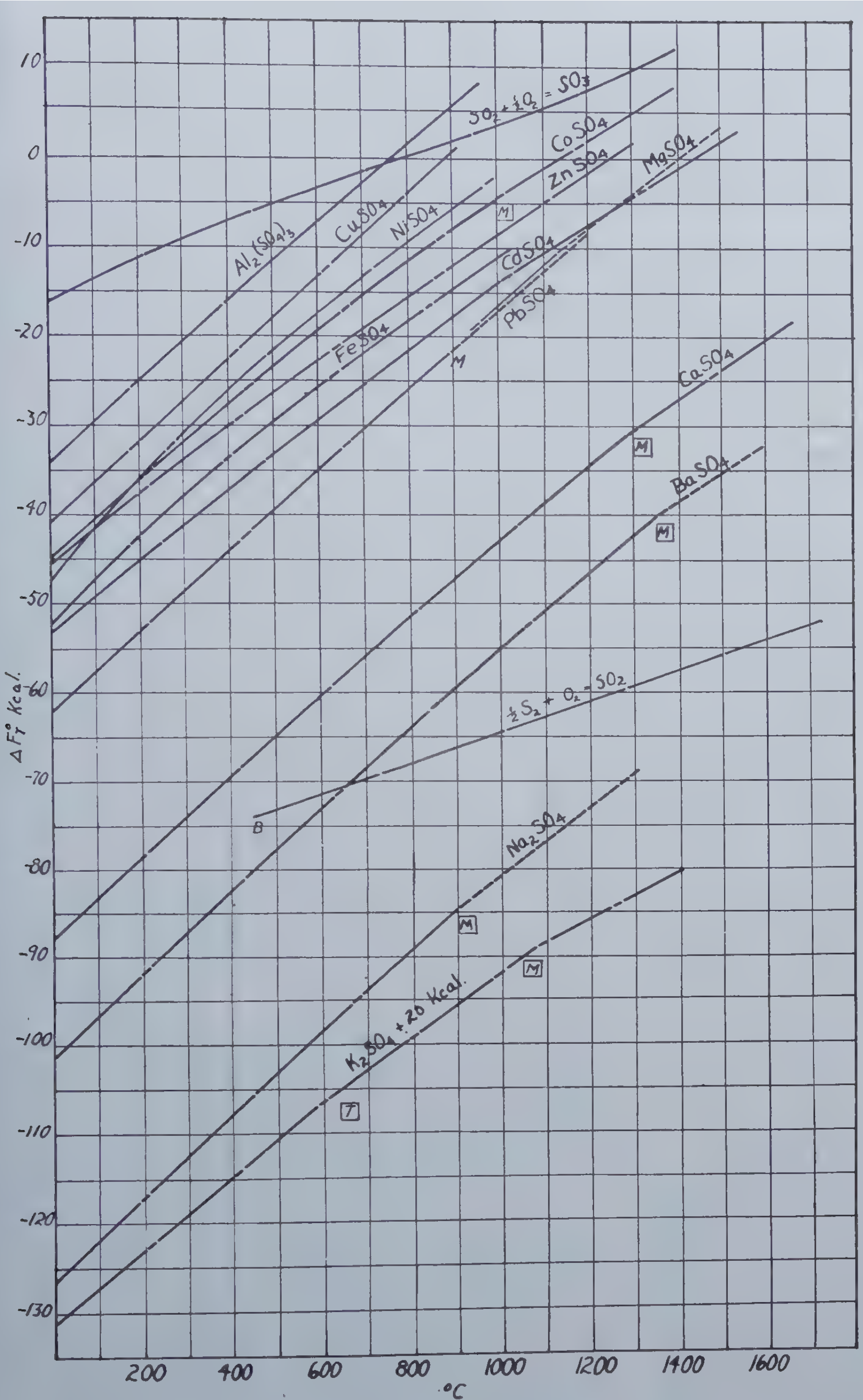

Fig. 4—Standard free energies of formation of metal sulphates from the oxide and SO_3, for the reaction involving 1 gram mol of SO_3 gas.

Table I. Key to Free Energy Diagrams

Changes of State	Element or Other Starting Material	Product
Melting Point	M	[M]
Boiling Point	B	[B]
Sublimation Point	S	[S]
Transition Point	T	[T]

Probable Accuracy of Data:

————————	± 1 kilocal
——— ———	± 3 kilocal
—— — ——	±10 kilocal
…………………………	>±10 kilocal

product, and subtracted if it concerns a reactant. Further, if a is less than unity, as in the case of gases at partial pressures less than 1 atm, or in solid or liquid solutions, the corrections must be read for the reciprocal of a, and added to ΔF°$_T$ if it concerns a reactant, and subtracted if it concerns a reaction product.

Conclusion

In conclusion, it must be emphasized that, while an attempt has been made to use the most reliable thermodynamic data available to draw the diagrams presented herein, there are certain apparently anomalous features which must be treated with caution. An example is the position of the alkali metal curves in the oxide diagram, fig. 1; these fall higher than would be expected. It must also be remembered that the phase transformation points shown in the diagrams are those of the pure substances, and the temperatures in practice will frequently be lowered by the mutual solubility of two or more substances. While the activity corrections involved in solutions may often be small in com-

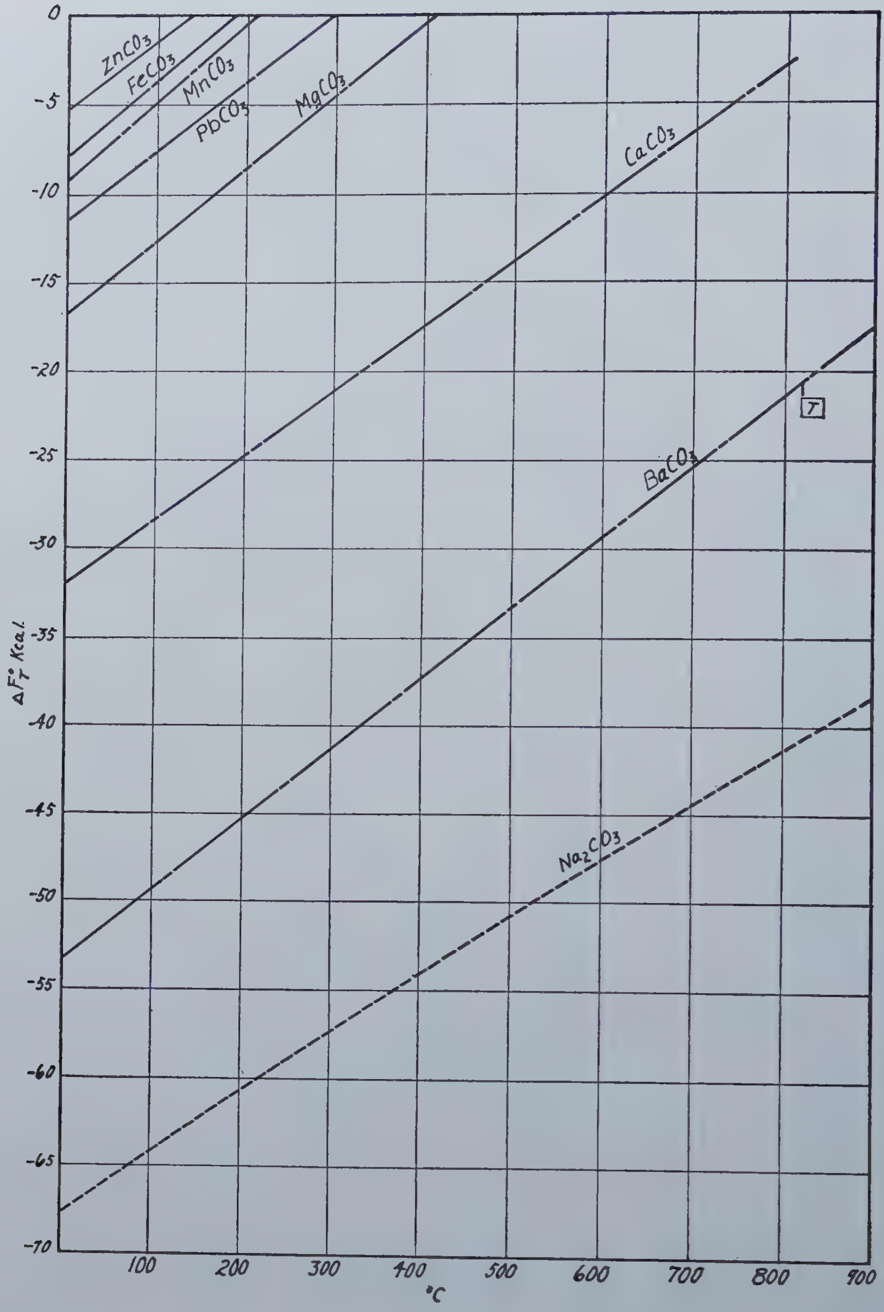

Fig. 5—Standard free energies of formation of metal carbonates from the oxide and CO_2, for the reaction involving 1 gram mol of CO_2 gas.

parison with the free energy of formation, they are frequently significant in considering displacements and other reactions involving smaller free energy changes, so that a detailed application of the diagrams requires a more detailed knowledge of the phase relations in the system.

However, the diagrams as they stand will furnish considerable useful information as to general tendencies. The only caution necessary here is that, if a metal can exhibit more than one valency in forming any type of compound, and if the curve shown is not that for the lowest valency compound, it may be possible for that particular metal to displace certain metals which lie lower on the diagram than does the given curve. This speculation may be applied to the lower oxides of titanium, for example. In the case of tin oxides, the curves for SnO and SnO_2 almost coincide, and only one curve is presented here.

Acknowledgments

The author desires to acknowledge his indebtedness to Professor Robert Lepsöe for suggesting this project and to A. B. Winterbottom and T. Smedsland for advice and assistance in the course of his work.

Table II. Sources of Data Used in Calculation

	DATA USED
Al_2O_3	ΔH_{298}^{51}; C_p: $Al_2O_3^{56}$, Al^{20}, O_2^{16}: $S^\circ_{298}{}^{24}$; equil., 1500-2073 °K^{64}
As_2O_3	ΔH_{298}^{3}; C_p: $As_2O_3^{20}$, As^{20}, O_2^{58}; $S^\circ_{298}{}^{24}$; $\Delta F^\circ_{298}{}^{28}$
BaO	ΔH_{298}^{3}; C_p: O_2^{58}, others Kopp's Rule; $S^\circ_{298}{}^{27}$, others^{24}
CdO	$\Delta H_{298}^{3,33}$; C_p: O_2^{16}, others^{20}; $\Delta F^\circ_{298}{}^{:32,33}$ and third law^{24}.
CaO	ΔF°_T, 298-1124 °K^{62}; high temperatures recalculated.
CO, CO_2	$\Delta F^\circ_T{}^{,62}$
CoO	ΔH_{298}^{3}; C_p: O_2^{16}, Co^{20}, CoO Kopp's Rule; equil.^{70}
Cu_2O	$\Delta H_{298}^{3,62,33}$; C_p: O_2^{16}, Cu^{20}, Cu_2O^{48}; $\Delta F^\circ_{298}{}^{62,33}$ and third law^{24}
CuO	ΔF°_T, 298-1357 °K^{62}; $\Delta H_{fus.}$, CuO^{48}
H_2O	$\Delta F^\circ_T{}^{62}$
Fe oxides	$\Delta F^\circ_T{}^{,46}$
PbO	$\Delta H_{298}^{3,33}$; C_p:O_2^{16}, Pb^{20}, PbO^{61}; $\Delta F^\circ_{298}{}^{62,33}$; red to yellow PbO, $\Delta F^\circ_{298}{}^{44}$
MgO	ΔH_{298}^{55}; Cp; O_2^{16}, others^{20}; $\Delta S^\circ_{298}{}^{24}$
MnO	ΔF°_T, 298-1500 °K^{57}; ΔF°_T, 1500 °K^{46}
HgO	ΔH_{298}^{3}; C_p:O_2^{16}, Hg^{20}, HgO^{11}; $\Delta F^\circ_{298}{}^{14}$; $\Delta F^\circ_{630}{}^{29}$; $\Delta S^\circ_{298}{}^{24}$
NiO	$\Delta F^\circ_T{}^{,62}$ corrected^{,40}
K_2O	ΔH_{298}^{3}; C_p: O_2^{16}, K^{20}; assume C_p and ΔS°_{298} for K_2O same as $Na_2O^{1,24}$
SiO_2	ΔH_{298}^{49}; C_p: O_2^{16}, others^{20}; $\Delta S^\circ_{298}{}^{24}$
Ag_2O	ΔH_{298}^{42}; C_p: O_2^{58}, Ag^{20}, Ag_2O^{42}; $\Delta F^\circ_{298}{}^{42,33}$
Na_2O	ΔF°_T, 298-1165 °K^{62}; high temperatures recalculated

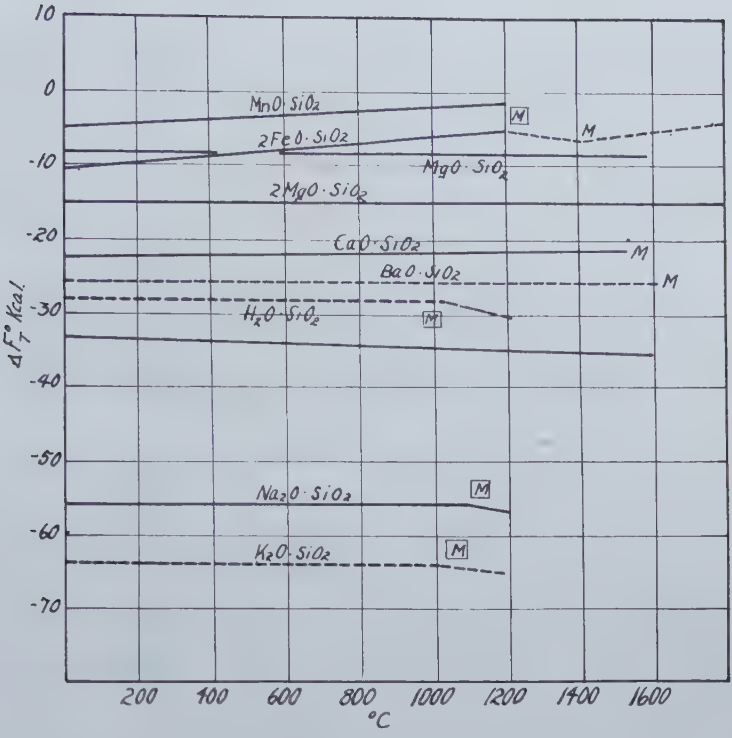

Fig. 6—Standard free energies of formation of metal silicates from the oxide and 1 gram mol of SiO_2.

Taken from Richardson[45]

SnO_2	ΔH_{298}^{3}; C_p: O_2^{16}, others[20]; ΔF°_{298}: equil.[62], emf[32], third law[24]
TiO_2	ΔH_{298}^{3}; C_p: O_2^{16}, Ti^{20}, TiO_2^{39}; ΔS°_{298}: TiO^{53}, others[24]
V_2O_3	$\Delta F^\circ_T{}^{46}$
ZnO	ΔH_{298}^{65}; C_p:O_2^{16}, others[20]; equil., emf, solubility[62,33], third law[24]
ZrO_2	$\Delta F^\circ_T{}^{62}$
SULPHIDES	
Sb_2,S_3,Cds,	CaS, CS_2, CoS, H_2S, PbS, MoS_2 use Kelley's[23] equations converted to formation from S_2, gas
Cu_2S	$\Delta F^\circ_T{}^{23,6}$
FeS	$\Delta F^\circ_T{}^{23,6}$
FeS_2	Mean of $\Delta F^\circ_T{}^{23}$ and ΔF°_T calculated from same experimental results[23], but assuming a known ΔH_{298}^{30} instead of a known ΔS°_{298}.
MnS	Cp: Mn^{62}, others[23]; S°_{298}:Mn^{54}, others[24]; equil.[6]
NiS	ΔH_{298}^{3}; C_p: S_2^{23}, others[20]; ΔF°_{298}: third law, assuming ΔS°_{298} as for FeS[24].
Ag_2S	ΔH_{298}^{34}; ΔC_p:[23], $\Delta F^\circ_{298}{}^{34}$; see also[47]
ZnS	ΔH_{298}^{19}; ΔC_p^{23}; ΔS°_{298} from[24]; see[31]
CHLORIDES	
$AlCl_3$	ΔH_{298}^{10}; C_p: Cl_2^{60}, Al^{20}, $AlCl_3$ (est.); S°_{298}:Al^8, Cl_2^{24}, $AlCl_3^{10}$; equil.[66]
$SbCl_3$	ΔH_{298}^{3}; C_p: Cl_2^{60}, others[20]; $\Delta F^\circ_{298}{}^{28}$.
$BaCl_2$	ΔH_{298}^{3}; C_p: Cl_2^{60}, $BaCl_2^{20}$, Ba (Kopp's Rule); S°_{298}: Cl_2^{24}, others[68]
$CdCl_2$	ΔH_{298}^{3}; C_p: Cl_2^{60}, Cd^{20}, $CdCl_2$ (Kopp's Rule); $S^\circ_{298}{}^{24}$.
$CaCl_2$	ΔH_{298}^{3}; C_p: Cl_2^{60}, Ca^{20}, $CaCl_2^{38}$; S°_{298}: $CaCl_2^{26}$, others[24]
C Cl_4	ΔH_{298}^{3}; C_p: Cl_2^{60}, C^{20}, CCl_4^{59}; S°_{298}:CCl_4^{12}, others[24]
$CoCl_2$	ΔH_{298}^{3}; C_p: Cl_2^{60}, Co^{20}, $CoCl_2$ (Kopp's Rule); $\Delta S^\circ_{298}{}^{24}$
CuCl	ΔH_{298}^{67}; C_p: Cl_2^{60}, Cu^{20}, CuCl (Kopp's Rule); $\Delta F^\circ_{298}{}^{67}$
$CuCl_2$	ΔH_{298}^{3}; C_p: Cl_2^{60}, Cu^{20}, $CuCl_2$ (Kopp's Rule); S°_{298}: $CuCl_2$ (est.), Cu^8, Cl_2^{24}
HCl	ΔH_{298}^{3}; C_p: all[60]; $\Delta F^\circ_{298}{}^{28}$; $\Delta S^\circ_{298}{}^{24}$
$FeCl_2$	ΔH_{298}^{3} C_p: Cl_2^{60}, $Fe^{41,15}$, $FeCl_2^{38}$; S°_{298}:$FeCl_2^{26}$, others[24]
$FeCl_3$	Cp,$FeCl_3$ (est.); equil. measurements[5,63]
$PbCl_2$	ΔH_{298}^{3}; C_p: Cl_2^{60}, others[20]; $\Delta F^\circ_{298}{}^{28}$
$MgCl_2$	ΔH_{298}^{55}; C_p: $MgCl_2^{38}$, others[20]; S°_{298}:$MgCl_2^{26}$, others[24]
$MnCl_2$	ΔH_{298}^{3}; C_p: Cl_2^{60}, Mn^{62}, $MnCl_2^{38}$; S°_{298}: $MnCl_2^{26}$, others[24]
$NiCl_2$	ΔH_{298}^{3}; C_p: Cl_2^{60}, Ni^{20}, $NiCl_2^{21}$; $\Delta S^\circ_{298}{}^{24}$
$SiCl_4$	ΔH_{298}^{3}; C_p: Cl_2^{60}, Si^{20}, $SiCl_4^{58}$; $\Delta S^\circ_{298}{}^{24}$
AgCl	ΔH_{298}^{3}; C_p: Cl_2^{60}, others[20]; $F^\circ_{298}{}^{28}$
NaCl	ΔH_{298}^{3}; C_p: Cl_2^{60}, others[20]; $\Delta F^\circ_{298}{}^{28}$
$TiCl_4$	ΔH_{298}^{3}; C_p: Cl_2^{60}, Ti^{20}, $TiCl_4^{58}$; $\Delta S^\circ_{298}{}^{24}$
$ZnCl_2$	ΔH_{298}^{2}; C_p: Cl_2^{60}, others[20]; $\Delta F^\circ_{298}{}^{2}$
SULPHATES	
SO_2	$\Delta F^\circ_T{}^{23}$
SO_3	ΔH_{298}^{17}; C_p: SO_3^{58}, SO_2^{23}, O_2^{20}; S°_{298}: $SO_3^{17,24}$, others[24]; also $\Delta F^\circ_T{}^{17}$
$BaSO_4$, $CdSO_4$,	$CaSO_4$ $CoSO_4$ $CuSO_4$, $PbSO_4$, $MgSO_4$, $NiSO_4$, $ZnSO_4$; these were all drawn from Kelley's equations[23], converted to the form: $MO + SO_3 = MSO_4$, using the above data for oxides and SO_3
$Al_2(SO_4)_3$	ΔH_{298}^{69}; Cp^{56}; $\Delta F^\circ_{298}{}^{52}$
$FeSO_4$	ΔH_{298}^{3}; assume Δ Cp and Δ S as for $CoSO_4$
$MnSO_4$	ΔH_{298}^{57}; Cp: $MnSO_4^{23}$, MnO^{20}, SO_3^{58};ΔF°_{298}:[23,35]; ΔS°_{298}, mean of all other sulphates[23]
K_2SO_4	ΔH_{298}^{69}; Cp^{56}; $\Delta F^\circ_{298}{}^{23}$
Na_2SO_4	ΔH_{298} and ΔF°_{298},[23,50]; Cp:[20], ([55] for K_2SO_4)
CARBONATES	
$BaCO_3$, $CaCO_3$	$FeCO_3$, $PbCO_3$, $MgCO_3$, $ZnCO_3$; $\Delta F^\circ_T{}^{25}$
$MnCO_3$	ΔH_{298}: $MnCO_3^{18}$, MnO^{57}, CO_2^{48}; Cp: $MnCO_3^{37}$, others[20]; $\Delta S^\circ_{298}{}^{24}$
Na_2CO_3	ΔH_{298}^{25}; Cp: $Na_2CO_3^{25}$, $Na_2O^{62,1}$, CO_2^4; $\Delta F^\circ_{298}{}^{25}$

References

[1] O. Barta: *Ztsch. Elektrochem.* (1937) **43**, 733.

[2] R. G. Bates: *Jnl.* Am. Chem. Soc. (1939) **61**, 1040.

[3] F. R. Bichowsky and F. D. Rossini: The Thermochemistry of Chemical Substances. Reinhold, N. Y., 1936.

[4] J. Chipman and M. G. A. Fontana: *Jnl.* Am. Chem. Soc. (1935) **57**, 48.

[5] A. Chretien and P. Galmiche: *Compt. Rend.* (1946) **223**, 802.

[6] E. M. Cox, M. C. Bachelder, N. H. Nachtrieb and A. S. Skapski: *Trans.* AIME (1949) **185**, 27. *Jnl. of Metals,* Jan. 1949.

[7] H. J. T. Ellingham: *Jnl.* Soc. Chem. Ind. (1944) **63**, 125.

[8] W. F. Giauque and P. F. Meads: *Jnl.* Am. Chem. Soc. (1941) **63**, 1897.

[9] S. Glasstone: Thermodynamics for Chemists. van Nostrand, N. Y., 1947.

[10] P. Gross, C. S. Campbell, P. J. C. Kent and D. L. Levi: Disc. Faraday Soc., No. 4, p. 206 (1948).

[11] P. Günther: *Ann. Physik* (1916) **51**, 828.

[12] J. F. G. Hicks, J. G. Hooley and C. C. Stephenson: *Jnl.* Am. Chem. Soc. (1944) **66**, 1064.

[13] C. D. Hodgman: Handbook of Chemistry and Physics. Chem. Rubber Publ. Co., 1947.

[14] F. Ishikawa and G. Kimura: The Sexagint. Kyoto Imp. Univ., p. 255, (1927).

[15] F. M. Jaeger, E. Rosenbohm and A. J. Zuithoff: *Rec. des Trav. chem. des Pays Bas* (1938) **57**, 1313.

[16] H. L. Johnston and M. K. Walker: *Jnl.* Am. Chem. Soc. (1935) **57**, 682.

[17] A. F. Kapustinskii: *Compt. rend.* acad. sci. U.R.S.S. (1946) **53**, 719.

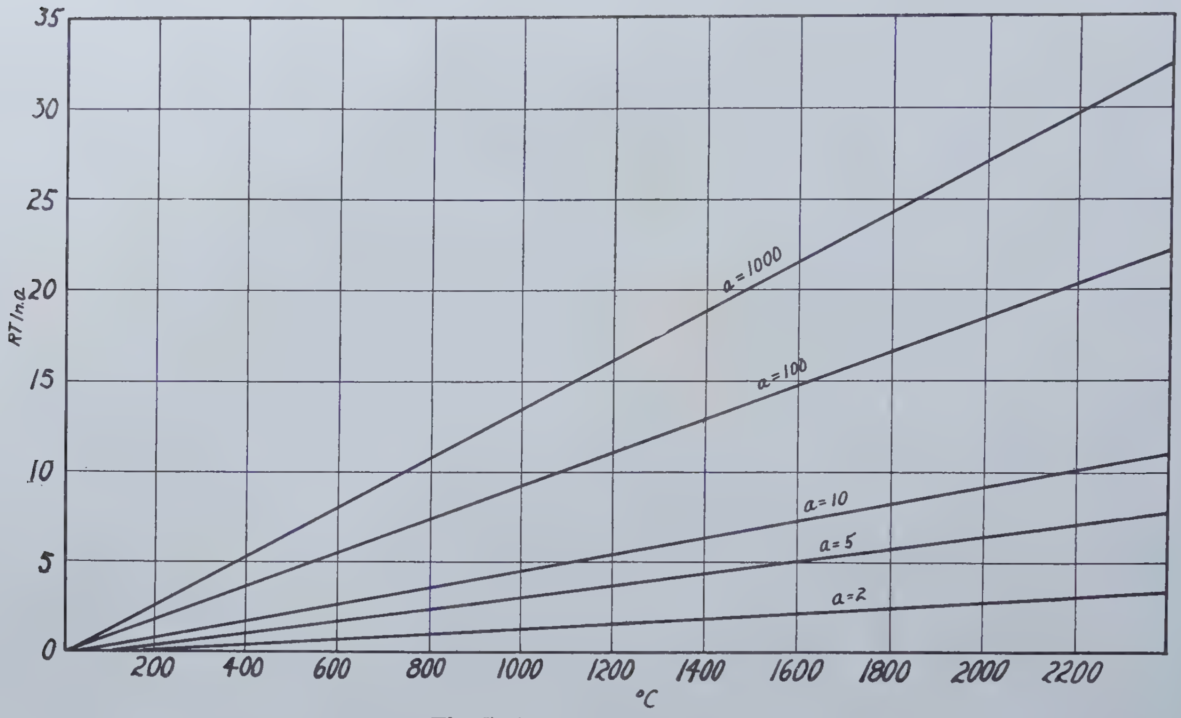

Fig. 7—Values of *RT* ln *a*.

To be used in correcting free energies for reactions involving substances not present at unit activity.

[18] A. F. Kapustinskii: *Jnl. Phys. Chem.* (U.S.S.R.) (1941) **15**, 220.

[19] A. F. Kapustinskii and Korshunov: *Jnl. Phys. Chem.* (U.S.S.R.) (1938) **2**, 220.

[20] K. K. Kelley: U. S. Bur. Mines Bull., No. 371 (1934).

[21] K. K. Kelley: U. S. Bur. Mines Bull., No. 383 (1935).

[22] K. K. Kelley: U. S. Bur. Mines Bull., No. 393 (1936).

[23] K. K. Kelley: U. S. Bur. Mines Bull., No. 406 (1937).

[24] K. K. Kelley: U. S. Bur. Mines Bull., No. 434 (1941/1948).

[25] K. K. Kelley and C. T. Anderson: U. S. Bur. Mines Bull., No. 384 (1935).

[26] K. K. Kelley and G. E. Moore: *Jnl.* Am. Chem. Soc. (1943) **65**, 1264.

[27] V. A. Kireev: *Jnl. Gen. Chem.* (U.S.S.R.) (1946) **16**, 1391.

[28] W. M. Latimer: The Oxidation States of the Elements and their Potentials in Aqueous Solutions. Prentice Hall, N. Y., 1938.

[29] G. N. Lewis and M. Randall: Thermodynamics and the Free Energy of Chemical Substances. McGraw-Hill, N. Y., 1923.

[30] S. V. Lipin, V. S. Uskov and V. R. Klokman: *Jnl. Appl. Chem.* (U.S.S.R.) (1942) **15**, 411.

[31] J. Lumsden: Disc. Faraday Soc., No. 4, p. 239 (1948).

[32] C. G. Maier: *Jnl.* Am. Chem. Soc. (1928) **51**, 194.

[33] I. A. Makolkin: *Jnl. Phys. Chem.* (U.S.S.R.) (1942) **16**, 13.

[34] I. A. Makolkin: *Jnl. Phys. Chem.* (U.S.S.R.) (1942) **16**, 18.

[35] G. Marchal: *Jnl. Chim. Phys.* (1925) **22**, 559.

[36] Metals Handbook, A.S.M., Cleveland, 1948.

[37] G. E. Moore: *Jnl.* Am. Chem. Soc. (1943) **65**, 1938.

[38] G. E. Moore: *Jnl.* Am. Chem. Soc. (1943) **65**, 1700.

[39] B. F. Naylor: *Jnl.* Am. Chem. Soc. (1946) **68**, 1077.

[40] C. J. Osborn: *Tid. Kjemi, Bergvesen og Metallurgi* (1949) **9**, 79.

[41] P. R. Pallister: *Jnl.* Iron & Steel Inst. (1949) **161** (*II*), 87.

[42] K. S. Pitzer and W. V. Smith: *Jnl.* Am. Chem. Soc. (1937) **59**, 2633.

[43] M. Randall, R. F. Nielson and G. H. West: *Ind. Eng. Chem.* (1931) **23**, 388.

[44] M. Randall and H. M. Spencer: *Jnl.* Am. Chem. Soc. (1928) **50**, 1572.

[45] F. D. Richardson: Disc. Faraday Soc., No. 4, p. 244 (1948).

[46] F. D. Richardson and J. H. E. Jeffes: *Jnl.* Iron & Steel Inst. (1948) **160**, 261.

[47] B. A. Rose, G. J. Davis and H. J. T. Ellingham: Disc. Faraday Soc., No. 4, p. 154 (1948).

[48] F. D. Rossini and R. S. Jessup: *Jnl.* Res. Nat. Bur. Standards (1938) **21**, 491.

[49] W. A. Roth and H. Troitzsch: Landolt-Bornstein Phys. Chem. Tab., supp. 3, p. 2749 (1936).

[50] E. Shibata, S. Oda and S. Furukawa: *Jnl.* Chem. Soc. Japan (1930) **51**, 289; also *Jnl. Sci.* Hiroshima Univ., Ser. A, (1930) **3**, 227.

[51] P. E. Snyder and H. Seltz: *Jnl.* Am. Chem. Soc. (1945) **13**, 683.

[52] C. H. Shomate: *Jnl.* Am. Chem. Soc. (1945) **67**, 765.

[53] C. H. Shomate: *Jnl.* Am. Chem. Soc. (1947) **69**, 218.

[54] C. H. Shomate: *Jnl. Chem. Phys.* (1945) **13**, 326.

[55] C. H. Shomate and E. H. Huffman: *Jnl.* Am. Chem. Soc. (1943) **65**, 1625.

[56] C. H. Shomate and B. F. Naylor: *Jnl.* Am. Chem. Soc. (1945) **67**, 72.

[57] J. C. Southard and G. E. Moore: *Jnl.* Am. Chem. Soc. (1942) **64**, 1769.

[58] H. M. Spencer: *Jnl.* Am. Chem. Soc. (1945) **67**, 1859.

[59] H. M. Spencer and G. N. Flannagan: *Jnl.* Am. Chem. Soc. (1942) **64**, 2511.

[60] H. M. Spencer and J. L. Justice: *Jnl.* Am. Chem. Soc. (1934) **56**, 2311.

[61] H. M. Spencer and W. M. Spicer: *Jnl.* Am. Chem. Soc. (1942) **64**, 617.

[62] M. de K. Thompson: The Total and Free Energies of Formation of the Oxides of Thirty-two Metals. Electrochem. Soc., N. Y., 1942.

[63] E. Thurmann-Nielsen: Thesis, N. T. H., Trondheim, 1943.

[64] W. D. Treadwell and L. Terebesi: *Helv. Chim. Acta* (1933) **16**, 922.

[65] E. C. Truesdale and R. K. Waring: *Jnl.* Am. Chem. Soc. (1941) **63**, 1610.

[66] T. Utne: Thesis, N. T. H., Trondheim, 1942.

[67] M. Watanabe: *Sci. Repts.* Tohoku Imp. Univ. (1933) **22**, 423.

[68] R. R. Wenner: Thermochemical Calculations. McGraw-Hill, N. Y., 1941.

[69] F. E. Young: *Jnl.* Am. Chem. Soc. (1945) **67**, 257.

[70] A. F. Kapustinskii and E. Gofman: *Jnl. Phys. Chem.* (U.S.S.R.) (1937) **9**, 713.

Conditioning Dwight-Lloyd Gases to Increase Bag Life

by R. E. Shinkoskey

This paper outlines the development of a program for increasing the life of woolen bags used for filtering Dwight-Lloyd gases by treating the bags and gases with hydrated lime. Methods and apparatus are described for determining alkalinity of dusts, acidity and breaking strength of bag cloth. Procedure and results, based on several years of operation, are presented.

DURING 1939, additional facilities were constructed in the Dwight-Lloyd Blast Furnace and Baghouse departments at the Selby, California, Plant of the American Smelting and Refining Co. In order to handle adequately the increased volume of gases from the resultant increase in production, it was necessary to increase gradually the amount of water used for cooling gases ahead of the sinter machine baghouse. As a result of this increased water cooling, the average bag life dropped from 27 months in 1939 to 14 months in 1941. (Table I). This drop in life meant an increased bag cost, as well as lower recovery of dust and some curtailment of operation.

During 1941, it was found new bags showed as high as 0.3 pct acidity* after two weeks of operation and as much as 2.0 pct acidity after some months of operation. This high acidity was present in spite of the fact that free oxide or relative alkalinity of the unburned dust ran from 5 to 6 pct.

In view of these circumstances, a twofold program was started in Nov. 1941.† Part one of this program consisted of vigorously dipping all new bags in a weak lime solution, containing 50 lb of hydrated lime per 50 gal of water. Part two consisted of feeding fine, dry, hydrated lime into the gas stream intake of the sinter baghouse fan. Apparatus for feeding this lime is shown in fig. 1. All baghouse chambers are shaken in rotation about once each hour. On alternate hours, the baghouse operator places 50 lb of hydrated lime (one sack) into the lime feeder, starts feeder and immediately starts the bag shaking machinery. The rate at which lime is fed is set to coincide with the approximate time necessary to shake all sinter baghouse chambers, or about 15 min. It is felt this method of lime addition is most effective for getting lime into the woolen bag fabric. The amount of lime so fed averages about 600 lb per day.

The amount of lime fed per day is varied to keep a minimum relative alkalinity of 9 pct in the unburned sinter dust. A daily dust sample is taken for alkalinity by allowing dust to accumulate in a sample pipe over a 24-hr period. This sample pipe, placed in any chamber cellar, is 2 in. in diam, 4 ft long, is sealed on the inner end, and capped on the outer end. It has a ½ in. slot cut for 18 in. along the tip end. This slot faces upward and allows the pipe to fill gradually with dust as bags are shaken.

Breaking strength of bags has, in most cases, been the deciding factor in bag replacement. Bags that normally test 100 psi breaking strength when new are replaced when they test under 35 lb. The method for determining breaking strength is shown in the description accompanying fig. 2.

Since the start of the liming program in 1941, bag life has increased from 14 months to an average of over 23 months, with a consequent material decrease in bag cost per year.

Table I. Drop in Bag Life

Year	Type of Bag	Total Bags in D & L Bag-house	Total Bags In-stalled	Life in Months of Bags Re-placed	Volume Gas Filtered cfm per Bag
1938	Wool-fulled	803	357	27	99
1939	Wool-fulled	803	255	27	117
1940	Wool-fulled	803	545	22	110
1941	Wool-fulled	1028	903	14	134
1942	Wool-fulled	1028	535	23	166
1943	Wool-fulled	1028	539	22	134
1944	Wool-fulled	953	521	24	105
1945	Wool-fulled	878	400	25	112
1946	Wool-fulled	878	498	23	115
1947	Wool-fulled	878	400	23	97

Table II. Method of Determining Per Cent Acidity in Bag Cloth

Acidity, as per cent sulphuric acid, may be determined by means of a Beckman pH meter as follows:

From a piece of bag cloth, which has been thoroughly cleaned of dust, a 5 g sample is weighed on a balance. Cut the sample into fine pieces and place in a 400 cc beaker. Add 100 cc (measured) of distilled water and stir vigorously. Filter on suction funnel, holding cloth pulp in beaker with a stirring rod. Wash cloth sample and filter wash water four additional times, each time with 20 cc distilled water, the last time squeezing cloth pulp over funnel. Discard pulp and rinse funnel and filter paper. Pour wash solution into measuring graduate and make up to exactly 300 cc with distilled water. Place into clean 600 cc beaker and measure the pH on meter. The per cent acid in bag cloth is read from the following table:—

pH	Pct Acid	pH	Pct Acid
2.0	3.72	3.0	0.37
2.1	2.95	3.1	0.30
2.2	2.34	3.2	0.23
2.3	1.86	3.3	0.19
2.4	1.48	3.4	0.15
2.5	1.17	3.5	0.11
2.6	0.93	3.6	0.09
2.7	0.74	3.7	0.07
2.8	0.59	3.8	0.06
2.9	0.47		

Should it be desired, the per cent acid may be determined by titrating the wash solution with standard sodium hydroxide solution.

---

* Methods for determining per cent acidity in bag cloth (table II) and per cent relative alkalinity of dust (table III) were developed by A. L. Labbe and J. J. Donoso of the American Smelting and Refining Co.

† This program was started largely as a result of work initiated by A. L. Labbe of the American Smelting and Refining Co.

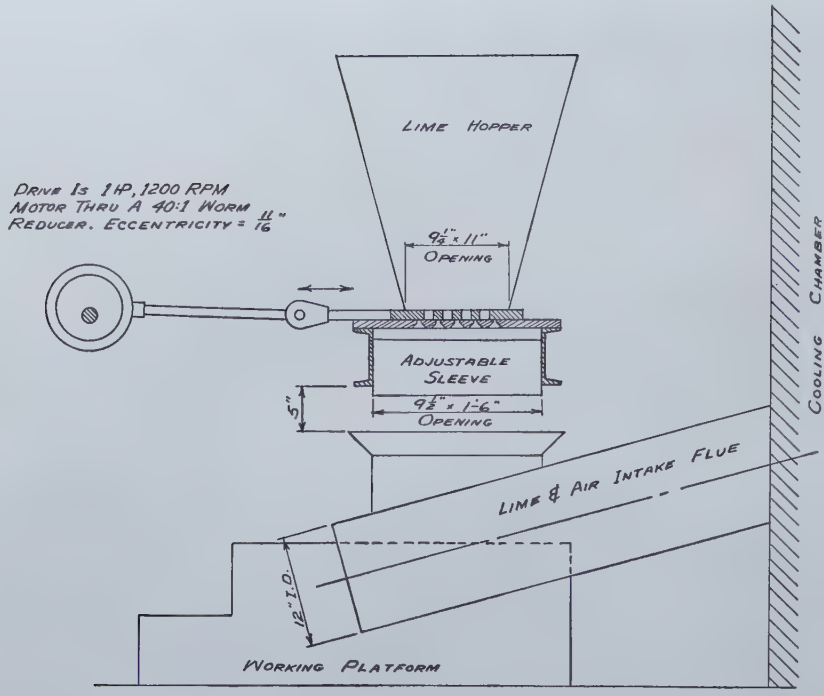

Fig. 1—Lime feeder.

R. E. SHINKOSKEY is associated with American Smelting and Refining Co., Selby Smelting Works, Selby, Calif.

AIME New York Meeting, Feb. 1950.

TP 2820 D. Discussion (2 copies) may be sent to Transactions *AIME before Apr. 1, 1950, and will be published Nov. 1950. Manuscript received Oct. 17, 1949.*

Method of Determining Breaking Strength of Bag Cloth

The breaking strength of bag cloth and seam is determined at Selby with a standard testing machine of the pendulum type, known as the Scott Model DH.

All specimens for testing are cut from a 12 in. vertical band, as shown on accompanying illustration. Individual test specimens are cut 4 in. wide and 6 in. long. Two sets of 5 specimens each are required; one set for warp breaking strength, having the long dimension parallel to warp yarns, and the other set for filling breaking strength and having the long dimension parallel to the filling yarns. Another set of 3 specimens for seam breaking strength is required. These specimens are to be 4 in. wide by 6 in. long, with the shorter dimension parallel to the seam and the seam forming a central axis.

The breaking strength in pounds per square inch of warp and fill is the average of each of the 5 test specimens, while the seam breaking strength is the average of the 3 test specimens.

Table III. Method of Determining Per Cent Relative Alkalinity of Baghouse Dusts

A 1 g sample of dust is weighed into a 250 cc beaker, 15 cc distilled water added and the solution stirred to break up lumps. Ten cc of half normal sulphuric acid are added and the solution brought to boil. It is then filtered through fine paper and washed three times with water. The filtrate, with 2 drops of methyl orange, is titrated with half normal sodium hydroxide. Per cent relative alkalinity is then given by the formula:

$$\text{Pct Rel. Alk.} = (X - \text{cc, NaOH}) \times 2.45$$

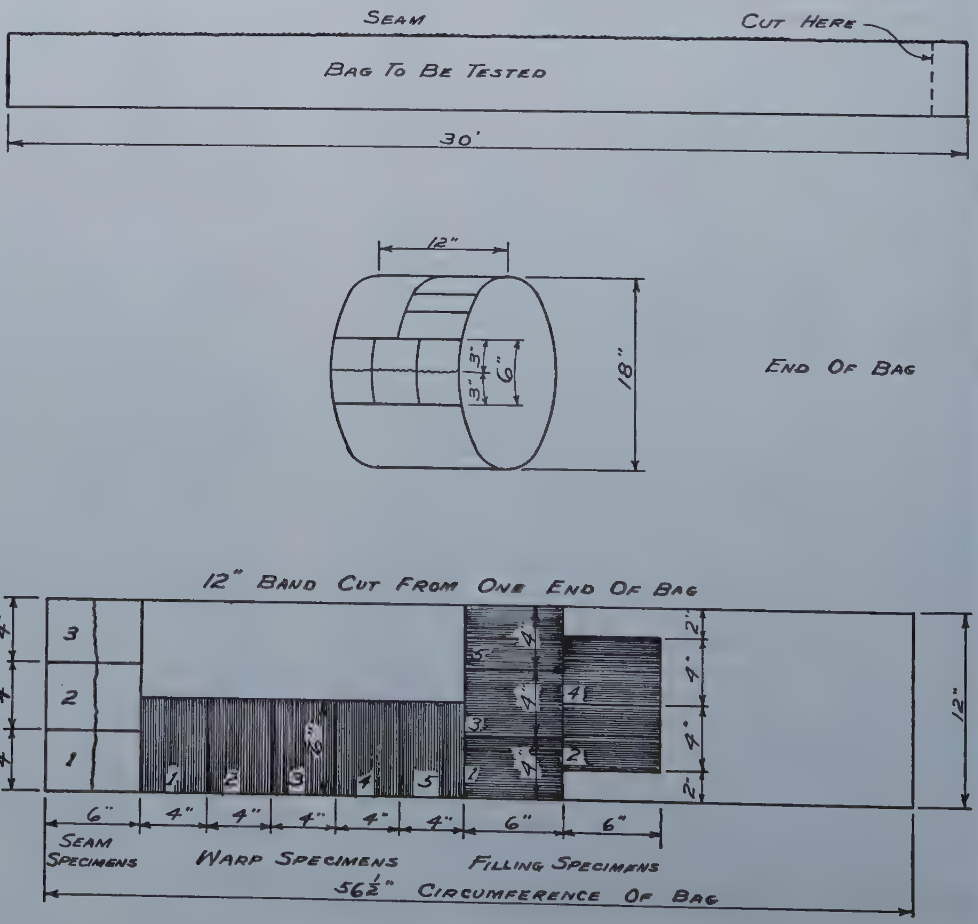

Fig. 2—Standard testing of woolen smelter bags.

An Improved Automatic Smoke Sampler

by J. J. Donoso

IN the operation of a smelter, continuous and accurate determination of smoke losses is essential for purposes of metals inventories and as a check on the efficiency of smoke recovery apparatus.

Previous to the development of a continuous and automatic smoke sampler by R. MacMichael, in 1924, two methods were in vogue, and still are in some smelters, for measuring solids passing out of a flue or stack. These are: (1) the so-called dust concentration method whereby the gas volume passing through the flue is first measured and then the total amount of solids carried in the smoke stream calculated from the weight of suspended matter filtered out of a measured volume of gas; (2) the balanced tube method is independent of gas volume flowing through the flue, and relies for its accuracy on the fact that a true smoke sample may be taken if the velocity of the gas in the sampling tube is constantly maintained at a known ratio of the average flue gas velocity. The total amount of solids passing through the flue is then proportional to the weight of filtered solids and to the ratio of the area of the flue to the area of the sampling tube, corrected for the velocity ratio.

The limitations of the first method lie in the uncertainty of the varying volume of gas arising from metallurgical operations and the unreliability of ordinary gas meters to hold their accuracy under

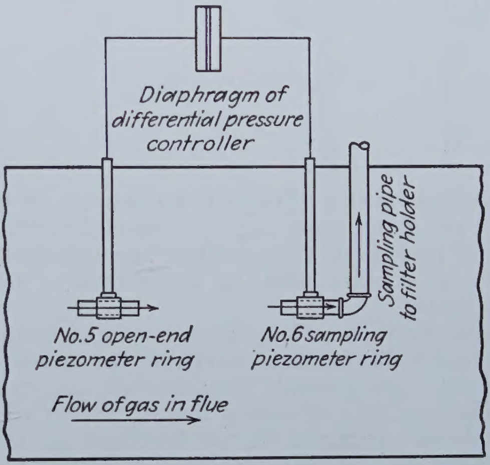
Diaphragm of differential pressure controller
Sampling pipe to filter holder
No.5 open-end piezometer ring
No.6 sampling piezometer ring
Flow of gas in flue

Fig. 1—Automatic smoke sampler— Piezometer rings.

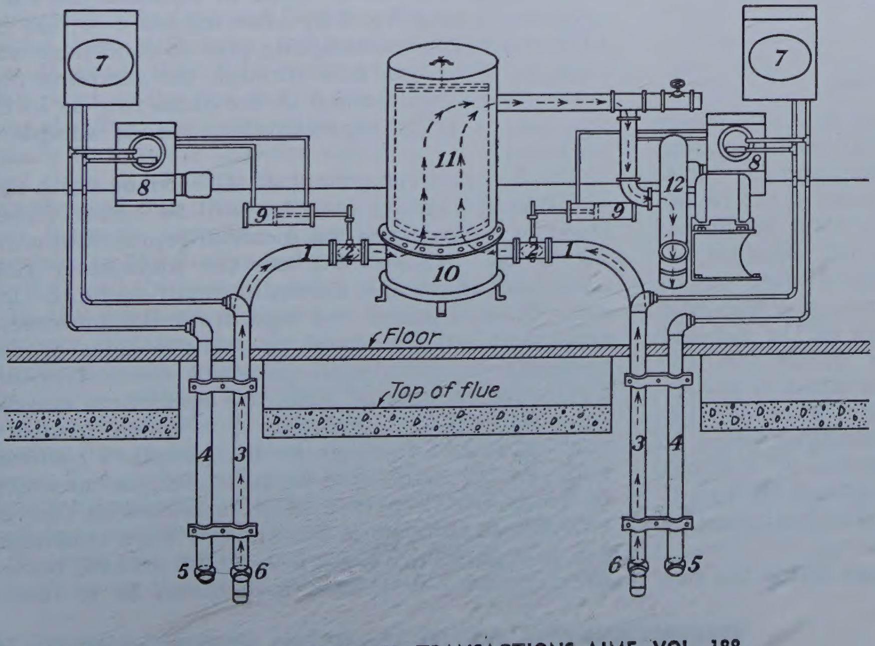

Fig. 2—Automatic multiple smoke sampler. General arrangement.

J. J. DONOSO is Metallurgist, American Smelting and Refining Co., Salt Lake City, Utah.

AIME New York Meeting, Feb. 1950.

TP 2823 D. Discussion (2 copies) may be sent to Transactions AIME before May 1, 1950, and will be published Nov. 1950. Manuscript received Oct. 17, 1949.

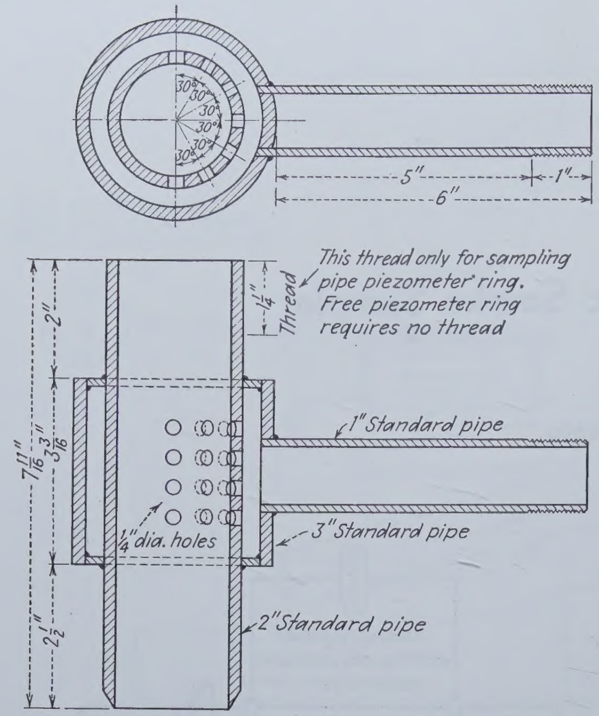

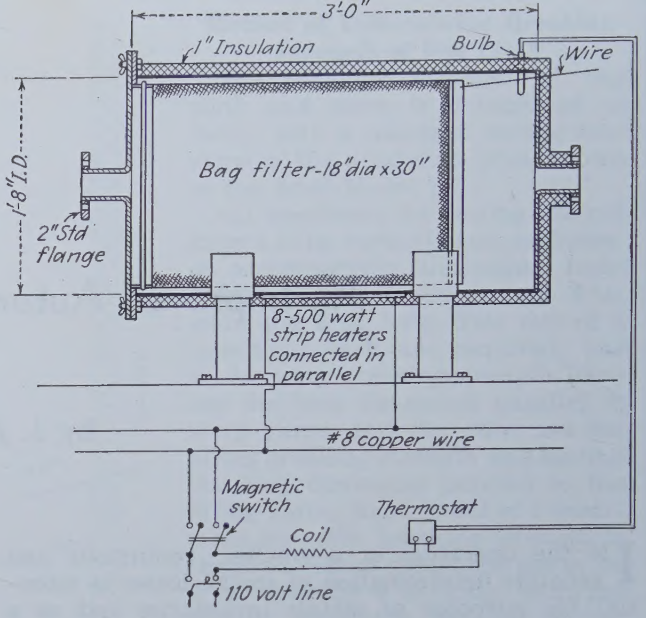

Fig. 3 (left)—Two-inch piezometer ring assembly.

Fig. 4 (above)—Filter holder for automatic smoke sampler.

such severe service. The impracticability of manually keeping the sampling and flue velocities equal for long periods of time renders the balanced-tube method of smoke sampling an indicative or spot check device.

MacMichael's sampler, in reality an automatically controlled balance tube, removed the human element and made possible the accurate and continuous determination of smoke losses. Essentially, the principle of operation of the MacMichael sampler is as described for the improved sampler, but the cumbersome and complicated electrical velocity-regulating device employed in his units gave rise to frequent interruptions and elaborate maintenance.

These objections have been overcome in the improved samplers now in use in a number of plants, both of American Smelting and Refining Co. and of others licensed by it. The utilization of modern fluid or pneumatic differential pressure controlling instruments not only makes the operation of the present sampler more trouble-free, but also allows for simultaneous sampling of multiple points or flues, using only one filter and one exhaust system.*

Theory and Operation

If a portion of the smoke stream is continuously withdrawn at a velocity constantly corresponding to the velocity of the gas in the flue, and the solids separated from the withdrawn portion of the smoke stream in a filtering medium, the total weight of solids being carried in the stream can then be determined from the weight of solids filtered out of the smoke sample in a known time, and the ratio of the area of the flue to the area of the opening through which the sample was taken. In the formula for smoke losses by this method, it is necessary to incorporate a factor which relates the average velocity of gas at the sampling point to the average velocity of gas in the flue as a whole. In practice, such a factor is determined by simultaneous Pitot tube explorations of flue and sampling point velocities.

Fig. 1 shows two piezometer rings inside the flue whose dust burden is to be measured. For clarity they are shown side by side on a horizontal plane, but in practice they are located on a vertical plane at right angles to the flow of gas in the flue and approximately 12 in. apart on a horizontal line. Ring No. 5 is open at both ends and measures only the static pressure in the flue since there is no impedance to the flow of gas through it. This ring is connected to one side of the diaphragm of a differential pressure controller. A static pressure of the same magnitude acts upon ring No. 6 because of its proximity to ring No. 5, but since ring No. 6 is connected to a filter system, resistance is offered to the flow of gas, so that unless gas is removed through it by the suction system at exactly the same velocity as gas flow in the flue, a dynamic pressure will be imposed which will distort the magnitude of the static pressure in ring No. 6 from that in ring No. 5. The impulse line of ring No. 6 is connected to the opposite side of differential pressure controller diaphragm. As the static pressure in ring No. 5 varies due to changes in flue gas velocity, the controller seeks to equalize the static pressure in ring No. 6 by allowing more or less gas to flow through the sampling pipe as conditions may require. Thus, gas flow through the sampling pipe is constantly maintained at the same rate as in the flue and a truly representative smoke sample is obtained.

The actual arrangement of the various units constituting the smoke sampler will be better understood by referring to the pictorial representation on fig. 1. No. 5-5 and 6-6 are the piezometer rings described above and shown in detail on fig. 2. Impulse lines 3-3 and 4-4 lead from the piezometer rings and are connected to opposite sides of diaphragms in differential pressure controllers 8-8. Connected in parallel with the controllers are differential pressure recorders 7-7 which furnish a running record to check on the sampler's performance. As the magnitude of the static head measured by rings 5-5 changes due to variations in flue gas velocity an impulse is transmitted from controllers 8-8 to regulating valves 9-9, which actuate butterfly dampers 2-2 in such a direction as to restore

---

* U. S. Pat. No. 1494855.

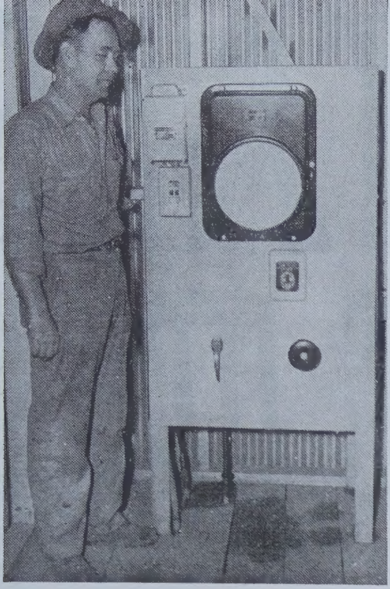

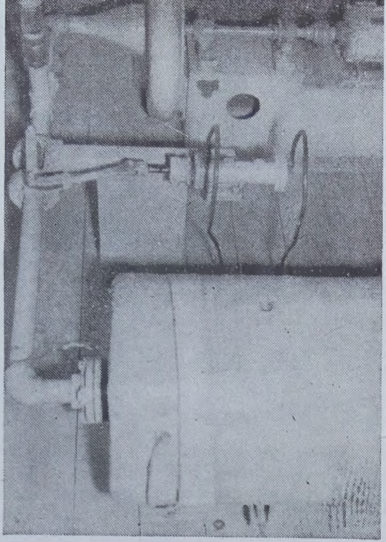

Fig. 5 (left)—Instrument cabinet.

Fig. 6 (right)—Exhaust fan, regulating valve and filter holder.

Fig. 7 (below) — Piezometer leads and insulated filter holder.

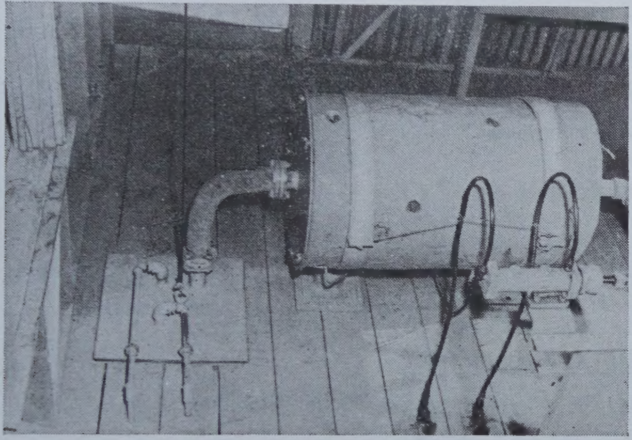

zero difference in static heads 5 and 6 by allowing more or less gas to flow through sampling pipes 1-1 as conditions may require. The sampling pipe, or pipes, discharge into a filter holder, 10, the solids being retained in the filter fabric, 11, and the clean gas passing through the suction system, 12, and evacuating at a point downstream from the sampling pipe.

As a direct check on the performance of the sampler installed at the Murray, Utah, plant of American Smelting and Refining Co. aside from the visual zero difference indicated by the recorder, simultaneous Pitot tube readings taken at the sampling point in the flue and in the sampling pipe outside the flue, over extended periods of time, gave results to indicate that the accuracy of the sampler was close to 100 pct. Actually, average velocity of gas through flue during testing period was 21.2 fps, and through sampling pipe 21.4 fps. The static pressure in the flue varied from 0.40 in. H_2O to 0.75 in. H_2O and the velocity head averaged 0.1 in. H_2O.

In the practical application of this sampler, experience dictates the size of piezometer rings and sampling pipes most adaptable to the particular conditions, although preliminary surveys may be made to determine volume and dust burden of gas passing flue to be sampled. For most practical purposes, 2 in. rings and sampling tube will suffice to obtain measurable amounts of dust filtered out of baghouse or Cottrell exhaust gases. (Fig. 3).

The size and material of the filter will again vary according to conditions, but generally a 30 in. bag of standard 18 in. diam woolen baghouse fabric is of sufficient size and durability to filter most metallurgical fumes. The filter is placed within a 20 x 36 in. steel drum with a detachable cover on which the filter bag is tied to a thimble, provision being made for periodic shaking of the bag by means of a wire tied to the bag and brought to the outside of the drum (fig. 4). The steel drum is electrically heated and insulated, and the temperature of the gas within the drum thermostatically controlled to insure a dry sample and longer filter life. (Fig. 5, 6, 7.)

A few days trial will determine the operating routine for a new sampler. The frequency with which a filter bag will have to be shaken will be shown by the differential pressure recorder, a deviation from zero difference indicating plugging up of the filter pores beyond the capacity of the exhaust system. Duration of a continuous sample is best determined by trial during the first few days operation; sufficient amount of dust should be accumulated to avoid weighing errors against the weight of the filter.

Having ascertained the effective flue area by sounding to eliminate area occupied by accumulated dust, and the Sampling Flue Factor by Pitot tube explorations, the formula for dust loss determination by the automatic balanced-tube method becomes:

$$\text{Dust Loss (lb per 24 hr)} = \frac{Ae}{As} \times \frac{24 \times W \times F_F}{Time}$$

Where,

Ae = Effective flue area (sq ft)
As = Area of sampling pipe (sq ft)
$Time$ = Duration of sampling (hr)
W = Weight of filtered sample (lb)
F_F = Flue factor, ratio of average overall flue gas velocity to average flue gas velocity at sampling point.